SOLAR THERMAL ELECTRIC POWER SYSTEMS

FINAL REPORT

VOLUME 3

APPENDICES

Prepared for

The National Science Foundation

Research Applied to National Needs

Washington, D. C.

Supported by NSF Grant GI-37815

Initiated May 1, 1973

Prepared by

Colorado State University

Fort Collins, Colorado

and

Westinghouse Electric Corporation

Pittsburgh, Pennsylvania

NOVEMBER 1974

Report: NSF/RANN/SE/GI-37815/FR/74/3

COLORADO STATE UNIVERSITY

Solar Energy Applications Laboratory

Engineering Research Center

SOLAR THERMAL ELECTRIC POWER SYSTEMS

FINAL REPORT

VOLUME 3

APPENDICES

Prepared for

The National Science Foundation
Research Applied to National Needs
Washington, D. C.

Supported by NSF Grant GI-37815
Initiated May 1, 1973

by

Colorado State University
Fort Collins, Colorado

and

Westinghouse Electric Corporation
Pittsburgh, Pennsylvania

NOVEMBER 1974

Report No: NSF/RANN/SE/GI-37815/FR/74/3

BIBLIOGRAPHIC DATA SHEET	1. Report No. NSF/RANN/SE/GI-37815/FR/74/3	2.	3. Recipient's Accession No.
4. Title and Subtitle	FINAL REPORT SOLAR THERMAL ELECTRIC POWER SYSTEMS		5. Report Date: November 1974 6.
7. Author(s)	Research Staff of Colorado State University and Westinghouse Electric Corporation		8. Performing Organization Rept. No. NONE
9. Performing Organization Name and Address	Solar Energy Applications Laboratory Colorado State University Engineering Research Center Fort Collins, Colorado 80523 Westinghouse Electric Corporation Pittsburgh, Pennsylvania 15112		10. Project/Task/Work Unit No. 11. Contract/Grant No. GI-37815
12. Sponsoring Organization Name and Address	The National Science Foundation Research Applied to National Needs Washington, D. C. 20550		13. Type of Report & Period Covered Final 5/1/73 - 11/30/74 14.

15. Supplementary Notes

16. Abstracts

The final report consists of three volumes: (1) an Executive Summary, (2) System Studies and Economic Evaluations, and (3) Appendices.

The objective of the research program is to develop design parameters of systems for thermal/mechanical conversion of solar energy to electric power at minimum cost per kilowatt-hour generated. Systems of 3MW to 300MW sizes in a public utility network are considered. Parametric performance and cost models are derived for key elements of the system. A sequential optimization program was developed using these models to determine optimum subsystem sets and combinations which yield the least capital cost plants. A dynamic simulation program was developed to determine annual electric power produced by solar power systems at specific locations. Electric energy cost comparisons are made to select promising systems for generation of electricity from solar energy.

17. Key Words and Document Analysis. 17a. Descriptors

Solar Thermal Conversion
Solar Energy
Power Generation
Optimization
Flat-Plate Collectors
Concentrating Collectors
Solar Collectors
Solar Power Plants

17b. Identifiers/Open-Ended Terms

STEPS (Solar Thermal Electric Power Systems)
Solar Thermal Conversion
Solar Power Plants

17c. COSATI Field/Group

18. Availability Statement	19. Security Class (This Report)	21. No. of Pages
Write to Mr. George Kaplan, Project Manager, Solar Thermal Projects, National Science Foundation, 1800 G Street, N. W. Washington, D.C. 20550	UNCLASSIFIED	
	20. Security Class (This Page) UNCLASSIFIED	22. Price

PREFACE

The final report for the study of Solar Thermal Electric Power Systems (STEPS), conducted by Colorado State University and Westinghouse Electric Corporation and financially supported by The National Science Foundtaion, Research Applied to National Needs, under Grant GI-37815, is in three main volumes and one supplementary volume. Volume 1 is an Executive Summary which contains brief summaries of the procedures, results, conclusions and recommendations developed from the study. Volume 2, titled System Studies and Economic Evaluations, contains descriptions of methodology, parametric performance and cost models, descriptions of solar power plants which have the potential to produce low-cost electric energy, and detailed conclusions and recommendations. Volume 3, Appendices, contains the details of the study which are summarized in Volumes 1 and 2. The Supplementary Volume, is a compilation of reprints of the computer printout from the optimization runs. Although each is self contained, reference to other volumes is sometimes made to guide the reader.

The final report was prepared by the staff of the Solar Energy Applications Laboratory at Colorado State University, Fort Collins, Colorado, in collaboration with the Westinghouse Electric Corporation. Westinghouse participants included the Georesearch Laboratory in Boulder, Colorado, the Research and Development Center, the Power Generation System Division and the Manufacturing Development Laboratory in Pittsburgh, Pennsylvania.

The International System of Units (SI) has been used throughout the report. Some English units are used in a few instances where it is considered to be in such common usage in the United States that results in unfamiliar metric units would handicap the reader unnecessarily.

TABLE OF CONTENTS

VOLUME 1 - EXECUTIVE SUMMARY

VOLUME 2 - SYSTEM STUDIES AND ECONOMIC EVALUATIONS

VOLUME 3 - APPENDICES

TABLE OF CONTENTS BREAKDOWN

TABLE OF CONTENTS

Appendix A. Preliminary Design Studies

Appendix B. The Sequential Optimization Process

TABLE OF CONTENTS (Continued)

Appendix C. Environmental Conditions

Appendix D. Flat-Plate Collectors

TABLE OF CONTENTS (Continued)

TABLE OF CONTENTS (Continued)

TABLE OF CONTENTS (Continued)

Appendix G. Heat Storage

TABLE OF CONTENTS (Continued)

TABLE OF CONTENTS (Continued)

Appendix H. Heat Engines

Table of Contents (continued)

Appendix I. Heat Rejection

Appendix J. Dynamic Simulations

Appendix K. Optimization Results

SUPPLEMENTARY VOLUME - OPTIMIZATION COMPUTER OUTPUT

LIST OF FIGURES

Appendix A. Preliminary Design Studies

LIST OF FIGURES (Continued)

Appendix B. The Sequential Optimization Process

Appendix C. Environmental Conditions

LIST OF FIGURES (Continued)

LIST OF FIGURES (Continued)

Appendix D. Flat-Plate Collectors

LIST OF FIGURES (Continued)

Appendix E. Concentrating Collectors

LIST OF FIGURES (Continued)

Appendix F. Heat Transport

LIST OF FIGURES (Continued)

Appendix G. Heat Storage

LIST OF FIGURES (Continued)

Appendix H. Heat Engines

LIST OF FIGURES (Continued)

Appendix I. Heat Rejection

Appendix J. Dynamic Simulations

Appendix K. Optimization Results

LIST OF TABLES

Appendix A. Preliminary Design Studies

Appendix C. Environmental Conditions

Appendix D. Flat-Plate Collectors

LIST OF TABLES (Continued)

Appendix E. Concentrating Collectors

LIST OF TABLES (Continued)

Appendix F. Heat Transport

Appendix G. Heat Storage

LIST OF TABLES (Continued)

Appendix H. Heat Engines

Appendix J. Dynamic Simulations

APPENDIX A

PRELIMINARY DESIGN STUDIES

BY

A. D. WATT,

R. F. LINFIELD,

G. L. WILCOX,

AND

S. KARAKI

1.0 INTRODUCTION

Preliminary system designs and analyses were made of specific configurations to establish limitations on the ranges of design parameters for practical solar thermal power plant systems. These limits were used as constraints for the optimization and dynamic simulation programs. From the preliminary system designs, subsystems which significantly affected capital costs of solar power plants were identified. Also, the effect of cost and performance factors on energy costs were examined.

The cost of electrical energy produced was estimated for solar plants located at Albuquerque, New Mexico using statistical hourly distributions of insolation for the year 1959. Materials and equipment costs were based on 1972-1973 prices, a rate of capital amortization of 16 cents per year per dollar was used, and all electric energy produced was assumed to be utilized in an electric network.

Collector costs were not investigated in detail for the preliminary designs. Therefore, a range of anticipated costs per unit area of collector was used to determine energy costs. The results indicated the range of collector costs which must be achieved for the solar plant to be competitive in bus-bar energy costs with conventional plants.

2.0 METHOD EMPLOYED

The method used to develop preliminary design concepts and to evaluate the performance of each system involved:

(1) Reviewing and selecting environmental and operating conditions for Albuquerque, New Mexico.

(2) Conceptually assembling a number of feasible solar power plants from compatible subsystems.

(3) Evaluating performance and cost trade-offs for the subsystems for a range of operating conditions.

(4) Determining the performance and system costs per unit of output power, and identifying major cost factors which affected energy production costs.

(5) Examining the effects of varying plant size and operating temperatures on energy costs.

2.1 Basic Plant Types Considered

Three types of solar thermal electric power systems were considered. They were:

(1) A low temperature (150^{o}C) flat-plate collector system in which the heat was transported by pressurized water. To achieve this temperature, collectors consisting of clear honeycomb between the absorber surface and cover glass with back insulation were designed. Orientation was assumed to be fixed at an azimuthal tilt equal to the latitude.

(2) A medium temperature (255°C) concentrating collector system (with a concentration ratio of 20) in which the heat was transported by steam. The collector consisted of a parabolic trough tilted to the latitude with single axis tracking.

(3) A higher temperature (350°C) system employing two axis tracking reflectors concentrating solar radiation on a central absorber mounted on a tower. Multiple tower plants were included in the analysis to achieve reductions of energy costs.

2.1.1 Preliminary Design Conditions

The design conditions used are tabulated below.

Location:	Albuquerque, New Mexico
Insolation:	Statistical distribution derived from 1959 measurements of total solar flux density on a horizontal plane.
Ambient Temperature:	10 °C
Sky Temperature:	-5 °C
Wind Velocity:	5 m/s
Storage Time:	Adjusted to obtain minimum energy costs.
Rated Capacity:	Varied to obtain minimum energy costs.
Collector Cost:	A parametric variable to establish relation to energy costs.

2.1.2 Performance and Cost Trade-Off Relationships

Preliminary performance and cost trade-offs were made for subsystems using the design parameters for the three preliminary systems

that were selected. Estimated performance and costs are expressed graphically in terms of the most significant system parameters. The performance curves were derived from theoretical and experimental data available in the literature. Subsystem costs per unit of power output were developed from discussions with material suppliers, component manufacturers and consultants in areas of interest. When the necessary data were not available, subsystem costs were derived using escalators on the basic materials costs and multipliers on cost estimates for the specific designs. Collector performance curves were used to determine collector efficiencies and to estimate available heat from solar radiation for a particular operating period. An important component in system cost is the cost of collectors. Rather than to provide detailed costs for collectors at this stage in the analysis, the cost for electric energy was expressed parametrically with unit collector costs. A range of 40 to 80 dollars per square meter was estimated to bracket the range of realistic collector costs.

The performance of a flat-plate honeycomb collector and a parabolic trough collector is shown in Figure 2-1. Thermal power output per unit area from the collector is shown as a function of incident solar flux density for the specific heat transport fluid temperatures chosen for these preliminary designs. The flat-plate collector was assumed to have a 5 cm. deep transparent honeycomb between the absorber surface and the glass cover. The absorbing surface was assumed to have an absorptivity of 0.95 and emissivity of 0.9. The back side was insulated with 10 cm. of glass wool. The parabolic trough collector had a concentration ratio of 20, intercept factor of 0.85 (the fraction of incident light intercepted by the absorber), surface reflectance of 0.75, absorptivity of 0.9. The transmissivity for the glass envelope

around the absorber tube was 0.95 , with a selective coating having an emissivity of 0.2. The ambient temperature was assumed to be 10 ^{o}C and sky temperature, -5 ^{o}C.

To determine heat transport costs and land costs, it was necessary to determine collector spacing in the field layout. Assuming that collectors are distributed in rows (east-west) and columns (north-south), the spacing between rows will be a function of latitude for polar mounted collectors, for no shading interference between rows. Spacing between columns is a function of the time of day, or hour angle. The spacing factors between rows, F_1, and between columns, F_2, are expressed in Figure 2-2 as functions of latitude and hour angle respectively.

Performance and cost estimates for the heat transport system were developed for different thermal power levels for both steam and pressurized hot water systems using a computer program as described in Appendix F. At each power level, the pipe size, flow rate, insulation thickness and costs associated with piping, pumping power, insulation and heat loss were calculated for the total transport system including the feedwater return. The results which are tabulated in Appendix F were used to determine heat transport costs as a function of field geometry.

The flat-plate collector system was designed for pressurized water transport with a heat exchanger boiler to generate steam to operate the turbine. Estimates for heat exchanger costs per unit of thermal power, as a function of inlet temperature and parametric in Δt, the difference between input and output steam temperatures, are shown in Figure 2-3.

A steam accumulator storage subsystem was assumed for each system.

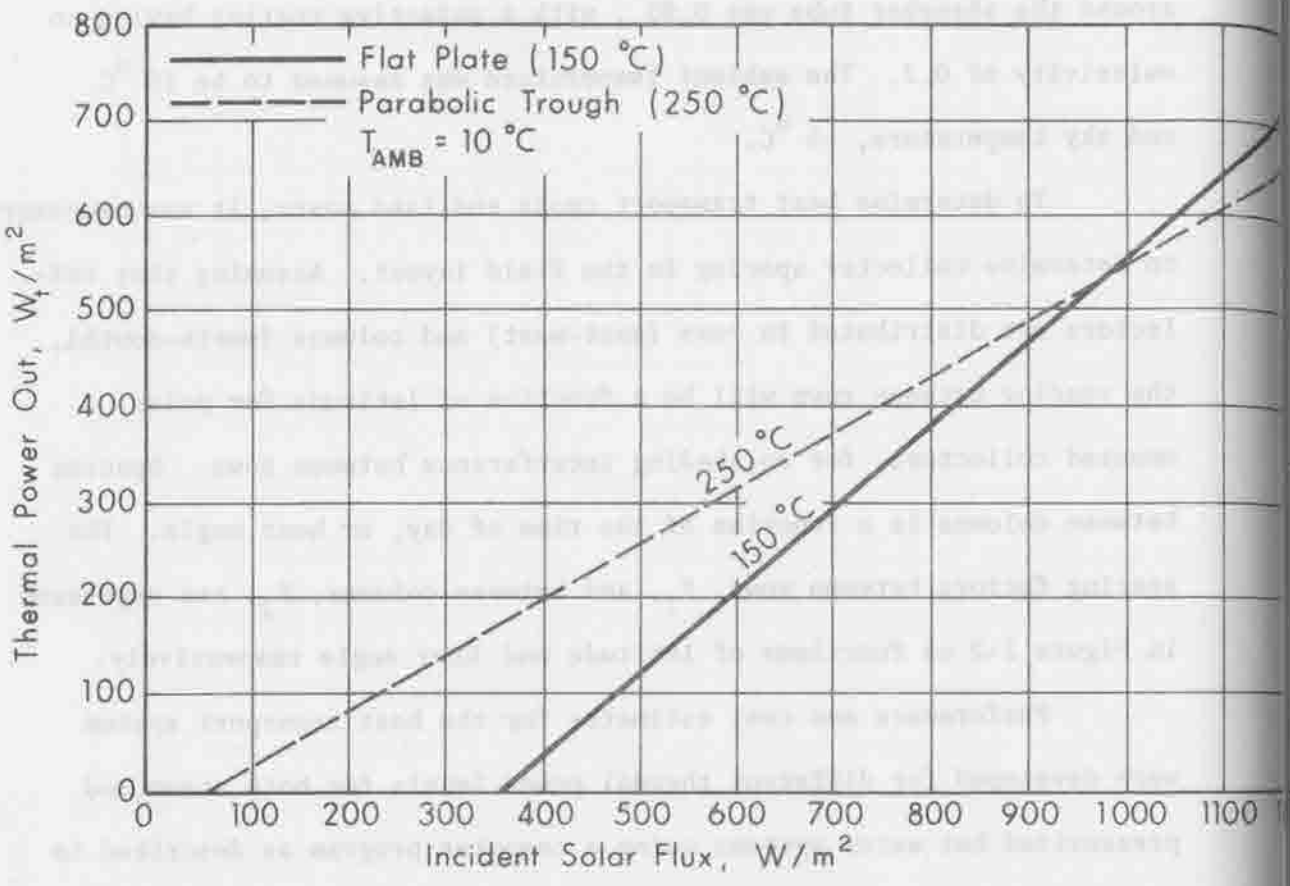

Figure 2-1 Collector Performance.

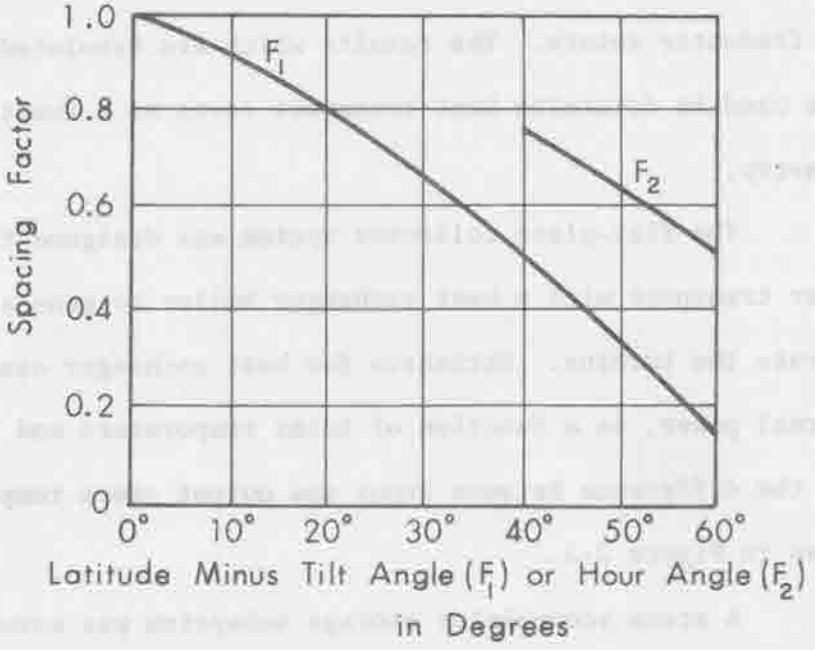

Figure 2-2 Collector Field Spacing Factors.

Estimated unit costs of steam accumulators and pressurized water storage units as a function of inlet temperature and parametric in Δt are shown in Figure 2-4. The efficiency of the storage subsystem was assumed to be 0.99 for each case. Different storage times were considered to evaluate its impact on electrical energy costs.

A Rankine-cycle turbine was selected as the prime mover. Cycle efficiency as a function of inlet steam temperature for a condensate return temperature of 50 ^{o}C is shown in Figure 2-5. The efficiency of the turbine-generator for multi-stage axial units as a function of percent operating load is given in Figure 2-6. Turbine-generator costs per unit of power output as a function of rated electrical generating capacity are shown in Figure 2-7. A tabulation of design parameters used to calculate the performance of the three basic system configurations is given in Table 2-1.

2.3 Solar Plant Capital Costs

The total area of collectors in square meters, A_c, required for a given installation was obtained from the relation

$$A_c = \frac{P_r R}{I' \eta_c \eta_{tr} \eta_s \eta_R \eta_{tg}} = \frac{P_r R}{I' \eta_o} \qquad (2\text{-}1)$$

where

P_r is the rated electrical generating capacity for the plant in kW

R is the ratio (with I=I') of collector output to rated turbine input

I' is the reference solar flux density (1 kW/m^2) for a typical clear day

η_c is collector efficiency with input I' (Figure 2-1)

η_{tr} is transport efficiency (Table 2-1)

η_s is storage efficiency (Table 2-1)

η_R is Rankine cycle efficiency (Table 2-1)

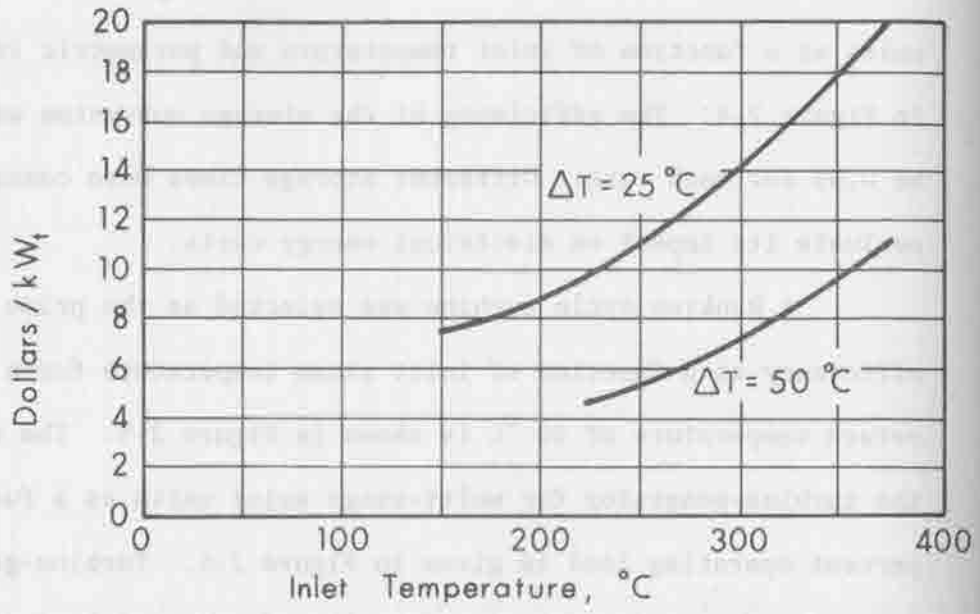

Figure 2-3 Heat Exchanger Costs

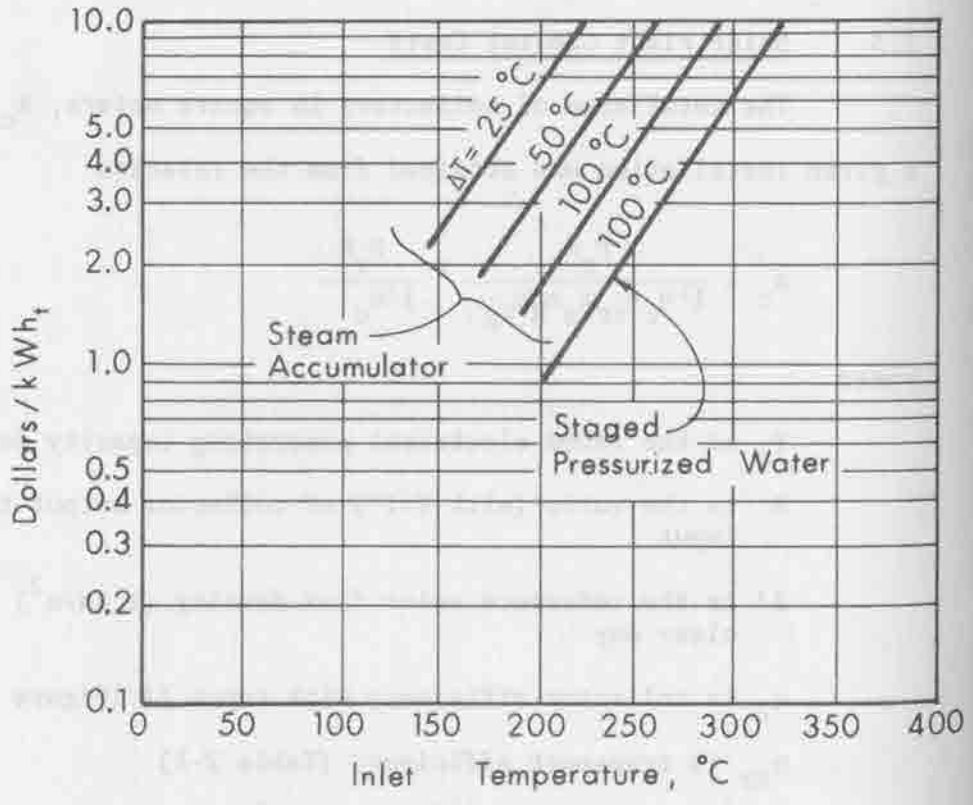

Figure 2-4 Storage System Costs

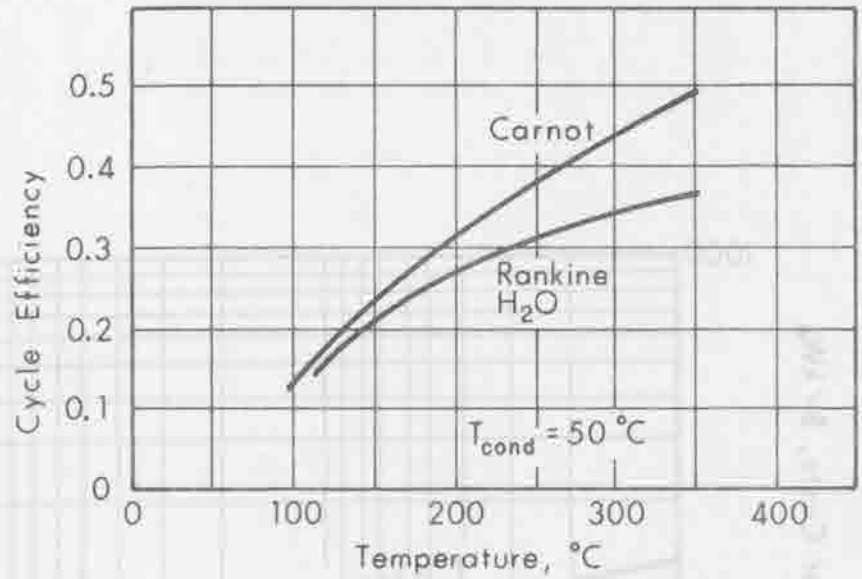

Figure 2-5 Turbine Cycle Efficiency as a Function of Inlet Temperature.

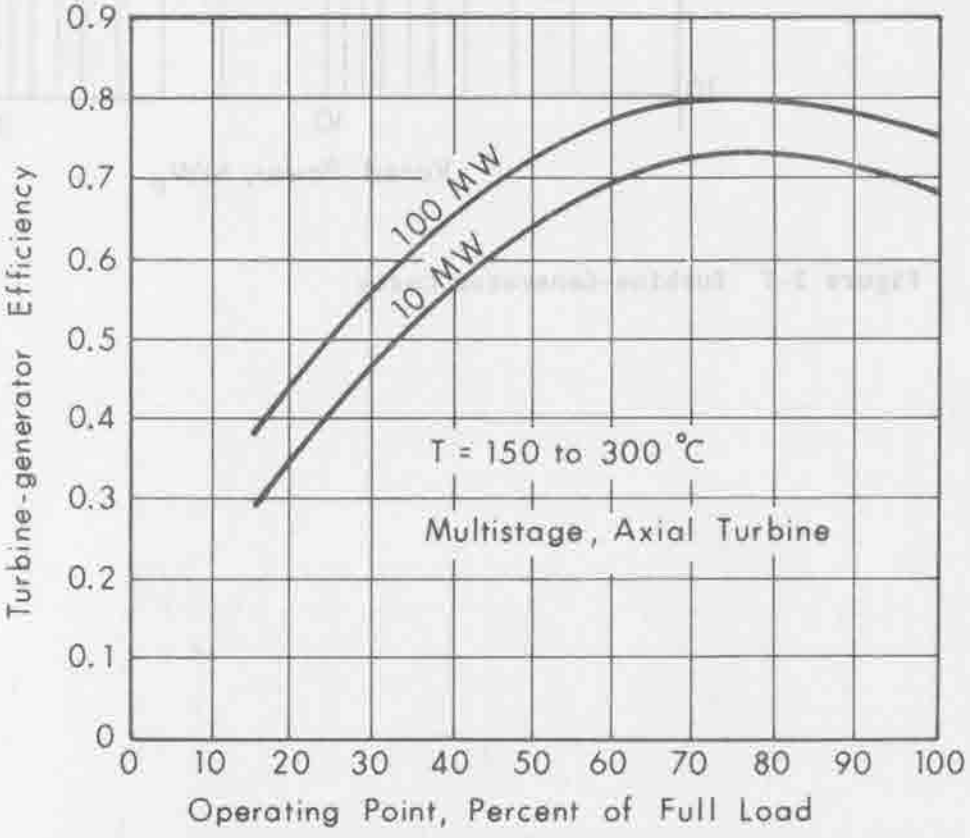

Figure 2-6 Turbine-Generator Efficiency as a Function of Operating Point. Rated Power Level = 80%; Maximum Power Level = 100%.

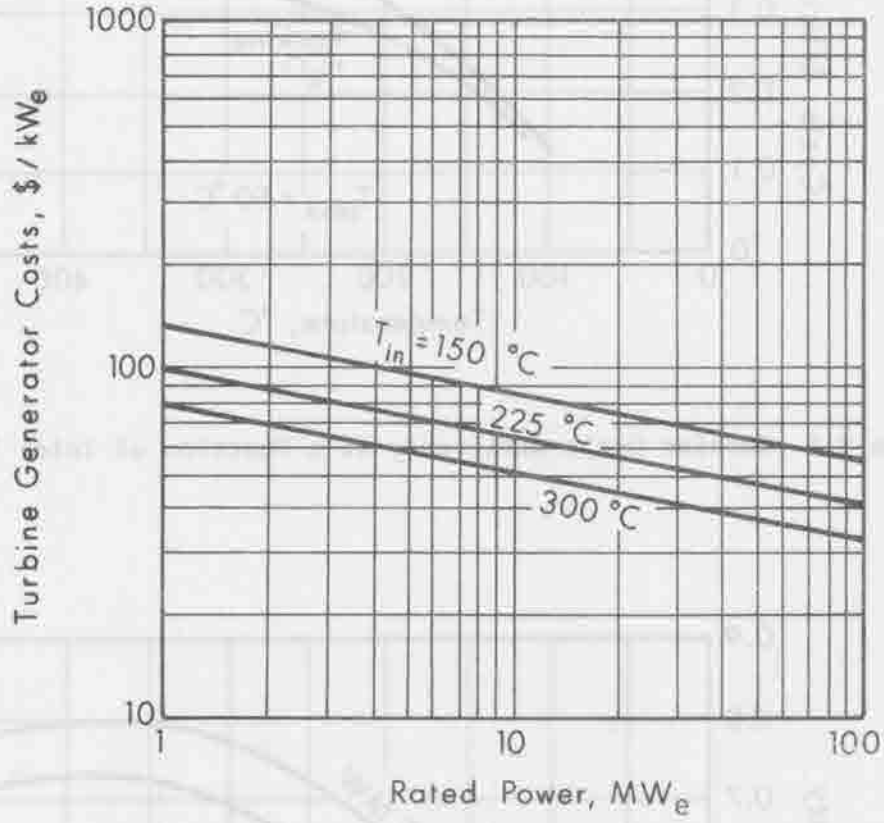

Figure 2-7 Turbine-Generator Costs

Preliminary System Design Parameters

	System #1	System #2	System #3
Concentration			
Type	Flat-Plate Honeycomb	Parabolic Trough	Reflector
Optics	Zero Curvature	Single Curvature	Heliostat
Concentration Ratio C	1	20	450
Intercept Factor γ	1	0.85	0.95
Surface Reflectivity ρ_{ave}	0.02 (glass)	0.75	0.8
Absorptivity α	0.95	0.95	0.95
Conversion	Tube in Plate	Linear Absorber	21 Towers
Emmissivity ε	0.95	0.2	0.99
Transmissivity τ	0.90	0.95	0.92
Transport			
Transfer Fluid	Water	Steam	Steam
Transport Temperature, T_f ^oC	150^o	250^o	350^o
Tracking	Fixed Tilt	Single Axis	Double Axis
Collector Efficiency η_c	0.55	0.55	0.58
Transport Efficiency η_{tr}	0.95	0.95	0.99

TABLE 2-1
(Continued)

	System #1	System #2	System #3
Storage and Exchange			
Heat Exchanger ΔT	20 °C	None	None
Heat Storage	Hot Water	Steam Acc.	Steam Acc.
η_s	0.99	0.99	0.99
Heat Engine and Generator			
Turbogenerator			
Rated Capacity	10 MW_e	10 MW_e	73 MW_e
Work Cycle	Rankine	Rankine	Rankine
η_R	0.2	0.30	0.37
η_{tg}	0.7	0.75	0.85
Waste Heat Disposal			
Condensate Return Temperature	50 °C	50 °C	50 °C
Cooling Towers T_{amb}	40 °C	40 °C	40 °C
T_{Wb}	35 °C	35 °C	35 °C
Control			
Collector Tracking	None	1 Axis	2 Axes

η_{tg} is turbine generator efficiency (Table 2-1)

η_o is overall efficiency

The reference solar flux density I' was assumed to be 1 kW/m^2 for the flat plate configuration which accepts both direct and diffuse radiation and 0.9 kW/m^2 for parabolic trough and the tower/heliostat systems. Numerical values for the parameters are listed in Table 2-1 with η_c shown in Figure 2-1. Collector costs were obtained by multiplying the collector area A_c by the cost per unit area. Values of 40 and 80 dollars per square meter were assumed.

The area of the collector field, A_f, is equal to the collector area divided by the spacing factors. Land costs were assumed to be 0.05 dollars per square meter which corresponds to 200 dollars per acre.

To calculate the piping required for the distributed collector systems, a square piping grid was established for the field. Assuming each collector to have the dimension of 2m by 4m, or $8m^2$, there are $A_c/8$ collectors connected to the grid. Power levels for major sections of the grid were selected and unit costs of piping, which include insulation and return line costs were multiplied by the length of line necessary for each power level. The total piping costs were multiplied by a factor of 1.5 to account for materials transport and construction costs at a remote site.

For the system using flat-plate collectors the heat exchanger costs in terms of rated capacity were determined by dividing the unit costs given in Figure 2-3, for the specified operating temperature, by $\eta_s\eta_R\eta_{tg}$.

Heat storage costs per hour of storage time were determined by dividing the unit costs obtained from Figure 2-4 by $\eta_R\eta_{tg}$. Total

storage costs depend on storage time selected. Turbine generator costs were obtained by multiplying the costs shown in Figure 2-7 by the rated generating capacity of the plant and adding 50 percent for cost of installation.

For the preliminary system evaluation, a cost of $28.00/kW$_e$ was assumed for the cooling subsystem. This corresponds to costs of $6.00/kW$_t$ of thermal capacity.

Estimates for the cost of site preparation, buildings, ancillary equipment, pumps and controls were assumed to increase with storage time. A summary of the preliminary plant costs obtained for the three basic system configurations is given in Table 2-2.

2.4 Electrical Energy Costs

The total cost of energy, R, produced at an electric power generating plant is given by

$$R = R_c + R_f + R_o + R_m \qquad (2\text{-}2)$$

where R is the cost of electrical energy in cents per kWh$_e$, R_c is the capital investment component, R_f is the fuel component, R_o is the operating component, and R_m is the maintenance component. The capital investment component was calculated by

$$R_c = \frac{C_p}{P_r} \frac{r_a}{8760\ C_f} \qquad (¢/kWh_e)$$

where C_p is the plant capital cost which includes direct costs of materials, installation, and indirect costs such as interest during construction, A&E fees, contingencies and spare parts. The fuel, operation, and maintenance costs are usually considered separately.

Summary of Plant Costs in $/kW$_e$ (rated)
(with 4 Hours Storage)

	System #1	System #2	System #5
Land	2.1	2.6	1.5
Structures and Improvements	12	12	12.5
Heat Concentration			
Collector (Reflectors)	R_{col}*	R_{col}*	R_{ref}**
Collector (Towers)	--	--	35
Collector (Absorbers)			9
Transport	54	28	9
Storage	16	74	40
Exchange	68	--	
Turbogenerator Plant			
Turbogenerator	135	75	50
Condenser and Cooling	42	28	17
Plant Equipment			
Pumps and Acc.	12	12	10
Switch Yard	6	6	6
Total vs. Collector Cost ***			
R_{ref} or R_{col} = 0	347	247.6	190
R_{ref} or R_{col} = \$40/m^2	1277	827.6	525
R_{ref} or R_{col} = \$80/m^2	2207	1407.6	860

* Costing Rate of the Collector
** Costing Rate of the Reflector
*** Excludes Architectural and Engineering fees and interest during construction

The rated plant capacity, P_r, in kW_e and r_a is a fixed annual charge in cents/year per dollar, and includes cost of money, depreciati insurance and taxes. This amortization rate varies from year to year, but for 1973-1974 is between 16 and 18¢/year per dollar. The number 8760 is the total hours in a year. The capacity factor C_f is the ratio of actual power generated to the amount it is possible to generate, considered on an annual basis.

The relationship between plant cost, capacity factor, and capital component of energy cost is shown in Figure 2-8. For a conventio coal powered plant C_f may be as large as 0.9, if the down time for maintenance and repair is small. Capacity factors of 0.8 are more typical for nuclear plants and 0.25 is typical for gas turbines which supply peaking power. The cost of power generation at typical conventional power plants, including fuel costs, is shown in Figure 2-9 using the Franklin Institute (1972) data.

The capacity factor for a solar plant may be expressed by

$$C_f = \frac{Q_e C_r}{P_r \times 8760} \quad , \tag{2-4}$$

where Q_e is the potential electrical energy produced in kWh_e/year. Be

$$Q_e = A_c \int_{1\ year} I\ \eta\ dt \tag{2-5}$$

and C_r is a system reliability factor;

then

$$C_f = \frac{Q'_{rad}\ \eta_e\ A_c}{P_r\ 8760} \tag{2-6}$$

where I is the effective incident solar flux density in kW/m^2 which

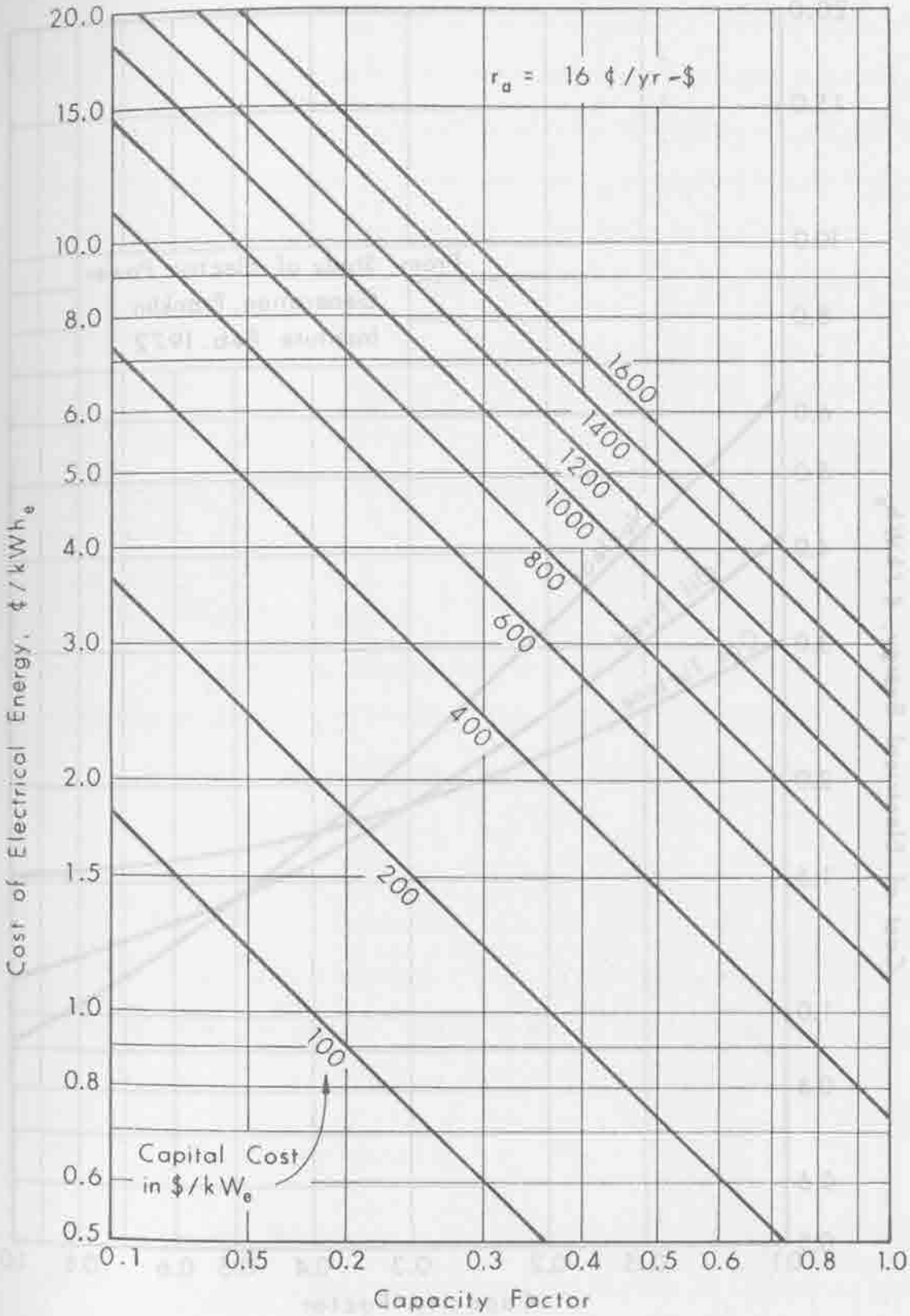

Figure 2-8. Capital Investment Component of Electrical Energy Costs.

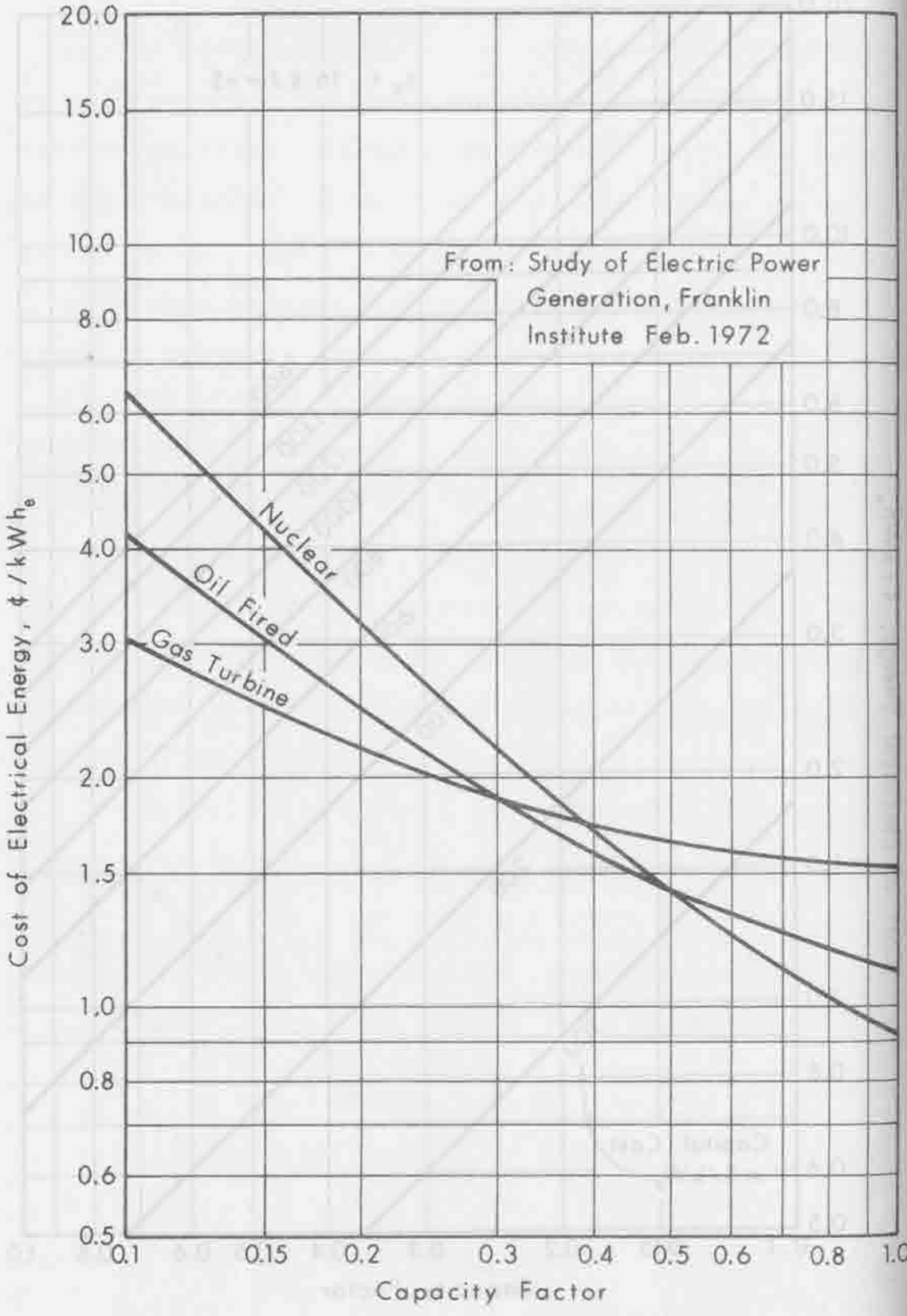

Figure 2-9 Electrical Energy Costs from Oil-Fired, Gas and Nuclear Power Plants

is a function of location and collector orientation. When integrated over the year, this yields the yearly average input energy density Q'_{rad} in kWh/m^2-year. The effective average overall plant efficiency over the same period is η_e. The total area of the collector field is expressed by A_c in square meters. The installed cost for the collectors of a solar plant is $C_c A_c$, where C_c is the unit collector cost in \$/m^2.

Substituting $C_c A_c$ for C_p in Equation (2-3) and the capacity factor determined by Equation (2-6) yields the collector component contribution (R_{cc}) to the capital energy cost.

$$R_{cc} = \frac{C_c \quad (r_a)}{Q'_{rad} \ \eta_e} \tag{2-7}$$

Preliminary insolation data from Albuquerque, New Mexico, (1959), indicated $Q'_{rad} \approx 7$ kWh/m^2-day or approximately 2580 kWh/m^2-year. Using this value and assuming r_a = 16¢/year per dollar,

$$R_{cc} = 0.0062 \frac{C_c}{\eta_e} \tag{2-8}$$

The solution to Equation (2-8) is shown in Figure 2-10. Cost corrections are required for different locations where Q'_{rad} differs from the yearly average of 7 kWh/m^2-day and for different collector capture potentials which depend upon collector orientation.

2.4.1 Plant Capacity Factor

The capacity factor is the ratio of the total annual energy ouput to the rated annual production from the plant. The total annual energy output for each of the three systems was obtained using the relative probability distribution shown in Figure 2-11. The frequency

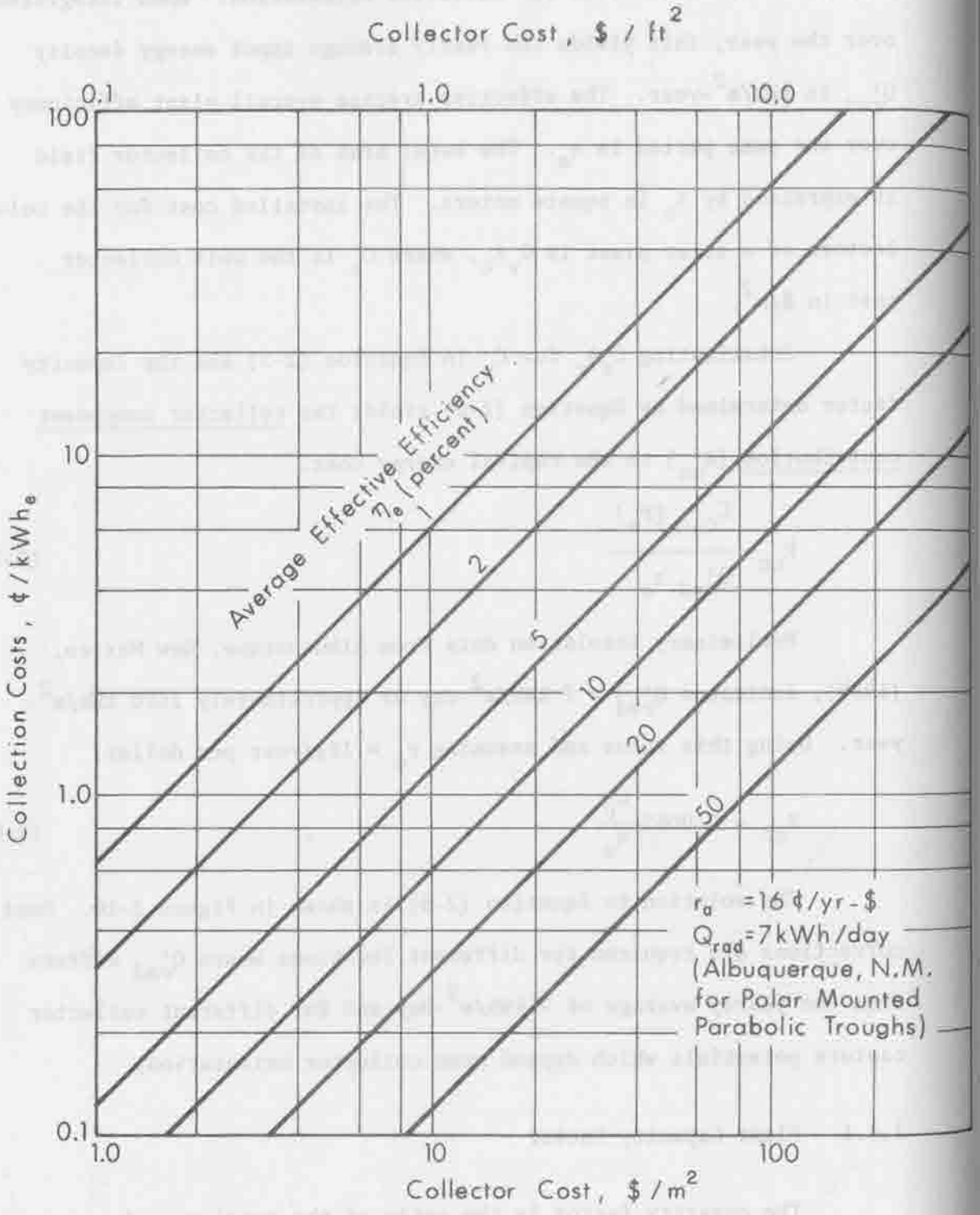

Figure 2-10 Collector Component of Electrical Energy Costs

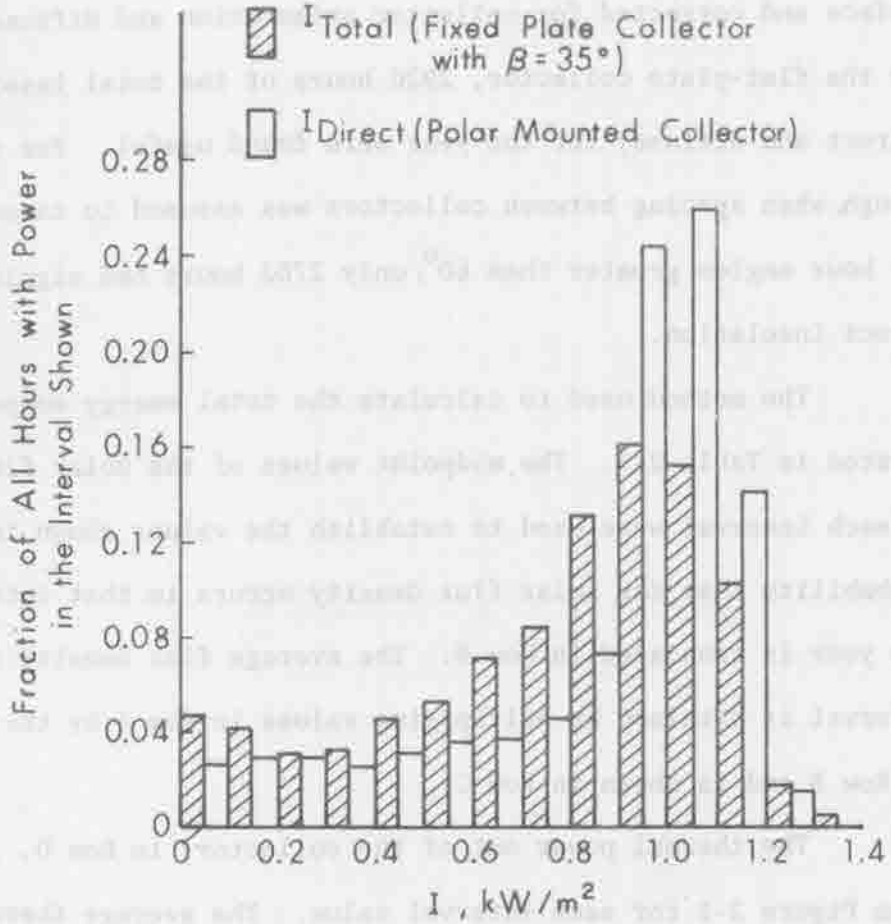

Figure 2-11 Relative Probability Distributions of Solar Flux Density (Data for 1959 at Albuquerque, N. M.).

distributions are for a flat-plate collector fixed at a tilt angle equal to the latitude and for a polar mounted parabolic trough at fixed tilt angle with single axis tracking. They were calculated from the 1959 Albuquerque total insolation measured on a horizontal surface and corrected for collector orientation and diffuse radiation. For the flat-plate collector, 2920 hours of the total insolation (direct and diffuse) for the year were found useful. For the parabolic trough, when spacing between collectors was assumed to cause shadowing for hour angles greater than 60^{o}, only 2702 hours had significant direct insolation.

The method used to calculate the total energy output is demonstrated in Table 2-3. The midpoint values of the solar flux density in each interval were used to establish the values shown in Row A. The probability that the solar flux density occurs in that interval during the year is tabulated in Row B. The average flux density in each interval is obtained by multiplying values in Row A by the probability in Row B and is shown in Row C.

The thermal power out of the collector, in Row D, is determined from Figure 2-1 for each interval value. The average thermal power from the collector is calculated by multiplying values in Row D by the probability density in Row B, as shown in Row E. The annual thermal energy output per year in Row F is obtained by multiplying Row E times 2702, the number of useful hours in a year for the parabolic collector.

The turbine operating point, in terms of percent of full load, is given in Row G and the efficiency from Figure 2-6 is tabulated in Row H. For a steam temperature of 250 ^{o}C the Rankine cycle efficiency is 0.30 from Figure 2-5. Overall turbine-generator efficiency for each

TABLE 2-5

Annual Energy Produced By 250 °C
Parabolic Trough System Configuration
(Albuquerque, N. M.)

(A) Interval Midpoint, W/m^2 (Fig. 2-11)	350	450	550	650	750	850	950	1050	1150	1250
(B) Probability at Midpoint (Fig. 2-11)*	.03	.03	.03	.04	.05	.08	.24	.27	.15	.02
(C) Average Solar Flux, W/m^2 (A x B)	10.5	13.5	16.5	26.5	37.5	68.0	228.0	283.3	172.5	25.0
(D) Thermal Power Out, W_t/m^2 (Fig. 2-1)	160	220	290	350	400	450	510	580	630	700
(E) Ave. Thermal Power Out, W_t/m^2 (B x D)	4.8	6.6	8.7	14.0	20.0	36.0	122.5	156	94.5	14.0
(F) Annual Energy Out, kWh_t/m^2-yr (B x 2702)	13	17.8	23.6	37.8	54	97.3	330	421	254	37.8
(G) Cummulative Energy Output	13	30.8	54.4	92.2	146.2	243.5	573.5	994.5	1248.5	1286.3
(H) Turbine Operating Point, (D)/700)	0.22	0.30	0.40	0.48	0.55	0.62	0.70	0.80	0.86	1.0
(I) Turbine - Generator Efficiency, (Fig. 2-6)	0.39	0.45	0.56	0.61	0.68	0.69	0.71	0.72	0.71	0.68
(J) Overall Efficiency (H x 0.3)	0.117	0.135	0.168	0.182	0.203	0.206	0.212	0.215	0.212	0.203
(K) Annual Electrical Energy kWh_e/m^2-yr (J x F)	1.5	2.4	4.0	6.9	11.0	20.0	70.0	90.7	54.0	7.7

Total Annual Production 268 kWh_e/m^2-yr

* Ratio of hours in interval to total hours of sunshine, 2920 hours for total and 2702 hours for direct radiation.

interval is given in Row I. The annual electrical energy produced in each interval is given in Row J.

The annual insolation per unit area is obtained by summing the values in Row C and multiplying by the number of hours of useful insolation which occurs during the year.

$$\Sigma \text{ Row C} \times 2702 = 2380 \text{ kWh/m}^2\text{-year}$$

The average thermal output is given by

$$\Sigma \text{ Row F} = 1283 \text{ kWh}_t/\text{m}^2\text{-year}$$

Therefore, the effective collector efficiency for the year is

$$\eta_c = \frac{1283}{2380} = 0.54$$

The total annual electrical energy produced is the sum of the values in Row J.

$$\Sigma \text{ Row J} = 268 \text{ kWh}_e/\text{m}^2\text{-year}$$

The average turbine-generator efficiency is then

$$\text{Ave. } \eta_R \eta_{tg} = \frac{268}{1283} = 0.209$$

This assumes a minimum storage capacity of one hour.

The overall system efficiency for the year is

$$\eta_o = \frac{268}{2380} \approx .10$$

The yearly electrical energy output, Q_e, can be determined by multiplying the electrical output per square meter by the collector area. As storage time increases, the turbine generator can be operated at a higher average efficiency by storing thermal energy and operating the turbine nearer maximum efficiency. This increased storage, however requires an increased collector area by an amount proportional to R_{∞} (1 + ts/8) where ts is the useful discharge time from storage accum-

ulated during 8 hours of operation during the day.

The capacity factor C_f can now be determined from

$$C_f = \frac{Q_e \times C_o}{P_r \times 8760} \qquad (2\text{-}9)$$

where Q_e is the electrical energy produced per year, P_r is the rated electrical generating capacity of the plant, 8760 is the total hours in a year and C_o is a reliability factor to account for down-time necessary for maintenance and repair.

The results obtained for the three basic system configurations are summarized in Table 2-4. It was assumed that four hours of storage capacity was achievable for each system.

2.4.2 Energy Cost Comparisons

Using the capital cost estimates for each system, along with the corresponding capacity factors, the electrical energy cost for the capital component can be computed, neglecting for the moment the Architectural and Engineering (A & E) costs, interest during construction (IDC), and Operation and Maintenance (O & M) fees. Results are summarized in Table 2-5 assuming collector costs of \$40/m^2 and \$80/m^2 and for 1-, 4- and 8-hour storage capacities and using an investment change rate of \$0.16/year per dollar.

It was estimated that the addition of A&E, IDC and O&M costs could add 20 to 50 percent to the total energy costs. Figures 2-12, 2-13, and 2-14 were prepared to show the impact of these added costs and the effect of collector costs on the total energy costs for the flat-plate (150°) and for the parabolic trough (250°) systems.

Preliminary comparisons of the electrical energy costs for the

TABLE 2-4

Summary of Annual Performance
(4 Hours Storage)

	10 MW System #1	10 MW System #2	73 MW System #3
Insolation (kWh/m^2-yr)	2150	2380	2380
Collector Thermal Output (kWh_t/m^2 yr)	1065	1283	1330
Electric Generator Output (kWh_e / m^2 yr)	107	270	417
Overall Efficiency (%)	5	11.3	17.5
Collector Area (m^2)	2.25×10^5	1.45×10^5	3.7×10^5
Total Electric Output (kWh_e/yr)	2.38×10^7	3.92×10^7	1.52×10^8
Actual Output to Rated Output	0.27	0.45	0.41
Outage Factor	0.9	0.9	0.95
Capacity Factor	0.24	0.41	0.34

TABLE 2-5

Energy Cost Summary ($¢/kWh_e$)

Excluding:

- Operation and Maintenance
- A & E Fee
- Interest During Construction

	Collector Cost	Storage Time		
		1 Hour	4 Hours	8 Hours
SYSTEM #1 (Flat plate)	$\$40/m^2$	10.5	8.6	6.6
	$\$80/m^2$	17.6	14.9	11.6
SYSTEM #2 (Parabolic trough)	$\$40/m^2$	3.8	3.75	3.7
	$\$80/m^2$	6.5	6.4	6.2
SYSTEM #3 (Tower Heliostat)	$\$40/m^2$	2.4	2.25	
	$\$80/m^2$	4.8	4.5	

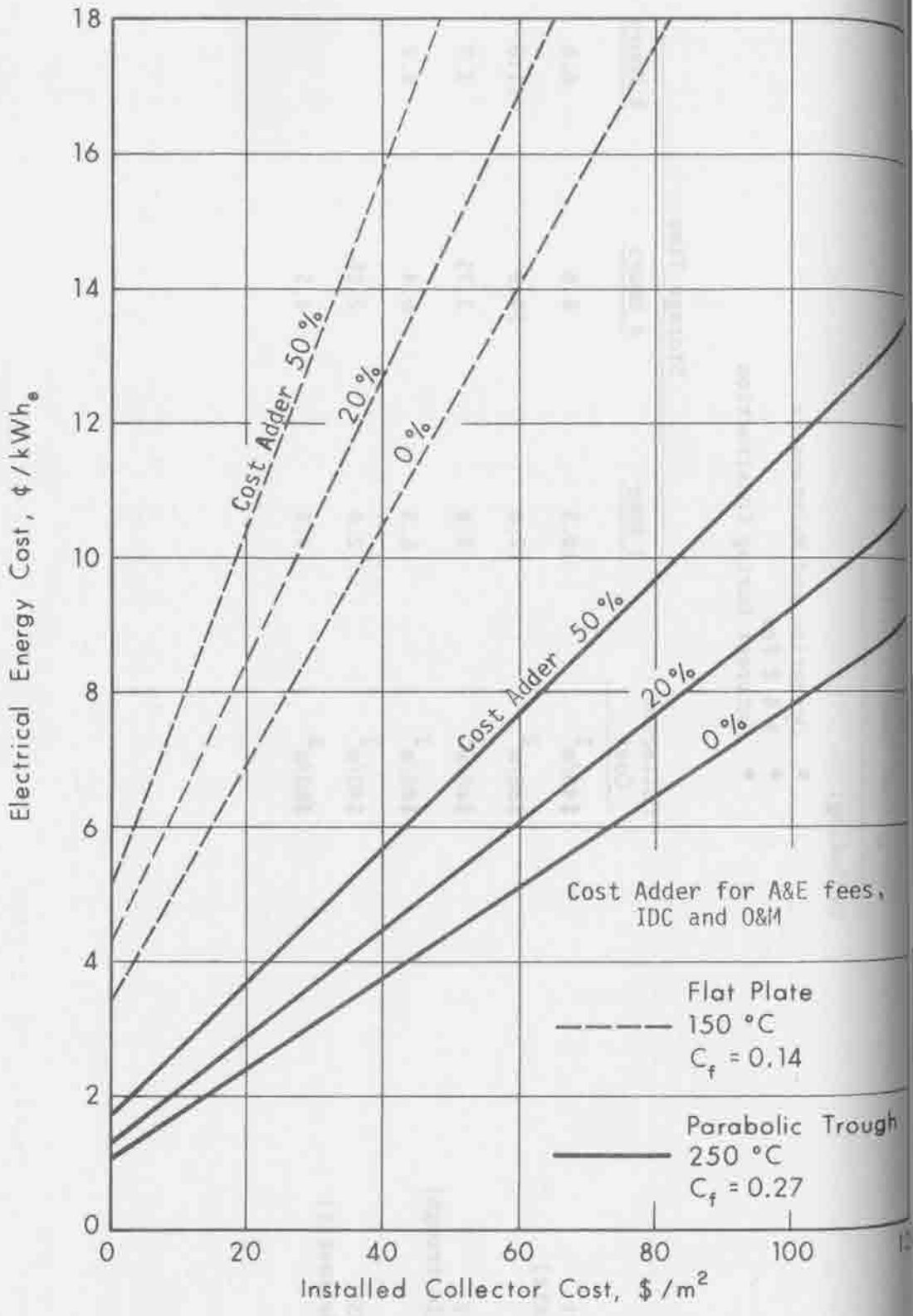

Figure 2-12 Energy Costs for Flat-Plate and Parabolic Trough Systems wi
1-Hour Storage.

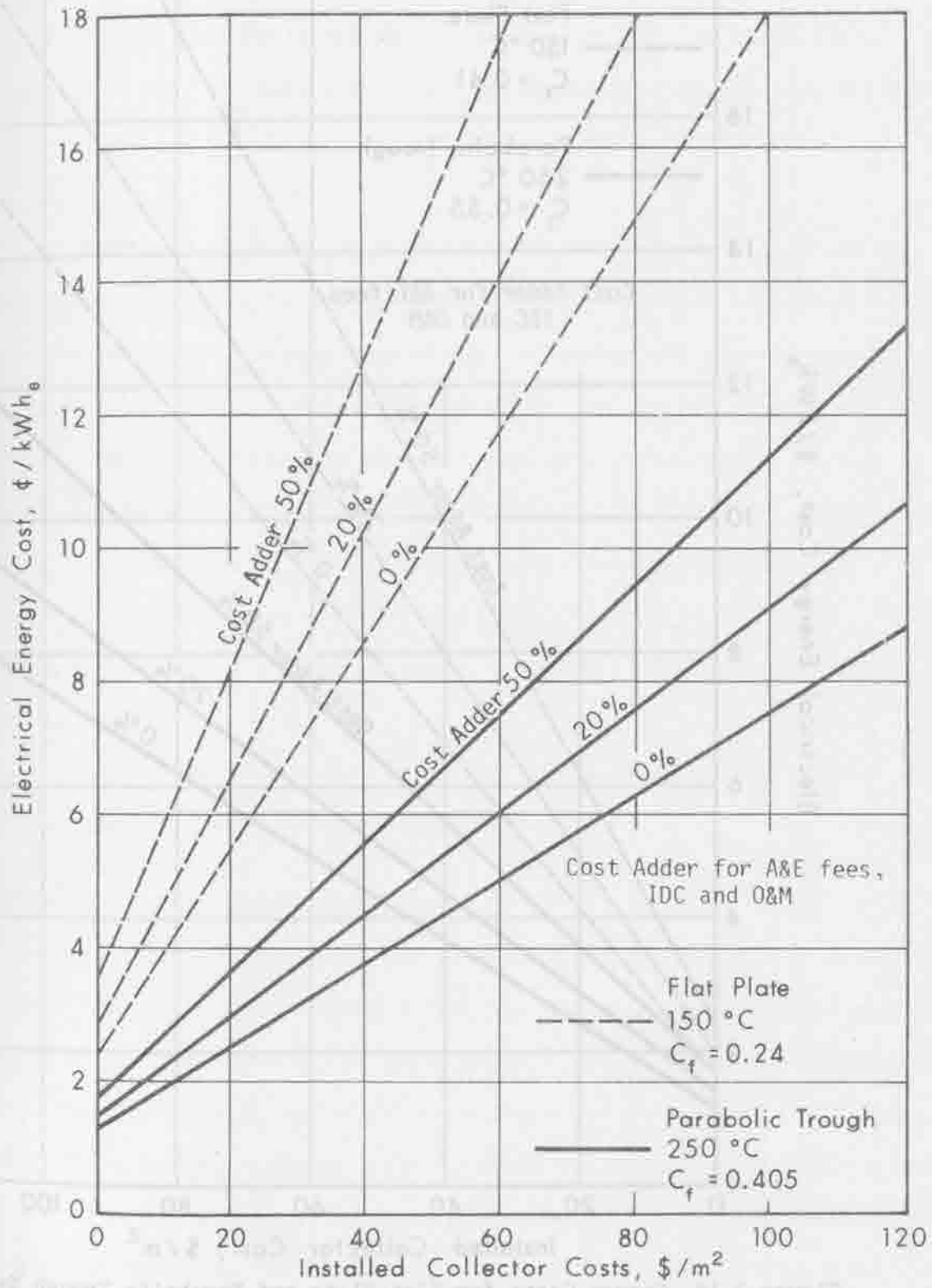

Figure 2-13 Energy Costs for Flat-Plate and Parabolic Systems for 4 Hours of Storage.

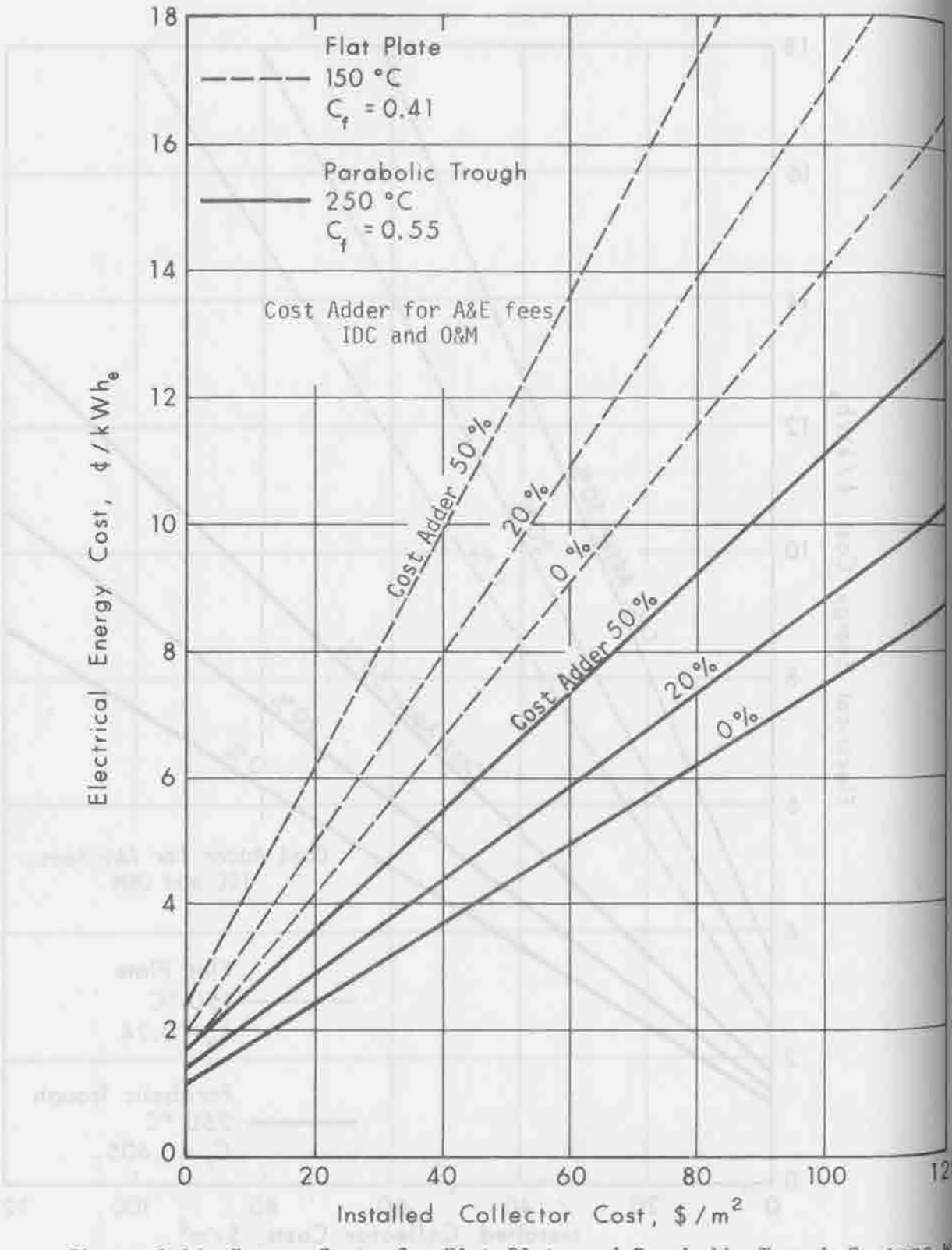

Figure 2-14 Energy Costs for Flat-Plate and Parabolic Trough Systems wi
8 Hours of Storage.

three systems are shown in Figure 2-15 using a 30 percent adder for A&E and IDC fees and assuming an amortization rate of $0.16/year per dollar for a 1973 base year. On this figure the storage time varies from 1- to 8-hours and collector costs from $40/m^2 to $80/m^2 for each system.

A comparison of solar plants for other plant sizes is shown in Figure 2-16. A collector cost of $40/m^2 was assumed for each plant. The tower/heliostat configuration was for 21 towers 100 meters high for the 73 MW plant and 21 towers 200 meters high for the 300 MW plant.

These results can be compared with fossil-fuel plants, both peaking and baseload, and a nuclear plant which are shown in Figure 2-17. The total cost of energy includes both the amortized capital investment and the fuel costs in terms of dollars/barrel of oil or dollar/lb. of uranium. The fuel costs, in ¢/kWh$_e$, were determined from Figure 2-18.

The comparative energy costs for an oil-fired peaking plant and baseload plant are shown in Figure 2-19.

2.5 Size and Temperature Effects

An estimate of solar power plant costs, in $/kWh$_e$, as a function of plant size is shown in Figure 2-20. The system consists of parabolic troughs with steam transport at approximately 250 ^{o}C and 4 hour storage capacity. Collector costs of $40/m^2 were assumed. The minimum total costs (top line on Figure 2-20) has a fairly broad range and occurs between 100 and 300 MW$_e$. The estimated performance in terms of efficiencies and costs for various operating temperatures for a parabolic trough system with

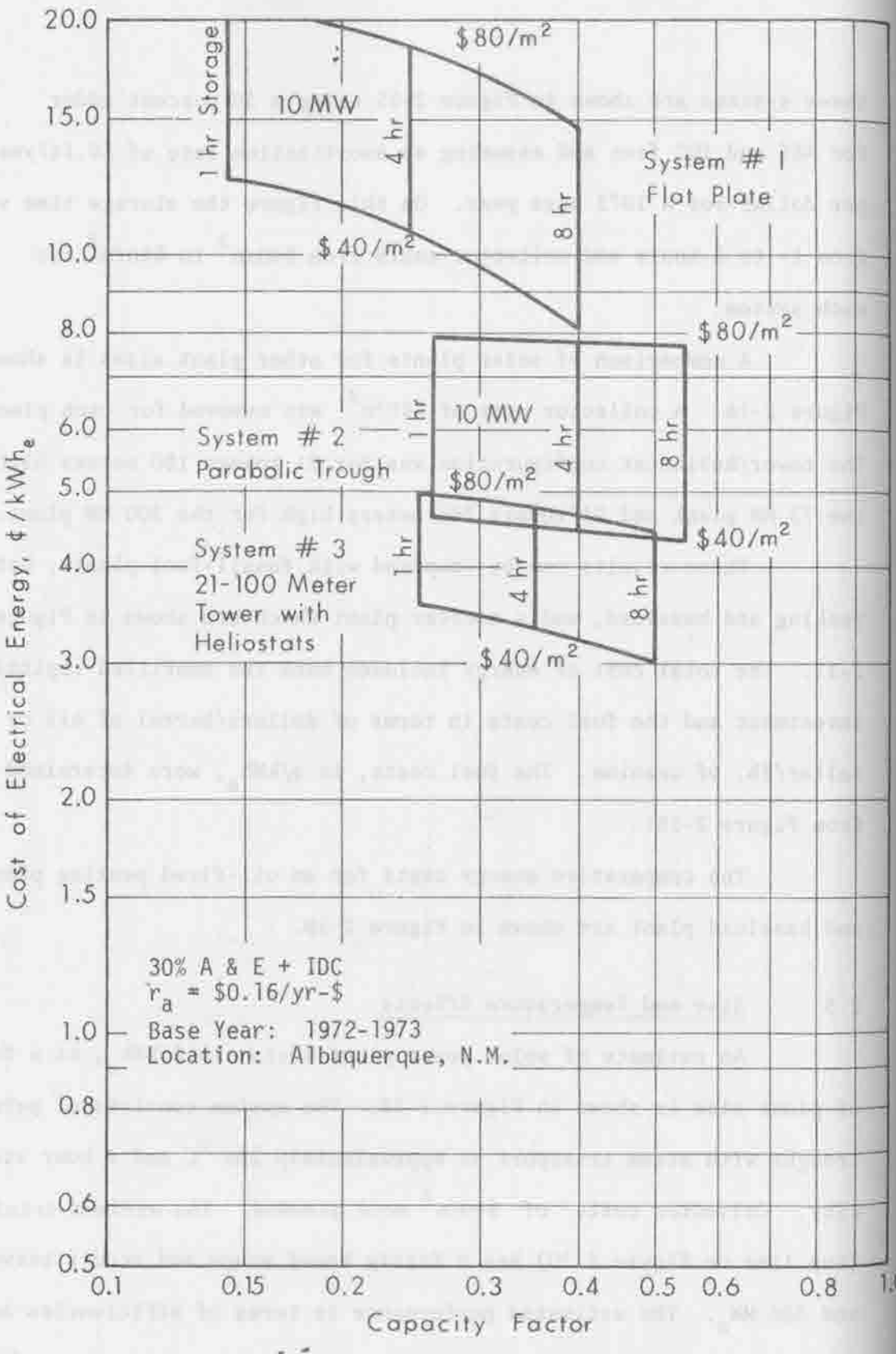

Figure 2-15. Preliminary Energy Cost Comparisons of Three System Configurations with Variable Collector Costs and Storage Time

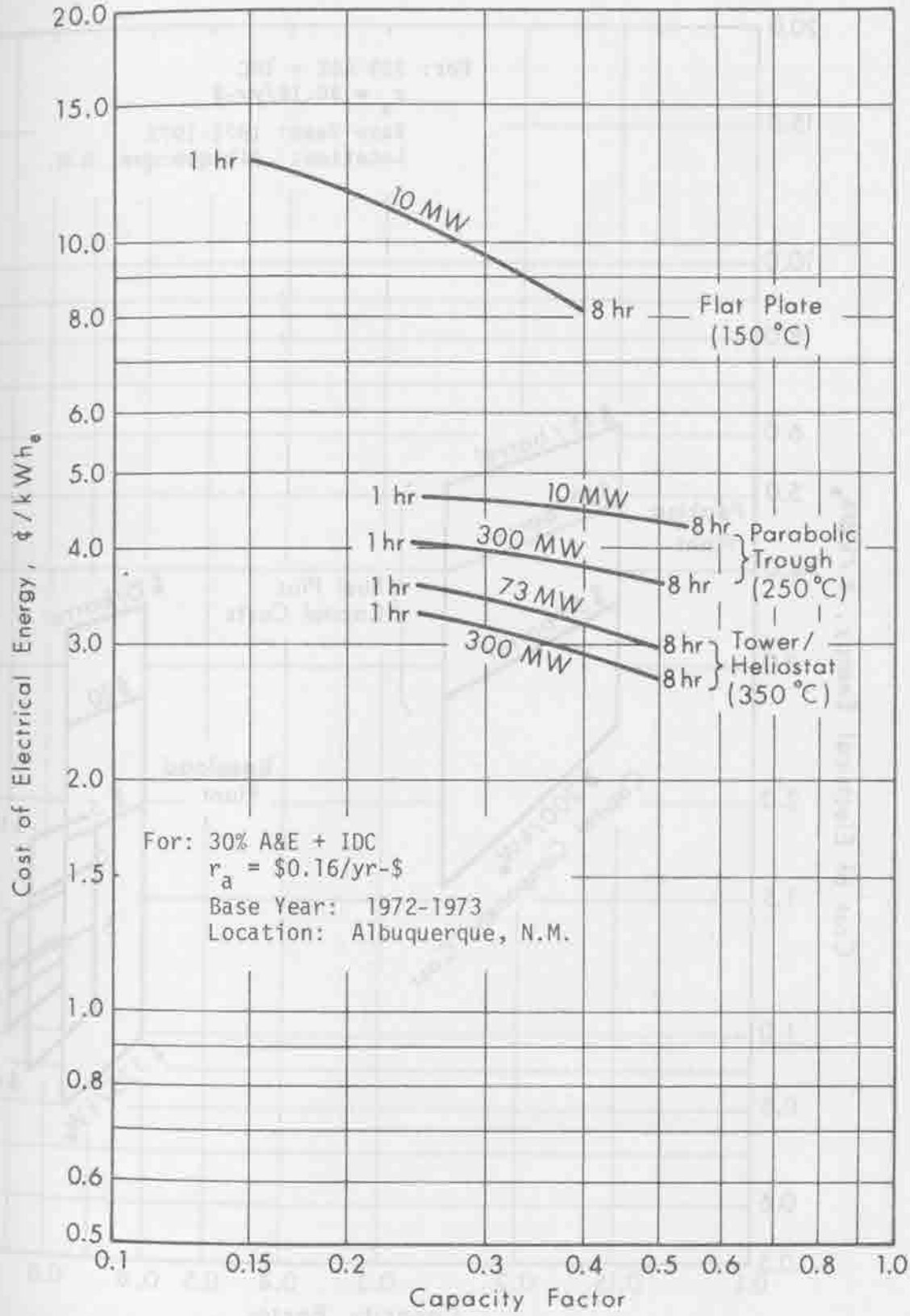

Figure 2-16 Preliminary Energy Cost Comparisons of Solar Plants Assuming Collection Subsystem Costs of $\$40/m^2$.

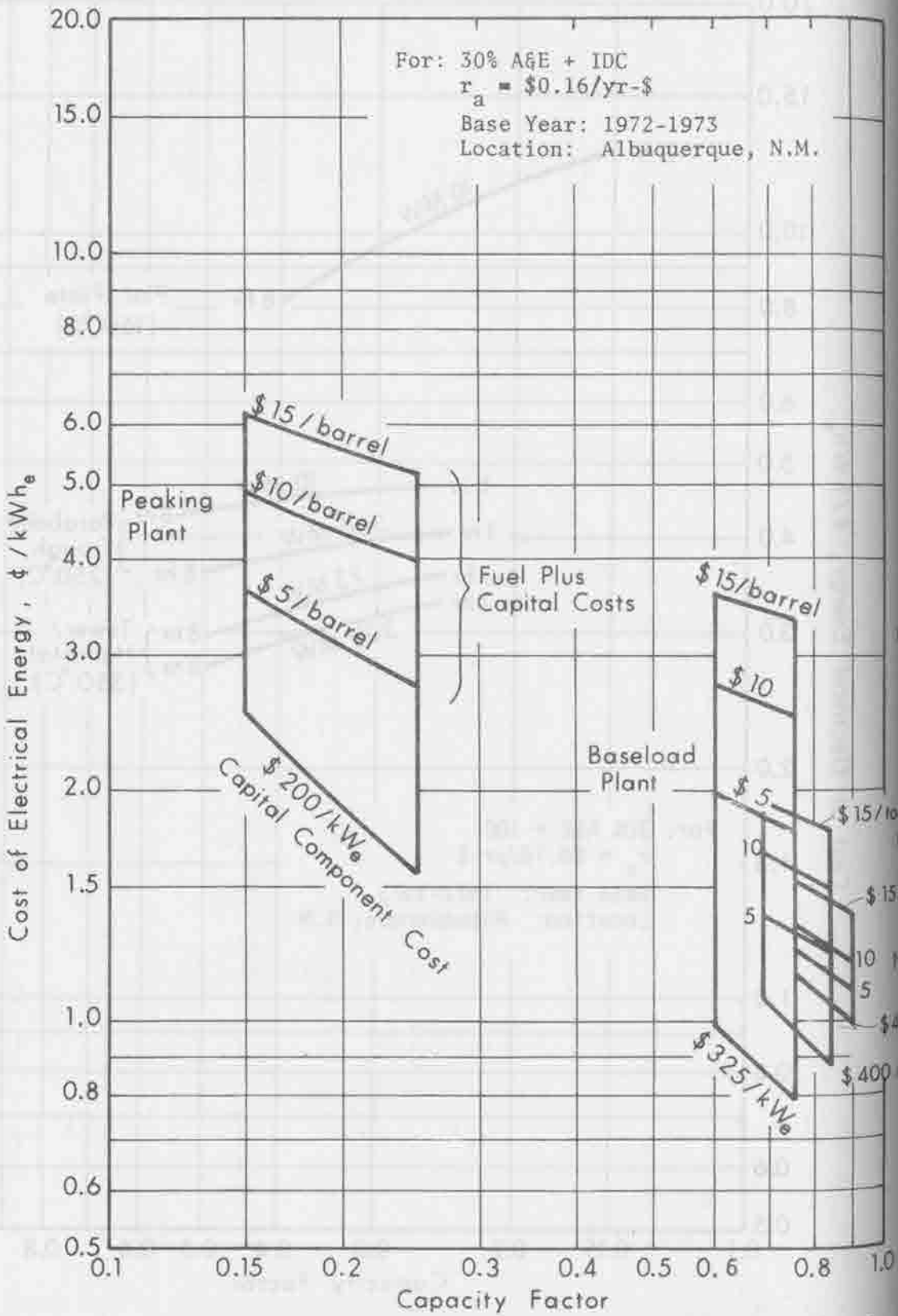

Figure 2-17 Estimated Electrical Energy Cost of Oil-fired, Coal and Nuclear Plants.

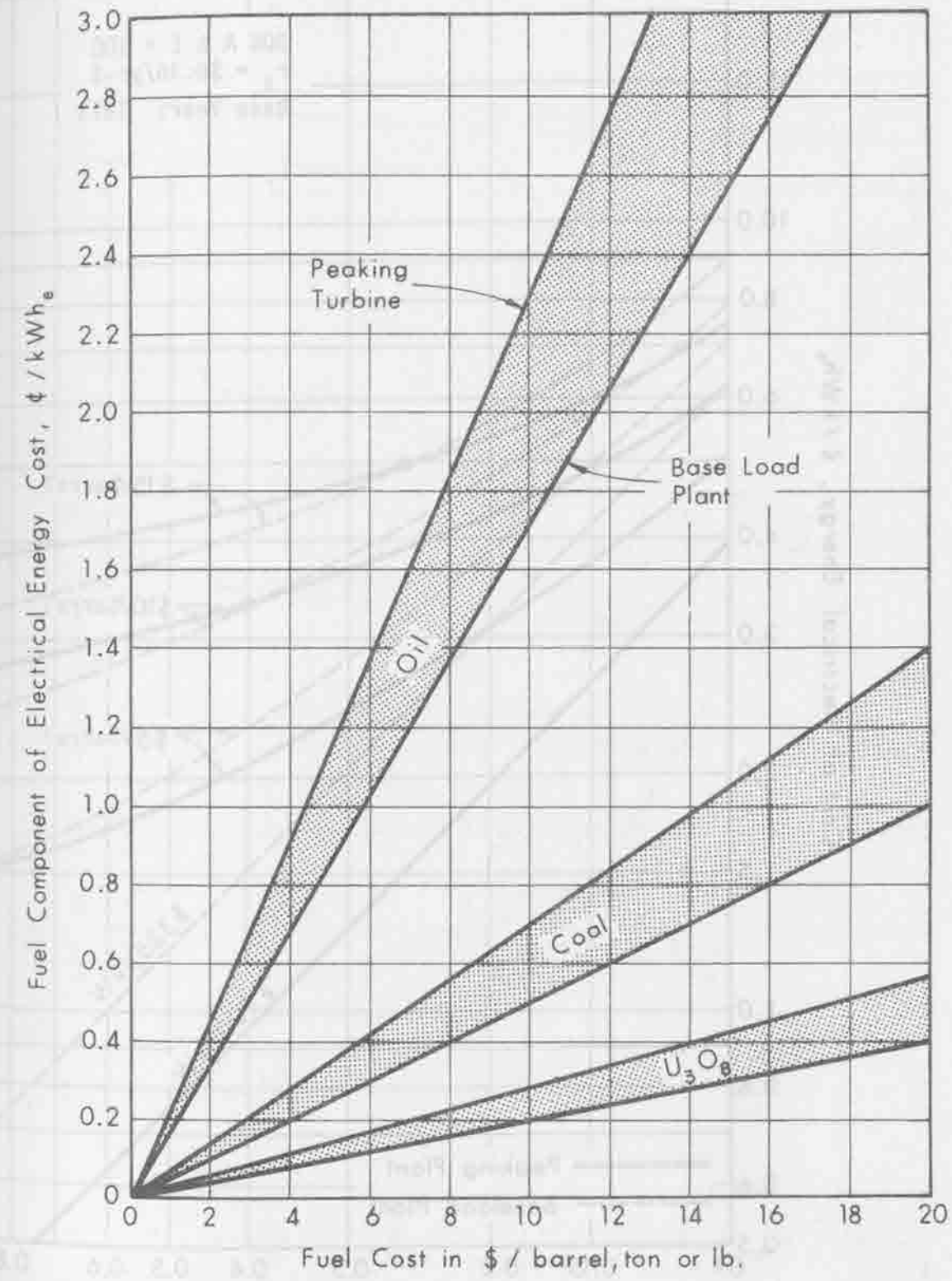

Figure 2-18 Fuel Component Costs.

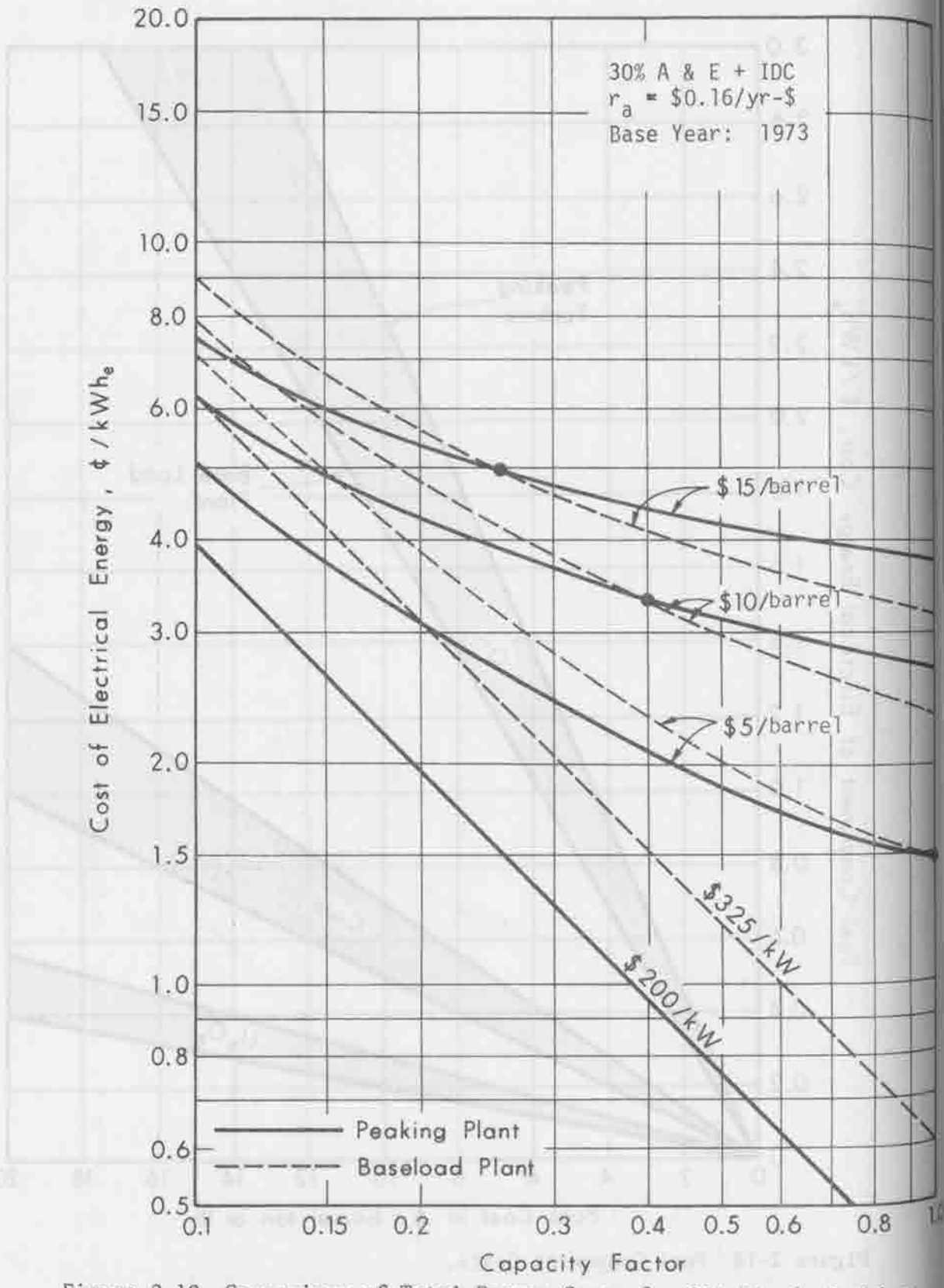

Figure 2-19 Comparison of Total Energy Costs for Oil-Fired, Peaking and Baseload Plants.

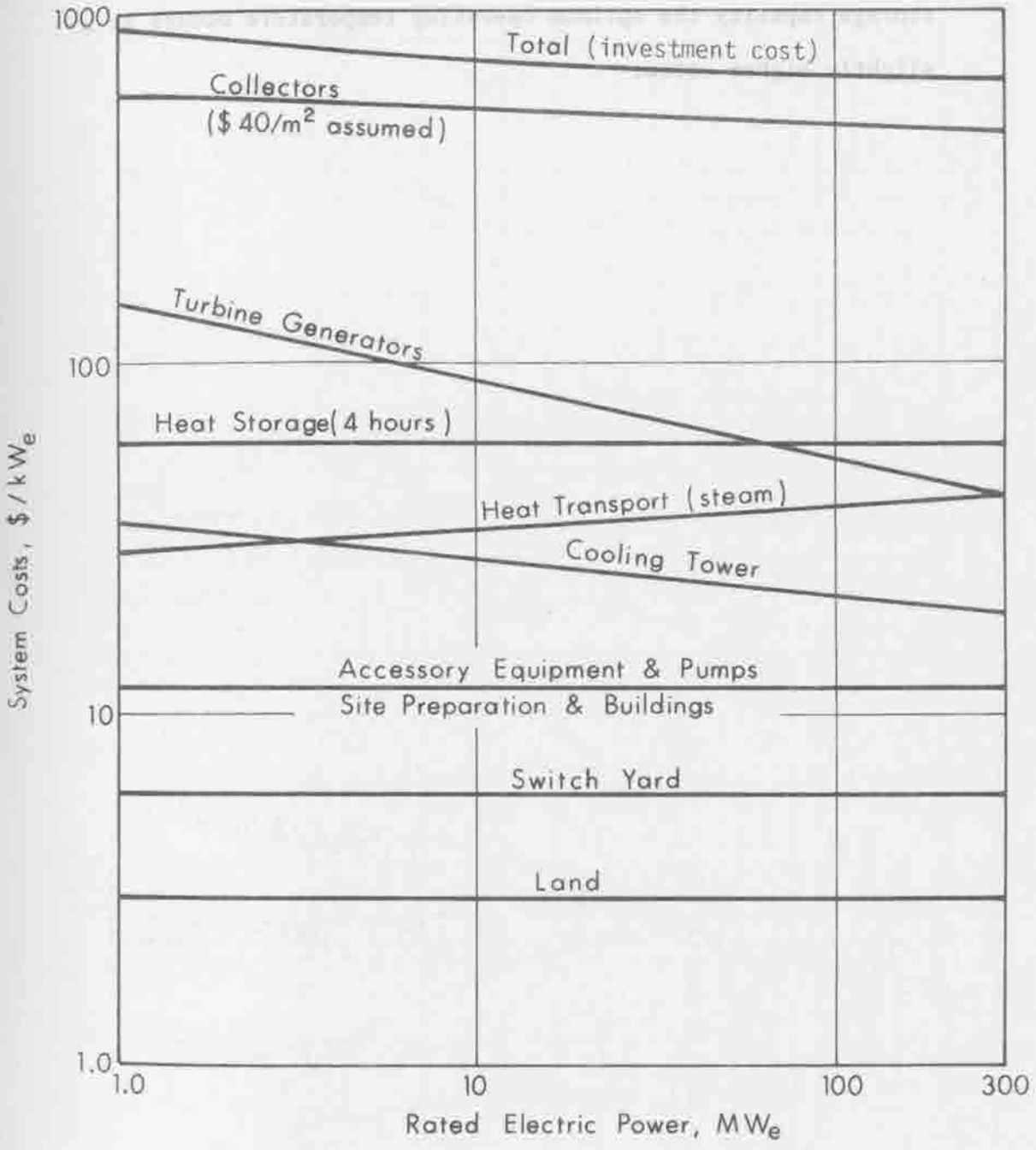

Figure 2-20. Costing Rate vs. Size for a Plant with Steam Transport at 250 °C and with Four Hours of Storage.

10 MW_e capacity is shown in Figure 2-21. The minimum plant cost occurs for a 250 ^{o}C system, for the conditions assumed. For less storage capacity the optimum operating temperature occurs at a slightly higher value.

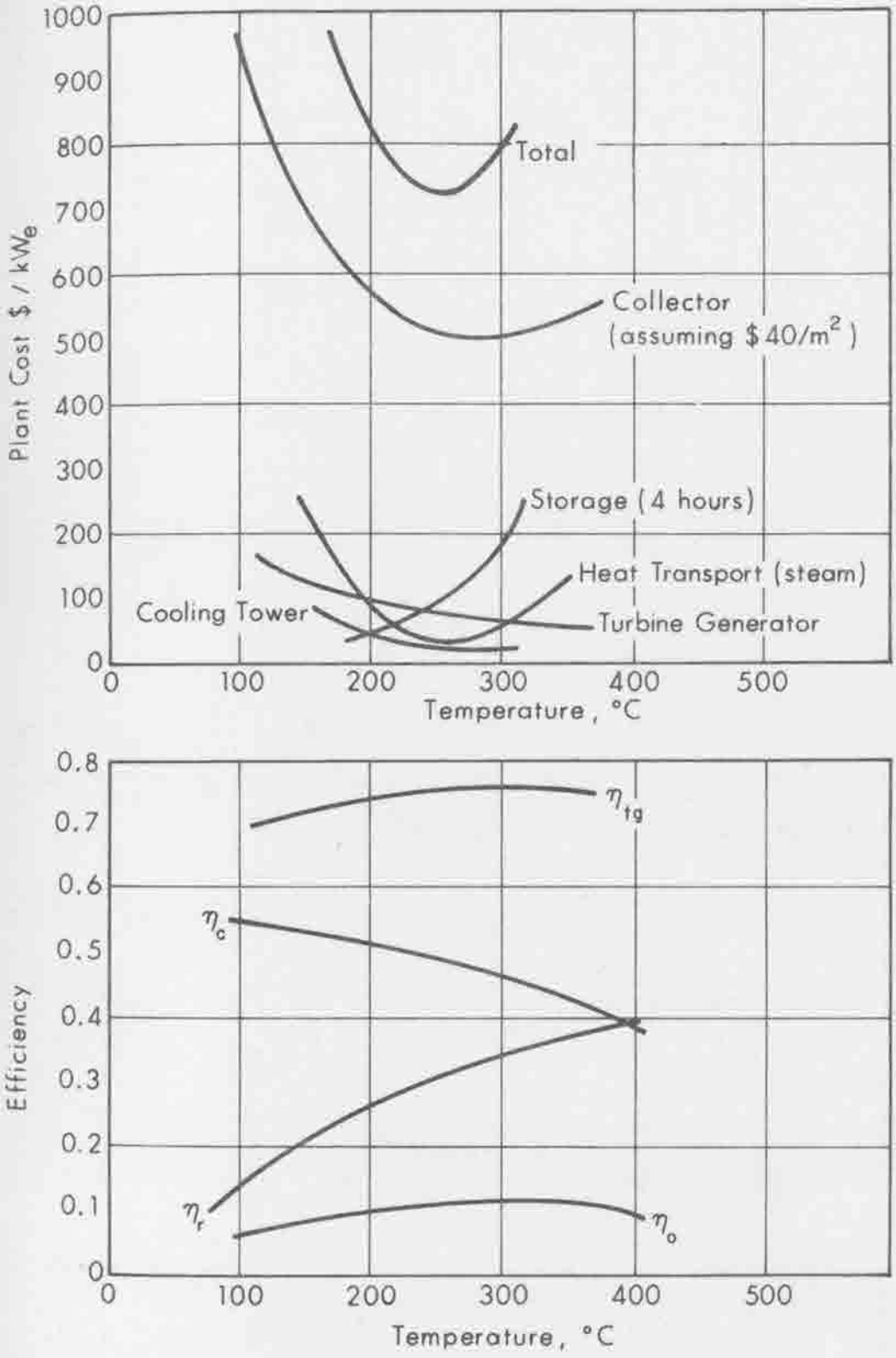

Figure 2-21. Estimated Performance and Costing Rate vs. Operating Temperature for 10 MW_e Rated Output, Steam Transport System, 4 Hours of Storage.

APPENDIX B

THE SEQUENTIAL OPTIMIZATION PROCESS

BY

W. S. DUFF,

G. L. WILCOX,

AND

S. B. THAYER

1.0 INTRODUCTION

The conversion of solar energy to electric power involves a complex interaction between a number of subsystems including solar concentrators, absorbers, heat transport, heat storage, prime movers and generators. The arrangements of subsystems for two general system types are depicted in Figures 1-1 and 1-2. The objectives of system optimization is to identify the design parameters of subsystems and the proper interconnection of these subsystems to produce electric output at minimum cost per kWh_e.

The problem of selection of the proper subsystems designs is more complex than simply assembling the minimum cost alternative for each subsystem. For example, the minimum cost collector design for a given set of performance parameters may force the adoption of an expensive heat transport system. Thus, system optimization is concerned with minimizing the total cost of the STEP System for a given output condition, not just identifying the minimum cost for each of the subsystems individually.

The multistage system optimization methodology described here is the first application of systematic optimization techniques to a total solar-thermal-electric power system. The principal advantage of the multistage optimization approach taken in this study over point design analysis is that a much wider variety of subsystems are given detailed consideration. The modern high-speed computer with its ability to make rapid computations and comparisons allows the multistage optimization process to identify the minimum total cost design, whereas point designs often overlook many of the possible combinations and

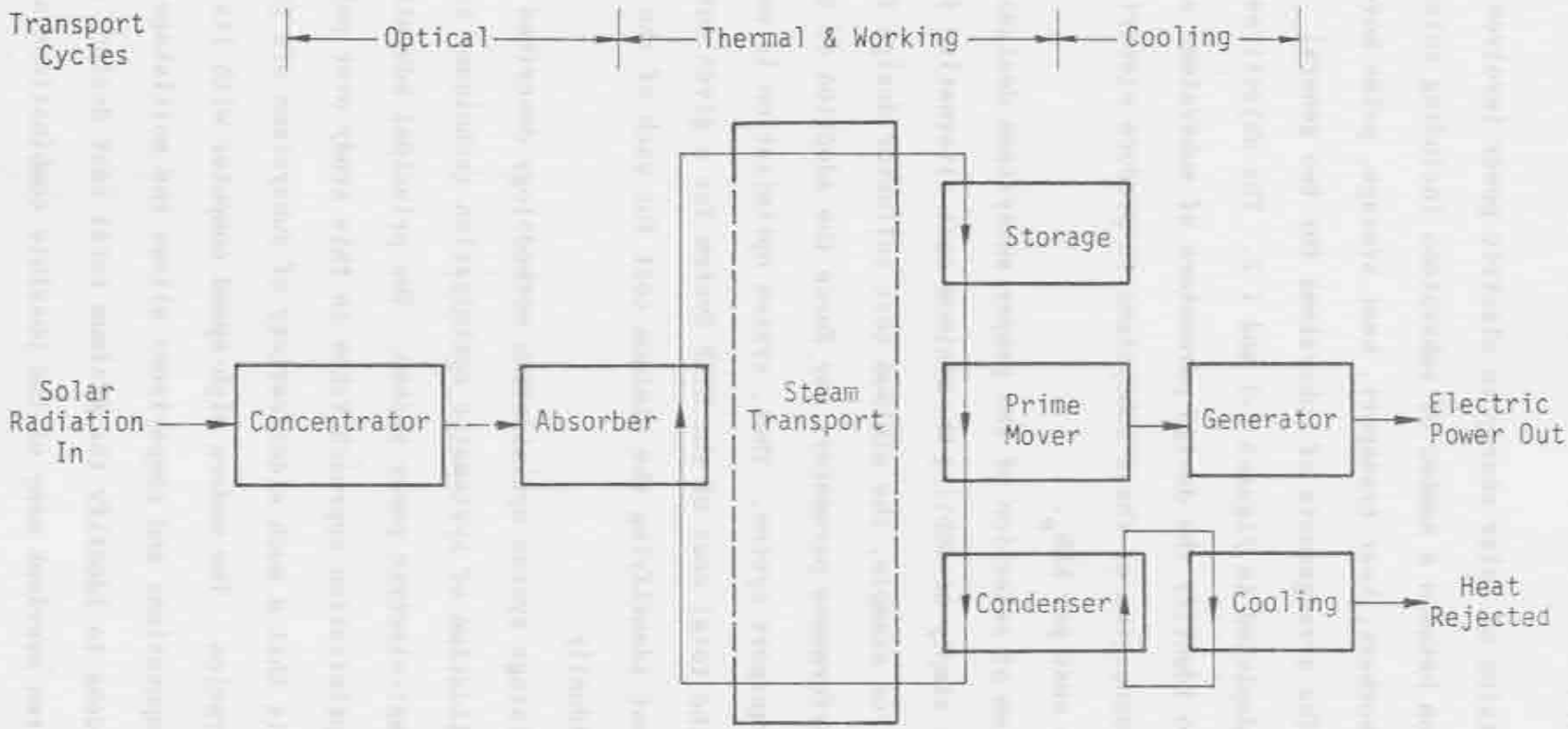

Figure 1-1. System Configuration with Steam Generated by the Collectors.

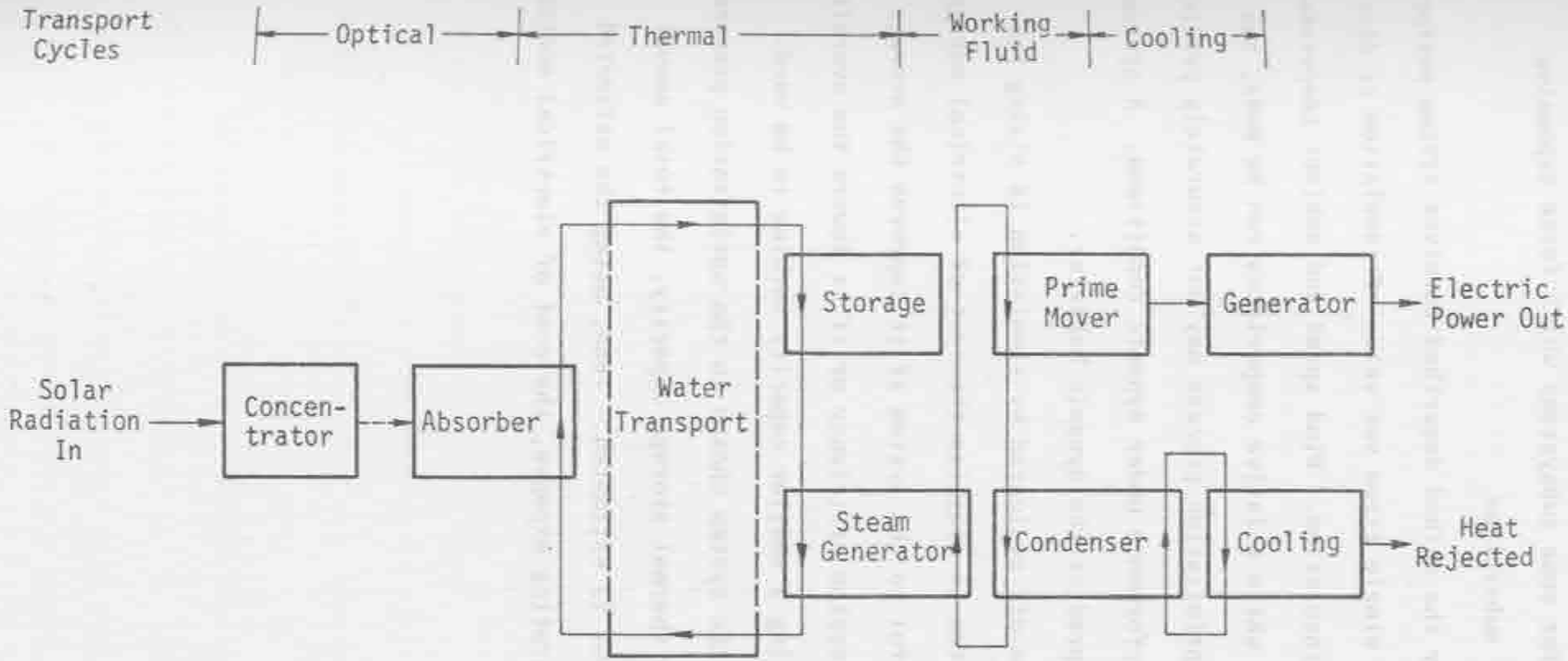

Figure 1-2. System Configuration Using Pressurized Water and Heat Exchanger.

may make poor choices for some subsystems which force expensive alternatives for other subsystems.

Optimization by the method described involves system performance characterization for a single fixed set value of insolation or distribution or of values for insolation. Wind speed and ambient temperature are also fixed. Thus, while relative comparisons can be made, the analysis used in the optimization process may not accurately predict the absolute system performance under dynamic conditions. A system simulation is used to predict the dynamic behavior.

The major trade-off evaluated by simulation is sizing the thermal storage subsystem to minimize the cost of electrical energy. Thermal storage is useful to the system if it improves the average turbine-generator conversion efficiency or if it lowers the overall system cost by permitting a smaller capacity turbine to be used.

By simulating the system chosen in the optimization process with variations in the thermal storage capacity, the total annual electrical energy output is estimated. Then, using the estimated annual capital and operating expense, the cost of electrical energy is found.

2.0 OPTIMIZATION METHODOLOGY

Mathematical models were developed to describe the performance of each of the alternative types of each of the STEP subsystems. Separate mathematical models were developed to describe the cost of each of the STEP subsystems as a function of its design variables. These performance and cost models are described separately in Appendices D through I of this report.

This appendix presents a methodology for finding minimum cost designs for solar thermal energy systems. This is a synthesis rather than an analysis approach and it is an alternative to traditional engineering approaches used in the determination of optimum system designs. In this synthesis approach a system is built up in stages and at each stage a minimum cost design is determined for a large number of different specified performances. At each subsequent stage the system comes closer to being completed and when the procedure is finished, the minimum cost system has been determined. This approach has been successfully used to analyze many other kinds of complex interrelated systems and it is believed that this is the first time it has been applied to solar thermal energy systems.

One traditional approach is to model the entire system in a simplified manner. This enables the experimenter to optimize the system by direct search or by graphical means since there are then only a few design parameters. Since most design parameters are fixed, only a few of the multitude of possibilities can be examined. In fixing most of the design variables, only an extremely small fraction of the possible designs are examined and the system's optimum is likely to be missed.

Alternatively more design variables could be included. However, this reduces or negates the usefulness of direct search.

Two problems arise when direct search is used to find an optimum in a system with many design variables. First, direct search becomes extremely ineffective if there are more than two or three design variables, Wilde (1964). This is characterized by Bellman (1957) as the curse of dimensionality. Second, direct search may not find an optimum when there are two or more design variables even if the response surface is unimodal, Wilde (1964). Palmquist and Beckman (1971) have demonstrated that there are multiple optima in radiative conductive systems. This makes the situation even worse for direct search since "such systems have not been studied with any success," Wilde (1964). Optimization using simulation is necessarily limited by these considerations.

Selcuk and Ward (1970) in a recent article employed simplified mathematical models of cost and performance to analyze the collection of solar energy and its conversion to electricity. The optimization was by direct search. This approach recognized the need to view the cost per unit of output as the primary criterion for optimization. This more complex problem, however, required that the cost and performance models be simplified and only a limited number of systems design variations could be examined.

Another approach that has been widely used in optimizing solar power generation systems is to fix several point designs and then perturb design variables until a systems optimum is converged upon. The nonlinear programming based techniques that are used permit more design variables to be considered than in direct search, but these techniques are still drawn to local optima (see Palmquist and Beckman

(1972) for examples of this happening in radiative-conductive systems.) Since multiple optima undoubtably exist in solar thermal energy systems, there is no assurance that a global optimum has been reached.

The dynamic programming, Bellman (1957), based methodology described in this appendix synthesizes or builds up the solar thermal energy system in stages. At each stage only a few of the many design variables need be considered. Thus, at each stage optimum systems are easily found.

A set of optimum concentrators indexed by properties of concentrated radiation they produce is found in the first stage. In the second stage, the absorber-heat exchanger is added to the concentrator, now characterized concisely by properties of concentrated radiation. A set of optimum collectors indexed by the properties of thermal power that they generate are then found. These minimum cost collectors are then used to find field designs that provide thermal power with specified properties at minimum cost. This minimum cost thermal power is then used in conjunction with turbine-generators and heat rejection systems to find minimum cost electric energy generating systems. Storage tradeoffs are then assessed by a dynamic simulation.

The prime requisite for using this approach is being able to find a concise parametric representation that conveys all of the performance information about the subsystems thus far put together. This permits a minimum cost to be associated with different values of the parameters so that optimization may be performed when the next subsystem is added. If this cannot be done an optimum system cannot be guaranteed. This parametric representation is developed in Section 2.1 and 2.2 of this appendix for collectors, in Sections 2.3.1 to 2.3.8 of this appendix for collector fields and in Section 2.4 for turbine-generator-cooling towers. The

detailed performance models that constitute these parametric representations are given in Appendix E, F, H and I respectively.

There are two major advantages to this approach. First, a vastly greater number of designs can be considered. This will be demonstrated below. Second, simplified performance and cost models are not required as is the case in some of the traditional approaches. Nonlinearities, discontinuities and equations that must be solved implicitly can be included and will fit in with the methodology quite easily. The primary consideration involved in performance and cost modeling is that of keeping computation times short.

2.1 Minimum Cost of Concentrated Radiation

The first subsystem to be examined is the concentrator: The concentrator is optimized parametrically by specifying the target shape, the type of focusing and two parameters, E and g. These characteristics are sufficient to describe the properties of concentrated radiation supplied to the next subsystem. Minimum costs are then computed for fixed values of the parameters, then the parameter values are changed and the process is repeated. Expressions (1) below indicate the functional dependence of these two performance parameters on the concentrator design variables.

$$E = (\rho_{ave}, A_p)^*$$

$$g = g(\theta_{max}, \sigma_\phi, \sigma_\lambda, \sigma_\delta, A_p, \text{target shape, concentrator type})^{**}$$

---

*$E = \rho_{ave} A_p$ for two axis tracking concentrators.

** This list also includes the heliostat size in the power tower concept

Specific mathematical equations for these functional relations may be found in Appendix E. These functional relations constitute the constraints in the optimization. That is, the values of E and g are fixed and designs are varied to find a minimum cost design.

Mathematically this may be expressed as

$$f_c(E, g, \text{target shape}) = \text{MIN } R_c(\theta_{max}, \rho_{ave}, A_p, \sigma_\phi, \sigma_\lambda, \sigma_\delta, \text{concentrator type}) \quad (2)$$

where the minimization is over designs yielding E and g for the specified target shape. Here f_c is the minimum concentrator cost as a function of E, g and target shape and R_c is the cost for specific values of θ_{max}, ρ_{ave}, A_p, σ_ϕ, σ_λ, σ_δ for a given concentrator type.

2.1.1 Tower-Heliostat Example

The optimization procedure for the tower-heliostat system was implemented on a computer as shown in Figure 2-1. The design variables are the field rim angle, θ_{max}; the average reflectivity of the heliostats, ρ_m; the width of the square heliostats, WP; the number of heliostats in a field, NW; the field aperture area, A_p; and the contour and pointing accuracy of the heliostats, $\sigma_{\phi,\lambda,\delta}$. A total of 12 values of θ_{max}, from 20^o to 75^o in steps of 5^o, were evaluated. One value of ρ_m, 0.90 was used. The field had one of 7 different heliostats sizes with a WP ranging from one to seven metres. With E and g fixed, different values of θ_{max}, ρ_m and WP are tested. With E, g, θ_{max}, ρ_m and WP fixed, NW, A_p and $\sigma_{\phi,\lambda,\delta}$ can be found directly (see Appendix E). Thus, a total 12 x 7 = 84 different field and heliostat combination sizes and designs were evaluated for each value of the E and g combinations. For

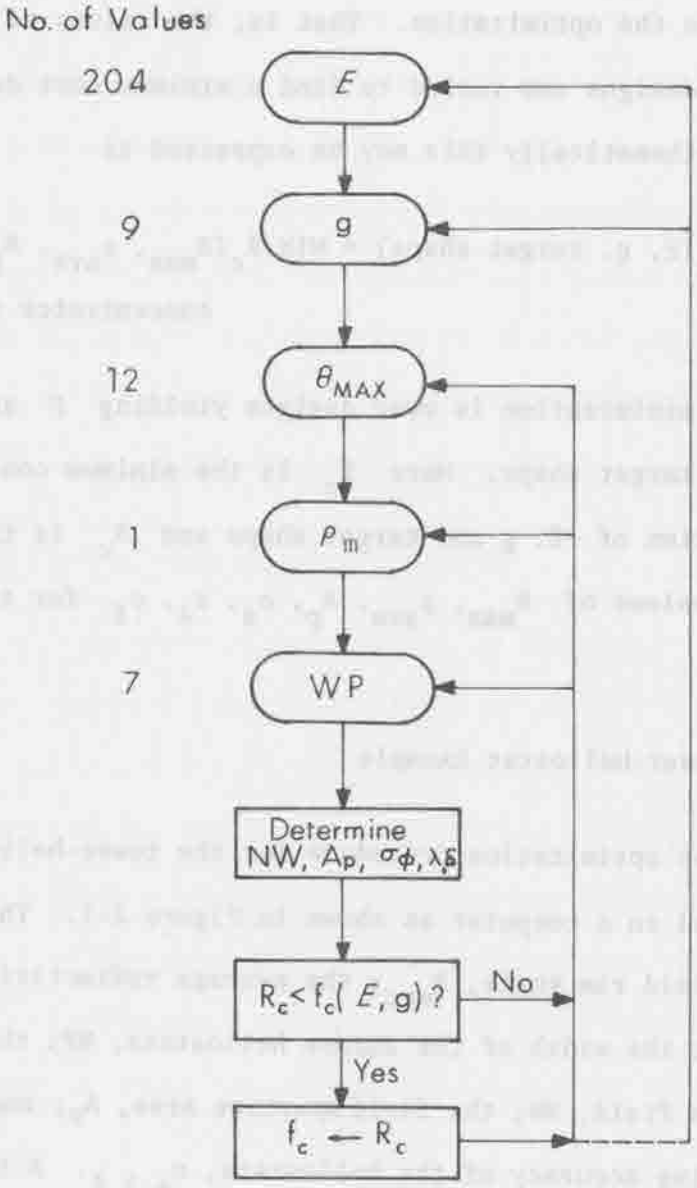

Figure 2-1. Minimum Cost of Concentrated Radiation from the Tower-Heliostat System.

other concentrator types, up to 720 different designs are evaluated for each E and g combination.

Each tower-heliostat system design may be fabricated in a range of sizes defined by g, E, ρ_m, θ_{max}, and WP. A total of 204 values of E were used in the evaluation of tower-heliostat systems. Each increment of E was 1.02 times the previous E value until 34 values in a target plant size range were evaluated. Then another 34 values of E were generated for a different target plant size range, and so on. Ranges of the target plant sizes have midpoints of 1, 3, 10, 30, 100 and 300 megawatts electric.

The parameter g is a measure of the spread of concentrated radiation and is a function of rim angle, contour errors, pointing errors, concentrator aperture, and concentrator type. A total of 9 values of g were examined for each E in the tower heliostat system, so a total of 204 x 9 or 1836 different E, g pairs were evaluated. For the example concentrator type, each of these 1836 pairs have 84 possible designs, or a total of 154,244 combinations.

With E and g fixed, the computer starts with the first value of θ_{max}, ρ_m, WP, A_p, $\sigma_{\phi,\lambda,\delta}$ and NW that yields E and g. It computes the cost to produce E and g and stores that cost value. (The cost models for concentrators are described in Appendix E). The mirror size, WP, is indexed by one while the other two design variables ρ_{ave} and θ_{max} are held constant; NW, A_p, $\sigma_{\phi,\lambda,\delta}$ are computed and then the corresponding cost is computed. The cost of E and g is compared to the previously calculated value and if less, the minimum cost is stored along with the values for θ_{max}, ρ_m, A_p, $\sigma_{\phi,\lambda,\delta}$, NW and WP. After all 84 combinations of θ_{max}, ρ_{ave}, A_p, $\sigma_{\phi,\lambda,\delta}$ and WP have been evaluated and the minimum cost for that E and g stored,

the value of g is incremented and the procedure repeated for the new combination of E and g. Eventually each of the 1836 pairs of E and g will be matched with one of the 154,244 designs.

An example computer printout for the results of this procedure is depicted in Figure 2-2 for the tower heliostat system. Shown is the minimum cost to produce a particular value of E and g along with the associated optimum design for that concentrator.

2.1.2 Quasi-Paraboloid Example

The optimization procedure for multiple mounted quasi-paraboloid concentrators was implemented on a computer as shown in Figure 2-3. As this procedure is carried out, a minimum cost of achieving performance of a concentrator characterized by various E and g combinations is determined. To find a minimum cost design for each concentrator type, 15 x 3 x 16 or 720 different designs were considered for each E and g pair. Thus, 272 different minimum cost concentrators, parametric in E and g, were determined.

In the figure it is shown that f_c, the minimum cost for a given E, g pair, is updated each time a new design is found that is superior to the previous designs examined. Though not shown in the diagram or in Figure 2-4, the minimum cost design that yielded the E, g combination is also saved for future reference. Thus, when an E, g pair is determined to be optimum for a particular application, such as a 10 MW solar-thermal electric power plant, the concentrator design that resulted in this minimum cost E, g pair can be retrieved.

PAGE 1 C9G2CP 09/25/74. 00.51.09.

PER MODULE COST FOR POINTING AND SURFACE ACCURACY 1.0
PER SQUARE METER COST FOR POINTING AND SURFACE ACCURACY 1.0

--PARAMETERS-- E/100	100G	VP	---OPTIMUM DESIGNS--- nW	Tm	Rm	AP/100	TWR	SIGMA	MIN		---COST/1000--- TWR	nELI	HT
500	500	1	68539	60	.90	1299	117	.083	469356	*	317	4212	48
500	700	2	17134	60	.90	1299	117	.063	435867	*	317	3955	48
500	980	1	68539	60	.90	1299	117	.153	4641		317	4212	48
500	1372	2	16954	55	.90	1248	140	.143	4325		340	3913	56
500	1921	3	7535	55	.90	1248	140	.148	4068		340	3686	56
500	2689	4	4238	55	.90	1248	140	.158	3864		340	3465	56
500	3765	6	1960	70	.90	1556	81	.148	3475		281	3154	38
500	5271	7	1398	60	.90	1299	117	.163	3211		317	2844	48
500	7379	7	1398	60	.90	1299	117	.285	3211		317	2844	48
510	510	1	69909	60	.90	1325	119	.084	478183	*	319	4296	49
510	714	2	17477	60	.90	1325	119	.065	444005	*	319	4034	49
510	1000	1	69909	60	.90	1325	119	.154	4728		319	4296	49
510	1399	2	17293	55	.90	1273	141	.144	4406		341	3991	57
510	1959	3	7686	55	.90	1273	141	.149	4165		341	3760	57
510	2743	4	4323	55	.90	1273	141	.160	3936		341	3534	57
510	3840	6	1967	65	.90	1414	99	.143	3510		299	3165	43
510	5376	7	1411	55	.90	1273	141	.151	3270		341	2871	57
510	7527	7	1411	55	.90	1273	141	.255	3270		341	2871	57
520	520	1	71306	60	.90	1352	120	.084	487197	*	320	4382	51
520	728	2	17827	60	.90	1352	120	.066	452315	*	320	4114	51
520	1020	1	71308	60	.90	1352	120	.154	4816		320	4382	51
520	1427	2	17639	55	.90	1299	142	.145	4489		342	4071	58
520	1998	3	7839	55	.90	1299	142	.151	4243		342	3834	58
520	2798	4	4409	55	.90	1299	142	.162	4010		342	3605	58
520	3917	6	2006	65	.90	1442	100	.148	3574		300	3238	45
520	5484	7	1439	55	.90	1299	142	.156	3330		342	2928	58
520	7677	7	1439	55	.90	1299	142	.268	3329		342	2928	58
531	531	1	72734	60	.90	1379	121	.085	496385	*	321	4470	52
531	743	2	18183	60	.90	1379	121	.068	460772	*	321	4197	52
531	1040	1	72734	60	.90	1379	121	.154	4909		321	4470	52
531	1456	2	17992	55	.90	1325	144	.146	4574		344	4153	60
531	2038	3	7996	55	.90	1325	144	.152	4322		344	3911	60
531	2854	4	4498	55	.90	1325	144	.164	4085		344	3678	60
531	3995	6	2046	65	.90	1471	101	.153	3641		301	3292	46
531	5593	7	1468	55	.90	1325	144	.161	3392		344	2987	60
531	7831	7	1468	55	.90	1325	144	.272	3391		344	2987	60
541	541	1	74189	60	.90	1406	122	.085	505761	*	322	4559	53
541	758	2	18547	60	.90	1406	122	.069	469483	*	322	4281	53
541	1061	1	74189	60	.90	1406	122	.155	5002		322	4559	53
541	1485	2	18352	55	.90	1351	145	.146	4660		345	4236	62
541	2079	3	8156	55	.90	1351	145	.153	4404		345	3990	62
541	2911	4	4588	55	.90	1351	145	.167	4162		345	3751	62
541	4075	6	2060	60	.90	1406	122	.144	3693		322	3315	53
541	5705	7	1496	55	.90	1351	145	.166	3456		345	3048	62
541	7987	7	1498	55	.90	1351	145	.275	3455		345	3043	62
552	552	1	75672	60	.90	1434	123	.086	515316	*	323	4650	55
552	773	2	18719	55	.90	1373	147	.056	477532	*	347	4320	63
552	1082	1	75672	60	.90	1434	123	.155	5097		323	4650	55
552	1515	2	18719	55	.90	1373	147	.147	4748		347	4320	63
552	2121	3	8319	55	.90	1373	147	.155	4487		347	4069	63
552	2969	5	3116	70	.90	1719	85	.144	4052		285	3731	44
552	4157	6	2102	60	.90	1434	123	.145	3763		323	3383	55
552	5819	7	1528	55	.90	1373	147	.170	3520		347	3109	63

Figure 2-2. Sample Computer Printout from the Heliostat-Tower Computer Optimization.

* A very large cost flags $\sigma_{\phi,\lambda}$ infeasibility.

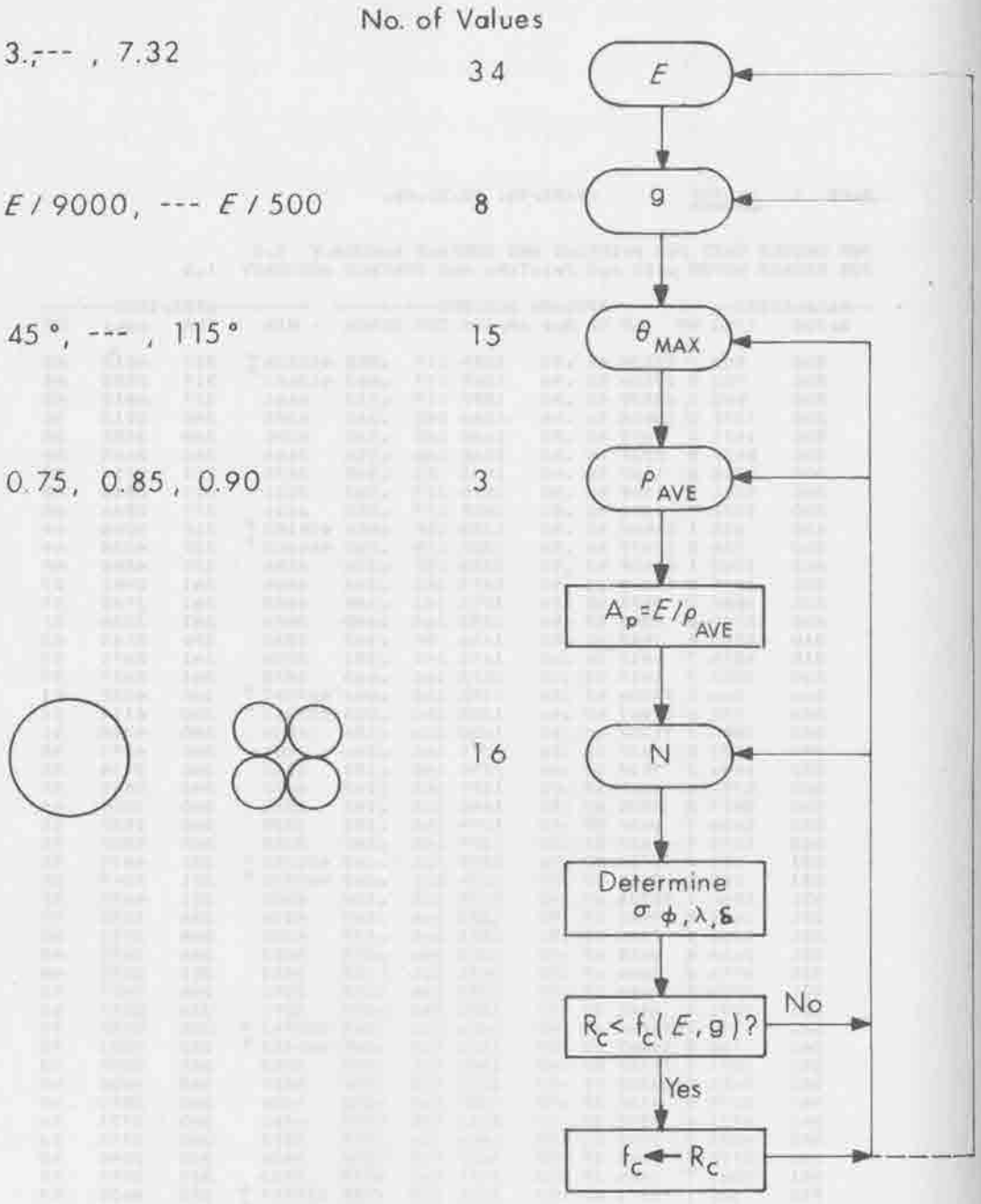

Figure 2-3. Concentrator Optimization Procedure for Multiply Mounted Quasi-Paraboloids.

2.2 Minimum Cost of Thermal Power from a Collector

A property of the STEP system is that it is arranged as a series of subsystems, and the output of the first sybsystem must be the input to the second and so forth. Thus each of the E , g output pairs from the concentrator may be inputs to an absorber-heat exchanger. Each absorber-heat exchanger design for a given E , g input will have different heat outputs described by $\dot{m}$, the mass flow rate of the heat transport fluid; T_{in}, the inlet temperature of the heat transport fluid; T_{out}, the outlet temperature and the state of the fluid, whether it is pressurized water or steam.

The minimum cost designs to yield various values of the concentrator performance parameters E and g are matched with compatible absorber designs. The result of this combination together with a specified insolation level, I_D, is a set of outputs ($\dot{m}$, T_{in} T_{out}) from the combined concentrator and absorber subsystems. Many of these outputs will be identical, indicating that there are different combinations of concentrator designs and absorber designs which will yield the same output. However, only one combination will yield the output at minimum cost, and this combination can be identified by adding together the cost of the absorber and the minimum cost of the concentrator. In subsequent analyses, only this minimum cost combination for each value of $\dot{m}$, T_{in} and T_{out}, is retained for incorporation in a compatible field layout with an appropriate heat transport subsystem.

The sequential optimization progresses by finding minimum cost concentrator-absorber-heat exchanger combinations. In this optimization, E , g and target shape are considered to be design variables. Thus, with the inclusion of the minimum cost of concentrated radiation having

properties E, g with a specified target shape, we can find many different collector designs all having a fixed output $\dot{m}$, T_{in} and T_{out}. These designs are then costed and the minimum cost collector with this output is then selected. Specific mathematical expressions that permit designs to be converted to values of $\dot{m}$, T_{in} and T_{out} under specified insolation levels and other ambient conditions are given in Appendix E.

Mathematically, the optimization may be expressed as

$$f_a(\dot{m}, T_{in}, T_{out}) = \text{MIN}\ [R_A(d,l,a,\varepsilon,\alpha,\tau,\dot{m},\text{absorber type, etc.}) + f_c(E,g,\text{target shape})] \qquad (2\text{-}3)$$

where the minimum is over designs, E, g, a, d, etc., yielding $\dot{m}$, T_{in} and T_{out}. Here f_a is the minimum collector cost for the given values, f_c is the minimum concentrator cost for the given values and R_A is the absorber-heat exchanger cost for a specified design.

2.2.1 Computer Implementation of the Absorber-Heat Exchanger Optimization

Movable point focus collectors using pressurized water will be used to illustrate the computer implementation of the optimization. The absorber-heat exchangers associated with these collectors have the least number of design variables. In all cases designs were enumerated for fixed values of $\dot{m}$, T_{in} and T_{out}. The enumerative search for designs that yielded a fixed value of $\dot{m}$, T_{in} and T_{out} for these collectors was implemented by selecting E, g and a as shown in the flow chart of Figure 2-4. As can be seen, a small and a large absorber can both produce the same T_{out} for fixed T_{in} and $\dot{m}$. The selection of a is accomplished by an interval search starting from $a = 0$ to find the appropriate small absorber and then from $a = 7g$ to find the appropriate large absorber. The number of a's considered in each interval search averages about ten.

For each $\dot{m}$, T_{in} and T_{out} the maximum number of designs considered is 272 x 2 = 544*. For each of the 544 designs the cost of the absorber-heat exchanger is computed and added to the minimum cost for concentrated radiation, $f_c(E,g)$, corresponding to that design's E and g. This total cost is the cost of the concentrator combined with the absorber-heat exchanger, that is, the cost of the collector. Out of these 544 designs the minimum cost design is selected as the collector producing thermal power with the characteristics $\dot{m}$, T_{out} and T_{in} at minimum cost. This process is then repeated for a total of 6 x 8 x (5 + 6 + 7 + 8) or 1248 values of $\dot{m}$, T_{out} and T_{in}.

Considerable savings in computation time has been achieved by synthesizing minimum cost collectors in two steps rather than all at once. The maximum number of designs examined can be seen from Figures 2-3 and 2-4. The maximum number of designs that are examined in the minimum cost of concentrated radiation analysis is 720 x 272 or 195,840 and 1248 x 544 or 678,912 for the minimum cost of thermal power from the collector analysis. This is a total of 874,752 designs. If this were done in one step and the same number of designs were examined as were effectively examined in this case, 1248 x 2 x 195,840 or 488,816,640 designs would be examined. Another way of putting this is that by condensing the 195,840 concentrator designs into 272, a savings of

---

* Many times this number are actually considered since about ten candidate a's are examined in the search procedure. In addition, other design variables such as absorber type, τ,α,ε, presence of a fin, etc. may be examined by rerunning the program with different settings. For movable collectors, the design parameter d was set to achieve turbulent flow at as large a diameter as was feasible. It could also have been iterated over a set of values, as was done in the tower-heliostat system. In the line focus case an additional design variable, absorber length L, must also be considered. Seven values of L are used in this case.

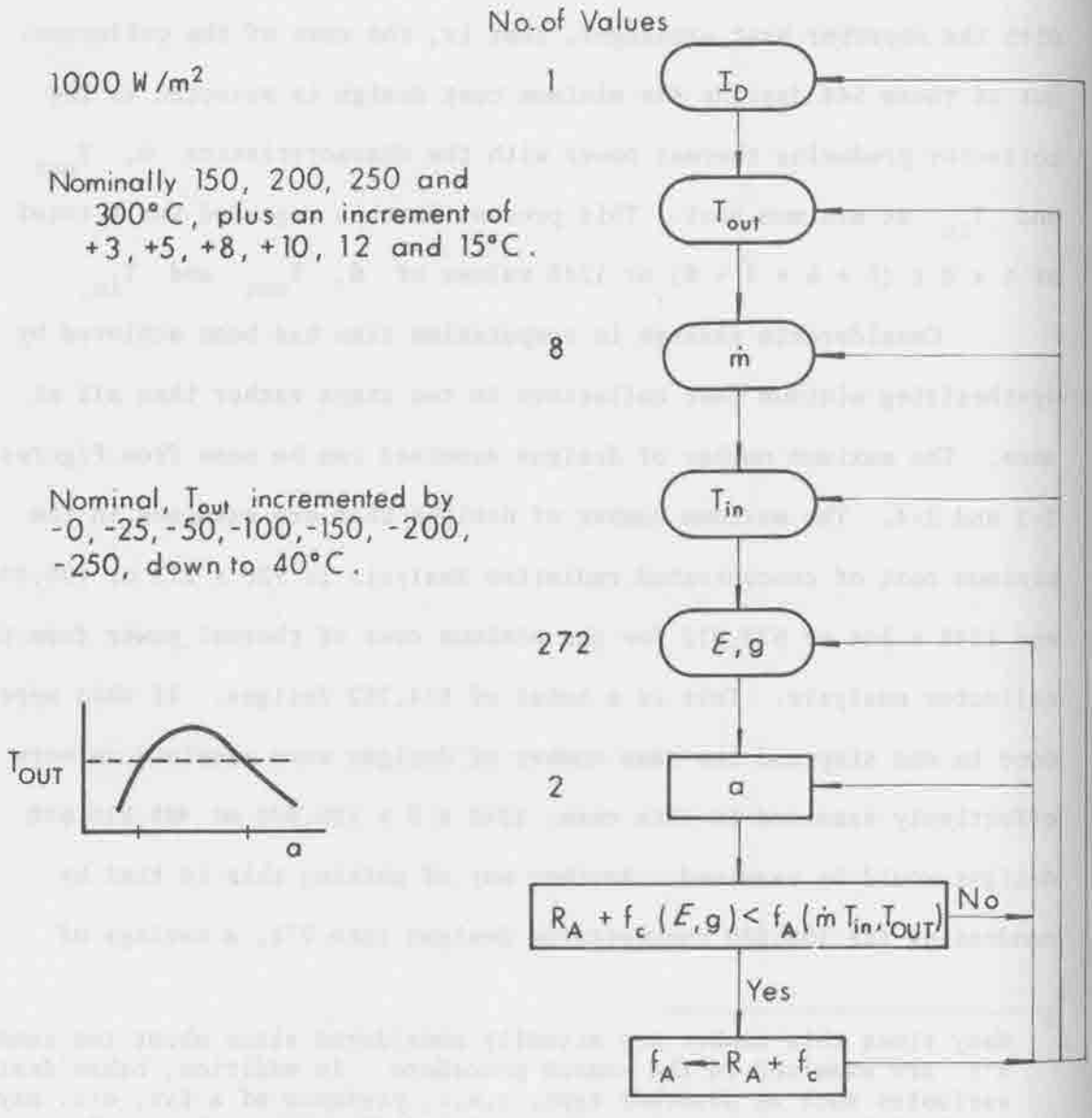

Figure 2-1. Computer Implementation of the Absorber-Heat Exchange Optimization for Movable Point Focus Collectors

about 560 to 1 in computational effort is achieved. This is possible since all of the characteristics of concentrated radiation necessary for the absorber-heat exchanger analyses can be expressed by E and g without losing any potential minimum cost collector designs.

This economy is actually greater than indicated, as the flow chart only indicates the analysis of a particular type concentrator or absorber-heat exchanger. In reality all concentrator designs and types that did not result in minimum cost of concentrated radiation having properties E and g for a particular target shape would be eliminated. So if ten different types of concentrators are considered then the information would be condensed from 1,958,400 total designs into 272 designs. The point here is that only the minimum cost designs need be retained. Thus, instead of 560 - 1 advantage there is now 5600 - 1 advantage.

2.2.2 Collector Optimization Example

An example of part of the output from the minimum cost of concentrated radiation analysis for Fresnel reflectors with pancake targets using the cost and performance models of Appendix E is shown in Figure 2-5. The output under the minimum cost column is the set of values of f_c. This analysis was repeated and similar tables generated for other point focusing concentrators delivering radiation to a pancake target. Another set of analyses was also performed on the same set of point focusing concentrators and tower-heliostat systems. The other computer outputs are given in Appendix K. After these analyses were completed the minimum costs for particular E and g combinations for each target shape were compared. That is, all spherical target analyses were compared to determine the minimum cost types and designs of concentrators delivering radiation to that type of target.

PAGE 1 CSG4P 08/14/74. 11.57.19.

PER MODULE COST FOR POINTING AND SURFACE ACCURACY 1.0
PER SQUARE METER COST FOR POINTING AND SURFACE ACCURACY 1.0

----PARAMETERS---- EAP *	G *	N	MP**	SCOS**	OPTIMUM DESIGNS---------- N**	TH*	RHO *	AP*	SIGMA*	MINIMUM COST	
7.04E+00	7.82E-04	1	1	.80	1	30	.95	7.41E+00	.077	5.58E+04	+
7.04E+00	1.10E-03	1	1	.80	1	40	.95	7.41E+00	.151	5.92E+02	
7.04E+00	1.53E-03	1	1	.80	1	35	.95	7.41E+00	.154	5.68E+02	
7.04E+00	2.15E-03	1	1	.80	1	30	.95	7.41E+00	.163	5.50E+02	
7.04E+00	3.00E-03	1	1	.80	1	25	.95	7.41E+00	.180	5.38E+02	
7.04E+00	4.21E-03	1	1	.80	1	25	.95	7.41E+00	.196	5.37E+02	
7.04E+00	5.89E-03	1	1	.80	1	25	.95	7.41E+00	.237	5.36E+02	
7.04E+00	8.25E-03	1	1	.80	1	25	.95	7.41E+00	.284	5.35E+02	
7.39E+00	8.21E-04	1	1	.80	1	30	.95	7.78E+00	.077	5.75E+04	+
7.39E+00	1.15E-03	1	1	.80	1	40	.95	7.78E+00	.151	7.13E+02	
7.39E+00	1.61E-03	1	1	.80	1	35	.95	7.78E+00	.154	6.83E+02	
7.39E+00	2.25E-03	1	1	.80	1	30	.95	7.78E+00	.163	6.67E+02	
7.39E+00	3.16E-03	1	1	.80	1	25	.95	7.78E+00	.180	6.54E+02	
7.39E+00	4.42E-03	1	1	.80	1	25	.95	7.78E+00	.196	6.53E+02	
7.39E+00	6.18E-03	1	1	.80	1	25	.95	7.78E+00	.237	6.52E+02	
7.39E+00	8.66E-03	1	1	.80	1	25	.95	7.78E+00	.284	6.51E+02	
7.76E+00	8.62E-04	1	1	.80	1	30	.95	8.17E+00	.077	6.92E+04	+
7.76E+00	1.21E-03	1	1	.80	1	40	.95	8.17E+00	.151	7.27E+02	
7.76E+00	1.69E-03	1	1	.80	1	35	.95	8.17E+00	.154	7.00E+02	
7.76E+00	2.37E-03	1	1	.80	1	30	.95	8.17E+00	.163	6.83E+02	
7.76E+00	3.31E-03	1	1	.80	1	25	.95	8.17E+00	.180	6.70E+02	
7.76E+00	4.64E-03	1	1	.80	1	25	.95	8.17E+00	.196	6.69E+02	
7.76E+00	6.49E-03	1	1	.80	1	25	.95	8.17E+00	.237	6.68E+02	
7.76E+00	9.09E-03	1	1	.80	1	25	.95	8.17E+00	.284	6.67E+02	
8.15E+00	9.06E-04	1	1	.80	1	30	.95	8.58E+00	.077	7.09E+04	+
8.15E+00	1.27E-03	1	1	.80	1	40	.95	8.58E+00	.151	7.45E+02	
8.15E+00	1.77E-03	1	1	.80	1	35	.95	8.58E+00	.154	7.17E+02	
8.15E+00	2.48E-03	1	1	.80	1	30	.95	8.58E+00	.163	6.99E+02	
8.15E+00	3.48E-03	1	1	.80	1	25	.95	8.58E+00	.180	6.86E+02	
8.15E+00	4.87E-03	1	1	.80	1	25	.95	8.58E+00	.196	6.85E+02	
8.15E+00	6.82E-03	1	1	.80	1	25	.95	8.58E+00	.237	6.84E+02	
8.15E+00	9.55E-03	1	1	.80	1	25	.95	8.58E+00	.284	6.83E+02	
8.56E+00	9.51E-04	1	1	.80	1	30	.95	9.01E+00	.077	7.29E+04	+
8.56E+00	1.33E-03	1	1	.80	1	40	.95	9.01E+00	.151	7.62E+02	
8.56E+00	1.86E-03	1	1	.80	1	35	.95	9.01E+00	.154	7.33E+02	
8.56E+00	2.61E-03	1	1	.80	1	30	.95	9.01E+00	.163	7.16E+02	
8.56E+00	3.65E-03	1	1	.80	1	25	.95	9.01E+00	.180	7.03E+02	
8.56E+00	5.11E-03	1	1	.80	1	25	.95	9.01E+00	.196	7.00E+02	
8.56E+00	7.16E-03	1	1	.80	1	25	.95	9.01E+00	.237	6.99E+02	
8.56E+00	1.00E-02	1	1	.80	1	25	.95	9.01E+00	.284	6.98E+02	
8.99E+00	9.98E-04	1	1	.80	1	30	.95	9.46E+00	.077	7.41E+04	+
8.99E+00	1.40E-03	1	1	.80	1	40	.95	9.46E+00	.151	7.79E+02	
8.99E+00	1.95E-03	1	1	.80	1	35	.95	9.46E+00	.154	7.49E+02	
8.99E+00	2.74E-03	1	1	.80	1	30	.95	9.46E+00	.163	7.31E+02	
8.99E+00	3.84E-03	1	1	.80	1	25	.95	9.46E+00	.180	7.17E+02	
8.99E+00	5.37E-03	1	1	.80	1	25	.95	9.46E+00	.196	7.16E+02	
8.99E+00	7.52E-03	1	1	.80	1	25	.95	9.46E+00	.237	7.14E+02	
8.99E+00	1.05E-02	1	1	.80	1	25	.95	9.46E+00	.284	7.13E+02	
9.43E+00	1.05E-03	1	1	.80	1	30	.95	9.93E+00	.077	7.57E+04	+
9.43E+00	1.47E-03	1	1	.80	1	40	.95	9.93E+00	.151	7.95E+02	
9.43E+00	2.05E-03	1	1	.80	1	35	.95	9.93E+00	.154	7.65E+02	
9.43E+00	2.88E-03	1	1	.80	1	30	.95	9.93E+00	.163	7.48E+02	
9.43E+00	4.03E-03	1	1	.80	1	25	.95	9.93E+00	.180	7.32E+02	

Figure 2-5. Minimum Cost of Concentrated Radiation from Fresnel Reflectors with Pancake Targets.

* $\xi, g, \theta_{max}, \rho_{ave}, \Lambda_p$ and $\sigma_{\phi,\lambda,\delta}$ θεσρεψτιχεωυ˜

** Used for the tower-heliostat analysis.

\+ Infeasible due to $\sigma_{\phi,\lambda,\delta}$

Figure 2-6 is a graph of minimum costs for several types of point focusing concentrators illustrating the comparisons that were made. Shown in the figure are a single mount paraboloid with a spherical target - C1G1 (a pancake target - C1G3), a multiple array of long focus quasi-paraboloids with a common spherical target - C3G2 (a pancake target - C3G4), a Fresnel lense with a spherical target - C7G2 (a pancake target - C7G4) and a Fresnel reflector with a spherical target - C5G2 (a pancake target - C5G4). As can be seen the Fresnel reflectors dominate all other types for the range of E's shown. This also holds true for other values of g. The costs for the two different target shapes differed only slightly and thus appear as single lines in the figure for each concentrator type. Thus the f_c's for Fresnel reflectors were carried into the absorber-heat exchanger optimization with other concentrator types being eliminated.

The example next moves to the generation of minimum cost thermal power from a collector. The minimum cost of thermal power designs for boiling collectors with pancake absorber-heat exchangers for different values of $\dot{m}$ and TBOIL with $I_D = 1000\ w/m^2$ is shown in Figure 2-7. An optimum design in Figure 2-7 has had appended to it a reference or trace back to the concentrator that delivered minimum cost radiation for the E and g that was chosen as part of the minimum cost collector design. Thus the design of a minimum cost concentrator can now be specified. A graphic illustration of this analysis for several point focus collector types is shown in Figure 2-8.

This example illustrates the synthesis approach to finding minimum cost collectors that has been described up to this point. To illustrate this procedure in more detail, a specific design will be selected from Figure 2-7, the collector in line 1. This is a partial

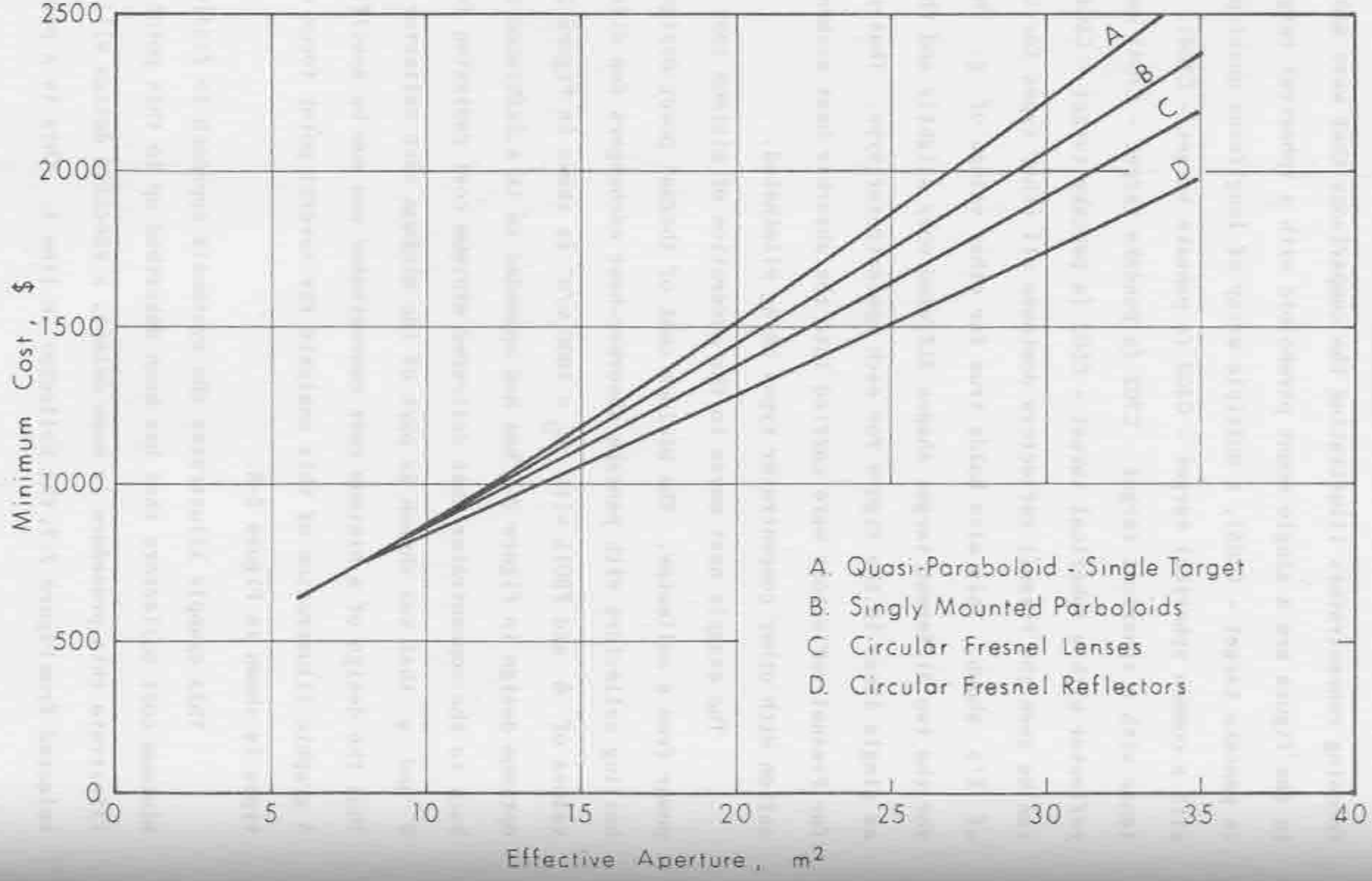
2500
2000
1500
1000
500
0
Minimum Cost, $
0
5
10
15
20
25
30
35
40
Effective Aperture, m²
A
B
C
D
A. Quasi-Paraboloid - Single Target
B. Singly Mounted Parboloids
C Circular Fresnel Lenses
D. Circular Fresnel Reflectors

07/04/79. 09.10.23.
PROGRAM ANCBL

CKDF FILE NAME
? C5GA
TYPE, COST MODEL
? 0,1
CAVITY
? 1

BOILING HEAT TRANSFER VERSION
RPIN= 811, EPSILON= .90, ALPHA= .93, TAU= 1.00, TAMB= 20,
FRACOL= 1.00, VELOCITY= 5.0, TYPE= 0, COST MODEL= CAI

ID= 1000

--PARAMETERS-- THRIL OF	HOST	D	L	LA	AL	Q	E	MINIMUM COST	TW	B	W	CR	MV	TR	DIR	AP	SIGMA	C. TYPE	PC	ETA	$/KW
150 .075	.040	.020	1.25		8.525E-02	8.246E-03	7.040E+00	6.350E+02	161	1	1	293	1	25	.95	7.41E+00	.284	C5GA	6.347E+02	.856	1.00E+02
150 .100	.040	.021	1.33		2.819E-02	5.369E-03	5.985E+00	7.159E+02	164	1	1	336	1	25	.95	9.46E+00	.196	C5GA	7.156E+02	.892	5.48E+01
150 .025	.080	.017	1.04		1.504E-02	8.246E-03	7.040E+00	6.349E+02	156	1	1	411	1	25	.95	7.41E+00	.284	C5GA	6.347E+02	.797	1.07E+02
150 .050	.080	.021	1.32		2.785E-02	5.369E-03	6.985E+00	7.159E+02	156	1	1	340	1	25	.95	9.46E+00	.196	C5GA	7.156E+02	.892	8.45E+01
150 .075	.080	.029	1.56		5.402E-02	1.633E-02	1.394E+01	8.013E+02	161	1	1	272	1	25	.95	1.47E+01	.234	C5GA	8.805E+02	.863	6.96E+01
150 .100	.080	.033	2.09		6.961E-02	2.110E-02	1.668E+01	1.076E+03	163	1	1	282	1	25	.95	1.97E+01	.284	C5GA	1.085E+03	.858	6.43E+01
150 .015	.160	.016	.65		1.177E-02	8.246E-03	7.040E+00	6.349E+02	153	1	1	429	1	25	.95	7.41E+00	.284	C5GA	6.347E+02	.853	1.23E+02
150 .020	.160	.022	1.37		2.996E-02	8.653E-03	7.393E+00	6.511E+02	154	1	1	260	1	25	.95	7.78E+00	.284	C5GA	6.508E+02	.868	9.64E+01
150 .025	.160	.028	1.75		4.586E-02	7.517E-03	8.985E+00	7.143E+02	154	1	1	194	1	25	.95	9.46E+00	.237	C5GA	7.143E+02	.892	8.47E+01
150 .035	.160	.035	2.22		7.367E-02	1.481E-02	1.214E+01	8.227E+02	156	1	1	169	1	25	.95	1.03E+01	.284	C5GA	8.219E+02	.855	6.96E+01
150 .050	.160	.033	2.09		6.939E-02	2.173E-02	1.865E+01	1.086E+03	158	1	1	283	1	25	.95	1.97E+01	.284	C5GA	1.085E+03	.855	6.43E+01
150 .075	.160	.043	2.72		1.175E-01	3.233E-02	2.760E+01	1.454E+03	162	1	1	247	1	25	.95	2.91E+01	.254	C5GA	1.453E+03	.872	5.74E+01
150 .010	.320	.022	1.37		2.990E-02	8.658E-03	7.392E+00	6.511E+02	152	1	1	280	1	25	.95	7.78E+00	.284	C5GA	6.505E+02	.868	9.64E+01
150 .015	.320	.029	1.83		5.357E-02	1.279E-02	1.092E+01	7.682E+02	153	1	1	213	1	25	.95	1.15E+01	.234	C5GA	7.652E+02	.871	7.59E+01
150 .020	.320	.032	2.04		6.643E-02	1.714E-02	1.464E+01	9.125E+02	154	1	1	232	1	25	.95	1.54E+01	.204	C5GA	9.115E+02	.876	6.74E+01
150 .025	.320	.033	2.09		6.927E-02	2.188E-02	1.868E+01	1.084E+03	155	1	1	284	1	25	.95	1.97E+01	.294	C5GA	1.085E+03	.857	6.43E+01
150 .035	.320	.034	2.17		7.479E-02	1.068E-02	2.503E+01	1.355E+03	156	1	1	352	1	25	.95	2.63E+01	.150	C5GA	1.354E+03	.897	5.73E+01
150 .005	.640	.022	1.37		2.990E-02	8.653E-03	7.392E+00	6.513E+02	151	1	1	260	1	25	.95	7.78E+00	.254	C5GA	6.508E+02	.867	9.63E+01
150 .010	.640	.032	2.04		6.622E-02	1.714E-02	1.464E+01	9.125E+02	152	1	1	232	1	25	.95	1.54E+01	.284	C5GA	9.115E+02	.876	6.74E+01
150 .015	.640	.033	2.39		9.074E-02	1.809E-02	2.163E+01	1.204E+03	153	1	1	251	1	25	.95	2.23E+01	.237	C5GA	1.203E+03	.890	5.94E+01
150 .020	.640	.050	3.17		1.591E-01	3.394E-02	2.891E+01	1.510E+03	154	1	1	198	1	25	.95	3.05E+01	.284	C5GA	1.511E+03	.835	5.60E+01
200 .075	.040	.016	1.03		1.717E-02	8.246E-03	7.040E+00	6.349E+02	209	1	1	432	1	25	.95	7.41E+00	.254	C5GA	6.347E+02	.784	1.08E+02
200 .100	.040	.023	1.43		3.389E-02	1.002E-02	8.557E+00	6.986E+02	211	1	1	271	1	25	.95	9.01E+00	.234	C5GA	6.980E+02	.859	9.02E+01
200 .025	.080	.015	.93		1.395E-02	8.246E-03	7.040E+00	6.349E+02	205	1	1	531	1	25	.95	7.41E+00	.284	C5GA	6.347E+02	.731	1.17E+02
200 .050	.080	.023	1.43		3.312E-02	1.002E-02	8.557E+00	6.986E+02	206	1	1	278	1	25	.95	9.01E+00	.204	C5GA	6.980E+02	.857	9.02E+01
200 .075	.080	.030	1.59		5.007E-02	1.401E-02	1.264E+01	8.232E+02	209	1	1	229	1	25	.95	1.33E+01	.234	C5GA	8.219E+02	.873	7.09E+01
200 .100	.050	.034	2.12		7.202E-02	1.984E-02	1.694E+01	1.013E+03	212	1	1	244	1	25	.95	1.78E+01	.254	C5GA	1.013E+03	.868	6.55E+01
200 .015	.160	.012	.78		9.810E-03	8.246E-03	7.040E+00	6.349E+02	202	1	1	750	1	25	.95	7.41E+00	.234	C5GA	6.347E+02	.627	1.27E+02
200 .020	.160	.019	1.18		2.251E-02	8.246E-03	7.040E+00	6.350E+02	203	1	1	329	1	25	.95	7.41E+00	.254	C5GA	6.347E+02	.836	1.03E+02
200 .025	.160	.023	1.43		3.304E-02	1.002E-02	8.557E+00	6.986E+02	203	1	1	273	1	25	.95	9.01E+00	.254	C5GA	6.980E+02	.859	9.02E+01
200 .035	.160	.027	1.66		4.460E-02	1.410E-02	1.204E+01	7.946E+02	205	1	1	284	1	25	.95	1.27E+01	.254	C5GA	7.937E+02	.855	7.33E+01
200 .050	.160	.034	2.12		7.256E-02	1.984E-02	1.694E+01	1.015E+03	206	1	1	246	1	25	.95	1.78E+01	.254	C5GA	1.013E+03	.858	6.55E+01
200 .075	.160	.033	2.38		9.146E-02	2.094E-02	2.503E+01	1.349E+03	210	1	1	285	1	25	.95	2.63E+01	.237	C5GA	1.346E+03	.891	5.31E+01
200 .100	.160	.052	3.24		1.701E-01	3.929E-02	3.355E+01	1.703E+03	212	1	1	208	1	25	.95	3.53E+01	.234	C5GA	1.698E+03	.877	5.50E+01
200 .010	.320	.019	1.15		2.251E-02	8.246E-03	7.040E+00	6.351E+02	202	1	1	329	1	25	.95	7.41E+00	.234	C5GA	6.347E+02	.836	1.03E+02
200 .015	.320	.023	1.43		3.330E-02	5.920E-03	9.904E+00	7.453E+02	202	1	1	313	1	25	.95	1.04E+01	.196	C5GA	7.447E+02	.891	8.02E+01
200 .020	.320	.030	1.87		5.692E-02	1.111E-02	1.277E+01	8.537E+02	203	1	1	246	1	25	.95	1.40E+01	.237	C5GA	8.524E+02	.808	6.79E+01
200 .025	.320	.034	2.11		7.775E-02	1.984E-02	1.694E+01	1.015E+03	204	1	1	247	1	25	.95	1.78E+01	.288	C5GA	1.013E+03	.865	6.35E+01
200 .035	.320	.039	2.44		9.653E-02	2.792E-02	2.354E+01	1.294E+03	205	1	1	260	1	25	.95	2.51E+01	.258	C5GA	1.297E+03	.864	5.97E+01
200 .050	.320	.051	3.22		1.576E-01	3.929E-02	3.355E+01	1.703E+03	207	1	1	211	1	25	.95	3.53E+01	.254	C5GA	1.696E+03	.877	5.50E+01
200 .005	.640	.019	1.10		2.245E-02	8.246E-03	7.040E+00	6.354E+02	201	1	1	330	1	25	.95	7.41E+00	.234	C5GA	6.347E+02	.836	1.03E+02
200 .010	.640	.030	1.87		5.957E-02	1.111E-02	1.327E+01	8.535E+02	202	1	1	267	1	25	.95	1.40E+01	.237	C5GA	8.524E+02	.838	6.79E+01
200 .015	.640	.035	2.19		7.749E-02	2.412E-02	2.059E+01	1.163E+03	202	1	1	279	1	25	.95	2.17E+01	.234	C5GA	1.161E+03	.857	6.26E+01
200 .020	.640	.040	2.69		1.002E-01	3.233E-02	2.760E+01	1.454E+03	203	1	1	290	1	25	.95	2.91E+01	.234	C5GA	1.453E+03	.853	5.73E+01
200 .025	.640	.051	3.20		1.566E-01	3.929E-02	3.325E+01	1.703E+03	204	1	1	219	1	25	.95	3.53E+01	.254	C5GA	1.696E+03	.877	5.50E+01
250 .075	.040	.014	.85		1.222E-02	8.246E-03	7.040E+00	6.350E+02	257	1	1	606	1	25	.95	7.41E+00	.284	C5GA	6.347E+02	.691	1.24E+02
250 .100	.040	.021	1.27		2.744E-02	6.184E-03	7.392E+00	6.527E+02	259	1	1	284	1	25	.95	7.78E+00	.237	C5GA	6.516E+02	.877	9.56E+01
250 .025	.080	.013	.79		1.052E-02	8.246E-03	7.040E+00	6.350E+02	254	1	1	703	1	25	.95	7.41E+00	.224	C5GA	6.347E+02	.645	1.33E+02
250 .050	.080	.021	1.27		2.725E-02	6.184E-03	7.390E+00	6.527E+02	255	1	1	286	1	25	.95	7.78E+00	.237	C5GA	6.516E+02	.877	9.56E+01
250 .075	.080	.026	1.57		4.157E-02	1.343E-02	1.147E+01	7.820E+02	257	1	1	288	1	25	.95	1.21E+01	.284	C5GA	7.800E+02	.849	7.64E+01
250 .100	.080	.021	1.31		2.977E-02	6.247E-03	1.464E+01	9.193E+02	260	1	1	326	1	25	.95	1.54E+01	.160	C5GA	9.182E+02	.826	6.73E+01
250 .020	.160	.015	.92		1.438E-02	8.246E-03	7.040E+00	6.351E+02	252	1	1	515	1	25	.95	7.41E+00	.204	C5G1	6.347E+02	.737	1.16E+02
250 .025	.160	.021	1.26		2.706E-02	6.184E-03	7.392E+00	6.527E+02	253	1	1	288	1	25	.95	7.78E+00	.237	C5GA	6.516E+02	.877	9.36E+01
250 .035	.160	.023	1.43		3.454E-02	8.702E-03	1.040E+01	7.584E+02	254	1	1	317	1	25	.95	1.09E+01	.237	C5GA	7.569E+02	.873	7.32E+01
250 .050	.160	.027	1.68		4.910E-02	8.766E-03	1.464E+01	9.180E+02	255	1	1	380	1	25	.95	1.54E+01	.196	C5GA	9.155E+02	.880	6.72E+01
250 .075	.160	.031	1.91		6.173E-02	1.900E-02	2.270E+01	1.248E+03	258	1	1	387	1	25	.95	2.39E+01	.237	C5GA	1.244E+03	.857	5.09E+01
250 .100	.160	.035	2.16		7.965E-02	2.546E-02	3.043E+01	1.579E+03	260	1	1	402	1	25	.95	3.20E+01	.237	C5GA	1.574E+03	.853	5.78E+01
250 .010	.320	.015	.92		1.437E-02	8.246E-03	7.040E+00	6.352E+02	251	1	1	516	1	25	.95	7.41E+00	.254	C5GA	6.347E+02	.737	1.15E+02
250 .015	.320	.025	1.54		4.079E-02	1.052E-02	8.985E+00	7.151E+02	252	1	1	235	1	25	.95	9.46E+00	.284	C5GA	7.132E+02	.866	8.72E+01
250 .020	.320	.028	1.72		5.057E-02	1.410E-02	1.205E+01	7.963E+02	252	1	1	251	1	25	.95	1.27E+01	.204	C5GA	7.937E+02	.860	7.29E+01
250 .025	.320	.027	1.66		4.701E-02	9.746E-03	1.464E+01	9.179E+02	253	1	1	326	1	25	.95	1.54E+01	.196	C5GA	9.155E+02	.826	6.72E+01
250 .035	.320	.030	1.79		5.461E-02	1.231E-02	2.059E+01	1.169E+03	254	1	1	397	1	25	.95	2.17E+01	.196	C5GA	1.166E+03	.822	6.12E+01
250 .050	.320	.035	2.16		7.940E-02	2.546E-02	3.043E+01	1.577E+03	256	1	1	403	1	25	.95	3.20E+01	.237	C5GA	1.574E+03	.853	5.70E+01
250 .005	.640	.015	.92		1.437E-02	8.246E-03	7.040E+00	6.346E+02	251	1	1	516	1	25	.95	7.41E+00	.254	C5GA	6.347E+02	.737	1.16E+02
250 .010	.640	.028	1.72		5.016E-02	1.410E-02	1.204E+01	7.964E+02	251	1	1	251	1	25	.95	1.27E+01	.234	C2GA	7.937E+02	.860	7.29E+01
250 .015	.640	.031	1.90		6.116E-02	1.688E-02	1.779E+01	1.054E+03	252	1	1	306	1	25	.95	1.87E+01	.237	C5GA	1.051E+03	.875	6.42E+01
250 .020	.640	.035	2.11		7.578E-02	1.994E-02	2.384E+01	1.299E+03	253	1	1	331	1	25	.95	2.51E+01	.237	C5GA	1.296E+03	.871	5.95E+01
250 .025	.640	.035	2.16		7.925E-02	2.546E-02	3.043E+01	1.579E+03	253	1	1	404	1	25	.95	3.20E+01	.237	C5GA	1.574E+03	.853	5.78E+01

END.

175.037 / 1379.662 / 61328
STOP

RUN TERMINATED.

Figure 2-7. Minimum Cost of Thermal Power from Boiling Collectors with Pancake Absorber Heat Exchangers.

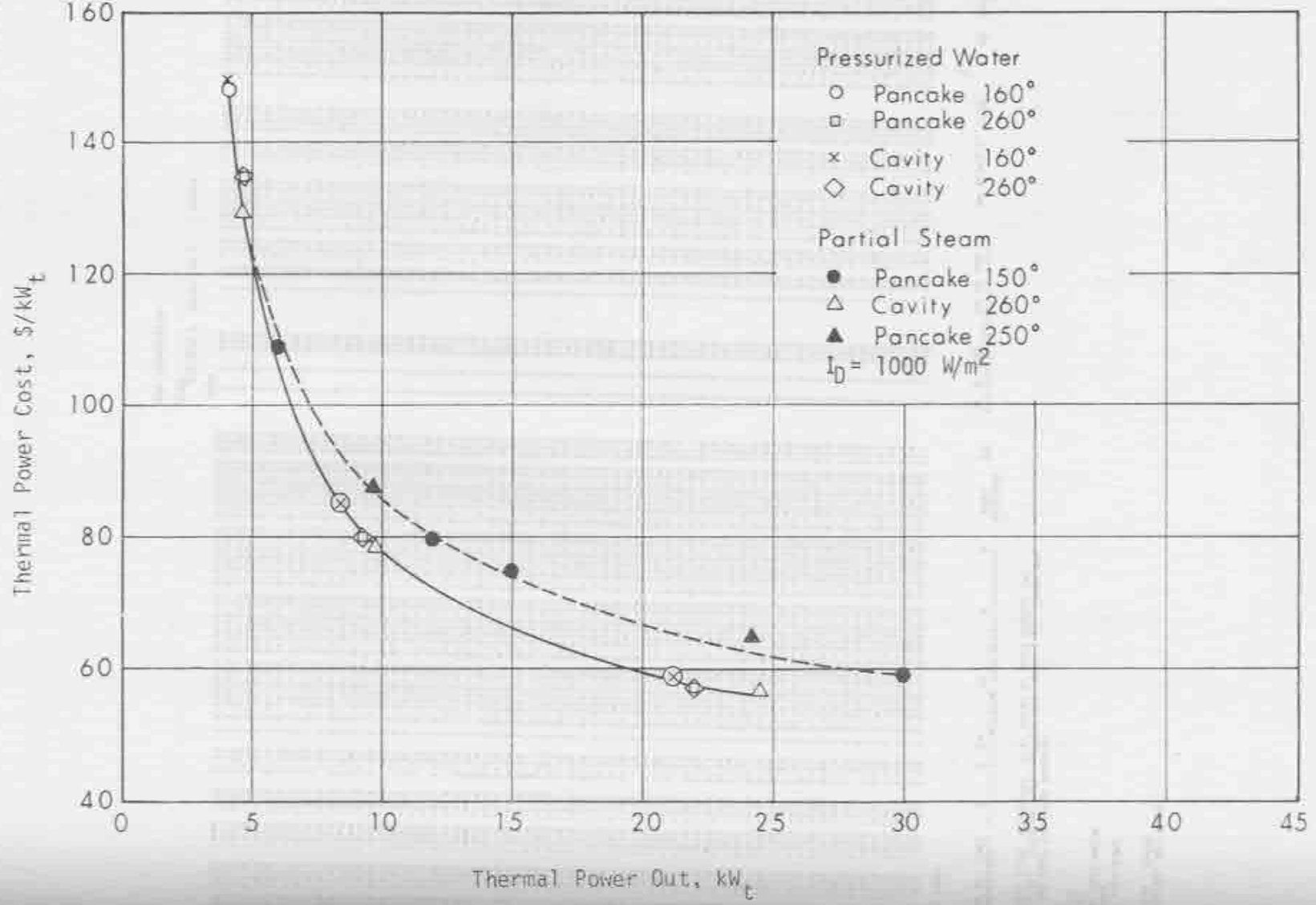

Figure 2-8. Minimum Cost of Heat from Ground Reflector Collectors with Various Receiver Types and Field Temperatures

boiling Fresnel reflector collector that produces a fluid temperature of 150 ^{o}C. The mass flow rate of this collector is .040 kg/sec and the fraction of latent heat added is .075. The absorber for this collector is a pancake shape with a helical arrangement of tubes around the surface having a .020 m diameter and length of 1.25 m. The parameters L and N are not used for this case. AL, the surface area of one side of the pancake absorber, is .02525 m^2 E and g are 7.040 m^2 and .008246 m^2 respectively. The minimum cost for delivering heat with characteristics TBOIL of 150 ^{o}C, QF of .075 and $\dot{m}$ of .040 kg/sec is $635. The power out, which can be calculated from TBOIL, QF and $\dot{m}^*$, is 6350 watts. The concentrator design which was available on a disk file is appended under the "trace back" heading. Thus, the concentrator providing concentrated radiation with characteristics E = 7.040 and g = .008246 at minimum cost is 7.41 m^2 in aperture area with a rim angle of 25^{o} and has a surface coating having a reflectivity of .95. The combined tracking and surface contour accuracy is about .284^{o}. The collector efficiency of 85.4%, the cost of thermal power of $100/kW and the concentration ratio A_p/a of 293 are quantities that can now be found from the combined information in the table. They are displayed for convenience.

As a second example, the second part of a tower-heliostat optimization output is shown in Figure 2-9. This system is analyzed in the optimization procedure in a similar manner to collectors.

At this point in the analysis a set of minimum cost collectors has been built up by first examining the concentrator subsystem and then adding the absorber-heat exchanger subsystem. This set of minimum cost collectors is indexed by the different values of the parameters $\dot{m}$, T_{in} and T_{out}. For movable collectors the set and its associated minimum

* TBOIL, QF and $\dot{m}$ take the place of T_{out}, T_{in} and $\dot{m}$ for the boiling analysis.

```
CMOM FILE NAME
 ? C0G2E
TYPE, C0ST M0DEL
 ? 1,9
MD0TL
 ? 166.

B0ILING HEAT TPANSFER VERSI0N
KFIN= 211, EPSIL0N= .90, ALPHA= .95, TAU= 1.00, TAMB= 20,
FRAUDL= 1.00, VEL0CITY=  5.0, TYPE= 1, C0ST M0DEL= CA9
```

PARAMETERS																							
		-------0PTIMUM DESIGNS------				MINIMUM				--------TRACE BACK--------													
TB0IL	MD3T	D	L	AL	100G	$/100	C0ST	$/KW	KW	WP	NW	CR	Tn	Rno	AP/100	TWP	Sigma	F0/1000	ETA	C0NC.	FILE
ID= 1000																							
150	166.0	.100	39079	3927	65534	6217	47464252	111	427347	7	17907	1971	70	.90	19349	286	.432	39133	.221	C9G2E
150	169.3	.140	39181	5512	58193	5520	36568661	84	435894	7	15901	1247	70	.90	17181	269	.429	34735	.254	C9G2E
150	172.6	.160	24940	4009	27429	5100	32784517	74	444441	7	14690	1534	70	.90	15873	259	.279	32059	.280	C9G2E
150	176.0	.200	29563	5941	59356	5631	35833327	79	452998	7	16219	1180	70	.90	17525	272	.429	35431	.255	C9G2E
150	179.3	.140	13142	1849	38407	7141	45731605	99	461535	7	20570	4809	70	.90	22225	306	.291	44995	.208	C9G2E
150	182.6	.140	28433	4000	75278	7141	46631217	99	470092	7	20570	2823	70	.90	22225	306	.436	44992	.212	C9G2E
150	185.9	.140	34931	4914	40245	5743	38248366	80	478629	7	16544	1485	70	.90	17875	275	.351	36144	.265	C9G2E
150	189.2	.220	15874	3509	91764	8705	55159808	113	487176	7	25075	3036	70	.90	27093	338	.441	54958	.180	C9G2E
150	192.6	.140	48664	6845	105390	7141	48204238	97	495723	7	20570	1299	70	.90	22225	306	.527	44990	.223	C9G2E
150	195.9	.140	13278	1868	45900	8534	54310548	109	504270	7	24633	5678	70	.90	26561	335	.296	53670	.190	C9G2E
150	199.2	.240	16468	3971	88200	8367	52995767	103	512816	7	24101	2623	70	.90	26041	331	.440	52797	.197	C9G2E
200	169.3	.180	17019	3111	45992	6095	38801898	87	443623	7	17556	2439	70	.90	18969	263	.353	38364	.234	C9G2E
200	172.6	.180	35123	6421	99311	6729	43300163	96	452321	7	19393	1305	70	.90	20943	297	.525	42376	.216	C9G2E
200	176.0	.180	8890	1625	45900	8534	54117628	117	461020	7	24553	6538	70	.90	26561	335	.296	53670	.174	C9G2E
200	179.3	.240	8330	2030	36916	6864	43449496	93	469718	7	19771	4209	70	.90	21362	300	.359	43234	.220	C9G2E
200	182.6	.120	26078	3178	51632	6864	46406107	97	478417	7	19771	2689	70	.90	21362	300	.357	43203	.224	C9G2E
200	189.2	.120	36076	4396	47746	8341	44723000	90	495814	7	16265	1796	70	.90	19735	286	.354	39920	.251	C9G2E
200	192.6	.140	17344	2466	36916	6864	44490334	88	504512	7	19771	3465	70	.90	21362	300	.209	43234	.236	C9G2E
200	195.9	.220	26334	5884	46810	6217	39316661	78	513211	7	17907	1315	70	.90	19340	286	.354	39134	.265	C9G2E
200	199.2	.160	37545	6101	73802	7001	45956624	88	521909	7	20167	1429	70	.90	21790	302	.435	44103	.240	C9G2E
250	166.0	.240	12895	3218	44992	5975	38365632	88	435819	7	17212	2312	70	.90	18597	260	.353	37609	.234	C9G2E
250	169.3	.140	30389	4424	43245	5743	38876342	86	444535	7	16544	1616	70	.90	17875	275	.351	36144	.249	C9G2E
250	172.6	.220	12850	2942	30254	5631	36103982	80	453251	7	16219	2303	70	.90	17525	272	.288	35434	.259	C9G2E
250	176.0	.220	9309	2130	35482	6597	42033061	91	461968	7	19003	3057	70	.90	20538	294	.288	41544	.225	C9G2E
250	179.3	.220	18292	4165	45392	6095	39326576	84	470684	7	17556	1613	70	.90	18969	263	.353	38364	.248	C9G2E
250	192.6	.220	13013	2977	60554	8042	51429398	102	505550	7	23165	3363	70	.90	25029	325	.361	50726	.202	C9G2E
250	195.9	.240	8844	2207	41573	7730	49276189	96	514266	7	22256	4360	70	.90	24057	319	.293	48739	.214	C9G2E
250	199.2	.180	17284	3235	60554	8042	51635575	99	522982	7	23165	3093	70	.90	25029	325	.361	50726	.209	C9G2E

EnD.

3663.742 / 29289.774 / 34936

costs can now be used to further build the system into a collector field delivering heat to a central point. The objective will be to determine the collectors, insulation thicknesses, pipe diameters, collector coupling and layouts that make up the minimum cost collector fields.

2.3 Heat Transport and Field Layout Optimization

A methodology is presented in this section for finding the

1. collectors,
2. heat transport fluids,
3. piping arrangements,
4. field geometries,
5. pipe diameters and,
6. insulation thicknesses

that make up a collector field delivering thermal power with a specified mass flow rate, inlet temperature and outlet temperature at minimum cost.

2.3.1 General Approach

Two slightly different optimization models are required for field optimization. The first synthesizes feeder line subsystems consisting of a collector and its associated heat transport segment into minimum cost feeder lines. The second, which requires inputs from the first, synthesizes trunk line subsystems consisting of a feeder line junction and its associated heat transport segment into minimum cost fields. The various subsystems and their interrelationships are shown in Figure 2-10.

To initiate the optimizations a collector (or collectors), heat transport fluid, piping arrangement, field mass flow rate, field outlet

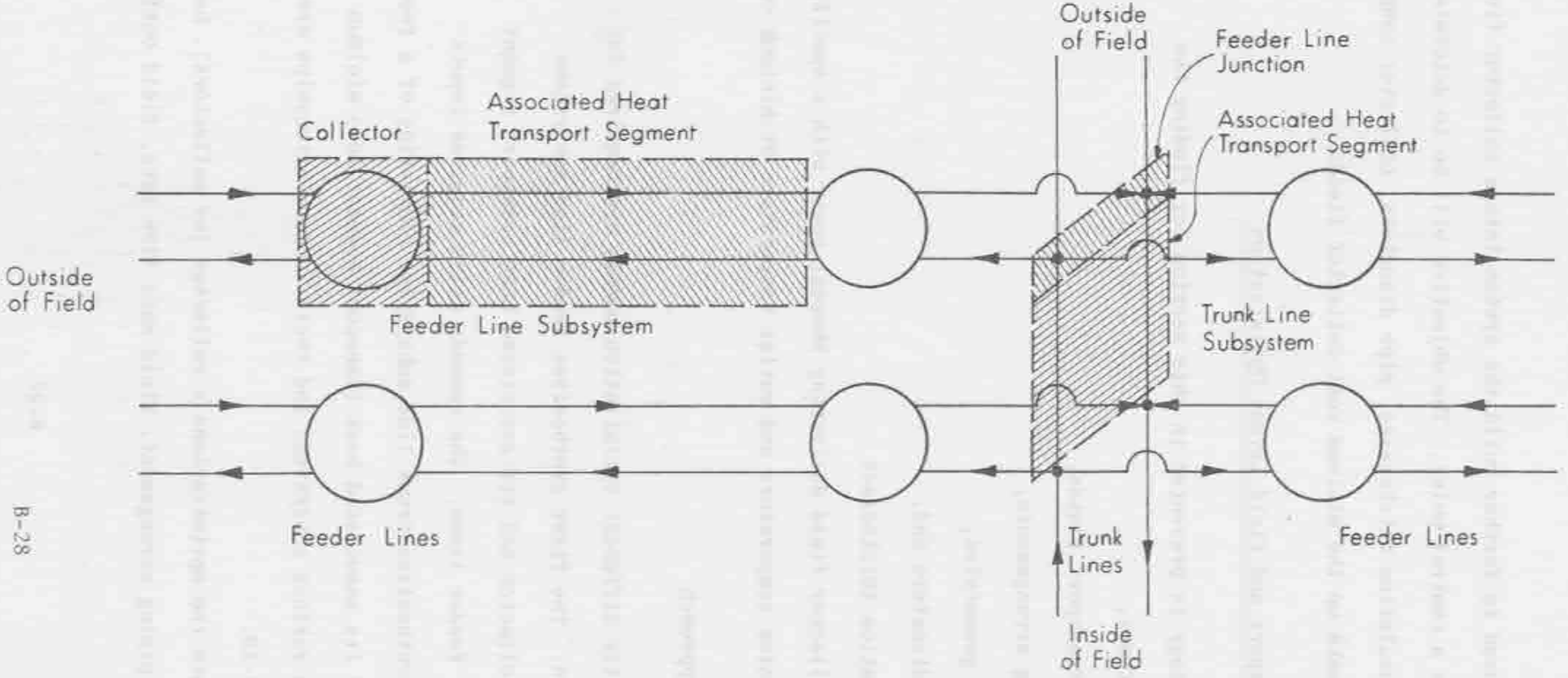

Figure 2-10. Heat Transport and Field Layout Optimization Subsystems.

temperature and field inlet temperature are specified. The feeder lines are synthesized and then the trunk lines are synthesized to find a minimum cost thermal power field for the specified field conditions. Other collectors, heat transport fluids and piping arrangements are selected and tested under the same conditions until the minimum cost collector field layout for the specified conditions is found. Another field mass flow rate outlet temperature and inlet temperature is then specified and the process repeated.

The method is quite general in that it will indicate the location in the field where the collector type should be switched when more than one collector type is specified. It can handle series, parallel, double parallel and more complex piping arrangements. It automatically determines optimum field geometries and it handles different heat transport fluids by minor changes in the performance models. Detailed development of performance and cost models that were used in this optimization procedure are given in Appendix F.

2.3.2 Interaction Between the High and Low Temperature Sides

Figure 2-11 is an illustration of the interaction between the high and low temperature sides for a parallel arrangement of collectors. It is intended to show the need to simultaneously consider both low and high temperature heat transport sides in the optimization. The vertical lines in the figure represent constant magnitude temperature rises across adjacent collectors in the feeder lines. Because the low temperature return line loses temperature, the output temperature of the collectors toward the outside of the field is lower than at the inside of the field. Just how much lower depends on the pipe sizes and insulation thicknesses of each heat transport segment.

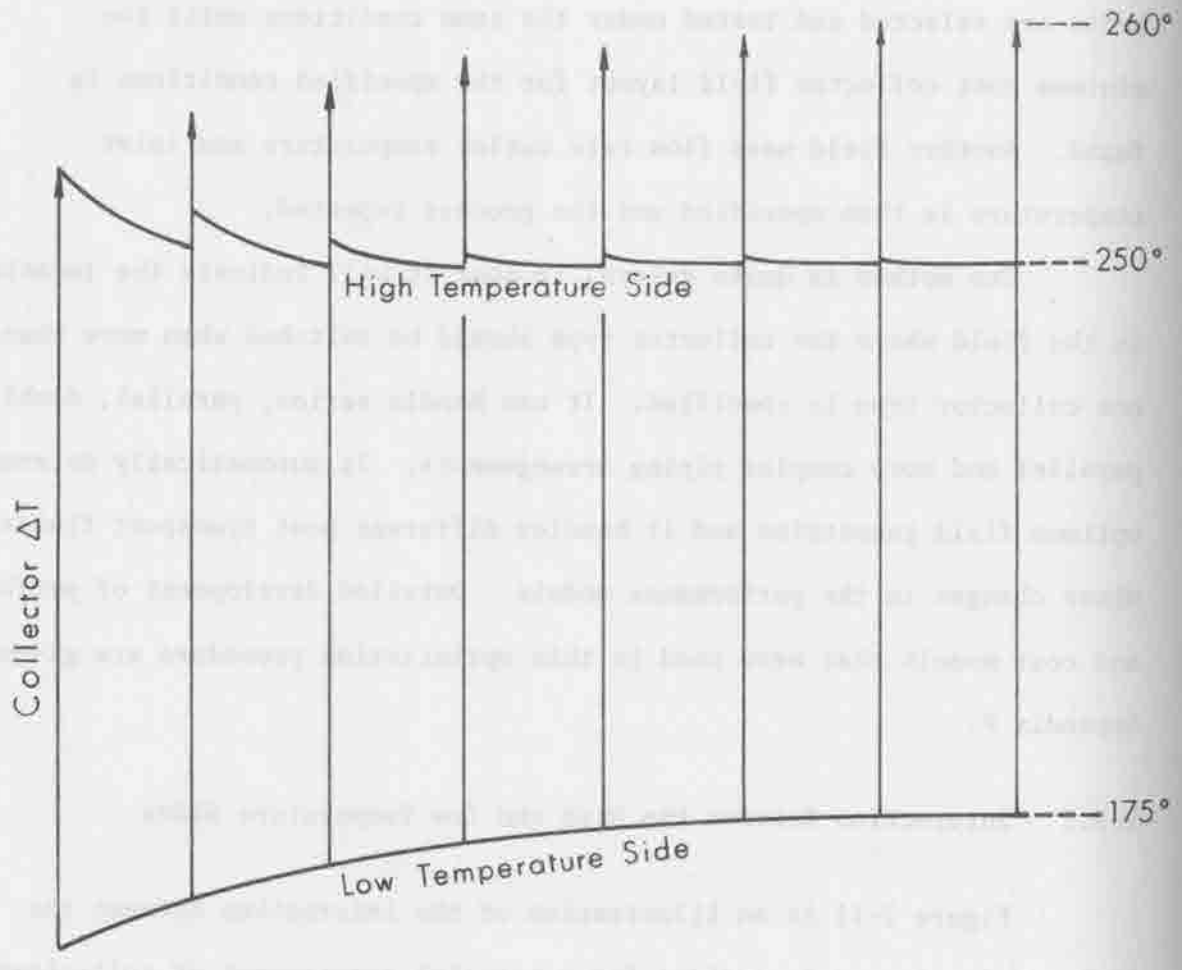

Figure 2-11. Interactions Between The High and Low Temperature for a Pressurized Water System.

The fluid in the high temperature line mixes with the fluid coming out of the collectors. The resultant temperature depends on the local temperature in the high temperature line, T_H; the outlet temperature of the collector, T_C (which in turn depends on the local temperature in the low temperature line, T_L); the mass flow rate through the collector $\dot{m}$; and the local mass flow rate in the high temperature line, $\dot{M}$. This relationship is shown in Equation 2-4,

$$T_M = \frac{\dot{m}\ (T_L + \Delta T_C) + \dot{M}\ T_H}{\dot{m} + \dot{M}} \qquad (2\text{-}4)$$

where T_M is the temperature after mixing. What the local temperature was before mixing is determined not only by the pipe size and insulation thickness on the previous heat transport segment, but also by all pipe sizes, insulation thicknesses, and mass flow rates on heat transport segments farther out in the feeder lines.

Thus, in the case of parallel piping arrangements, it is necessary to simulatneously consider both high and low temperature side heat transport segment designs--especially when return temperatures are high. This is also true on the trunk lines since mixing takes place there as well. Mixing does not take place in series systems and temperature drops do not occur with saturated or two phase flow systems. The optimization can be simplified in these cases as will be shown in Sections 2.3.7 and 2.3.8.

2.3.3 Changes in Available Thermal Power

Three variables, mass flow rate $\dot{m}$, high side temperature T_H, and low side temperature T_L measure the available thermal power from

a field or any intermediate collection subsystems in the minimum cost field synthesis*. A change in one, two or all three of these variables indicates a change in the availability of the thermal power. That is, there is a change in its potential for accomplishing an end use, such as generating electric power. Thus, in the synthesis procedure, changes in these quantities will be of interest.

The points in a parallel field subsystem where changes in available thermal power are about to occur or have just occurred are shown in Figure 2-12. The temperature and mass flow rate of the heat transport fluid into the n^{th} subsystem are T^{n-1} and $\dot{M}^{n-1}$ respectively.** The temperature and mass flow rate out of a collector or collectors (or out of feeder lines if trunk lines are being synthesized) are T_c^n and $\dot{m}^n$ respectively. The temperature and mass flow rate after mixing are T_M^n and $\dot{M}^n$ respectively. The temperature out of the subsystem is T^n. The following relationships are obvious from the diagram

$$\dot{M}^n = \dot{M}^{n-1} + \dot{m}^n \tag{2-5a}$$

$$T_M^n = \frac{\dot{m}^n T_c^n + \dot{M}^{n-1} T^{n-1}}{\dot{M}^n} \tag{2-5b}$$

$$\Delta T^n = T^n - T^{n-1} \tag{2-5c}$$

$$\Delta T_M^n = T^n - T_M^n \tag{2-5d}$$

T_M^n can be eliminated from 2-5d by 2-5b.

---

* For boiling systems the analogous quantities would be the boiling temperature, the enthalpy and the mass flow rate.

**Superscripts will be used in the rest of this section to indicate the subsystem index.

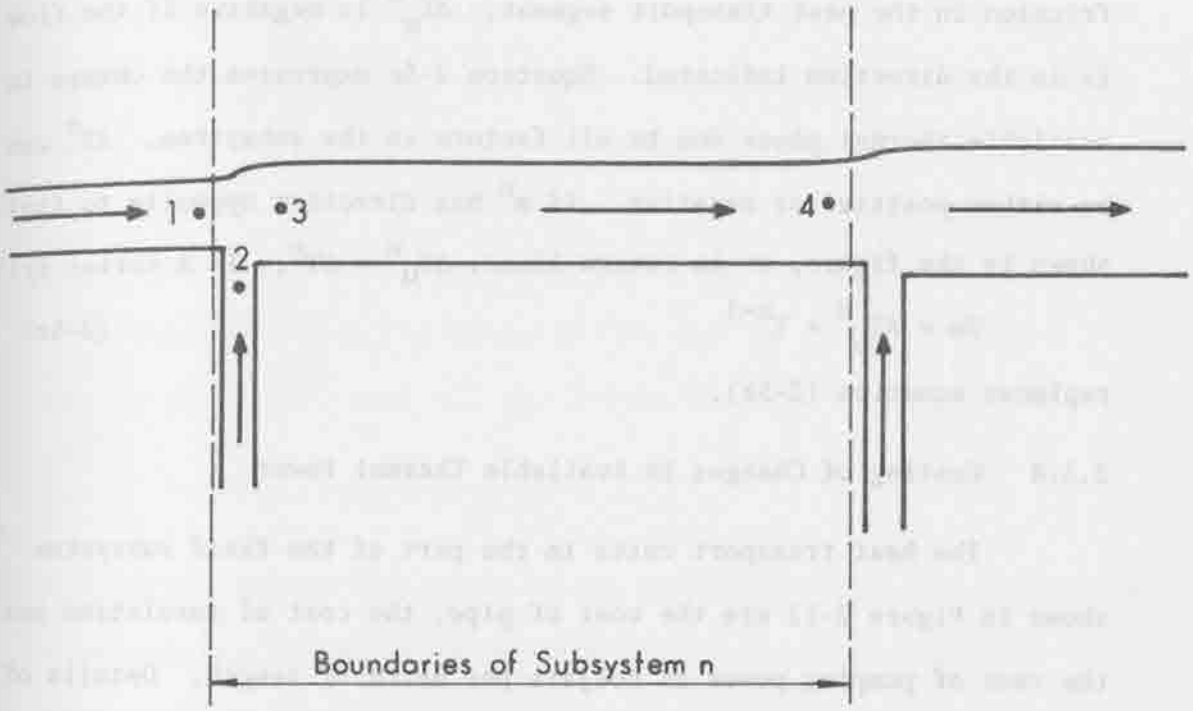

Point	Temperature	Mass Flow Rate
1	T^{n-1}	$\dot{M}^{n-1}$
2	T_c^n	$\dot{m}^n$
3	T_M^n	M^n
4	T^n	$\dot{M}^n$

Figure 2-12. Available Thermal Power Changes Across Field Subsystem n.

Equation 2-5a indicates a change in available thermal power due to a change in mass flow rate. Equation 2-5d indicates a change in available thermal power due to losses through the insulation and due to friction in the heat transport segment. ΔT_M^n is negative if the flow is in the direction indicated. Equation 2-5c expresses the change in available thermal power due to all factors in the subsystem. ΔT^n can be either positive or negative. If $\dot{m}^n$ has direction opposite to that shown in the figure, as in return lines, $\Delta T_M^n = \Delta T^n$. In a series system

$$Tm = \Delta T_c^n + T^{n-1} \qquad (2\text{-}5e)$$

replaces equation (2-5b).

2.3.4 Costing of Changes in Available Thermal Power

The heat transport costs in the part of the field subsystem shown in Figure 2-12 are the cost of pipe, the cost of insulation and the cost of pumping power in dollars per metre of length. Details of the cost models for these costs are given in Appendix F.* These costs are a function of ΔT_M^n, T^n, $\dot{M}^n$ and pipe diameter for subsystem n.** Pipe diameter may be eliminated as a dependent variable by performing a minimization operation over pipe diameter on the sum of the costs for fixed values of ΔT_M^n, T^n and $\dot{M}^n$. Thus a cost that is functionally dependent on ΔT_M^n, T^n and $\dot{M}^n$ was found. This function of dependence is shown below

$$C_{HT} = C_{HT}(\Delta T^n, \dot{m}^n, T^n, \dot{M}^n) \qquad (2\text{-}6)$$

---

* A cost of heat lost was used as an approximation in Appendix F. Such an approximation is unnecessary since the methodology of this appendix makes up for losses with additional feeder line subsystems.

**They are also dependent on other variables, such as ambient temperature, that were held constant in this analysis.

Equation 2-6 is expressed in terms of ΔT^n and $\dot{m}^n$ rather than $\Delta T_M{}^n$ for purposes of the optimization. Examination of Equations 2-5 shows that this substitution can be made. Since field subsystems have two heat transport lines, a high temperature side and a low temperature side, Equation 2-6 must be generated for both lines.

A most useful characterization of the costs of heat transport for a field subsystem now exists. Equation 2-6 along with the collector cost directly yields the change in the cost of available thermal power for fixed T^n, $\dot{M}^n$ and $\dot{m}^n$ for different ΔT^n's.

2.3.5 Feeder Line Optimization

The feeder line optimization procedure begins with the outermost subsystem and builds up the minimum cost feeder line, subsystem by subsystem, until the innermost subsystem has been reached. At each stage, n, in the feeder line synthesis, a range of $T_H{}^n$'s and $T_L{}^n$'s are considered and costs as a function of $T_H{}^n$ and $T_L{}^n$ are determined. These costs are then used in stage n+1 to determine costs as a function of $T_H{}^{n+1}$ and $T_L{}^{n+1}$.

At the beginning of the feeder line optimization a temperature grid is chosen for both the high and low temperature sides. The grid consists of a temperature increment δT_H or δT_L and a temperature range $[\underline{T_H}, \overline{T_H}]$ or $[\underline{T_L}, \overline{T_L}]$. The range and the increment determine the number of temperature points on the grid. Appropriate values for δT and the range will depend on the temperatures, mass flow rates, collector temperature rises and feeder line lengths and will be different for different values of these variables. Collector costs, dimensions, mass flow rates, temperature rises, field North/South and

East/West fill factors and the piping arrangement are also specified.

The optimization begins with the outermost subsystem shown in Figure 2-13. The high and low temperature side mass flow rates are equal and are designated by $\dot{M}^1$. The minimum cost $f_1 (T_H^1, T_L^1)$ is computed for the various values of T_H^1 and T_L^1 in the low and high side grids by

$$f_1 (T_H^1, T_L^1) = \underset{(\Delta T_H^1, \Delta T_L^1)}{\text{MIN}} [C_{HT} (\Delta T_H^1, T_H^1, \dot{M}^1) + C_{HT} (\Delta T_L^1, T_L^1, \dot{M}^1) + NC_A] \qquad (2\text{-}7)$$

where C_A is the collector cost and N is the number of collectors in a subsystem.* Not evident in Equation 2-7 is the interdependence of the high and low temperature side heat transport functions, C_{HT}. This interdependence is shown in Equations 2-4 and 2-5 and these equations constitute constraints in the minimization operation of Equation 2-7.

The argument $\dot{m}^1$ is not shown in the function C_{HT}. In fields made up of only one collector design it is a constant. To maintain simplicity of the notation, this will be assumed to be the case and $\dot{m}^n$ will be suppressed in the subsequent development. In field optimizations where two or more collectors are considered, $\dot{m}^1$ would appear in C_{HT}. It would also be an additional design variable so that the minimization would then be over ΔT_H^1, ΔT_L^1 and $\dot{m}^1$. The state variables T_H^1 and T_L^1 would also then include $\dot{M}^1$.

---

* This is dictated by the piping arrangement. There is one collector in a subsystem for series or single parallel piping arrangement, two for double parallel and so forth.

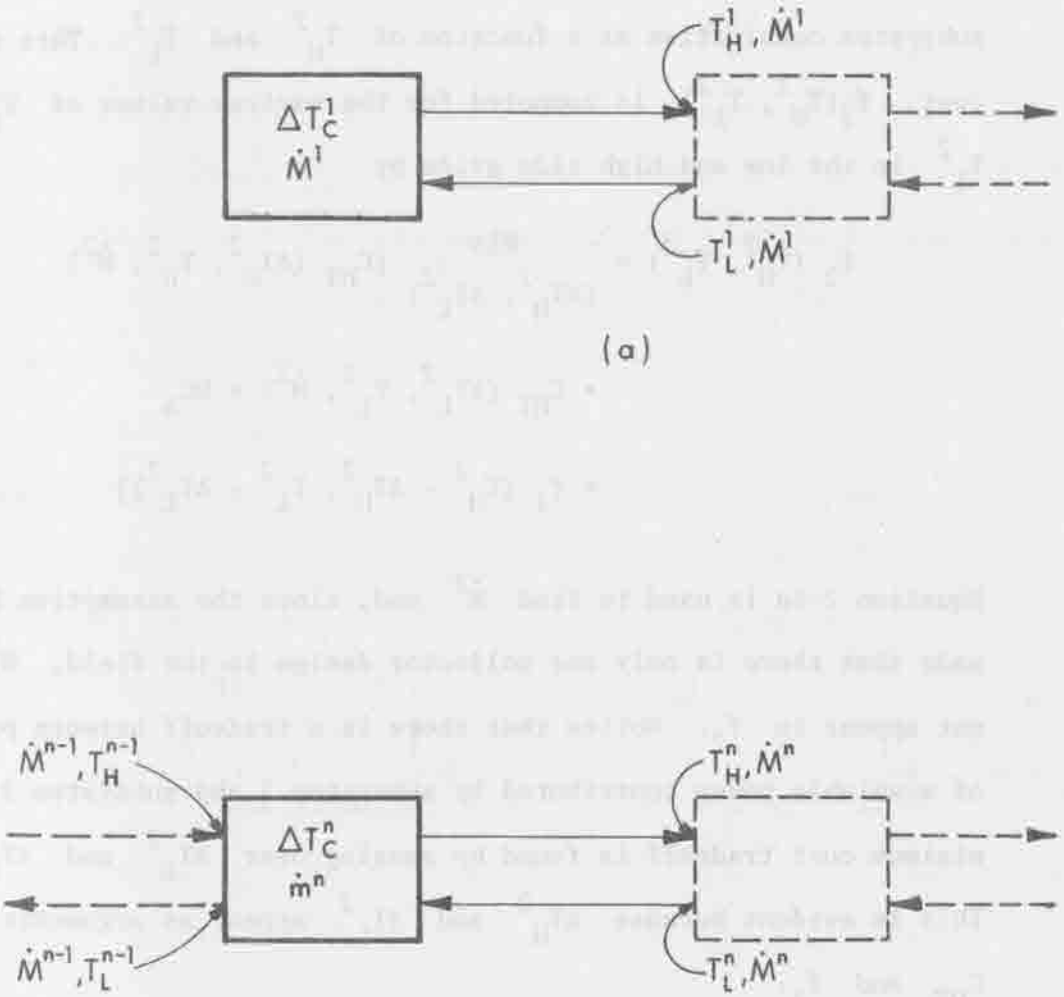

Figure 2-13. Feeder Line Subsystems.

The next step in the optimization is to add the second subsystem to the first in such a way as to find the minimum costs of the two subsystem combination as a function of T_H^2 and T_L^2. This minimum cost, $f_2(T_H^2, T_L^2)$, is computed for the various values of T_H^2 and T_L^2 in the low and high side grids by

$$f_2 (T_H^2, T_L^2) = \underset{(\Delta T_H^2, \Delta T_L^2)}{\text{MIN}} [C_{HT} (\Delta T_H^2, T_H^2, \dot{M}^2) + C_{HT} (\Delta T_L^2, T_L^2, \dot{M}^2) + NC_A + f_1 (T_H^2 - \Delta T_H^2, T_L^2 - \Delta T_L^2)] \quad (2\text{-}8)$$

Equation 2-5a is used to find $\dot{M}^2$ and, since the assumption has been made that there is only one collector design in the field, M^2 does not appear in f_2. Notice that there is a tradeoff between proportions of available power contributed by subsystem 1 and subsystem 2 and the minimum cost tradeoff is found by ranging over ΔT_H^2 and ΔT_L^2. This is evident because ΔT_H^2 and ΔT_L^2 appear as arguments in both C_{HT} and f_1.

Continuing in this manner, the minimum costs of the combination of the first n subsystems are found by

$$f_n (T_H^n, T_L^n) = \underset{(\Delta T_H^n, \Delta T_L^n)}{\text{MIN}} [C_{HT} (\Delta T_H^n, T_H^n, \dot{M}^n) + C_{HT} (\Delta T_L^n, T_L^n, \dot{M}^n) + NC_A + f_{n-1} (T_H^n - \Delta T_H^n, T_L^n - \Delta T_L^n)] \quad (2\text{-}9)$$

Thus, minimum cost feeder lines consisting of n subsystems can be built up, or synthesized, in this way. The theoretical justification

for this procedure is given in most introductory texts covering dynamic programming. For instance, see Bellman (1957).

Thus far only the minimum costs have been discussed and not the optimum designs that produced the minimum cost feeder lines. In dynamic programming the designs that produced the minimum costs are recorded as they are determined in the same parametric manner as the minimum costs themselves. Thus the optimum designs can be retrieved at any place in the analysis of the feeder lines by a trace back procedure. This trace back yields the optimum pipe diameters and insulation thicknesses on each of the heat transport segments of the minimum cost feeder lines.

This retention of the optimum designs proceeds as follows: As Equations 2-7 and 2-9 are calculated, an optimum design $(\Delta T_H^n, \Delta T_L^n)^*$ is retained in an array $u_n(i,j)$ by

$$u_n(T_H^n, T_L^n) = (\Delta T_N^n, \Delta T_L^n)^* \qquad (2\text{-}10)$$

for each value of T_H^n and T_L^n in the grid. The optimum high and low temperature side insulation thicknesses for the heat transport segment can be calculated from $(\Delta T_H^n, \Delta T_L^n)^*$, T_H^n, T_L^n and $\dot{M}^n$. Optimum pipe diameters can also be calculated from these quantities via equations developed in the minimization operation discussed in Section 2.3.4.

The trace back of the optimum designs proceeds as follows: Suppose a minimum cost feeder line consisting of N subsystems has been synthesized. The optimum pipe diameters and insulation thicknesses for the innermost feeder line subsystem are found from $(\Delta T_H^n, \Delta T_L^n) = u_n(a,b)$, where a and b are the desired high and low temperature side temperatures at the innermost feeder line subsystem. The optimum pipe

diameters and insulation thicknesses for the next closest feeder line subsystem are found from $(\Delta T_H^{n-1}, \Delta T_L^{n-1}) = u_{n-1}(a',b')$, where $a' = a - \Delta T_H^n$ and $b' = b - \Delta T_L^n$. For the next subsystem, these quantities are found as $(\Delta T_N^{n-2}, \Delta T_L^{n-2}) = u_{n-2}(a'',b'')$, where $a'' = a' - \Delta T_H^{n-2}$ and $b'' = b' - \Delta T^{n-2}$. This iterative retrieval procedure using the array $u_n(i,j)$ continues until $(\Delta T_H^1, \Delta T_L^1)$ is calculated.

A flow chart development of the optimization procedure for hot water feeder lines is shown in Figure 2-14. This procedure can be simplified for series boiling as will be shown in Section 2.3.7.

Now that the optimization has synthesized minimum cost feeder lines consisting of any number of subsystems, trunk line optimization can be initiated. Notice that we have the minimum costs for $n = 1, \ldots,$ subsystems for all values of T_H^n and T_L^n in the high and low side grids and that we know $\dot{M}^n$ from Equation 2-5a.

2.3.6 Trunk Line Optimization

As was the case with feeder line optimization, trunk line optimization starts with the outermost subsystem and builds up the minimum cost trunk line, subsystem by subsystem, until the innermost subsystem has been reached. It can be seen in Figure 2-10 that a trunk line subsystem is identical to a feeder line subsystem if the feeder lines entering the subsystem are considered to be the analogue of collectors. Thus the situations depicted in Figures 2-11 and 2-12 and Equations 2-4, hold where the term "collector" is placed by "feeder line". Equation 2-6 is also identical, except in the case of parallel feeder lines, where $\dot{m}^n$ identifies the length of and mass flow rate out of the feeder line and thus is not suppressed.

Figure 2-14

Field Optimization Flow Chart-
Hot Water Feeder Lines

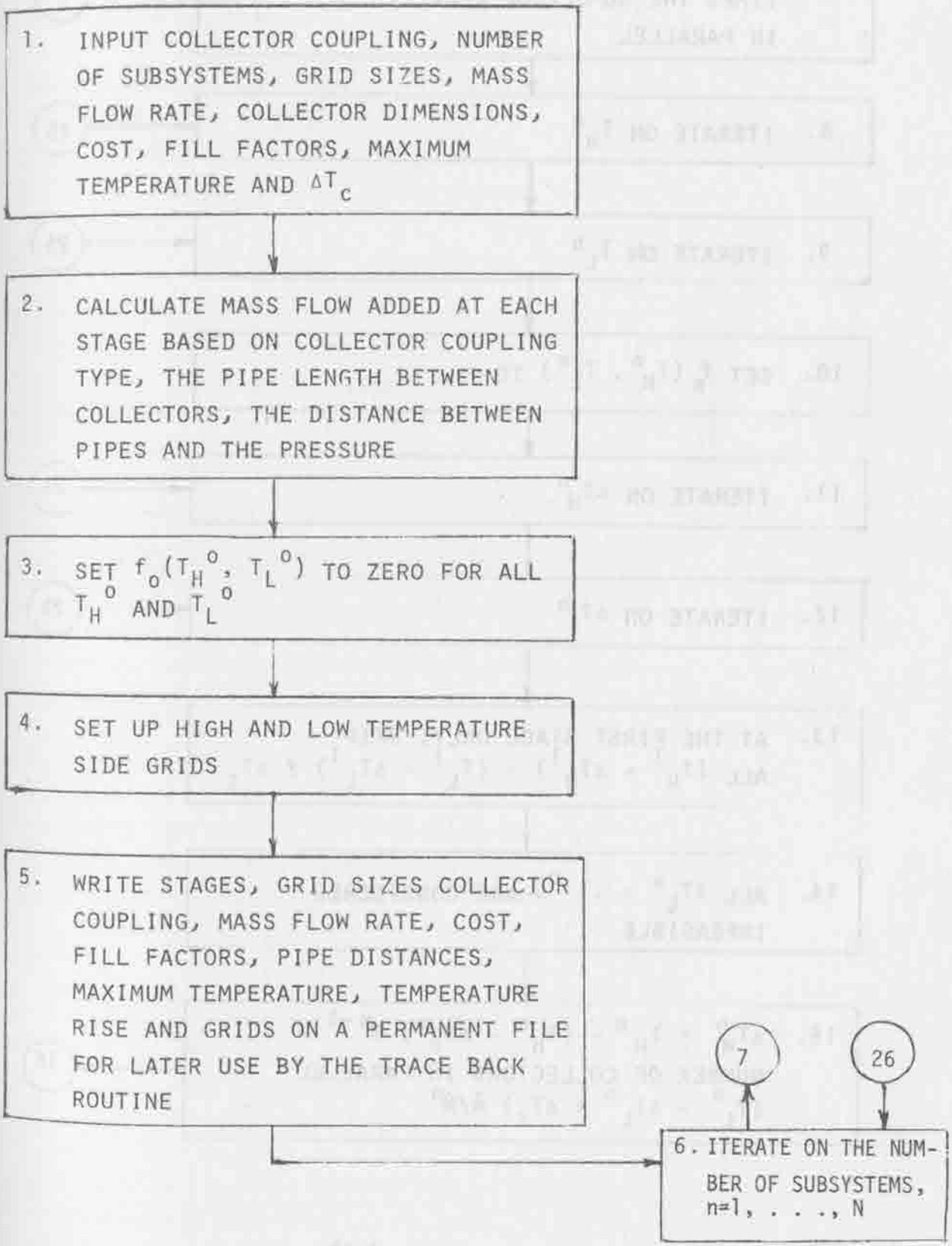

Figure 2-14 (Continued)

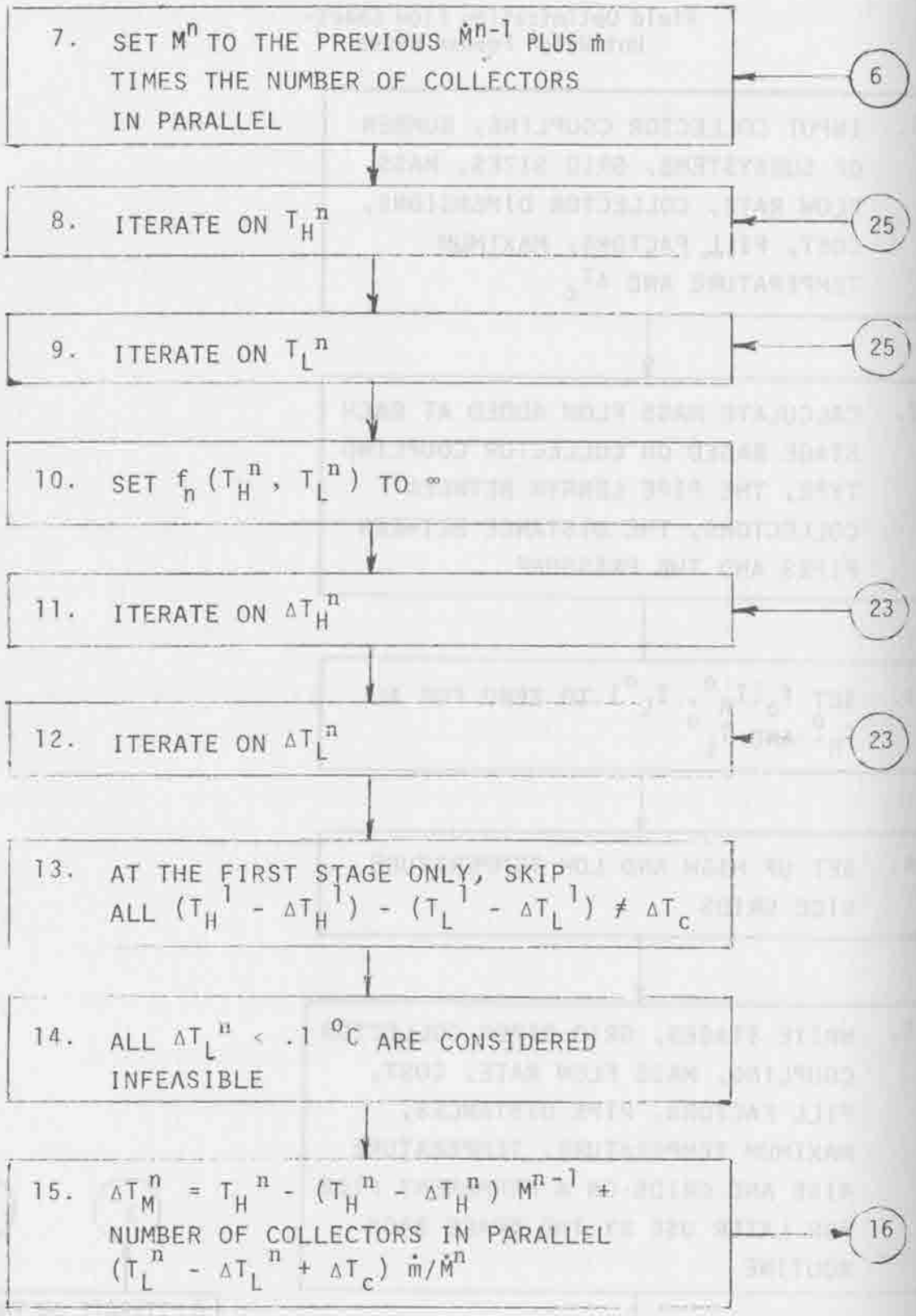

Figure 2-14 (Continued)

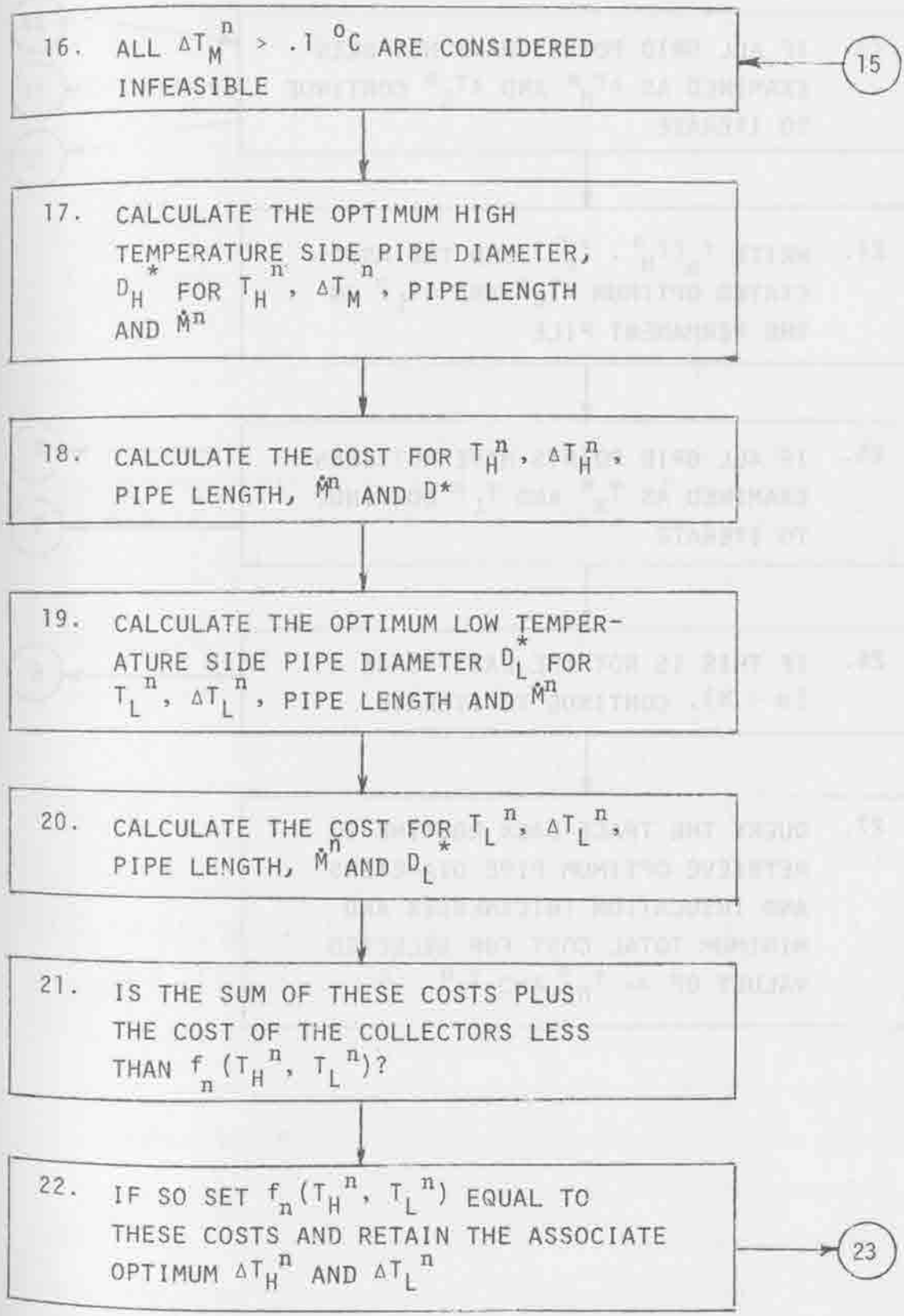

Figure 2-14 (Continued)

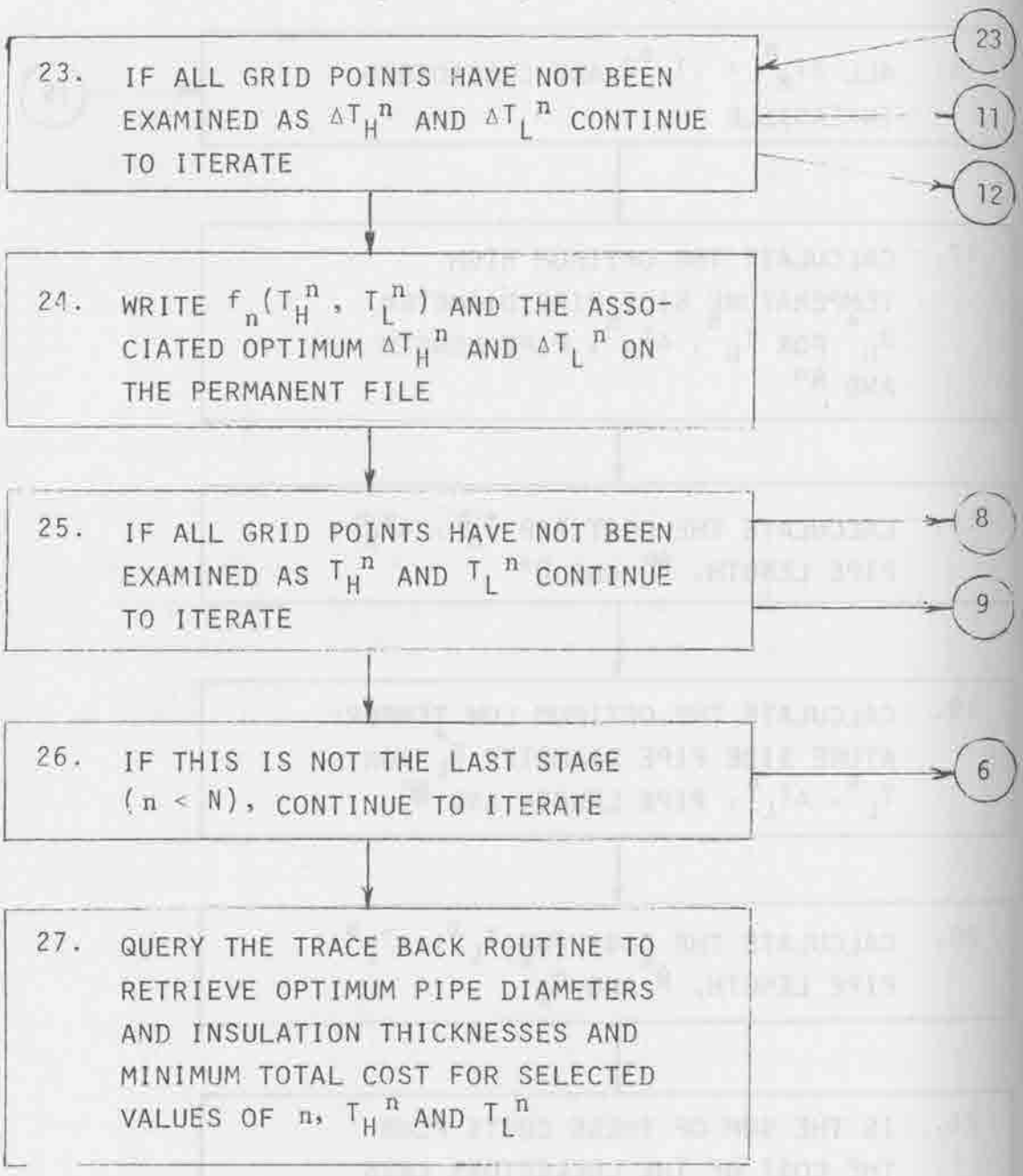

The analogous equations to 2-7, 2-8, and 2-9 are

$$F_1(T_H^1, T_L^1, 2k^1) = \underset{(\Delta T_H^1,\ \Delta T_L^1)}{\text{MIN}} [C_{HT}(\Delta T_H^1, k^{1\bullet}m, T_H^1, k^{1\bullet}m) + C_{HT}(\Delta T_L^1, k^{1\bullet}m, T_L^1, k^{1\bullet}m) + 2f_k(a,b)] \tag{2-11}$$

$$F_2(T_H^2, T_L^2, 2k^2) = \underset{(\Delta T_H^2,\ \Delta T_L^2,\ j^2)}{\text{MIN}} [C_{HT}(\Delta T_H^2, 2j^{2\bullet}m, T_H^2, 2k^{2\bullet}m) + C_{HT}(\Delta T_L^2, 2j^{2\bullet}m, T_L^2, k^{2\bullet}m) + 2f_j(a,b) + F_1(T_H^2 - \Delta T_H^2, T_L^2 - \Delta T_L^2, 2k^2 - 2j^2)]. \tag{2-12}$$

and

$$F_n(T_H^n, T_L^n, 2k^n) = \underset{(\Delta T_H^n,\ \Delta T_L^n,\ j^n)}{\text{MIN}} [C_{HT}(\Delta T_H^n, 2j^{n\bullet}m, T_H^n, 2k^{n\bullet}m) + C_{HT}(\Delta T_L^n, 2j^{n\bullet}m, T_L^n, k^{n\bullet}m) + 2f_j(a,b) + F_{n-1}(T_H^n - \Delta T_H^n, T_L^n - \Delta T_L^n, 2k^n - 2j^n) \tag{2-13}$$

where a and b are fixed temperatures such that ΔT_C in Equation 2-4 is replaced by $a - b$ and $\dot{m}$ is the mass flow rate that is put through one feeder line subsystem's collectors. Alternatively a and b could be considered as design choices and would appear under the minimization. The mass flow from a feeder line into the n^{th} trunk line subsystem is given by $j^{n\bullet}m$ where j^n is the number of subsystems in the feeder lines--that is, j^n determines the number of collectors or analogously the length of the feeder lines. The quantity

$2k^n \dot{m}$ expresses the mass flow rate through the n^{th} trunk line's heat transport segment where $2k^n$ is the total number of feeder line subsystems that have been added to the system as of trunk line subsystem n. The use of $2k^n$ and $2j^n$ rather than k^n and j^n, expresses the situation shown in Figure 2-10 where there are two feeder lines for each trunk line subsystem.

A simplification of Equations 2-11, 2-12 and 2-13 is possible for boiling systems. This is discussed in Section 2.3.8.

Notice that the tradeoff between proportions of available power contributed by subsystem 1 and subsystem 2, as depicted in Equation 2-12, now involves the length of the feeder lines in subsystem 2 and the length of the feeder lines in subsystem 1, j^2 and $k^2 - j^2$ respectively. Thus, the optimum field geometry is being found for trunk lines consisting of two trunk line subsystems and $2k^2$ feeder line subsystems. Again, by the principles of dynamic programming, Equation 2-13 is the situation where the optimum field geometry is being found for trunk lines consisting of n trunk line subsystems and $2k^n$ feeder line subsystems. For example, if a parallel piping arrangement was being examined and an output temperature of A, an input temperature of B and a mass flow rate of C was required of the trunk line, the minimum cost system could be found by iteratively calculating Equations 2-11 and 2-13 and then finding

$$F^* = \underset{N}{\text{MIN}} \{F_N(A, B, C)\} \qquad (2\text{-}14)$$

The trace back procedure for the trunk lines not only yields the optimum pipe diameters and insulation thicknesses on each of the heat

transport segments of the minimum cost system, as was the case with feeder lives, it also yields the optimum field geometries.

When Equations 2-11 and 2-13 are calculated, an optimum design $(\Delta T_H^n, \Delta T_L^n, j^n)^*$ is retained in array $U_n(i,j,k)$ by

$$U_n(T_H^n, T_L^n, 2k^n) = (\Delta T_H^n, \Delta T_L^n, j^n)^* \qquad (2\text{-}15)$$

for each value of T_H^n, T_L^n and k^n in the grid. The additional optimum design variable j_n is the optimum length of the feeder lines for trunk line subsystem n when the high side temperature is T_H^n, the low side temperature is T_L^n and there are $2k^n$ feeder line subsystems in the system.

Suppose N^* was the optimum value of N in Equation 2-14. The trace back would proceed as follows: The optimum pipe diameters and insulation thicknesses for the innermost trunk line subsystem are found from $(\Delta T_H^{N^*}, \Delta T_L^{N^*}, j^{N^*}) = U_{N^*}(A, B, C)$. The optimum feeder lines into this subsystem would have length given by $n = j^{N^*}$. The optimum pipe diameters and insulation thicknesses of each of the heat transport segments of these feeder lines are found as discussed in Section 2.3.5.

The optimum pipe diameters and insulation thicknesses for the next closest trunk line subsystem are found from $(\Delta T_H^{N^*-1}, \Delta T_L^{N^*-1}, j^{N^*-1}) = U_{N^*-1}(A', B', C')$, where $A' = A - \Delta T_H^{N^*}$, $B' = B = \Delta T_L^{N^*}$ and $C' = C - j^{N^*}$. The rest of the optimum trunk line subsystem designs $(\Delta T_N^{N^*-2}, \Delta T_L^{N^*-2}, j^{N^*-2})$, ----, $(\Delta T_H^1, \Delta T_L^1, j^1)$ and their associated optimum feeder line designs are then iteratively generated this way until the optimum field geometry pipe diameters and insulation thicknesses have been traced back.

2.3.7 Series Boiling Feeder Line Simplifications

In order to get high boiling collector efficiencies it was found that a relatively high mass flow rate through the collectors was required. This meant that a number of collectors in series were needed to add the required latent heat to produce saturated steam. Thus, series feeder lines were analyzed for boiling collector fields.

In boiling $\Delta T_H^n = 0$ and therefore T_H^n is equal to T_H^{n-1}. In series systems $\dot{M}^n$ is equal to $\dot{M}^{n-1}$. Examination of the heat transport cost (See Appendix F) shows that ΔT_H affects the expression for $C_{HT}(T_H, \Delta T_H, M)$ through the average fluid temperature for the heat transport segment, $T_H - \Delta T_H/2$, and the heat lost through the insulation $\dot{M}C_p\Delta T_H$. For boiling, only the second effect is relevant and it is expressed as $\dot{M}\Delta h$, where h is enthalpy. Thus, for series boiling, C_{HT} can be re-expressed as $C_{HT}(T_H, \Delta h, \dot{M})$ or, more simply, as $C_{HT}(\Delta h)$, since $\dot{M}$ is constant for collectors in series and T_H is constant for boiling.

It has been found that C_{HT} is convex* for all reasonable values of Δh, T_H and $\dot{M}$. This is not apparent from the expression for C_{HT}** but has been verified experimentally. The convexity of C_{HT} permits a significant compuational simplification of the feeder line cost minimization. This simplification proceeds as follows:

---

* A function, $f(x)$ is convex on Ω if for all x and y in Ω and for $0 \leq \lambda \leq 1$, $f(\lambda x + (1 - \lambda)y) \leq \lambda f(x) + (1 - \lambda)f(y)$.

** C_{HT} is a complicated expression of Δh since Δh appears both directly and indirectly via the pipe diameter optimization.

1. Fixing the value of N, the number of subsystems in a feeder line, fixes the total thermal power loss through the insulation. This thermal power loss Δh_{TOT} is

$$\Delta h_{TOT} = NQ_A - \dot{M}(h_g - h_\ell) \qquad (2\text{-}16)$$

where Q_A is the thermal power added per collector, h_g is the enthalpy of saturated steam at T_H and h_ℓ is the enthalpy of water at T_H.

2. Thus the problem becomes one of apportioning Δh_n over Δh_{TOT} or

$$\sum_{n=1}^{N} \Delta h_n = \Delta h_{TOT} \qquad (2\text{-}17)$$

3. Equation 2-9 now becomes

$$f_n(H^n) = \underset{\Delta h_n}{\text{MIN}} \left[C_{HT}(\Delta h_n) + f_{n-1}(H^n - h_n)\right] \qquad (2\text{-}18)$$

subject to 2-17, where H^n is the enthalpy loss as of subsystem n.

4. For C_{HT} convex, the solution to 2-10 for $n = N$ and $H^N = \Delta h_{TOT}$ is well known and is $\Delta h_i = \Delta h_{TOT}/N$, $i = 1, \text{----}, N$.

This suggests the following, considerably shorter, computational procedure for series boiling feeder lines.

1. Consider that the return line pipe diameter and insulation thickness is constant. This is reasonable since T_L is close to T_a and hence T_L^1 would be close to T_L^N. Thus ΔT_L^1 would be close to ΔT_L^N. Also, $\dot{m}^n$ is constant for all n.

2. Assume that the solution $\Delta h_i/N$ holds when the series subsystems that raise the temperature of the return water to boiling is added to the series boiling feeder line. Equation 2-16 is appropriately modified to include the sensible heat addition. The justification for this approximation is that the latent heat addition is much greater than the sensible heat addition. Alternatively, the two parts of the series feeder line could be handled individually.

3. Start with the smallest N such that Δh_{TOT} is positive in 2-16.

4. For a range of ΔT_L's compute

$$Z_N = N\, C_{HT}(\Delta h_{TOT}/N) + C_{HT}(T_L, \Delta T_L), \qquad (2\text{-}19)$$

where $C_{HT}(T_L, \Delta T_L)$ is computed for the length of the entire feeder line. Select as Z_N^*, the minimum Z_N in the ΔT_L range.

5. Set N to $N + 1$ and repeat step 4.

6. When $Z_{N+1}^* > Z_N^*$, stop. An N stage feeder line is optimal. As N increases, the values of Z_N will at first decrease and then increase. For feeder lines having only a few subsystems, the first N will occasionally be the minimum cost system. Examples of this optimization procedure are shown in Section 2.3.9.

2.3.8 Trunk Line Simplifications for Boiling

For boiling system trunk lines, the mass flow will increase as more and more feeder lines feed into the trunk line. Now C_{HT} depends on $\dot{m}^n$ and the solution to 2-16 is not known apriori even though $C_{HT}(\Delta h_n, \dot{M}^n)$ is convex in Δh_n. Thus, the dynamic programming iterative equations will be required.

A simplification in these equations does arise, however, since the series boiling feeder lines are of a fixed length when a constant feeder line mass flow rate is used. This is because saturated steam must be produced. Thus $2k^n$ and $2j^n$ need not appear explicitly and considerable computation time is saved.

Even further savings in computation time can be realized by taking advantage of the low temperature of the return line. However, an approach different from the last section is required. A $\Delta T_L^n = \Delta T_L$ and a $T_L^n = T_L$ are fixed for all subsystems n and the dynamic programming analysis implied by

$$f_n(H^n) = \underset{\Delta h_n}{\text{MIN}} [C_{HT}(\Delta h_n, \dot{M}^n) + C_{HT}(T_L, \Delta T_L, \dot{M}^n) + f_{n-1}(H^n - \Delta h_n)] \qquad (2\text{-}20)$$

is run. Then the analysis of 2-20 is repeated for other values of ΔT_L and the minimum cost value chosen. This results in different pipe diameters and insulation thicknesses for each high and low side heat transport segment.

Different values of H^N, where N is the number of trunk line subsystems, will result in steam of different qualities. The cost of a separator $C_s(H^n)$, to yield saturated steam is added to $f_N(H^N)$ and

these costs are compared for various values of H^N. The lowest value of $[f_N(H^N) + C_s(H^N)]/\dot{M}^N$, where $\dot{M}^N$ is the mass flow rate after the separator, is a measure of the minimum cost of thermal power out of the trunk line. Examples of this optimization procedure are shown in Section 2.3.9.

2.3.9 Sample Results

A feeder line optimization run for pressurized water is shown in Figure 2-15. The piping arrangement is single parallel with minimum cost point focusing collectors having an aperture area of 30.5 m^2, a mass flow rate of .05 kg/sec., a collector ΔT of 112°C and a cost of $1554. The field fill factor is .5 m in each coordinate direction. The fill factor and aperture diameter yield a heat transport segment length of $2\sqrt{A_p/\pi}/.5 = 12.5$ m. The high temperature side grid was [210, 209, 208, ----, 200] and the low temperature side grid was [100.00, 99.75, 99.50, ----, 85.00].

The first trace back in part (a) of the figure is for a feeder line consisting of 20 subsystems. For the innermost subsystem the optimum values, $\Delta T_H^{20} = 0°C$ and $\Delta T_L^{20} = .25°C$, for $T_H^{20} = 200°C$ and $T_L^{20} = 100°C$ are given in the first line of columns two and five respectively. For the next subsystem the optimum values, $\Delta T_H^{19} = 0°C$ and $\Delta T_L^{19} = .25°C$, for $T_H^{19} = T_H^{20} - \Delta T_H^{20} = 200°C$ and $T_L^{19} = T_L^{20} - \Delta T_L^{20} = 99.75°C$ are given in the second line and so forth until the outermost subsystem with optimum values, $\Delta T_H^1 = -5°C$ and $\Delta T_L^1 = 2°C$, has been traced back. As mentioned previously, the optimum pipe diameters and insulation thicknesses for subsystem n can be found from T_H^n, ΔT_H^n, T_L^n, ΔT_L^n and M^n. These have been computed

```
FILE NAME
 ? f2s.093
NEW EXPERIMENT
 ? 1
NX,NXL,NNX,FTYPE,FM,T0,TRISE,TII,TIIL
 ? 11,61,20,2,.05,.013,.113,1,.25
YD,XD,FNG,FEN,CC
 ? 1,30.5,.5,.5,1554
GUESS
USE IN EXECUTION.
ACCUM. CPU SECONDS =   939.472

TRACE BACK STAGE AND DESIGN T AND TL
 ? 20,200,100

TRACE BACK FROM STAGE  20  COST     42331  DESIGN T AND TL 200.00 100.00

STAGE---HIGH SIDE DT, D, TI---LOW SIDE DT, D, TI
 20  0.   .0238  .0319   .25 .0232  .0360
 19  0.   .0232  .0312   .25 .0223  .0400
 18  0.   .0225  .0305   .25 .0213  .0423
 17  0.   .0217  .0297   .25 .0203  .0459
 16  0.   .0210  .0330   .25 .0192  .0492
 15  0.   .0202  .0333   .25 .0181  .0520
 14  0.   .0195  .0335   .25 .0170  .0565
 13  0.   .0187  .0337   .25 .0157  .0623
 12  0.   .0179  .0339   .25 .0145  .0694
 11  0.   .0170  .0340   .25 .0131  .0789
 10  0.   .0162  .0340   .25 .0117  .0919
  9  0.   .0153  .0340   .25 .0102  .1106
  8  0.   .0143  .0338   .25 .0080  .1290
  7  0.   .0132  .0353   .50 .0128  .0405
  6  0.   .0119  .0368   .50 .0110  .0497
  5  0.   .0107  .0383   .50 .0090  .0655
  4  0.   .0093  .0396   .50 .0060  .1174
  3  1.00 .0060  .1774   .75 .0080  .0770
  2  1.00 .0030  .0786  1.00 .0060  .1095
  1 -5.00 .0080  .0757  2.00 .0060  .1021

TRACE BACK STAGE AND DESIGN T AND TL
 ? 15,200,100

TRACE BACK FROM STAGE  15  COST     30225  DESIGN T AND TL 200.00 100.00

STAGE---HIGH SIDE DT, D, TI---LOW SIDE DT, D, TI
 15  0.   .0210  .0290   .25 .0180  .0533
 14  0.   .0200  .0281   .25 .0166  .0581
 13  0.   .0195  .0281   .25 .0156  .0640
 12  0.   .0184  .0281   .25 .0143  .0715
 11  0.   .0178  .0280   .25 .0130  .0814
 10  0.   .0170  .0278   .25 .0116  .0951
  9  0.   .0159  .0267   .50 .0159  .0307
  8  0.   .0143  .0296   .50 .0144  .0350
  7  0.   .0137  .0305   .50 .0128  .0411
  6  0.   .0123  .0313   .50 .0109  .0506
  5  0.   .0112  .0321   .50 .0089  .0669
  4  1.00 .0080  .1413   .75 .0093  .0415
  3  1.00 .0030  .0679  1.00 .0083  .0360
  2  1.00 .0080  .0509  1.50 .0080  .0332
  1 -5.00 .0080  .0746  2.75 .0080  .0385

TRACE BACK STAGE AND DESIGN T AND TL
 ? 10,200,100

TRACE BACK FROM STAGE  10  COST     19210  DESIGN T AND TL 200.00 100.00

STAGE---HIGH SIDE DT, D, TI---LOW SIDE DT, D, TI
 10  0.   .0176  .0282   .50 .0142  .0280
  9  0.   .0164  .0267   .50 .0123  .0313
  8  0.   .0154  .0253   .50 .0103  .0357
  7  0.   .0144  .0256   .50 .0107  .0421
  6  0.   .0131  .0260   .50 .0103  .0513
  5  0.   .0117  .0275   .75 .0115  .0315
  4  1.00 .0080  .0306   .75 .0080  .0402
  3  1.00 .0030  .0460  1.00 .0053  .0366
  2  1.00 .0080  .0354  1.50 .0080  .0330
  1 -6.00 .0080  .0435  3.50 .0080  .0516

TRACE BACK STAGE AND DESIGN T AND TL
 ? 5,200,100

TRACE BACK FROM STAGE   5  COST      9306  DESIGN T AND TL 200.00 100.00

STAGE---HIGH SIDE DT, D, TI---LOW SIDE DT, D, TI
  5  0.   .0166  .0139  1.00 .0126  .0265
  4  1.00 .0095  .0371  1.00 .0100  .0263
  3  1.00 .0089  .0269  1.25 .0092  .0254
  2  1.00 .0080  .0081  1.75 .0080  .0247
  1 -7.00 .0080  .0028  3.00 .0080  .0339
```

(a) (b) (c) (d)

Figure 2-15. Sample Results for a Pressurized Water Feeder Line Optimization.

and are also shown in the figure. For the innermost subsystem, 20, the high temperature side optimum pipe diameter and insulation thickness are .0238 m and .0319 m respectively. For the low temperature side the corresponding values are .0232 m and .0380 m respectively.

Optimum design trace backs for various length feeder lines from this run are shown in parts (a), (b), (c), and (d) of the figure. The five stage, or subsystems, trace back of part (d) of the figure is displayed graphically in Figure 2-16. This figure illustrates the high and low temperature side interactions discussed in Section 2.3.2.

Two feeder line optimization runs for series boiling are shown in Figure 2-17. The point focusing collectors used have an aperture area of 37.1 m^2, cost $1781 and add 2.5 and 5 percent of the required latent heat. The corresponding mass flow rates through the collectors are .64 kg/sec and .32 kg/sec. and boiling takes place at 250°C. The fill factors are again .5 and the length of the heat transport segment is 13.7 m. The thermal power added per collector is 27.3 kw. The optimum number of subsystems for minimum cost feeder lines are indicated in the figure and are 68 and 33 respectively.

A trunk line optimization run for boiling collectors is shown in Figure 2-18. Each minimum cost feeder line provides saturated steam to the trunk lines at a mass flow rate of .32 kg/sec, a temperature of 200°C and a cost of $61,601. The trunk line subsystem heat transport length of 12.71 m is determined from the point focusing collector size and the fill factors. $C_p \Delta T$ at 200°C is used to approximate Δh for computational convenience. Thus ΔT is shown in the figure rather than Δh. The DESIGN T specification in the trace back indicates the amount of latent heat lost in the trunk line for that

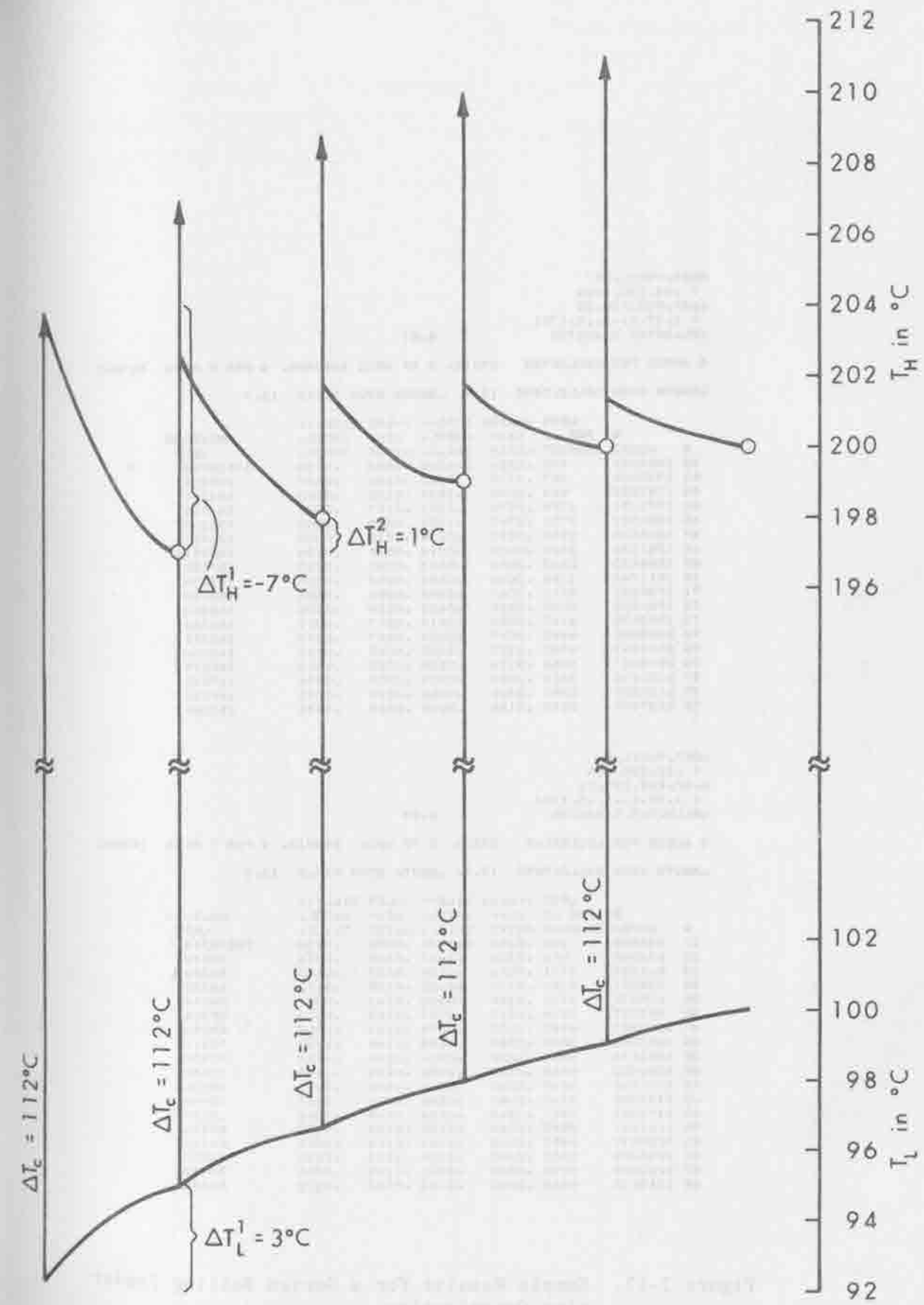

Figure 2-16. Trace Back T_H, T_L Results.

```
MDOT,TOIL,OF
 7 .64,250,.025
LAP,FNS,FEW,CC
 7 1,37.1,.5,.5,1781
COLLECTOR DIAMETER                6.87

Q ADDED PER COLLECTOR   27311, Q TO BOIL 1092425, Q FOR T RISE  587840

LENGTH BTWN COLLECTORS  13.7, LENGTH BTWN PIPES  13.7

                LOSS --HIGH SIDE-- --LOW SIDE---
          Q   PER MT  DIA-  INSUL.  DIA-  INSUL.        MINIMUM
 N     ADDED SEGMENT METER THICK. METER THICK.           COST
 62 1693259     188 .0354 3.4710 .0080  .2154       51636294
 63 1720569     597 .1775  .3793 .0164  .0547         210379
 64 1747880     994 .2250  .1957 .0193  .0293         153286
 65 1775191    1399 .2574  .1331 .0197  .0300         141963
 66 1802501    1771 .2743  .1031 .0212  .0202         138227
 67 1829812    2152 .2858  .0838 .0212  .0206         136957
 68 1857122    2503 .2930  .0714 .0219  .0154         136791 X
 69 1884433    2843 .2982  .0623 .0223  .0123         137251
 70 1911744    3192 .3020  .0551 .0223  .0126         138074
 71 1939054    3513 .3047  .0498 .0226  .0104         139146
 72 1966365    3844 .3069  .0452 .0226  .0106         140383
 73 1993676    4147 .3084  .0417 .0227  .0091         141743
 74 2020986    4460 .3097  .0386 .0227  .0093         143191
 75 2048297    4747 .3107  .0362 .0228  .0081         144708
 76 2075607    5044 .3116  .0339 .0228  .0083         146277
 77 2102918    5315 .3123  .0321 .0229  .0074         147889
 78 2130229    5597 .3129  .0304 .0229  .0075         149535
 79 2157539    5872 .3134  .0289 .0229  .0076         151209


MDOT,TOIL,OF
 7 .32,250,.05
LAP,FNS,FEW,CC
 7 1,37.1,.5,.5,1781
COLLECTOR DIAMETER                6.87

Q ADDED PER COLLECTOR   27311, Q TO BOIL  546212, Q FOR T RISE  293920

LENGTH BTWN COLLECTORS  13.7, LENGTH BTWN PIPES  13.7

                LOSS --HIGH SIDE-- --LOW SIDE---
          Q   PER MT  DIA-  INSUL.  DIA-  INSUL.        MINIMUM
 N     ADDED SEGMENT METER THICK. METER THICK.           COST
 31  846629     188 .0254 2.4839 .0080  .2154       18075314
 32  873940     958 .1702  .1461 .0146  .0210          68510
 33  901251    1771 .2020  .0759 .0155  .0147          65329 X
 34  928561    2503 .2137  .0520 .0159  .0114          65737
 35  955872    3192 .2189  .0400 .0161  .0091          66914
 36  983182    3844 .2217  .0327 .0163  .0077          68354
 37 1010493    4460 .2232  .0278 .0163  .0067          69992
 38 1037804    5044 .2240  .0244 .0164  .0059          71677
 39 1065114    5597 .2244  .0216 .0164  .0054          73407
 40 1092425    6140 .2250  .0198 .0164  .0056          75169
 41 1119736    6657 .2255  .0182 .0164  .0057          76951
 42 1147046    7145 .2260  .0166 .0164  .0059          78749
 43 1174357    7617 .2262  .0158 .0164  .0061          80557
 44 1201667    8065 .2264  .0148 .0164  .0063          82374
 45 1228978    8492 .2265  .0141 .0164  .0064          84193
 46 1256289    8902 .2267  .0134 .0163  .0065          86027
 47 1283599    9293 .2268  .0128 .0163  .0065          87860
 48 1310910    9669 .2268  .0123 .0163  .0070          89696
```

Figure 2-17. Sample Results for a Series Boiling Feeder Line Optimization.

```
FILE NAME ? CONIT2

NEW EXPERIMENT ? 1

KMX,NMX,SM,TB,TII,DTL ? 201,13,.32,200,.1,.1

L,AP,FNS,FEW,CSIDE ? 1,31.7,.5,.5,61601

LENGTH BETWEEN BRANCHES  12.71

TRACE BACK STAGE ? 13

DESIGN T AND DTL ? 180,.1

COST      3207833
```

	---HIGH SIDE----			----LOW SIDE----		
STAGE	DT	DIA.	TI	DT	DIA.	TI
13	-1.40	1.2001	.0168	.10	.1365	.0016
12	-1.50	1.1585	.0165	.10	.1305	.0016
11	-1.50	1.1022	.0173	.10	.1242	.0017
10	-1.50	1.0438	.0182	.10	.1178	.0018
9	-1.50	.9829	.0193	.10	.1110	.0019
8	-1.50	.9189	.0205	.10	.1038	.0020
7	-1.50	.8515	.0220	.10	.0963	.0021
6	-1.50	.7797	.0238	.10	.0883	.0022
5	-1.50	.7024	.0262	.10	.0796	.0024
4	-1.60	.6244	.0277	.10	.0701	.0027
3	-1.60	.5290	.0320	.10	.0595	.0031
2	-1.60	.4177	.0394	.10	.0471	.0035
1	-1.60	.2821	.0513	.10	.0312	.0054

```
FRACTION OF LATENT HEAT LOST .0091

MASS FLOW RATE OUT OF SEPARATORS  16.4867

TRACE BACK STAGE ? 13

DESIGN T AND DTL ? 182.5,.1

COST      3208213
```

	---HIGH SIDE----			----LOW SIDE----		
STAGE	DT	DIA.	TI	DT	DIA.	TI
13	-1.30	1.1369	.0174	.10	.1365	.0016
12	-1.30	1.1321	.0190	.10	.1305	.0016
11	-1.30	1.0773	.0199	.10	.1242	.0017
10	-1.30	1.0202	.0209	.10	.1178	.0018
9	-1.30	.9606	.0221	.10	.1110	.0019
8	-1.30	.8981	.0235	.10	.1038	.0020
7	-1.30	.8321	.0251	.10	.0963	.0021
6	-1.30	.7619	.0272	.10	.0883	.0022
5	-1.30	.6862	.0298	.10	.0796	.0024
4	-1.40	.6108	.0313	.10	.0701	.0027
3	-1.40	.5172	.0362	.10	.0595	.0031
2	-1.40	.4079	.0447	.10	.0471	.0038
1	-1.60	.2755	.0576	.10	.0312	.0054

```
FRACTION OF LATENT HEAT LOST .0078

MASS FLOW RATE OUT OF SEPARATORS  16.5108

TRACE BACK STAGE ? 13

DESIGN T AND DTL ? 185,.1

COST      3208709
```

	---HIGH SIDE----			----LOW SIDE----		
STAGE	DT	DIA.	TI	DT	DIA.	TI
13	-1.10	1.1069	.0204	.10	.1365	.0016
12	-1.10	1.1024	.0222	.10	.1305	.0016
11	-1.10	1.0489	.0230	.10	.1242	.0017
10	-1.10	.9934	.0244	.10	.1178	.0018
9	-1.10	.9353	.0258	.10	.1110	.0019
8	-1.10	.8744	.0274	.10	.1038	.0020
7	-1.10	.8101	.0293	.10	.0963	.0021
6	-1.10	.7415	.0317	.10	.0883	.0022
5	-1.10	.6677	.0348	.10	.0796	.0024
4	-1.20	.5956	.0368	.10	.0701	.0027
3	-1.20	.5037	.0418	.10	.0595	.0031
2	-1.30	.4024	.0480	.10	.0471	.0038
1	-1.40	.2678	.0658	.10	.0312	.0054

```
FRACTION OF LATENT HEAT LOST .0063

MASS FLOW RATE OUT OF SEPARATORS  16.5344

TRACE BACK STAGE ? 13

DESIGN T AND DTL ? 190,.1

COST      3210398
```

	---HIGH SIDE----			----LOW SIDE----		
STAGE	DT	DIA.	TI	DT	DIA.	TI
13	-.70	1.0299	.0311	.10	.1365	.0016
12	-.70	1.0255	.0333	.10	.1305	.0016
11	-.70	.9757	.0353	.10	.1242	.0017
10	-.70	.9233	.0371	.10	.1178	.0018
9	-.70	.8696	.0391	.10	.1110	.0019
8	-.70	.8126	.0415	.10	.1038	.0020
7	-.70	.7523	.0444	.10	.0963	.0021
6	-.80	.7035	.0420	.10	.0883	.0022
5	-.80	.6328	.0460	.10	.0796	.0024
4	-.80	.5555	.0525	.10	.0701	.0027
3	-.80	.4655	.0611	.10	.0595	.0031
2	-.90	.3752	.0693	.10	.0471	.0038
1	-1.00	.2479	.0934	.10	.0312	.0054

```
FRACTION OF LATENT HEAT LOST .0036

MASS FLOW RATE OUT OF SEPARATORS  16.5505

TRACE BACK STAGE ? 13

DESIGN T AND DTL ? 195,.1

COST      3215576
```

	---HIGH SIDE----			----LOW SIDE----		
STAGE	DT	DIA.	TI	DT	DIA.	TI
13	-.30	.8960	.0679	.10	.1365	.0016
12	-.30	.8914	.0737	.10	.1305	.0016
11	-.30	.8472	.0771	.10	.1242	.0017
10	-.30	.8010	.0811	.10	.1178	.0018
9	-.30	.7527	.0857	.10	.1110	.0019
8	-.40	.7033	.0839	.10	.1038	.0020
7	-.40	.6529	.0958	.10	.0963	.0021
6	-.40	.6231	.0814	.10	.0883	.0022
5	-.40	.5505	.0900	.10	.0796	.0024
4	-.40	.4673	.1021	.10	.0701	.0027
3	-.40	.4063	.1012	.10	.0595	.0031
2	-.50	.3297	.1206	.10	.0471	.0038
1	-.60	.2146	.1678	.10	.0312	.0054

```
FRACTION OF LATENT HEAT LOST .0038

MASS FLOW RATE OUT OF SEPARATORS  16.6062
```

Figure 2-18. Sample Results for a Boiling Trunk Line Optimization.

run and DTL is ΔT_L. The amount of latent heat lost can be calculated by subtracting this number from 200°C, the boiling temperature, and multiplying by C_p at 200°C.

The minimum costs in the figure are for the two trunk lines, one on each side of the turbine generator, that make up the field. Trace backs were made for various amounts of latent heat lost in the trunk lines by changing the DESIGN T input. The interpretation of the columns and rows of the figure is the same as for the feeder line case of Figure 2-16.

The trunk line optimization for pressurized water was not implemented since it was evident from these three types of optimization runs that boiling fields would have lower costs. (See Volume II.)

2.4 Optimization Methodology for Steam Generator and Heat Engine

The optimization process for the steam generator and heat engine uses as inputs the outputs from the energy collection and transport subsystems. To limit the iterative search for the minimum cost design, the inlet steam temperature of the steam generator was restricted to four values (150, 200, 250 and 300°C), and its outlet (condenser) temperature was restricted to three values (30,40 and 50°C). The optimization of the steam generator is performed separately from that of the heat engine but both share the same restricted set of engine operating temperatures. These are mass flow rate $\dot{m}$, temperature T_o, phase state, steam or water, and initial temperature of the fluid returned to the collector field.

The steam generator optimization program is outlined in Figure 2-19. First a set of turbine-generator operating parameters

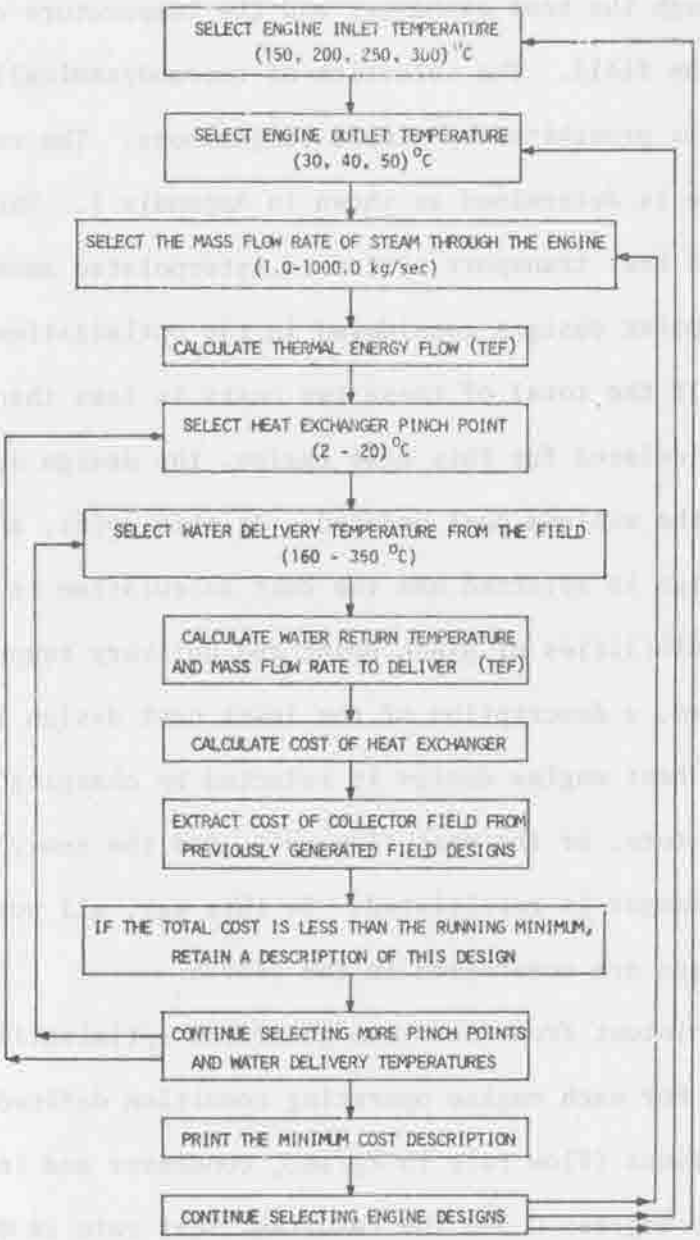

Figure 2-19. Steam Generator Optimization.

are selected (inlet temperature, outlet temperature and mass flow rate). These parameters determine the size of the turbine and the heat flow through it. Next the water delivery temperature and heat exchanger pinch point are selected. This selection determines the mass flow rate of water through the heat exchanger and the temperature of the water returned to the field. The selection of thermodynamically impossible combinations is prohibited by simple comparisons. The cost of the heat exchanger is determined as shown in Appendix I. The cost of the collectors and heat transport system is interpolated among the many minimum cost point designs considered in the optimizations of those subsystems. If the total of these two costs is less than any cost previously calculated for this heat engine, the design description is retained and the minimum cost updated. At this point, another heat exchanger design is selected and the cost calculation is repeated. After all possibilities of pinch point and delivery temperature have been considered, a description of the least cost design is printed out. Then, another heat engine design is selected by changing the inlet or outlet temperature, or the mass flow rate, and the search for a minimum cost heat exchanger is reinitiated. In this way, all possible combinations of designs are considered in the search.

The pointout from the steam generator optimization is shown in Figure 2-20. For each engine operating condition defined by the first four columns (flow rate in kg/sec, condenser and inlet temperature in degrees C and the resultant heat rate in MW thermal) the minimum cost combination of field and heat exchanger conditions are printed. These conditions consist of the flow rate of water in the field in kg/sec and the low and high side temperatures in degrees

ENGINE				FIELD				FIELD	HT-EXCH	TOTAL
FLOW	T-CND	T-IN	P(MWT)	FLOW	T-RET	T-IN	P(MWT)	$/KW$_T$	$/KW$_T$	($1000)
3	30	250	8.0	9.7	197	350	8.0	322.86	3.25	2597.26
3	30	300	7.9	15.2	261	350	7.9	505.22	4.76	4043.02
3	40	250	7.8	9.7	199	350	7.8	321.95	3.29	2550.16
3	40	300	7.8	15.1	263	350	7.8	503.95	4.82	3970.59
3	50	250	7.7	9.6	202	350	7.7	321.02	3.33	2502.64
3	50	300	7.7	15.1	264	350	7.7	502.66	4.88	3997.57
10	30	150	26.1	21.4	105	350	26.1	213.98	2.33	5553.20
10	30	200	26.8	25.8	147	350	26.8	257.90	2.66	6900.51
10	30	250	26.5	32.3	197	350	26.5	322.86	3.25	8657.50
10	30	300	26.4	50.6	261	350	26.4	505.22	4.76	13478.73
10	40	150	25.7	21.4	108	350	25.7	213.47	2.36	5551.90
10	40	200	26.4	25.8	150	350	26.4	257.26	2.69	6877.53
10	40	250	26.1	32.2	199	350	26.1	321.95	3.29	8580.03
10	40	300	26.0	50.4	263	350	26.0	503.95	4.82	13220.09
10	50	150	25.3	21.3	112	350	25.3	212.94	2.39	5449.51
10	50	200	26.0	25.7	153	350	26.0	256.63	2.73	6746.29
10	50	250	25.7	32.1	202	350	25.7	321.02	3.33	8342.14
10	50	300	25.6	50.3	264	350	25.6	502.66	4.88	12991.93
30	30	150	78.3	64.3	105	350	78.4	213.98	2.33	16959.66
30	30	200	80.4	77.4	147	350	80.5	257.90	2.66	20980.52
30	30	250	79.6	97.0	197	350	79.6	322.86	3.25	25972.60
30	30	300	79.2	151.7	261	350	79.3	505.22	4.76	40430.20
30	40	150	77.1	64.1	108	350	77.2	213.47	2.36	16655.69

Figure 2-20. Printout of the Steam Generator Optimization.

centigrade. The capital costs of the field and heat exchanger (steam generator) in $/kW thermal and the total cost in 1972 millions of dollars are shown in the last three columns.

The procedure for optimizing the turbine-generator-cooling system is outlined in Figure 2-21. A design is selected from the field optimization of boiling collector fields or collector fields using hot water and a steam generator. This design consists of the inlet temperature, the steam mass flow rate, the condensing temperature and the total cost of the collector field, heat transport system and heat exchanger. From the inlet temperature, mass flow rate and the condenser temperature, the basic turbine generator cost and electric output are calculated using the relationships described in Appendix H. At this point, the cooling system operating temperatures are chosen (i.e., the range and the terminal temperature difference) and the resulting cooling tower approach to the wet bulb temperature is calculated. The turbine generator efficiency is chosen (between 0.7 and 0.9) and the associated turbine-generator cost multiplier is selected from the curve shown in Appendix H. The final turbine generator cost, electric output and heat rejected is now calculated using multipliers obtained from Appendix H. Using the heat rejected and the chosen cooling system operating temperature, the cost of the condenser cooling-tower system including the cost of pumping, is calculated using data in Appendix I.

The generator output and an annual frequency distribution of hour by hour insolation data is used to calculate the approximate annual energy output. No correction is made for lower turbine-generator efficiencies at lower insolation levels so that the apparent capacity factor is 0.37. This has no significant effect

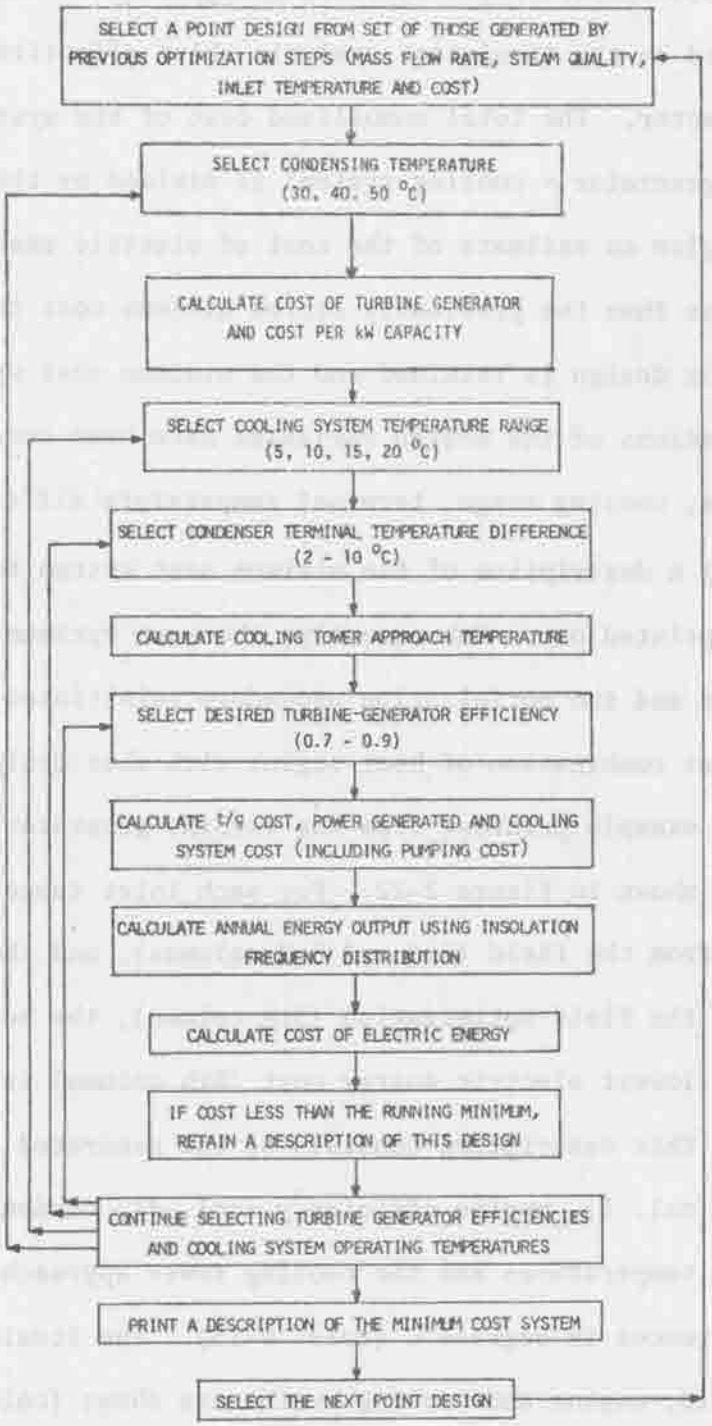

Figure 2-21. Turbine-Generator-Cooling System Optimization.

on the cost of energy comparisons between systems, but it does result in an understatement of the absolute energy costs. This deficiency is corrected in the simulation analysis which effectively lowers the capacity factor. The total annualized cost of the system (field + turbine - generator + cooling system) is divided by this total energy output to give an estimate of the cost of electric energy. If this cost is less than the previously stored minimum cost then a description of this design is retained and the minimum cost updated. After all combinations of the design variables have been considered (condenser temperature, cooling range, terminal temperature difference and engine efficiency) a description of the minimum cost system for this point design is printed out. Subsequently, the next optimum field design is selected and the optimization procedure reinitiated to find the minimum cost combination of heat engine with that design.

An example printout from the turbine generator optimization program is shown in Figure 2-22. For each inlet temperature and steam flow rate from the field (2nd and 3rd columns), and the cost of that field from the field optimization (5th column), the heat engine design giving the lowest electric energy cost (8th column) is described in the printout. This description consists of the generated electric power in megawatts (col. 1), engine efficiency (col. 4), condenser steam, inlet and outlet temperatures and the cooling tower approach and range temperature differences in degrees C (cols. 9-13). The itemized capital cost of the field, engine and cooling system are shown (cols. 5-7) in dollars per kilowatt electric rated.

1	2 *	3 *	4	5 *	6	7	8	9	10	11	12	13
ELECT	STEAM	INL	ENG	FIELD	TUR-GEN	C0OLNG	ELECT	C	0	N	D	E N S E R	APPR
POWER	FLOW	TMP	EFF	COSTS	COSTS	COSTS	COST	TEMP	INL	OUT	RNG		TMP
MW-E	KG/SEC	D-C		$/KWE	$/KWE	$/KWE	$/KWH	DEGREES		CENTIGRADE			
31.5	43.4	250	.84	232.19	92.43	27.93	.024	40	28	38	10		3**
31.5	43.4	250	.84	232.16	92.46	27.97	.024	40	28	38	10		3
31.6	43.5	250	.84	231.72	92.44	27.97	.024	40	28	38	10		3
31.7	43.6	250	.84	231.71	92.40	27.96	.024	40	28	38	10		3
110.1	148.1	250	.86	297.00	83.31	24.15	.024	40	28	38	10		3
110.2	148.2	250	.86	296.76	83.30	24.15	.024	40	28	38	10		3
110.4	148.5	250	.86	296.16	83.27	24.14	.024	40	28	38	10		3
110.7	148.8	250	.86	296.39	83.23	24.14	.024	40	28	38	10		3
95.3	147.8	200	.86	313.61	90.12	29.46	.026	40	28	38	10		3
95.4	147.9	200	.86	313.38	90.11	29.46	.026	40	28	38	10		3
95.6	148.2	200	.86	312.81	90.08	29.46	.026	40	28	38	10		3
96.4	149.5	200	.86	310.11	89.94	29.45	.026	40	28	38	10		3
75.7	147.6	150	.86	356.59	104.45	40.01	.030	40	28	38	10		3
75.8	147.7	150	.86	356.35	104.44	40.01	.030	40	28	38	10		3
75.9	148.0	150	.86	355.75	104.41	40.01	.030	40	28	38	10		3
76.0	148.3	150	.86	355.08	104.38	40.01	.030	40	28	38	10		3
27.3	43.4	200	.84	294.84	98.95	33.95	.026	40	28	38	10		3
27.4	43.4	200	.84	294.57	98.93	33.95	.026	40	28	38	10		3
27.4	43.5	200	.84	294.10	98.90	33.94	.026	40	28	38	10		3
27.5	43.6	200	.84	294.08	98.86	33.93	.026	40	28	38	10		3
21.7	43.4	150	.84	345.96	112.37	45.30	.030	40	28	38	10		3
21.8	43.4	150	.84	346.10	112.35	45.79	.030	40	28	38	10		3
21.8	43.5	150	.84	345.55	112.32	45.79	.030	40	28	38	10		3
21.8	43.6	150	.84	345.21	112.28	45.77	.030	40	28	38	10		3

* Columes 2, 3, and 5 are input data from collector field optimization.

** The 3 ^{o}C is a smaller approach than normally encountered in practice. This has resulted in part from the coarse grid (10^{o}) for condenser temperature and 5^{o} grid for range used in the initial run of this program.

Figure 2-22. Printout of the Turbine Generator/Cooling System Optimization, T wet bulb = 25 ^{o}C.

References

1. Wilde, D.J., Optimum Seeking Methods, Prentice-Hall, 1964.

2. Bellman, R., Dynamic Programming, Princeton University Press, 1957.

3. Palmquist, R.W. and W.A. Beckman, "Optimum Thermal Design of Radiative-Conductive Systems," Trans. of the ASME: Journal of Engineering for Industry, May, 1972.

4. Selcuk, M.K. and G.T. Ward, "Optimization of Solar Terrestial Power Production Using Heat Engines," Trans. of the ASME: Journal of Engineering for Power, April, 1970.

APPENDIX C

ENVIRONMENTAL CONDITIONS

BY

C. D. BEACH,

J. BAXTER,

AND

S. SHIEH

1.0 INTRODUCTION

Weather records obtained for the project were in the form of magnetic tape recording of hourly values for 15-year periods at El Paso, Texas, Phoenix, Arizona, and Albuquerque, New Mexico. During the project, a tape for Inyokern, California, was obtained from the Aerospace Corporation. It was felt by the project team and consultants that the differences between these locations in the southwest would have marginal effect on system performance. It was decided to first compare the systems against one another using typical conditions for the region and then simulate the best systems using the weather data from one location. For initial designs, data for 1959 from Albuquerque, New Mexico, was chosen because a tape for that year was obtained that had been checked for consistency and completeness.

Albuquerque data was used in three forms:

1) Point data was used to represent typical hourly conditions of insolation, ambient temperature and wind velocities.
2) Three typical clear days were selected to represent mid-summer, mid-winter and equinox conditions.
3) Statistics were derived from the complete year for insolation on collectors of various orientation as well as temperature, wind velocity and relative humidity.

These 1959 Albuquerque data were applied to preliminary system and subsystem performance analysis. Albuquerque is located at a latitude of 35.05 ^{o}N and longitude of 106.62 ^{o}W. Subsequently, the same analyses of insolation statistics were made for Albuquerque 1962, El Paso, 1959, and the Inyokern data.

Where point designs were made for subsystem comparisons, the following conditions were assumed:

1. Direct normal insolation 1000, 700 or 400 W/m^2
2. Diffuse insolation, 100 W/m^2
3. Ambient temperature 20 ^oC, and 40 ^oC
4. Sky temperatures 20 ^oC below ambient temperature
5. Wind speed 5 m/sec (10 mph)

2.0 TYPICAL CLEAR DAYS

To compare collector subsystem performance without using the entire year of data, three days were chosen from the records to represent a clear summer day, a clear winter day and a clear spring (or fall) day. Hourly values of total insolation on a horizontal surface are shown in Figure 2-1 for each of the days.

To compute the insolation on tilted collectors, it is necessary first to subtract the diffuse component of the measured total, horizontal insolation. The diffuse component has to be estimated because neither the diffuse nor direct radiation is measured separately. The method described by Liu and Jordan (1960) was used to estimate the diffuse component of the total radiation when the measured value was less than 0.8 of the extra-terrestrial value. For measured radiation greater than 0.8 of extra-terrestrial, the diffuse was assumed to be a constant five percent of the extraterrestrial value. The hourly variations of the estimated direct and diffuse solar radiation on a horizontal surface are shown in Figure 2-2 for the three typical days.

The use of the approximations above is supported by the data of Liu and Jordan only when the total insolation is between 0.4 and 0.8 of extraterrestrial insolation. When total insolation is greater than 0.8 of the extraterrestrial value, the diffuse radiation does not continue to decrease as would be indicated by an extension of the correlation proposed by Liu and Jordan. In fact, during partly cloudy days, the direct sun may be as stong as for a clear day while forward scatter from clouds may contribute a significant portion to the total radiation and cause the total radiation to approach the extraterrestrial value. When the total insolation drops below 0.3 of the extraterrestrial value, the

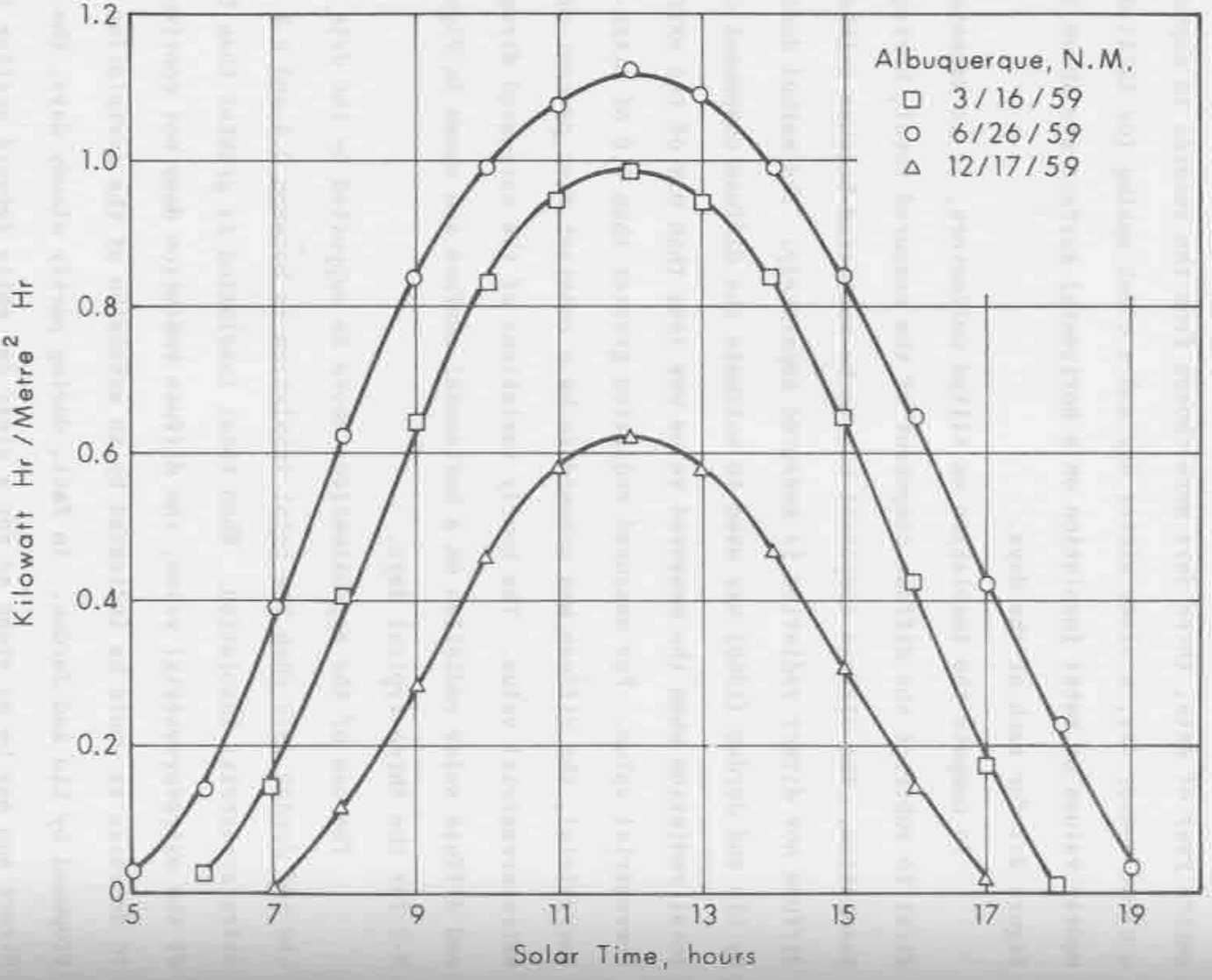

Figure 2-1. Hourly Variations of Total Solar Radiation on a Horizontal Surface for Three Typical Clear Days.

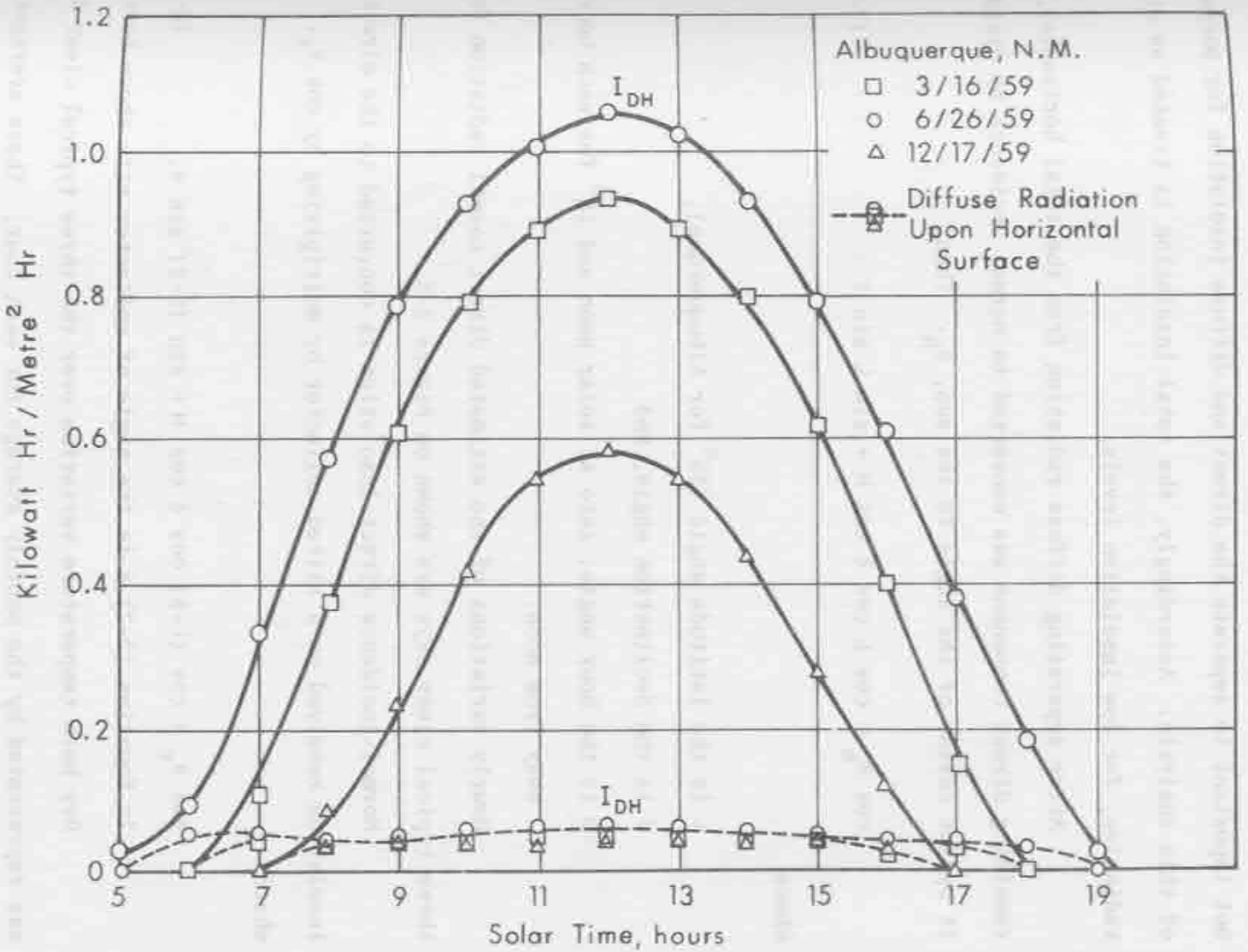

Figure 2-2. Hourly Variations of Direct and Diffuse Solar Radiation on a Horizontal Surface for the Three Typical Days.

energy available for electric power generation is very likely below the threshold of usefulness in most collector designs. In that case, it is not important to separate the direct and diffuse insolation for purposes of this analysis. Accordingly, the total insolation is treated as diffuse radiation, for low insolation levels.

After separating diffuse radiation from the total horizontal, the remaining direct component was converted to normal incidence by dividing it by the cosine of the angle to the sun, θ_h. Then,

$$\cos \theta_h = \cos L \cos \delta \cos H + \sin L \sin \delta \qquad (2\text{-}1)$$

where

L is the latitude angle (35^o for Albuquerque),

δ is the declination angle, and

H is the hour angle; zero at solar noon and 15^o for each hour away from noon.

Hourly variations of the estimated direct normal radiation for the three typical clear days are shown on Figure 2-3.

Normal-incidence direct insolation is converted to the direct insolation received on a tilted collector by multiplying by $\cos \theta_t$, where

$$\cos \theta_t = \cos (L-\beta) \cos \delta \cos H + \sin (L-\beta) \sin \delta. \qquad (2\text{-}2)$$

In Equation (2-2) β is the angle of collector tilt above horizontal.

Dry bulb temperature variation over the three typical clear days was represented by the monthly average for each hour. These averages are shown in Figure 2-4. Relative humidity values were also averaged for each hour to represent typical conditions for each of the days chosen.

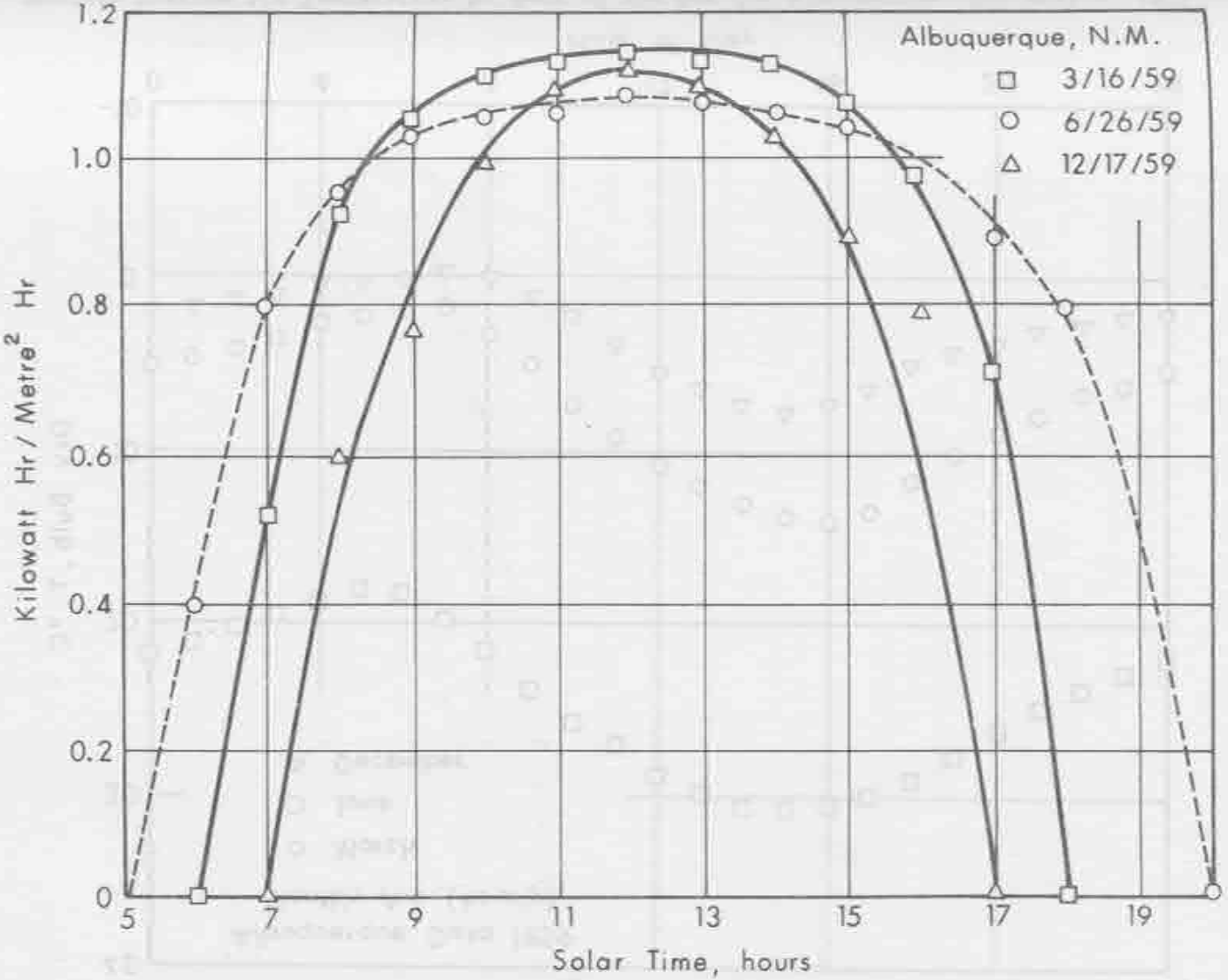

Figure 2-3. Hourly Variations of the Direct Normal Radiation for Three Typical Clear Days.

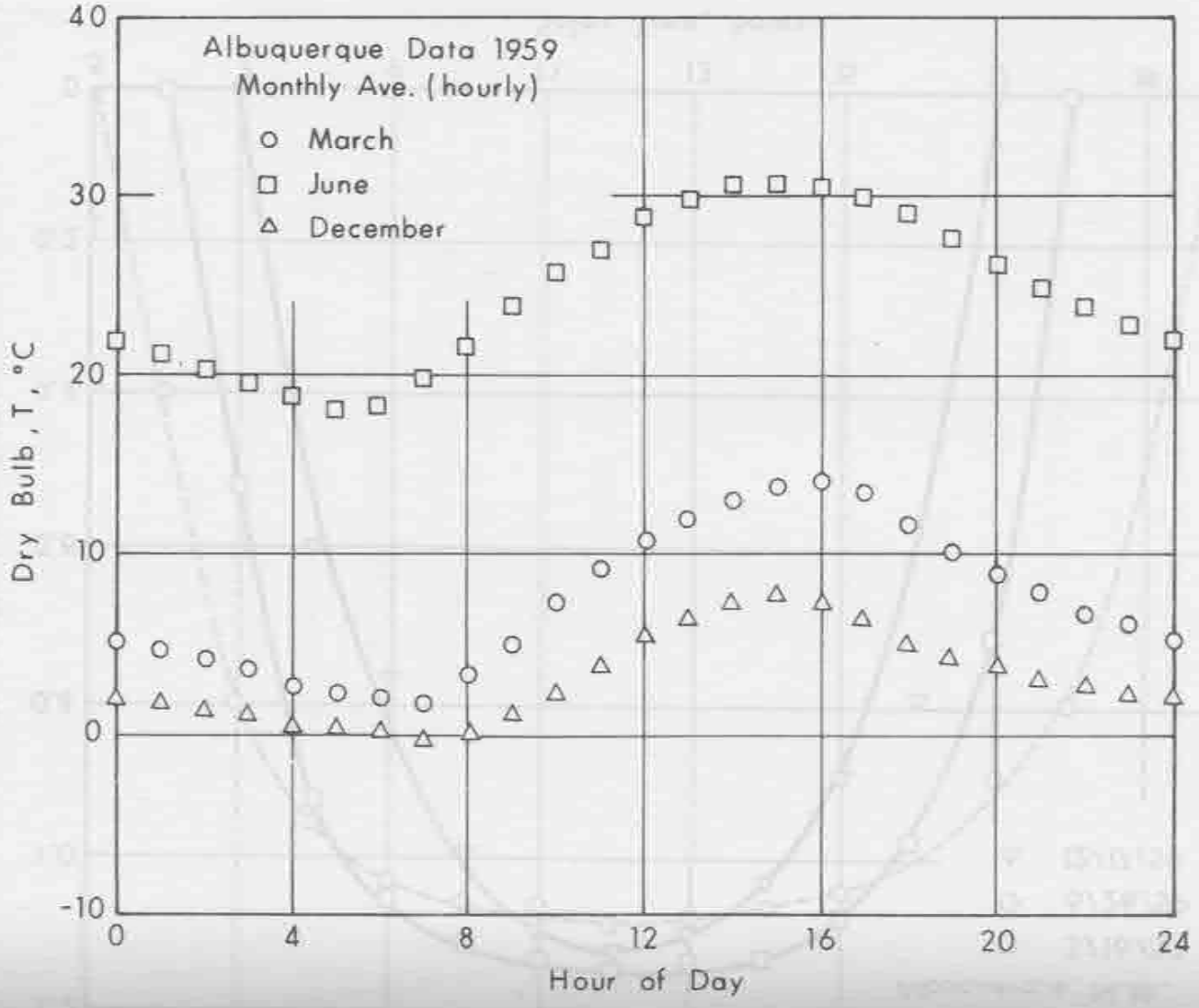

Figure 2-4. Monthly Average Air Temperature by Hour of the Day for Albuquerque, New Mexico, 1959.

These are shown in Figure 2-5. A steady wind speed of 5m/sec (≈10 mph) was chosen for performance calculations during the typical days. This is somewhat higher than the median value for the year as shown in the next section.

Sky temperatures were computed to represent the three typical days. A computer code developed at the National Oceanic and Atmospheric Administration (NOAA) in Boulder, Colorado, was used by NOAA personnel to estimate the sky radiation temperature from radiosonde data obtained from the National Weather Service. At NOAA recommendations, 1972-1973 radiosonde data was used instead of 1959 data, because of greater accuracy in more recent instruments. Clear days selected for sky temperature calculations were June 19, 1973, March 12, 1973 and December 13, 1972.

The calculated values, Table 2-1, are 25° to 30 °C below the dry bulb temperature at the time the radiosonde data was taken, and 35° to 40 °C below the average daytime temperatures shown by Figure 2-4. This suggests that the use of sky temperatures 20 °C below ambient temperatures may not be low enough for very clear days.

TABLE 2-1

CALCULATED SKY TEMPERATURE

Month	Sky Temperature	Dry Bulb (6PM)
June	-13.0 °C	12.9
March	-23.7 °C	2.8
December	-33.1 °C	-4.2

Sky temperature was assumed to be very nearly constant during the day because it depends strongly on absolute humidity numbers which vary slowly. Furthermore, radiosonde data is only available every 12 hours, so hourly sky temperatures would have to be interpolated.

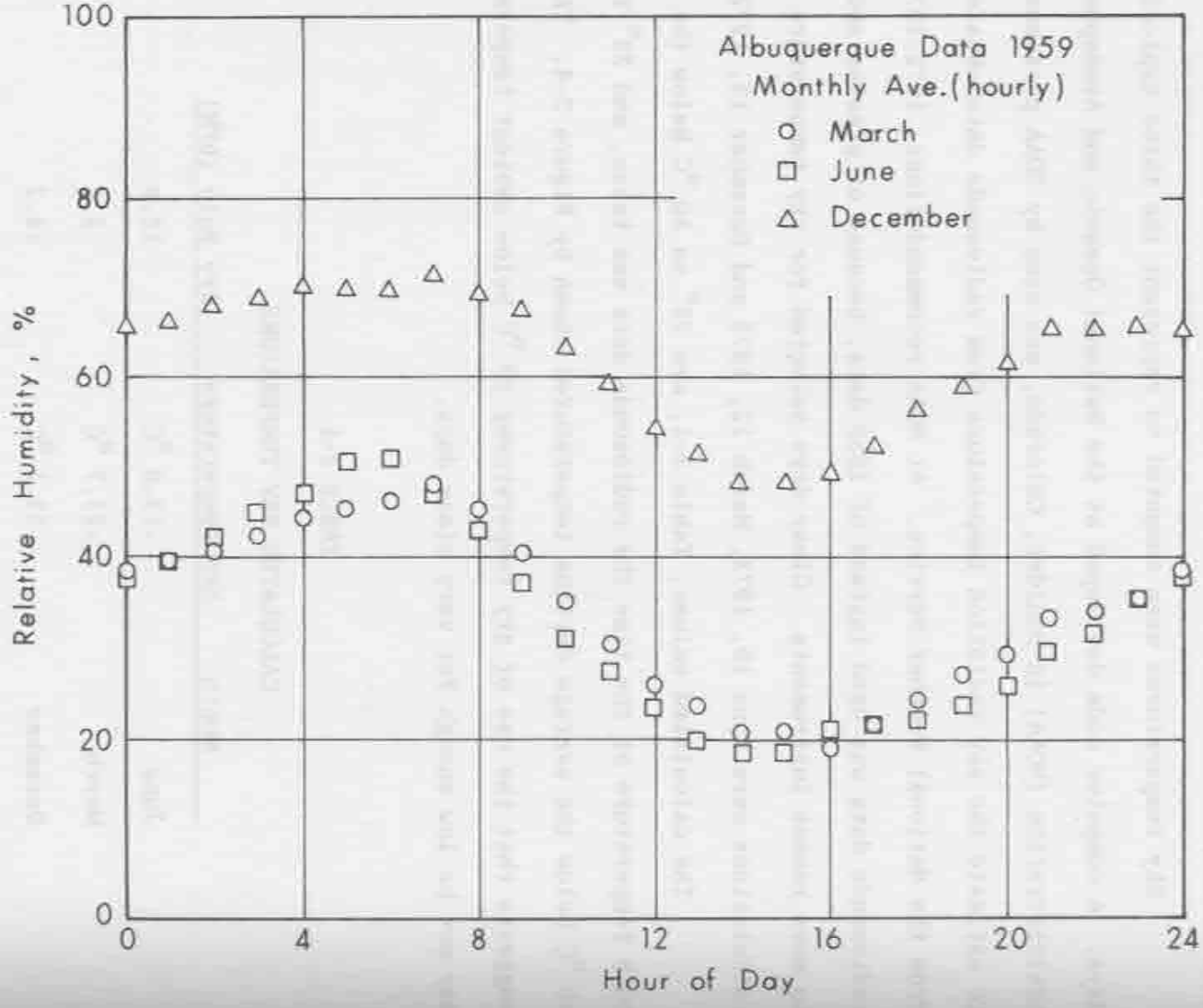

Figure 2-5. Monthly Average Relative Humidity by Hour of the Day for Albuquerque, New Mexico, 1959.

3.0 ANNUAL STATISTICS

More useful collector subsystem performance, and in some cases total system performance, can be obtained from the statistics of the whole year rather than only three days.

For seven different flat-plate collector orientation conditions and five focusing collector tracking conditions, the 1959 Albuquerque insolation data were corrected for collector angles and sorted according to the frequency of occurence of different values.

On the focusing collectors the insolation is

$$I_{fo} = I_{on} \cos \theta_t \quad W/m^2, \tag{3-1}$$

and the total insolation on flat-plate collectors is estimated to be

$$I_{fe} = I_{on} \cos \theta_t + 0.5\, I_d \quad W/m^2 \tag{3-2}$$

where

I_{on} = Direct normal insolation, W/m^2

θ_t = Angle between the normal to the collector and the sun

I_d = Diffuse insolation, W/m^2

Except for the horizontal collector, only one-half the diffuse radiation was included because the tilted collector does not see the whole hemisphere of sky.

The diffuse insolation was estimated from the total insolation using the relationship given by the curve in Figure 3-1. The solid part of the curve was adapted from the data of Liu and Jordan (1960), and the remainder was estimated. Where the total insolation is less than 0.5 of the extraterrestrial insolation, it is not useful for power generation, so the estimated diffuse is not important. Where it exceeds 0.8 of the extraterrestrial value the diffuse radiation is made constant because it does not realistically continue to decrease as extrapolation of

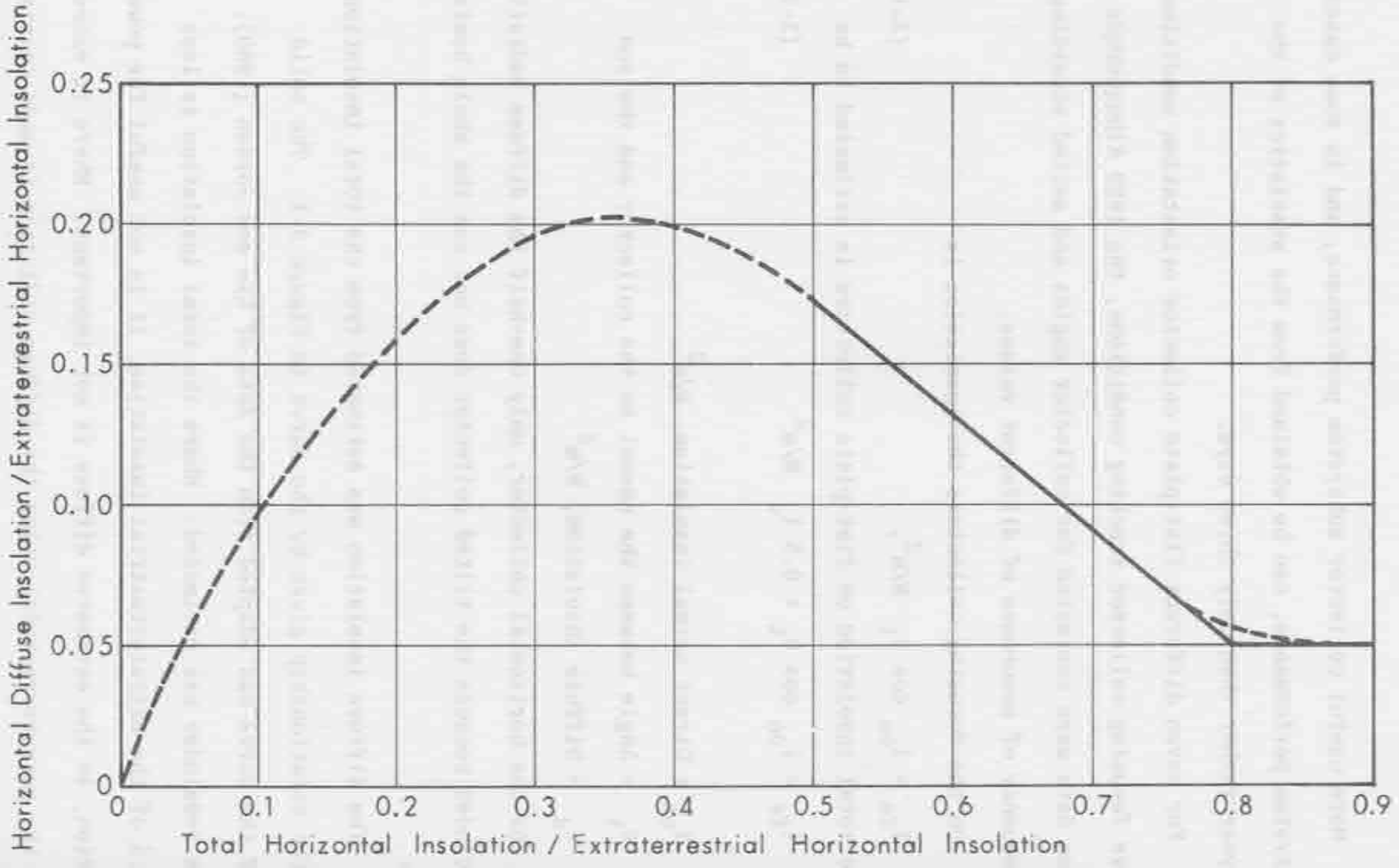

Figure 3-1. Diffuse Insolation vs. Total Insolation, Normalized by Extraterrestrial Insolation. Adapted from Liu and Jordan (1960).

the solid line would indicate.

Extraterrestrial insolation on a horizontal surface is estimated from

$$I_{oh} = 1.353\ r_c \cos \theta_h \qquad (3\text{-}3)$$

where r_c is a multiplier to account for variation in distance to the sun, see Table 3-1, and $\cos \theta_h$ is defined by Equation (2-1), above.

In the expression for the cosine of the angle to the sun from the vertical, Equation (2-1), the declination angle, δ, varies throughout the year as shown in Table 3-1. The hour angle, H, is based on mean solar time which also varies seasonally. These seasonal differences between solar time and clock time are caused by orbital and rotational variation. The difference is called the equation of time, and is also tabulated in Table 3-1. Then, the hour angle is found, for Albuquerque, by

$$H = 15(T-12.5 + ET) + 105 - LON^* \qquad (3\text{-}4)$$

where

T is clock time in hours, Mountain Standard Time

ET is the equation of time adjustment, Table 3-1, and

LON is the longitude, 106.62°.

The collector orientations and tracking conditions for which the frequency distribution of insolation values were made are listed in Table 3-2. Also given in the table are the expressions for $\cos \theta_t$ in Equations (3-1) and (3-2) as they apply to each collector type and orientation.

The computed frequency distributions (histograms) are given in

---

* The insolation data recorded on tape for 12:00 is the average for the preceding hour and therefore better represents the value for 11:30. For the recorded data solar noon falls between the 12:00 and 13:00 records.

TABLE 3-1

Solar Declination, Distance Multiplier
For Solar Constant, and Equation of Time

Date	δ	r_c	ET (hrs.)
Jan. 22	-19.85°	1.0300	-0.191
Feb. 22	-10.47°	1.0207	-0.228
Mar. 22	0.33°	1.0057	-0.120
Apr. 22	11.93°	0.9875	0.022
May 22	20.23°	0.9727	0.058
Jun. 22	23.45°	0.9670	-0.028
Jul. 22	20.43°	0.9692	-0.105
Aug. 22	12.05°	0.9785	-0.051
Sep. 22	0.62°	0.9945	0.116
Oct. 22	-10.78°	1.0133	0.256
Nov. 22	-19.97°	1.0267	0.234
Dec. 22	-23.45°	1.0327	0.030

TABLE 3-2

Collector Orientation and Tracking Conditions

Condition	$\cos \theta_c$	Notes
Fixed, South Facing		
1. Horizontal	$\cos L \cos \delta \cos H + \sin L \sin \delta$	a
2. Fixed Tilt; $\beta = L$	$\cos \delta \cos H$	a,b
3. Seasonal Adj.; $\beta = L - \delta$	$\cos^2 \delta \cos H + \sin^2 \delta$	a,b
Single Axis Tracking		
4. Horizontal, N-S Axis	$[1-(\sin L \cos \delta \cos H - \cos L \sin \delta)^2]^{1/2}$	c,d
5. Horizontal, E-W Axis	$\cos (L-\beta)\cos \delta \cos H + \sin (L-\beta) \sin \delta$	e,f
6. Tilted N-S Axis, $\beta = L$	$\cos \delta$	c,e
7. Adjusted N-S Axis, $\beta = L - \delta$	$[1-\sin^2 \delta \cos^2 \delta (1-\cos H)^2]^{1/2}$	c,e
Two Axis Tracking		
8. Normal at all times	1.	c,e

Notes:

a) Flat-plate collectors only
b) Limit hour angle to $\pm 90^{\circ}$
c) Limit tracking to $\pm 60^{\circ}$ to prevent shading
d) Focusing collector only
e) Both focusing and flat-plate collectors
f) $\beta = \text{Tan}^{-1} [(\sin L \cos \delta \cos H - \cos L \sin \delta)/(\cos L \cos \delta \cos H + \sin L \sin \delta)]$

Figures 3-2 through 3-13 for the various collector deployment schemes. For the tracking collectors, only hour angles less than 60^{o} were considered useful because shadowing is expected to become excessive for greater angles. These data are suitable for estimating annual collector output, and unless storage is involved, the complete system operation can be estimated. When storage is used, so the thermal output is not necessarily used in the hour of its output, system performance is difficult to estimate from these statistics.

For the ambient air temperature and wind speed, frequency distributions of the hourly values were made for the 1959 Albuquerque data. These are shown in Figures 3-14 and 3-15.

From Figure 3-14 the average temperature appears to be about 14 ^{o}C. However, the average temperature for the hours of collector operation would be higher than the average for all hours. Figure 2-4 indicates a difference between daytime mean and daily mean of slightly more than 1 ^{o}C, which suggests 15 ^{o}C as a reasonable average ambient temperature for systems operating in Albuquerque.

Maximum wind velocity for structural requirements has been placed at 60 m/s (≈120). This is a condition for survival of components and not an operating condition. As observation of the data in Figure 3-15 suggests that, If 1959 is a typical year, winds exceeding 15 m/s (30 mph) are rare and this velocity might be an acceptable upper limit on design for operation.

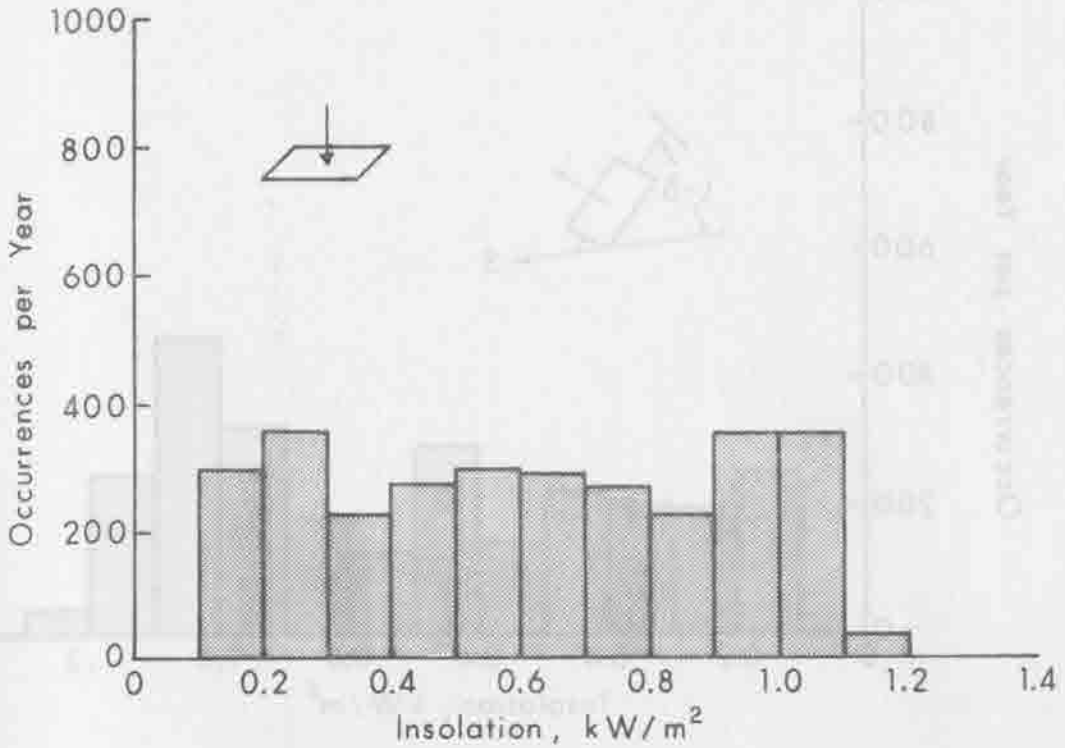

Figure 3-2. Hourly Insolation Statistics, Horizontal Flat-Plate Collector. Albuquerque Data, 1959.

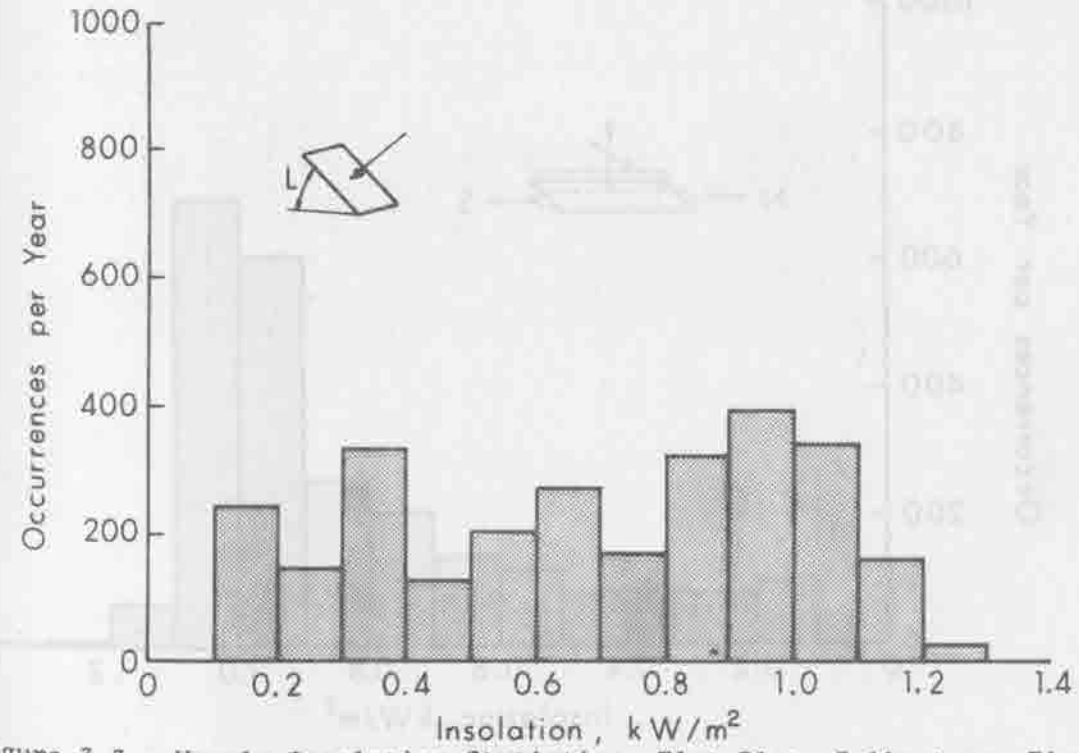

Figure 3-3. Hourly Insolation Statistics, Flat-Plate Collectors, Fixed Tilt Equal to Latitude. Estimated from Albuquerque Data, 1959.

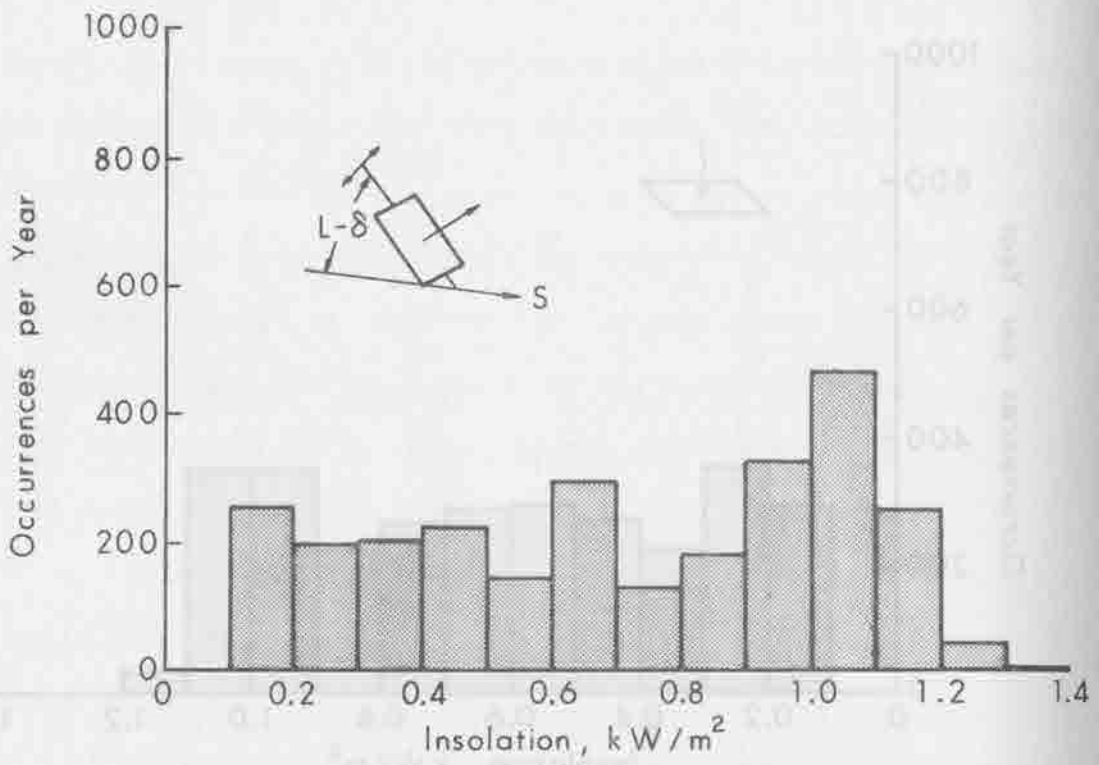

Figure 3-4. Hourly Insolation Statistics, Flat-Plate Collector, Seasonally Adjusted Tilt Equal to Latitude Minus Declination. Estimated from Albuquerque Data, 1959.

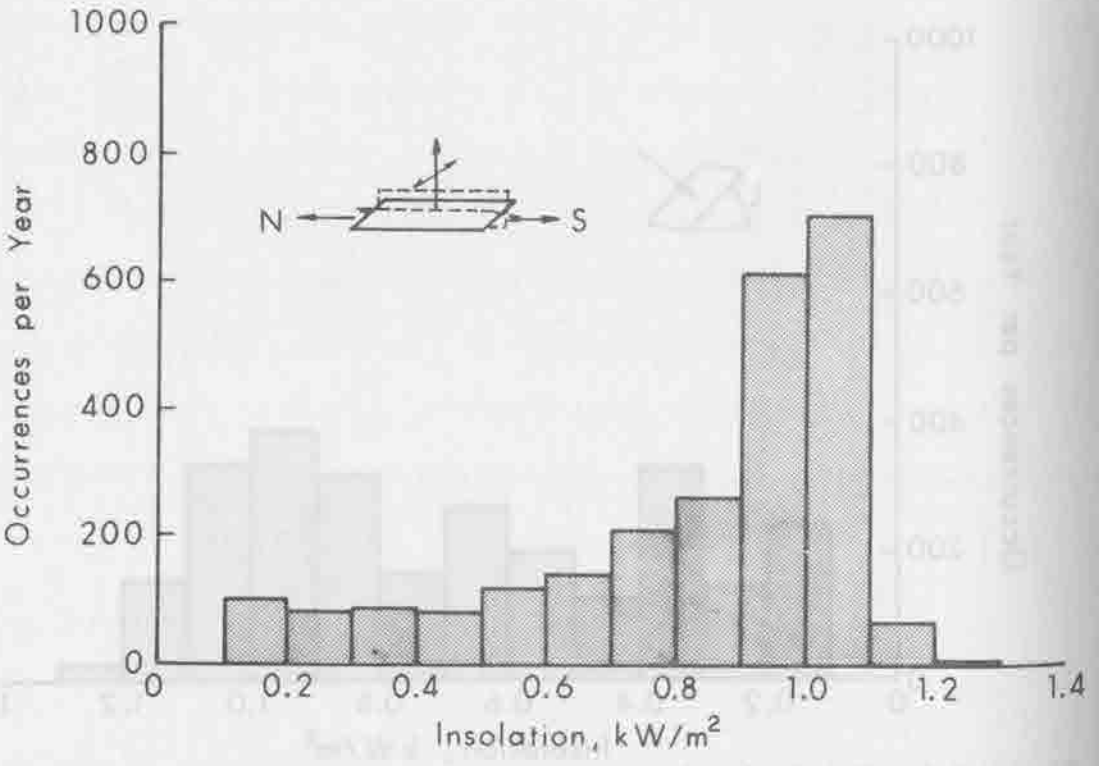

Figure 3-5. Hourly Insolation Statistics, Focusing Collector, North-South Horizontal Axis, East-West Tracking. Estimated from Albuquerque Data, 1959.

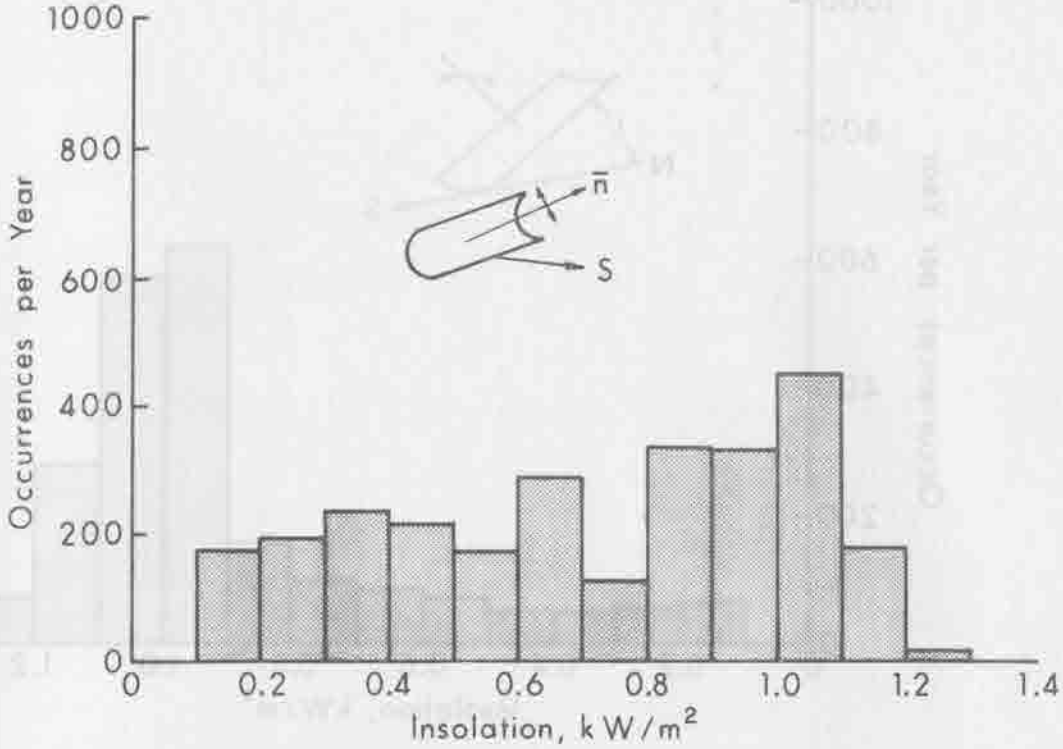

Figure 3-6. Hourly Insolation Statistics, Focusing Collector, East-West Axis, Tilt to Sun Elevation Angle. Estimated from Albuquerque Data, 1959.

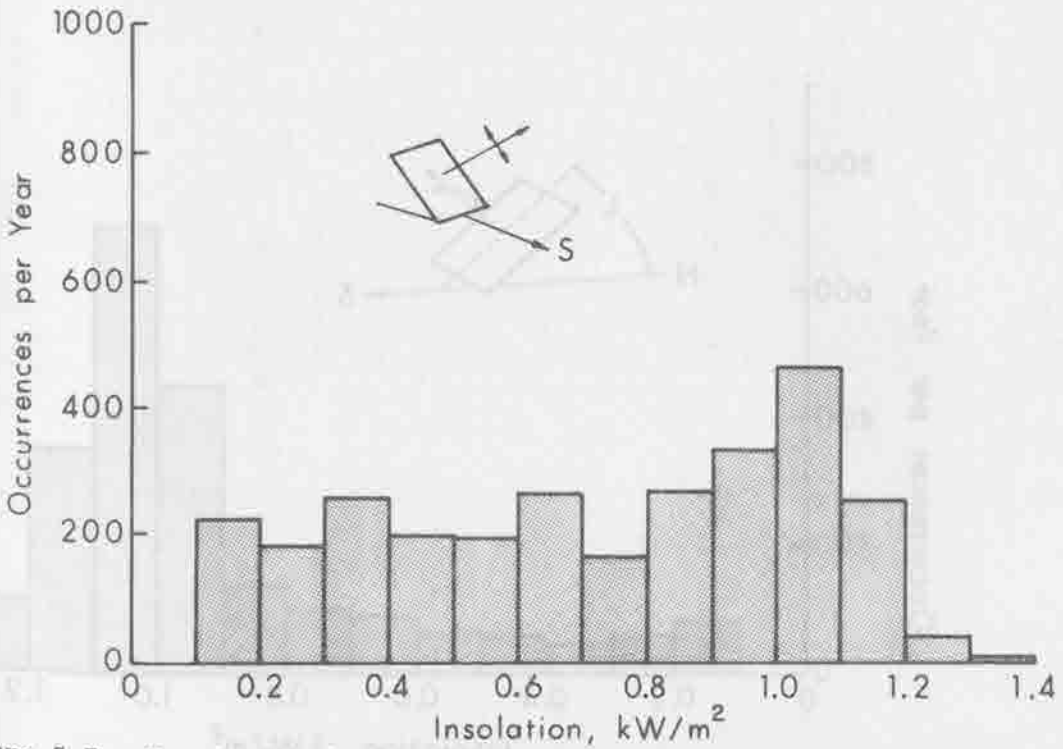

Figure 3-7. Hourly Insolation Statistics, Flat-Plate Collector, Tilt Continuously Adjusted to Sun Elevation Angle. Estimated from Albuquerque Data, 1959.

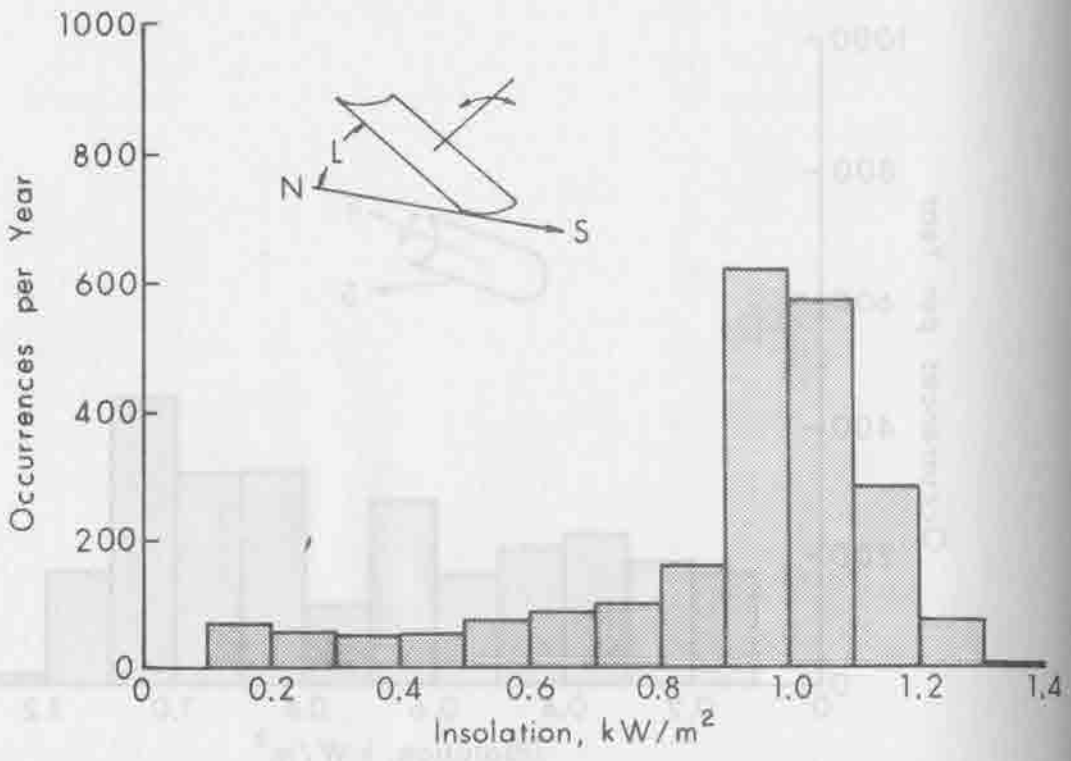

Figure 3-8. Hourly Insolation Statistics, Focusing Collector, Tilted on North-South Axis, Tracking East to West. Estimated from Albuquerque Data, 1959.

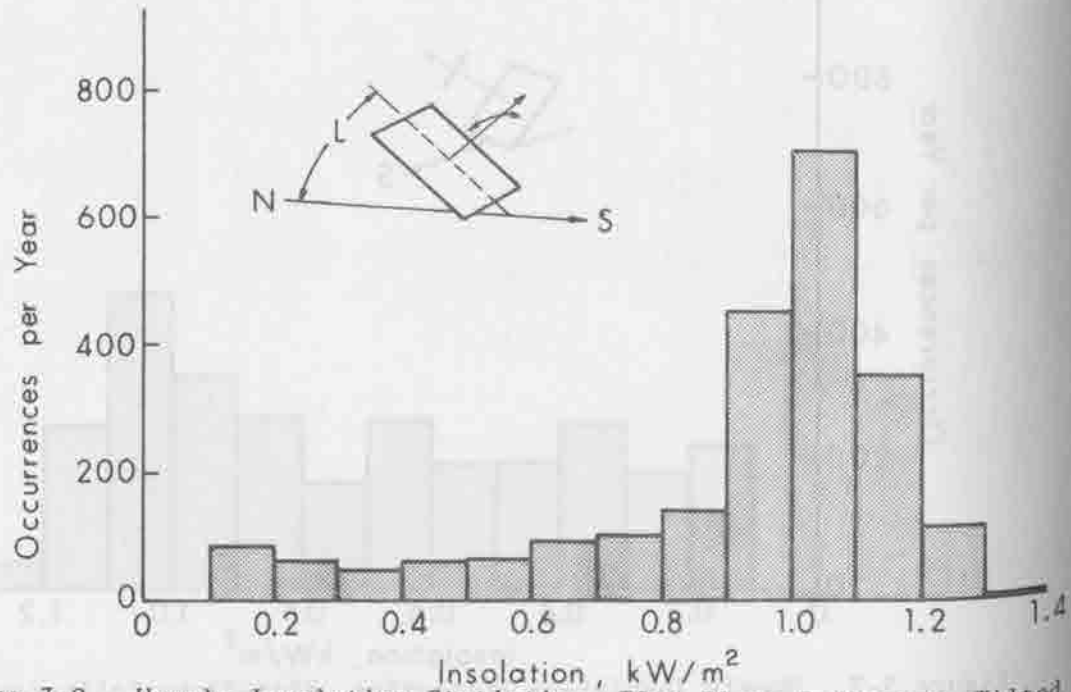

Figure 3-9. Hourly Insolation Statistics, Flat-Plate Collector, Tilted on North-South Axis, Tracking East to West. Estimated from Albuquerque Data, 1959.

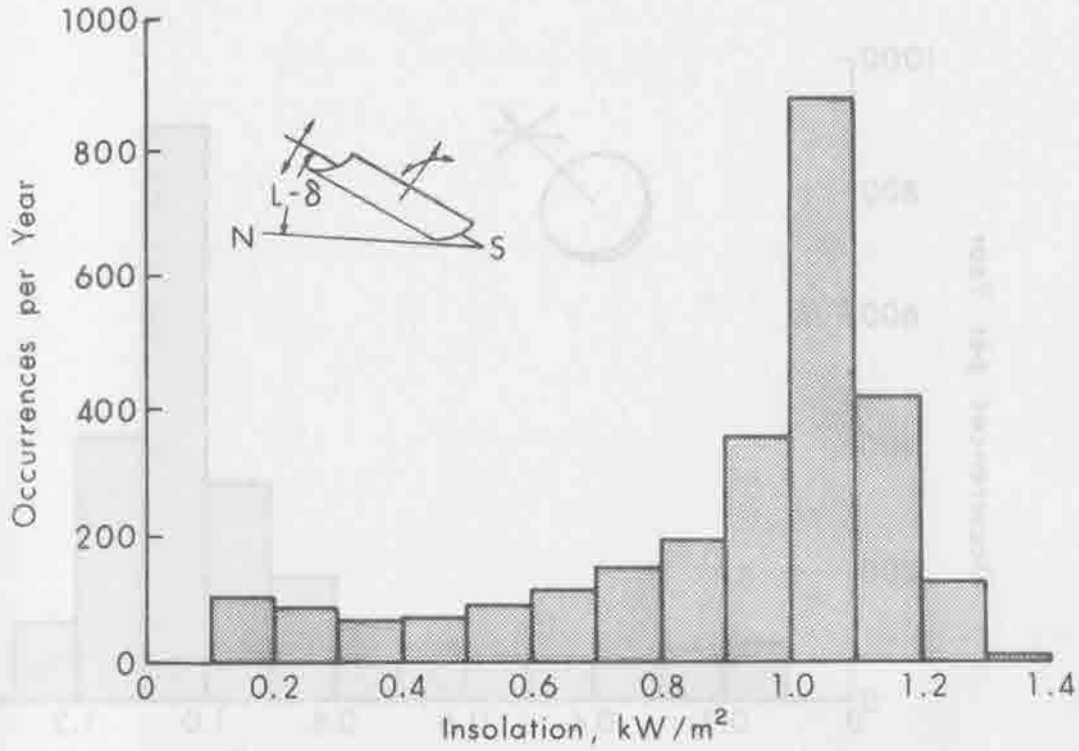

Figure 3-10. Hourly Insolation Statistics, Focusing Collector on Seasonally Adjusted Tilt, North-South Axis. Estimated from Albuquerque Data, 1959.

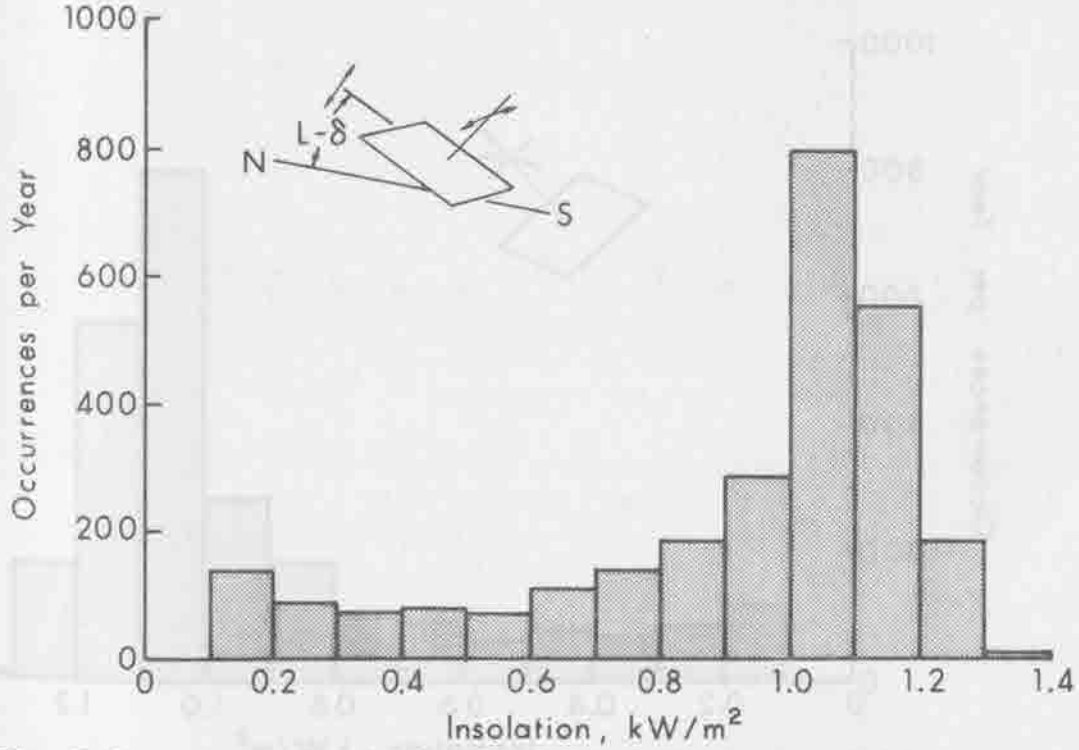

Figure 3-11. Hourly Insolation Statistics, Flat-Plate Collector on Seasonally Adjusted Tilt, North-South Axis. Estimated from Albuquerque Data, 1959.

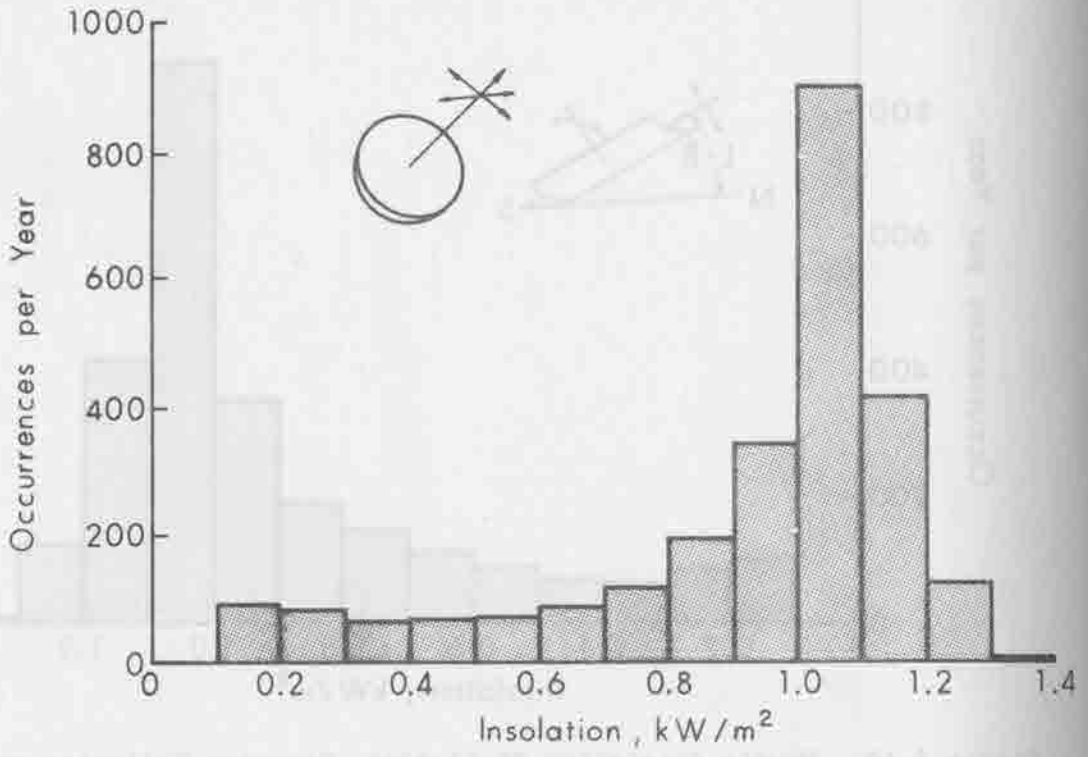

Figure 3-12. Hourly Insolation Statistics, Focusing Collector, Two-Axis Tracking. Estimated from Albuquerque Data, 1959.

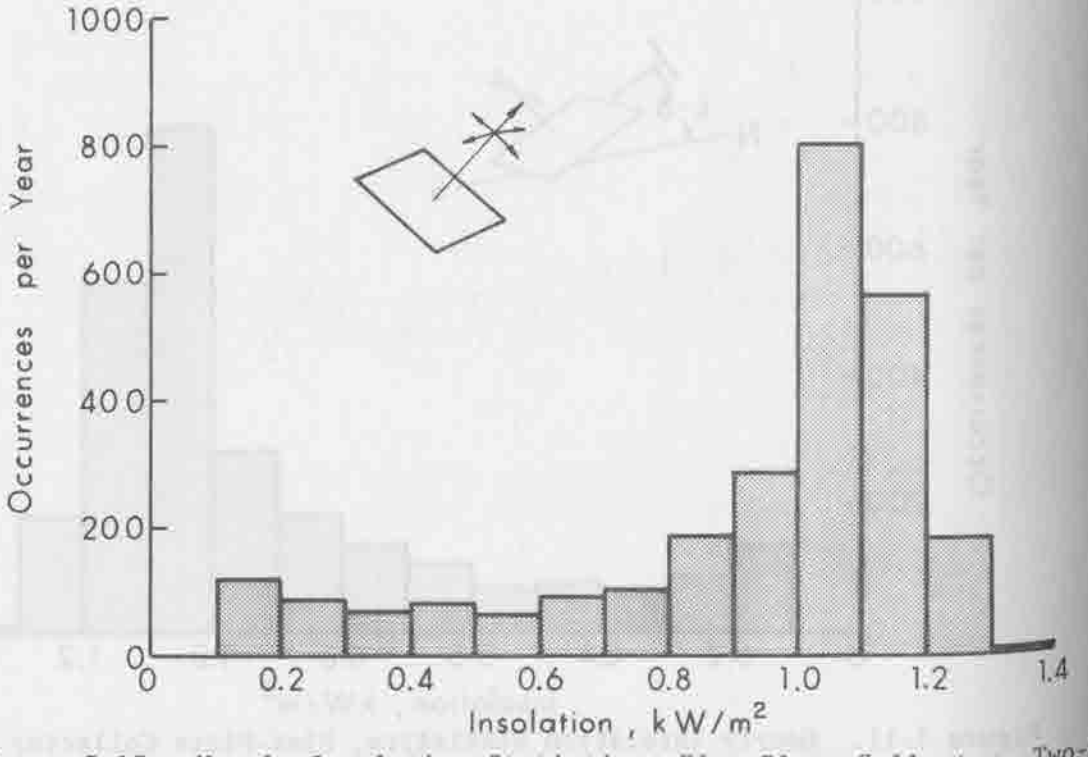

Figure 3-13. Hourly Insolation Statistics, Flat-Plate Collector, Two-Axis Tracking. Estimated from Albuquerque Data, 1959.

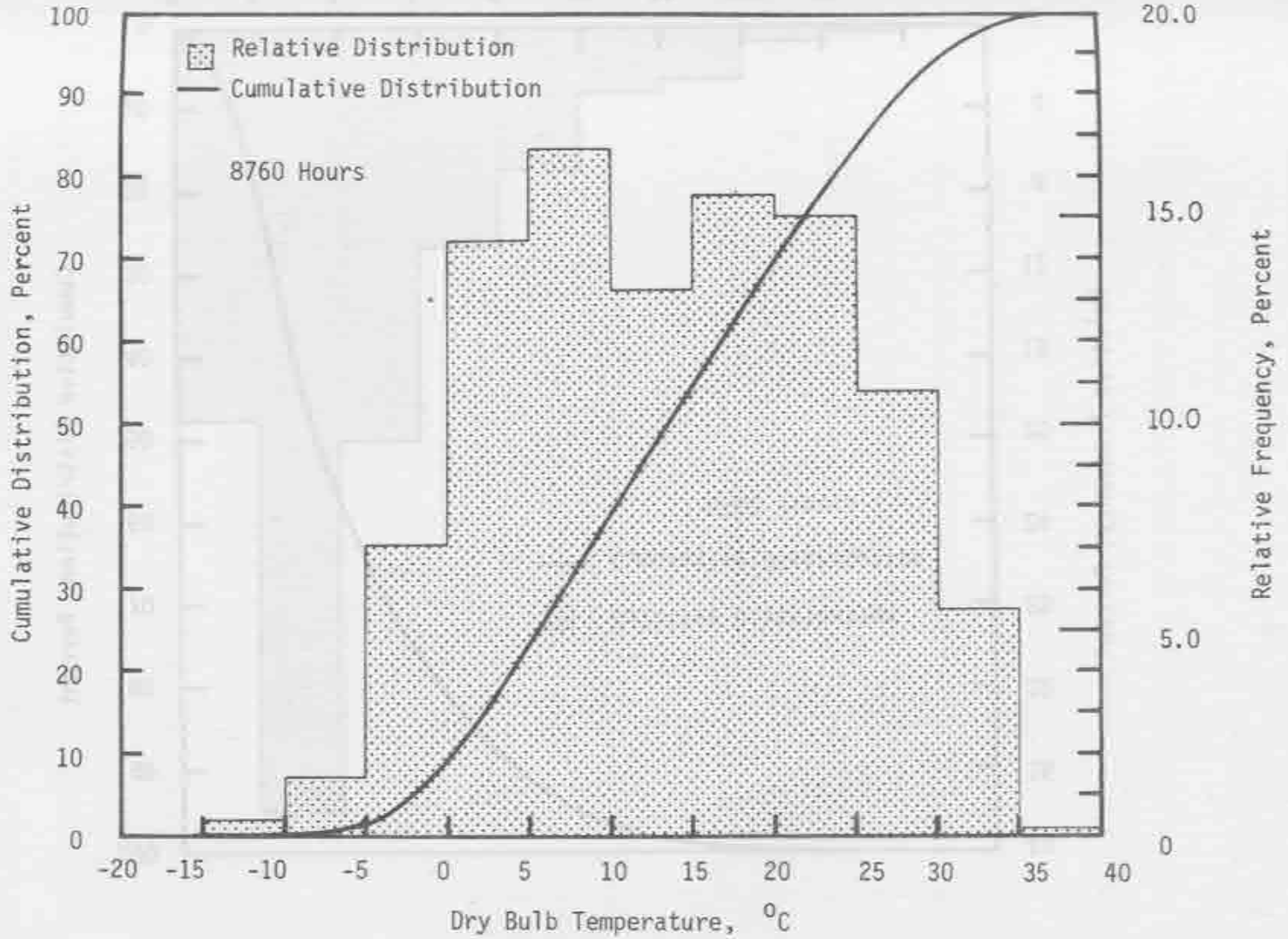

Figure 3-14. Ambient Temperature Data, Albuquerque, N.M., 1959

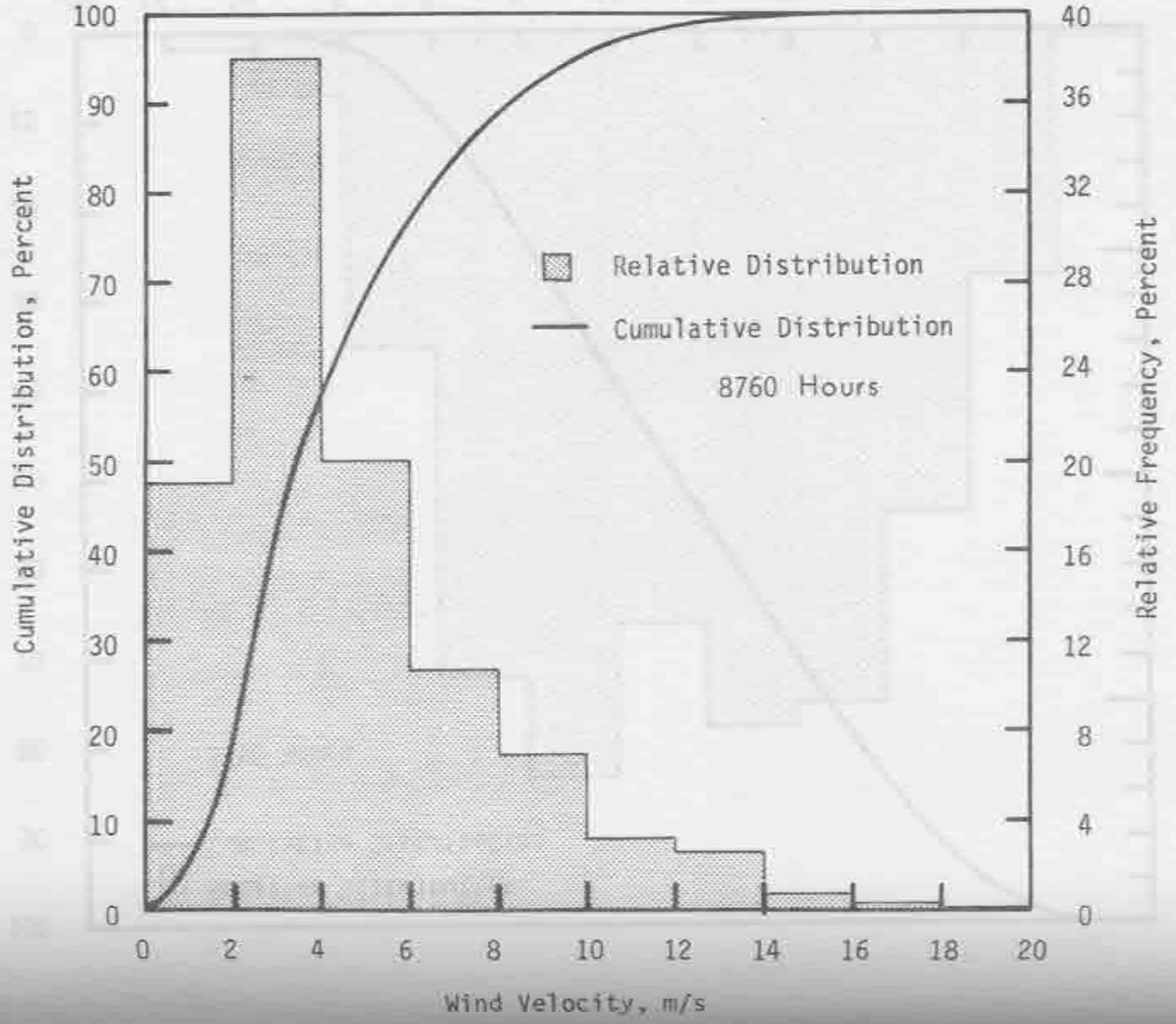
Cumulative Distribution, Percent
Relative Frequency, Percent
Relative Distribution
Cumulative Distribution
8760 Hours
Wind Velocity, m/s
0
10
20
30
40
50
60
70
80
90
100
0
4
8
12
16
20
24
28
32
36
40
0
2
4
6
8
10
12
14
16
18
20

4.0 MARKOV INSOLATION MODEL

It was noted above that the statistics taken from the insolation data are reliably used for system performance estimates only if heat storage is not employed. A statistical description of insolation which could be usable even with storage is the Markov model.

In this model the insolation is described by the probabilities that it will have a certain value during a given hour. The probabilities of occupying a given level may be different for each hour of daylight, in which case the model is non-stationary. Furthermore, in a first-order Markov model, the probabilities depend on the insolation value of the previous hour. In a second-order model the dependence would go back to the two previous hours.

If a practical Markov model were developed it could represent as many years of data as were available for a site and the model could be used to compute the output of a complex system in lieu of an hour-by-hour simulation.

The data for 1959 was analyzed to see whether, as a Markov process the model was first or second order and whether it was stationary. Conditional transition probabilities were calculated which indicated that the process was first-order but non-stationary. In addition, the transition probabilities depended upon the season as indicated by the declination angle.

Therefore to describe the process, a probability matrix must be determined for each combination of four to six declination angles ranges and eight to twelve hours of the day. In this application, the Markov model apparently has no advantage over direct simulation with one year of data.

5.0 CONCLUSIONS AND RECOMMENDATIONS

The site which received the most detailed data analysis was Albuquerque, New Mexico. Data for other sites is available for simulation of the most suitable candidate systems and preliminary analyses have been made for El Paso and Inyokern data.

In the analysis of any of the insolation data, the greatest shortcoming is the necessity for estimating diffuse insolation in order to compute direct insolation and adjust it to various collector angles. Where accurate systems analyses are required either direct or diffuse insolation must be known as well as the total, so that realistic estimates of direct normal insolation are available.

APPENDIX D

FLAT-PLATE COLLECTORS

BY

C. D. BEACH

AND

L. BALL

1.0 INTRODUCTION

Flat-plate (non-concentrating) collectors are suitable for producing heat at temperatures to 100 °C or in some cases 150 °C. In solar thermal electric power generation, flat-plate collectors could be used to heat water or another working fluid from the condenser fluid outlet temperature to the 100 - 150 °C range. If this is the maximum temperature required by the plant design, the whole collector field might consist of flat-plate collectors. If higher temperatures are needed the output of the flat-plate collectors could be delivered to concentrating collectors.

A great number of articles have been published regarding the collection of heat by flat-plate collectors (see for example, Hottel and Woertz (1942) and Whillier (1967)), so this appendix only outlines the methods used during this project to analyze the performance of flat-plate collectors.

Optimization depends upon cost estimates as well as performance estimates and, of the two, cost estimates are the harder to verify. In the later sections of this appendix some example cost estimates are shown and related to the performance to indicate the general range of the lowest cost heat from flat-plate collectors.

2.0 COLLECTOR DESIGN CONCEPTS

The goal of flat-plate collector design is to reduce energy losses to the limit that is practical with low cost, long-lasting materials and simple construction. Losses considered are described in the succeeding section in three categories: optical losses, conduction-convection losses and radiation losses.

The basic flat-plate collector consists of a heat absorbing surface with arrangements to reduce thermal losses. The absorbing surface contains channels or tubes for the flow of fluid to remove the collector heat. Figure 2-1 illustrates the concept using two pieces of glass to reduce losses through the front and insulation to reduce losses through the back. Some variations on this basic concept are described below.

2.1 Loss Reduction Techniques

Losses which reduce collector efficiency were listed above in three categories; optical loss, conduction-convection loss and radiation loss.

2.1.1 Optical Losses

The optical loss factor accounts for the fraction of incident radiant energy that is never absorbed by the collector. This factor depends upon

1) Transmittance of the glazing surfaces as affected by surface reflectivity and internal absorption. Transmittance depends, in part, on angle of incidence.
2) Absorptivity to solar radiation, α, of the absorbing surface,
3) Losses attributable to dirt on the glazing and the shading of the absorber by side walls and cover supports.

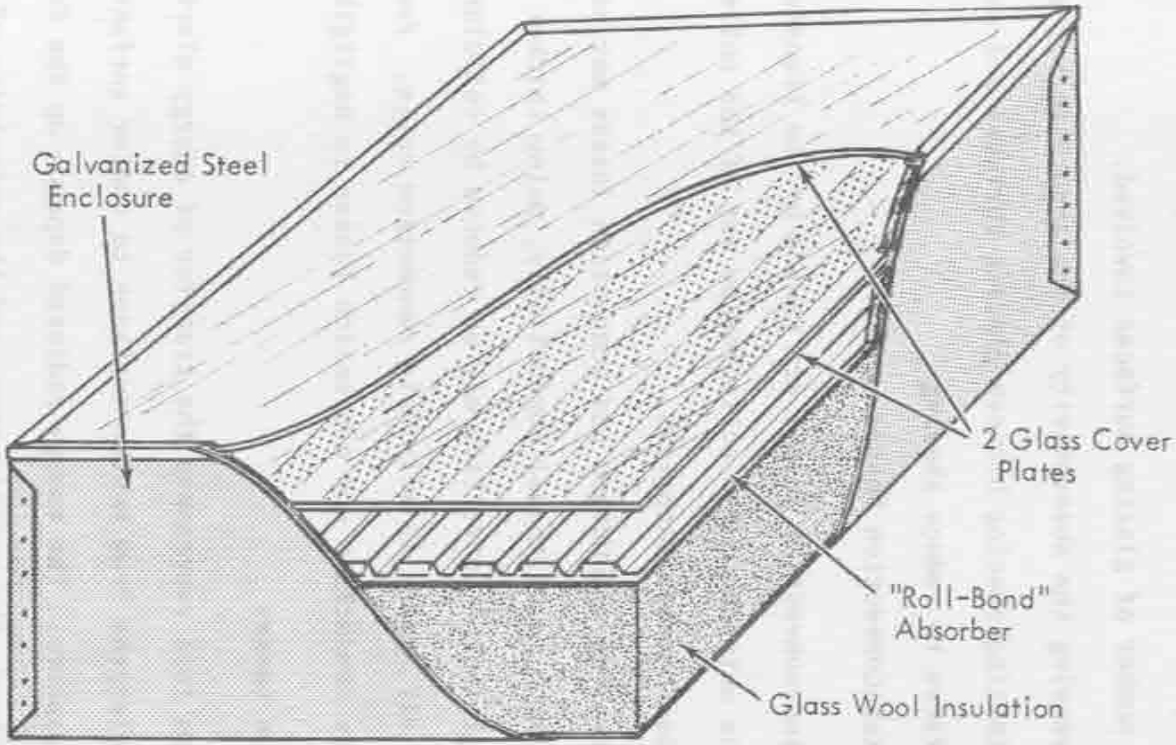

Figure 2-1. Flat Plate Collector with Two Glass Cover Plates.

Optical losses are of special concern because the represent high quality energy that is available, but rejected by the collector. Reduction of these losses is possible by:

1) Increasing transmittance of glazings. This means reducing surface reflectivity by special chemical processes, reducing absorptivity of the glass by reducing iron content and reducing the number of glazing surfaces involved.
2) Increasing the absorptivity of the absorbing surface.
3) Minimizing spacing between glazing surfaces and absorbing surfaces to reduce shading.

2.1.2 Conduction-Convection Losses

Conduction-convection losses are caused by the transfer of heat from the inside to the outside of the collector by way of the collector materials and the air spaces between materials.

The control of conduction and convection losses may be accomplished by using materials with lower themal conductivity, using thicker insulation and more layers of glazing. Convection may be reduced by cellular structures such as honeycomb in air spaces to eliminate convection cells. Evacuation of air spaces may reduce conduction and convection losses to negligible levels.

2.1.3 Radiation Losses

Radiation loss represents the transfer of energy electromagnetically at infrared wavelengths from hotter surfaces to cooler surfaces on to the surrounding atmosphere. The energy radiated depends on the fourth power of absolute temperature, the surface area, and the emissivity of the surface.

Radiation losses are reduced by surface treatments that decrease the emissivity and by shielding the absorber with more layers of glazing. Some surface geometric arrangements are helpful to reducing radiation by keeping hotter surfaces radiating toward only slightly cooler ones. Honeycomb structures, for example, provide some reduction of radiation loss as well as the reduction in convection loss.

From the brief description of losses, above, it is apparent that there is a trade-off necessary between the optical losses and the thermal losses (radiation, conduction and convection). For example using more layers of glazing reduces thermal losses but increases the optical losses. Similarly a honeycomb structure between the absorber and the glazing lowers thermal losses, but it adds to optical losses by blocking some of the incident energy before it reaches the absorber. Even the reduction of heat radiation losses by lower surface emissivity to infrared wavelengths cannot be accomplished without some penalty in the absorptivity of the surface to the solar spectrum.

2.2 Collector Orientation

The intensity of radiation on flat-plate collectors is reduced by the cosine of the angle from the collector to the sun. There may be an advantage to having the collector tilt fixed, however, because the expense of installing and maintaining a large number of flexible pipe joints may not be justifiable. These effects are analyzed quantitatively in subsequent sections. An additional effect of collector orientation is the reduced transmittance of glass and reduced absorptivity of surfaces at angles of incidence greater than about 45^{o}. These effects are evaluated below.

2.3 Design Classification

One approach to classification of suitable flat-plate collector types is shown in Table 2-1. The table includes variations in the absorber design, the loss control techniques and the orientation or deployment conditions. Because this project is a study of electric power generation, only collectors designed for heating liquids were considered.

Also for purposes of this study, plastic glazings were excluded. Clear plastics are deteriorated by ultra-violet light and have not been

TABLE 2-1

CLASSIFICATION OF SOLAR FLAT-PLATE COLLECTORS
(Non-Focusing)

1. Types of Absorbers
   a. Metal surfaces with internal tubes
   b. Metal surfaces with attached tubes
   c. Individual metal tubes

2. Types of Glazings
   a. Single layer of glass
   b. Multi-layers of glass

3. Types of Surfaces
   a. Flat black paints, oxides, enamels
   b. Selective black, low emittance coatings
   c. Transparent honeycomb
   d. Scratched, finned, or roughened surface

4. Types of Deployment
   a. Horizontal
   b. Stationary, tilted
   c. Periodic tilt angle adjustment
   d. Continuous tilt angle adjustment
   e. Continuous, single-axis, east-west adjustment, constant tilt angle
   f. Continuous double-axis adjustment

5. Radiation Augmentation
   a. Adjacent non-specular reflective areas
   b. Adjacent specular reflective areas

6. Special Collector Combinations
   a. Evacuated glass tube with internal flat absorber-liquid or gas heater, Speyer (1964)
   b. Evacuated plate, Blum et al (1973)
   c. Liquid heater using semi-transparent surfaces, Lumsdaine (1969)
   d. Collector irradiated from both faces, Souka and Safwat (1969)

shown to offer life-cycle cost advantages over glass. Used behind glass, plastics may perform acceptably, but since the use of plastic does not greatly reduce overall collector costs, this analysis has been made with glass for glazings, and the sensitivity to the cost of the glazing is shown in the final section on estimated costs.

3.0 ANALYTICAL MODELS

Mathematical analysis of flat-plate collector performance is very well summarized by Whillier (1967). His methods were used with a few variations described below to write computer programs that predict heat losses and collector efficiency under the full range of ambient conditions and for the design variables described in Table 2-1, above.

3.1 Collector Heat Balance

Under static operating conditions the useful heat removed per unit area of collector is the difference between the absorbed energy and the thermal losses.

$$q_u = IF_e \cos \theta_c - U_L(T_c - T_a) \qquad (3\text{-}1)$$

where

I is the incident solar radiation, watt/m^2

F_e is the effective net absorptivity of the collector

θ is the angle between the sun and the collector normal

U_L is the total collector loss rate at temperature T_c, $W/m^2\ ^oC$

T_c is average collector surface temperature ^oC, and

T_a is ambient temperature, ^oC.

The useful heat can be expressed as an enthalpy change in the collector fluid, but for liquid flow it is approximately correct to write

$$q_u = \dot{m}\, C_p(T_o - T_i) \qquad (3\text{-}2)$$

where

$\dot{m}$ is fluid flow rate, kg/hr

C_p is specific heat of the fluid at the average temperature W-hr/kg ^oC

T_o is fluid outlet temperature, ^oC, and

T_i is fluid inlet temperature, ^oC.

The remainder of this section is a description of the computation of thermal loss coefficient, U_L, and the elimination of the collector temperature dependence in Equation 3-1.

3.2 Optical Losses

The fraction of the incident energy that is absorbed by the collector depends on the transmissivity of glazing, the absorptivity of the absorber surface, and the angle of incidence of the insolation on the collector.

Figures 3-1 through 3-4 show the calculated absorbed energy as a fraction of incident energy for one through four glass covers, and plate absorptivities of 0.9 and 0.95. Normal and low reflectivity glass are compared, both with attenuation in the glass of 0.2 per inch. Glass 1/8 inch thick is assumed. The absorbed energy begins to decrease markedly for angles of incidence greater than 45 degrees. Computed energy capture is based on the methods described by Whillier (1967) and account for multiple reflections between glazing-air interfaces.

The angular dependence of the optical losses in the curves of Figures 3-1 through 3-4 is for F_e only and is in addition to the cos θ_c dependence shown in Equation (3-1).

3.3 Conduction-Convection Losses

Conduction and convection losses depend on:

1) Average temperature of the absorbing plate
2) Ambient air temperature and wind speed
3) Number of glass covers and, to a minor extent, their spacing
4) Rear and edge insulation

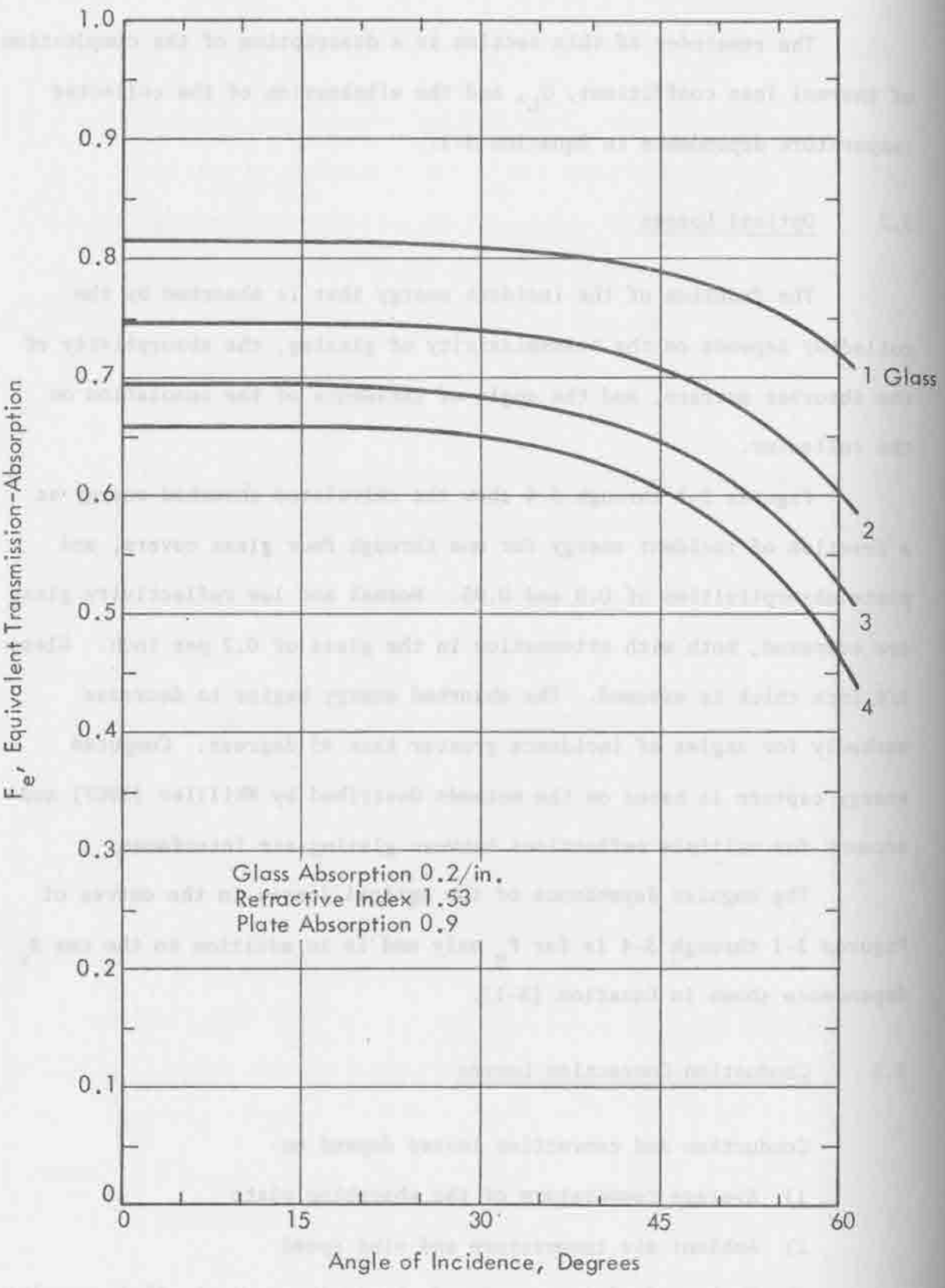

Figure 3-1. Fraction of Incident Energy Absorbed by a Flat-Plate Collector.

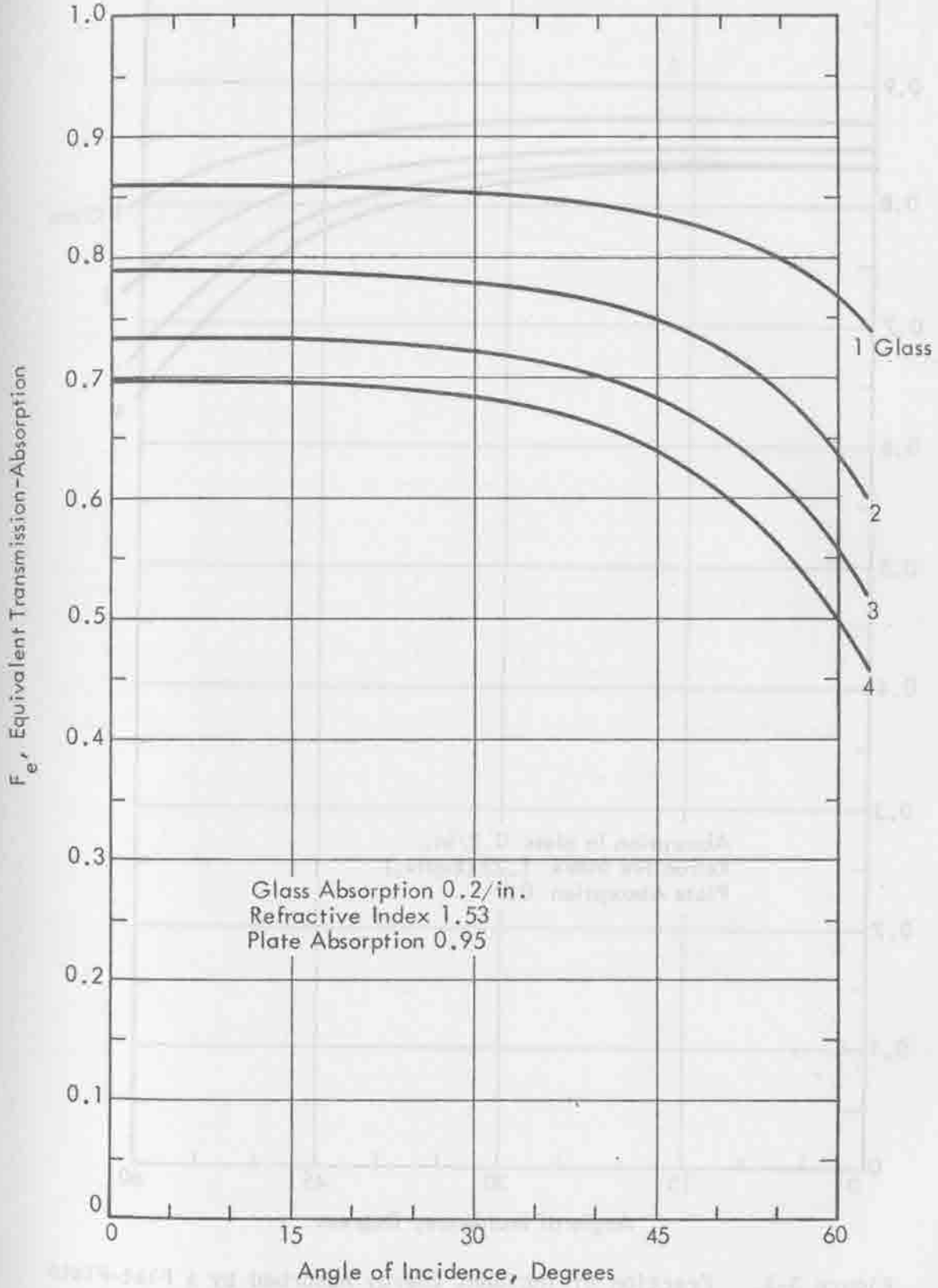

Figure 3-2. Fraction of Incident Energy Absorbed by a Flat-Plate Collector.

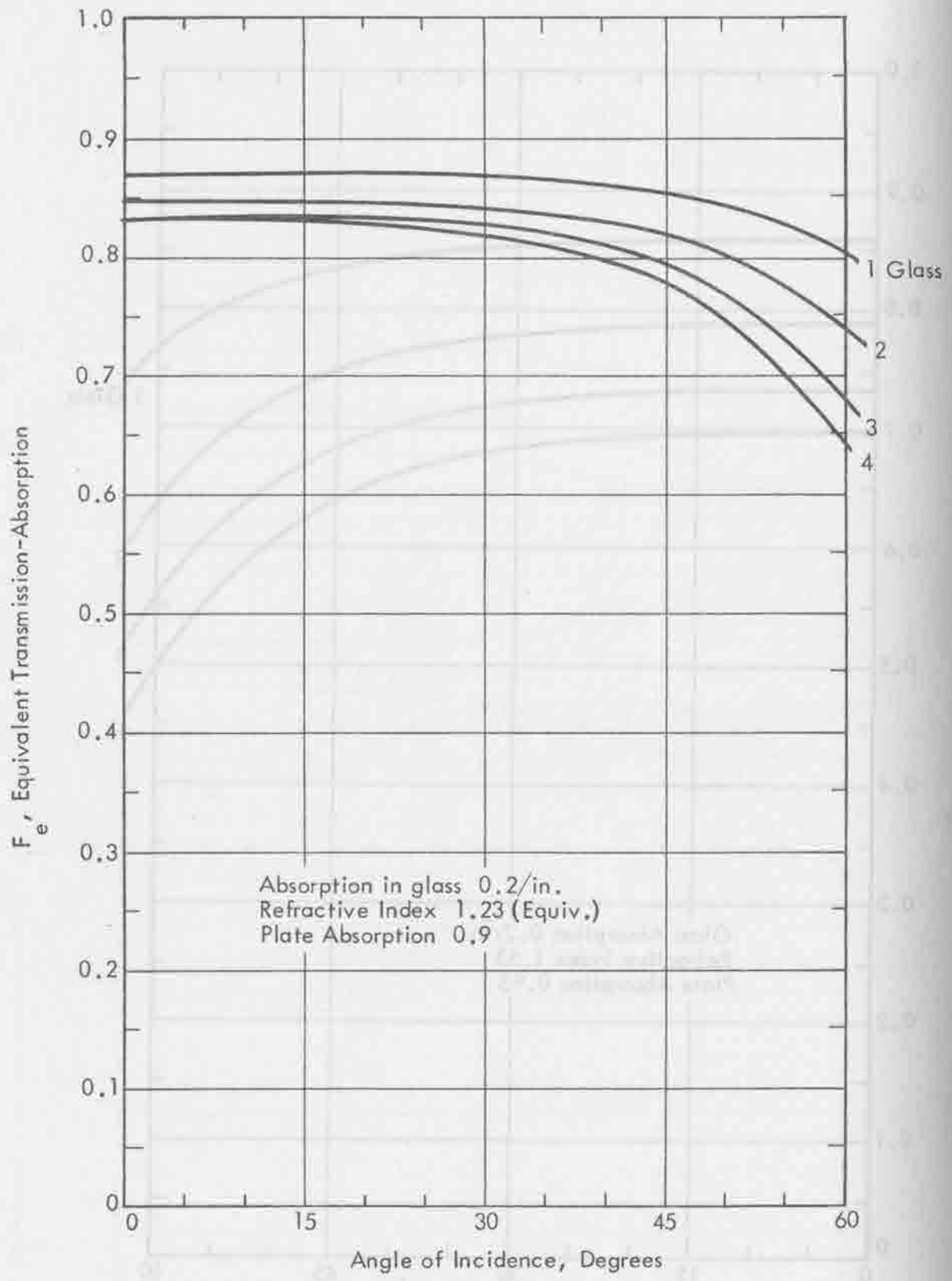

Figure 3-3. Fraction of Incident Energy Absorbed by a Flat-Plate Collector with Low Reflectivity Glass.

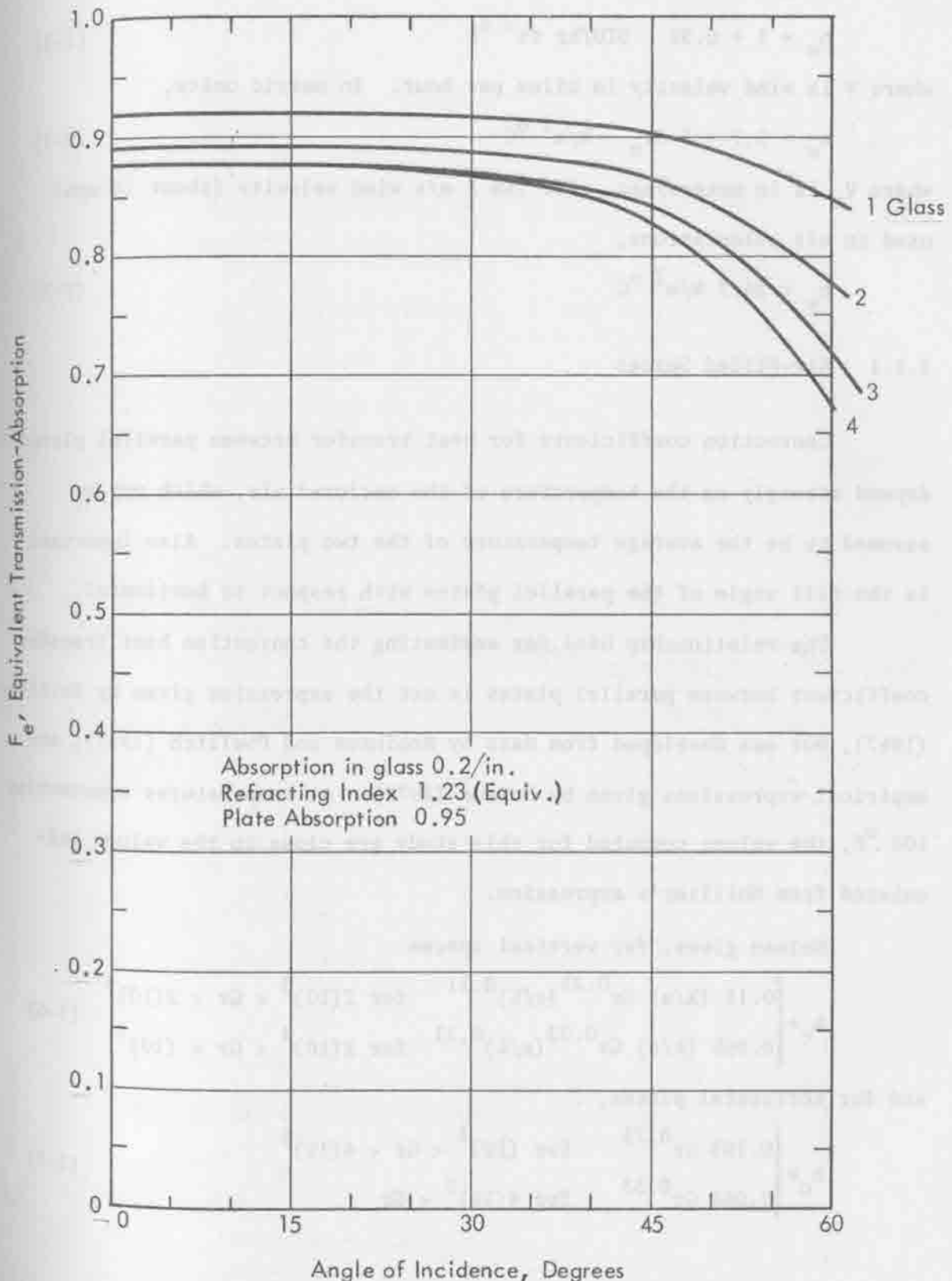

Figure 3-4. Fraction of Incident Energy Absorbed by a Flat-Plate Collector with Low Reflectivity Glass.

The convection loss coefficient from the outer glass surface to the air is given by Whillier (1967) as

$$h_w = 1 + 0.3V \quad \text{BTU/hr ft}^2\,^{\circ}\text{F} \tag{3-3}$$

where V is wind velocity in miles per hour. In metric units,

$$h_w = 5.7 + 3.8V_m \quad \text{W/m}^2\,^{\circ}\text{C} \tag{3-4}$$

where V_m is in meters/sec. For the 5 m/s wind velocity (about 10 mph) used in all calculations,

$$h_w = 24.7 \text{ W/m}^2\,^{\circ}\text{C} \tag{3-5}$$

3.3.1 Air-Filled Spaces

Convection coefficients for heat transfer between parallel plates depend strongly on the temperature of the enclosed air, which may be assumed to be the average temperature of the two plates. Also important is the tilt angle of the parallel plates with respect to horizontal.

The relationship used for estimating the convection heat transfer coefficient between parallel plates is not the expression given by Whillier (1967), but was developed from data by Robinson and Powlitch (1957), and empirical expressions given by Holman (1972). At temperatures approaching 100 $^{\circ}$F, the values computed for this study are close to the values calculated from Whillier's expression.

Holman gives, for vertical spaces

$$h_c = \begin{cases} 0.18\ (k/s)\ Gr^{0.25}(s/L)^{0.11} & \text{for } 2(10)^3 < Gr < 2(10)^4 \\ 0.065\ (k/s)\ Gr^{0.33}(s/L)^{0.11} & \text{for } 2(10)^4 < Gr < (10)^7 \end{cases} \tag{3-6}$$

and for horizontal plates,

$$h_c = \begin{cases} 0.195\ Gr^{0.25} & \text{for } (10)^4 < Gr < 4(10)^5 \\ 0.068\ Gr^{0.33} & \text{for } 4(10)^5 < Gr \end{cases} \tag{3-7}$$

where Gr is the dimensionless Grashof number given by

$$Gr = \frac{9.8\, s^3}{\nu^2} \frac{(T_1 - T_2)}{T_{av}} \qquad (3\text{-}8)$$

and

s = plate spacing, meters

k = thermal conductivity of air at T_{av}, in W/m ^{o}K

L = length of vertical rise in plates, meters

ν = kinematic viscosity of air at T_{av}, in m^2/sec

T_1, T_2 = plate temperatures, ^{o}K, and

$T_{av} = (T_1 + T_2)/2$ in ^{o}K

Within the range of temperatures of interest for flat-plate collector operation, Gr varies from 5000 to 40,000 and the useful tilt angles vary from horizontal to vertical. The data of Robinson and Powlitch (1957) for parallel plate at 45^{o} tilt show variations in heat transfer with $(T_1 - T_2)$ to leave an exponent 0.3, intermediate between the 0.25 and 0.33 exponents in the equations above. To simplify computation, $Gr^{0.3}$ was used for all temperatures and tilt angles in the flat-plate collector analysis.

Both k and ν vary with average temperature so their temperature variation was included in the expression for h_c. Over the range of $250\ ^{o}K < T_{av} < 450\ ^{o}K$,

$$k = 1.83(10)^{-4}\, T_{av}^{0.87} \qquad W/m\ ^{o}K \qquad (3\text{-}9)$$

and

$$\nu = 7.2(10)^{-10}\, T_{av}^{1.75} \qquad m^2/sec. \qquad (3\text{-}10)$$

Then using a heat transfer coefficient of the form

$$h_c = \frac{C\, k}{s}\, Gr^{0.3} \qquad (3\text{-}11)$$

and substituting Equations (3-8), (3-9) and (3-10), the expression becomes

$$h_c = C' \frac{(T_1-T_2)^{0.3}}{T^{0.48}} \quad W/m^2\ {}^oK \tag{3-12}$$

Calculating the value of C' from the data of Robinson and Powlitch (1957) gives

$$C' = \begin{cases} 12, \text{ Vertical plates} \\ 17, \ 45^o \text{ Tilt to plates} \\ 20, \text{ Horizontal plates} \end{cases} \tag{3-13}$$

The constants in Equation (3-12) apply to spacings greater than 2 cm and change very little with increased spacing except for horizontal collectors. For horizontal collectors, the heat transfer coefficient decreases by the factor $(0.02/s)^{0.1}$ with spacing greater than 2 cm. Reducing the plate spacings below 2 cm. begins to suppress the convection, and the conduction eventually becomes the limiting effect. Then the heat transfer rate depends on 1/s.

3.3.2 Evacuated Spaces

As the air pressure is reduced between the absorber and the glass covering, first the convection heat transfer is eliminated and finally the conduction is reduced. With flat glass and flat absorber plates the pressure can be reduced only if the glass is supported. Some experimenters have done this (Blum et al, (1973)) to the extent of suppressing convection losses. However, using a cylindrical configuration, Speyer (1964) built experimental collectors with sufficient vacuum to make the conduction-convection losses negligible.

Figure 3-5 shows the decrease in heat transfer as the air pressure is reduced. The heat transfer coefficient approaches that of conduction only, as the air pressure is reduced to 0.01 atmosphere. Conduction effects, however, remain unchanged until the molecular mean free paths are comparable to the dimensions of the air space.

(see Teagan (1967)). At 10^{-7} to 10^{-6} atmospheres (10^{-4} to 10^{-3} Torr) the conduction loss is only about one percent of the conduction loss at atmospheric pressure.

Whether the pressure is reduced to 10^{-1} atmosphere or 10^{-7} atmosphere does not materially affect the structural support required to prevent implosion. However, a higher vacuum does require a higher quality seal, and implies a higher degree of difficulty in maintaining the vacuum.

3.4 Radiation

Heat exchange by thermal radiation between two surfaces depends on their temperatures, areas and the long wave emissivities of both surfaces. For extensive parallel plates the heat exchange rate is

$$Q_p = \frac{A\,\sigma\,(T_1^4 - T_2^4)}{\frac{1}{\varepsilon_1} + \frac{1}{\varepsilon_2} - 1} \quad \text{watts} \qquad (3\text{-}14)$$

where

A is the surface area of each plate, square meters

σ is the Stefan-Boltzmann constant, $5.67(10)^{-8}$ $W/m^2\ {}^oK$

T_1, T_2 are plate temperatures, ^oK, and

ε_1, ε_2 are surface emissivities at the respective plate temperatures.

For long concentric cylinders, Speyer (1964) for example, the equivalent expression is

$$Q_c = A_1\,\sigma\,(T_1^4 - T_2^4) \begin{cases} \dfrac{1}{\frac{1}{\varepsilon_1} + \frac{A_1}{A_2}\left(\frac{1}{\varepsilon_2} - 1\right)} & A_2 \text{ diffuse} \\ \dfrac{1}{\frac{1}{\varepsilon_1} + \frac{1}{\varepsilon_2} - 1} & A_2 \text{ specular} \end{cases} \qquad (3\text{-}15)$$

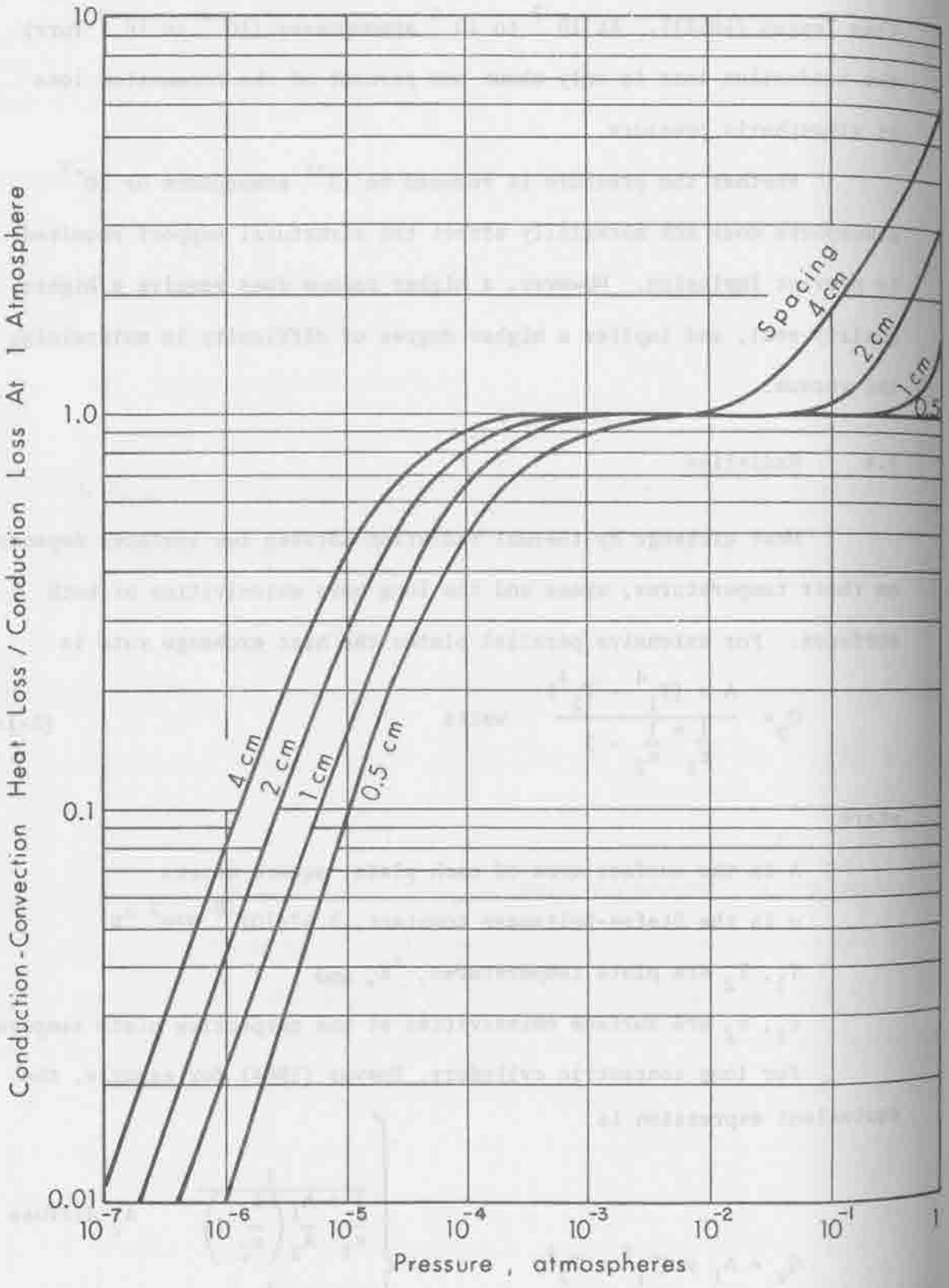

Figure 3-5. Relative Heat Loss vs. Pressure and Spacing. (Air Temperature less than 100°C).

where A_1 is the surface area of the inner cylinder and A_2 is the surface area of the outer cylinder. The expressions are unchanged when A_1 is specular or diffuse, but the heat transfer is reduced when A_2 is specularly reflecting.

In the evacuated tubes designed by Speyer, part of the glass tube was silvered to reduce radiation losses. However, when only a part of A_2 is reflective, there may be an insignificant reduction in radiated heat loss. Much of the reflected radiation escapes around the sides of the inner surface and is absorbed in the diffuse, upper portion of the glass envelope.

Radiation from a heated body to the surrounding atmosphere depends on the effective sky radiation temperature, T_s, and the heat loss expression is,

$$Q_s = A_1 \sigma \varepsilon_1 (T_1^4 - T_s^4) \quad \text{watts} \qquad (3\text{-}16)$$

Sky temperature determination is discussed in Appendix B. An accurate determination is tedious and was not attempted on a day-to-day basis. For most of the collector modeling, sky temperature was assumed to be 20 °C below the ambient temperature. The total collector heat loss is relatively insensitive to sky temperature. For example, in a collector with two glass covers, the heat loss is increased by about 7 percent by a 40 °C reduction in sky temperature. For 3 glass covers, the corresponding increase in losses is only about 4 percent.

3.5 Total Thermal Loss Coefficient, U_L

To compute the total collector heat loss rate, the convection and radiation loss coefficients are combined in parallel and series to represent the total heat conductance between the absorber to the surrounding air. See Whillier (1967), for example. However, the heat transfer coefficients depend on the temperatures of the surfaces involved,

and the estimated temperatures, in turn, are determined by the values of the heat transfer coefficient.

The solution, both for surface temperatures and inter-surface heat transfer coefficients, was determined by iteration - computing first the heat transfer coefficients from estimated temperatures, then the temperatures from the heat transfer coefficients. This was repeated until the estimated surface temperatures had changed less than 0.5 ^{o}C from the prior iteration.

After the heat loss rate through the front of the collector was determined by the iterative calculation described above, the loss coefficient was increased by ten percent to account for heat conducted through the back and sides of the collector. This represents a different insulation thickness for different collector designs, but varies between about 5 cm. and 20 cm..

3.6 Collectors Modeled

The types of flat-plate collectors specifically modeled for estimates of annual thermal energy output under conditions of fixed tilt, equal to the 35 degree latitude of Albuquerque, New Mexico, were:

1. Absorber with imbedded tubes, surface emissitivities of 0.9, 0.2 and 0.1, protected by 1, 2, 3 or 4 glass cover plates.
2. Honeycomb (transparent) between absorber and glass cover, Cunnington and Streed (1973). Optical properties of mylar were used although its temperature limits are inadequate for this application.
3. Evacuation between absorber and supported glass plate, a hypothetical and possibly impractical case.
4. Evacuated glass tubes with absorbers inside. Speyer (1964)

3.6.1 Multi-Layered Glass Covered Model

Heat loss coefficients were calculated for flat-plate collectors with varying number of glass covers and varying surface emissivities. The back and side losses were assumed to be ten percent of the loss through the glass covers. These loss rates are shown in Figures 3-6 through 3-8 for collector temperatures from 50 ^{o}C to 150 ^{o}C.

3.6.2 Honeycomb Designs

The placement of a honeycomb structure between the absorber plate and the cover glass controls heat losses in two ways:

1. Small honeycomb cells prevent the formation of air convection cells and reduce the conduction - convection loss to the conduction loss of the air in parallel with the conduction loss through the honeycomb material. This means the honeycomb material should be very thin-walled and have low thermal conductivity. The cells should be made small, but this increases the honeycomb material used and blocks more of the incoming light.
2. The honeycomb intercepts most of the re-radiated energy from the absorber before it can reach the cover glass. This produces an effective emissivity lower than that of the absorber plate alone. The honeycomb material should be opaque to infrared energy and have low reflectivity.

Several types of honeycomb materials have been tested by Cunnington and Streed (1973) to intercompare their performance. Even transparent honeycombs have a more limited allowable angle of incidence

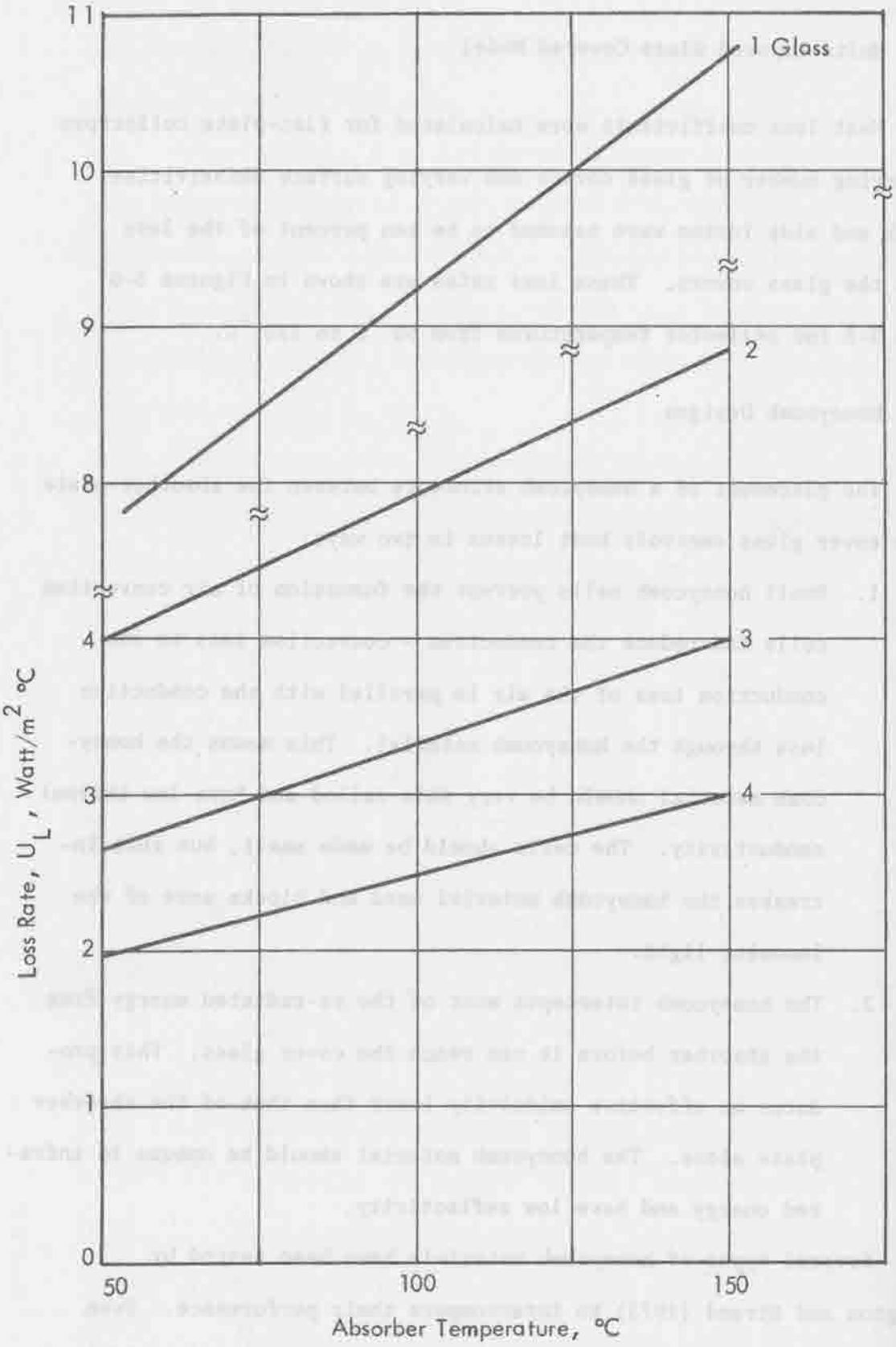

Figure 3-6. Flat-Plate Collector Loss Rates, ε = 0.9, Wind = 5m/s.

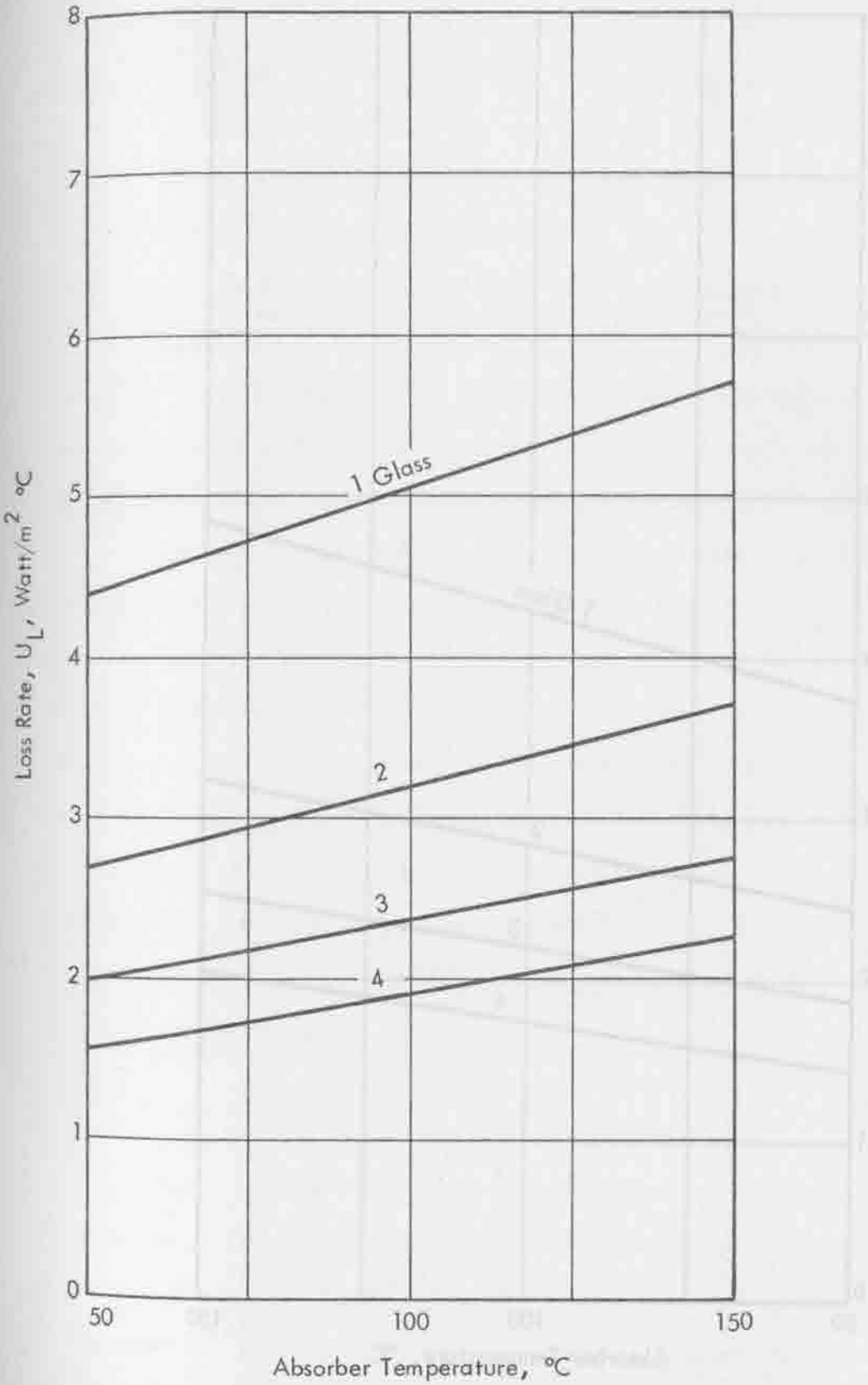

Figure 3-7. Flat-Plate Collector Loss Rates, ε = 0.2, Wind = 5m/s.

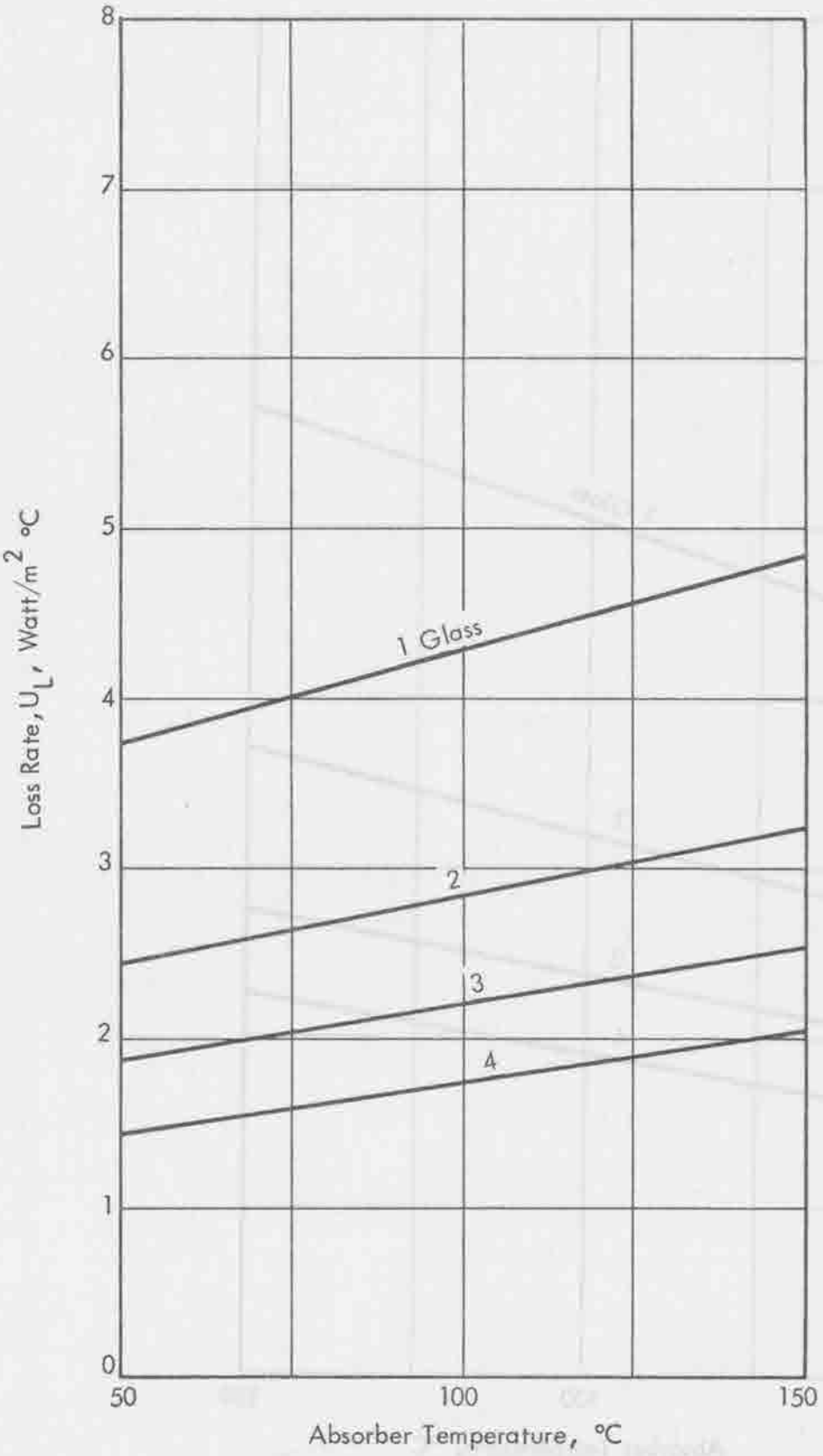

Figure 3-8. Flat-Plate Collector Loss Rates, ε = 0.2, Wind = 5m/s.

than flat-plate collectors with multiple glass covers. This problem could be overcome by having a movable collector, but movable collectors, in turn, produce other problems. Based on the results of Cunnington and Streed, the reduction in equivalent absorptivity for a honeycomb behind one piece of glass is shown in Figure 3-9. The result for low reflectivity glass was estimated from the measured data for normal glass

Mylar appears to be the most suitable honeycomb material tested, but it is certainly not ideal. One quality not evaluated was its performance at elevated temperatures and in this category mylar may be inadequate for use in solar thermal power generating applications.

The heat loss coefficient for honeycomb was estimated by calculating conduction and radiation loss, but no convection loss between the absorber and the glass cover. The radiation loss was estimated as though the absorber had a reduced equivalent emissivity. Loss coefficients are shown in Figure 3-10 for an equivalent emissivity of 0.5 over the temperature range 50 ^{o}C to 150 ^{o}C. Based on the experimental results of Cunnington and Streed (1973), an emissivity of 0.5 corresponds approximately to a cell depth-to-width ratio of 1.5 to 2. This range includes the ratio 1.7 for which the angle of incidence measurments of Figure 3-9 were made.

3.6.3 Evacuated Collectors

Evacuating the space between the absorber and the glass covering reduces the conduction-convection loss from the front of the collector to a negligibly small value. Dominant losses are then caused by radiation heat transfer and conduction through any materials separating the absorber and the glass or the collector housing.

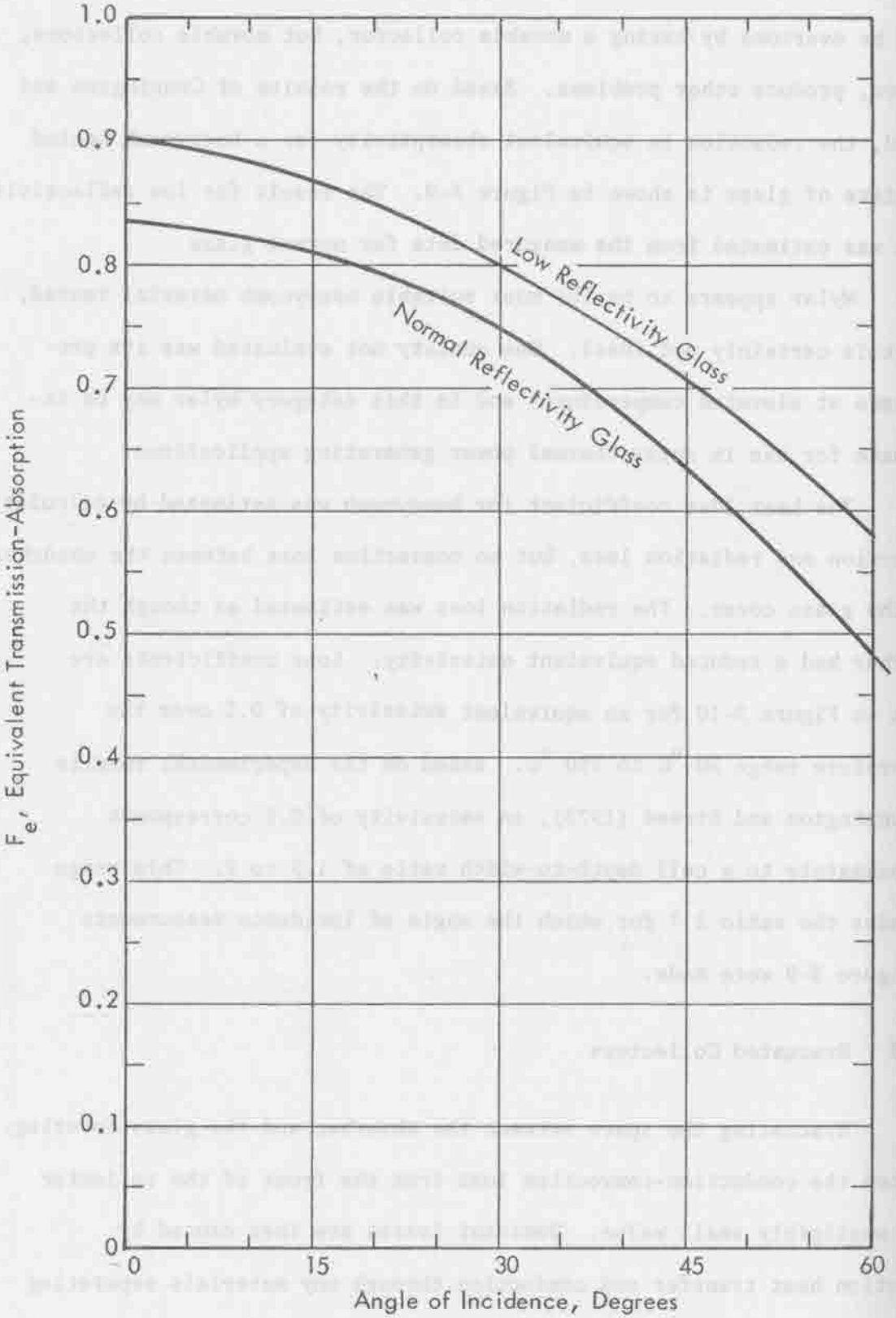

Figure 3-9. Fraction of Incident Energy Absorbed by Flat-Plate Collector with Mylar Honeycomb under One Glass Sheet. Honeycomb Cell Depth/Width = 1.7.

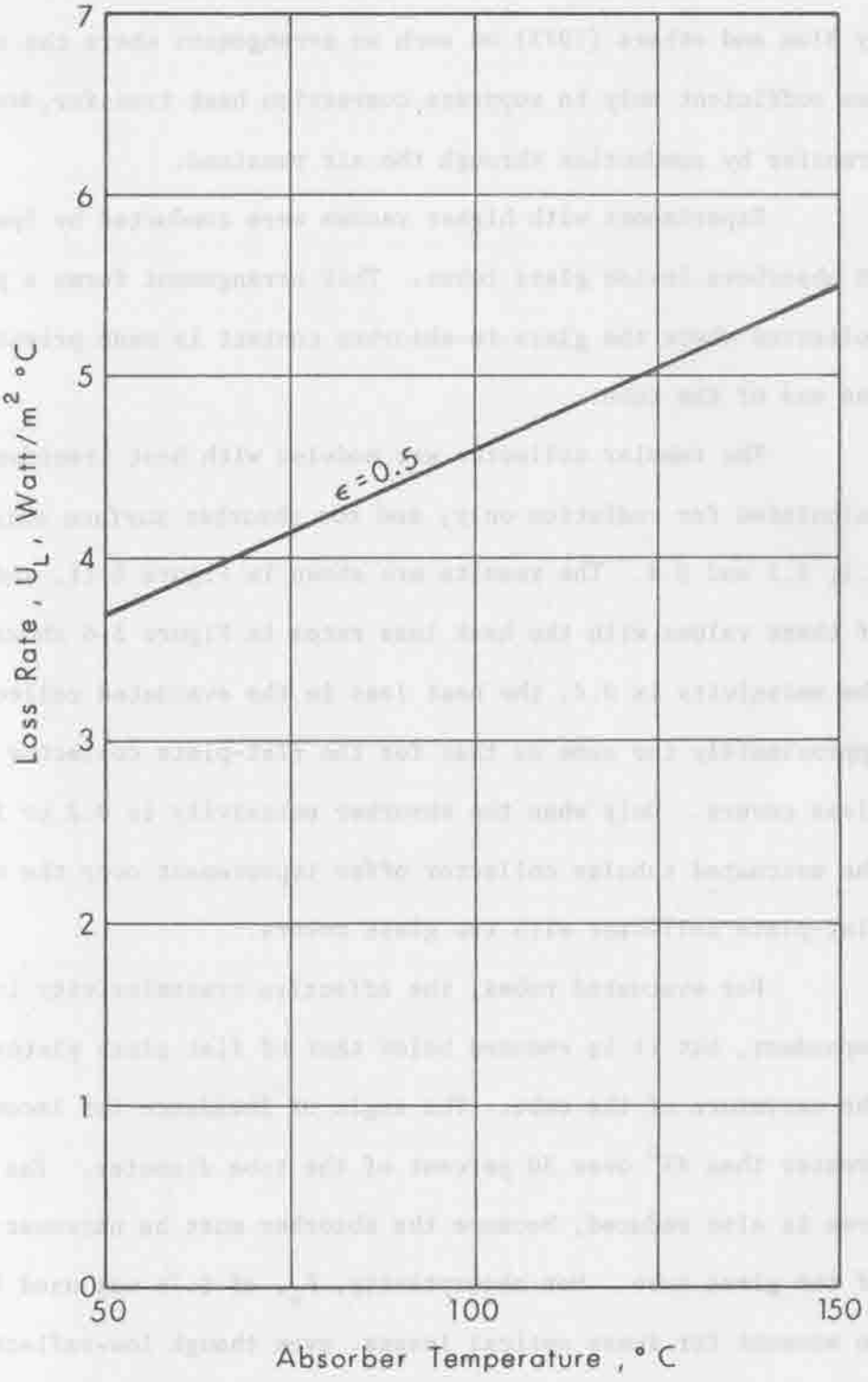

Figure 3-10. Thermal Loss Rates, Flat-Plate Collector with Mylar and Evacuated Plate. Honeycomb between Absorber and Glass.

A flat absorber and a flat glass plate can be assembled so that the space between them may be evacuated. Experiments were conducted by Blum and others (1973) on such an arrangement where the evacuation was sufficient only to suppress convection heat transfer, and heat transfer by conduction through the air remained.

Experiments with higher vacuum were conducted by Speyer (1964) on absorbers inside glass tubes. This arrangement forms a practical collector where the glass-to-absorber contact is made primarily at only one end of the tube.

The tubular collector was modeled with heat transfer coefficients calculated for radiation only, and for absorber surface emissivities of 0.1, 0.2 and 0.4. The results are shown in Figure 3-11, and a comparison of these values with the heat loss rates in Figure 3-6 shows that when the emissivity is 0.4, the heat loss in the evacuated collector is approximately the same as that for the flat-plate collector with two glass covers. Only when the absorber emissivity is 0.2 or lower does the evacuated tubular collector offer improvement over the non-evacuated flat-plate collector with two glass covers.

For evacuated tubes, the effective transmissivity is not angle dependent, but it is reduced below that of flat glass plates because of the curvature of the tube. The angle of incidence for incoming radiation is greater than 45^{o} over 30 percent of the tube diameter. The effective absorber area is also reduced, because the absorber must be narrower than the diameter of the glass tube. Net absorptivity, F_e, of 0.76 was used in the modeling to account for these optical losses, even though low-reflectivity glass was assumed for the tubes.

A heat loss coefficient for the flat-plate collector with partial vacuum was not computed although the computer program would easily

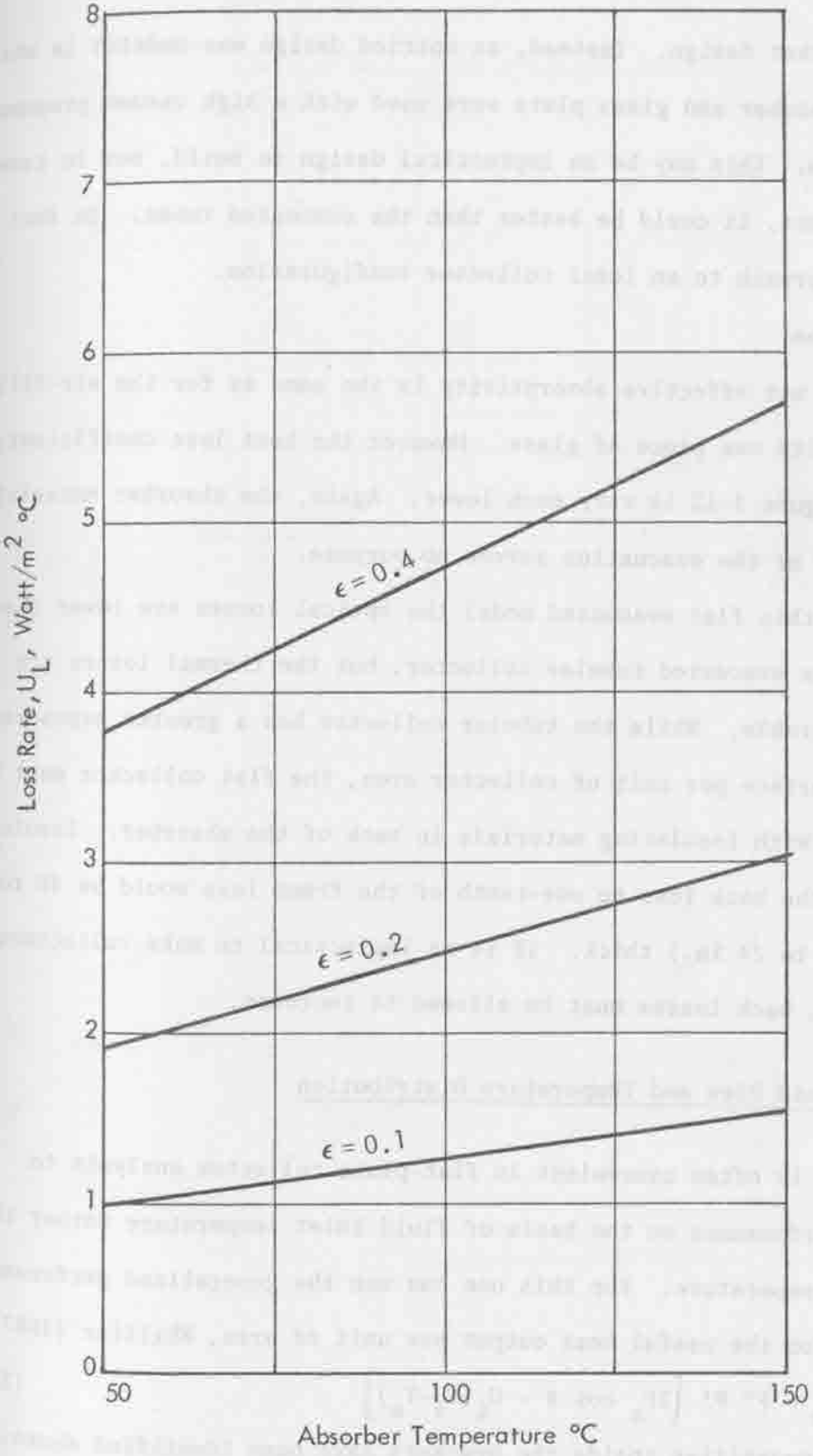

Figure 3-11. Loss Rates, Collectors with Evacuated Glass Tubes (Speyer, 1964), Wind = 5m/s.

accomodate that design. Instead, an untried design was modeled in which the flat absorber and glass plate were used with a high vacuum presumed between them. This may be an impractical design to build, but in terms of performance, it could be better than the evacuated tubes. In fact it is an approach to an ideal collector configuration.
configuration.

The net effective absorptivity is the same as for the air-filled collector with one piece of glass. However the heat loss coefficient, shown in Figure 3-12 is very much lower. Again, the absorber emissivity must be low or the evacuation serves no purpose.

In this flat evacuated model the optical losses are lower than those of the evacuated tubular collector, but the thermal losses are about comparable. While the tubular collector has a greater exposure of glass surface per unit of collector area, the flat collector must be in contact with insulating materials in back of the absorber. Insulation to reduce the back loss to one-tenth of the front loss would be 40 to 60 cm. (15 to 24 in.) thick. If it is impractical to make collectors this thick, back losses must be allowed to increase.

3.7 Fluid Flow and Temperature Distribution

It is often convenient in flat-plate collector analysis to compute performance on the basis of fluid inlet temperature rather than absorber temperature. For this one can use the generalized performance equation for the useful heat output per unit of area, Whillier (1967),

$$q_u = F'' F' \left[I F_e \cos \theta - U_L (T_i - T_a) \right] \qquad (3\text{-}17)$$

where the quantities inside the brackets have been identified above. The difference from the form of Equation (3-1) is in using T_i, the fluid

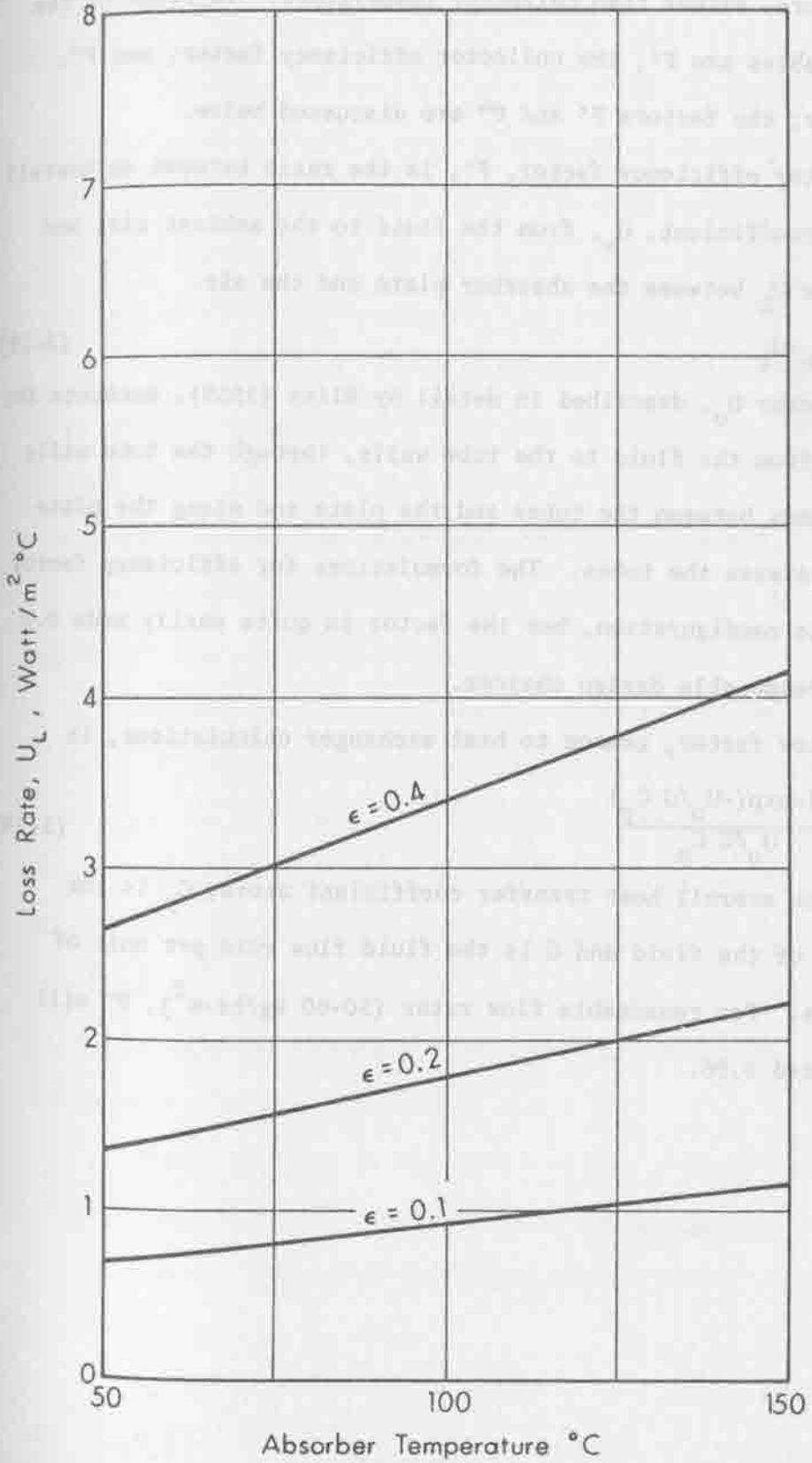

Figure 3-12. Flat-Plate Collector Loss Rates, Wind = 5m/s, Honeycomb and Evacuated Plate.

inlet temperature, rather than collector temperature. In front of the bracketed variables are F', the collector efficiency factor, and F", the flow factor; the factors F' and F" are discussed below.

Collector efficiency factor, F', is the ratio between an overall heat transfer coefficient, U_o, from the fluid to the ambient air, and the loss factor U_L between the absorber plate and the air.

$$F' = U_o/U_L \tag{3-18}$$

The factor U_o, described in detail by Bliss (1959), accounts for heat transfer from the fluid to the tube walls, through the tube walls through the bonds between the tubes and the plate and along the plate in the space between the tubes. The formulations for efficiency factor vary with plate configuration, but the factor is quite easily made 0.9 or better by reasonable design choices.

The flow factor, common to heat exchanger calculations, is

$$F'' = \frac{1-\exp(-U_o/G\ C_p)}{U_o/G\ C_p} \tag{3-19}$$

where U_o is the overall heat transfer coefficient above, C_p is the specific heat of the fluid and G is the fluid flow rate per unit of collector area. For reasonable flow rates (50-60 kg/hr·m^2), F" will generally exceed 0.96.

4.0 COLLECTOR HEAT OUTPUT

Collector design variables described in the preceding sections were the number of glass cover plates, the transmissivity of the glass, the absorptivity and emissivity of the absorber plate and the orientation or deployment of the collector. Some special configurations for loss control were considered such as honeycombs and evacuation.

To compare flat plate collectors quantitatively, estimates were made of the annual output of the heat at 100°C for a range of collector designs from one with a single glass cover to an (idealized) evacuated collector. Comparisons were made for five different deployment conditions to show the relative gains in total output possible by varying the collector angle either seasonally or continuously and on one or two axes.

In Table 4-1 are listed, for different collector deployment schemes, the hours per year when the estimated insolation flux density (this includes $\cos\theta_c$ dependence) fell into each intensity range. These numbers are the raw data from which histograms in Appendix C, Figures 3-2, 3-3, 3-4, 3-7, 3-9, 3-11 and 3-13 were plotted. The given data is the first column and applies to a horizontal collector. The other four columns were estimated from the horizontal data. Albuquerque 1959 data were used.

Since the data in the fourth column closely resembles that in the third column and the data in the sixth is very similar to that in the seventh, the collector output were estimated only for the data in columns 1, 2, 3, 5, and 6.

To estimate the annual output at 100°C from the data of Table 4-1, the weighted output were summed according to the equation

TABLE 4-1

Frequency of Occurrence of Insolation Levels, Hourly Values, Estimated from 1959 Albuquerque Data

Insolation kw/m^2	1 Horizontal Tilt= 0	2 Fixed,* Tilt=L	3 Seasonal* Tilt=L-δ	4 Continuous* Tilt=β	5 Single Axis** Track Tilt=L	6 Single Axis** Track Tilt=L-δ	7 Continuous** Track Two Axes
0-0.1	5785	6034	5937	5896	6507	6047	6097
0.1-0.2	296	244	257	227	84	139	120
0.2-0.3	356	145	197	183	60	87	89
0.3-0.4	226	332	205	259	46	74	70
0.4-0.5	272	127	225	199	59	81	81
0.5-0.6	297	205	145	195	64	71	65
0.6-0.7	288	270	296	267	93	110	96
0.7-0.8	269	168	130	166	100	142	106
0.8-0.9	227	321	280	269	139	187	189
0.9-1.0	352	393	327	337	450	286	287
1.0-1.1	354	340	465	463	685	794	802
1.1-1.2	38	155	251	254	353	549	563
1.2-1.3	0	25	41	41	113	184	186
1.3-1.4	0	1	4	4	7	9	9

L = Latitude angle, 35°

δ = Declination angle. See Table 3-1 App.B

$$\beta_o = \tan^{-1}\frac{(\sin L \cos\delta \cos H - \cos L \sin\delta)}{(\cos L \cos\delta \cos H + \sin L \sin\delta)}$$

(maximizes $\cos\theta_z$ at any hour angle, H.)

* Limited to hour angles ± 90° or less Insolation zero for great angles

** Limited to hour angles ± 60°. Insolation zero for greater angles

$$Q_o = \overline{\tau\alpha} \sum_{i=1}^{h} I_i \, Hr_i - U_L(100 - T_a) \sum_{i=1}^{h} Hr_i \; kWh_t \qquad (4\text{-}1)$$

where Q_o is the output thermal energy in kilowatt hours per year

$\overline{\tau\alpha}$ is the effective transmissivity-absorptivity product of the collector for normal incidence (see Table 4-2 below).

I_i is the insolation level, midpoint in each range, for the left hand column of Table 4-1,

U_L is the collector heat loss rate (see Table 4-2 below).

T_a is the ambient temperature, chosen for these calculations to be 15°C, and

Hr_i is the hours (Table 4-1) in the year estimated to have an average insolation, I_i.

The summation proceeds from the highest insolation values, the bottom of Table 4-1, to the limiting insolation level I_h where the heat loss rate 85 U_L is equal to the absorbed energy, $I_h \, \overline{\tau\alpha}$. For lower insolation levels the collecter does not, on the average, collect any heat and would not be operated. Then the limiting insolation level is

$$I_h = 85U_L / \overline{\tau\alpha} \; . \quad kW/m^2 \qquad (4\text{-}2)$$

Table 4-2 lists, for 14 types of flat plate collectors, the estimated output for the following five deployment conditions:

1. Horizontal
2. South facing, tilted 35° from the horizontal
3. South facing, tilt adjusted seasonally to the difference between the latitude and the declination (normal to the sun at solar noon)
4. Single-axis tracking about a north-south axis tilted at 35° from horizontal

TABLE 4-2

Annual Heat Output from Flat-Plate Collectors

TYPE	No. of Glass Covers	Reflectivity of Glass γ	Absorptivity α	Emissivity ε	Net Absorption $\overline{\tau\alpha}$ [3]	Loss Rate, U_L $W/m^2°C$ [4]	Estimated Annual Output, kWh_t/m^2 [5][6] Horizontal	Fixed Tilt=L	Seasonal Tilt=L-δ	Single Axis Track Tilt=L	Single Axis Track on adj. Tilt
I. Tube-in-Plate	1	0.02	0.9	0.1	0.86	4.3	620	720	800	980	1170
2.	2	0.08	0.9	0.1	0.73	2.9	670	740	820	970	1150
3.	2	0.02	0.9	0.1	0.83	2.9	840	920	1010	1170	1390
4.	3	0.08	0.95	0.95	0.72	3.1	610	680	760	910	1090
5.	3	0.08	0.9	0.1	0.68	2.2	710	790	860	980	1180
6.	3	0.02	0.95	0.95	0.86	3.1	850	930	1030	1190	1420
7.	3	0.02	0.9	0.1	0.81	2.2	950	1020	1120	1260	1490
8.	4	0.08	0.95	0.95	0.67	2.5	640	710	790	920	1090
9.	4	0.08	0.9	0.1	0.64	1.8	730	800	870	980	1170
10.	4	0.02	0.95	0.95	0.85	2.5	950	1040	1130	1280	1530
11.	4	0.02	0.9	0.1	0.80	1.8	1020	1090	1190	1310	1560
12.Transparent Honeycomb	1	0.02	0.95[1]	0.95[2]	0.86	4.6	570	670	750	930	1110
Evacuated:											
13.Tubes	1	0.02	0.9	0.1	0.76	1.3	1100	1160	1260	1360	1620
14.Plate	1	0.02	0.9	0.1	0.86	0.9	1320	1390	1500	1600	1900

Notes: (1) Reduced by the honeycomb to 0.9 effective
(2) Reduced by the honeycomb to 0.5 effective
(3) Normal incidence; this is reduced for angles greater than 30°.
(4) Computed for 15°C ambient, 5 m/sec wind speed.
(5) Albuquerque, N.M. data 1959
(6) Accuracy estimated to be ± 5 percent for data used.

5. Single-axis tracking about a tilted north-south axis, adjusted seasonally to the difference between the latitude and the declination.

After normalizing the outputs for all other deployment conditions to that for fixed tilt at 35^{o}, the average increase or decrease in annual output was computed and is listed in Table 4-3.

The averages in Table 4-3 indicate the approximate limit on the increase in collector cost that could be allowed and still not have a higher cost of heat than the cost of heat from the collector with a fixed tilt.

TABLE 4-3

Comparison of Annual Output for Different Collector Deployment Conditions

Deployment	Average, Compared to Fixed Tilt	Variation for Different Collector Types
Horizontal	0.91	± 0.04
Seasonal ($\beta = L-\delta$)	1.10	± 0.02
Single Axis Tracking	1.27	± 0.12
Single Axis, Adj. Tilt	1.51	± 0.15

5.0 FLAT-PLATE COLLECTOR COST ESTIMATE

Several detailed cost estimates have been made for flat-plate collectors with different design and complements of materials. It was found that for the present manufacturing techniques, the collector cost is materials intensive, with the cost of installation and assembly costs ranking second and third.

A major problem encountered concerned estimates for the cost of a new process for large quantity production. For example, the application of low reflectivity coatings to glass has been done for some time by the Optical Coating Laboratory, Inc. for relatively small orders on small glass samples using a batch process. They have recently been applying low reflectivity coatings with a continuous process on glass up to 30 in. x 40 in. (0.76m x 1.0m). This could be done for about \$0.50 per ft^2 (\$5.38 per m^2) for quantities on the order of 10^6 square feet for coatings on one side. To process larger glass sheets would require a new machine; however, the large quantity price was estimated to be the same. Some manufacturers are now able to produce low reflectivity with surface etching, but none is offering this in quantity. The cost has been estimated to be as low as \$0.10/ft^2 for treatment of both sides, but it is difficult to establish an accurate 1973 cost.

Other pricing problems included the absorber, selective absorbing surfaces, and manufacturing costs; however, various independent estimates made for similar collector designs were reasonably close, and it is felt that, for the assumptions made, the present cost estimate should be within 20 percent of what would actually have been obtained if the collectors were built and installed in 1973 with large quantity manufacturing processes.

The following assumptions were used to limit the number of design variables. Additional assumptions are stated in subsequent sections.

1. The solar plant would be located in the southwest near Albuquerque, New Mexico.
2. The flat-plate collectors and support frame would be assembled at an on-site fabrication facility. This would eliminate post-fabrication transportation costs and facilitate service during installation.
3. Shipping charges for major materials (glass, absorber subassembly, sheet metal, construction stell, etc.) were estimated for Chicago or Pittsburgh to Albuquerque.
4. The design variables carried through for illustration here are:
   (a) Three or four glass plates
   (b) Low reflectivity treatment on all glass plates, or all plates untreated
   (c) Absorber coated with nonselective black or with a selective surface, t = 0.1 to 0.2.
   (d) The general configuration is show in Figure 5-1a, b
5. All materials are to be purchased in large enough quantities to obtain lowest base prices.
6. Entire cost estimate is based on 1973 dollar values.

The following section delineate the designs and costs for the absorber, glass, insulation, collector housing, fabrication, and field installation.

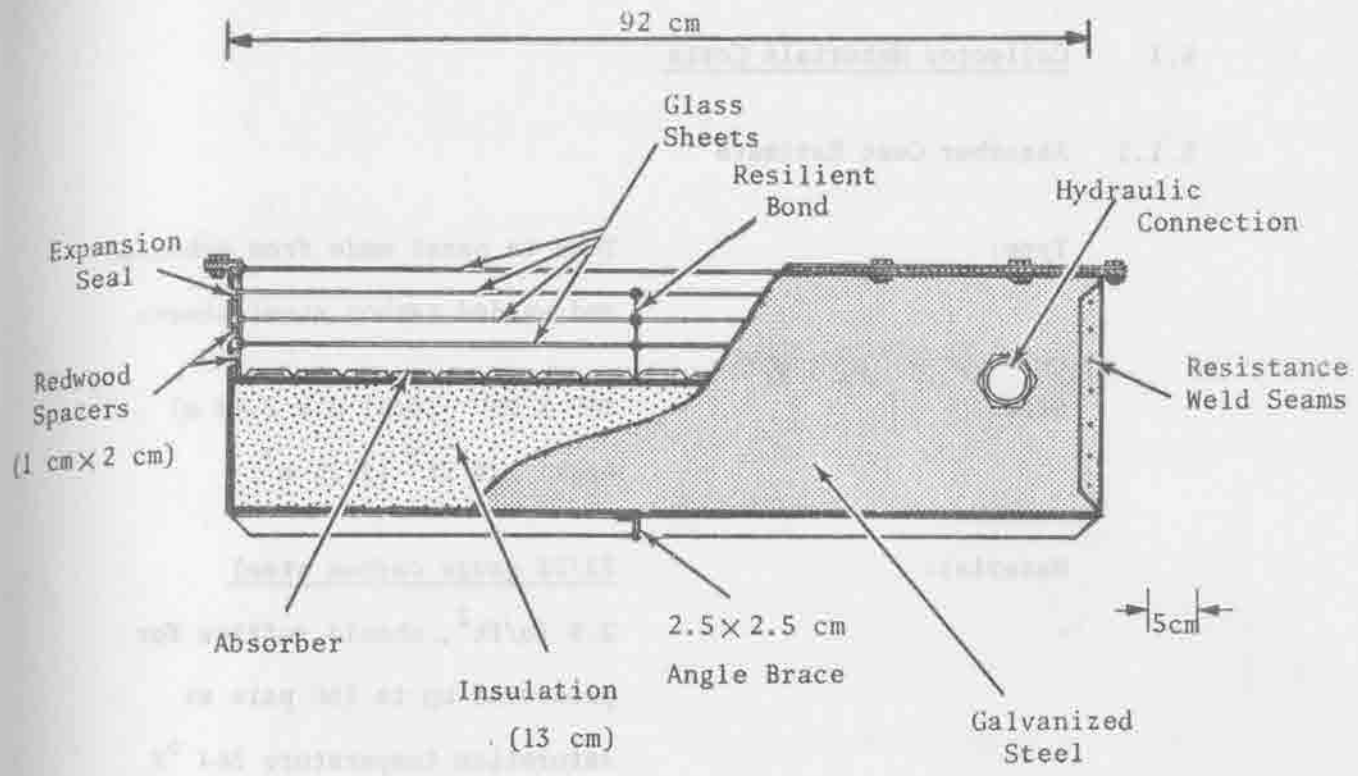

Figure 5-1a. Concept for Construction of Flat-Plate Collector.

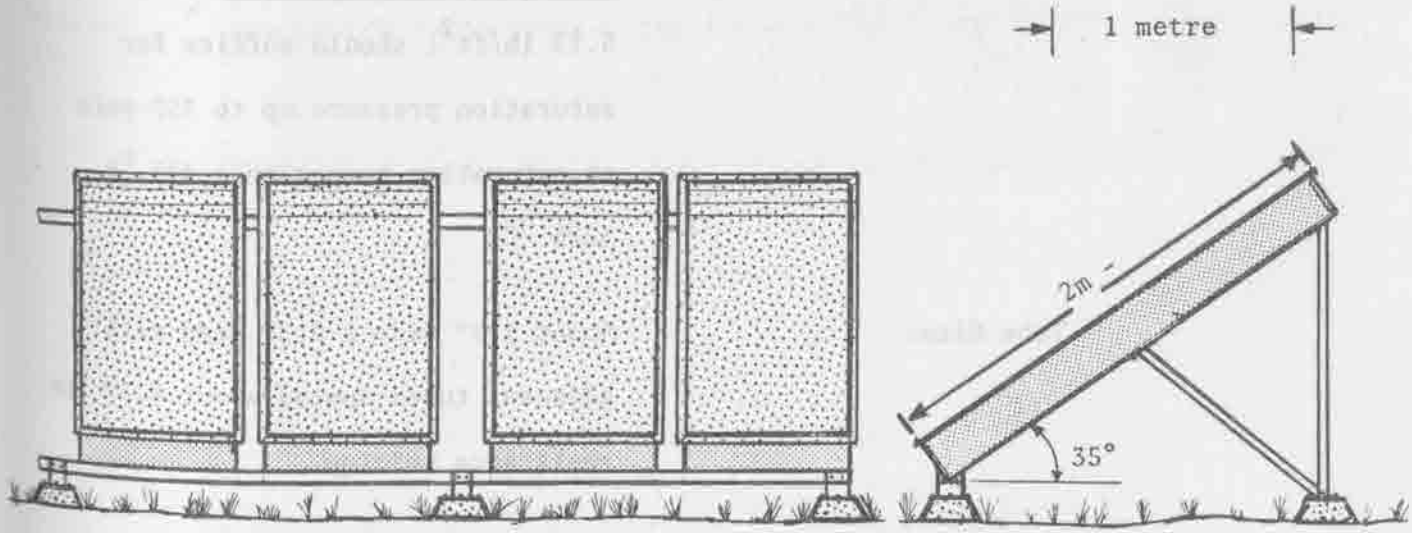

Figure 5-1b. Concept for Flat-Plate Collector Installation.

5.1 Collector Materials Costs

5.1.1 Absorber Cost Estimate

Type:	Tube in panel made from embossed and welded carbon steel sheets.
Size:	36" x 96" (0.91 m x 2.44 m) Area: 24 ft^2 (2.23 m^2)
Material:	22/22 gauge carbon steel 2.5 lb/ft^2, should suffice for pressures up to 160 psia at saturation temperature 364 ^oF (184 ^oC) 18/14 gauge carbon steel 5.13 lb/ft^2, should suffice for saturation pressure up to 350 psia at saturation temperature 427 ^oF (225 ^oC)
Tube Size:	About 1.3" wide x 0.3" deep with adjacent tubes spaced about 0.3" for resistance welding.
Tube Pattern:	Not specified.
Manufactured Cost:	(without absorbing surface) 22/22 gauge, \$1.00/ft^2 (\$10.76/m^2) Based on budget estimate for carload quantities from Tranter Manufacturing, Inc., Lansing, Michigan, August 1975.

18/14 gauge, $2.03/ft^2 ($21.85/m^2)

Based on the additional material cost and same manufacturing complexity factor as for 22/22 gauge.

Absorbing Surface: (Applied)

Black paint ($\alpha = \varepsilon \simeq 0.95$), $0.01/ft^2 ($0.107/m^2)

Selective surface ($\alpha = 0.9$ $\varepsilon = 0.2$) $0.15/ft^2 ($1.62/m^2), based on estimate from Alcoa for treating aluminum panels.

Freight: Rail freight for steel is about $0.035/T-mi (Oct. 1973). For 1300 mi from Chicago to Albuquerque, freight rate is $0.022/lb.

	Freight Charge	
Gauge	$/ft^2	$/m^2
22/22	0.055	0.59
18/14	0.113	1.22

Summary and Recommendation for Absorber:

The use of 18/14 gauge will allow higher temperature operation and longer life; however, the added costs are probably not justified for the established 150 ^{o}C operating limit for flat-plate collectors. The following table gives the total cost of an absorber panel made from 18/14 steel and 22/22 gauge steel and shipped to a fabrication facility in Albuquerque.

TABLE 5-1

Cost per Absorber Panel

Item	18/14 gauge $/m^2	22/22 gauge $/m^2
Panel	21.85	10.76
Absorbing surface:		
Nonselective	0.11	0.11
Selective	1.62	1.62
Freight	1.22	0.59
Total, nonselective	23.18	11.46
Total, selective	24.69	12.97

5.1.2 Glass Cost Estimate

Type: Outer layer - tempered 1/8" water clear, similar to PPG Herculite K

Inner layers - double strength B quality (DS-B), 1/8" thick (0.0032 m) water clear

Low reflectivity coatings estimated at about $0.20/ft^2, applied at the glass factory.

Size: Herculite K is available in sheets up to 68" x 96". Use 36" x 96" (0.91 m x 2.44 m) to be compatible with absorber.

DS-B is available in sheets up to 60" x 80". Use two 36" x 48" (0.91 m x 1.22 m) per layer. Join sheets with impermeable, resilient bond.

Cost: The following table gives the cost for carload quantities and shipping to Albuquerque. Glass costs were obtained from PPG Industries Inc., June 1973.

TABLE 5-2

Cost of Carload Quantities of Glass

Type	Weight lbs/ft^2	Weight kg/m^2	$/ft^2	$/m^2	$/lb	$/kg
Herculite K	1.65	8.06	0.40	4.31	0.242	0.535
DS-B	1.65	8.06	0.221	2.38	0.134	0.295
Low ρ Coating (add)			+ 0.20	+ 2.15		

For shipping from Pittsburgh to Albuquerque, add $0.022/lb. ($0.0485/kg.)

Summary of Glass Cost:

TABLE 5-3

Cost of Glass for Collectors
(Includes Shipping)

Item	kg/m^2	$/m^2 Noncoated	$/m^2 All coated
1 Sheet (Herculite K)	8.06	4.70	6.85
1 Sheet (DS-B)	8.06	2.77	4.92
2 Sheets (1 Herculite K, 1 DS-B)	16.12	7.47	11.77
3 Sheets (1 Herculite K, 2 DS-B)	24.18	10.24	16.69
4 Sheets (1 Herculite K, 3 DS-B)	32.24	13.01	21.61

5.1.3 Insulation Cost Estimate

Type: Fiberglass flat sheets with no foil backing.

Thickness: The most economical thickness has recently been studied, using 1972-73 economic data, by the Thermal Insulation Manufacturers' Association (TIMA) (1973). Their recommendations were tabulated for two classes of insulation (mineral wool and fiberglass, calcium silicate and cellular glass) and three applications (commercial, process, and utility).

For utilities, with an operating temperature of 50 ^{o}C, (305 ^{o}F), TIMA recommends 5" (0.13 m) thick fiberglass, or mineral wool, as optimum.

Cost: The Building Cost File (1974) gives about \$9/m^3 for 5" thick insulation. This is for less than carload quantities in 1974 including shipping. For carload quantities in 1973, use a material cost of 80% of the above and de-escalate at 8%. Thus, cost = \$9.00 x 0.8/1.08 = \$6.70/m^3. For a thickness of 0.13 m, the unit cost is \$6.70 x 0.13 = \$0.87/m^2.

5.1.4 Collector Housing Cost Estimate

Type: Box break formed from cold rolled carbon steel sheet. The sheet should be galvanized or otherwise coated to prevent rusting.

Size: Large enough to accept 36" x 96" abosrber, the various layers of glass, and various insulation thicknesses. Assume 2 cm. spacing between glass layers and allow for 0.13 m insulation. The following chart gives total housing depths in metres for 150 ^{o}C operation.

TABLE 5-4

Depth of Housing for 3 and 4 Sheets of Glass

No. of Glass Layers	Depth Metres	Steel Sheet Area m^2
3	0.19	3.8
4	0.21	4.0

Material: Sheetmetal - Use about 18 gauge carbon steel (galvanized). This is 0.0478 inches (0.0012 m) thick and weighs 2.0 lb/ft^2 (9.76 kg/m^2).

Bracing: Use 1" x 1" x 1/8" steel angle which weighs 0.8 lb/ft. Each box will require about 11 ft. or 8.8 lbs.

Spacers: Use redwood spacers glued to sides of box (2 cm. x 1 cm.).

Cost:

TABLE 5-5

Cost of Materials for Housing

Material	Unit Cost	Total $ 3 Glass Sheets	Total $ 4 Glass Sheets
Galvanized Steel	$ 0.15/lb	12.27	12.91
Bracing	0.17/lb	1.50	1.50
Spacers	Negligible	--	--
Total: $		13.77	14.42
$/m^2 surface area (2.23 m^2)		6.17	6.47
$/m^2 shipping (@ $0.03/lb.)		1.04	1.08
Total $/m^2		7.21	7.55

5.1.5 Summary of Materials Costs

TABLE 5-6

Summary of Materials Costs

Item	$/m^2$ 3 Glass Sheets	4 Glass Sheets
Absorber (22/22) Nonselective	11.46	11.46
Absorber (22/22) Selective	12.97	12.97
Glass-Noncoated	10.24	13.01
Glass-Coated	16.69	21.61
Insulation	0.87	0.87
Housing	7.21	7.55
Lowest combination Total	29.78	32.89
Highest combination Total	37.74	43.00

5.2 Cost of Collector Fabrication and Installation

5.2.1 Fabrication Cost

Assume that materials are shipped to an on-site fabrication facility. The following estimate is for the time required to construct the first unit (with no major problems) and the labor estimate will be based on the time for the 1000th unit (0.365 of the first) using a 90% learning curve. Union scale wages will be assumed only for specialized trades where construction may be controlled by codes.

The time estimate in Table 5-7 is based upon the manufacturing flow chart shown in Figure 5-2. The labor rates at Albuquerque are about 96% of those in the Denver area (Building Cost File, 1974). From Table 5-7, the labor cost for factory fabrication is calculated below using 13-1/2% fringe benefits, 80% overhead, and a labor efficiency of

75% productive time (estimated by Westinghouse Manufacturing Development Laboratory, 1973).

Item	Cost $\$/m^2$
Labor	1.97
Fringe Benefits @ 13-1/2%	0.27
	2.24
Overhead, 80%	1.79
	4.03
Efficiency, 75%	x 4/3
Total Labor	\$ 5.37 per metre^2

The total cost for the fabricated collector including materials is shown in Table 5-9 for the eight configurations considered. The burdens include 10% G&A added to labor plus materials, and 10% profit. This is a total factor of 1.21 times the direct labor, overhead, and materials.

5.2.2 Installation Cost

The installation costs are based on field labor for site preparation and collector installation, plus the cost of materials such as concrete footings, steel supports, and plumbing connections to the main heat transport lines and are itemized in Table 5-9. Fabrication cost of the support frame is estimated in Table 5-8.

5.3 Total Installed Cost

The total installation cost of \$20.59 is combined with fabrication costs in Table 5-10 to give total estimated installed cost. For the three and four plate collectors, there is less than 20 percent variation

TABLE 5-7

Labor Estimate for Fabrication of 36" x 96" Flat-Plate Collector

Item/Operation	Estimated Hours Unit 1	Estimated Hours Unit 1000	Labor Rate $/Hr.	Total Cost 1000th Unit
Receive, Inspect and Store				
Sheet steel	0.1	0.04		
Glass	0.2	0.08		
Angle Iron	0.05	0.02		
Absorbers	0.1	0.1		
Test and Inspect	0.2	0.08		
	0.65	0.32	5.00	1.60
Fabrication				
Cut and drill steel	0.2	0.08		
Form steel	0.1	0.04		
Weld corners	0.1	0.04		
Weld braces	0.2	0.1		
Install Insulation	0.02	0.006		
Install Absorber	0.1	0.04		
	0.72	0.306	5.00	1.53
Glass Installation				
Glue Spacer	0.03	0.01		
Glass Sheet	0.03	0.01		
	0.06	0.02		
3 Sheets	0.18	0.06		
4 Sheets	0.24	0.08		
Install Top Seal	0.03	0.01		
Subtotal				
3 Sheets	0.21	0.07	4.00	0.28
4 Sheets	0.27	0.09		0.36

TABLE 5-7
(Continued)

Final Test and Inspection				
Test	0.2	0.1		
Inspection	0.2	0.05		
Totals:	0.4	0.15	7.50	1.13
3 Sheets		0.846		4.54 x 0.96 = 4.36
4 Sheets		0.866		4.62 x 0.96 = 4.44

$/m^2$ @ 4.40/2.23 m^2 = $1.97/$m^2$

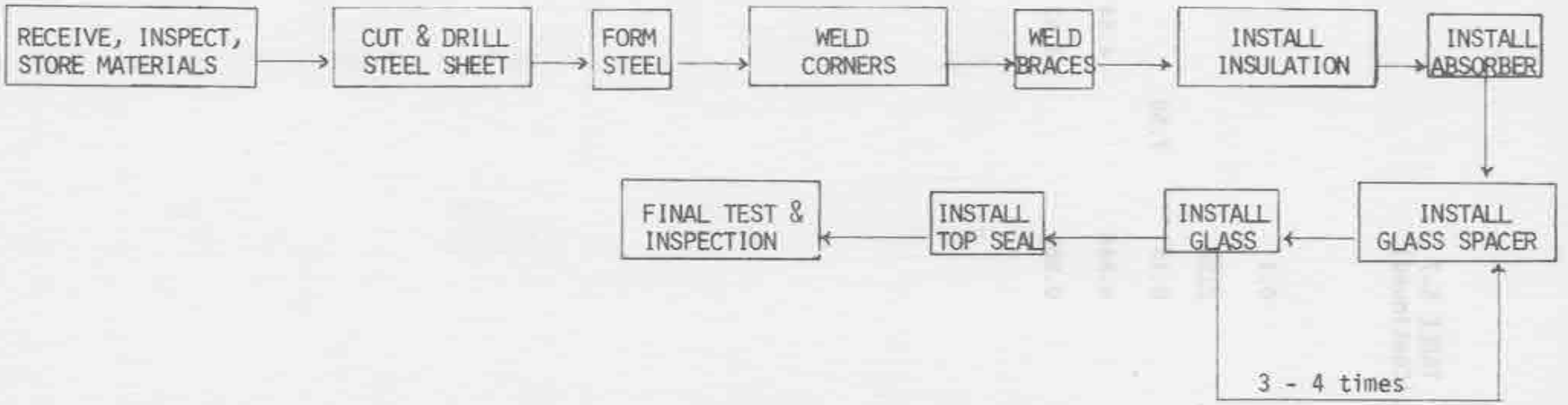

Figure 5-2. Flow Chart for Flat-Plate Collector Manufacture.

in cost between the collector with the non-selective surface, and non-treated glass compared to the one with selective surface and treated glass.

In Table 5-11 the three and four plate collectors costs are broken down by percentages to show the sensitivity of collector cost to components.

TABLE 5-8

Cost Estimate for Support Frame Assembled at On-Site Facility

Item	Weight, lbs.	Cost, $
Angle, 1" x 1" x 14'	11.2	
Angle, 2" x 2" x 1/8" x 19'	31.4	
Pipe, 1" x 0.133" x 8'	13.4	
Footing Plates, 1/4" x 2" x 3" 5 each	3.6	
	59.6 lbs.	
Total Steel Price @ $0.10 per lb.		5.96
Shipping @ $0.022/lb.		1.31
Total Materials		7.27
Labor		5.07
Overhead (100%)		5.07
Total Direct Costs		17.41

TABLE 5-9

Cost Estimate for Field Installation

	Total Each	$/m^2
Site Preparation (0.33 m-hr*)	1.32	
Assemble Frame (0.4 m-hr.)	1.60	
Install Collectors (0.2 m-hr.)	0.80	
Make Plumbing Connection (0.2 m-hr.)	0.80	
Labor Subtotal	4.52	
Overhead, 80%	3.62	
	8.14	
Efficiency, 75%	x 4/3	
Total Direct Labor	10.85	4.87
Concrete Footings	0.44	0.20
Prefabricated Frame Materials (Table 5-8)	17.41	7.81
		12.88
Burden (10% G&A, 10% Profit)		2.70
Total		15.58

* Man-hours at $4.00 per hour for the 1000th unit.

TABLE 5-10

Summary of Cost Estimate

Total Cost of Fabricated and Installed Flat-Plate Collector

(Dollars/Metre^2 of Collector Area)

	3 Plates				4 Plates			
	Non-sel		Sel		Non-sel		Sel	
	NC	C	NC	C	NC	C	NC	C
Labor & Overhead	5.37	5.37	5.37	5.37	5.36	5.37	5.37	5.37
Direct Materials	21.78	36.23	31.29	37.74	32.89	41.19	34.40	43.00
Sub Total	35.15	41.60	36.66	43.11	38.26	46.56	39.77	48.37
Total Fabrication Cost (Includes burden factor of 1.21)	42.53	50.34	44.36	52.16	46.29	56.34	48.12	58.53
Installation	15.58	15.58	15.58	15.58	15.58	15.58	15.58	15.58
Total Installed Cost ($/m2)	58.11	65.92	59.94	67.74	61.87	71.92	63.70	74.11

3, 4 Plates - Glass Plates including 1 sheet of Herculite K.

Non-sel - Absorber painted black (22/22).

Sel - Absorber etched with a selective surface (22/22).

NC - Non-treated Glass Sheets

C - All Glass Sheets treated to reduce reflectivity.

TABLE 5-11

Sensitivity of Flat-Plate Collector
Cost to each of Component

Cost Components	Percentage of Total	
Collector Fabrication		
Materials		
Absorber Plate (non-selective)	20	
Glass (3 plates untreated)	18	
Housing and Insulation	14	
	51*	
Labor and Overhead	9	
Burden and Profit	13	
Total Fabrication		73
Installation		
Support Frame Materials	6	
Support Frame Assembly	8	
Installation Labor	8	
Burden and Profit	5	
Total Installation		27
TOTAL		100

* Totals may not be sum of parts because of round-off.

5.4 Flat-Plate Collector Cost Reduction

To reduce the collector costs given in Table 5-10 a greater volume of production must be assumed as well as a cost reduction for manufacturing experience.

In Table 5-12 collector costs are broken into increments. In the first column are the increments that went into the cost estimate for the fabrication and installation of collectors for one power plant. In the second column are the increments as limited by estimated material costs. Substitution of materials might take possible the further reduction of some of these numbers. The third column contains an estimate of incremental costs based on a higher volumn of production and increased experience. Combining these incremental costs results in installed collector costs which are 50 to 70 percent of the costs estimated for a single plant.

TABLE 5-12

Flat-Plate Collector Cost Increments

Item	Cost, $/m^2 One Plant	Materials Cost	Continuous Production
• Absorber, Flat black, Housing and Insulation	20	8	12
Add for Selective Coat, $\varepsilon = 0.2$	2	0.2	1
Add for Selective Coat, $\varepsilon = 0.1$	4	0.5	2
Add for Honeycomb	32	3	106
Add for Evacuation	10	1	4
• Glass, per sheet	4	2	3
Add for Treatment to reduce reflectivity	2.5	0.2	1
• Installation	16	4	10

6.0 COST OF HEAT

Using the approximate cost relationships of Table 5-12 for continuous production of flat plate collectors, an estimate of installed collector cost can be made for each of the collector types of Table 4-2 above. Then from the estimated annual output, Table 4-2 and the annualized cost, 16 percent of the investment, the approximate cost of heat can be compared for flat plate collector types. The results are shown in Table 6-1, with the cost of heat at the collector given by

$$C_h = C_I(0.16)/Q_o \qquad \$/kWh_t \qquad (6\text{-}1)$$

where C_I is the installed collector cost per square metre and Q_s is the total annual thermal output. The collector efficiency was estimated for normal incidence insolation at 1 kW/m^2, so it is not an average for all operating conditions. Using an average ambient temperature of 15 ^oC the efficiency may be computed from

$$\eta = [1000(\overline{\tau\alpha}) - U_L\ (85)]/10 \quad \text{percent} \qquad (6\text{-}2)$$

and the cost per kW (thermal) in the last column of Table 6-1 is computed from

$$\$/kW = 100 \times \text{Installed cost/Efficiency} \qquad (6\text{-}3)$$

After acknowledging the possible errors in estimating both the annual heat output and the installed collector cost, it is difficult to draw an absolute conclusion as the the best flat-plate collector type.

Making relative comparisons, within the limits of the cost and performance assumptions, one could conclude that:

1. A low cost treatement to reduce the reflectivity of the glass should be sought.

2. Honeycombs are probably not cost effective unless a better material than mylar is found.
3. Where several layers of glass are used, the emissivity of the absorber surface is not important to performance or cost.
4. If reliable, low-cost evacuation is possible it promises the lowest cost of heat from flat plate collectors.

An over all consideration of the average cost of heat from flat plate collectors and the low efficiency of energy conversion at these temperatures makes it difficult for STEPS system using flat-plate collectors to compete with systems using concentrating collectors. However, Clark, et.al., (1974), have proposed some low cost flat-plate collectors which they estimate to be competitive with concentrating systems.

TABLE 6-1

Estimated Cost of Heat from Flat Plate Collectors, 100°C, Fixed Tilt

TYPE	No. of Glass Covers	Reflectivity of Glass γ	Absorptivity α	Emissivity ε	Efficiency for 1 kW/m^2 Insolation	Annual[3] output tilt=35° kWh$_t$	Estimated Installed cost $/m^2	Cost of Heat mills/kWh$_t$	Installed[4] cost/output $/kW$_t$
1. Tube-in-Plate	1	0.02	0.9	0.1	49	720	28	6.2	57
2.	2	0.08	0.9	0.1	48	740	30	6.5	62
3.	2	0.02	0.9	0.1	58	920	32	5.6	55
4.	3	0.08	0.95	0.95	46	680	31	7.3	68
5.	3	0.08	0.9	0.1	49	790	33	6.7	67
6.	3	0.02	0.95	0.95	60	930	34	5.8	57
7.	3	0.02	0.9	0.1	62	1020	36	5.6	58
8.	4	0.08	0.95	0.95	46	710	34	7.7	74
9.	4	0.08	0.9	0.1	49	800	36	7.2	74
10.	4	0.02	0.95	0.95	64	1040	38	5.8	60
11.	4	0.02	0.9	0.1	65	1090	40	5.9	62
12. Transparent Honeycomb	1	0.02	0.95[1]	0.95[2]	47	670	32	7.6	68
Evacuated:									
13. Tubes	1	0.02	0.9	0.1	67	1160	42	5.8	63
14. Plate	1	0.02	0.9	0.1	78	1390	42	4.8	54

Notes: (1) Reduced by the honeycomb to 0.9 effective

(2) Reduced by the honeycomb to 0.5 effective.

(3) Albuquerque, N.M. data 1959.

(4) For 1 kW/m^2 insolation, normal incidence

REFERENCES

Bliss, Raymond W. Jr., (1959): The Derivation of Several "Plate Efficiency Factors" Useful In the Design of Flat Plate Solar Heat Collectors, Solar Energy Vol. 3, No. 4, p. 55.

Blum et al (1973): Design and Feasibility of Flat Plate Solar Collectors to Operate at 100 - 150 c. Paper No. E 18, International Congress "The Sun in the Service of Mankind," Paris, France (July 1973)

Building Cost File, (1974): Western Edition, Construction Publishing Co., Inc. Two Park Avenue, New York, New York 10016

Clark, A. F., J. A. Day, W. C. Dickinson and L. F. Wonters, (1974): A Shallow Solar Pond Energy Conversion System: An Analysis of Conceptual 10 MW_e Plant. Report No. UCR6-51533, Lawrence Livermore Laboratory, Livermore, California, 25 January 1974.

Cunnington, G. R., and E. R. Streed, (1973): Experimental Performance of a Honeycomb Covered Flat Plate Solar Collector. Conference Paper (October). International Congress "The Sun in The Service of Mankind," Paris, France (July 1973)

Holman, J. P., (1972): Heat Transfer, 3rd Edition, McGraw Hill Book Co., New York.

Hottel, H. C., and B. B. Woertz, (1942): The Performance of Flat Plate Solar Heat Collectors, Transactions of ASME, p. 91, (February 1942)

Lumsdaine, (1968): Solar Heating of a Fluid Through a Semi-Transparent Plate--Theory and Experiment, Solar Energy, Vol. 12, No. 4, p. 457.

Robinson, H. E. and F. J. Powlitch, (1957): "The Thermal Insulating Value of Air Spaces," Housing Research Paper 32, U.S. Housing and Home Finance Agency.

Souka and Safwat, (1969): Theoretical Evaluation of the Performance of a Double Exposure Flat Plate Collector Using a Single Reflector, Solar Energy, Vol. 12, No. 3, p. 347.

Speyer, E. (1964): Solar Energy Collection With Evacuated Tube, ASME Paper No. 64-WA/Sol-2.

Teagan, W. P. and G. S. Springer, (1967): "Plane Layer Type Apparatus for Gas Thermal Conductivity Measurements," Review of Scientific Instruments, Vol. 38, No. 3.

Thermal Insulation Manufacturers Association, (1973), 7 Kirby Plaza, Mt. Kisco, N. Y. 10549

APPENDIX E

CONCENTRATING COLLECTORS

BY

W. S. DUFF,

W. W. SHANER,

C. D. BEACH,

G. WILCOX,

AND

S. B. THAYER

1.0 INTRODUCTION

The relationships that are required to translate a solar concentrating collector design into performance and cost are developed in this appendix. The approach developed here is quite general and can be used to analyze such diverse collector types as a paraboloid and a tower-heliostat system. This approach makes it possible for the first time to express concentrating collector performance and cost in concise soluable mathematical form strictly in terms of the collector design variables. This achievement is crucial in being able to effectively find minimum cost solar thermal electric power systems.

The collector performance analysis is divided into the analysis of two subsystems, the concentrator and the absorber-heat exchanger. This is done to make the number of design variables in the optimization manageable. This can be seen in Appendix B. The decoupling of the concentrator and absorber-heat exchanger is accomplished by a Hottle-Whillier-Bliss analysis and the specification of two parameters, one that indicates the amount of radiation that a concentrator can deliver and the other that specifies the distribution of the concentrated radiation in the target area. These two parameters along with target shape convey all of the information about the concentrator subsystem that is needed in the absorber-heat exchanger subsystem analysis. These performance relationships are developed in Sections 2 and 3 of this Appendix.

In order for the optimization approach of Appendix B to be efficient, the computation in costing of a specific design must be accomplished rapidly. This is achieved by generating parametric

cost models from the manufacturing cost estimation analysis. Mathematical expressions and tables that relate concentrator and absorber-heat exchanger costs to design parameters are given in Section 4 of this Appendix.

2.0 CONCENTRATOR PERFORMANCE

Concentrated solar radiation has three fundamental features which distinguish it from nonconcentrated radiation: (1) greater intensity, (2) intensity variation as a function of position, and (3) directional variation of delivered concentrated radiation. The intensity of concentrated radiation varies from a maximum at the theoretical focus of the concentrator, to a much smaller value a short distance away from the focus. Actual intensity variation is, of course, functionally related to the size, configuration and accuracy of a particular concentrator.

The performance of other subsystems in a system using solar concentrators depends on the values of the three properties of concentrated radiation, irrespective of the concentrator design features. This latter point can not be overemphasized as it is the key to the general applicability of the method presented for concentrator performance comparison. Thus, the determination of these three measures of concentrated radiation provides the basis for concentrator performance comparison.

Consider first the equation for useful thermal power from a collector:

$$Q_u = F' [I_D A_p \rho_{ave} \tau \alpha \gamma \pi - U_L A_L (T_{ave} - T_a)] \qquad (2\text{-}1)$$

The original form of this equation was used to characterize flat-plate collectors and is due to Hottel and Whillier (1958) and Bliss (1959). It is also valid in this form for concentrating collectors as may be seen in the development by Duff (1974).

Equation (2-1) may be rewritten as:

$$Q_u = F' [I_D E \tau\alpha G(g,a) \eta - U_L A_L (T_{ave} - T_a)] \quad (2-2)$$

where E is the effective aperture and is equal to A_p times the average fraction over the concentrator aperture of direct radiation reflected or transmitted. G is a statistical distribution in a with a parameter g, a measure of spread of the concentrated radiation. It will be shown below that, in contrast to the intercept factor γ, G is an expression whose form depends only on the type of concentrator and not on the properties of the absorber-heat exchanger. It will also be shown that g depends on the design and type of concentrator and on only the "shape" of the target. I_D is independent of both the concentrator and absorber-heat exchanger properties and η depends on the type of collector tracking. The rest of the quantities in equation (2-2) depend only on the properties of the absorber-heat exchanger. Thus, by specifying E,g and target shape, the concentrator may be decoupled from the absorber-heat exchanger and any subsequent subsystems. Table 2-1 is a breakdown of specific types of collectors into catagories that are implied by the decoupling operation.

When delivered concentrated radiation is fully specified by assigning values to the parameters E and g and when target shape and concentrator focus types are both given, it is possible to find designs that will provide the given delivered radiation for various concentrator types. For example, for given E, g, target shape and concentrator focus type, many different designs for Fresnel lenses, Fresnel reflectors and paraboloids can be determined that result in the desired out-

TABLE 2-1

Categories for the Concentrator Subsystems by Collector Type

CONCENTRATOR TYPE	POINT FOCUS		LINE FOCUS	
	Spherical Target	Pancake Target	Round Target	Flat Target
Parabolic (multiple or single reflector elements)	• Paraboloid	• Paraboloid	• One and two axis tracking parabolic troughs.	• One and two axis tracking parabolic troughs.
Planar (Multiple or single reflector/ refractor types)	• Multiple flats with structurally integrated common focus. • Fresnel circular reflectors and lenses. • Multiple flats with fixed common focus (tower concept). • Small quasi paraboloid array with common focus.	• Multiple flats with structurally integrated common focus. • Fresnel circular reflectors and lenses. • Multiple flats with fixed common focus (tower concept). • Small quasi paraboloid array with common focus.	• One and two axis tracking Fresnel strip reflectors and lenses. • Multiple flats in a strip array.	• One and two axis tracking Fresnel strip reflectors and lenses. • Multiple flats in a strip array.

radiation. Each design can then be costed and the minimum cost design selected to provide the desired radiation output.

The relationship of various rays from the sun are shown in Figure 2-1. The angle between the reflected random ray, o-d, from the random plane, and the reflected ray, o-a, from a perfect optical surface is $2\phi + \psi$. The angles ψ and ϕ are shown in the figure. The surface irregularity over a finite area of the reflector can be expected to be random, and the solar rays within the confines of the sun diameter may also be considered random. Thus, if ψ and ϕ are assumed to be normally distributed with mean zero, then the standard deviation of the angle of a reflected random ray from a reflected perfect optics ray from the sun center is $\sqrt{4\sigma_\phi^2 + \sigma_\psi^2}$ where σ_ψ is the standard deviation of the distribution of radiation across the diameter of the sun and σ_ϕ is the standard deviation of the concentrator surface irregularities expressed in terms of angular deviation from a perfect surface.

The reflected radiation intercepted by spherical targets can be closely approximated by those intercepted by a plane, A, normal to the perfect optics ray from the sun center and having the dimensions of the projected cross-section of the target. The distribution of reflected radiation on the plane is expressible as analytic function, $G(g,a)$, where g is the measure of spread of the reflected radiation.

The function $G(g,a)$ is a probability distribution of concentrated radiation which includes the absorber dimension, a, as well as g. This distribution takes on two different forms, normal or exponential, depending on whether point or line focusing concentrators are used. The expression for g changes for different types of targets and optical arrangements.

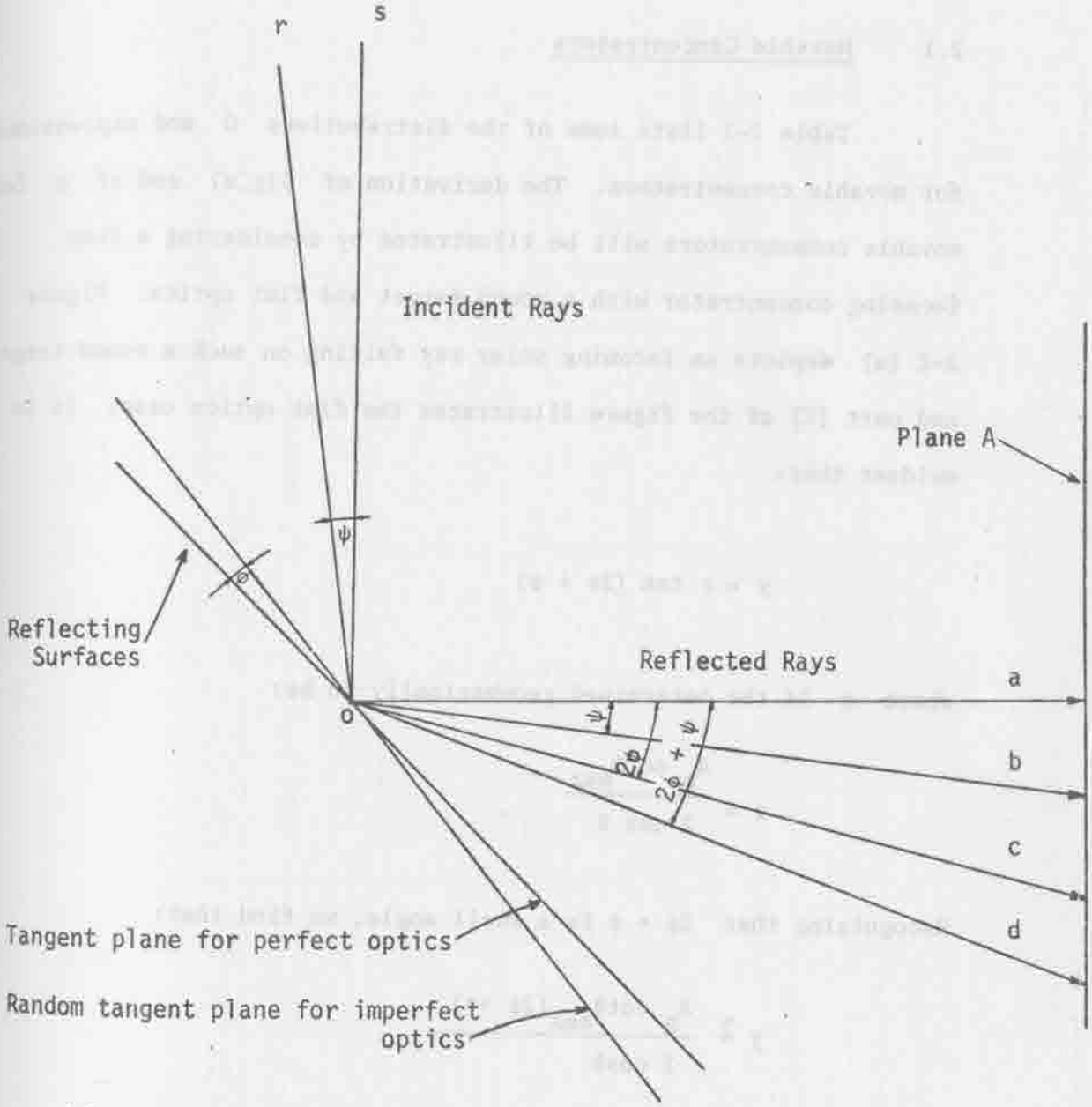

Line:

o-s	Ray from sun center
o-r	"Random" ray from sun
o-a	Reflected ray from sun center for perfect optics plane
o-b	Reflected random ray
o-c	Reflected ray from sun center for random plane
o-d	Reflected random ray for random plane

Figure 2-1. Geometric Representation of the Angular Deviation of a Solar Ray.

2.1 Movable Concentrators

Table 2-2 lists some of the distributions G and expressions g for movable concentrators. The derivation of G(g,a) and of g for movable concentrators will be illustrated by considering a line focusing concentrator with a round target and flat optics. Figure 2-2 (a) depicts an incoming solar ray falling on such a round target and part (C) of the figure illustrates the flat optics case. It is evident that:

$$y = r \tan (2\phi + \psi) \tag{2-3}$$

where r is the determined geometrically to be:

$$r = \frac{A_p \cot\theta_{max}}{2 \cos \theta} \tag{2-4}$$

Recognizing that $2\phi + \psi$ is a small angle, we find that:

$$y \approx \frac{A_p \cot\theta_{max} (2\phi + \psi)}{2 \cos\theta}$$

Using Equation (2-5), the variance of the sum of independent normally distributed random variables is found to be:

$$\sigma_y^2 = \frac{A_p^2 \cot^2 \theta_{max} (4\sigma_\phi^2 + \sigma_\psi^2)}{8\,\theta_{max}} \int_{-\theta_{max}}^{\theta_{max}} \frac{d\theta}{\cos^2\theta} \tag{2-6}$$

TABLE 2-2

Parameters for Concentrators

DESCRIPTORS	POINT FOCUS		LINE FOCUS	
	Spherical Target	Pancake Target	Round Target	Flat Target
G(g,a)	$1 - e^{-\frac{a}{g}}$		Area under the $\mu=0$, $\sigma=g$ normal distribution between $-a/2$ and $a/2$	
a	Cross-sectional area of sphere	Area of circle	Diameter	Width
g (for parabolic concentrator shapes, multiple or single reflector elements	$\frac{2A_p(4\sigma_\phi^2+\sigma_\psi^2) \cdot (2+\cos\theta_{max})}{3\theta_{max}\sin\theta_{max}}$	$\frac{2A_p(4\sigma_\phi^2+\sigma_\psi^2)}{\sin^2\theta_{max}}$ (Note 1)	$\left\{\frac{A_p^2(4\sigma_\phi^2+\sigma_\psi^2) \cdot (2+\cos\theta_{max})}{12\theta_{max}\sin\theta_{max}}\right\}^{1/2}$	(Notes 2 and 3)
g (for linear concentrator shapes, multiple or single reflector/refractor elements)	$\frac{2A_p\cos\theta_{max} \cdot (4\sigma_\phi^2+\sigma_\psi^2)}{\theta_{max}\sin\theta_{max}}$	$\frac{2A_p(1+\cos^2\theta_{max}) \cdot (4\sigma_\phi^2+\sigma_\psi)}{3\theta_{max}\cos\theta_{max}\sin\theta_{max}}$ (Note 3)	$\left\{\frac{A_p^2\cos\theta_{max} \cdot (4\sigma_\phi^2+\sigma_\psi^2)}{4\theta_{max}\sin\theta_{max}}\right\}^{1/2}$	$\left\{\frac{A_p^2(1+2\cos^2\theta_{max}) \cdot (4\sigma_\phi^2+\sigma_\psi^2)}{12\theta_{max}\cos\theta_{max}\sin\theta_{max}}\right\}^{1/2}$ (Note 3)
A_p	Aperture Area		Aperture Width	
E	$A_p \rho_{ave}$			

Notes for Table 2-2:

(1) This expression is due to Aparisi (See Umarov, 1967), and has been verified by different derivations (see Teplyakov, 1971 and Grilikhes, 1966) and experiments (see Zakhidov and Teplyakov, 1966). The exponential form of the distribution, obtained by Aparisi, is identical to that derived here, although a different was used. The approximation expression for this case is:

$$\frac{2A_p(4\sigma_\phi^2+\sigma_\psi^2)}{\theta_{max}\tan^2\theta_{\frac{max}{2}}}\left[\frac{1}{3\sin^3\theta_{max}\cos\theta_{max}}+\frac{2}{3\sin^3\theta_{max}}\right.$$

$$+\frac{2}{\sin\theta_{max}}-\frac{\cos\theta_{max}}{3\sin^3\theta_{max}}-\frac{2\cos\theta_{max}}{\sin\theta_{max}}+\frac{4\sin\theta_{max}}{3\cos\theta_{max}}$$

$$\left.-\ln\tan\left(\frac{\pi}{4}+\frac{\theta_{max}}{2}\right)+\ln\tan\left(\frac{\pi}{4}-\frac{\theta_{max}}{2}\right)\right]$$

(2)

$$\left\{\frac{A_p^{\,2}(4\sigma_\phi^2+\sigma_\psi^2)}{4\theta_{max}\tan^2\theta_{\frac{max}{2}}}\left[\frac{-1}{3\sin^3\theta_{max}\cos\theta_{max}}+\frac{2}{3\sin^3\theta_{max}}\right.\right.$$

$$+\frac{2}{\sin_{max}}-\frac{\cos\theta_{max}}{3\sin\theta_{max}}-\frac{2\cos\theta_{max}}{\sin\theta_{max}}+\frac{4\sin\theta_{max}}{3\cos\theta_{max}}$$

$$\left.\left.-\ln\tan\left(\frac{\pi}{4}+\frac{\theta_{max}}{2}\right)+\ln\tan\left(\frac{\pi}{4}-\frac{\theta_{max}}{2}\right)\right]\right\}^{\frac{1}{2}}$$

(3) Approximate expressions.

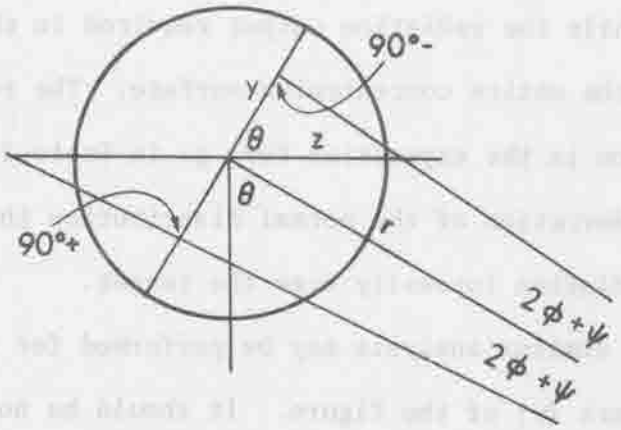

(a)

Round and Flat Targets

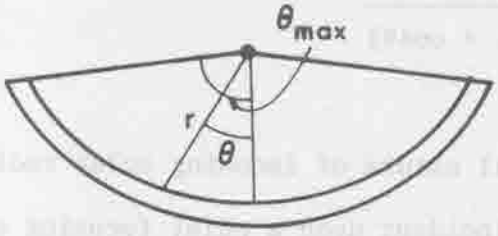

(b)

Parabolic Optics

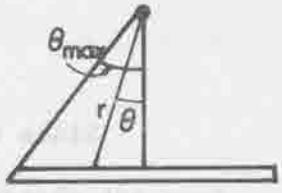

(c)

Flat Optics

Figure 2-2. Optics of Parabolic and Flat-Concentrators and Incidence of a Solar Ray on a Round or Flat Target.

The above integration is required in order to effectively sum over all incident points of incoming radiation on the concentrator surface. Figure 2-2 showed that the derived distribution for y is a function of θ, while the radiation output required in the analysis is the sum over the entire concentrator surface. The result of the above integration is the expression for g in Table 2-2. Here g is the standard deviation of the normal distribution that describes the variation in the radiation intensity over the target.

A similar analysis may be performed for the parabolic optics case in part (b) of the figure. It should be noted that the method is the same. Only the expression for r needs to be altered to account for the geometrical differences. The new expression for r is:

$$r = \frac{A_p(1 + \cos\theta_{max})}{2 \sin\theta_{max}(1 + \cos\theta)} \qquad (2\text{-}7)$$

Since the statistical nature of incoming solar radiation does not change when it is incident upon a point focusing concentrator as opposed to a line focusing concentrator (see Dudko and Dudko, 1968), it is obvious that the expressions for g in the point focusing case will be functionally related to the line focusing case just derived. The form of the transformation is πr^2 and this transformation results in an exponential distribution with the parameters given in Table 2-2.

As can be seen in Figure 2-2, an approximation of the form:

$$z \stackrel{\sim}{=} \frac{y}{\cos\theta} \qquad (2\text{-}8)$$

is possible for the case of a line focusing concentrator with

a flat target. Thus, an approximation expression for the variance of the radiation intensity of a line focus concentrator with flat optics and a flat target is

$$\sigma_z^2 = \frac{A_p^2 \cot^2\theta_{max} (4\sigma_\phi^2 + \sigma_\psi^2)}{8\,\theta_{max}} \int_{-\theta_{max}}^{\theta_{max}} \frac{d\theta}{\cos^4\theta} \qquad (2\text{-}9)$$

Performing the indicated integration yields:

$$\sigma_z^2 = \frac{A_p^2 (4\sigma_\phi^2 + \sigma_\phi^2)}{2\,\theta_{max}} \left[\frac{2 + \cos 2\,\theta_{max}}{3 \sin 2\,\theta_{max}} \right] \qquad (2\text{-}10)$$

An expression for parabolic optics if found in a similar manner. It should be emphasized that the goodness of the apprximation hinges on the angle in Figure 2-2 being close to 90^o. Figure 2-3 compares the point focusing concentrator expressions for g from Table 2-2 using a normalized form of the expressions. Notice that, as might be expected, all expressions are the same for small rim angles. Notice also that the approximation agrees closely with Aparisi's expression (see Umarov, 1967) up to a rim angle of about 45^o. Since this expression has been verified experimentally, (see Zakhidov and Teplyakov, 1966) it serves as a verification of the results developed here.

To illustrate the method, assume that an average radiation intensity of 60 kW/m^2 from a concentrator with an effective aperture, E, of 2 metres squared and a radiation dispersion, g, equal to .02 metres squared is required. Using the expression derived, it is possible to find an infinite number of point designs which will result in the required radiation output. For example, consider a spherical target with area = .022 m^2. A paraboloidal concentrator with $\theta_{max} = 90^0$,

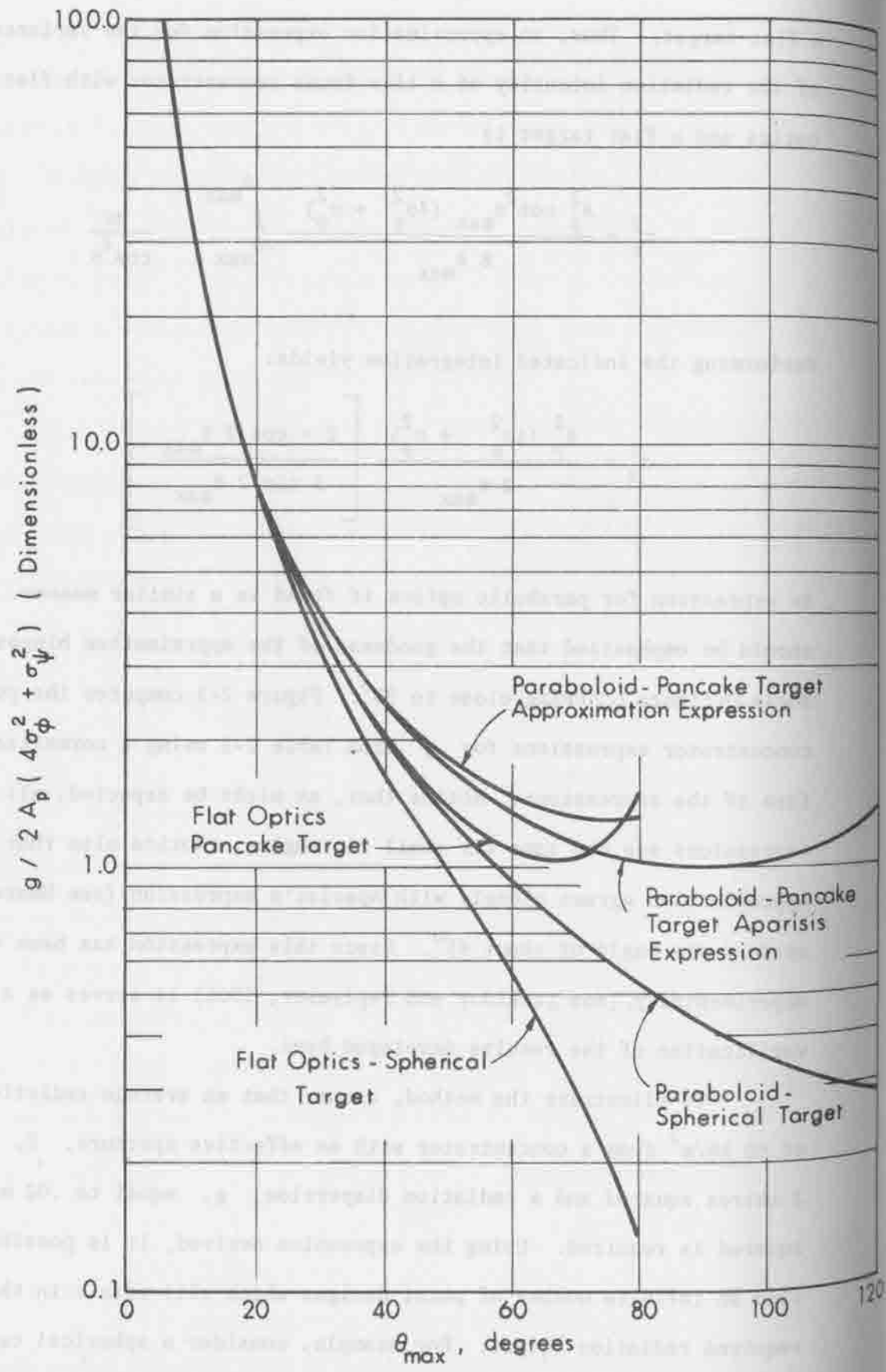

Figure 2-3. Comparisons of Point-Focus Concentrators with Different Targets.

$\rho_{ave} = .85$, $A_p = 2.35\ m^2$, and $\sigma_\phi = 1^o$ would yield the desired radiation. Similarly, a circular Fresnel reflector with $\theta_{max} = 50^o$ and all other design parameters the same will also result in the same radiation output. The concentrator optimization procedure of Appendix B developes a large number of concentrator designs that achieve a desired $\bar{E}$ and g, costs each design and selects the design with minimum cost.

2.2 Tower/Heliostat System

Because the sun is not constantly normal to the plane of the heliostat field, the analytical model lacks the symmetry of the models for the Fresnel reflector or the paraboloid. A considerable effort has been made by other research teams to optimize field shape, tower placement, and heliostat spacing. See for example Sheldahl-Foster Wheeler (1974) and University of Houston-McDonnel Douglas (1973).

In the modeling done for this project an optimization of the above factors was not attempted. Instead a round field with a tower at the center was assumed. Average reflecting area and mirror spacing factors were estimated and expressed as functions of the rim angle. From these expressions the effective aperture, $\bar{E}$, and spread factor g were calculated for use in the search for the tower height, field size and heliostat size producing the lowest cost electrical output.

As a starting point, the heliostat array analysis by Sheldahl-Foster Wheeler (1974) was used for basic geometric relationships and for its expressions for ideal performance of close-packed mirrors. The field geometry is expressed in terms of the unit vectors $\bar{n}$, $\bar{t}$, and $\bar{s}$, indicating respectively the directions normal to the mirror, toward the tower top from the mirror and toward the sun from the mirror. Figure

2-4 shows the relationships and the angles of azimuth, β, and zenith, θ, for each vector. While $\bar{s}$ is the same for each mirror at a particular time, $\bar{t}$ uniquely expresses the position of the mirror in the field.

In a field of closely packed mirrors, that is, when mirror area equals ground area, varying amounts of the mirror surface are in use at different times of day and for different locations in the field. There are losses when (1) a mirror shadows a neighboring mirror from the sun or (2) light striking a mirror is screened from the tower because it hits the back of a neighboring mirror.

The analysis by the Sheldahl team of closely packed mirrors produced expressions for losses owing to shading and screening and an average utilization factor, which is plotted in Figure 2-5. This efficiency η is converted to reflected solar power by

$$Q_r = \eta \rho_m A_f I_D \text{ watts}$$

where

ρ_m is the average specular reflectivity of the mirrors,

A_f is mirror field area, m^2, and

I_D is direct insolation, W/m^2.

The curve for $\theta_s = 0$ applies to a Fresnel reflector.

The efficiency curves of Figure 2-5 are parametric in sun's zenith angle. The sun will never be normal to a horizontal field. In fact, the most probable angles for the sun are between 40^o and 70^o depending on the latitude. See Threlkeld (1970) for example. The relative frequency of the sun's zenith angle falling in a given angular range for all daylight hours of the year is plotted in Figure 2-6 for

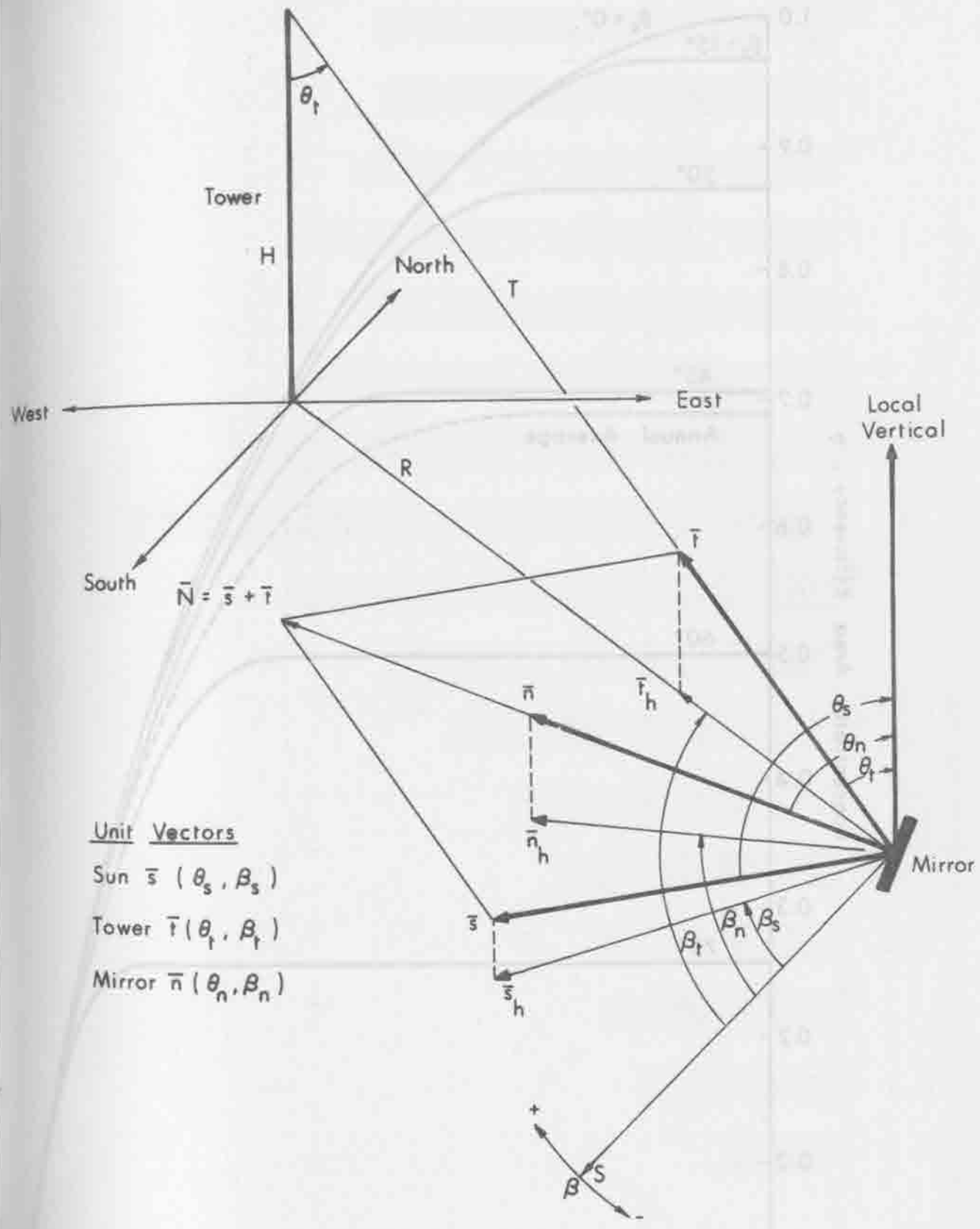

Figure 2-4. Tower-Heliostat Field Geometry.

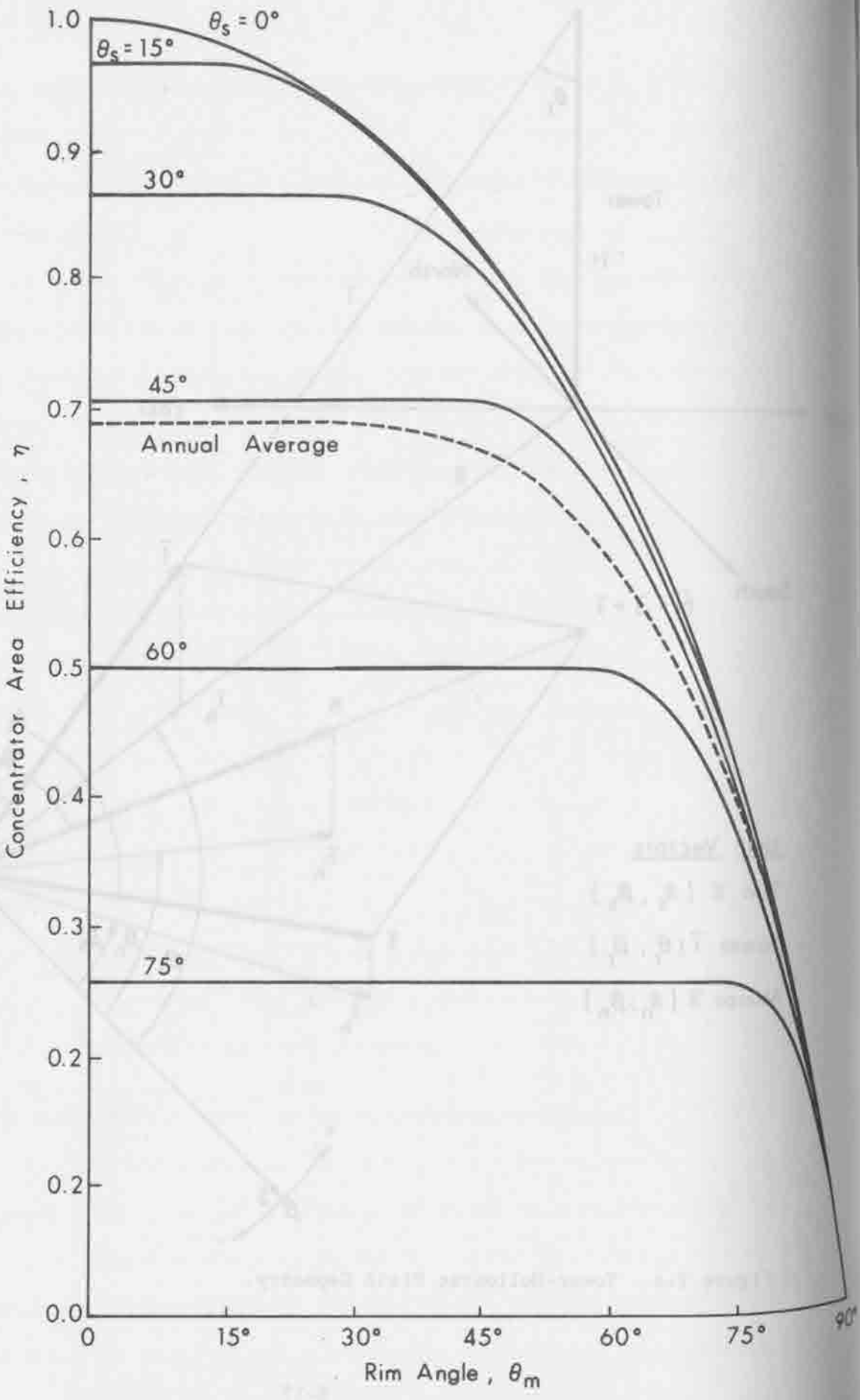

Figure 2-5. Concentrator Area Efficiency.

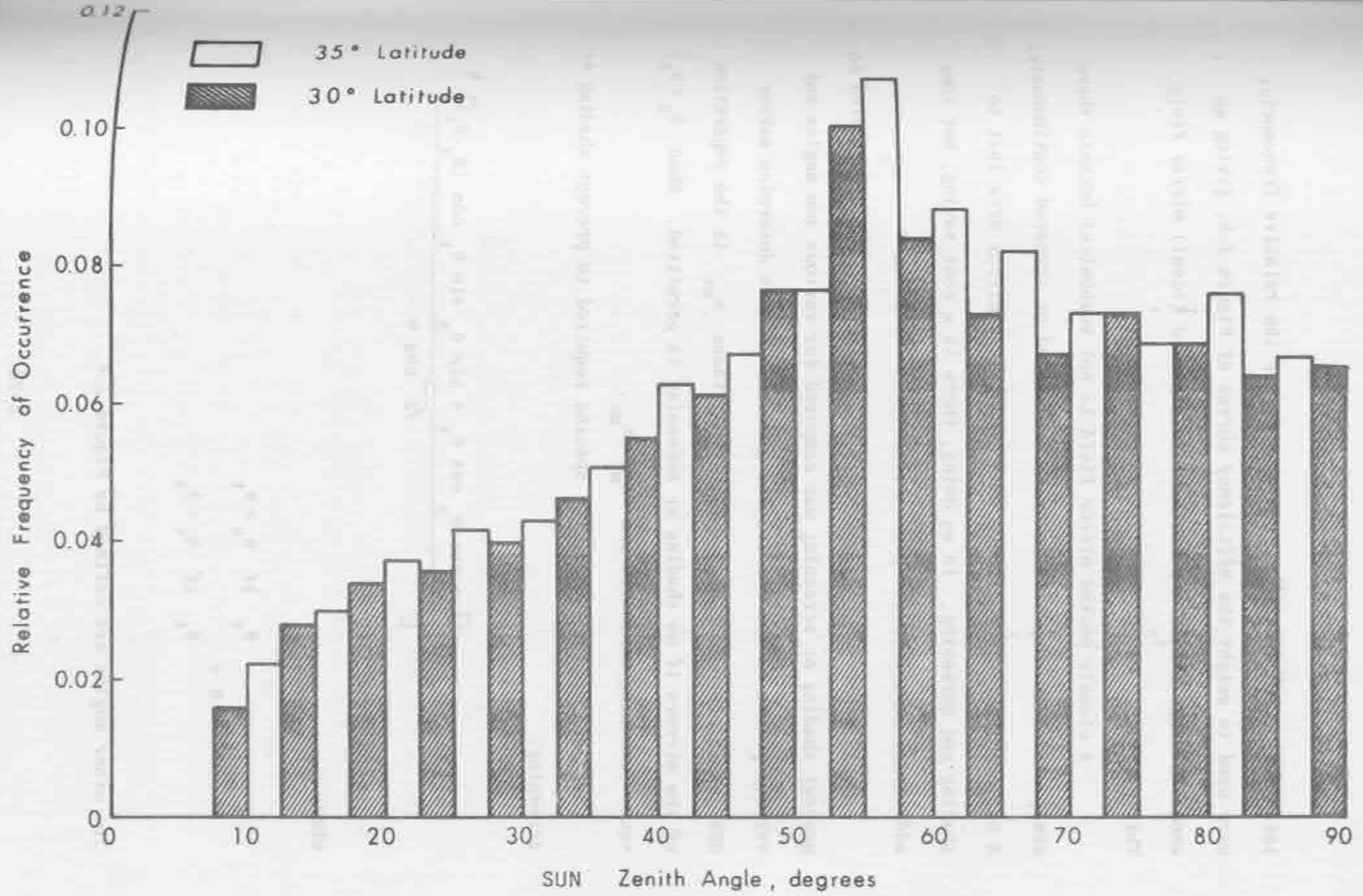

Figure 2-6. Relative Frequency of the Sun Zenith Angle.

latitudes of 30^{o} and 35^{o}. From this figure the relative frequencies were used to weight the efficiency curves of Figure 2-5, giving an annual average efficiency for a closely packed (ideal) mirror field. This average is the dashed line in Figure 2-5.

A closely packed mirror field is not economical because there are portions of many mirrors which are shaded or screened continuously. A better placement of mirrors would reduce the mirror area lost to shading and screening. In so doing, there is a cost saving, but some additional loss of solar power reflected to the target.

To provide a reasonable mirror spacing the spacing required to prevent shading or screening was computed for various sun angles and various points in the field. The geometry used to determine mirror spacing is shown in Figure 2-7. The distance x_{mt} is the separation of the mirrors if no shading or screening is permitted. When $\theta_s < \theta_t$, tower screening dominates and $x_{mt} > x_{ms}$.

Then let x_m equal the spacing required to prevent shading or screening:

$$x_m = \left[\frac{1 + \cos\theta_s \cos\theta_t + \sin\theta_s \sin\theta_t \cos(\beta_s - \beta_t)}{\sqrt{2}\cos\theta}\right]^{\frac{1}{2}}$$

where

$$\theta = \begin{cases} \theta_s & \text{if } \theta_s > \theta_t \\ \theta_t & \text{if } \theta_t > \theta_s \end{cases}$$

The other angles are defined by Figure 2-4.

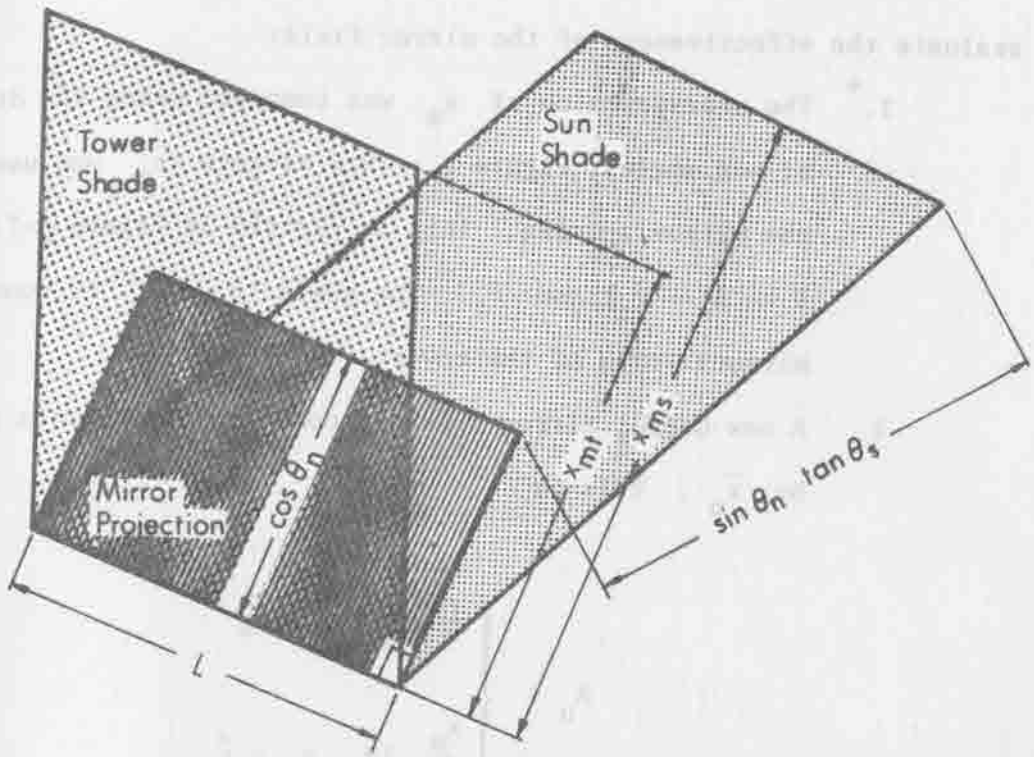

a) Plan View

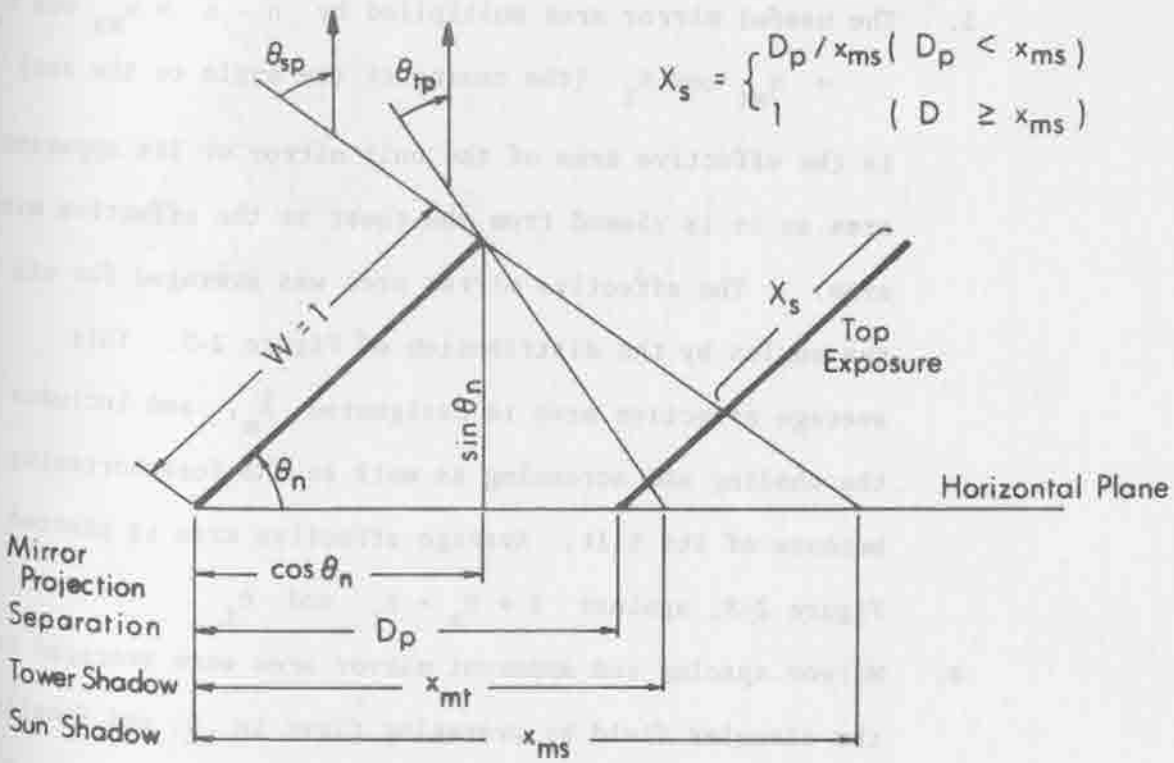

b) Side View

Figure 2-7. Geometry for Mirror Spacing.

The following procedure was used to establish a mirror spacing and evaluate the effectiveness of the mirror field:

1. The average value of x_m was computed using the distribution of sun angles, Figure 2. This average $\bar{x}_m$ was used as the mirror spacing. This is plotted in Figure 2-7 a, against $\beta = \beta_s - \beta_t$ and θ_t. The angle $\beta = 0^o$ at noon for mirrors North of the tower.

2. A new useful mirror area was computed for mirrors spaced by $\bar{x}_m$. This is

$$A_u = \begin{cases} 1 & \text{if } x_m \leq \bar{x}_m \\ \dfrac{\bar{x}_m}{x_m} & \text{if } x_m \geq \bar{x}_m \end{cases}$$

3. The useful mirror area multiplied by $\bar{\eta} \cdot \bar{s} = x_{ms} \cos \theta_s = x_{mt} \cos \theta_t$ (the cosine of the angle to the sun) is the effective area of the unit mirror or its apparent area as it is viewed from the tower is the effective mirror area. The effective mirror area was averaged for all sun angles by the distribution of Figure 2-5. This average effective area is designated $\bar{A}_m$, and includes the shading and screening as well as the foreshortening effect because of its tilt. Average effective area is plotted in Figure 2-8, against $\beta = \beta_s - \beta_t$ and θ_t.

4. Mirror spacing and apparent mirror area were averaged over the circular field by averaging first in β and finally in θ_t, weighting the values by the increase in area as θ_t

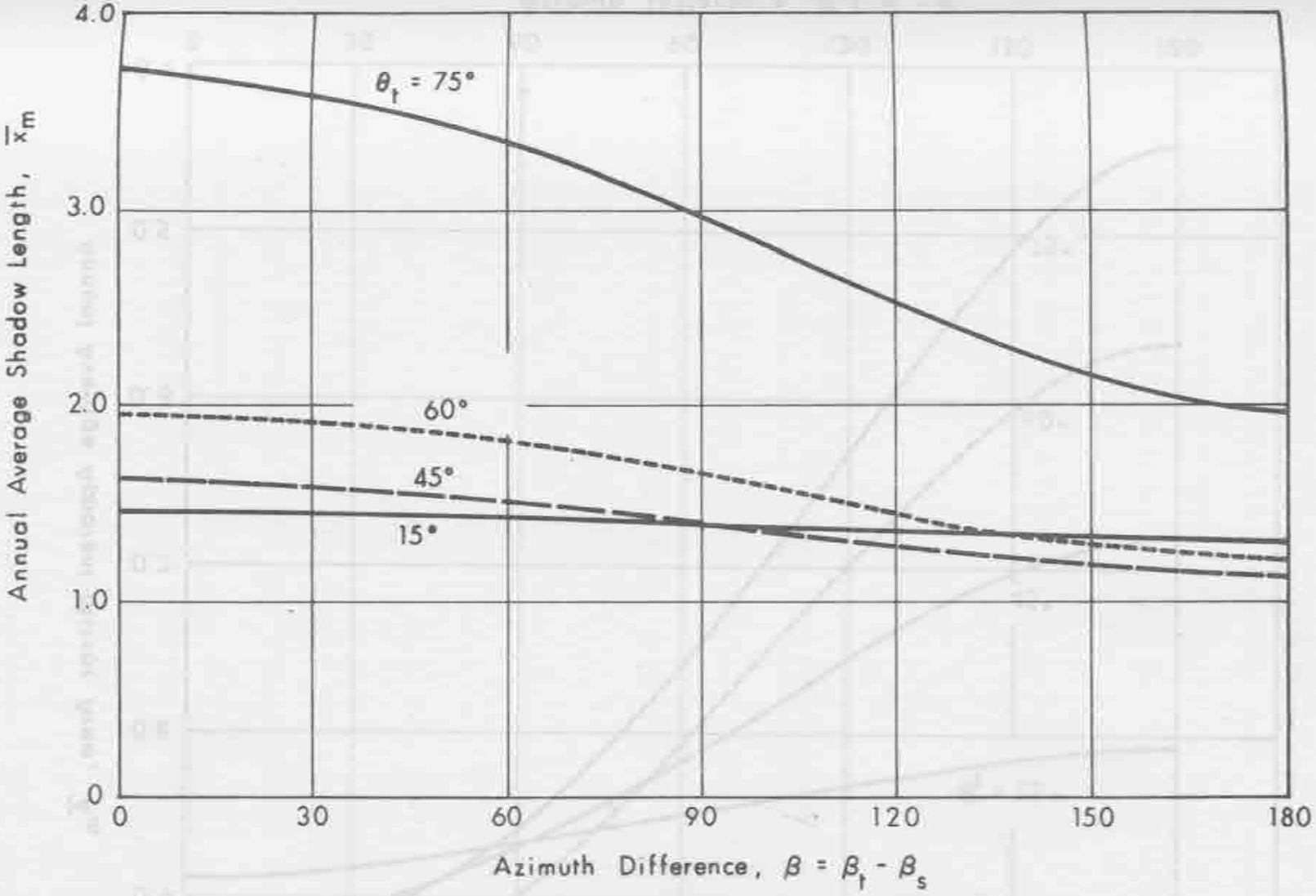

Figure 2-7a. Average Mirror Shadow Length in Mirror Units for Circular Heliostat Field with Central Tower.

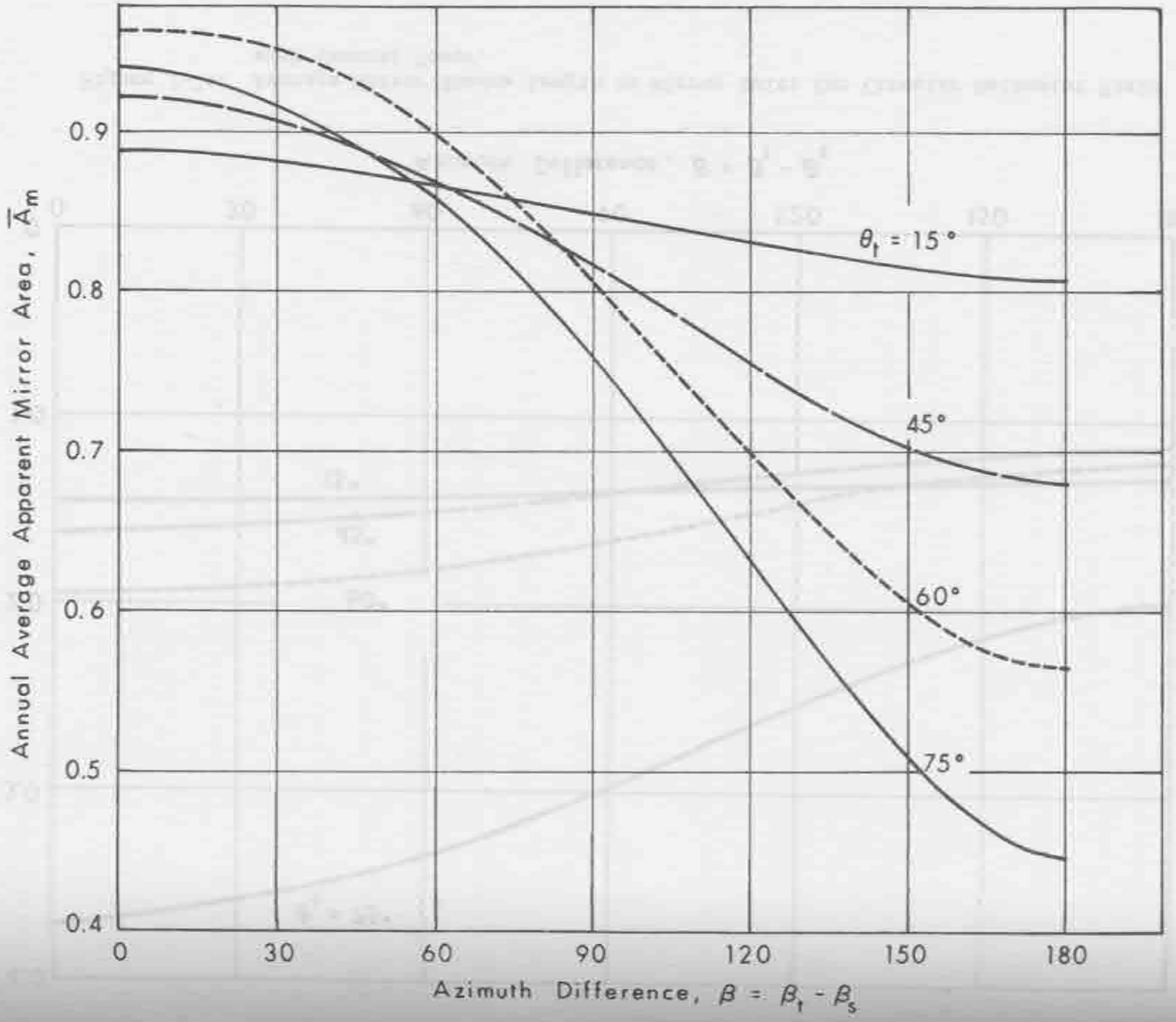

Figure 2-8. Average Apparent Area of a Unit Mirror as Viewed by Tower, for Circular Heliostat Field with Central Tower.

increases. The weighting factor for the ring of mirrors between θ_1 and θ_2 is proportional to $(\tan^2 \theta_2 - \tan^2 \theta_1)$.

Averages, over the year and over the mirror field, of mirror spacing and apparent area are plotted against rim angle, θ_{max}, in Figure 2-9. These factors are used in computing the field effective aperture, E, as follows:

The number of mirrors in a field is

$$N = A_f/(1.2\ A_m \bar{S})$$

where

A_m is actual mirror area

$\bar{S}$ is average mirror spacing to reduce shadowing (Figure 2-9)

The factor 1.2 accounts for an arbitrary mirror spacing side to side.

The solar flux reflected to the target area is

$$Q_r = NI_D\ \rho_m\ A_m\ \bar{A}_e$$

or

$$Q_r = A_f\ I_D\ \rho_m\ \bar{A}_e/1.2\ \bar{S}$$

where $\bar{A}_e$ is the average effective mirror area (Figure 2-9) and the other factors have been discussed above.

The effective aperture for the tower heliostat field is

$$E = A_f\ \rho_m\ \bar{A}_e/1.2\ \bar{S} \quad .$$

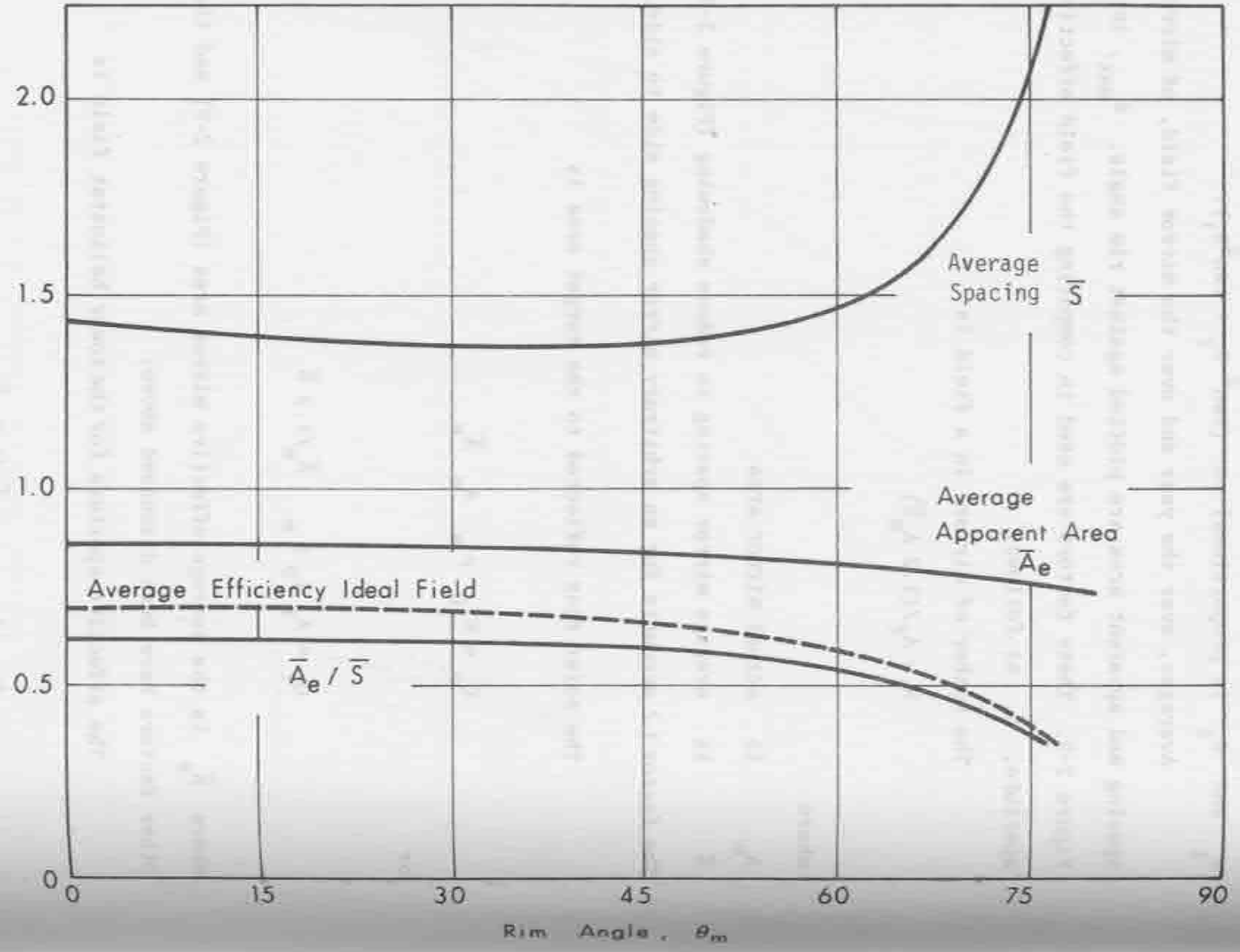
2.0
1.5
1.0
0.5
0
0
15
30
45
60
75
90
Rim Angle, θ_m
Average Spacing $\overline{S}$
Average Apparent Area $\overline{A}_e$
Average Efficiency Ideal Field
$\overline{A}_e / \overline{S}$

As a comparison to the efficiency of the ideal, close packed, field represented by Figure 2-5, the average efficiency of the spaced mirrors is (neglecting the 1.2 for side spacing)

$$\eta_s = \overline{A}_e/\overline{S} \quad .$$

This efficiency is plotted in Figure 2-6 and compares to the average efficiency plotted in Figure 2-5.

The spread factor, g, for the radiation at the top of the tower is

$$g = \pi\sigma_m^2$$

where σ_m^2 is the mean-squared spread of the radiation from all the mirrors in the plane of the target.

First the spread from a single mirror will be derived; then the average effect for the whole field will be found. In Figure 2-10, the side view of a plane mirror reflecting the sunlight to the target area is shown. Each side of the mirror is W meters in length and the ray distance from the center of the target to the ray intercept point is shown in one dimension only. The actual distance in the plane of the target from the center to the striking point of the ray is

$$r_t = [(x+2L\phi_x)^2 + (y+2L\phi_y)^2]^{\frac{1}{2}}$$

where y is the distance normal to x in the plane of the target and ϕ_y is the surface error of the mirror measured in the plane normal to the planes of ϕ_x and the mirror. The errors ϕ_x and ϕ_y are assumed to be independent with Gaussian distributions.

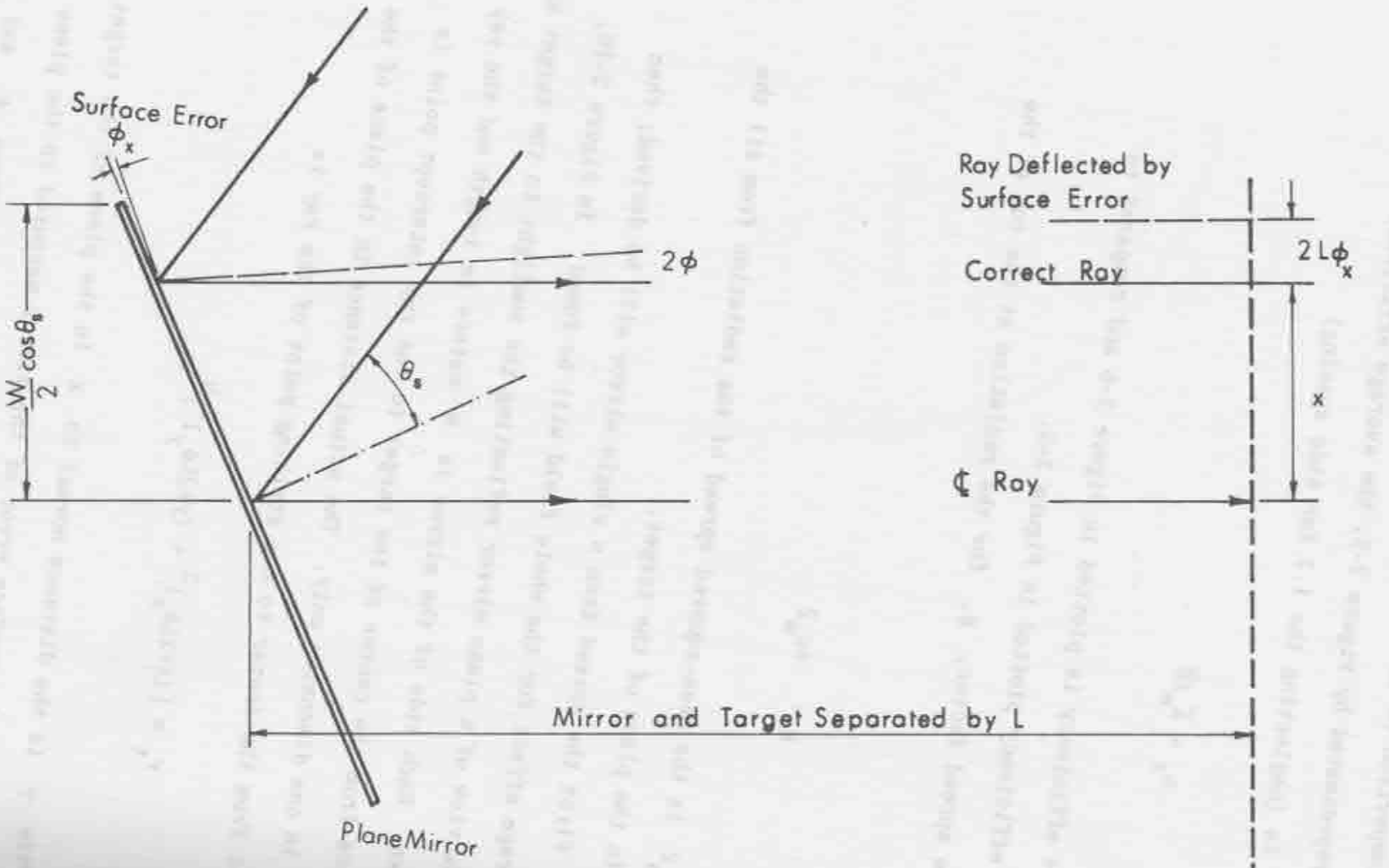

Figure 2-10. Diagram for Derivation of Spread of Solar Radiation at Target as R... by Plane Mirror.

Since it may be assumed that each ray from the mirror has an equal intensity at the target, the mean squared value of r_t is

$$\overline{r_t^2} = \mathcal{E}\left[(x + 2L\,\phi_x)^2 + (y+2L\,\phi_y)^2\right]$$

where $\mathcal{E}$ is the expected value operator. For the mirror represented in Figure 2-10 with angle between the sun and the target in the plane of the diagram,

$$\mathcal{E}(x^2) = \frac{(WA_m)^2}{12}$$

where A_m is the effective height of the mirror as viewed by the tower. Then

$$\overline{r_t^2} = \mathcal{E}\left[\frac{W^2}{12}(1+A_m^2) + 4L^2\,\sigma_\phi^2\right]$$

Effective mirror height A_m is a function of position in the mirror field and L is a function of θ_t, the angle to the tower. To find σ_m^2, the average spread of the radiation from all mirrors, $\overline{r_t^2}$ is averaged over the field, weighting the contribution from each element of the field by the average radiation density reflected from that element. This means each contribution is divided by the mirror spacing at that point in the field. Then

$$g = 2\pi\ \text{Avg}\left[\frac{W^2}{12}\left(\frac{1+A_e^2}{s}\right) + \frac{H^2\sigma_e^2}{s\cos^2\theta_t}\right]$$

where L has been replaced by $H/\cos\theta_t$ and

$$\sigma_e^2 = 4\,(\sigma_\phi^2 + \sigma_\psi^2)$$

to represent both surface and pointing errors in the mirror.

Avg [ ] is the average effect over the entire heliostat field and produces a value of g which is independent of azimuth because it has been averaged over all azimuths, as it was averaged over all sun angles.

After averaging, g may be expressed by

$$g = A_1 A_m + A_2 H^2 \sigma_e^2$$

where A_1 and A_2 are tabulated below for different rim angles.

θ_m	A_1	A_2
15	0.906	6.53
30	0.987	7.35
45	0.879	9.49
60	0.832	15.65
75	0.724	45.68

Using curve fitting techniques the coefficient A_1 and A_2 may be represented by

$$A_1 = 0.573 + 0.671 \cos\theta_{max} - 0.338 \cos^2\theta_{max}$$

and

$$A_2 = 2.02 + 1.82/\cos \theta_{max} + 2.45/\cos^2 \theta_{max} \quad .$$

Thus, the expressiong for E and g for the tower-heliostat concentrating system as expressed above were used with the cost equations in the optimization procedure to determine the optimum tower height and field size to provide lowest cost electrical output.

A logical refinement of the technique would be the inclusion of the tower position in the field as another variable.

3.0 ABSORBER-HEAT EXCHANGER PERFORMANCE

The other solar collector subsystem is the absorber-heat exchanger. The performance parameters, E and g, of the concentrator subsystem can be considered to be design parameters of the absorber-heat exchanger subsystem since they convey all the information about the concentrated radiation that is needed in the absorber analysis. Because of this, a Hottel - Whillier - Bliss analysis can be used as a basis for a generalized treatment of absorber-heat exchanger performance.

The Hottel-Whillier-Bliss approach has been used extensively to analyze the performance of flat-plate collectors. It can be extended to concentrating collectors as was suggested in Löf and Duffie (1963). Section 3.1 below verifies this by deriving the detailed H-W-B relationships for concentrating collectors that were developed as part of this study.

The types of absorber-heat exchangers that were considered in this study are given in Table 3-1.

Section 3.2 details the heat transfer and other models that were required as part of the H-W-B analysis. Also included in this section are other heat transfer models that were required to complete the absorber-heat exchanger analysis, such as tube wall burn-out checks.

3.1 Hottel-Whillier-Bliss Analysis

The flat-plate H-W-B relations extend in a fairly straight forward manner to most concentrating collector absorber-heat exchangers now that expressions for E, g and G have been developed. The situation where the heat exchanger tube is non-uniformly radiated and the heat transfer fluid is water, is somewhat more complicated. Since the development for this case is representative of the development for

TABLE 3-1

Categories for the Absorber-Heat Exchanger Subsystem by Collector Type

POINT FOCUS		LINE FOCUS	
Spherical	Pancake	Round	Flat
• Heat exchanger tubes in series on the surface of a sphere *†	• Helical heat exchanger back insulated*†	• Bare tube †	• Heat exchanger tubes in series on the surface of a flat *†
• Heat exchanger tubes in parallel on the surface of a sphere *†	• Helical heat exchanger uninsulated *†	• Non-evacuated tube with cover †	• Insulated and jacketed tube (Meinel type)
	• Cavity heat exchanger	• Evacuated tube with cover †	

* With or without a fin between tubes.

† With or without selective surfaces.

the uniform intensity case and the changes for the uniform intensity case are fairly obvious, this case will be used to illustrate the general development of the H-W-B relations for concentrating collectors. A schematic representation of this case is given in Figure 3-1.

The tube that transports the fluid in flat-plate collectors and the absorber-heat exchangers of line focusing solar collectors are exposed to a uniform lengthwise radiation. Even in the case of spherical absorber-heat exchangers in point focusing collectors the assumption of a uniform lengthwise radiation may be a reasonable approximation. Here there is often a cyclical variation of radiation intensity over many cycles and the integrated effect may be approximated by assuming a constant radiation level along the tube length. This is not the case of a pancake absorber with a helical heat exchanger tube.

Figure 3-2 is a schematic representation of the distribution of radiation from a point focusing concentrator on a pancake absorber. As can be seen the intensity of the radiation is highest at the center of the pancake absorber and drops off toward the outer edges. Thus, the radiation intensity varies from one end of the heat exchanger tube to the other and increases rapidly near the tube outlet as was indicated in Figure 3-1. The flow direction of the fluid is taken to be from the outside of the pancake absorber to the inside as in counterflow heat exchangers. This maximizes the amount of energy exchanged and provides an added advantage that will be discussed below.

Let x be the distance along the tube from the fluid inlet at the outside of the absorber toward the outlet at the center of the absorber. For a constant radial spacing of the helix, the expression for the local useful rate of energy gain per unit area is

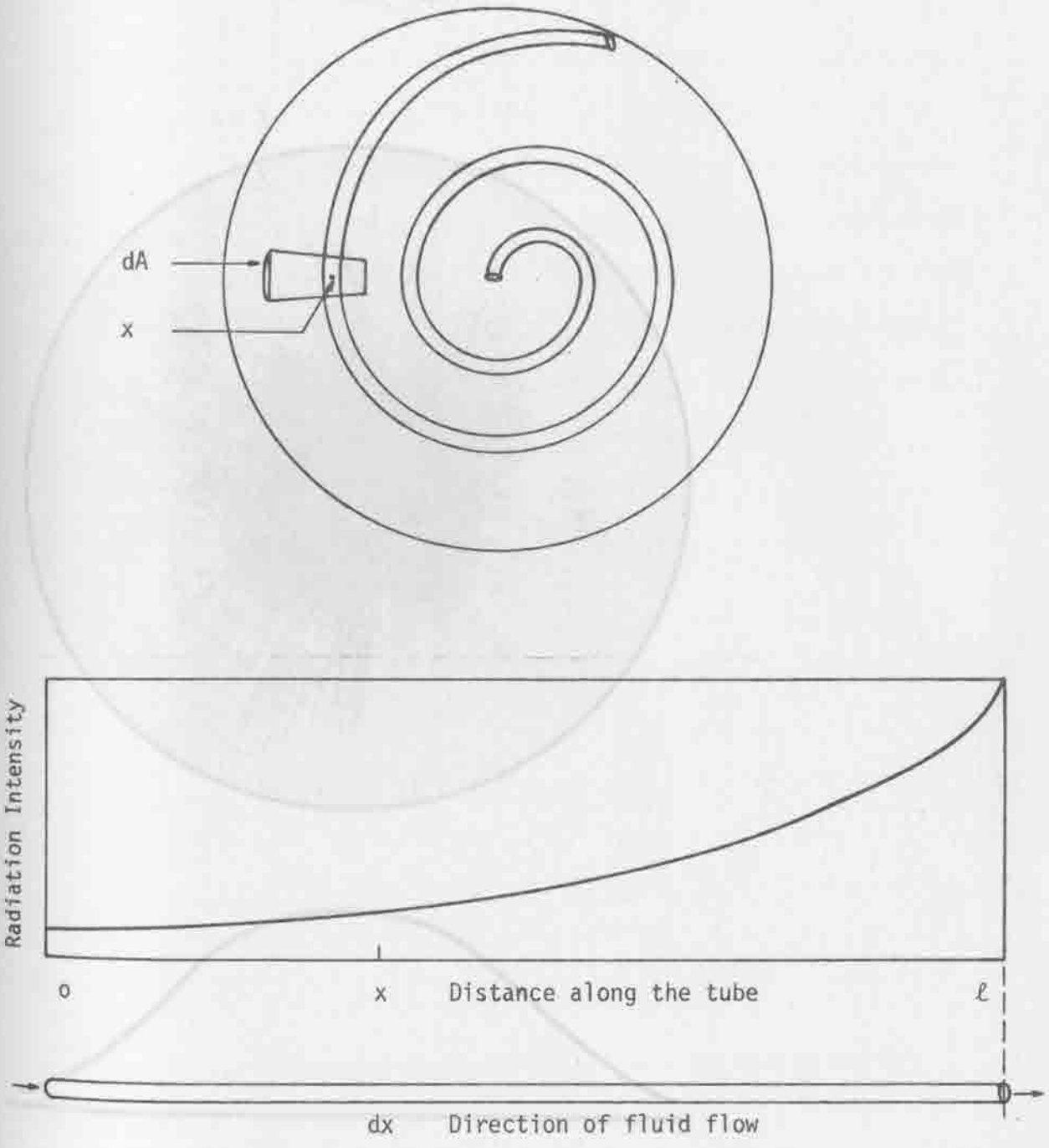

Figure 3-1. Pancake Absorber with a Helical Heat Exchanger Tube

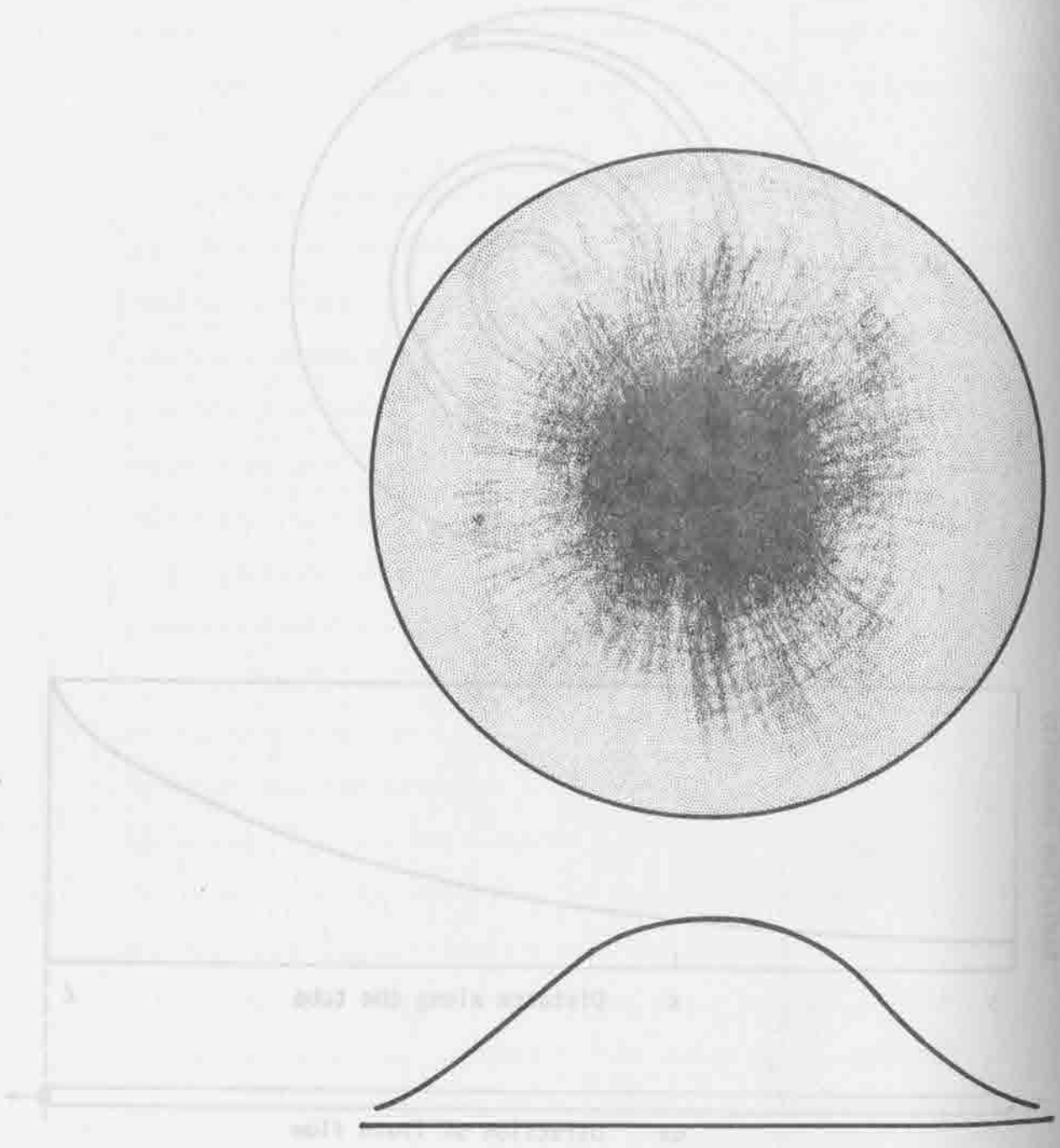

Figure 3-2. Non-Uniform Radiation Intensity on a Pancake Target.

$$q_u = \frac{\ell \dot{m} C_p}{A_L} \cdot \frac{dT_b(x)}{dx}$$

$$= F'' \left[I_D E \alpha \tau \exp(-(\ell - x)A_L/\ell g)/g - U_L(T_b(x) - T_a) \right] \qquad (3\text{-}1)$$

The original form of this equation was used to characterize flat-plate collectors and is due to Hottel and Whillier (1958) and Bliss (1959). The expression $I_D E \alpha \tau$ represents the total radiation delivered to the focal zone. The expression $\exp(-(\ell - x)A_L/\ell g)/g$ is the radiation intensity at x normalized by $I_D E \alpha \tau$. This expression arises from the fact that the normalized radiation intensity for point focusing collectors follows an exponential distribution with parameter g. This was shown by Duff and Lamerio (1974) and in section 2 of this appendix.

F'' in equation 3-1 is given as

$$F'' = \frac{F(A_L - \ell d)}{A_L} + \frac{\ell d}{A_L} \qquad (3\text{-}2)$$

in equation 3-2, F is the fin efficiency factor.

$$F = \frac{\tanh\left[\sqrt{U_L/k_{fin} t_{fin}} \; (A_L - \ell d)/2\ell\right]}{\sqrt{U_L/k_{fin} t_{fin}} \; (A_L - \ell d)/2\ell} \qquad (3\text{-}3)$$

Equation 3-1 may be written in terms of the local fluid temperature rather than the local fin base temperature.

$$q_u = \frac{\ell \dot{m} C_p}{A_L} \cdot \frac{dT_f(x)}{dx}$$

$$= F'[I_D E \alpha \tau \exp(-(\ell - x)A_L/\ell g)/g - U_L(T_f(x) - T_a)] \qquad (3\text{-}4)$$

Here F' is

$$F' = F'' \quad \frac{I + F'' U_L A_L}{h_o \pi \ell d} \tag{3-}$$

The above factors F, F' and F'' have been generalized from the factors for flat-plate collectors that are available in the literature -- for instance see Kline, Duffie and Beckman (1974). The factors are those where the heat exchanger tube is integral with the fin. These generalized forms of the factors are applicable to most types of absorber-heat exchangers including pancake or spherical absorbers for point focusing collectors, flat or round absorbers for line focusing collectors and for flat-plates.

Solving Equation 3-4 for the local fluid temperature we have

$$T_f(x) = \frac{F' I_D E \alpha \tau \exp(-A_L/g)}{F' U_L g + \dot{m} C_p} \exp(A_L x/\ell g) - \exp(-F' U_L A_L x/\ell \dot{m} C_p)$$

$$+ (T_{in} - T_a) \exp(-F U_L A_L x/\ell \dot{m} C_p) + T_a \tag{3-}$$

The average temperature of the fluid in the tube, T_{ave} may then be determined by integrating along the tube length and dividing by the tube length.

$$T_{ave} = \frac{F' I_D E \alpha \tau \exp(-A_L/g)}{F' U_L g + \dot{m} C_p} \frac{g}{A_L} [\exp(A_L/g) - 1]$$

$$+ \frac{\dot{m} C_p}{F' U_L A_L} [\exp(-F' U_L A_L/\dot{m} C_p) - 1]$$

$$- \frac{(T_{in} - T_a) \dot{m} C_p}{F' U_L A_L} [\exp(-F' U_L A_L/\dot{m} C_p) - 1] + T_a \tag{3-}$$

The total useful rate of energy gain of the absorber may now be expressed as

$$Q_u = F' \left[I_D \bar{\varepsilon\alpha\tau} \left[1-\exp(-A_L/g)\right] - U_L A_L \left(T_{ave} - T_a\right) \right] \qquad (3\text{-}8)$$

Again the expression $1 - \exp(-A_L/g)$ arises from the fact that the radiation is exponentially distributed with parameter g. This expression is the fraction of available radiation that is intercepted by the absorber. T_{ave} is found by successively approximating the average temperature on the right hand side of Equation 3-7. T_{ave} is then used to find Q_u in Equation 3-8. The average fluid temperature is used for evaluating U_L in Equations 3-7 and 3-8 since it usually differs very little from the average fin base temperature.

These equations are useful for conducting performance comparisons, as will be shown below, as well as for the optimization. The performance of pancake absorbers with helical heat exchangers and water as the heat transfer fluid is illustrated in Table 3-2 for 10 design variations. The first design in the table is for the A_L that yields maximum performance in terms of useful heat output with the other design parameters held constant. The design parameters were then varied one at a time using this design as a base. The effect on performance of each design variation is also given in the table.

A further comparison is made with the performance predicted by Equations 3-7 and 3-8 and the performance using analogous equations derived under the assumption of uniform radiation. These comparisons are also shown in the table. These differences are expressed in percentage change from the nonuniform radiation performances. As can be seen, the average

TABLE 3-2

Nonuniform and Uniform Irradiance Performance Comparisons

		DESIGN VARIATIONS									
		1	2	3	4	5	6	7	8	9	10
DESIGN PARAMETERS	E	8.0	4.0	8.0	8.0	8.0	8.0	8.0	8.0	8.0	8.0
	g	.010	.010	.002	.010	.010	.010	.010	.010	.010	.010
	A_L	.070	.070	.070	.095	.070	.070	.070	.070	.070	.070
	ℓ	7.0	7.0	7.0	9.5	5.0	14.0	7.0	7.0	7.0	7.0
	d	.010	.101	.010	.010	.010	.005	.010	.010	.010	.010
	t_{in}	40.0	40.0	40.0	40.0	40.0	40.0	200.0	40.0	40.0	40.0
	t_a	20.0	20.0	20.0	20.0	20.0	20.0	20.0	0.0	20.0	20.0
	$\dot{m}$	.010	.010	.010	.010	.010	.010	.010	.010	.005	.010
	α	.90	.90	.90	.90	.90	.90	.90	.90	.90	.90
	ε	.90	.90	.90	.90	.90	.90	.90	.90	.90	.10
	τ	1.0	1.0	1.0	1.0	1.0	1.0	1.0	1.0	1.0	1.0
	t_{fin}	---	---	---	---	.005	---	---	---	---	---
	k_{fin}	---	---	---	---	211.0	---	---	---	---	---
NONUNIFORM IRRADIANCE	T_{out}	204.3	121.6	205.0	204.0	202.1	207.0	343.4	203.6	365.8	205.8
	T_{ave}	63.0	51.2	44.3	56.7	62.7	63.4	216.9	62.6	85.6	63.3
	Q_u	6.87	3.41	6.90	6.86	6.78	6.98	6.44	6.84	6.82	6.93
UNIFORM IRRADIANCE	$\%\Delta T_{out}$	-2.2	-1.2	-2.5	-2.8	-2.1	-2.3	-4.0	-2.2	-7.7	-1.7
	$\%\Delta T_{ave}$	91.5	56.9	172.6	111.5	90.8	92.4	22.4	92.2	123.9	92.3
	$\%\Delta Q_u$	-1.8	-1.7	-2.2	-2.7	-1.7	-1.9	-3.1	-1.8	-4.3	-1.2

temperature of the absorber-heat exchanger predicted by each of the assumptions varies quite significantly. Also, the performance differences between the two assumptions is accentuated when the inlet temperature is elevated or when the mass flow rate is lowered.

A significant result of the comparison between the uniform and nonuniform radiation assumptions is illustrated in Figure 3-3. In this figure it can be seen that the optimum size of the pancake absorber when the other design parameters are fixed at their values in the base design is quite different depending upon which assumption is made. The optimum size pancake absorber under the more realistic assumption of nonuniform radiation turns out to be 30% larger than the optimum absorber under the assumption of uniform radiation. Also, there is a difference between the maximum performance predicted in each case of 1.5%. The most significant aspect of this comparison, however, is the fact that the nonuniform radiation assumption predicts a very gradual fall off in performance as the absorber increases in size beyond the optimum, whereas the uniform radiation assumption predicts a steep fall off. This is rather important in terms of actually manufacturing an absorber-heat exchanger for a solar collector. In manufacturing solar collectors, variations in the amount of spread of the radiation distribution from one collector to another will occur. It is very useful to know that the absorber can be made oversize to compensate for this variation without penalizing the optimal performance of an individual collector to a significant degree.

The reason for this difference is illustrated in Figure 3-4. Shown in this figure is the fact that the absorber temperature is always lower for nonuniform radiation and thus radiative and convective losses will

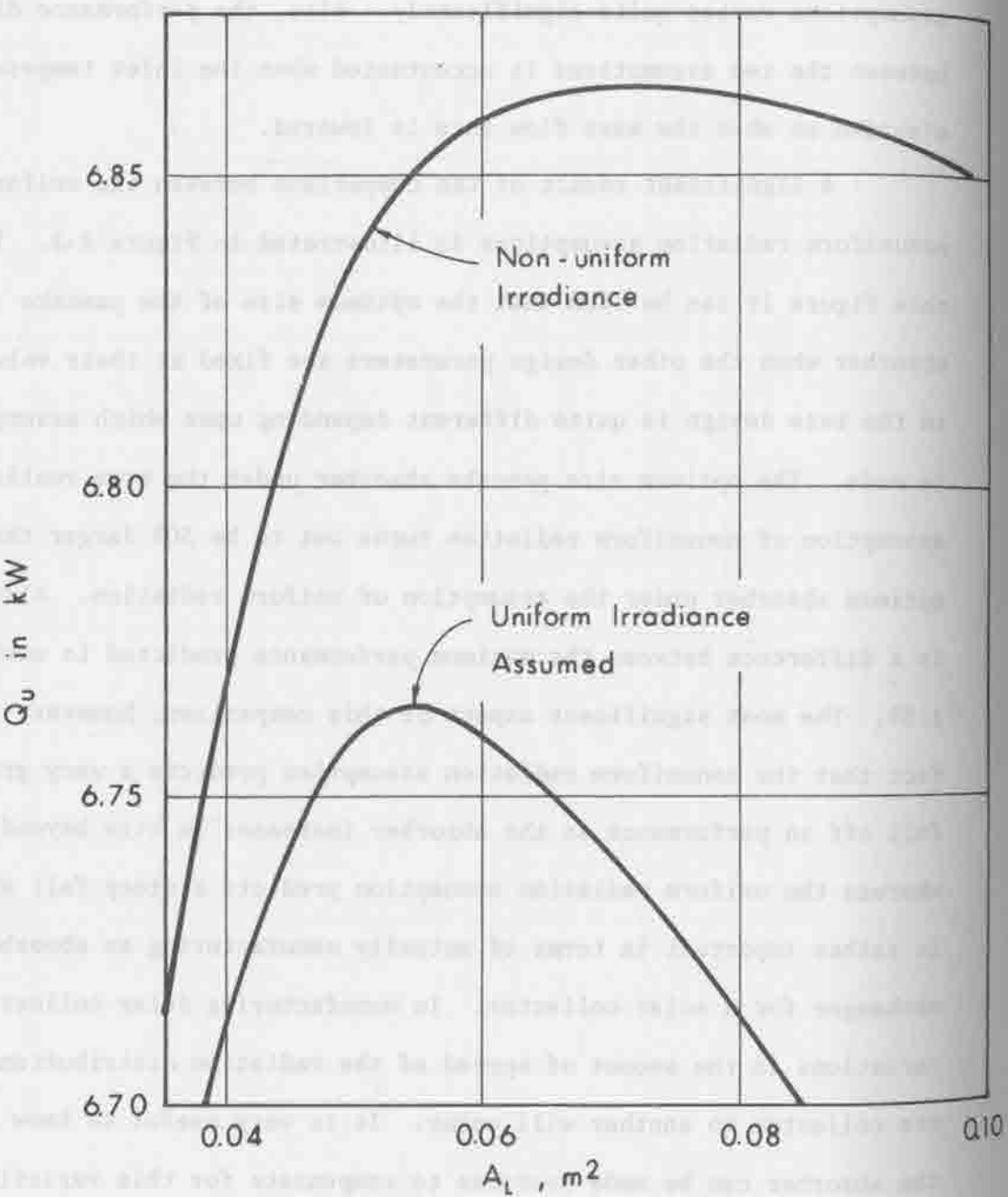

Figure 3-3. Non-Uniform Irradiance Pancake Absorber Helical Heat Exchanger Performance.

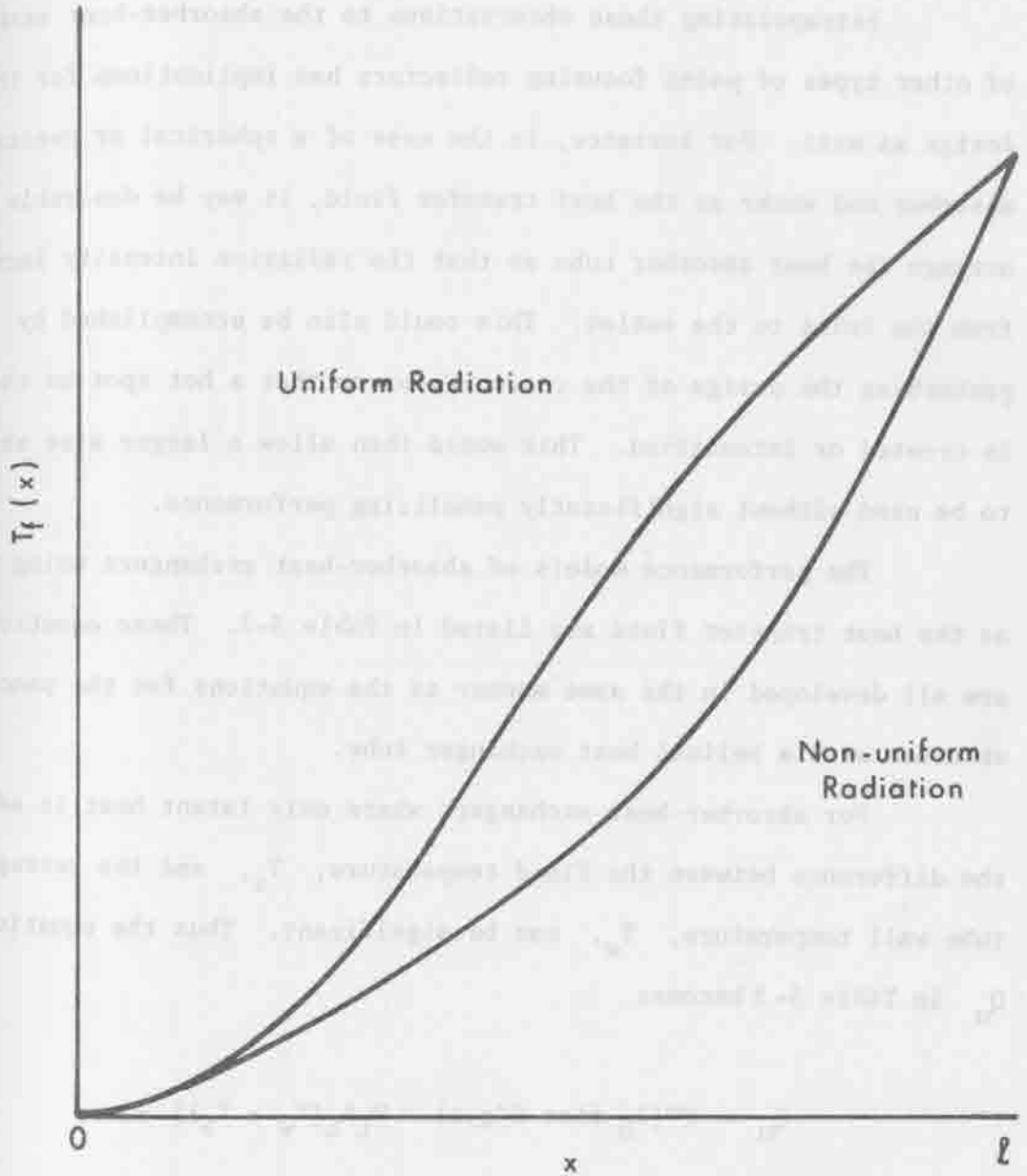

Figure 3-4. Fluid Temperature Distribution Along the Heat Exchanger Tube.

be lower. When the absorber is made larger these differences are accentuated.

Extrapolating these observations to the absorber-heat exchangers of other types of point focusing collectors has implications for their design as well. For instance, in the case of a spherical or conical absorber and water as the heat transfer fluid, it may be desirable to arrange the heat absorber tube so that the radiation intensity increases from the inlet to the outlet. This could also be accomplished by perturbing the design of the concentrator so that a hot spot on the absorber is created or intensified. This would then allow a larger size absorber to be used without significantly penalizing performance.

The performance models of absorber-heat exchangers using water as the heat transfer fluid are listed in Table 3-3. These equations are all developed in the same manner as the equations for the pancake absorber with a helical heat exchanger tube.

For absorber-heat exchangers where only latent heat is added, the difference between the fluid temperature, T_s, and the average tube wall temperature, T_w, can be significant. Thus the equation for Q_u in Table 3-3 becomes

$$Q_u = F''[I_D E L\alpha\tau G(g,a) - U_L A_L (T_w - T_a)] \quad (3-9)$$

For boiling absorber-heat exchangers, Q_u can also be expressed as

$$Q_u = \pi d\ell h_B (T_w - T_s) \quad (3-10)$$

TABLE 3-3

Absorber-Heat Exchanger Equations

DESCRIPTORS	PANCAKE ABSORBER	SPHERICAL ABSORBER	FLAT LINEAR ABSORBER	CIRCULAR LINEAR ABSORBER	FLAT-PLATE COLLECTOR
L	1		Absorber Length		
G(g,a)	$1 - e^{-\frac{a}{g}}$		area under the $\mu=0$, $\sigma=g$, normal distribution between $-a/2$ and $+a/2$.		1
a	area of circle	cross sectional area of sphere	width	diameter	---
$T_f(x)$	$\frac{F'I_D\xi\tau\alpha e}{F'U_L g+\dot{m}C_p}\left(e^{\frac{-A_L}{g}\left(\frac{A_L x}{g}\right)} - e^{\frac{-F'U_L A_L x}{\ell \dot{m} C_p}}\right) + (T_{in} - T_a)\, e^{\frac{-F'U_L A_L x}{\ell \dot{m} C_p}} + T_a$		$\frac{I_D\xi\tau\alpha G(g,a)}{U_L A_L}\left(1 - e^{\frac{-F'U_L A_L x}{\ell \dot{m} C_p}}\right) + (T_{in} - T_a)\, e^{\frac{-F'U_L A_L x}{\ell \dot{m} C_p}} + T_a$		
T_{ave}	$\frac{F'I_D\xi\tau\alpha e}{F'U_L g + \dot{m} C_p}\left[\frac{g}{A_L}\left(e^{\frac{A_L}{g}} - 1\right) - \frac{F_R}{F'}\right]^{-\frac{A_L}{g}} + (T_{in} - T_a)\,\frac{F_R}{F'} + T_a$ (Note 1)		$\frac{I_D\xi\tau\alpha G(g,a)}{U_L A_L}\left[1 - \frac{F_R}{F'}\right] + (T_{in} - T_a)\,\frac{F_R}{F'} + T_a$ (Note 1)		
Q_u	$F'\left[I_D\xi\tau\alpha G(g,a) - U_L A_L (T_{ave} - T_a)\right]$ (Note 2)				

Notes for Table 3-3

(1)

$$F_R = \frac{\dot{m} C_p}{U_L A_L} \left[1 - e^{\frac{- F' U_L A_L}{\dot{m} C_p}} \right]$$

(2) For the uniform radiation case only, Q_u can be written as

$$Q_u = F_R \left[I_D E L \alpha \tau G(g,a) - U_L A_L (T_{in} - T_a) \right]$$

Combining Equations 3-9 and 3-10, gives

$$T_w = \frac{\pi d \ell \pi h_B T_B + F'' I_D \bar{E}L \alpha\tau G(g,a) + F'' U_L A_L T_a}{\pi d \ell h_B + F'' U_L A_L} \qquad (3\text{-}11)$$

T_w is then found by successively approximating the average temperature on the right hand side of Equation 3-11. T_w is then used to find Q_u in equation 3-9 or 3-10.

3.2 Physical Property Models

The major physical property models required to use the performance models are given below. These models are drawn from many different sources. As is often the case in the thermal sciences, a number of alternative choices were available for most models. The choice of a particular model was based on two considerations: (1) its adequacy in reflecting relative differences between designs and (2) the speed of computation. As mentioned previously, computational speed enhances the efficiency of the optimization procedures.

Minimum tube internal diameter to insure turbulent water flow:

$$.007 \dot{m} T_{out} \quad (m)$$

Minimum tube diameter to avoid clogging by internal impurity build up:

$$.002 \quad (m)$$

Where tube diameters were still too large compared to the size of the absorber, the diameter was decreased to provide sufficient wrap around length:

Minimum tube wall thickness to withstand pressure p in bars:

$d_p/2040$ (m)

Minimum tube wall thickness for structural ridgity:

.0001 (m)

Radiative component of U_L:

$$\varepsilon\sigma[(T_{ave}+273.15)^4 - (T_a+268.15)^4]/(T_{ave}-T_a) \quad (W/m^2-{}^oC)$$

U_L for nonevacuated covered absorber-heat exchanger tubes when the wind velocity is 5 m/sec (regression curve fit to curves on pages 53 and 54 of the October 1973 STEPS report):

$$7.0867 + [.0547\ (T_{ave} + 273.15) - 15.4987\ ]\varepsilon \quad (W/m^2-{}^oC)$$

U_L for evacuated covered absorber-heat exchanger tubes when the wind velocity is 5 m/sec (regression curve fit to curves on pages 53 and 54 of the October 1973 STEPS report):

$$.6492 + [.0547\ (T_{ave} + 273.15) - 15.4987\ ]\varepsilon \quad (W/m^2-{}^oC)$$

Heat transfer coefficient between circulating water and the tube wall for laminar flow in the entrance region * (Whillier, ASHRAE):

$$\frac{k_f}{d}\left[4.36 + \frac{.0668d\ Pr\ Re/\ell}{[1+.04(dPrRe/\ell)]^{.66}}\right] \quad (W/m^2-{}^oC)$$

Heat transfer coefficient between circulating water and the tube wall for laminar flow * (McAdams, Heat Transmission):

---

* The values of the various quantities in these expressions are a function of temperature.

$$3.66 \frac{k_f}{d} \quad (W/m^2\text{-}^oC)$$

Heat transfer coefficient between circulating water and the tube wall for turbulent flow * (McAdams, Heat Transmission):

$$0.23 \frac{k_f}{d} Pr^{.4} Re^{.8} \quad (W/m^2\text{-}^oC)$$

Heat transfer coefficient for the convection component of U_L for a flat absorber-heat exchanger * (Rohsenow and Choi):

$$.916 Pr^{1/3} Re^{\frac{1}{2}} \frac{k}{d}, \quad Re \leq 5 \times 10^5$$

$$\frac{.937 C_p \rho V}{Re^{.2} Pr^{2/3}} \quad Re > 5 \times 10^5 \quad (W/m^2\text{-}^oC)$$

Heat transfer coefficient for the convection component of U_L for a spherical absorber-heat exchanger * (Eckert and Drake, Analysis of Heat and Mass Transfer):

$$.37 Re^{.6} \frac{k}{d} \quad (W/m^2\text{-}^oC)$$

Heat transfer coefficient for the convection component of U_L for a cylindrical absorber-heat exchanger * (Holman):

$$.3 Re^{.56} Pr^{.33} \frac{k}{d} \quad (W/m^2\text{-}^oC)$$

* The values of the various quantities in these expressions are a function of temperture.

Heat transfer coefficient between circulating unsaturated steam and the tube wall* (Strack, NASA-TN D-5813) :

$$.0828 \frac{k_f}{d} Pr^{.4} Re^{.8} \left(Re \frac{d^2}{d_m^2}\right)^{.05} \quad (W/m^2\text{-}^oC)$$

Value of radiation intensity where tube burnout occurs (Lowdermilk et.al., NASA TN-4382):

$$2{,}365{,}000 \quad (W/m^2)$$

The maximum radiation intensity on the absorber-heat exchanger is

$$\frac{I_D E}{g} \quad (W/m^2)$$

for point focus concentrators and

$$\frac{I_D E}{\sqrt{2\pi g}} \quad (W/m^2)$$

for line focus concentrators as can be easily derived from G(g,a).

---

* The values of the various quantities in these expressions are a function of temperature.

4.0 COST MODELS

The objective in costing the concentrating collectors is to provide the optimizing model with costs on a wide range of alternative collector designs with different performance characteristics in such a way that biases are not introduced favoring one type of collector over another.

Concentrator designs were selected to cover the range of economically attractive possibilities in terms of performance, configuration, materials, and manufacturing techniques. Types considered for analysis included paraboloids, partial spheres, catenaries of revolution, heliostats for power towers, troughs, Fresnel lenses and reflectors, and inflated plastic cylinders. Estimates were obtained for paraboloids set both collectively on supporting racks and individually on their own mounts. Focusing possibilities included parallel and series absorbers for each reflector, as well as more than one reflector focusing on a common absorber. Linear absorbers for troughs included exposed pipe, shielded pipe, and pipe inside an evacuated glass tube.

This selection of reflectors and absorbers covers the range of the more relevant possibilities as of this date. As life tests on thin reflective films under tension become available, these too could warrant consideration. Partial spheres and catenaries of revolution were dropped from the list early in the study because they possess little, if any, cost advantage over the paraboloids in compensation for their poorer performance; and inflated plastic cylinders were dropped because of their short anticipated life and consequently high replacement and maintenance costs.

Alternative parameters considered for the reflective shells

were those of aperture width, rim angle*, reflectivity, contour accuracy and tracking accuracy. Aperature widths ranged from ten centimeters to 7.5 meters. Rim angles were from 45 to 115 degrees. Reflectivities in the neighborhood of 85 to 90 percent resulted from the choice of reflective materials. Contour accuracy of 0.1 degree is obtainable from standard manufacturing processes for paraboloidal shells; but lesser accuracies result when fabricating sections and when mounting more than one shell on a common frame. Reliable estimates of effective contour accuracies require experimental testing, which was not part of this research effort. Similarly, tracking accuracy of 0.1 degree can be obtained from proper selection of motor drives and gears; but actual tests of performance are required to estimate overall accuracy.

The principal parameters influencing the costs of absorbers were those of temperature and pressure. Temperatures that were considered extended from a low of 100 ^{o}C to a high of 315 ^{o}C, while pressures ranged from 14.7 psia to 2,365 psia. Parameters less important to overall costs were absoptivity and emissivity, which were on the order of 95 percent and 10 percent respectively.

Wind loads of 45 meters per second were used in estimating the structural and foundation requirements of the installations. For loadings above this level, low-cost shear-pin assemblies were assumed to protect the installations by allowing a collector to position itself more favorably to the wind. Wind loads for performance were not parameterized in comparing the costs of alternative designs. Structural

---

*The rim angle is then formed by the ray extending vertically through the focus and the ray from the focus to the rim of the reflector when the reflector is in the horizontal position.

design coupled with wind-tunnel testing would probably be required to arrive at reliable estimates of cost-performance relationships.

The relevant costs for comparison of the various alternatives include those of investment, maintenance, operation, and replacement. Given the significance of investment to overall costs coupled with the lack of information on component lives and maintenance procedures, most of the costing effort centered on initial investment. Investment costs cover manufacturing, field facilities and structures, and installation. Comparative costs substantially favor manufacture and pre-assembly over field construction. Accordingly, collectors were assumed to be built in modular units ready for quick assembly in the field. Transportation clearances of 4.3 meters limited the maximum size of modular units to approximately 3.65 meters on one side. Two 3.65 x 7.3 meter sections could be shipped and installed in the field to give a frame with multiple reflectors that is 7.3 meters square or a circular section 7.3 meters in diameter. To the extent practicable, the absorbers would be part of this pre-assembled package. Field structures and facilities would include the supports and foundations for the modules and tracking and electrical installations.

Normal maintenance and operating costs were assumed to be similar to other outdoor facilities, such as those encountered in the electric utility industry. Similarly, estimates of the lives of structures, gears, motors, electrical connections, and the like were obtained from industry sources. Overall life of the installations was assumed to be 30 years. Estimating the maintenance and replacement costs of the reflective surfaces, however, presented a more difficult problem because of the lack of experience and data on such items. A sensitivity analysis (Section 4.7.3)

indicates that frequent cleaning of the surfaces is not as economical as allowing the surfaces to become dirty and building additional surface area to make up for the loss in reflectivity. Non-routine cleaning of the surfaces following particularly unfavorable conditions, such as heavy dirt deposits from combined rain and dust storms, would be done. The effective lives and the costs of replacing the reflective surfaces are even more difficult to estimate with confidence. As a first approximation, these costs have been assumed to be similar for all types of installations and have been omitted from the analysis until more reliable information is obtained.

4.1 Methods of Estimation

The large collection of reference material on solar energy (technical journals, conference proceedings, etc.) located at C.S.U. was screened for relevant data on concentrating collectors. Categories of data collected included: types of concentrators and absorbers, materials, dimensions, performance, tracking methods and devices, methods of manufacture, manufacturers of concentrators, reflective materials, absorber components, operation and maintenance procedures, and costs.

Cost data obtained from this search served as points of reference, but could not be used directly in the modelling because of the general lack of detail and its specificity to particular designs. Accordingly, reliance for costing information was shifted to three alternative and complementary sources: the Manufacturing Development Laboratory (MDL) of the Westinghouse Electric Corporation, data currently being developed by investigators of point designs such as Black and Veatch (Consulting Engineers), and project staff at C.S.U. MDL pro-

vided cost estimates for the large-scale manufacture of collectors driving and control mechanisms, and for maintenance and operation of the system. Black and Veatch, among other things, made available their detailed estimates of piping connections to the collectors and costs on power towers. C.S.U. staff provided estimates of absorber, field, and installation costs, as well as developed the cost functions for the range of parameters required for the optimizing model.

Cost data derived from the foregoing sources were used as building blocks for the various collector designs. For instance, costs for modular frames, drives, and tracking were first developed for sets of small parabaloids mounted on racks. These costs were essentially the same as for heliostats used to focus on the power towers. Such costing procedures wherein only the differences in conditions require additonal cost estimates reduced the amount of costing effort and yielded consistency among the alternatives.

All cost values were adjusted to estimates in dollars. In making these estimates, large-scale production was assumed. That is, if economically or otherwise feasible, solar energy plants were assumed to comprise a significant amount of new generating capacity. This led to an admittedly crude estimate of annual installations of 17.5 million square meters of projected surface area.* This level of installation is sufficiently large to confirm that installation of solar facilities

*Five percent of the projected average annual additions to utility generating capacity for the 1970 to 1980 period in the United States was arbitrarily selected, Federal Power Commission, (1971). This amounts to 1,750 megawatts of solar generating capacity being installed on the average each year, using a conversion ratio of 10 percent from solar radiation to electrical energy and peak solar radiation of one kilowatt per square meter.

at this rate indeed involves large-scale production on the part of potential manufacturers of concentrating collectors.

Westinghouse staff specialized in the fields of materials, production equipment, and manufacturing processes combined their knowledge to select what in their opinions were the most suitable materials and processes for concentrating collectors over the aforementioned ranges of parameters. Conceptual designs were set and from these flowed estimates of quantities of materials, labor, and equipment. Methods of production, such as in-house forming of structural frames and cutting of gears, large quantity costs for materials, labor rates, and production equipment costs were obtained through suitable contacts within Westinghouse and from other organizations. Estimates of overhead rates, profit levels, and other costs of the manufactured collectors and absorbers came from a variety of sources. Throughout, emphasis was on breadth of coverage and consistency of estimates rather than on detailed estimates for a limited number of designs.

4.2 Paraboloids

The paraboloid was the first type of concentrating collector studied by the CSU/Westinghouse team. As a result, it serves as a basis for developing portions of the cost data for other types of concentrating collectors--particularly the heliostat and circular Fresnel lenses and reflectors. Moreover, the analytical approach to design and costing for paraboloids is more thoroughly studied and described than for other types of collectors. This does not mean, however, that the results for the other types are less reliable, since the paraboloid was used as a learning process in developing the design and costing metho-

odologies. The sections that follow reflect these circumstances and include discussions of manufacturing materials and processes for concentrators and absorbers, field structures and installations, cost breakdowns for two of the lower-cost alternatives, and parametric relationships for aperture width, reflectivity and rim angle.

4.2.1 Manufacturing Materials and Processes for Concentrators

Alternative materials and processes were systematically listed and described, followed by a review of the most suitable combinations for the ranges of parameters being considered. Eight characteristics (e.g., reflectivity, costs per square meter of applied surface, and useful life) for 19 surface materials (e.g., silver, aluminum, chromium and rhodium) were tabulated. Similarly, 22 characteristics (e.g., costs per kilogram, ease of forming, coefficients of thermal expansion, and tensile strength) for 32 shell materials (e.g., aluminum, steel, cast iron, glass, epoxies, and lightweight concrete were also tabulated. For both categories of materials an initial weighting system was applied to the various characteristics to identify those materials apparently most favorable for the requisite conditions. The weighting served to highlight various possibilities rather than to serve as the basis for the final selection. For example, thermally evaporated silver and chromium plating ranked high as potential surface materials, while pressed glass and fiber glass reinforced cement ranked high as shell materials.

Descriptions of alternative manufacturing processes were obtained from published sources to identify the relevant possibilities. Of primary concern were accuracy of forming, rates of output per machine, and costs per machine. Assuming that production of collectors

is to come from five plants strategically located across the United States, annual output for 250 working days per year would be 14,000 square meters of projected area per day.* By knowing the nominal production rate and the limits of a machine's capabilities to produce different aperture widths, the number of machines required for different aperture widths can be determined. Thirteen alternative processes are plotted in Figure 4-1. By way of illustration, injection molding of collectors with one meter aperture would call for about 10 machines each producing at the rate of 2 per minute; whereas, the same process producing collectors with apertures of 10 centimeters would call for about 100 machines each producing at the rate of 20 per minute. The foregoing machines operating on a two-shift basis would in both cases turn out 14,000 square meters of projected surface area each day.

The foregoing information was augmented by discussions with process technologists to arrive at production techniques and materials most suitable for the various sets of collector parameters. The coice for the smallest aperture range (10 to 30 centimeters) was pressed glass with vapor deposited aluminum for reflectivity of 85 percent and silver for reflectivity of 90 percent.

Aluminum sheets were selected for the shell material for the paraboloids of medium (0.5 to 3 meters) and large (3.5 and 7.5 meters) apertures. Diaphragm hydro-drawing would be used in shaping the medium sizes and spin forming would be used for the larger sizes. Initially, explosion forming had been favored for the latter, but was dropped

---

* 1,750 megawatts per year at 10 percent conversion would require about 17.5 million square meters. Five plants operating 250 days per year would each have a daily output of 14,000 square meters.

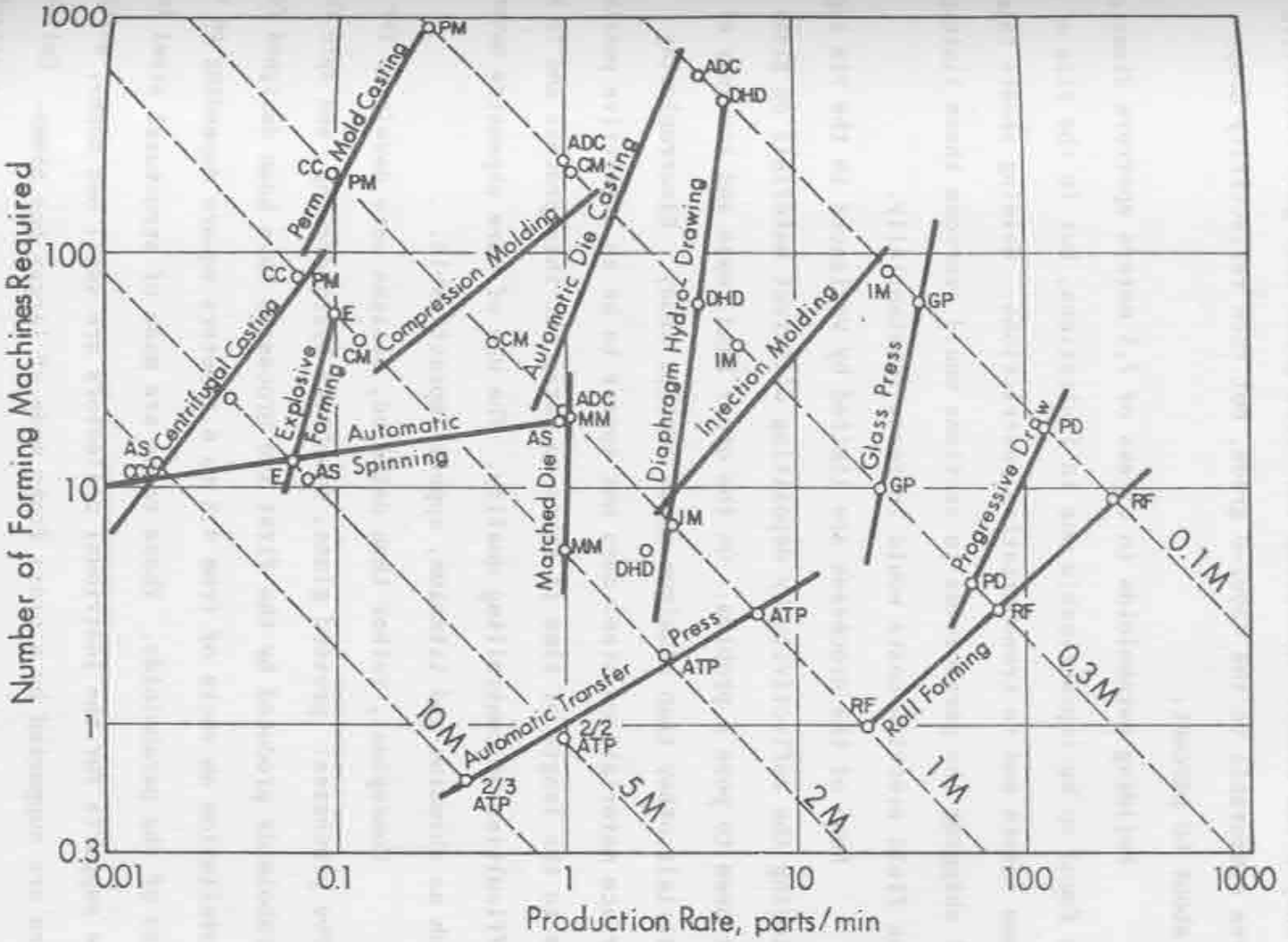

Figure 4-1. Production of Paraboloidal Collectors 14,000 m^2/plant/day.

because of excessive costs. Aluminum alloy #3002-0 is reflector grade and when highly buffed and anodized will give reflectivities of 85 percent for several years. A less expensive grade of aluminum, alloy #1100, gives reflectivities from 75 to 85 percent when buffed and not anodized. Duration of such reflectivities are short, being on the order of only a few weeks. Anodizing the #1100 grade will give reflective lives comparable to the #3002-0 grade, but then reflectivity drops to about 60 percent.

Building paraboloids in excess of 7.5 meters aperture diameter was found to be impracticable due to limitations, but in the size of aluminum sheets and to transportation restrictions. Welding sheets together and shipping the paraboloids in sections would overcome these limitations, then field erection costs would increase substantially.

None of the processes are limited by variances in the rim angle. Altering the reflectivity by depositing different materials on glass does not seem to pose a problem. On the other hand, ease and accuracy of shaping materials other than aluminum needs further study. Electroplating surface materials on steel does not appear to be an attractive possibility due to the length of time it takes to carry out this process and to the difficulties of controlling quality. The use of more expensive materials, such as chromium and titanium, appear impracticable.

Conceptual, rather than detailed, designs were developed for the three processes: pressed glass, diaphragm hydro-drawing, and spin forming. Paraboloids produced by the first two processes have been designed for installation on racks of from 4.5 to 6.1 meters square depending on the size of the paraboloids. These racks are made of structural steel in which the supports for the individual collectors are small box beams, which in turn are supported by a cross frame made of larger box beams. Collectors are positioned in the openings between the small box beams and attached

by means of simple fasteners. Each rack is mounted on balanced gimbled joints that are driven by either high-torque stepping motors or synchronous gear motors, depending on the particular tracking control system adopted.

4.2.2 Types and Characteristics of Absorbers

The characteristics of "point" focusing absorbers for paraboloids depend upon the types of collectors and the means for circulating the absorbing fluid. If the paraboloid is singly mounted and the absorber remains in a fixed position, flexible hoses and couplings can be omitted; but if the absorber moves as the paraboloid tracks the sun, flexible hoses and couplings are needed. Where multiple paraboloids with individual absorbers are set in a frame and the frame tracks the sun, then flexible couplings are also needed. On the other hand, where multiple paraboloids focus on a single absorber, the possibilities are similar to those for singly mounted paraboloids.

The multiple paraboloids could be connected in series or in parallel, and the amount of material would vary accordingly. If the rim angle is less than 90 degrees, the absorber could be in the form of a continuous pipe with suitable openings and surface coating. But if the rim angle is more than 90 degrees, the absorber spurs would have to branch into the reflector or else portions of the reflector would have to be notched out.

Components of the absorber unit are the absorber pipe or tubing, the coating, connecting pipe or tubing, insulation, and connections. Valves between the main pipeline network and collector modules are included as part of the piping network. For singly mounted paraboloids, the absorber would be a single unit located at the focal point. The size

of the absorber depends on the concentration ratio. For modelling purposes three types of paraboloidal absorbers were considered: the sphere, helix, pancake and cavity. Whatever the shape, manufacturing techniques are available to meet practical requirements. Paints for low temperatures and metalizing processes for higher ones are under study elsewhere. Overall costs are not sensitive to the types of coatings on "point" focusing absorbers because of the small amount of material and processing involved.

The absorber and connecting pipe would be of stainless steel to prevent corrosion and to guard against fouling of the lines. Calcium silicate with protective aluminum jackets was selected for the insulating material. If the absorbers are stationary, standard tees and elbows would be used for connections; but if the absorber moves, flexible couplings of braided metal and either synthetic rubber or thermoplastics would be used. Costs escalate rapidly as the temperatures and diameters of flexible hose and couplings increase. In fact, those manufacturers of flexible connections that were contacted during the study do not offer warranties for their products when operating temperatures exceed 230 ^{o}C for more than brief periods.

4.2.3 Field Structures and Installations

The assembly of paraboloidal shell (or shells) and absorber (or absorbers) would be mounted on heavy-walled pipe machined at the top to accept the assembly inserts. The pipe would first have been set in the ground and backfilled with a chemical foaming material known as "Poleset". This material is reported to have long life, is easy to use, and develops strength greater than the surrounding soil at a cost that is

competitive with conventional backfilling material, Forward Enterprises, Inc. (1974). The possibility of setting the pipe supports in heavy concrete slabs was eliminated because of the excessive amounts of concrete required to resist overturning during high winds if the slabs are at the surface. Buried slabs could be smaller, but this would require considerable excavation. Also, the use of precast piles driven into the ground would generally be more expensive than augering and backfilling. Piles would therefore not be used except where soil conditions do not permit the cheaper method.

Setting the pipe, installing the modules, and connecting the motors, tracking devices, and other components would be done by contractors. Close supervision would be required to insure that the absorbers and reflectors were in proper alignment. If properly planned, the installation of pipe and the setting of the collector modules is expected to be accomplished at a fairly rapid pace. Three-man crews operating with a truck and crane are expected to be able to install and align four of the larger-sized modules per day. Ten such crews installing models with 7.3 meter aperture widths would be able to complete the collector field for a 50 megawatt plant in approximately one year. This ought to be well within the construction schedule for power plants of this capacity.

Tracking can be accomplished in a number of ways. One way would be to install optical sensors and power amplifiers on each model. Another way would be to use a mini-computer to program and actuate the modules according to a pre-programmed schedule based on the known position of the sun relative to each module location. This latter arrangement is estimated to be more economical for paraboloidal collectors. To improve upon the reliability of the tracking system, five telescopes were assumed to be

located in the collector field to act as feed-back mechanisms. Eventually additional study will be justified to review the practicality and costs of alternative tracking methods.

4.2.4 Breakdown of Lowest-Cost Alternatives

Least costs for the various methods of manufacturing and installing reflective shells tend to approach a value of $50.00 per square meter of projected area, as shown in Figure 4-2. This result applies to the small pressed-glass reflectors, the somewhat larger hydro-drawn reflectors, the groups of four spin-formed reflectors, and the large singly-mounted reflectors. Savings in unit costs occur as the size of the reflectors and modules increase. Breaks in the curve are caused by limitations in the manufacturing processes and by transportation restrictions. Thus, the pressed-glass process is applicable only up to 30 centimeters; the hydro-forming process can only be used for sizes up to 2.0 meters; and modular units are limited by bridge and other clearances of 3.65 meters.

A more critical factor in total costs is the variance in absorber costs according to the type of module. Providing absorbers for the arrays of small paraboloids is expensive, approaching the cost of the modules themselves, which was the basis for eliminating this type of module. Also, unit absorber costs decrease as do the number of reflectors per module, to the point where the cheapest absorber cost per square meter of reflective area is for the largest, singly-mounted reflector. Representative absorber costs are $8.70 per square meter of reflective area for the modules of four and $4.30 per square meter of reflective area for the singly-mounted 7.3 meter paraboloid.

The singly-mounted paraboloid with an aperture width of 7.3 meters

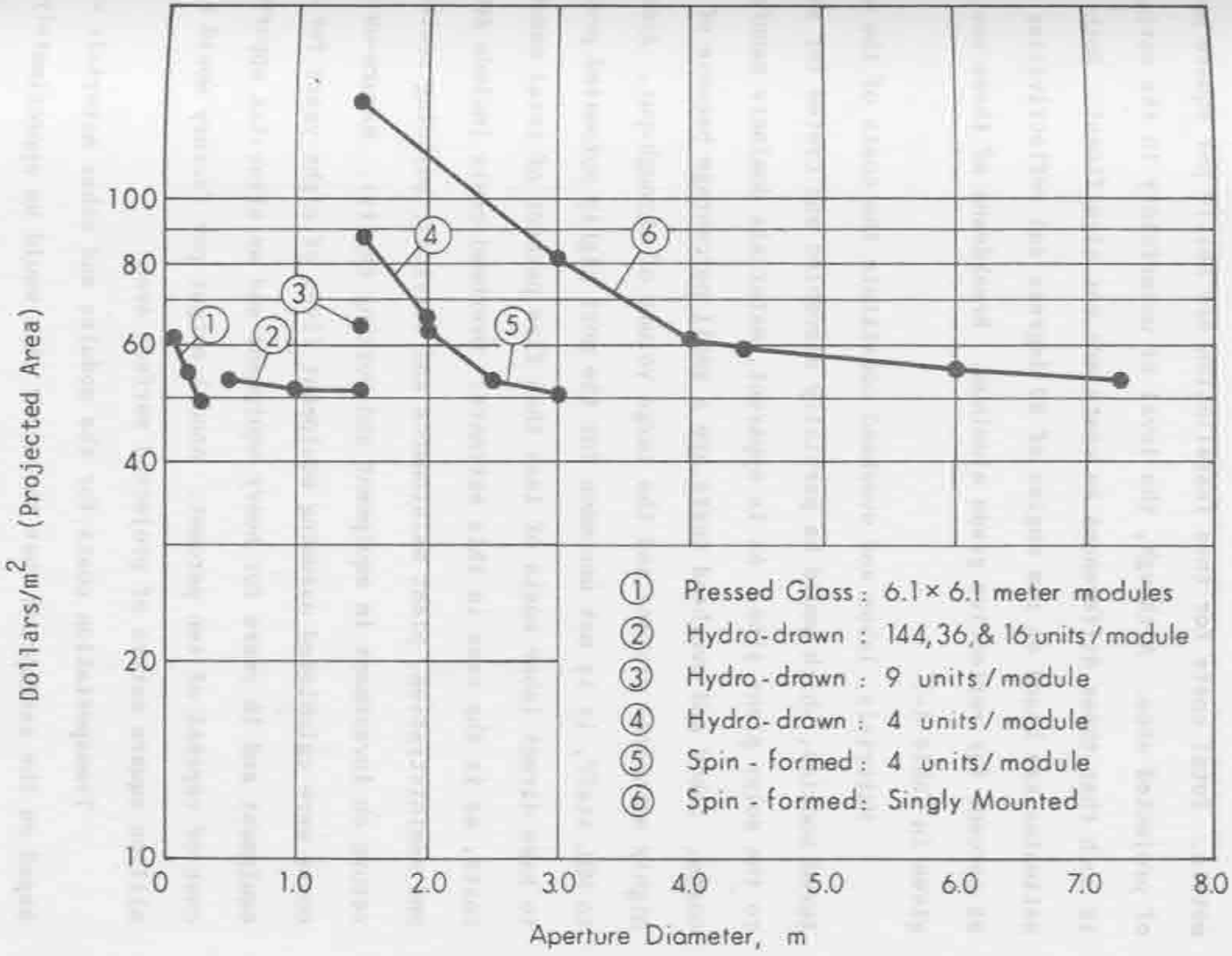

Figure 4-2. Cost-Aperture Relationships for Paraboloidal Concentrators ($\rho_{ave} = 0.85$, $\theta_{max} = 80^{o}$).

and fixed absorber is the lowest cost alternative of this group, with a total cost of $58.10 per square meter of projected area. The next lowest type is the module of four paraboloids each with aperture widths of 3.0 meters. Total costs for this installation are $61.10 per square meter of projected area. Although, the level of uncertainty in the estimates is such that these differences in costs are not significant. Both estimates are based on rim angles of 80 degrees and reflectivities of 85 percent for reflective grade aluminum. Breakdowns of these costs are given in Table 4-1.

Materials, labor and overhead constitute the costs of the manufactured modules, which would be partially assembled and crated for shipment to the solar plant site. As is apparent, materials dominate manufacturing costs. Labor and overhead costs are a small percentage because of the highly automated process and the large volume of through-put. According to MDL staff, it is not uncommon for the most highly automated processes to have direct labor costs of less than five percent of total manufacturing costs, as is the case in this estimate. Overhead costs include general and administration, plant maintenance and services, building rental, and return on investment in equipment and working capital. Return-on-investment costs were calculated assuming equipment lives of eight years for light equipment and 16 years for heavy equipment and an after-tax opportunity cost of capital of ten percent. Annual output per factory would be 3.5 million square meters of projected surface area.

Transportation costs for the modules and other materials were based on the assumption that the solar site would be approximately 350 miles from the factory producing the modules and that the average rate for this distance is $20.00 per ton. These are admittedly approximate figures

TABLE 4-1

Itemized Costs for Minimum-Cost Paraboloids with Reflectivity of 85% and Rim Angle of 80°

Item	$/m^2$ Singly Mounted (7.5m)	$/m^2$ 4 Units of 3.0 m Each
Installed Cost, Without Absorbers		
Materials		
Aluminum shell	18.50	11.90
Framing for shell	1.20	1.20
Gears and motors	4.70	6.90
Other	1.10	1.50
Labor and overhead to manufacture	4.90	3.80
Pipe support	6.40	7.20
Foundation	6.40	7.20
Tracking mechanisms and controls	2.90	3.70
Transportation	0.90	1.10
Installation of modules	4.00	5.00
Subtotal	51.00	49.20
Contingency (5 percent)	2.60	2.50
TOTAL	53.60	52.00
Absorbers		
Materials	2.90	6.20
Labor and overhead to manufacture and install	1.40	2.50
Subtotal	4.30	8.70
Contingency (5 percent)	0.20	0.40
TOTAL	4.50	9.10
GRAND TOTAL	58.10	61.10

but the relative magnitude of transportation costs is not critical to the overall estimate.

In contrast, field construction and installation costs proved to be much higher than originally anticipated. While it is possible that these costs can be reduced through more careful analysis and consideration of other alternatives, their overall significance to the total estimate is expected to remain.

As noted earlier, absorber costs will vary according to the pressures and temperatures of the working fluid, the diameters of the connecting tubing or pipe, and whether or not flexible couplings are required. The values shown in Table 4-1 were for pressures of about 500 psia and temperatures below 250 ^{o}C. The diameter of absorber pipe assumed for the 7.3 meter paraboloid was 6 centimeters, while those for the 4-unit modules were 2.5 centimeters. Absorber costs for pipe, insulation, connections, and the absorber are fairly evenly divided for the 7.3 meter paraboloid; but for the 4-unit module, the costs for flexible couplings and for insulation are relatively more important than the other two cost items.

The contingency factor of five percent is included to cover oversights and unexpected difficulties in production and installation. It is an estimate reflecting expectations that costs will actually be higher than those tabulated; it is not an allowance for inflation or to cover whatever financial difficulties might arise should costs exceed the estimates.

4.2.5 Cost-Parameter Relationships

Sensitivity of collector costs to changes in aperture width and module size were shown in Figure 4-2, based on rim angle of 80 degrees

and reflectivity of 85 percent. Figure 4-3 shows that as rim angles increase or decrease from 80 degrees the costs vary accordingly. Changes in the amount of material required for shells with different rim angles are primarily responsible for these cost changes. Equipment selected for each process are, for the most part, capable of producing the different rim angles without difficulty and at essentially the same speed.

Figure 4-4 shows the effect on costs of changing the reflectivity from 85 percent to 60 percent. These changes also are the result of different material costs. Reduced costs result from using aluminum alloy #1100 that yields reflectivities on the order of 60 percent. Cost reductions are greater as the rim angles increase and as the aperture width of the spin-formed paraboloids increase. A single curve is shown for hydro-drawn paraboloids because the thickness of the shell material is approximately the same over the relevant range of 0.5 to 1.5 meters aperture width; but for the spin-formed paraboloids shell thickness increases with larger diameters. Reflectivities for aluminum that are of sufficiently long duration lying between 60 and 85 percent may exist, but were not uncovered during the study.

Figures 4-2, 4-3, and 4-4 can be used to obtain costs for various aperture widths, reflectivities, and rim angles. For example, the cost of a spin-formed paraboloid of 7.3 meters width, reflectivity of 60 percent, and rim angle of 115 degrees would cost $57.00 per square meter of projected area. This involves adding $58.10 from Table 4-1 and $5.30 from Figure 4-3, and subtracting $6.40 from Figure 4-4. Or, if reflectivity of 85 percent is desired, the cost would be the sum of the first two values; namely, $63.40 per square meter.

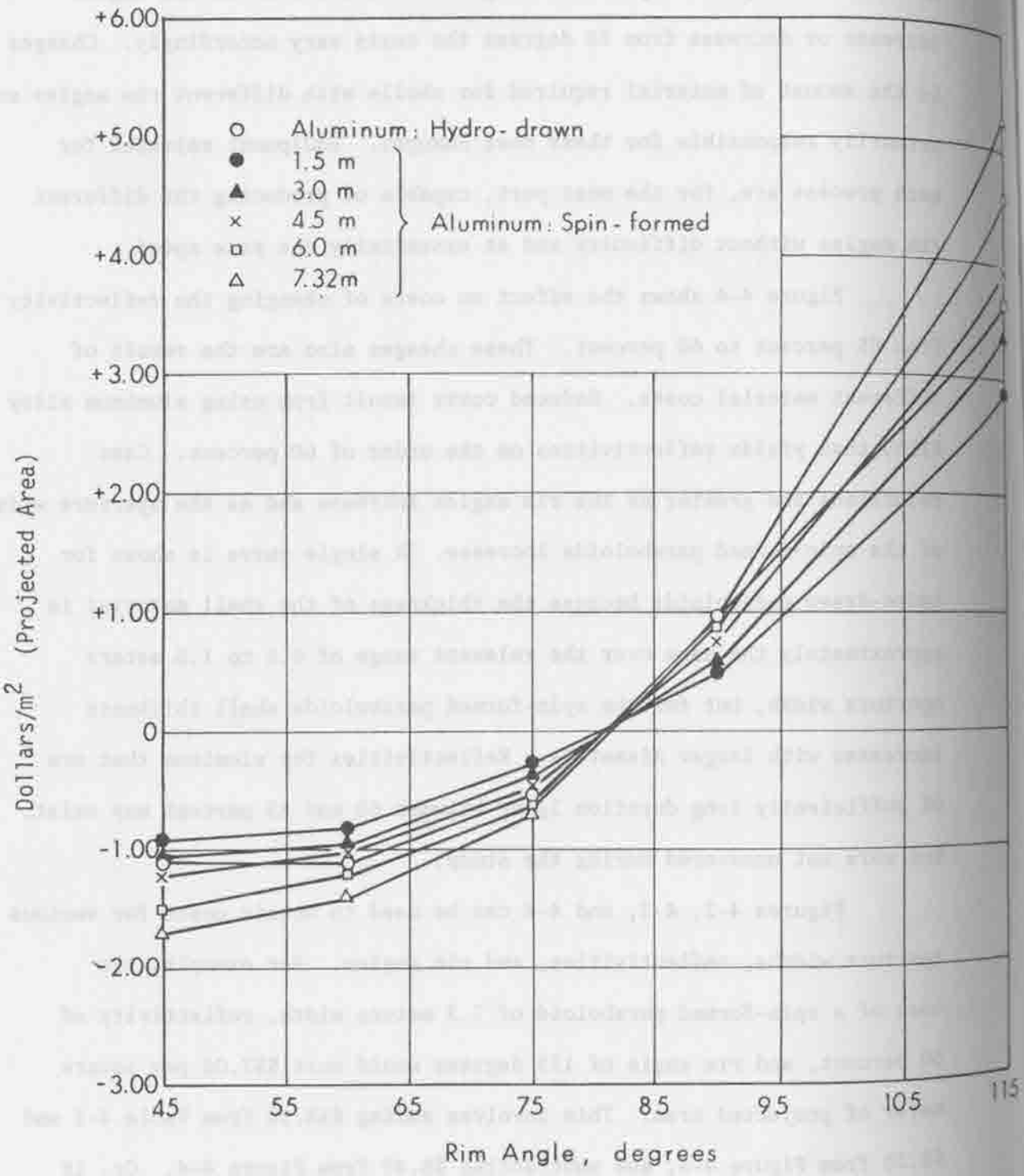

Figure 4-3. Cost Increments for Rim Angles of Various Paraboloid Sizes. (ρ_{ave} = 0.85).

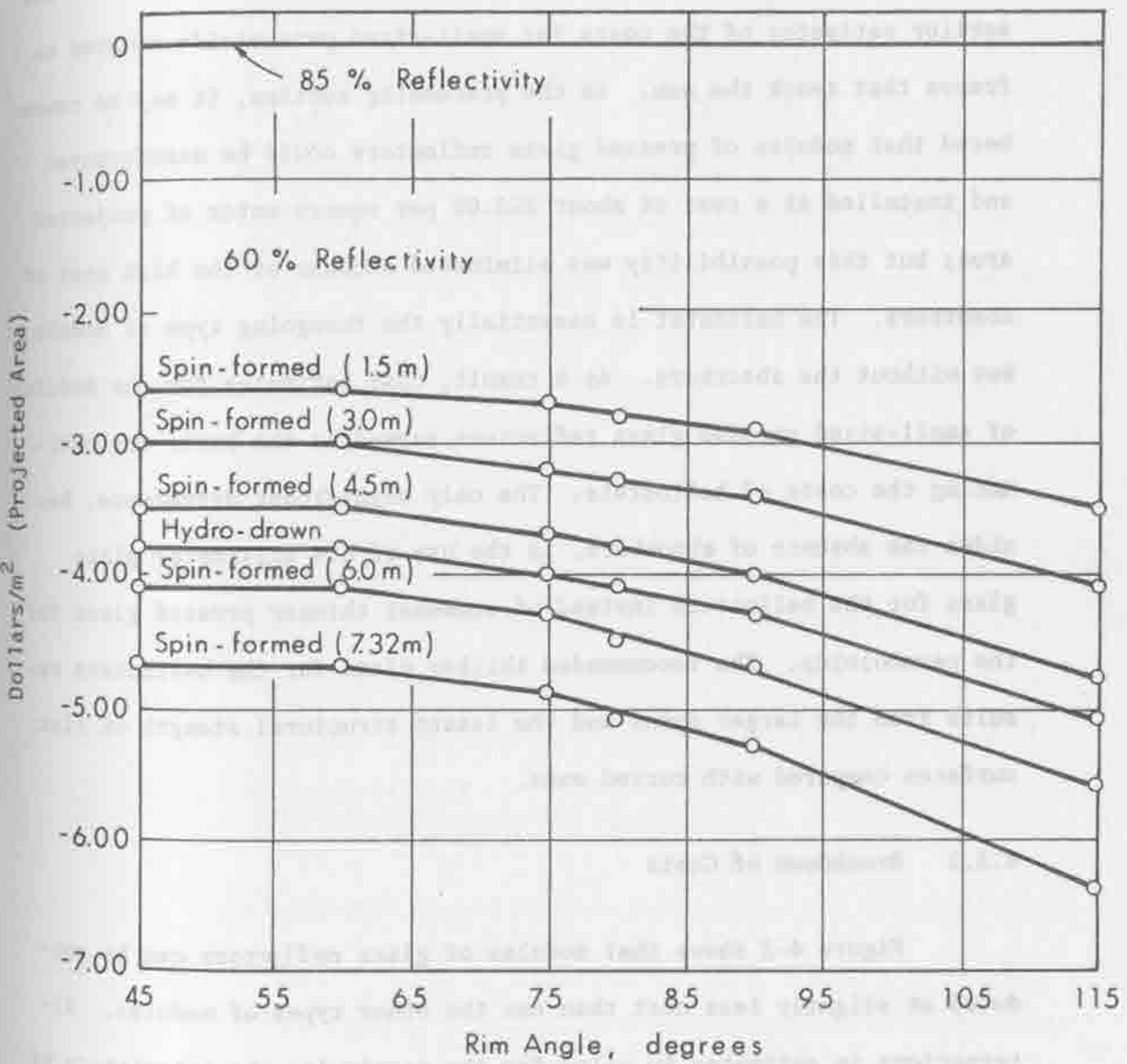

Figure 4-4. Cost Increments for Rim Angle and Reflectivity for Various Paraboloid Sizes.

4.3 Heliostats

4.3.1 Description and Method of Estimation

The estimates of costs for heliostats flowed directly from the earlier estimates of the costs for small-sized paraboloids mounted on frames that track the sun. In the preceeding section, it may be remembered that modules of pressed glass reflectors could be manufactured and installed at a cost of about $50.00 per square meter of projected area; but this possibilitiy was eliminated because of the high cost of absorbers. The heliostat is essentially the foregoing type of module, but without the absorbers. As a result, cost estimates for the modules of small-sized pressed glass reflectors served as the basis for estimating the costs of heliostats. The only significant difference, besides the absence of absorbers, is the use of 6.4 millimeter plate glass for the heliostats instead of somewhat thinner pressed glass for the paraboloids. The recommended thicker glass for the heliostats results from the larger spans and the lesser structural stength of flat surfaces compared with curved ones.

4.3.2 Breakdown of Costs

Figure 4-2 shows that modules of glass reflectors can be produced at slightly less cost than can the other types of modules. Alternations in estimates to allow for the particular characteristics of the heliostat bring overall costs back into the range of $50.00 per square meter of projected area. One of the adjustments is the slightly thicker plate glass. Another is the use of back-silvered glass to obtain a reflectivity of 90 percent in place of 85 percent reflectivity obtained by back-coating with aluminum. Overall material costs are somewhat

lower than for the paraboloids, but the cost of installation and field adjustments to individual reflectors is higher. The cost breakdown shown in Table 4-2 is for an overall module size of 6.1 meters square with individual reflectors that are 1.5 meters square.

4.3.3 Cost Parameter Relationships

Cost-design relationships were tested for variances in reflectivity and in module and reflector sizes. Thermal-evaporated aluminum on glass can be substituted for back-silver glass to give reflectivities of about 85 percent at a savings on the order of $0.90 per square meter. Variances in costs due to changes in module and reflector sizes are expressed by the following formula:

$$\text{Cost} = 68.4 - 3.3W + 1.26\ (W + d)/Wd + (0.59 + 0.23)/d^2$$

Where, costs are in 1972 dollars per square meter of projected area; W is the length of the square module in meters, and d is the length of the square reflector in meters.

4.4 Circular Fresnel Lenses and Reflectors

Alternative to curved surface reflectors, such as paraboloids, are Fresnel lenses and reflectors. Plastic disks molded under conditions similar to the production of phonograph records could be placed on modular racks as were the small-sized paraboloids. Current manufacturing techniques limit the size of Fresnel disks to approximately 2.3 meters diameter. Thus, the alternatives for multiply mounted Fresnel lenses with individual absorbers would be either to mount four of these 2.3 meter disks on a frame of 4.7 x 7.4 meters, or to mount nine, six-

TABLE 4-2

Itemized Costs for Heliostats
Module Size, 6.1 metres; Reflector Size, 1.5 metres and Reflectivity, 90 percent

Item	$/m^2
Materials	
Back-silvered glass	4.20
Fasteners and supports	1.10
Main structure	1.20
Gears and motors	7.40
Other	2.40
Labor and overhead to manufacture	4.00
Pipe supports	7.00
Foundation	7.00
Tracking mechanisms and controls	3.70
Transportation	1.60
Installation and adjustments	7.70
Subtotal	47.30
Contingency (5 percent)	2.40
TOTAL	49.70

teen, or more smaller disks on larger frames. In either case, costs per square meter of projected are not competitive with other types of concentrating collectors because of high unit absorber costs. Overall unit costs increase as the size of the frame decreases and as the number of absorbers per module increase.

4.4.1 Description of a Viable Fresnel Lens Arrangement

An alternative that does not suffer from the foregoing drawbacks involves the assembly of individual Fresnel lenses in facet form that focus on a common absorber located at the center of the module. Each lens would have grooves that, when combined, form concentric circles. A laminate of glass and polycarbonate was found to be more economical than a single sheet of plastic with sufficient thickness to maintain sufficient rigidity. The glass has higher structural strength and is lower in cost. Six-millimeter plate glass backed by three-millimeter polycarbonate should be reasonably resistant to breakage. The plastic material would be placed so that the grooves are nearest the absorber. This positioning is favored on three counts: 1) the glass will shield the plastic from ultraviolet rays, 2) dirt and other particles are less apt to accumulate in the grooves, and 3) the grooves do not interfere with the path of the sun's rays, as shown in Figure 4-5. However, when positioned in this manner, the focal length must be greater than roughly 0.4 times the diameter of the widest groove. This limitation is set by the index of refraction for the polycarbonate material.

As with small paraboloidal reflectors, the laminate would be supported by small steel cross-beams. Other portions of the module are

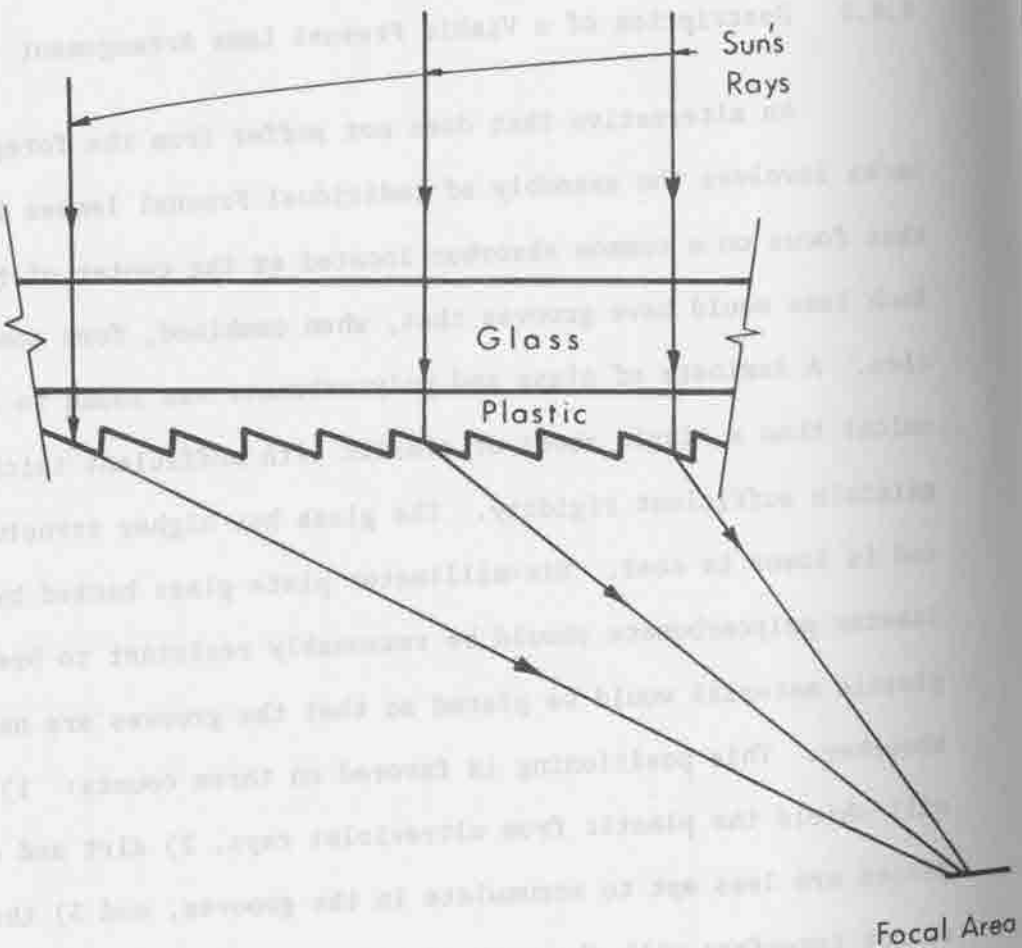

Figure 4-5. Non-Interference with the Sun's Rays through a Fresnel Lens.

assumed to be the same as for the racks of paraboloids, except that a more elaborate supporting structure is required to permit the central absorber to be positioned below the lens instead of above the assembly.

4.4.2 Breakdown of Costs for Fresnel Lens Module

Large singly focusing modules of Fresnel lenses appear to have a slight cost advantage over large singly mounted aluminum paraboloids (Compare Table 4-3 with Table 4-1). Total costs for the lenses are $54.30 per square meter of surface area compared with $58.10 per square meter of projected area for the paraboloids. However, the structural design for this type of Fresnel lens arrangement may be more complex than for the large paraboloids, which could reduce this apparent cost advantage. Firmer conclusions must await more detailed structural design.

Various comments on Table 4-3 follow: Costs of glass and plastic making up the Fresnel lens are based on large-volume purchases and through-put. Structural framing costs reflect the more complex nature of the supports relative to that for the 7.3 meter paraboloid. Gears and motors are slightly more costly because of the greater torque. MDL staff indicate that a Fresnel lens of a size comparable to that of a spin-formed paraboloid would take about three times as long to produce. This, and the extra labor required, account for the higher cost figure for labor and overhead to manufacture. Pipe supports are shorter for the Fresnel lens, thus the lower cost. Transportation costs are somewhat higher because of the heavier weight and more fragile material. Other costs are not substantially different.

TABLE 4-3

Itemized Costs for Circular Fresnel Lens
7.3-metre Module with Single Focus

Item	$/m^2$
Installed Cost, Without Absorber	
Materials	
Fresnel lens and metal supports	11.70
Structural frame	4.10
Gears and motors	5.40
Other	1.10
Labor and overhead to manufacrure	6.50
Pipe supports	4.00
Foundation	6.40
Tracking mechanisms and controls	2.90
Transportation	1.80
Installation of modules	4.00
Subtotal	47.90
Contingency (5 percent)	2.40
TOTAL	50.30
Absorber	
Materials	2.60
Labor and overhead to manufacture and install	1.20
Subtotal	3.80
Contingency (5 percent)	0.20
TOTAL	4.00
GRAND TOTAL	54.30

4.4.3 Cost-Parameter Relationships for Lenses

Of the various parameters under consideration, two were costed out for singly mounted, single focusing Fresnel lenses. Some provisional values for various module widths and focal lengths are shown below. Focal lengths are in terms of module widths. Costs, in 1972 dollars per square meter of surface area, are for the installed module including absorber. Absorber and Fresnel laminate costs are roughly constant over the indicated ranges of values. Structural, installation, and other such costs account for the variances in costs.

In addition to the above, different thicknesses of plastic and glass and different spacings of steel supports were tested for their cost effects on contour accuracies. In this case, contour accuracy was taken as being the weighted average amount of sag in the lens surface. Results were not particularly cost sensitive so that the foregoing values apply to conditions of 0.1 degree contour error. No evaluations were made for variances in tracking error, for the reasons given earlier.

4.4.4 Description of Fresnel Reflectors

From a construction standpoint, the Fresnel reflector has a number of advantages over the lens and paraboloids that in some instances more than offset its disadvantages. Favorable factors include: 1) the plastic material can be lower-cost since it does not have to be transparent, 2) because transparency is not a factor, effective life of the plastic should be longer, 3) lack of transparency requirements also mean that supportive materials less expensive than glass can be used, and 4) structures supporting the Fresnel material are less complex for reflectors than for lenses. Countering these advantages are: 1) un-

certainties about whether or not high quality, durable reflectors can be made, 2) effective area is reduced by interference of the grooves, and 3) higher absorber costs.

The literature search on concentrating collectors carried out by CSU/Westinghouse staff turned up little on the practicality of constructing such reflectors; although, the possibilities seem encouraging. In view of the favorable outcome of certain cost estimates, further study is surely warranted. The overall effects of groove interference in the paths of portions of the reflected rays can be quantified. The cause of the interference is illustrated in Figure 4-6. The functional relationship between the percentage reduction of reflective area due to groove interference and the ratio of focal length to reflector radius is given in Figure 4-7. The higher the ratio, the lower the reduction. But, as the ratio increases the cost of the absorber unit increases: the length of the connecting tubing and the amount of insulation increase and the structural support to keep the absorber in place becomes larger. The cost effects of these increases are not great, however, and optimal designs will probably indicate rather long focal lengths. Results are not particularly sensitive to the number of grooves per inch.

4.4.5 Cost Breakdown for Fresnel Reflector Module

Various configurations of Fresnel reflector assemblies were considered. The more interesting possibilities are those employing small diameter, medium and low pressure tubing for a single absorber mounted on a large circular reflector of fron silvered plastic. Rotating the reflector about a fixed absorber does not appear to be practicable, which means that flexible hose and couplings are needed for absorber connections. These costs are modest for combinations of pres-

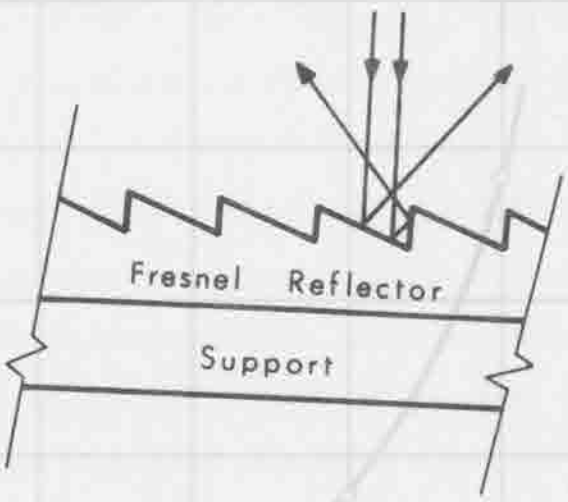

Figure 4-6. Interference with the Sun's Rays on a Fresnel Reflector.

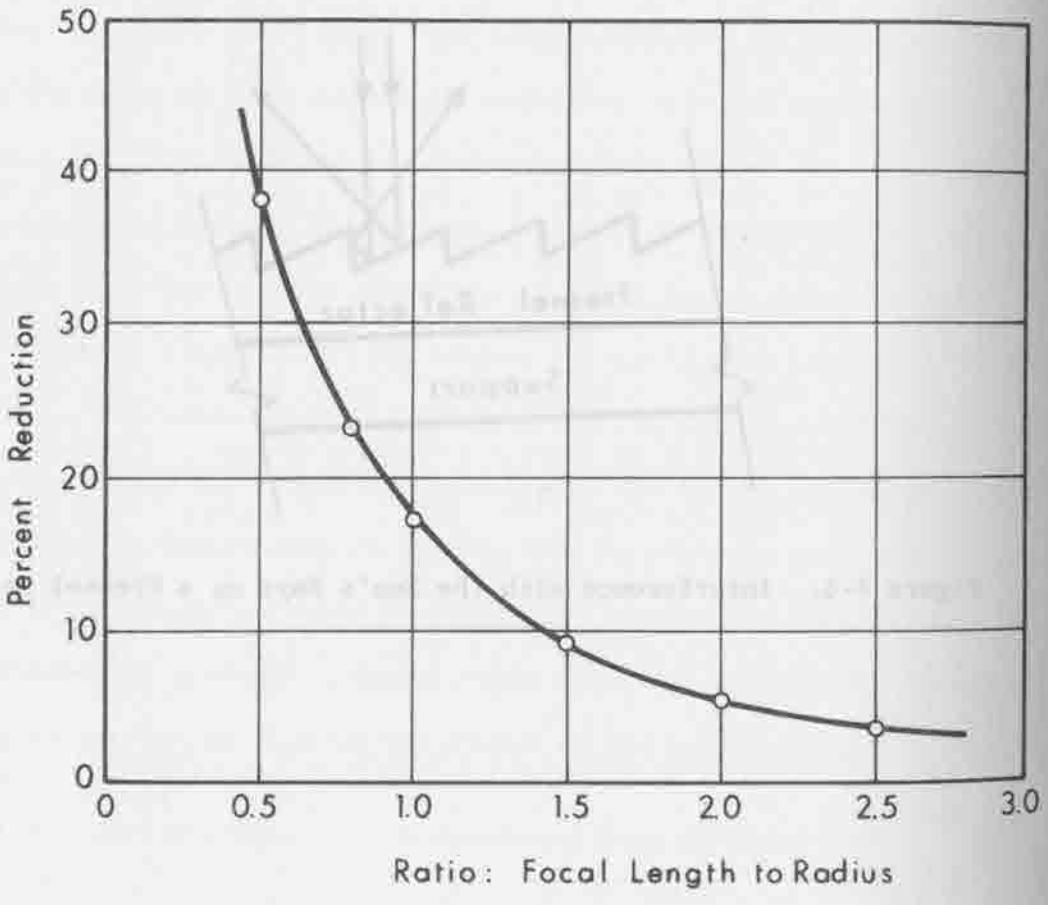

Figure 4-7. Reduction in Reflectivity of Fresnel Reflector from Groove Interference. (100 Grooves per Inch).

sures below 500 psia and diameters less than 2.5 centimeters. Accordingly, the cost breakdown in Table 4-4 is for an absorber that utilizes 1.3 centimeter tubing operating under pressures less than 500 psia.

Total costs of $48.50 per square meter of surface area shown in Table 4-4, are almost $10.00 below those for the large paraboloid whose costs are shown in Table 4-1. For comparison purposes, however, three factors should be noted: first, the paraboloid does not require flexible couplings and therefore can accommodate larger absorber tubing and pressures without significant increases in unit costs, whereas the Fresnel reflector cannot; second, interference of the Fresnel grooves reduces the effective area of the reflector; and third, reflectivities of front-silvered plastic and reflective grade aluminum are probably not comparable over extended periods. The first factor eliminates the Fresnel reflector for high pressure, large diameter combinations. The second factor can be taken into account by using the information contained in Figure 4-7. For example, if a focal length to Fresnel radius were 1.5, the costs of $48.50 should be divided by 91 percent to obtain an equivalent cost of $53.30 per square meter of reflective area. Finally, experimentation is required for long-term comparisons of different reflective surfaces. Most of the individual costs are similar in one way or another to those for other types of concentrating collectors. Only a few comments will be added. The Fresnel reflector is assumed to be made of PVC, placed on low-cost material, and supported by small tubular steel cross-members. Large volume purchase of PVC is about 45 percent of the cost of polycarbonate. Costs for the reflector and supports are reasonably firm. Labor and overhead to manufacture are less certain and might well be reduced by further investigation. The absorber support could be an insulated steel pipe through which

TABLE 4-4

Itemized Costs for Circular Fresnel Reflectors
Single Focus, 7.3-metre Width; 1.3-Centimeter Absorber
Tubing Under Pressures Less than 500 psia, Reflectivity Over 90 percent

Item	$/m^2
Installed Cost, Without Absorber	
Materials	
Fresnel reflector and supports	6.80
Structural frame	0.60
Gears and motors	4.70
Other	1.10
Labor and overhead to manufacture	6.50
Pipe supports	6.40
Foundation	6.40
Tracking mechanisms and controls	2.90
Transportation	1.20
Installation of modules	4.00
Absorber support	0.90
Subtotal	41.50
Contingency (5 percent)	2.10
TOTAL	43.60
Absorber	
Materials	3.10
Labor and overhead to manufacture and install	1.60
Subtotal	4.70
Contingency (5 percent)	0.20
TOTAL	4.90
GRAND TOTAL	48.50

the absorber tubing passes. Its principal function is to keep the absorber from moving when subjected to dead weight and wind loadings.

4.4.6 Cost-Parameter Relationships for Reflectors

Cost-parameter relationships parallel those for Fresnel lenses regarding module sizes. Minor adjustments are required to account for differences in the costs of absorbers and supporting absorber pipe. Unit costs for varying focal lengths are primarily affected by the percentages shown in Figure 4-7. Front-silvered plastic was assumed to have a reflectivity of over 90 percent, which is some 5 to 10 percent above that anticipated for an aluminized surface. The applied cost of deposited silver is about $1.00 per square meter higher than that for deposited aluminum. Warping of the material supporting the plastic refelctor could be a problem in obtaining high contour accuracies. This factor, together with tracking errors, has not been quantified.

4.5 Parabolic Troughs

A number of alternatives were considered under the general heading of single curvature reflectors. Circular and catenary shapes were discarded after MDL staff considered them to have no cost advantage over the more efficient parabolic trough. Relying on knowledge gained from double curvature reflectors, the smaller range of troughs was not investigated. Instead, attention was directed to parabolic troughs with aperture widths of one meter and larger. Cost estimates for Fresnel strip lenses and reflectors showed no cost savings. In fact, strip lenses proved slightly more expensive than some of the troughs due primarily to the compactness of the trough and the consequent savings in structural materials. As a result, the remaining portions

of this section are devoted to the parabolic trough in its various forms.

4.5.1 Description of Two Types of Troughs

Conceptual designs were obtained for two basic types of parabolic troughs. One of these involves an assembly line of roll-form equipment to produce troughs that have aperture widths of two meters and are 18.3 meters long. The trough would be formed by top and bottom sheets of aluminum and a honeycomb core material of "Hexcell" aluminum. The top would be highly reflective aluminum roll sheets of the same quality as that used for obtaining the 85 percent reflectivity for the paraboloids. The trough would be mounted on oil-less journal bearings, driven by worm gears and 1/8th horsepower stepping motors, and supported by ten centimeter aluminum channels. This assembly in turn would be set on individual concrete beams designed to resist overturning due to high winds.

The foregoing process is applicable for widths not exceeding two meters. For greater widths, a less automated process is required. Cost estimates were prepared for an assembly 7.5 meters wide by 29.2 meters long. Eight half-sections, designed to meet railway and highway clearance requirements, would be fabricated in the shop and delivered for assembly in the field. These sections would be made of structural steel ribs and stringers that support highly reflective aluminum sheets. They would be set on du-type oil-less slider bearings and driven by drive gears and gear motors with 50:1 reduction. Five such sets would be required per installation. Six-inch channels set on individual concrete beams would support the structure at each of five points.

Four different linear absorbers were considered for these reflectors. One would simply be an unprotected stainless steel pipe with a suitable absorptive coating. An insulated pipe shield with a bottom opening could encase the absorber to reduce convective losses. A third type would involve enclosing the absorber in an evacuated glass tube. This type would require suction pumps installed in the field to maintain the required vacuum. The fourth type of absorber is the combination of stainless steel absorber pipe, evacuated glass tubing, and a pipe shield around them. All would require flexible couplings, since the absorber moves with the reflector. Rotating the reflector about a fixed absorber would require relatively more expensive structures and hence higher overall costs, except for installations with large diameter absorbers operating in high pressure ranges.

Field structures and installations would be somewhat different from those described for paraboloids and circular Fresnels. Concrete beams as mounts for the troughs and to resist overturning would be set in the ground similar to railroad ties. Wind forces acting on the larger troughs would be considerably greater than for the largest paraboloids. Pairs of piles sitting under each support were found to be more costly an alternative than these concrete beams. Installation would be accomplished by contractors who, because of the greater number of field connections and more awkward nature of the sections, would require comparatively more time, on a square meter basis, than would be needed to install the paraboloids. One-axis tracking for the smaller-sized troughs would make use of the type of mini-computer noted earlier. However, for the larger-sized troughs a lower-cost alternative is the installation of individual sensory devices on each

trough. Finally, troughs can be positioned horizontally or be inclined, if the latter, the inclination can be fixed, or varied with the seasonal position of the sun. Varying the inclination was assumed to be accomplished automatically rather than manually.

4.5.2 Cost Breakdown

Unit costs for varying aperture widths are shown in Figure 4-8. These costs are for troughs with reflectivities of 85 percent and rim angles of 80 degrees. The automated process by which parabolic cross sections are turned out was found to be the least cost approach; and increasing the width of the trough produces the lowest costs. Unfortunately, this process can be employed for widths only up to two meters. Unit costs for the structural steel method decline as the widths approach the 7.5 meter limit. But at $53.00 per square meter of projected area, this method is still $6.00 above the unit costs of $47.00 for the smaller alternative. It may have been observed that these costs are not significantly below those for the paraboloids.

Low pressure absorbers made of stainless steel pipe with pipe shields would cost $12.80 per square meter of projected area for the larger trough, compared with $7.80 per square meter for the smaller trough. This difference increases the overall advantage for the smaller trough to $11.00. Higher pressures and smaller concentration ratios would further increase the spread in absorber costs for these two types of troughs.

The nature of the various cost components is not unlike that described earlier for the paraboloids. Some additional comments pertinent to the troughs are in order, however. Material costs for the two types of troughs are roughly the same (see Table 4-5). The

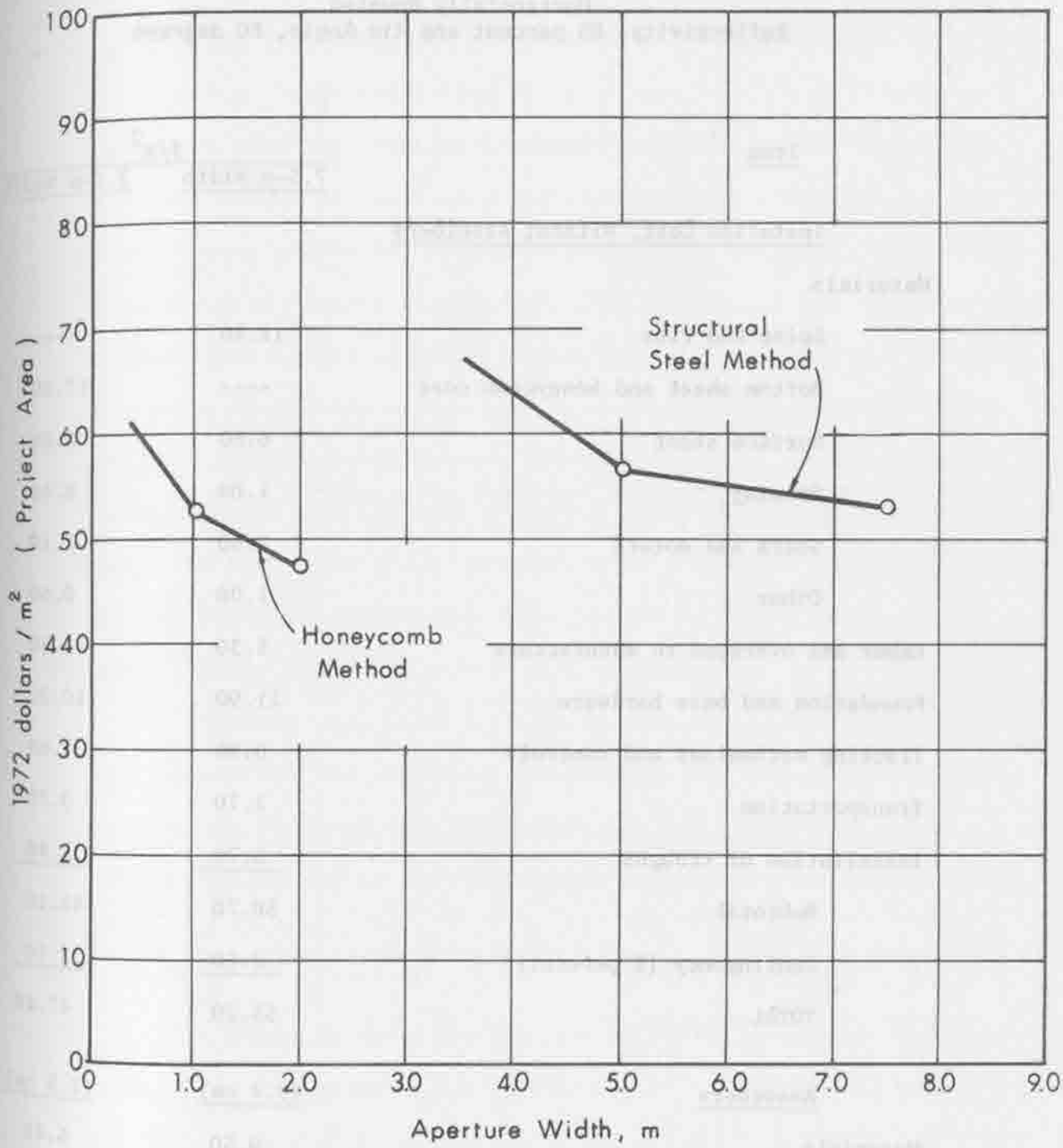

Figure 4-8. Costs of Parabolic Troughs Mounted Horizontally. (ρ_{ave} = 85%, θ_{max} = 80°).

TABLE 4-5

Itemized Costs for Parabolic Troughs
Horizontally Mounted
Reflectivity, 85 percent and Rim Angle, 80 degrees

Item	$/m^2$ 7.5-m Width	2.0-m Width
Installed Cost, Without Absorbers		
Materials		
Spine and ribs	11.80	----
Bottom sheet and honeycomb core	----	12.40
Surface sheet	6.80	6.80
Framing	1.00	0.40
Gears and motors	3.60	2.10
Other	1.00	0.60
Labor and overhead to manufacture	5.30	2.50
Foundation and base hardware	11.90	10.20
Tracking mechanisms and controls	0.90	3.60
Transportation	1.70	0.70
Installation of troughs	6.70	5.80
Subtotal	50.70	45.10
Contingency (5 percent)	2.50	2.30
TOTAL	53.20	47.40
Absorbers	(9.4 cm)	(2.5 cm)
Materials	9.50	5.40
Labor and overhead to manufacture and install	2.70	2.00
Subtotal	12.20	7.40
Contingency (5 percent)	0.60	0.40
TOTAL	12.80	7.80
GRAND TOTAL	66.00	55.20

greater volume of structural material for the 7.5 meter trough is offset by its lower cost per pound, compared with the aluminum sections. Being heavier, the troughs require larger gears and motors. Major savings in labor and overhead to manufacture accrue to the automated process. Foundation costs are surprisingly high for both types. This result occurs because of the need to protect the installations against overturning, or lateral displacement, from high winds. Further examination of foundation designs is needed before fianlly accepting these estimates. Unit costs of tracking mechanisms are considerably less for the larger troughs because fewer of them are needed. Individual sensor units costing $200.00 each are part of the 7.5 meter design; for the 2.0 meter design the mini-computer is the lower-cost alternative. Transportation and installation costs are also less for the 2.0 meter trough because of its lighter weight and greater ease of handling.

Absorber costs shown in Table 4-5 are only illustrative, since many alternatives are possible. Higher costs for large diameter pipe and flexible couplings more than offset the savings in unit costs arising from individual absorber lengths that serve wider sections.

4.5.3 Cost-Parameter Relationships

Variances in costs arising from different rim angles, reflectivities, types of absorbers, and positioning of the trough were examined, in addition to the changes relating to different aperture widths previously shown in Figure 4-8. Below are the alternations in unit costs that should be made when considering different rim angles and reflectivities. These apply to both types of parabolic troughs and should be added (or subtracted) to the grand totals in Table 4-5.

Reflectivity	Rim Angle 45°	60°	75°	80°	90°	115°
85%	-1.15	-1.10	-0.50	0	+0.80	+2.80
60%	-3.75	-3.70	-3.20	-2.10	-2.10	-0.50

Considering the magnitude of total costs for troughs, the alternations are not great. Cost savings from using standard grade aluminum (#1100) instead of the reflective grade (#3002-0) do not justify the loss in reflectivity. Future examination of other reflective surfaces would probably turn up cases in which the drop in reflectivity is not so great.

Unit absorber costs for the parabolic trough are a function of a number of variables: namely, width and length of trough, operating pressure and temperature, diameter of stainless steel pipe or tubing, length of supports, diameter and length of flexible hose and couplings, type of absorptive coating, and sizes of insulated pipe shield and evacuated glass tubing if they are used. Cost functions were developed for the optimizing model that made use of cost tables for the above factors. No attempt was made to express all of these various combinations in graphical form. Rather than doing so here, some examples of costs for different components will be given so as to reveal their relative importance. To illustrate, unit absorber costs from Table 4-5 are made up of the following components:

Parameters	Values	
Absorber diameter	9.4 cm.	2.5 cm.
Pressure	100 psia.	100 psia.
Module length	29.3 m.	18.3 m.
Module area	219.5 sq.m.	36.6 sq.m.
Cost Item	**$/m²**	
Flexible hose and couplings	4.65	0.80
Absorber pipe	2.45	2.00
Pipe shield	1.80	1.40
Insulation around shield	0.45	1.05
Absorptive coating	0.10	0.10
Pipe supports	0.05	0.05
Total	9.50	5.40

If pressure is increased to 566 psia., flexible hose and couplings must be of higher strength. Such a change would add $2.50 and $0.50 per square meter of projected area to the larger and smaller aperture troughs, respectively. Placing the absorber in an evacuated glass tube and providing the necessary vacuum pumps would add $2.00 per square meter of projected area to the larger trough compared with $10.50 for the smaller trough. The greater number of pumps per unit area account for this significant increase.

Finally, the costs of additional structures to place the trough on a fixed tilt (according to latitude) were estimated. Adding to these estimates were the costs of power units to mechanically adjust the tile according to the season of the year. Comparisons of unit costs for different aperture widths and for the three types of installations are shown below:

	$/m^2		
	Type of Mounting		
Aperture Width (meters)	Horizontal	Fixed Tilt	Adjustable Tilt
1.0	52.60	53.10	83.00
2.0	47.00	48.30	64.10
5.0	56.80	60.30	69.30
7.5	52.90	59.30	66.30

The large increase in unit costs for the smallest trough with adjustable tilt results from the greater number of power units per solar field. Structures for the largest trough with fixed tilt must be stronger, as well as being higher, which accounts for their higher unit costs.

As with most of the earlier cases, the effects on costs of variances in contour and tracking accuracies were not estimated in other than cursory fashion.

4.6 Annualized Costs of Operation

As mentioned elsewhere in this report, an objective of this research effort is to compare the costs of alternative solar thermal electric power systems. Costs are to be in dollars (cents or mils) per kilowatt-hour. To obtain the necessary cost data associated with the foregoing investments in concentrating collectors, two other types of data are needed. These are the economic lives of the installations and the annual costs of their operation, maintenance, and replacement.*

4.6.1 Economic Lives of Concentrating Collectors

The economic life of an asset is the length of time it "pays" to keep the asset in service. Even though the asset may be able to continue its physical performance, its economic life for the intended purpose has ended once it becomes more economical to replace it with either an improved unit or a new unit of the same type.

In conformance with industry standards, the assumed life of the solar installation is assumed to be 30 years. This may well be an optimistically long life, inasmuch as the initial versions of new technologies are often quickly replaced by improved versions. Countering this argument, however, is the nature of this type of installation in which the predominant costs are associated with initial investments rather than annual operating costs. If this is indeed the case, once the system has been installed it could economically remain in service even

---

* Additional these requirements are estimates of 1) the capitalization factor for the relevant types of electric utilities, 2) rates and types of utilization of the solar powered systems, and 3) other investment lives and costs and the costs of their maintenance, operation, and replacement.

though less expensive versions subsequently become available.

In estimating the economic lives of system components, the reasonable assumption has been made that the solar field will be properly maintained. Furthermore, maintenance procedures and economic lives of many of the components are expected to be similar to field installation already owned and operated by existing public utilities and the U.S. Bureau of Reclaimation. The following estimates of lives were obtained primarily from such sources:

Item	Economic Life (years)
Motors	> 10
Gears	> 20
Bearings	> 10
Exposed cables	> 30
Underground cables	> 30
Steel structures	> 30
Aluminum structures	> 30

More difficult to estimate, and crucial to the selection of STEPS alternatives, are the lives of different types of reflective surfaces. Experimental data of sufficiently long duration are only now becoming available. Several years of testing probably are still required before reasonably accurate data can be fed into optimizing models. Until such information is available, reliable designs for reflective materials and means for their efficient replacement cannot be made. For want of such data, and in the light of current judgement about surface lives exposed to the elements, the assumption has been made that all surface types will have to be replaced or refinished

every 10 years. That is, no allowances are made for what will surely be economic advantages for some surface types.

4.6.2 Annual Costs

Annual operating costs associated with concentrating collectors comprise their operation, routine and special maintenance, and replacements. Operating costs would not be great since the collectors are assumed to operate automatically. A minimum staff of sixteen workers are assumed to be needed for a 50 megawatt plant to operate the minicomputer and related equipment, to adjust the modules when they fail to function properly, and for other tasks. Little basis currently exists for distinguishing between alternative concentrator types. Thus, an annual cost of $150,000.00 per year is uniformly assumed for this activity.

Maintenance of reflective surfaces and other components of the concentrating collectors is also considered to require only minimal effort. As noted in Section 4.7, the sensitivity analysis suggests that the apparently most economic alternative is to allow the reflective surfaces to remain dirty rather than attempt to keep them cleaned.

Maintenance of other components will cover such tasks as periodic painting of steel structures, greasing and adjustments of certain types of equipment, and so on. However, it should be noted that the climate in a number of the assumed locations is arid and thus problems of corrosion, requiring careful attention to protective coatings, would not be serious. Moreover, wherever possible, sealed and maintenance-free types of components suitable for outdoor conditions have been part of the conceptual design and costed accordingly. Fouling

of moving parts from dust and sand particles is a consideration that eventually deserves study. As with operating costs, no attempt has been made to distinguish among different types of concentrator designs in estimating annual costs of maintenance. Special and routine maintenance of components other than surfaces is assumed to be $50,000.00 annually.

Replacement of components at the end of their useful lives involves the costs of the components themselves, as estimated for the original investment, to which delivery and installation costs should be added. For want of more precise information, delivery and installation costs are assumed to be ten percent of the original equipment cost.

When considering costs that occur over time, the question of how to allow for inflation arises. Two approaches are possible. If the assumption is made that inflation uniformly affects all costs, including the capital market, then present-day costs and a deflated cost of capital can be employed. If this assumption is unrealistic, then differential rates of inflation must be applied to all future expenditures and the cost of capital should incorporate anticipated inflationary effects on the capital market. The optimizing model employed for this project is capable of handling either approach. Considering the uncertainty of much of the annual and replacement information, the similarities in components, and the difficulties of predicting future inflation rates, the constant cost approach has been applied.

4.7 Breakeven Analyses on Whether or Not to Clean the Reflective Surfaces

When reasonably accurate estimates of costs are difficult to make, a breakeven analysis will sometimes yield sufficient information for choosing among alternatives. This proved to be the case in the choice between cleaning the reflective surfaces of the collectors and allowing them to remain dirty. The question of cleaning the surfaces arises as a result of the degradation of reflectivity due to the accumulation of dirt and other foreign matter.

The approach, described below, consists of setting the equivalent uniform annual cost of investing in additional collectors equal to the annual cost of cleaning them. The results show that neither manual nor automatic washing is as cheap as allowing the surfaces to remain dirty and providing additional surface area to obtain comparable levels of radiation.

4.7.1 Additional Surface Versus Manual Washing

Assume installed collector and absorber costs of $60.00 per square meter broken down as follows: surface and shells with a cost of $15.00 per square meter and lives of five years; motors, gears, and similar items with a cost of $15.00 per square meter and lives of ten years; and basic structure and other components with a cost of $30.00 per square meter and lives of 30 years. Let the required before-tax return on investment for the typical electric utility by 15 percent. Then, the equivalent uniform annual cost per square meter of projected area would be:*

* The following notation is more or less standard for calculations in engineering economy. For example, see the text by Grant and Ireson (1970).

$30(A/P, 15%, 30 years) = 30 x 0.1523 = $ 4.57

$15(A/P, 15%, 10 years) = 15 x 0.1993 = 2.99

$15(A/P, 15%, 5 years) = 15 x 0.2983 = 4.48

Total = $12.04/Square Meter

where, for example, the term (A/P, 15%, 30 years) is the capital recover factor that converts an initial amount, P, into an equivalent uniform annual amount, A, using an interest rate of 15 percent and a life of 30 years. The formula for obtaining the value of 0.1523 is $15\%(1 = 15\%)^{30} \cdot ((1 + 15\%)^{30} -1)^{-1}$. In this case P = $30 and A = $4.57.

Additional to investment are the costs of maintaining the extra surface area and the labor to replace the worn out shells, motors, and other items having lives of 5 and 10 years. Equivalent uniform annual costs per square meter of projected area are as follows:

Labor to replace reflectors every 5 years:

$2.00(A/F, 15% 5 years) = 2 x 0.148 = $0.30

Labor to replace motors, etc. every 10 years:

$1.00(A/F, 15%, 10 years) = 1 x 0.049 =$0.05

Marginal maintenance cost for extra surface area:

5% x $60.00 (original investment) = $3.00

Total = $3.35/Square Meter

where the term (A/F, 15%, 5) is the sinking fund factor that converts a future amount, F, into an equivalent uniform annual amount, A, using an interest rate of 15 percent and a life of 5 years. The formula for obtaining the value of 0.148 is $15\%((1 + 15\%)^{5} -1)^{-1}$. In this case F = $2.00 and A = $0.30.

Combining the annualized investment costs of $12.04 with maintenance and replacement costs of $3.35 gives a total of $15.39 per square meter of projected area.

With an average reflectivity of 85 percent when initially installed and a reduction of 8 percent to a level of 78.2 percent in 9 weeks that stabilizes at this level, then the average reflectivity of the surface that is cleaned every 9 weeks would be 81.6 percent, provided the rate of degradation is uniform over this 9-week period. This last assumption actually favors cleaning, since it is more likely that the degradation is more rapid at the outset so that the average reflectivity of the washed surface would be less than 81.6 percent.

Comparable radiation would result from the two maintenance procedures (i.e., washing and no washing) if the projected surface area for the case of no washing were increased by 4.3 percent (i.e., 81.6% ÷ 78.2% -1). The equivalent uniform annual cost of this increased area is $0.66 per square meter (i.e., 4.3% x $15.39). For a module of 16 collectors of 1.5 meters aperture width, the projected surface area is 28.2 square meters and the equivalent uniform annual cost would be $18.61 per module (i.e., $0.66 x 28.2).

The foregoing value can now be compared with the cost of manually washing the surfaces. Assume a comprehensive field labor cost of $8.00 per hour in which the hours of actual cleaning are 80 percent of total hours on the job. With the modules being cleaned every nine weeks, the total number of cleanings per year would be 5.8. One can now find the breakeven point in terms of the length of time to clean such a module:

($8.00/hour x 5.8 times per year x H hours/module) ÷ 80% = $18.61

H = 0.32 hour or about 19 minutes of washing time per module.

Nineteen minutes per module is quite a short time and certainly does not allow for the type of hand cleaning assumed for the Honeywell experiments. Thus, it seems safe to conclude that hand cleaning of the reflector surfaces is not justified.

4.7.2 Additional Surface Versus Automated Washing

Assume that a simple system of one-inch diameter piping is placed adjacent to the reflectors in four rows of approximately 6.0 meters length each for a total of 24 meters of piping for each module and that about 16 meters of connecting pipe are required, giving a total of 40 meters per reflector. With an installed cost for such a piping system of $6.50 per meter and a cost of $40.00 for valves and solenoids, the total cost per module would be $300.00. The equivalent uniform annual cost of this installation, assuming an interest rate of 15 percent and a life of 15 years, would be:

$$\$300 \times (A/P, 15\%, 15 \text{ years}) = 300 \times 0.17102 = \$51.30.$$

This annual amount, which excludes costs of water and other services, is greater than the annual cost of $18.61 per square meter for increasing the area of collector surface. In conclusion, automated washing would also appear to be an inferior alternative, even if the washing were to be so frequent as to raise the reflectivity to approximately its original value.

4.8 A Note on the Construction and Costs of Tall Towers

There are many factors involved in the design and construction of tall towers. One of the primary factors which largely influences the cost, is the type of loading which the tower will encounter. These include top vertical loads, horizontal pull-off loads, wind loading, and

seismic stresses.

Another important influence upon the structure and costs is the risk factor involved. For antenna towers in remote locations where there are no structures or people living near the tower, the safety factor employed is usually less than that used for towers in cities. The remoteness of the location can have a significant impact upon costs. For remote areas the logistics involved raise both the material and labor costs.

A summary of the amounts of material and the approximate costs on a number of steel towers is given by Watt (1967) and based on tall towers. No attempt is made here to describe the detailed procedures of tower design, but rather to show how certain factors determine the amount of materials which may be involved in their construction. Three types of towers are considered: (a) guyed steel towers; (b) self-supporting steel towers; and (c) steel reinforced concrete towers. The guyed steel towers usually require the least amount of material over the height and loading range generally considered for antennas. They have a good performance record when properly designed and installed; however, there have been a number of cases where marginally designed guyed steel towers have collapsed. In Figure 4-9, the weight of structural material involved as a function of tower height is shown for several conditions. The lower dashed curve indicates the amount of structural steel involved over a range of heights for a number of actually designed and installed guyed steel towers, with a top horizontal pull-off capability in the range of 40 tons. The amount of material appears to vary in an exponential form where for this particular condition the amount of steel required for the guyed steel towers is $W_t = 18 \times 10^{h/200}$. The initial constant (18

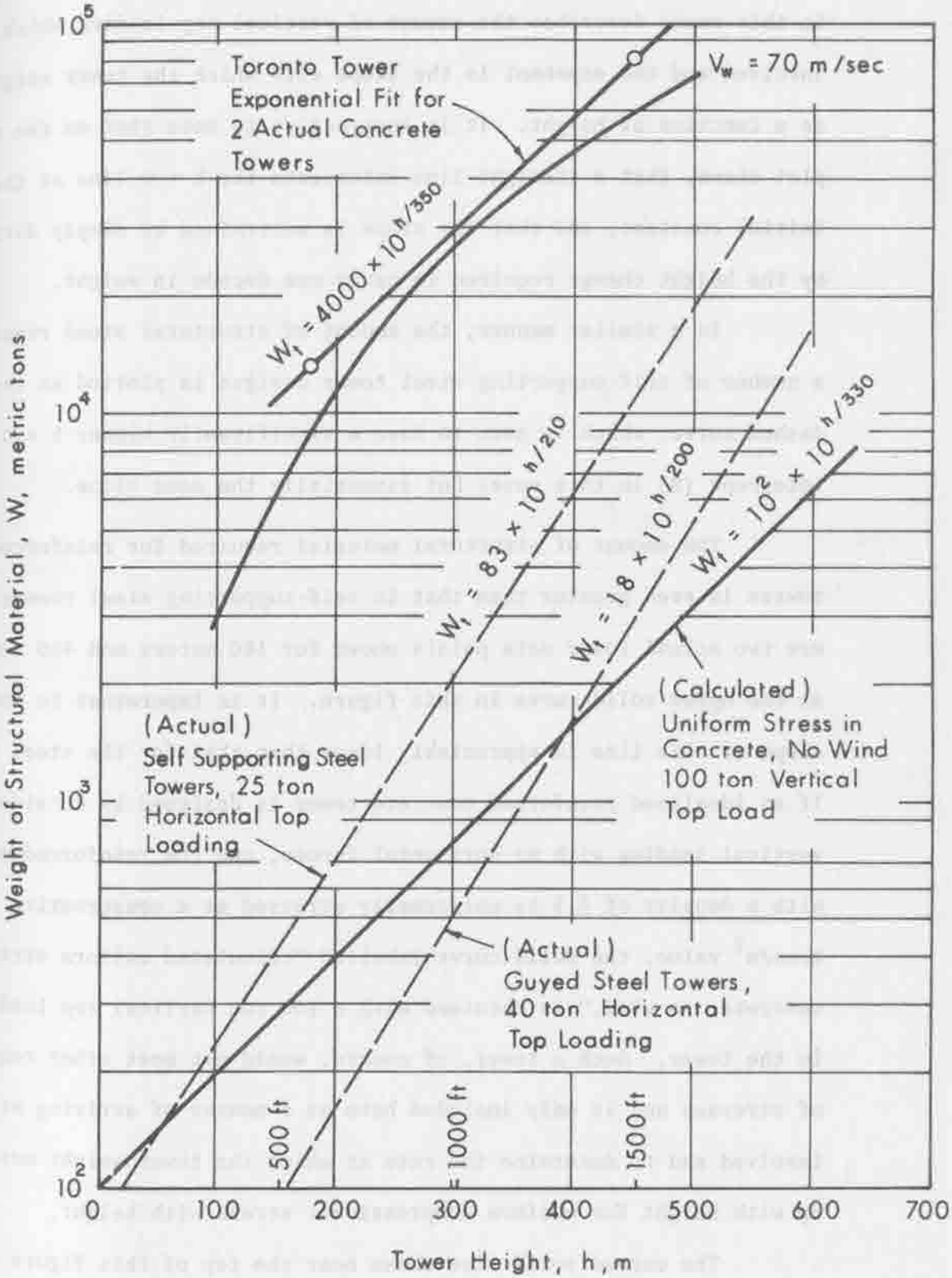

Figure 4-9. Weight of Tower Materials.

in this case) describes the amount of vertical top loading which may be involved and the exponent is the slope with which the tower weight increases as a function of height. It is instructive to note that on the semi-log plot shown, that a straight line intersects the h = 0 line at the initial constant, and that the slope is determined by simply dividing 1 by the height change required to cover one decade in weight.

In a similar manner, the amount of structural steel required for a number of self-supporting steel tower designs is plotted as the upper dashed curve, which is seen to have a significantly higher h = 0 intercept (83 in this case) but essentially the same slope.

The amount of structural material required for reinforced concrete towers is even greater than that in self-supporting steel towers. There are two actual tower data points shown for 180 meters and 450 meters as the upper solid curve in this figure. It is imporatnat to note that the slope of this line is appreciably lower than that for the steel towers. If an idealized reinforced concrete tower is designed by considering only vertical loading with no horizontal forces, and the reinforced concrete with a density of 3.5 is uniformally stressed at a conservative 350 metric tons/m^2 value, the solid curve labelled "calculated uniform stress in concrete, no wind," is obtained with a 100 ton vertical top load is applied to the tower. Such a tower, of course, would not meet other requirements of stresses and is only included here as a manner of arriving at the slope involved and to determine the rate at which the tower weight must build up with height for uniform compressional stress with height.

The curved solid line shown near the top of this figure represents the tower weight required to safely withstand wind loading for a trapizoidal tower with a 10 percent taper. This curve is for a wind velocity

of 70 metres per second. Typical design winds range from 50 to 100 m/sec. For the case where the concrete does not go into tension, the tower weights required are calculated as follows:

The upsetting moment due to the wind is calculated on the basis of a wind pressure $p = 0.06\ V^2$; where p is in kg/m^2 and V is the wind velocity in /second. The force exerted on a cylindrical segment of the tower is calculated using an effective area 1.5 times the actual area, i.e., $1.5D\ \Delta h$, where D is the tower diameter at the height being considered, and Δh is the differential height of the segment.

For a conical shaped tower with a 10 percent taper, the differential upsetting moment is

$$\Delta M_u = 1.5 \times 0.06\ V^2 \times 0.1\ (h_t - h)h\ \Delta h$$

the resulting total moment is

$$M_u = 9 \times 10^{-3}\ V^2 \int_o^{h_t} (h_t - h)h\ \Delta h = 1.5 \times 10^{-3} V^2 h_t^{\ 3}.$$

The righting moment due to tower weight W_t and the base diameter which equals $0.1\ h_t$ is $M_r = W_t \times 0.1\ h_t/2$. For a safe tower, this moment is chosen as twice the upsetting moment. As a result

$$W_t \times 0.1\ h_t/2 = 2 \times 1.6 \times 10^{-3} V^2 h_t^{\ 3},$$

$$\text{and } W_t = 6 \times 10^{-2} V^2 h_t^{\ 2}.$$

If V = 50 m/sec, $W_t = 150\ h_t^{\ 2}$, and the tower weight in metric tons is $0.15\ h^2$, for a wind velocity of 70 m/sec (=168 mph), $W_t \approx 0.3\ h^2$.

It is important to note that the square law relationship derived on the basis of wind loading only will not provide for sufficient increase

in concrete with height for heights above 400 meters to meet the uniform safe compressional stress criteria. This means that the calculations of required structural mass on a basis of wind alone is not sufficient. There are many other factors, of course, which enter into the amount of materials required, including dynamic stresses, torsion, wind vibrations and wind and inertial loading of structures on the top of the tower, which must be considered carefully in arriving at the eventual design. Since the tower structural weight cannot continue to rise at only a square law relation for large tower heights, but must have a rate of increase with height that is at least equal to the exponential of the uniform compressional loaded tower the weight is expected to follow the shape of the upper curve on Figure 4-9.

The cost of towers is shown in Figure 4-10. The costing is obtained by employing a value of $1,000.00 per ton of structural steel for the total installed cost and $66.00 per ton ($\approx$ $180/yd^3$) for concrete. The solid curve, marked, "steel, self-supporting" shows the constructed costs in 1972 dollars for a heavy duty self-supporting steel tower. By way of reference, the cost in height for the steel self-supporting Tokyo TV tower is shown to fall quite close to this curve. The curve labelled, "concrete", is that for steel reinforced concrete towers. The upper circle is for the Toronto tower, and the lower circle represents a detailed reinforced concrete tower design cost at the height shown. It is important to note that the transition point where the cost of the tower increases more rapidly than h^2 which is a crucial point in tall tower solar plant design, occurs in the 200 meter region for the steel towers. On the other hand, it appears that the transition for concrete towers is somewhat higher perhaps in the 250 meter height range. The

TABLE 7-2

Heat Transport Optimization Printout for a Thermal Power Level of 1.0 MW

THE FOLLOWING DATA ARE COMPUTED AT A TRANSFERRED POWER OF 1.00MW

STM TMP DEG C	RET TMP DEG C	FLOW RATE KG/ SEC	ENG EFF %	INS THCK CM OUT	INS THCK CM RET	PIPE DIA CM OUT	PIPE DIA CM RET	OPT VEL M/ SEC	PIPE COST $/YR /M	PUMP COST $/YR /M	INS COST $/YR /M	HEAT COST $/YR /M	RET COST $/YR /M	TOTAL COST $/YR /M
100		0.412	12	5.4	2.7	25.2	2.6	14.2	5.465	0.63	0.825	1.16	1.065	9.15
90	94	43.461	10	5.3	5.1	21.4	18.6	1.3	4.694	0.45	0.705	1.03	6.07412.	
80	84	14.770	8	4.9	4.5	12.8	11.2	1.2	2.930	0.27	0.437	0.72	3.799	8.16
70	74	9.038	5	4.7	4.1	10.1	9.2	1.2	2.388	0.21	0.352	0.63	3.080	6.66
60	64	6.585	2	4.6	3.8	8.7	8.1	1.1	2.103	0.18	0.308	0.57	2.684	5.85
		FLOW	EFF	INSUL		DIAMETER		VEL	PIPE	PUMP	INS	HEAT	RET	TOTAL
150		0.400	21	6.0	2.7	14.8	2.5	8.9	3.333	0.35	0.620	1.05	1.048	6.40
140	144	39.413	20	6.3	6.0	20.1	17.1	1.4	4.425	0.42	0.828	1.28	6.15013.	
130	132	13.397	18	5.7	5.3	12.0	10.6	1.3	2.767	0.25	0.512	0.92	3.902	8.35
120	121	8.193	16	5.5	5.0	9.5	8.7	1.3	2.257	0.20	0.414	0.80	3.190	6.86
110	110	5.963	14	5.3	4.7	8.2	7.6	1.2	1.987	0.17	0.363	0.74	2.797	6.06
100	100	4.726	12	5.2	4.4	7.3	6.9	1.2	1.816	0.15	0.330	0.70	2.534	5.52
90	90	3.940	10	5.1	4.2	6.7	6.5	1.2	1.695	0.14	0.307	0.67	2.339	5.11
80	81	3.398	8	5.1	3.9	6.3	6.1	1.2	1.605	0.13	0.290	0.65	2.185	4.84
		FLOW	EFF	INSUL		DIAMETER		VEL	PIPE	PUMP	INS	HEAT	RET	TOTAL
200		0.392	27	6.2	2.7	9.9	2.5	6.4	2.351	0.23	0.507	1.02	1.037	5.14
190	193	34.708	26	7.0	6.7	18.9	15.9	1.4	4.176	0.39	0.909	1.49	6.16613.	
180	180	11.886	25	6.4	6.0	11.3	10.0	1.4	2.625	0.23	0.568	1.09	3.975	8.56
170	168	7.312	24	6.1	5.6	9.0	8.2	1.3	2.148	0.19	0.462	0.96	3.271	7.05
160	157	5.346	22	5.9	5.3	7.7	7.2	1.3	1.896	0.16	0.406	0.89	2.889	6.22
150	145	4.250	21	5.8	5.1	6.9	6.6	1.3	1.734	0.14	0.371	0.84	2.628	5.66
140	135	3.551	20	5.7	4.8	6.4	6.1	1.3	1.620	0.13	0.345	0.81	2.433	5.24
130	124	3.066	18	5.6	4.6	6.0	5.8	1.3	1.535	0.12	0.326	0.78	2.279	5.01
120	114	2.710	16	5.5	4.4	5.6	5.5	1.3	1.468	0.12	0.311	0.76	2.152	4.81
110	105	2.438	14	5.5	4.2	5.4	5.3	1.2	1.415	0.11	0.299	0.74	2.045	4.61
100	95	2.223	12	5.4	4.1	5.1	5.1	1.2	1.371	0.11	0.289	0.73	1.951	4.44
		FLOW	EFF	INSUL		DIAMETER		VEL	PIPE	PUMP	INS	HEAT	RET	TOTAL
250		0.391	31	6.4	2.6	7.3	2.1	4.8	1.804	0.16	0.439	1.02	1.023	4.49
240	242	28.255	31	7.6	7.2	17.3	14.3	1.5	3.850	0.36	0.944	1.64	6.30013.	
220	215	6.129	29	6.6	5.9	8.3	6.8	1.4	2.015	0.17	0.492	1.09	3.364	7.41
200	190	3.643	27	6.2	5.4	6.5	5.4	1.4	1.644	0.13	0.399	0.96	2.699	5.91
180	167	2.671	25	6.0	5.0	5.6	4.7	1.4	1.465	0.12	0.354	0.90	2.349	5.15
160	145	2.146	22	5.9	4.6	5.1	4.3	1.3	1.355	0.10	0.327	0.86	2.114	4.70
140	126	1.817	20	5.8	4.3	4.7	4.1	1.3	1.280	0.10	0.308	0.83	1.940	4.41
		FLOW	EFF	INSUL		DIAMETER		VEL	PIPE	PUMP	INS	HEAT	RET	TOTAL
300		0.400	34	6.4	2.5	5.4	1.9	3.6	1.426	0.12	0.385	1.02	1.004	3.97
290	291	20.628	34	7.5	7.4	10.9	10.8	3.1	3.703	1.61	0.691	1.44	7.29918.	
270	259	4.674	32	6.9	6.2	7.5	5.9	1.5	1.850	0.16	0.501	1.18	3.260	6.97
250	231	2.873	31	6.6	5.6	5.9	4.7	1.5	1.533	0.12	0.414	1.06	2.648	5.78
230	206	2.165	30	6.4	5.2	5.2	4.1	1.4	1.381	0.11	0.372	1.00	2.323	5.19
210	184	1.779	28	6.3	4.9	4.7	3.7	1.4	1.289	0.10	0.346	0.96	2.104	4.75
190	163	1.532	26	6.2	4.6	4.4	3.5	1.4	1.225	0.09	0.329	0.93	1.940	4.43
170	143	1.358	24	6.1	4.3	4.2	3.3	1.4	1.178	0.09	0.315	0.91	1.808	4.19
150	125	1.229	21	6.0	4.1	4.0	3.1	1.4	1.141	0.08	0.305	0.89	1.700	4.01
		FLOW	EFF	INSUL		DIAMETER		VEL	PIPE	PUMP	INS	HEAT	RET	TOTAL
350		0.430	36	6.5	2.5	4.2	1.9	2.7	1.178	0.09	0.347	1.03	1.070	3.72
340	338	12.237	35	7.6	7.4	8.5	8.4	3.7	4.200	1.73	0.612	1.42	7.66913.	
320	300	3.145	35	6.7	6.2	4.8	4.5	3.0	1.545	0.62	0.384	1.09	3.234	6.93
300	269	2.056	34	6.8	5.8	5.4	3.9	1.6	1.416	0.11	0.419	1.14	2.624	5.74
280	241	1.610	33	6.7	5.4	4.8	3.5	1.6	1.296	0.10	0.383	1.09	2.328	5.09
260	217	1.362	32	6.5	5.0	4.4	3.2	1.6	1.222	0.09	0.360	1.05	2.128	4.65
240	195	1.201	31	6.5	4.8	4.2	3.0	1.5	1.171	0.09	0.345	1.02	1.979	4.32
220	175	1.087	29	6.4	4.5	4.0	2.9	1.5	1.134	0.08	0.333	1.01	1.858	4.06
200	156	1.000	27	6.3	4.3	3.8	2.7	1.5	1.105	0.08	0.324	0.99	1.758	3.85
180	139	0.931	25	6.3	4.1	3.7	2.7	1.5	1.081	0.08	0.317	0.98	1.672	3.67

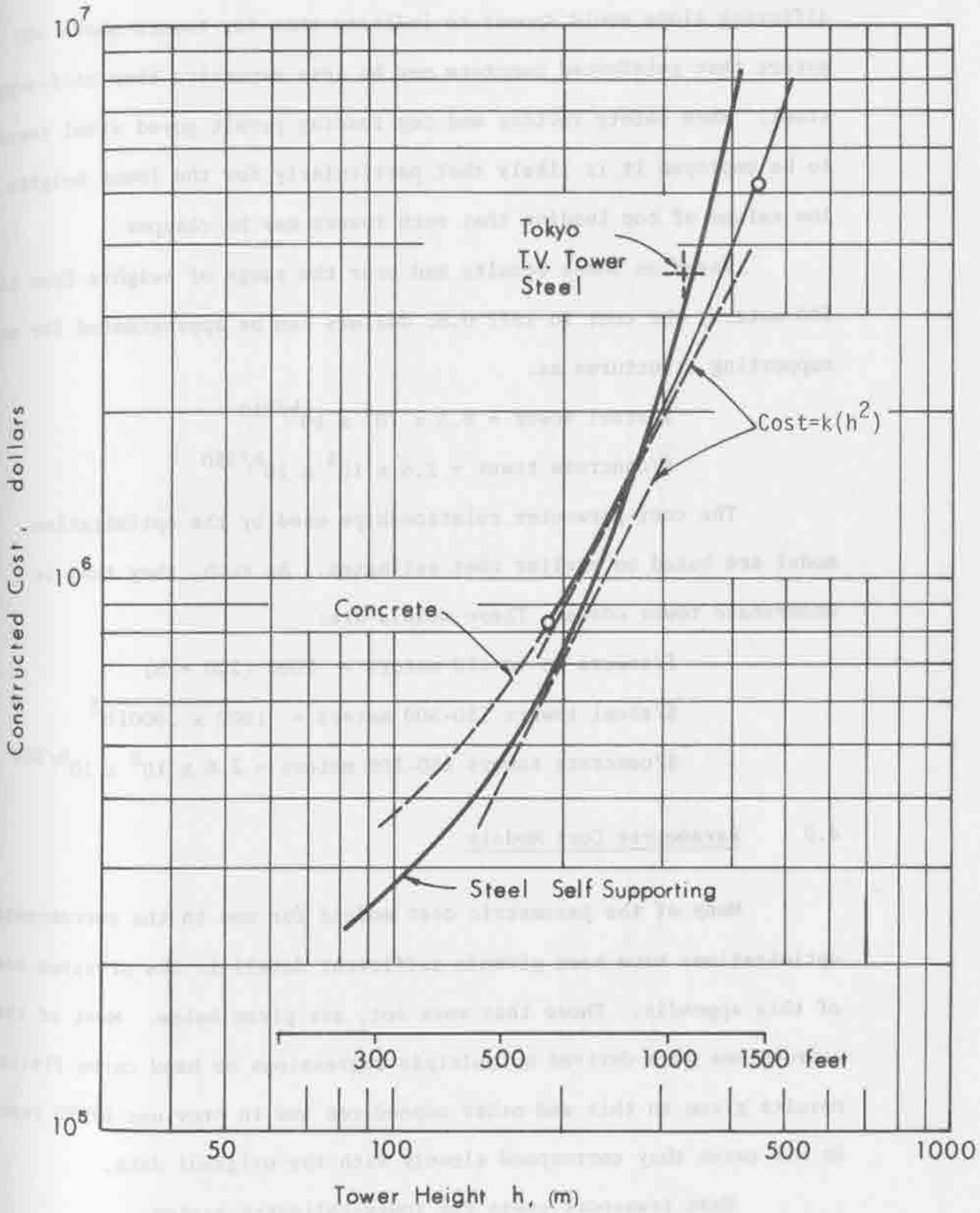

Figure 4-10. Estimated Costs of Steel and Steel Reinforced Concrete Towers.

TABLE 7-3

Heat Transport Optimization Printout for a Thermal Power Level of 10.0 MW

THE FOLLOWING DATA ARE COMPUTED AT A TRANSFERRED POWER OF 10.00MW

STM IMP DEG C	RET TMP DEG C	FLOW RATE KG/ SEC	ENG EFF %	INS THCK CM OUT	INS THCK CM RET	PIPE DIA CM OUT	PIPE DIA CM RET	OPT VEL M/ SEC	PIPE COST $/YR /M	PUMP COST $/YR /M	INS COST $/YR /M	HEAT COST $/YR /M	RET COST $/YR /M	TOTAL COST $/YR /M
100		4.118	12	5.8	3.3	57.6	6.6	27.2	17.069	7.47	1.858	2.24	2.15	830.80
90	94	34.611	10	5.7	5.6	48.9	48.9	2.4	12.370	5.38	1.579	1.95	21.15	142.43
80	84	147.700	8	5.6	5.1	38.8	33.8	1.3	8.238	0.81	1.257	1.62	10.34	622.27
70	74	90.376	5	5.5	4.7	30.7	26.8	1.3	6.594	0.64	1.001	1.35	8.19	917.79
60	64	65.850	2	5.4	4.4	26.5	23.2	1.2	5.728	0.55	0.866	1.21	7.03	715.39

	FLOW	EFF	INSUL		DIAMETER		VEL	PIPE	PUMP	INS	HEAT	RET	TOTAL
150	3.999	21	6.7	3.3	36.0	6.4	15.0	6.840	3.10	1.436	1.96	2.11	215.44
140	144394.128	20	6.9	6.8	46.3	46.3	2.6	11.131	4.83	1.839	2.38	20.07	440.25
130	132133.968	18	6.7	6.2	36.4	31.1	1.4	7.745	0.76	1.452	1.97	10.36	322.30
120	121 81.929	16	6.5	5.8	28.8	24.8	1.4	6.196	0.60	1.157	1.66	8.24	017.85
110	110 59.634	14	6.4	5.5	24.8	21.2	1.3	5.378	0.52	1.001	1.49	7.08	615.47
100	100 47.262	12	6.3	5.2	22.2	19.2	1.3	4.857	0.46	0.911	1.37	6.33	313.94
90	90 39.404	10	6.3	5.0	20.4	17.7	1.3	4.491	0.43	0.841	1.29	5.78	812.84
80	81 33.979	8	6.2	4.7	19.1	16.6	1.3	4.219	0.40	0.789	1.24	5.36	812.01

	FLOW	EFF	INSUL		DIAMETER		VEL	PIPE	PUMP	INS	HEAT	RET	TOTAL
200	3.924	27	7.4	3.3	30.2	6.3	6.9	6.481	0.71	1.405	2.06	2.08	012.74
190	193347.075	26	7.8	7.7	43.5	43.5	2.7	9.860	4.53	2.004	2.70	18.97	138.07
180	180118.865	25	7.6	7.1	34.3	28.9	1.5	7.314	0.72	1.588	2.26	10.30	022.18
170	168 73.123	24	7.4	6.7	27.2	23.1	1.5	5.866	0.57	1.276	1.91	8.22	517.84
160	157 53.461	22	7.2	6.4	23.4	19.7	1.4	5.101	0.49	1.113	1.72	7.09	315.51
150	145 42.503	21	7.1	6.1	21.0	17.8	1.4	4.611	0.44	1.006	1.60	6.35	214.01
140	135 35.510	20	7.0	5.8	19.3	16.4	1.4	4.266	0.40	0.930	1.51	5.81	512.92
130	124 30.659	18	6.9	5.5	18.1	15.3	1.4	4.006	0.38	0.872	1.45	5.39	912.10
120	114 27.098	16	6.9	5.3	17.1	14.5	1.4	3.804	0.36	0.827	1.40	5.06	611.45
110	105 24.377	14	6.8	5.1	16.3	13.9	1.4	3.641	0.34	0.792	1.36	4.79	110.92
100	95 22.234	12	6.8	4.9	15.6	13.3	1.3	3.508	0.32	0.762	1.32	4.55	710.47

	FLOW	EFF	INSUL		DIAMETER		VEL	PIPE	PUMP	INS	HEAT	RET	TOTAL
250	3.912	31	7.5	3.2	16.9	5.6	8.9	3.913	1.82	0.924	1.62	2.13	810.41
240	242282.552	31	8.4	8.3	35.6	35.5	3.6	16.277	7.12	1.849	2.68	27.71	155.64
220	215 61.291	29	7.7	7.2	18.8	18.6	2.7	4.795	2.13	1.022	1.73	9.24	618.92
200	190 36.429	27	7.7	6.7	19.7	16.1	1.5	4.337	0.41	1.064	1.78	6.59	114.18
180	167 26.705	25	7.5	6.2	17.0	13.9	1.5	3.792	0.35	0.930	1.63	5.62	912.33
160	145 21.462	22	7.4	5.7	15.4	12.6	1.4	3.460	0.32	0.843	1.53	5.01	911.18
140	126 18.167	20	7.3	5.3	14.3	11.7	1.4	3.232	0.30	0.792	1.46	4.58	010.36

	FLOW	EFF	INSUL		DIAMETER		VEL	PIPE	PUMP	INS	HEAT	RET	TOTAL
300	4.003	34	7.6	3.2	11.7	5.6	7.8	4.220	1.85	0.736	1.49	2.16	110.46
290	291206.279	34	8.9	8.7	28.7	28.5	4.5	23.687	9.81	1.672	2.58	37.08	074.82
270	259 46.744	32	8.0	7.5	15.5	15.1	3.5	7.103	3.03	0.941	1.75	12.03	924.86
250	231 28.734	31	7.7	6.9	12.7	12.2	3.2	4.883	2.04	0.788	1.56	8.37	917.65
230	206 21.648	30	7.5	6.4	11.2	10.8	3.1	3.886	1.69	0.707	1.46	6.77	114.51
210	184 17.787	28	7.4	6.0	10.4	10.0	3.0	3.371	1.45	0.661	1.40	5.82	612.70
190	163 15.318	26	7.3	5.7	9.8	9.4	2.9	3.035	1.29	0.628	1.36	5.18	611.49
170	143 13.583	24	7.2	5.3	9.3	8.9	2.8	2.798	1.18	0.604	1.32	4.71	710.62
150	125 12.292	21	7.2	5.0	8.9	8.6	2.8	2.579	1.14	0.581	1.29	4.356	9.95

	FLOW	EFF	INSUL		DIAMETER		VEL	PIPE	PUMP	INS	HEAT	RET	TOTAL
350	4.316	36	7.6	3.1	8.7	5.0	6.4	4.303	1.78	0.618	1.43	2.62	510.75
340	338122.368	35	9.1	8.9	22.3	21.8	5.5	26.637	11.04	1.428	2.42	39.91	881.45
320	300 31.450	35	8.2	7.6	12.7	12.0	4.3	8.937	3.62	0.862	1.75	13.46	328.63
300	269 20.564	34	7.9	7.0	10.6	9.8	4.1	6.301	2.67	0.735	1.58	9.57	020.86
280	241 16.103	33	7.7	6.6	9.6	8.8	3.9	5.227	2.19	0.675	1.51	7.84	917.45
260	217 13.619	32	7.6	6.2	9.0	8.1	3.7	4.612	1.92	0.638	1.46	6.83	815.46
240	195 12.012	31	7.6	5.9	8.6	7.7	3.6	4.205	1.74	0.612	1.42	6.15	814.13
220	175 10.870	29	7.5	5.6	8.2	7.4	3.6	3.920	1.61	0.593	1.39	5.66	113.17
200	156 10.002	27	7.4	5.3	8.0	7.1	3.5	3.709	1.51	0.578	1.37	5.27	812.44
180	139 9.318	25	7.4	5.0	7.7	6.9	3.5	3.473	1.50	0.561	1.35	4.97	111.85

differing slope would appear to indicate that for towers above 300 meters that reinforced concrete may be less expensive than self-supporting steel. When safety factors and top loading permit guyed steel towers to be employed it is likely that particularly for the lower heights and low values of top loading that such towers may be cheaper.

Based on these results and over the range of heights from 150 to 500 meters, the cost in 1972 U.S. dollars can be approximated for self-supporting structures as:

$$\$/\text{steel tower} = 8.3 \times 10^4 \times 10^{h/210}$$

$$\$/\text{concrete tower} = 2.6 \times 10^5 \times 10^{h/350}$$

The cost-parameter relationships used by the optimization model are based on earlier cost estimates. As such, they tend to understate tower costs. These models are:

$$\$/\text{towers up to 150 meters} = 1000\ (200 + h)$$

$$\$/\text{steel towers 150-500 meters} = 1000 \times .0001h^3$$

$$\$/\text{concrete towers 150-500 meters} = 2.6 \times 10^5 \times 10^{h/350}$$

4.9 Parametric Cost Models

Many of the parametric cost models for use in the concentrator optimizations have been given in sufficient detail in the previous sections of this appendix. Those that were not, are given below. Most of these expressions were derived by multiple regressions or hand curve fitting of results given in this and other appendices and in previous STEPS reports. In all cases they correspond closely with the original data.

Heat transport costs for tower-heliostat system:

$$7.73h\left(\frac{A_p}{850}\right)^{.79}, \quad A_p < 6{,}000$$

region of Figure 7-4. In this small pipe regime, steam is superior only above 175 °C. In the large pipe regime (10 MW), on the other hand, steam is superior above 150 °C and the differential is much larger at higher temperatures.

The above results were necessary for the consideration of preliminary systems designs. They are also important data for the verification of results of the more complex total system optimization. Many of the formulations developed for this heat transport subsystem optimization have been included in the overall system optimization.

$$21.76h\left(\frac{A_p}{850}\right)^{.308}, \quad A_p \geq 6{,}000$$

Fresnel Strip reflector costs:

f/Ap	Ap 1.0	3.0	5.0	7.5
.5	53.00	47.20	57.30	53.10
.75	49.60	44.20	53.60	49.70
1.00	48.30	43.00	52.20	48.40
1.25	47.60	42.40	51.40	47.70
1.75	46.40	41.30	50.10	46.50

Add-on costs for inclining and making the collectors mobile are the same as for parabolic troughs.

Concentrator related absorber-heat exchanger costs for point focus concentrators (except for Fresnel reflectors):

$$66 + 3.08\ (x + .6096)$$

where

$$x = A_p/2 \quad , \theta_{max} > 90^o$$

$$A_p/2 \sin\theta_{max}, \quad \theta_{max} \leq 90^o$$

Concentrator related absorber-heat exchanger costs for Fresnel circular reflectors:

$$70.5 + 3.08\ (f + .6096)$$

Surface contour error add-on cost for movable concentrators:

$$(a + bA_p)\ \frac{.00247}{\sigma_{\phi,\lambda}}, \quad \sigma_{\phi,\lambda} \geq .00247$$

$$\infty, \quad \sigma_{\phi,\lambda} < .00247$$

where a is the cost per concentrator and b is the cost per m^2 of concentrator aperture for accuracy tolerances of $\sigma_\phi = .1^o$ and $\sigma_\lambda = .1^o$.

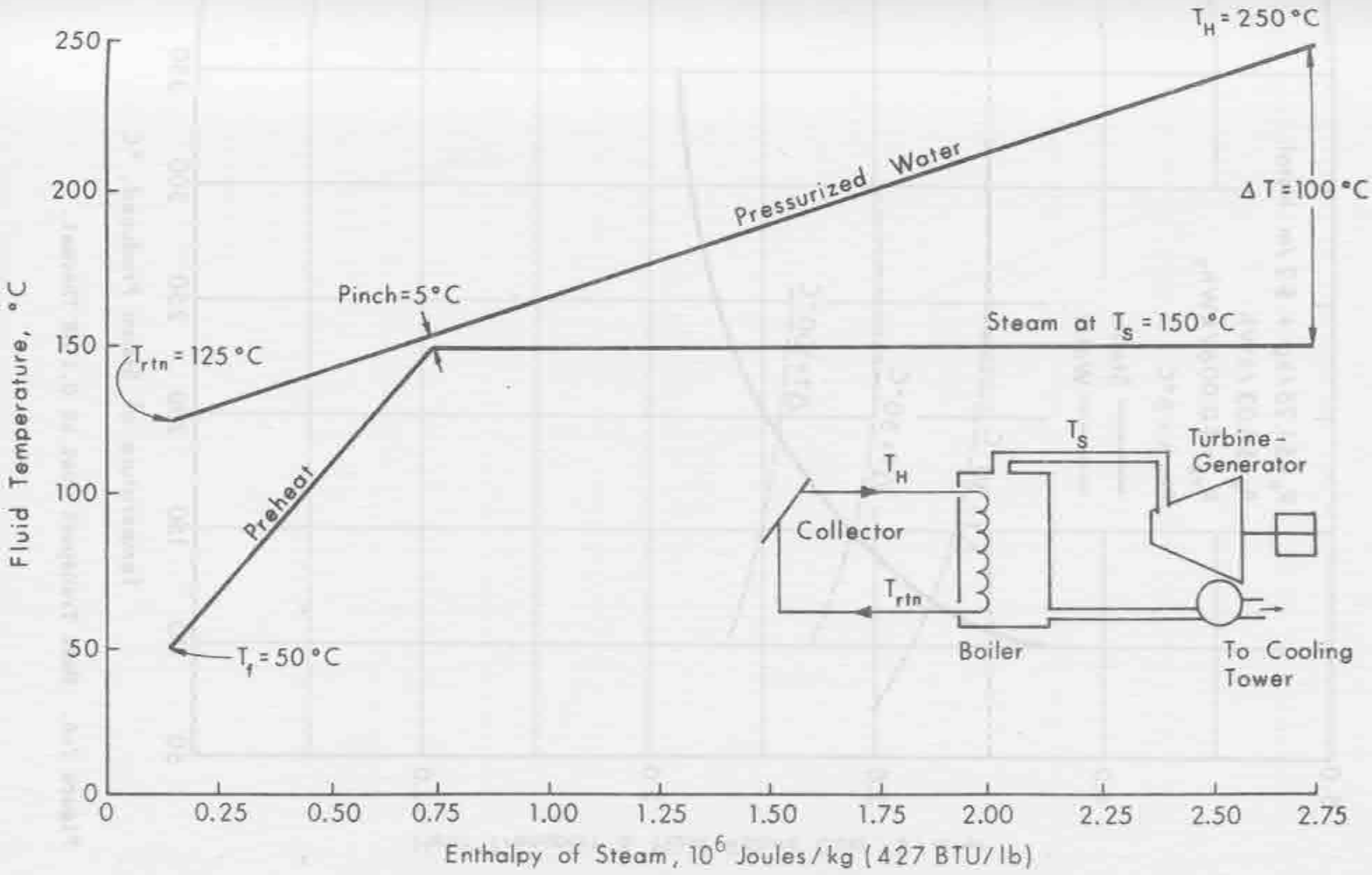

Figure 7-5. Heat Exchanger Performance is Presented as the Hot Water Input (upper line) at T_H Heating Feed Water from 50 °C to T_S and Boiling it (lower line). Lower Scale Applies only to Lower Trace. Upper Trace is Superimposed.

Increasing the flow rate in the transport loop decreases the slope of this upper line, rotating it about the pinch point.

Surface contour error add-on cost for heliostat fields:

$$(a + bW^2)N_w \quad \frac{.00247}{\infty} \quad , \sigma_{\phi,\lambda} \geq .00247 \quad , \sigma_{\phi,\lambda} < .00247$$

where a is the cost per heliostat and b is the cost per m^2 of hel area for accuracy tolerances of $\sigma_\phi = .1^o$ and $\sigma_\lambda = .1^o$

Point focus concentrator absorber-heat exchanger costs le concentrator related costs:

$$48331 \ell dt_w$$

Pumping costs for absorber-heat exchangers:

$$.0357d^{.8} V_f^{2.8} \cdot (D_{A_p} + 1.2192 + \ell)/.16$$

Non-evacuated covered cylinder absorber-heat exchanger co

$$.006\ (1.27\ d)^3\ L + (1.27d)^2 + 1.27d$$

Evacuated covered cylinder absorber-heat exchanger cost:

$$.006\ (1.27d)^3\ L + 285(1.27d)^2 + 1.27d$$

Meinel-type absorber-heat exchanger cost:

$$.0357d^{.8}V_f^{2.8}\ (D_{Ap} + 1.2192 + L)\ /.16 + (100d)^{1.3}\ L + 7680d - 139$$

REFERENCES

The Aerospace Corporation, (1974): Solar-Thermal Conversion Mission Analysis, Volume IV: Mission/System and Economic Analysis. El Segundo, California.

The Aerospace Corporation, (1972): Task I Report: Comparative Systems Analyses. El Segundo, California.

Bliss, R. W., Jr., (1959): "The Derivation of Several 'Plate Efficiency Factors' Useful in the Design of Flat-Plate Solar Heat Collectors," Solar Energy Journal, Vol. 3, p. 55.

Dudko, Yu. A. and O. A. Dudko, (1968): "Designing Concentrating Systems," Geliotekhnika, Volume 4, Number 6.

Duff, W. S., (1974): "The Analysis of the Performance of a Pancake Absorber-Heat Exchanger for a Solar Collector," ASME paper number 74WA-SOL/1.

Duff, W. S. and G. F. Lameiro, (1974): "A Performance Comparison Method for Solar Concentrators," ASME paper number 74WA-SOL/4.

The Federal Power Commission, (1971): The 1970 National Power Survey: Part I. Washington, D. C.

Grant, E. L. and W. G. Ireson, (1970): Principles of Engineering Economy, 5th Ed. The Ronald Press, New York.

Grilikhes, V. A., (1966): "A Method of Calculating Radiant Flux Distribution in Receivers of Solar Installations," Geliotekhnika, Volume 2, Number 1.

Hildebrandt, A. F., et al., (1972): Large-Scale Concentration and Conversion of Solar Energy. EOS, Trans. Am. Geophys. Union 53(7):684-691.

Hottel, H. C. and A. Whillier, (1958): "Evaluation of Flat-Plate Solar Collector Performance," Proceedings of the Conference on the Use of Solar Energy, U. of Arizona, Vol. II, p. 74.

Klein, S. A., J. A. Duffie and W. A. Beckman, (1974): "Transient Considerations of Flat-Plate Solar Collector," Accepted for publication in the Trans. of the ASME: J. of Engineering for Power.

Löf, G. O. G. and J. A. Duffie, (1963): "Optimization of Focusing Solar Collector Design," Trans. of the ASME: J. of Engineering for Power, (July).

Sheldahl-Foster Wheeler, (1974): NSF/RANN/SE/GI-41019/PR/74/2, Semi-Annual Progress Report, "Solar Power Array for the Concentration of Energy, July.

Teplyakov, D. I., (1971): "Concentration Ratio of Paraboloidal Solar Concentrators Deduced from Geometric Optics," Geliotekhnika, Volume 7, Number 6.

Threlkeld, James L., "Thermal Environmental Engineering", Second edition, Prentice-Hall, Inc.

Umarov, G. Y., (1967): "Problems of Solar Energy Concentration," Geliotekhnika, Volume 3, Number 5.

University of Houston-McDonald Douglas, (1974): NSF/RANN/SE/GI-39456/PR/73/4, Progress Report #1, "Solar Thermal Power Systems Based on Optical Transmission, February.

University of Minnesota and Honeywell, (1973): Research Applied to Solar-Thermal Power Systems: Progress Report No. 2. Minneapolis

Watt, A. D., (1967): VLF Engineering, Section 2.2.2, Pergamon Press.

Zakhidov, R. A. and D. I. Tephyakov, (1966): "Power Characteristics of Solar Reflecting Devices under Operative Tracking Conditions," Geliotekhnika, Volume 2, Number 4.

APPENDIX F

HEAT TRANSPORT

BY

A. D. WATT,

G. L. WILCOX, JR.,

AND

D. Q. HOOVER

1.0 INTRODUCTION

The natural resource being harvested by solar energy systems has a low average power density with appreciably greater peak power values. With insolation values in the U.S. ranging from 2 to 4 kWh/m^2-day in January to 6 to 7 in July, the average power flux over 24 hours ranges from 80 to 300 W/m^2 of horizontal surface. Clear day average values may range as high as 400 W/m^2. Instantaneous values of up to 1400 W/m^2 have been recorded for short periods of time, but a more normal clear sky summer noon value is 1100 W/m^2 for direct plus diffuse radiation.

The area of the collector field A_f over which the heat must be transported can be arrived at in several different ways. A preliminary estimate of field size, A_f in square meters, can be made from the relation

$$A_f = \frac{P_{rated}\, C_f}{P'_h\, \eta_o\, (1 - S_f)} \quad m^2$$

where: P_{rated} is the rated electrical output in watts, C_f is the capacity factor; i.e., the effective fraction of time that the plant operates at a rated output, P'_h is the average solar power density on a horizontal surface, in W/m^2, η_o is the average overall conversion efficiency, and S_f is a spill factor which is equal to the average fraction of insolation within the field area which misses the collectors.

For example, if P_{rated} = 100 MW, C_f = 0.5, η_o = 0.17, P'_h = 300 W/m^2, and S_f = 0.5, the required area is 2 x 10^6 m^2. If a rectangular field and piping system is employed, the field is 1.4 km on a side and this is also the distance over which heat must be transported from the farthest

collector (if a rectangular pipe layout is used and the heat engine is located in the center of the field).

The magnitude of the transport piping involved can be obtained by considering a square layout as in Figure 1-1. The number of collectors, N_c, is equal to the field area divided by the area of each collector unit, A_c, divided by a fill factor F_f. The length of piping one way is equal to the number of collectors times the distance between collector centers. Since in a square grid this distance is approximately $(A_c/F_f)^{1/2}$, the one way length of pipe on a rectangular grid is

$$L = N_c \, (A_c/F_f)^{1/2} = A_f \, (F_f/A_c)^{1/2} \quad m$$

$$= \frac{P_{rated} \, C_f \, F_f}{P'_h \, \eta_o \, (1 - S_f) \, A_c^{1/2}} \quad m$$

Using the values given for the 100 MW example and: $A_c = 25\ m^2$, and $F_f = 0.25$, yields 20,000 collectors and 2×10^5 metres of pipe for the going and also for the return paths.

The thermal power levels involved range from the individual collector output which, with a solar flux density of 1000 W/m^2, a collector area of 25 m^2, and a collector efficiency η_e of 0.5, is 12.5 kW_t. The maximum thermal power into the turbine and storage is

$$P_{tm} = P'_{max} \, A_c \, N_c \, \eta_c \quad \text{Watts}$$

If $P'_{max} = 1200\ W/m^2$, $A_c = 25$, $N_c = 40{,}000$ and the collector efficiency, η_c, is 0.5, the maximum thermal power from the field, P_{tm}, is 600 MW_t.

The range of temperatures involved is limited by either collector performance, heat transport material characteristics or the heat engine and its working fluid. Since collector output temperatures may range from a hundred to more than a thousand degrees C, the temperature limits

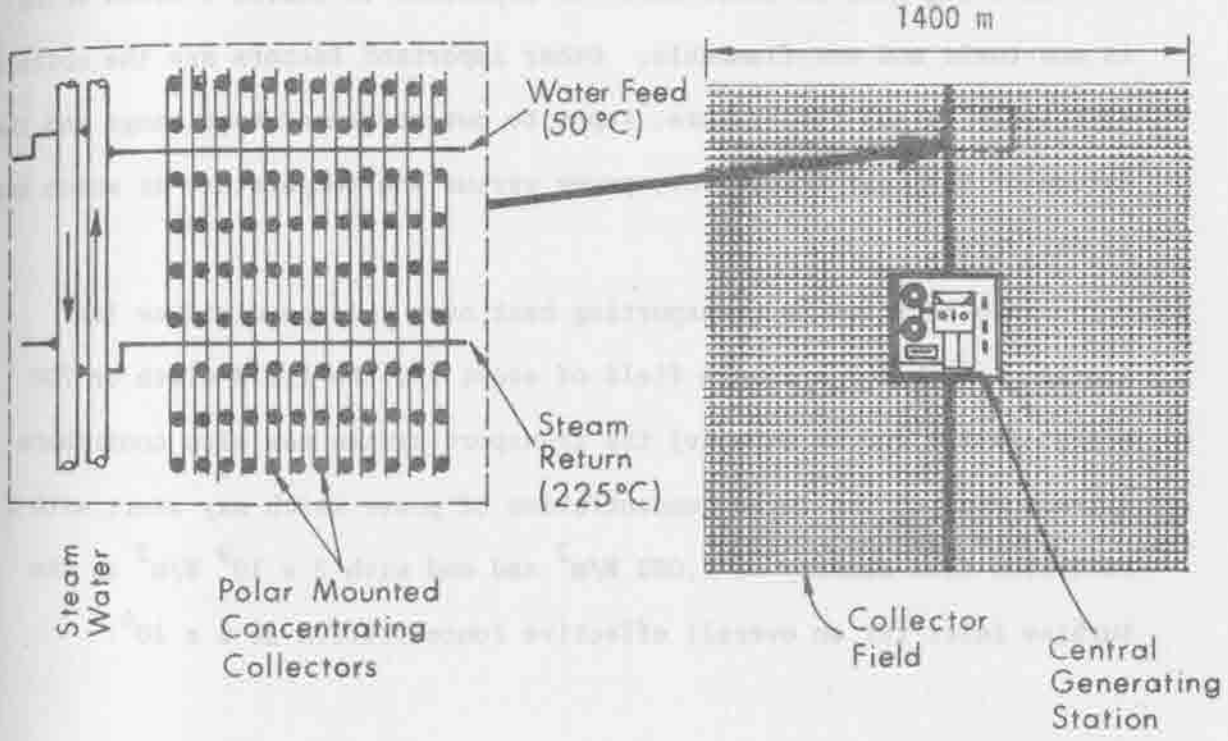

Figure 1-1. Solar Thermal Electric Power System.

will be largely imposed by the materials in the heat absorber, heat transport, or heat engine.

There are many factors which enter into the choice of heat transport materials. For a 100 MW plant, 2,000 to 20,000 tons of transport fluid must be circulated at high temperatures, velocities, and in some cases, high pressure. The possibility of pipe failure and the resulting loss of fluid makes it important to choose a fluid which is non-toxic and non-flammable. Other important factors are the collector efficiency versus temperature, input to output temperature range and the nature of the heat load, i.e., power versus the temperature at which heat is delivered.

In addition to transporting heat over a large distance (an average length for a square field of about 1/2 the field width or 700 metres in the 100 MW example) the transport system may also contribute a great deal of the large concentration of power which may start with a radiation flux density of 1,000 W/m^2 and end with 2×10^9 W/m^2 at the turbine inlet for an overall effective concentration of 2×10^6.

2.0 TRANSPORT METHODS AND FUNDAMENTALS

There are three well known methods of heat transport: conduction, convection, and radiation. The transfer of energy from the sun to earth is by radiation which in systems involving optical concentration is redirected by reflection or refraction to an absorbing surface. In systems such as the tower mounted absorber, much of the transfer of energy is by radiation.

The three methods have differing performance characteristics and cost relationships which should be considered in a well balanced heat transport design. The normal sequence involved is first, radiation to the absorber, next, conduction in the absorbing material, and then transfer via a film coefficient to some convective fluid which may also be the heat engine working fluid. If another working fluid is used, further transfer via film coefficients and conduction is involved in heat exchangers or steam generators.

The temperature drop for conduction in a uniform cross-section is

$$\Delta T = (P_t/A)\ \ell/\sigma \approx P'\ \eta_c\ \ell/k_i \qquad {}^{o}C$$

where ΔT is in degrees C, (P_t/A) or $P'\ \eta_c$ is the heat power flux density in W/m^2, ℓ is the transfer length, k_i is the thermal conductivity in watts per metre degree C, P' is the solar flux in watts/m^2, and η_c is the collector efficiency. For steel, k_i is in order of 50, and as a result,

$$\Delta T/\ell \approx 0.02\ (P_t/A). \qquad {}^{o}C/m$$

For conduction through a thin sheet in a flat-plate collector where the heat flux density may be 500 W/m^2, the temperature drop is

only 10 ^{o}C/m, or a fraction of a degree for a normal wall thickness. If a tube on sheet arrangement is employed, the temperature rise with distance, ℓ, from the tube center on a sheet of thickness S is

$$\Delta T = P' \eta_c \ell/2k_i S. \qquad ^{o}C$$

For $P' \eta_c$ = 500 W/m^2, ℓ = 0.1 metre, k_i = 50 W/m ^{o}C, and S = 5 x 10^{-4} metres, ΔT is 100 ^{o}C. Using a copper sheet would change the temperature difference to about 10^{o} and an aluminum sheet would result in a ΔT of 20 ^{o}C. It is apparent from this discussion that the transfer or concentration of heat by conduction is fine for distances in the order of a centimeter or so, but that it is impractical for long distances.

Transfer of heat by forced connection, as we shall see, is usually not desirable for short distances and low power levels. In Section 7.1, it is shown that for a pumped fluid

$$\Delta T = \frac{P_t}{C_p \rho (\pi/4) d^2 V} \qquad ^{o}C$$

where C_p is the specific heat of the fluid in watt - sec/kg. ^{o}C. ρ is its density in kg/m^3, d is the pipe diameter in metres and V is the effective fluid velocity in metres/sec.

For water, $C_p \rho$ is relatively constant at 4 x 10^6 in the temperature range of 100 to 300 ^{o}C and a good velocity is 1 m/sec. The resulting temperature difference is

$$\Delta T \approx 3 \times 10^{-7} P_t/d^2 \qquad ^{o}C$$

or solving for transfer power yields

$$P_t = 7.5 \times 10^6 \Delta T d^2. \qquad W$$

Note that if ΔT = 20 ^{o}C, and the pipe diameter d = 1 cm that P_t = 15 kW, which is the order of magnitude for a single collector output, and if d = 1 metre, P_t = 150 MW. These values are not optimum but are shown to indicate the order of magnitude of diameters and power levels involved. Because of the fact that the cost of small pipes (less than 1 cm dia.) is insensitive to diameter, and in the range 1 to 30 cm, varies only as the first power of diameter, the cost of transporting heat by forced convection in \$/kW decreases almost directly with power level in the range from 1 kW to 1 MW. This makes it very important in heat transport field layout design to combine the outputs of collectors quickly and have a minimum length of low power level piping.

If there is a need for moderate distance heat transport (0.5 to 5 metres) with a low temperature drop, natural convection in a heat pipe may be a good choice. In this distance region, conduction will be very expensive, and for a single path the initial cost of a pump for forced convection will make such a solution very expensive on a unit length basis. When multiple moderate length paths are involved and pumping power is needed for associated long distance transport, a system of capillaries may be most effective provided the capillaries are not too small.

Insulation of heat transport lines is an important factor in solar system design. The thermal conductance per metre length of pipe diameter d_1 with an insulating jacket diameter d_2 and thermal conductance k_i is

$$G/_{\ell} = 2\pi\, k_i\, \ell n\, (d_2/d_1) \quad W/m\ ^{o}C$$

as an example, when d_2/d_1 = 2, and k_i = 0.04 W/m ^{o}C (typical for glass

wool), $G/_{\ell}$ = 0.17 W/m ^{o}C. If the temperature drop across the insulation is 200 ^{o}C, the power loss per metre length of pipe is 35 W/m. Such a loss is negligible for a large pipe carrying 100 MW where η_t (efficiency of transport) for a km long pipe would be 0.9996. For a small pipe carrying 10 kW, a length of 10 metres has a transfer efficiency of 0.96. Thicker insulation can be used to reduce the heat loss; however, increasing the diameter ratio by 10 (i.e., to 20) only reduces the loss by a factor of 4. From this it can be seen that insulation with a low value of k_i is important for small pipes. The large percentage heat losses from small pipe is another reason why it is desirable to combine heat flow into larger pipes as soon as feasible.

From these considerations, it is apparent that forced convection of some heat transport fluid through insulated pipes must serve as the major thermal transport mechanism. In "tall tower" type systems, much of the transport, as well as concentration, is carried out with the electromagnetic energy.

3.0 MATERIALS - PROPERTIES AND PRICES

A wide variety of materials are available to transport heat. Conductive transport is of primary interest in collectors and heat exchangers, and only a few materials and their thermal conductivity are listed in Table 3-1.

TABLE 3-1

Thermal Conductivity in the 200 k_i ^{o}C Region

Material	W/m ^{o}C
water	0.65
glass	1.2
stainless steel	18
iron	65
zinc	100
aluminum	260
copper	400

Some materials used in forced convection are listed in Table 3-2. The second set of values, H ρ, gives a relative comparison of the volumetric merit of the materials for heat transport, where

$$H = \int_{o}^{T} C_p dT$$

is the heat content of the material at temperature T in Watt-sec/kg, relative to that at T = $0^{o}C$. Water stands out above all the others in this comparison. When pressure is added to the figure of merit in the last set, it is seen that for this figure of merit water drops off a great deal at the high temperatures. Steam, which increased markedly in the previous comparison, remains rather uniform in the region of 0.42. The liquid metals and vegetable oils rate better as temperature increases due to their low vapor pressures. It is essential that oils be kept as free of fatty acid as possible if they are to be used near their upper temperature

TABLE 3-2

Comparison of Heat Transfer Properties of a number of Fluids. Primarily for comparison purposes, as some of the values were obtained by the product of averages in place of a precise integration.

	H^*, kWh/kg			$H\rho$, kWh/m^3			$H\rho p^{-1}$, kWh/m^3-atm		
Material T, °C =	100	200	300	100	200	300	100	200	300
Water	0.116	0.234		110	200	260	110	12	2.9
Steam (saturated)	0.74	0.769		0.44	6.02	37	0.44	0.41	0.42
Na	0.037			32	60		32	60	
Therminol 77				45	95		45	95	
Soybean Oil				51	105		51	105	
Ammonia	0.41			40					
Air	0.028			0.03	0.027	0.024	0.03	0.027	0.024
CO_2	0.024			0.04					
H_2	0.406			0.024					
He	0.015			0.02					

* energy content relative to that at 0 °C.

limits of 200 to 250 °C. This can be done by a special refining process during use.

Using still another figure of merit derived in Section 7.8, which includes viscosity and pumping loss, a number of fluids are compared over the temperature range of interest in Figure 7-2. This figure of merit, which is valid for pipe diameters of 0.1 metre or greater, represents relative pipe and pumping costs, and also includes the transport material costs. The factor which increases the cost of the sodium transport is the requirements for stainless steel pipe. For example, stainless may cost 15 times as much as carbon steel. This fact raises the cost of sodium transport above the steam and water curves as shown.

The approximate cost of a number of heat transport fluids is given in Table 3-3. To compare transport material cost with pipe, pumping and heat loss costs given in Section 7, the cost per metre length of pipe is given in Table 3-4.

TABLE 3-3
Approximate Cost of Materials in 1973 U.S. Dollars

Material	$/kg	$/m^3
Water & steam	0.001*	1
Na	0.6	540
Therminol (77)	0.3 to 1.2 (5.0)	200 to 1200, (5000)
Dowtherm	0.7 to 1.0	900 to 1200
Soybean oil	0.45	390
CO_2	0.07	0.001
H_2	5	0.8
He	12	2.00

* for treatment and ion control

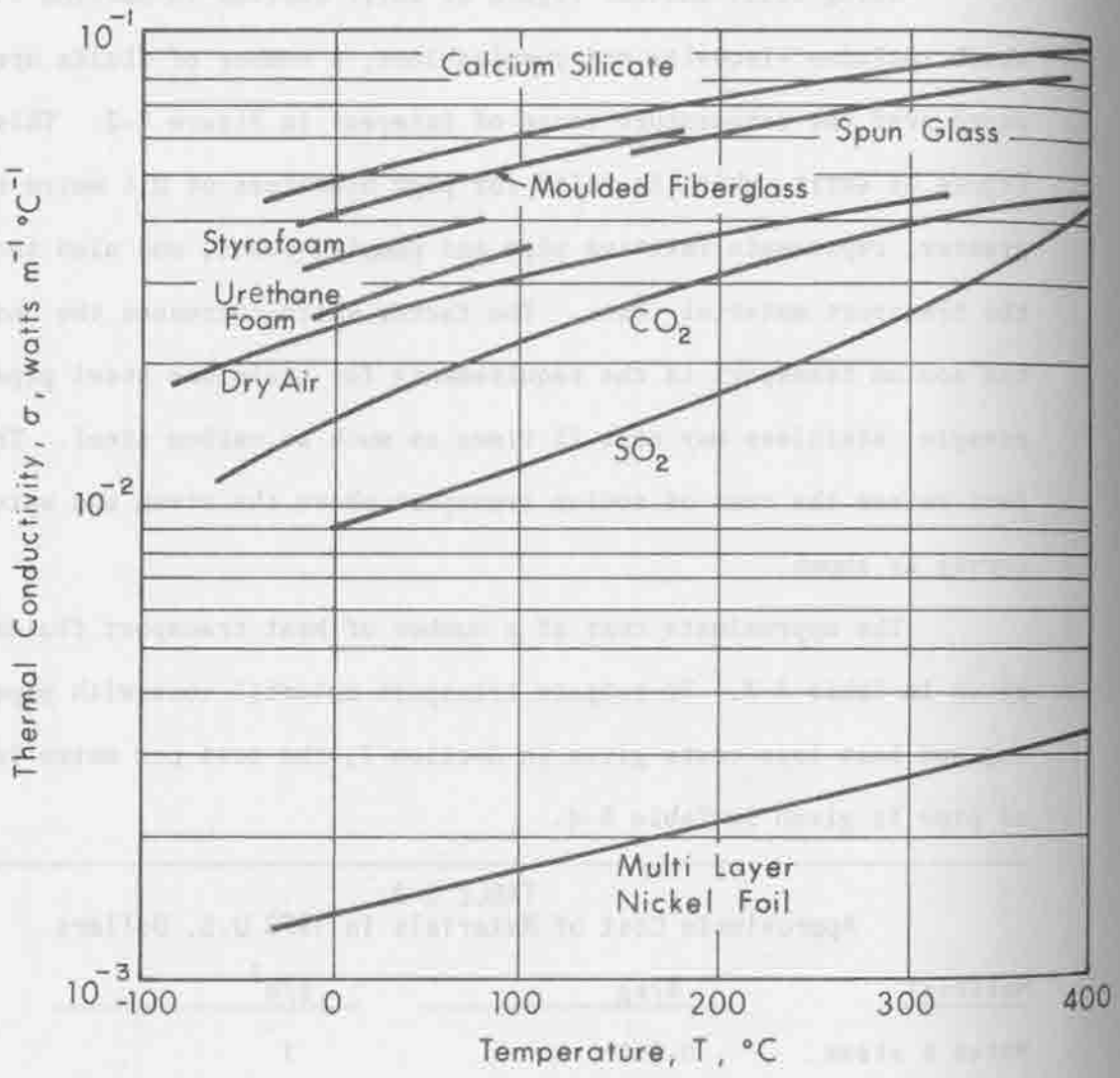

Figure 3-1. Thermal Conductivity of Various Insulating Materials.

TABLE 3-4
Cost of Metre Length of Pipe

Pipe diameter metres	Vol/m m^3/m	$/m Na	$/m Dowtherm
10^{-2}	7.8×10^{-5}	4×10^{-2}	9.4×10^{-2}
10^{-1}	7.8×10^{-3}	4.2	9.4
1.0	0.78	420	940

The above costs can be annualized by multiplying by 0.16 for a direct comparison with the other piping costs in $/m-yr. When this is done, the cost of transport materials is seen to be small for pipes less than 10^{-1} metres in diameter. For the larger pipe, 1 metre diameter, the transport material cost becomes dominant for Dowtherm.

The effective cost of pipe materials in $/kg varies with pipe diameter, being higher at the smaller diameters in some cases by about 1.5 to 1. The average 1973 cost of seamless pressure piping using A 106 steel is about 0.4 to 0.5 $/kg. Stainless steel (304) is estimated to cost about $8/kg in the same time interval. For hot rolled steel, the ultimate tensile strength is about 35×10^6 kg/m^2, with a working strength, t_w, of 6×10^6 kg/m^2. The material density is 7.8×10^3 kg/m^3.

The thermal conductivity of insulating materials over their useful temperature range are shown in Figure 3-1. For temperatures below 100 ^oC the urethane and styrofoams are good. Molded fiberglass is useful into the 200 ^oC region. Spun glass can be used up to about 400 ^oC and calcium silicate can be used at temperatures as high as 1,000 ^oC.

The cost of insulating materials has about doubled in the past

few years, and it is difficult to get an accurate costing which yields a precise comparison of the various materials. Another factor is the large range of quoted costs for a given material. The values quoted in Table 3-5 for the large volume case were arrived at after lengthy discussions and analysis of several price estimates by potential suppliers. Because of the large amount of material, a special factory is envisioned along with an automated installation procedure which has a far different costing rate than that involved in one-of-a-kind petrochemical plants with complex piping.

TABLE 3-5

Costs of Insulating Materials

1974 U. S. Dollars

Material	Normal quote Bulk	Molded	automated installation
	$/m^3	$/m^3	$/m^3
Urethane foam	100	180	150
Styrofoam	60	110	90
Molded fiberglass	60	110	90
Spun glass	80	160	120
Calcium silicate	100	200	150

The insulation of piping is required to control the heat loss which occurs via several different mechanisms and paths. First, there is the transfer of heat from the fluid itself through a convective film to the inside wall of the pipe. Next, via conduction, the heat is transferred through the pipe wall to the inside surface of the insulating jacket. At this point, the primary control mechanism occurs,

which is the resistance to the flow of heat through the insulating jacket from its inside to the outside surfaces. At the outside surface, heat is lost by two mechanisms to the surroundings. First, there are convective losses to the air itself, and in parallel with this loss, a transfer of energy via radiation from the outer surface of the insulation to the surroundings.

The first two mechanisms involved can usually be neglected and we can write the power loss per length of pipe for the remaining three mechanisms as

$$P/\ell = \underset{\text{conduction}}{\Delta T_1 \; k_i \; 2\pi/\ell n \; (1 + 2t/d)} \qquad W/m \qquad (3\text{-}1)$$

where k_i is the thermal conductivity of the insulation. The other symbols are defined in Figure 3-2. The power loss from the outer surface of the insulation to the air can be approximated as

$$P/\ell \underset{\text{convection}}{} \approx \Delta T_2 \; 10\pi \; d_o \; (1 + 0.1/d_o)^{0.5} \; V_w^{\;0.67}, \; W/m \qquad (3\text{-}2)$$

In parallel with this convective flow is a radiative loss which is

$$P/\ell \underset{\text{radiation}}{} = \pi d_o \; 5.67 \times 10^{-8} \; \varepsilon (T_2^{\;4} - T_3^{\;4}) \qquad W/m$$
$$\approx \pi d_o \; 2.3 \times 10^{-7} \varepsilon \; \Delta T_3 \; T_2^{\;3}.^{*} \qquad (3\text{-}3)$$

where $\Delta T_3 = (T_2 - T_3) \approx \Delta T_2$ and ε is the surface emissivity. The latter two power loses must add up to equal the conduction loss, which is equal to the total power loss from the pipe. The conduction loss is seen to be directly proportional to the temperature difference between the inner and

* Note T_2 must be in ^{o}K.

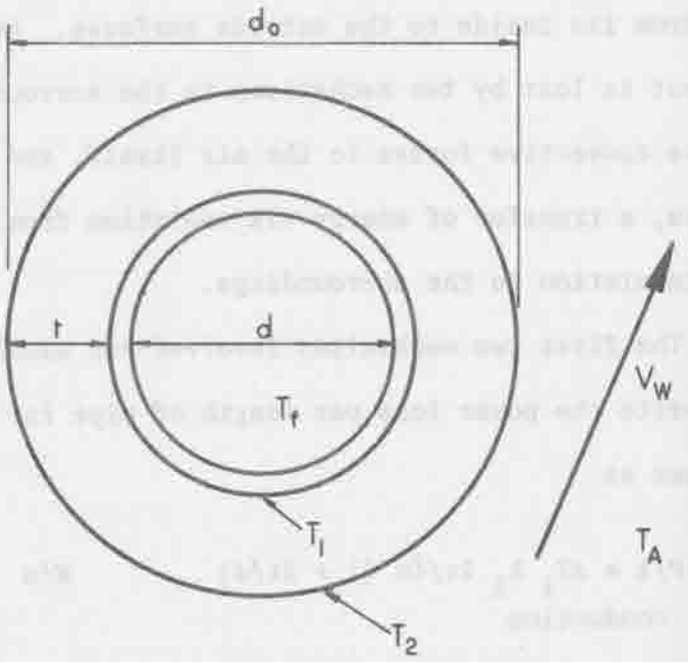

$\Delta T_1 = T_1 - T_2$

$\Delta T_2 = T_2 - T_A$

T_F = Fluid Temperature

T_A = Ambient Air Temperature

V_W = Wind Velocity, m/sec

d = Pipe Diameter

d_o = Insulated Pipe Diameter

t = Thickness of Insulation

Figure 3-2. Definition Sketch for Symbols.

outer surfaces of the insulation, ΔT_1, as well as to the conductivity of the insulation. The geometric factor which controls heat loss is the logarithm of the ratio of inner to outer diameters, or (1 + 2t/d), where t is the thickness of insulation. The amount of insulation contained in a jacket with these dimensions is important in determining the cost of reducing the heat loss. Both of these factors, the heat loss factor F_l and the volume factor F_v are shown in Figure 3-3. Also shown in this figure is the insulation effectiveness factor, which starts at 1 for very thin layers of insulation, and progressively becomes less effective as the thickness to diameter ratio increases. For example, it can be seen that by the time that the thickness equals the diameter, the insulation as a whole has become about 3/10 as effective as it was for the first initial layer.

In determining the ΔT_1 to use, it is necessary to first check the temperature differentials ΔT_2 and ΔT_3 which are involved in the convection and radiation transfers of heat from the outer surface of the pipe to the environment surrounding it. For normal wind velocities V_w, the convective heat loss is seen to be directly proportional to the diameter for large diameter pipe and insulation, and increases with wind velocity. For pipe of a 1 metre outside diameter, the power loss per meter length of pipe with a 5 metre per second wind is equal to $95\Delta T_2$. If the outer diameter, on the other hand, is reduced to 1 cm, the power lost by convection becomes $3.1\Delta T_2$.

The amount of heat lost via radiation is directly proportional to the outside diameter and to ΔT_3, which is usually about equal to ΔT_2, as well as to the outside surface temperature cubed. For a 1 metre diameter pipe with a surrounding temperature of 0 ^{o}C, the power loss for ΔT_3=10 ^{o}C is 150 watts per metre length of pipe. The power loss as a function of temperture differential

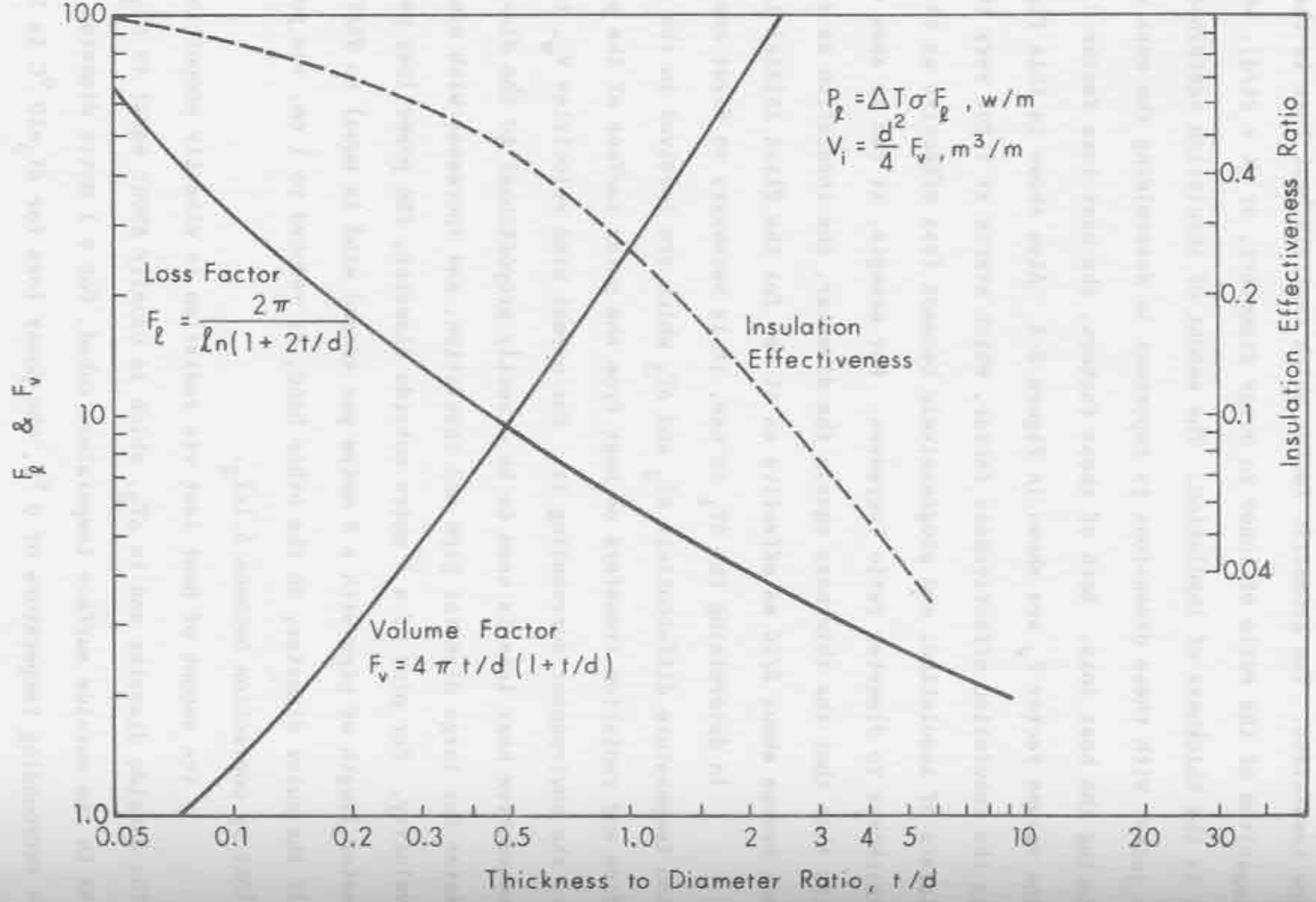

Figure 3-3. Heat Loss and Insulation Volume Factors, and an Insulation Effectiveness Factor - Vs - Thickness.

can be obtained with the aid of Figure 3-4 for all three mechanisms. The insert correction factor is to be used for the radiation values when the surrounding temperature T_3 is not equal to zero. The amount of loss occuring for a 0.1 metre diameter pipe at 200 ^{o}C and $T_3 = 0$ is solved by a few iterations. Choosing a $\Delta T_2 = \Delta T_3 = 20^{o}$ yields a $P/\ell = 60$ watts per metre for P radiation plus P convection. The remaining ΔT, yields a $P/\ell = 80$. If $\Delta T_2 = 25$, P/ℓ conv + rad = 75 watts per metre, the remaining $\Delta T_1 = 75$ yields a $P/\ell = 76$ watts per metre which is well within the limits of the expressions used.

The preliminary optimization of insulation thickness can be visualized by looking at Figure 3-3. If the loss factor F_1 is assigned a given value in terms of dollars per kWh of energy lost, and the volume factor is assigned a cost related to the amount of insulation in \$/m^3, we have two cost factors which can be annualized by proper methods to arrive at the cost of heat loss on a \$/metre-yr basis, as well as the cost of insulation on a \$/metre-yr basis. The minimum of the sum of these two will, for example, on the figure shown occur near the cross-over point. As the thickness to diameter ratio changes and the cost of heat or the cost insulation shift, the slopes at the cross-over point may not be equal, in which case there will be a displacement of the cost minimum from the cross-over. In such a case, the total cost per year will not be precisely equal to twice the value at the cross-over point. It is important to note that in the optimization procedure, that it is the minimization of the cost of heat output of the transport section which is important. This follows from the relation

$$\$/kWh_{out} = \frac{\$/kWh_{in} + \ell_1 R_T/P_t C_f 8760}{\eta_t} \qquad (3\text{-}4)$$

where ℓ_1 is the length of transport piping, R_T is the annualized cost of heat transport defined in Section 7.7 (equation 7-21), P_t is the thermal power transfer rate in kW, and C_f is the capacity factor of the transport line. The transfer efficiency of this length of piping is given by:

$$\eta_t = \frac{P_{in} - (P/\ell)\ell_1}{P_{in}} \qquad (3\text{-}5)$$

It is useful to examine how the cost of thermal energy varies along a transmission line. In Equation (3-4) we assume the cost of input thermal power is \$0.006/kWh, the length is 100 metres, the cost of transfer piping is \$3/m-yr for a 100 kW level of transfer (see Table 7-1), and the capacity factor is 0.25. If η_t is equal to 0.96, the resulting cost of thermal energy out of this 100 metre length of pipe is seen to have increased appreciably to \$0.0077/kWh_t. It can be seen that by proper iteration, the minimum cost of thermal energy out of this segment of pipe can be readily obtained.

The results of the preliminary optimizing of pipe costs, pumping cost insulation, etc. will be described in detail in Section 7. It is instructi to note, however, that, from Figure 3-4, if the cost of insulation and/or heat are increased by a given ratio that the total cost of transport due to these two components will increase by approximately the square root of the ratio by which the increases occurred, provided that the thickness-to-diameter ratio is in the vicinity of 0.5. As the actual ratio departs from this value, the cost becomes more sensitive to the cost of insulation at higher thickness-to-diameter ratios and more sensitive to energy cost at the lower thickness-to-diameter ratios.

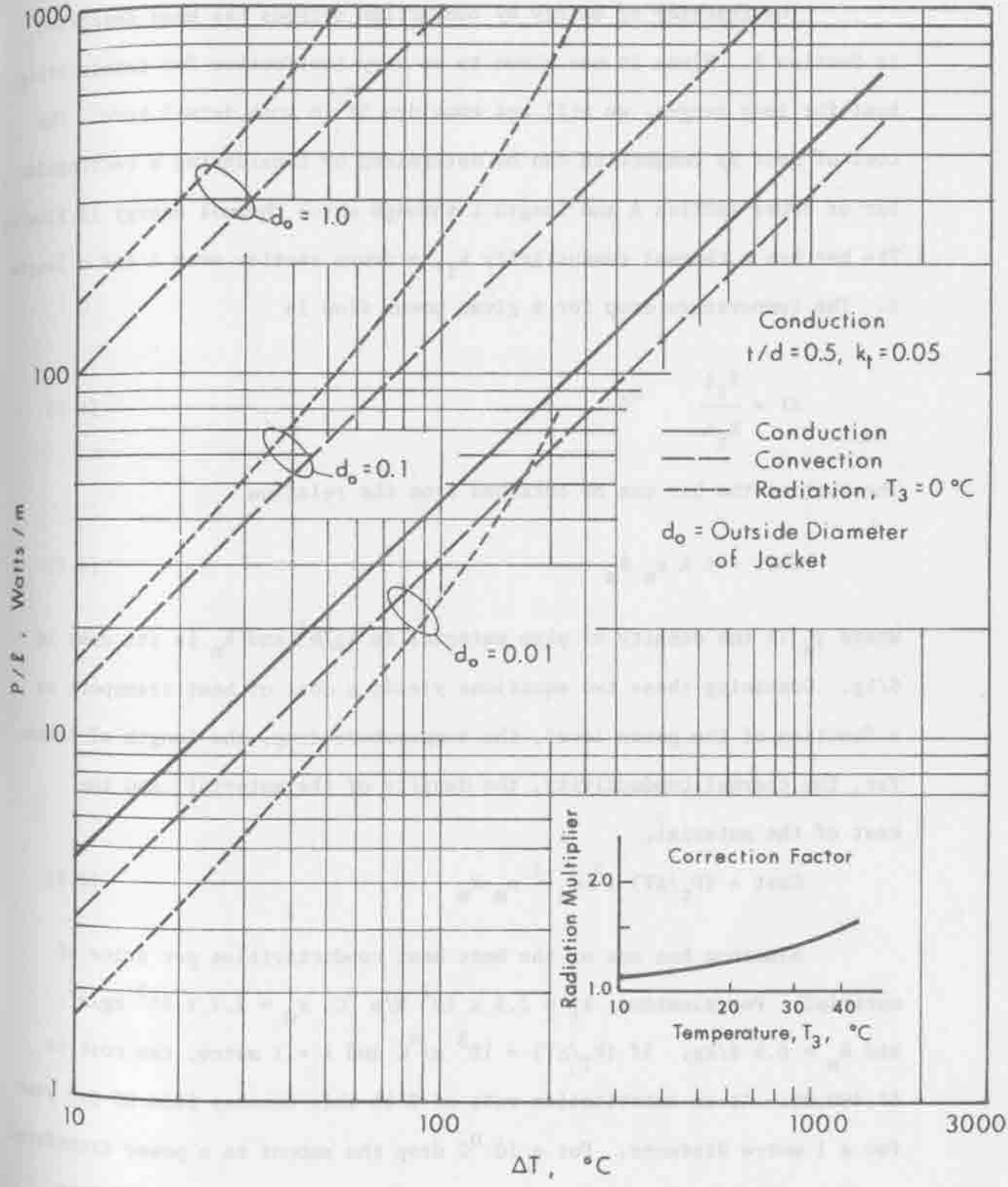

Figure 3-4. Thermal Power Transfer in Watts per Metre Length of Pipe.

4.0 CONDUCTION METHODS

The transfer of energy by conduction methods has been described in Section 2. Since it was shown to be very ineffective for transmitting heat for long ranges, we will not consider it in much detail here. The cost of heat by conduction can be determined by considering a rectangular bar of cross section A and length L through which thermal energy is flowing. The bar has a thermal conductivity k_i, a cross section area A and a length ℓ. The temperature drop for a given power flow is

$$\Delta T = \frac{P_t \ell}{k_i A} \quad {}^{o}C \tag{4-1}$$

The cost of the bar can be obtained from the relation

$$\text{Cost} = \ell \, A \, \rho_m \, R_m \tag{4-2}$$

where ρ_m is the density of pipe material in kg/m^3 and R_m is its cost in \$/kg. Combining these two equations yields a cost of heat transport as a function of the power level, the temperature drop, the length of transfer, the thermal conductivity, the density of the material, and the cost of the material.

$$\text{Cost} = (P_t/\Delta T) \, \ell^2 \, k_i^{-1} \, \rho_m \, R_m \tag{4-3}$$

Aluminum has one of the best heat conductivities per price of material. For aluminum, $k_i = 2.5 \times 10^2$ W/m ^{o}C, $\rho_m = 2.7 \times 10^3$ kg/m^3, and $R_m = 0.5$ \$/kg. If $(P_T/\Delta T) = 10^3$ w/^{o}C and $\ell = 1$ metre, the cost is \$5,400.00. At an amortization rate of 0.16 this becomes \$864.00 per year for a 1 metre distance. For a 10 ^{o}C drop the amount to a power transfered would be only 10 kW, and it can be readily seen that the cost of heat transport by conduction is very high.

5.0 FILM COEFFICIENTS

The exact relations for the transfer of heat via film coefficients from a fluid to a solid surface are very complex and will not be treated in detail here since considerable literature is available on the subject. Several simplified relations will be given which can be used in determining either order-of-magnitude solutions or trends required in overall optimization. These results can be applied either at the initial pickup of heat by the transfer fluid on the collector absorber, or in the transfer from one fluid to another in a heat exchanger.

For forced convection, the film coefficient can be rather well approximated by the relation.

$$P/\ell = k\, d\, (1 + 0.1/d)^{1/2} V^{0.67} \quad W/m$$

where d is the pipe diameter in metres, V is the velocity of the fluid in metres per second, and k is a constant which is 3,000 for water and 30 for air. For flat surfaces the relation can be employed by using a film coefficient which is $h = 1{,}000\ V^{0.67}$ for water, and $h = 10\ V^{0.67}$ for air, where both film coefficients are in watts/m^2 ^oC.

6.0 CONVECTION METHODS

The transport of heat via forced convection is covered in considerable detail in Section 7 and we will only summarize here some of the results on the basic properties. In Section 7 it is shown that the basic transfer of heat is cheaper via pressurized water as compared to steam. This result is valid provided that the heat load extracts heat energy over a temperature range in a uniform manner, rather than extracting a large amount of heat at a constant temperature as is the case for the production of steam. Under such conditions where a steam generator is required, either a large differential temperature is required between the going and return paths, or else large volumes of pressurized water must be circulated with concommitant pumping losses and effective increase in the cost of transporting heat energy for the production of steam. The basic cost versus length, which was seen to vary with ℓ^2 in the conduction case, is now linearly related to length so that convection methods are more cost effective for long distances.

The sensitivity of the costing rate to various factors can be obtained from relations derived in Section 7.7. For large pipes, where the wall thickness is determined by pressure, the costing rate in \$/m-yr is

$$R_{T_{min}} = \frac{2.72\mu^{0.06}}{\rho^{0.6}} \left(\frac{C_f R_e}{\eta_p}\right)\left(\frac{R_p \rho_p r_a p}{t_w}\right)^{0.7}\left(\frac{P_t/\Delta T}{C_p}\right)^{0.8} \text{ \$/m-yr} \quad (6\text{-}1)$$

where μ is the fluid viscosity, kgm/sec, ρ is density, kg/m^3, C_f is the loss factor, R_e is the cost of electrical energy in \$/kWh electric, η_p is pumping efficiency, R_p is the cost of pipe materials, ρ_p their density, t_w their tensile strength, r_a is the rate of amortization, p is the pressure

in kg/m^2 and C_p is the average specific heat of the fluid in joules/kg ^oC. $P_t/\Delta T$ is the power transfer rate per degree C. It can be noted that the cost of transferring energy increases with the power level to the 0.8 power and with the increase in pressure to the 0.7 power. If the load factor or cost of electrical energy varies, the costing rate varies as the .3 power of these factors. This solution is an analytic one derived for the case where the cost of transfer fluid or the cost of thermal insulation are negligibly small compared to the cost of pipe and pumping power. A similar relation for small pipe, where the wall thickness is determined by manufacturing techniques, as opposed to pressure, is

$$R_{T_{min}} = 34.4 \frac{\mu^{0.34}}{\rho 0.34} \left(\frac{C_f R_e}{\eta_p}\right)^{0.17} \left(r_a R_p\right)^{0.83} \left(\frac{P_t}{C_p \Delta T}\right)^{0.48} \quad \$/m\text{-}yr \quad (6\text{-}2)$$

It can be seen that under these conditions the cost minimum is independent of pressure, is less sensitive to the costs of electricity, and is also less sensitive to the cost of money. The sensitivity to power level is also lower for small pipe than it is for large pipe.

The costing derived by the iterative program described in Section 7 is summarized in Figure 6-1, where the cost of steam pipe only, as well the steam plus return pipe, insulation, and pumping costs, are shown as a function of power transfer level ranging from 1 kW to 100 MW. The costing rate in \$/m-yr-kW is also shown on this curve, using the right-hand ordinate. It is instructive to note the rather rapid decrease in the costing rate as a function of power level. This decrease is one of the reasons, as we shall see in the field layout section, that it is important to combine the flow of thermal power whenever feasible.

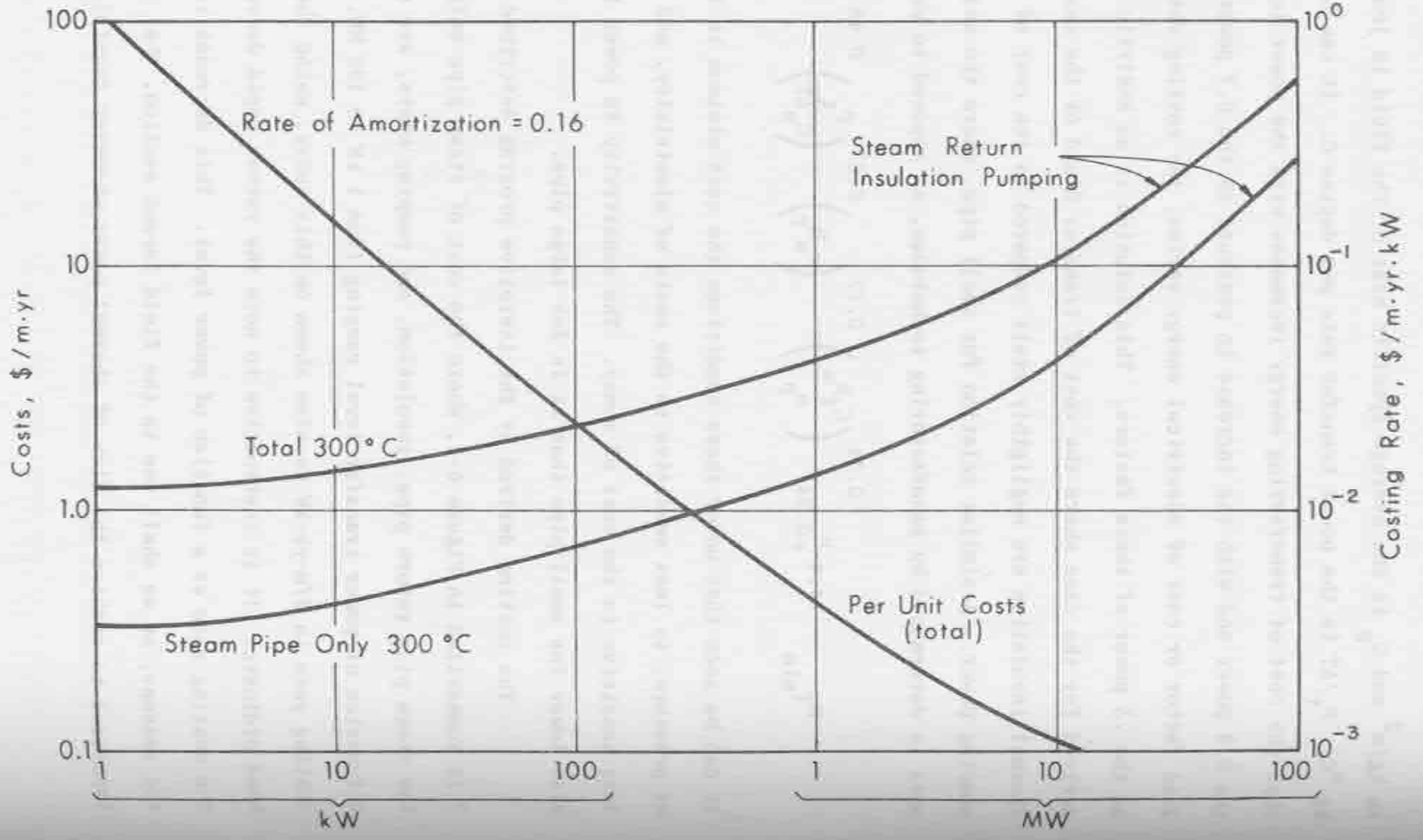
100
10
1.0
0.1
Costs, $/m·yr
Rate of Amortization = 0.16
Steam Return
Insulation Pumping
Total 300 °C
Steam Pipe Only 300 °C
Per Unit Costs
(total)
10^{0}
10^{-1}
10^{-2}
10^{-3}
Costing Rate, $/m·yr·kW
1
10
100
kW
1
10
100
MW
Power Transfer Level, thermal

7.0 HEAT TRANSPORT PRELIMINARY OPTIMIZATION

Early in this research program the relationships among the physical and economic heat transport variables were formulated analytically. The resulting equations were incorporated into a computer program for the purpose of selecting the minimum cost combination of pipe size and insulation thickness for the transport of heat using forced convection of steam or water. The derivation of some of these equations was presented in Appendix C of the original CSU/Westinghouse proposal to the National Science Foundation.

7.1 Transport Velocity Equation

The heat rate transport equation for water or steam is:

$$P_T = (\Delta H \rho) \frac{\pi d^2 V}{4} \quad \text{watts} \tag{7-1}$$

where P_T is the power transferred from collector to the heat engine or heat exchanger in watts; ΔH is the enthalpy drop through the engine and exchanger in joules/kg; ρ is the density of the fluid in kg/m^3; d is the diameter of the transfer pipe in metres; and V is the mean velocity of the transfer fluid in the pipe in metres per second. Solving for the velocity in terms of diameter yields

$$V = \frac{4 P_T}{\Delta H \rho \pi d^2} \quad m/s \tag{7-2}$$

7.2 Pumping Cost

Pumping power is added at the heat engine condenser or at the steam generator exit. This power is furnished by electricity obtained

from the heat engine. Conversion efficiency for thermal to electrical power is assumed here to be $0.8\ \eta_r$, the Rankine cycle efficiency. If all of the pumping power is conserved as the heat of friction in the transfer, then the cost of pumping is $(1 - 0.8\ \eta_r)/\eta_p$ times the cost of electricity (η_p is the efficiency of the pump). The relationship between pumping cost and piping cost suggests a minimum cost exists because smaller, less expensive pipes necessitate more pumping power to transport a given amount of heat.

The pumping power required with a cylindrical pipe or duct can be obtained by first noting that the friction head can be obtained from

$$h_f = \frac{f \ell V^2}{2\ g\ d} \quad \text{metres} \tag{7-3}$$

where

- f is a friction factor shown in Figure 7-1 as a function of the Reynolds number, N_{Re}, and parametric in relative pipe roughness, ε/d,
- ℓ is the length of pipe,
- V is the velocity of the heat transfer fluid,
- g is the acceleration due to gravity = 9.8 m/sec^2, and
- d is the pipe diameter.

The friction head on a per unit length basis is given by

$$h_f/\ell = 5.1 \times 10^{-2}\ f\ V^2\ d^{-1} \tag{7-4}$$

For smooth pipes, an approximation for the friction factor is

$$f \approx \frac{0.2}{N_{Re}^{1/5}} \tag{7-5}$$

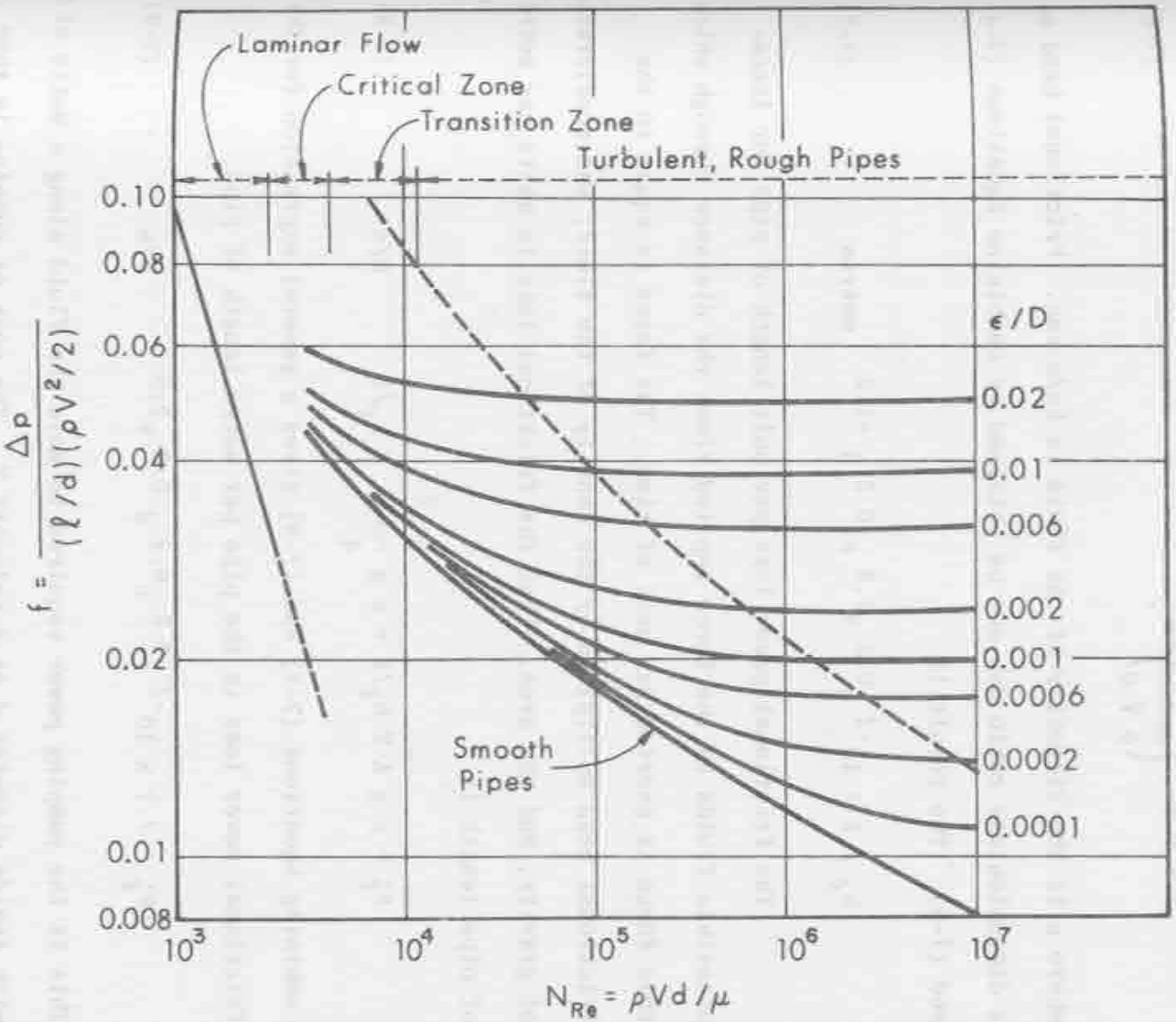

Figure 7-1. Friction Factor vs. Reynolds Number (N_{Re}) for Fluids Flowing in Pipes.

which is valid for Reynolds numbers greater than 10^4 and less than 10^7. Since $N_{Re} = \rho V d/\mu$, the friction factor becomes

$$f \approx 0.2 \left(\frac{\mu}{\rho V d}\right)^{\frac{1}{5}}, \qquad (7\text{-}6)$$

where μ is the viscosity of the fluid in kg/m-sec. Frictional head as a dimensionless ratio can now be obtained by combinine Equations (7-4) and (7-6). The result is

$$h_f / \ell \approx 10^{-2} \mu^{0.2} V^{1.8} \rho^{-0.2} d^{-1.2} \quad \text{metres} \qquad (7\text{-}7)$$

The frictional power loss per unit length of pipe for incompressible fluids is the force applied times the distance through which this force is exerted per unit of time. The force is equal to the frictional head multiplied by the density of the fluid, the acceleration of gravity, and the area. Then the frictional loss in watts per metre of pipe length is

$$P'_f \approx \rho g A V h_f/\ell = \rho g \frac{\pi d^2}{4} V h_f/\ell \qquad \text{W/m} \qquad (7\text{-}8)$$

Combining Equations (7-7) and (7-8) gives a general expression for the frictional power loss in the pipe per metre length of pipe.

$$P'_f \approx 7.7 \times 10^{-2} \rho^{0.8} \mu^{0.2} d^{0.8} V^{2.8} \qquad \text{W/m} \qquad (7\text{-}9)$$

This is the pumping power required to move the fluid along a metre of pipe with inside diameter d at a velocity V. The cost of pumping is then

$$R_{pump} (\$/\text{yr m}) = 8.76 P'_f C_f R_e \frac{(1 - 0.8 \eta_r)}{\eta_p} \qquad (7\text{-}10)$$

where R_e is the cost of electricity in \$/kWh, C_f is the diurnal capacity factor, and η_p is the mechanical efficiency of the pump. The factor 8.76 is used to convert \$/kWh to \$/W-yr.

7.3 Pipe Cost

The cost of pipe for transferring thermal energy from a collector field depends on the amount required, and the type of material used. For the case where the pipe thickness s is small compared to the diameter d, the force per unit length tending to push the pipe apart is simply p times d where p is the pressure and d is the diameter. The restraining tension of the material can be considered as divided equally between the two halves of a pipe and as a result the wall thickness required is

$$s = \frac{p\,d}{2\,t_w} \quad \text{metres} \tag{7-11}$$

where the pressure is in kg/m^2, the diameter and thickness are in metres, and t_w is the working tensile strength of the pipe material in kg/m^2. For steel, the ultimate tension, t_u, is approximately equal to 30×10^6 kg/m^2, and if $t_w = 0.2\ t_u$, it equals 6×10^6 kg/m^2. For these conditions,

$$s = 8.3 \times 10^{-8}\ p\ d \quad \text{metre} \tag{7-12}$$

The cost of pipe can now be obtained from the relation

$$\text{Pipe Cost} = \pi d\ s\ \rho_p\ R_p$$

$$= \frac{1.57\ d^2\ P\ \rho_p\ R_p}{t_w} \tag{7-13}$$

where ρ_p is the density of the material in kilograms per cubic metre, and R_p is the cost of the materials in dollars per kilogram. As an example, for steel pipe, $\rho_p = 7.8 \times 10^3$ kg/m^3 and $t_w = 6 \times 10^6$ kg/m^2, so the annualized pipe cost in dollars per metre per year becomes

$$R_{pipe}\ (\$/m\ yr) = 1.75 \times 10^{-3}\ p\ d^2\ R_p\ r_a, \tag{7-14}$$

where r_a is the rate of return on investment.

7.4 Insulation Cost

Using an insulating material whose costing rate is C_{ins} \$/m^3, the cost of insulating a one metre length of pipe of diameter d with insulation f thickness t is

$$R_i = C_{ins}\ \pi(d + t)\ t. \tag{7-15}$$

and annualized with a rate of return on investment of r_a,

$$R_I = r_a\ C_{ins}\ \pi(d + t)\ t. \tag{7-16}$$

7.5 Heat Loss Cost

The thermal power loss from a one metre section of cylindrical pipe is given by

$$P'_{loss} = \frac{2\pi\ k_i\ \Delta T}{\ln\ (r_2/r_1)} = \frac{2\pi\ k_i\ \Delta T}{\ln\ (1 + \frac{2t}{d})} \tag{7-17}$$

where k_i is the thermal conductivity of the insulating material in W/m ^oC, ΔT is the difference in temperature between the pipe and the surrounding air in ^oC. The radii, r_1 and r_2 are respectively, the inside and outside diameter of the insulation, and t is the thickness of insulation.

In order to compute the cost of heat lost, a reasonable value for the cost of thermal energy, R_{te}, of \$0.006/kWh$_t$ was assumed. Accurate field layout optimization requires R_{te} to be determined at each point in the field, which cannot be done in a non-parametric optimization. The assumed value was arrived at from two directions: first, using reasonable costs for collector components (\$50/m^2, 16 percent rate of return on investment and 5.5 kWh/day); second, assigning a competitive busbar electric energy cost of \$0.03/kWh$_e$ and a conversion efficiency of 20 percent (so thermal energy costs 20 percent of electric energy). The cost of heat loss per metre length of pipe is:

$$R_H = \frac{2\pi\ k_i\ \Delta T\ R_{te}\ 8.76\ C_f}{\ln\ (1 + \frac{2t}{d})} \qquad \$/m\text{-}yr. \qquad (7\text{-}18)$$

if the plant is in use a fraction of the year equal to C_f.

7.6 Heat Transport Materials Cost

The volume of transport material per unit pipe length is $V/\ell = (\pi/4)\ d^2$. If its density is ρ, the cost per metre of transport material is

$$R_{tm}\ (\$/m\ yr) = r_a\ (\pi/4)\ \rho\ R_{tm}\ d^2, \qquad (7\text{-}19)$$

where R_{tm} is the cost of transport material in dollars per kilogram.

7.7 Total Transport Cost

An analytical solution for the cost of transporting heat energy in dollars per metre of pipe per year can be obtained by combining Equations (7-10), (7-14), (7-16), (7-18) and (7-19). The annualized total cost of heat transport is then given by:

$$R_T = R_{pump} + R_{pipe} + R_I + R_H + R_t$$

$$= 8.76\, C_f \left(P'_{pf}\, R_e \frac{1 - 0.8\,\eta_r}{\eta_p} + \frac{2\pi\, k_i\, \Delta T\, R_{te}}{\ln\left(1 + \frac{2t}{d}\right)} \right)$$

$$+ r_a \left[C_{ins}\, \pi (d + t)\, t + d^2 \left(\frac{\pi\, \rho\, R_{tm}}{4} + 1.75 \times 10^{-3}\, p\, R_p \right) \right] \qquad (7\text{-}20)$$

For the purpose of solving for the lowest cost with respect to pipe material and pumping power (i.e., no insulation, no heat loss and negligible fluid costs) we obtain the following cost:

$$R_{pp}\ \left(\frac{\$}{yr\text{-}m}\right) = 1.75 \times 10^{-3}\, pd^2\, R_p\, r_a$$

$$+ (7.7 \times 10^{-2})\ (8.76) \left(\frac{4}{\pi} \cdot \frac{P_T}{\Delta H} \right)^{2.8} \frac{\mu^{0.2}\, C_f R_e\, (1 - 0.8\eta_r)}{\eta_p\, \rho^2\, d^{4.8}} \qquad (7\text{-}21)$$

To obtain the minimum cost solution, we take the derivative of the cost with respect to pipe diameter and solve when the derivative is equal to zero.

$$0 = 2 \times 1.75 \times 10^{-3}\, pd\, R_p\, r_a$$

$$- (8.76)\ (7.7 \times 10^{-2}) 4.8 \left(\frac{4\, P_T}{\pi \Delta\, H} \right)^{2.8} \frac{\mu^{0.2}\, C_f\, R_e\, (1 - 0.8\, \eta_r)}{\eta_p\, \rho^2\, d^{5.8}} \qquad (7\text{-}22)$$

Solving for d_{opt} we obtain:

$$d_{opt} = 3.02 \left(\frac{P_T}{\Delta H} \right)^{0.41} \left(\frac{R_e\, C_f\, (1 - 0.8\eta_r)}{r_a\, p\, R_p\, \eta_p} \right)^{0.15} \left(\frac{\mu^{0.03}}{\rho^{0.29}} \right) \qquad (7\text{-}23)$$

Substituting back into Equation (7-2), we obtain the expression for optimum transport velocity

$$V_{opt} = \frac{4\ P_T}{\pi \Delta H \rho} \left(\frac{1}{d_{opt}^2} \right) \tag{7-24}$$

The fluid flow rate in kg/sec is given by

$$F = \pi\ \rho\ V_{opt}\ d_{opt}^2/4. \tag{7-25}$$

The cost of heat transfer can be obtained by substituting the optimum diameter obtained from (7-23) into Equation (7-21). After simplification this cost minimum is

$$\$_T\ (\$/m \cdot yr) = \frac{1.1 \times 10^{-6}\ \mu^{0.06}}{\rho^{0.56}} \left(\frac{C_f\ R_e}{\eta_p} \right)^{0.28} (P_T/\Delta H)^{0.8}\ (\rho_p\ R_p\ p\ r_a)^{0.72}$$

$$+ 2.4 \times 10^{-6} \left(\frac{C_f\ R_e}{\eta_p} \right)^{0.3} (\rho_p\ R_p\ p\ r_a)^{0.7}\ \frac{(P_T/\Delta H)^{0.8}\ \mu^{0.06}}{\rho^{0.6}} \tag{7-26}$$

Since the exponents of both halves of the summation of pipe and pumping costs have approximately the same value, an approximate solution can be written as

$$\$_T\ (\$/m \cdot yr) = \frac{4.9 \times 10^{-5}\ \mu^{0.06}}{\rho^{0.6}} \left(\frac{C_f\ R_e}{\eta_p} \right)^{0.3} (R_p\ \rho_p\ r_a\ p)^{0.7}\ (P_T/\Delta H)^{0.8} \tag{7-27}$$

7.8 Preliminary Results

Before the completion of the above formulation and its implementation in a computer program, approximations were made to obtain preliminary data and to verify computer generated data. A working fluid was

selected using a relative costing figure derived from Equation (7-27),

$$R_{pp}\ (\$/m\ yr) \quad .'. \quad \frac{p^{0.7}\ \mu^{0.06}\ C^{0.7}}{\rho^{0.6}\ \Delta H^{0.8}}, \qquad (7\text{-}28)$$

where p is the pressure, μ the viscosity, ρ the density, ΔH the enthalpy change from the high temperature to 50 ^{o}C (all in consistent units), and C the relative pipe material cost (carbon steel = 1.0). This costing rate includes the cost of plumbing and pumping, and in the case of Dowthe the cost of the fluid itself. Cost comparisons of transport using variou are presented in Figure 7-2. Only relative costs are shown. The Dowthern curve (plotted for a 1 metre diameter pipe) reflects the higher fluid costs for this material. Because of the abundance of technical data for water and steam and since no fluid is clearly less expensive, water and steam were selected for detailed study.

7.9 Preliminary Estimates of Pipe Size and Insulation Thickness

Before the complete heat transport preliminary optimization had been implemented on the computer, it was necessary to create graphical estimates of minimum cost heat transport designs. The cost of installed insulated pipe was initially estimated using Figures 7-3 and 7-4. Assumin a pipe diameter, d, in order to find the minimum cost design, the point must be found where the sum of the cost of heat lost, R_H, and insulation cost, R_I, have a zero slope:

$$\frac{d}{dt}\ [R_H + R_I] = 0, \qquad (7\text{-}29)$$

where t is the insulation thickness in metres. Using Equations (7-16) for R_I and (7-18) for R_H and differentiating yields the relation

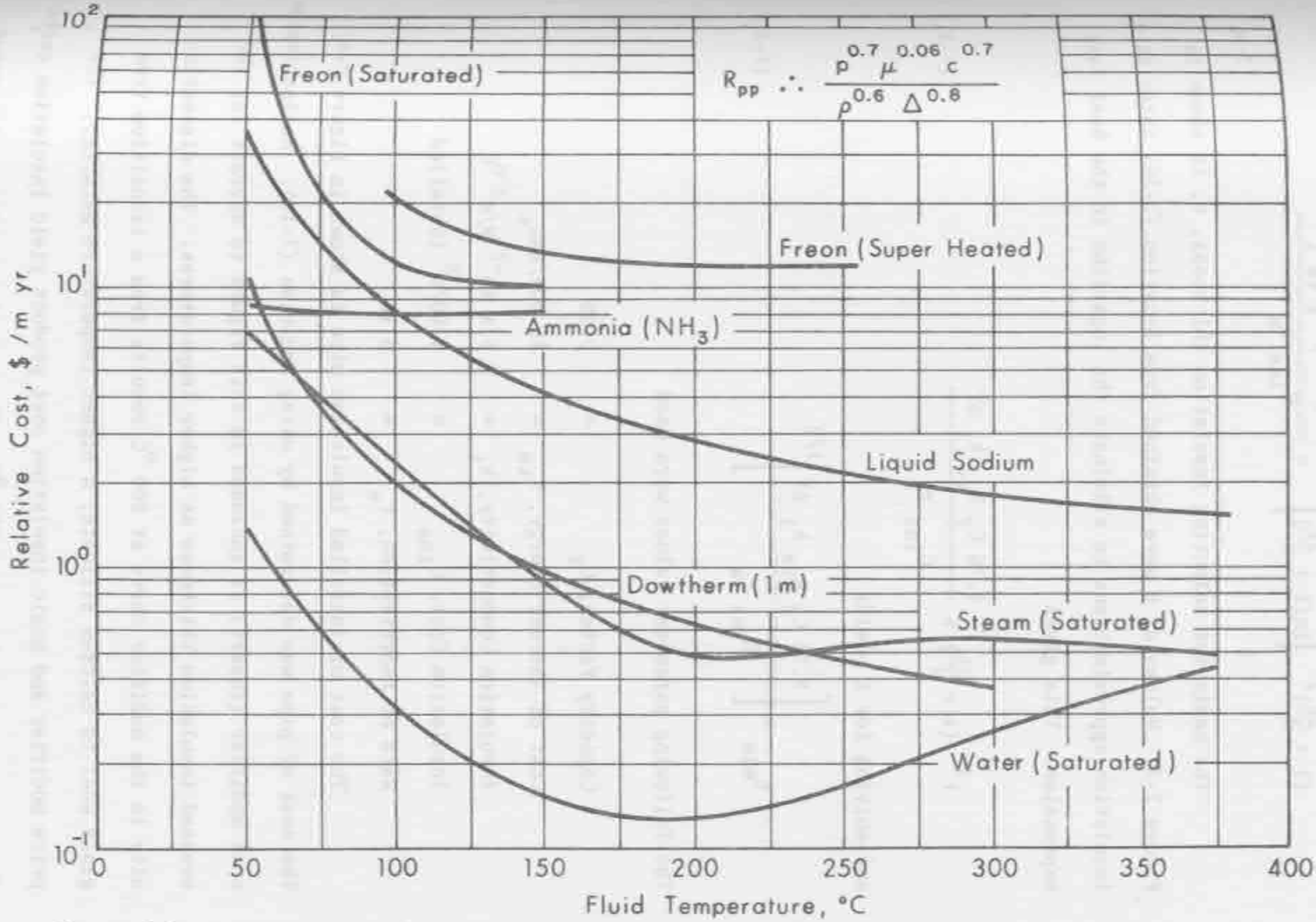

Figure 7-2. Relative Cost of Heat Transport Excluding Fluid Cost (Valid for Pipe Diameters of 0.1 m or Greater).

$$(1 + \frac{2t}{d})^2 \left[\ln(1 + \frac{2t}{d})\right]^2 = \frac{4\ (8.76)\ C_f R_{te} k_i \Delta T}{C_{ins}\ r_a} \tag{7-30}$$

The basis for selecting insulation thickness, t, is shown in Figure 7-3. Values of t were obtained from Equation (7-30) using thin insulation approximations to eliminate the logarithm in the heat loss expression. This gives

$$t^2 \ (1 + \frac{2t}{d}) = \frac{8.76\ C_f\ R_{te}\ k_i\ \Delta T}{C_{ins}\ r_a} \tag{7-31}$$

and solving for t yields

$$t_{min} = \left[\frac{8.76\ C_f\ R_{te}\ k_i\ \Delta T}{C_{ins}\ r_a}\right]^{1/2} \tag{7-32}$$

The following parameter values were used

Capacity Factor, C_f	=	0.25
Cost of Thermal Energy, R_{te}	=	\$0.006/kWh$_t$
Insulation Conductivity, k_i	=	5×10^{-2} W/m^2 ^oC
Insulation Cost, C_{ins}	=	\$100/m^3 installed
Rate of Amortization, r_a	=	0.16

The cost of installed insulation pipe is shown in Figure 7-4. The cost of pipe was determined by using Equation (7-13). An insulation cost modifier (insert) is included in this figure to correct for increased insulation thickness at higher temperatures. The discontinuity in the modifier curve at 500 ^oC results from a transition from glass wool to calcium silicate, a higher temperature material. The price modifier and basic insulation cost product yield insulation costs for temperatures other than 200 ^oC. The knee in the insulation curve

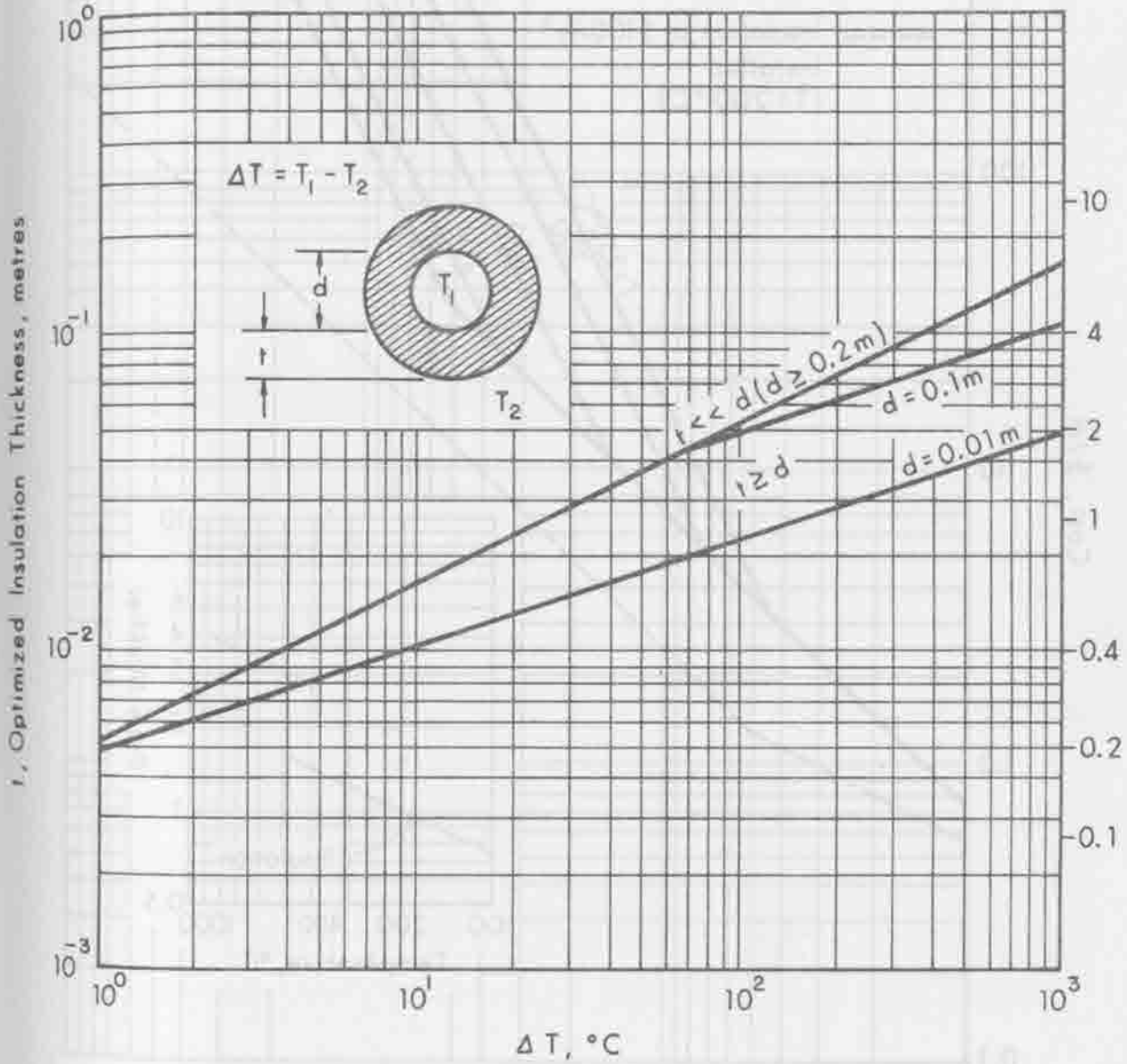

Figure 7-3. Optimum Insulation Thickness as a function of ΔT.

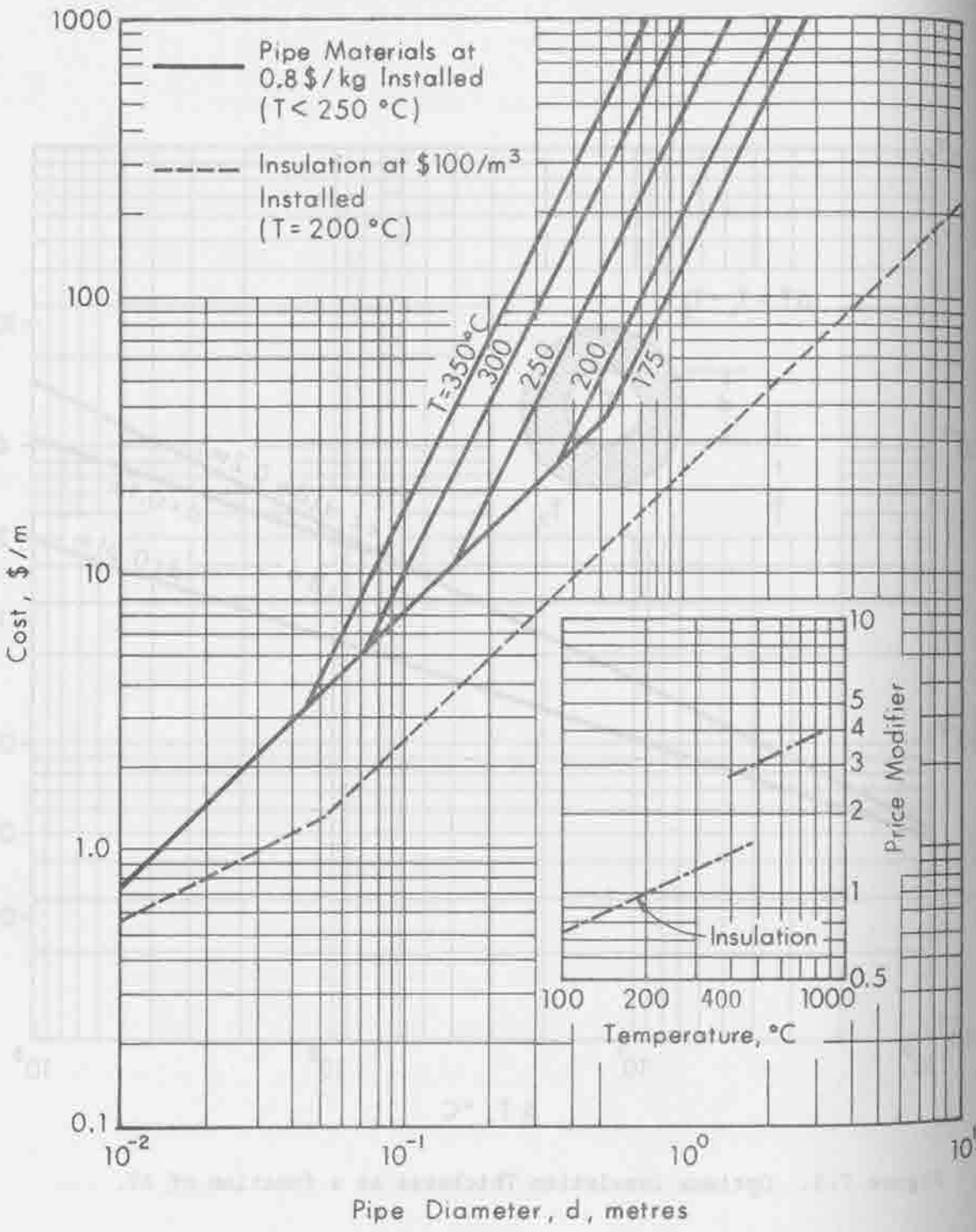

Figure 7-4. Insulation and Pipe Costs for Various Pipe Diameters. Different Temperature Lines allow for Elevated Pressures of Saturated Steam and Water.

which occurs at a pipe diameter of 6 cm, corresponds to the point at which the insulation thickness approaches the pipe diameter. The different temperature lines for pipe costs include the costs of additional wall thickness at the elevated pressures of saturated steam and water at those temperatures. Pipes with less than 10^5 kg/m^2 stressing are not manufactured, and the 175 ^{o}C pipe is the thinnest walled obtainable. Smaller pipes are not manufactured with a wall thickness less than 0.39 cm (0.154") and therefore the lower portion of the solid curve indicates that the cost varies directly as pipe diameter.

7.10 Final Costing of Steam and Hot Water Heat Transport

The heat transport preliminary optimization program determines the flow rate, pipe diameter, and fluid velocity required to deliver a given amount of energy at a given temperature with a given fluid using Equations (7-24), (7-25) and (7-26). This pipe diameter, along with the given temperature, is then used to calculate the optimum insulation thickness. An initial insulation thickness is estimated using Equation (7-33). The result of an iterative search is an optimum choice of insulation for this pipe diameter. Another outer iteration is employed to find the minimum total cost. Other pipe diameters are used to compute new costs of pipe, pump, heat, and insulation until a minimum overall cost is attained:

$$R_T = \min \left[R_H + R_I + R_{pipe} + R_{pump} \right] \qquad (7\text{-}33)$$

Final costs of a preliminary optimized heat transport subsystem were generated by the computer program for different thermal power levels from 10 kW to 20 MW. At each power level, the pipe size, flow rate, insu-

lation thickness, and the costs associated with piping, pumping power, insulation, and heat loss were computed. The 0.1, 1.0 and 10.0 MW results are shown in Table 7-1, 7-2, and 7-3 for steam and water transport for various temperatures. The transport fluid temperature is shown in the first line of each section of the print-out (i.e., 100, 150, etc.). The first line of each section represents the case of steam generation in the collector and direct transport to the turbine. In the case of hot water transport in the field (lower lines in each print-out section), the flow rate necessary to create turbine steam via a steam generator is calculated using the thermodynamic model shown in Figure 7-5. The different flow rates (3rd column) imply different steam temperatures (1st column), different field return temperatures (2nd column), different heat engine efficiencies (4th column), different return system costs (next to last column), and different total transport costs (last column).

The results of transport cost computations for 0.1, 1.0, and 10 MW power levels and for various transport temperatures are shown in Figures 7-6, 7-7 and 7-8. These results differ from those presented in the semiannual report because of the inclusion of a $2/m installation charge in the pipe cost and the addition of return pipe costs. The solid curves represent direct steam transport and the dashed curves show the cost of hot water transport for different steam generator temperature drops. The abcissa shows the temperature of steam produced, not the transport fluid temperature; they are the same only in the case of steam. The lower temperature drops in the steam generator are associated with higher transport costs because of the higher required flow rate. The 0.1 and 1.0 MW curves are essentially similar since these power levels require pipe diameters mostly in the lower

TABLE 7-1

Heat Transport Optimization Printout for a Thermal Power Level of 0.1 MW

THE FOLLOWING DATA ARE COMPUTED AT A TRANSFERRED POWER OF 0.10MW

STM TMP DEG C	RET TMP DEG C	FLOW RATE KG/ SEC	ENG EFF %	INS THCK CM OUT	INS THCK CM RET	PIPE DIA CM OUT	PIPE DIA CM RET	OPT VEL M/ SEC	PIPE COST $/YR /M	PUMP COST $/YR /M	INS COST $/YR /M	HEAT COST $/YR /M	RET COST $/YR /M	TOTAL COST $/YR /M
100		0.041	12	4.5	2.2	8.3	1.0	13.1	2.016	0.20	0.294	0.56	0.661	3.73
90	94	4.346	10	4.4	4.3	7.1	6.7	1.2	1.762	0.15	0.255	0.51	2.438	5.11
80	84	1.477	8	4.0	3.7	4.2	4.3	1.1	1.180	0.09	0.163	0.39	1.681	3.50
70	74	0.904	5	3.8	3.4	3.3	3.6	1.1	1.002	0.07	0.135	0.35	1.422	2.98
60	64	0.659	2	3.7	3.1	2.9	3.1	1.1	0.908	0.06	0.120	0.33	1.271	2.68

		FLOW	EFF	INSUL		DIAMETER		VEL	PIPE	PUMP	INS	HEAT	RET	TOTAL
150		0.040	21	4.8	2.2	4.9	1.0	8.2	1.313	0.12	0.233	0.57	0.655	2.88
140	144	3.941	20	5.1	5.0	6.6	6.4	1.2	1.673	0.14	0.303	0.66	2.559	5.33
130	132	1.340	18	4.6	4.4	4.0	4.1	1.2	1.127	0.08	0.197	0.52	1.797	3.72
120	121	0.819	16	4.4	4.1	3.1	3.4	1.2	0.958	0.06	0.164	0.47	1.534	3.19
110	110	0.596	14	4.2	3.8	2.7	3.0	1.1	0.870	0.06	0.146	0.44	1.380	2.89
100	100	0.473	12	4.1	3.6	2.4	2.7	1.1	0.813	0.05	0.135	0.42	1.271	2.69
90	90	0.394	10	4.0	3.4	2.2	2.5	1.1	0.773	0.05	0.127	0.40	1.187	2.54
80	81	0.340	8	4.0	3.2	2.1	2.4	1.1	0.744	0.04	0.121	0.39	1.119	2.42

		FLOW	EFF	INSUL		DIAMETER		VEL	PIPE	PUMP	INS	HEAT	RET	TOTAL
200		0.039	27	4.9	2.2	3.3	1.0	5.9	0.989	0.08	0.203	0.60	0.651	2.51
190	193	3.471	26	5.7	5.6	6.2	6.0	1.3	1.591	0.13	0.339	0.80	2.653	5.51
180	180	1.189	25	5.1	4.9	3.7	3.9	1.3	1.080	0.08	0.224	0.63	1.895	3.90
170	168	0.731	24	4.8	4.6	3.0	3.2	1.2	0.923	0.06	0.188	0.57	1.630	3.37
160	157	0.535	22	4.6	4.3	2.5	2.8	1.2	0.839	0.05	0.168	0.54	1.474	3.07
150	145	0.425	21	4.5	4.1	2.3	2.5	1.2	0.786	0.05	0.155	0.51	1.363	2.87
140	135	0.355	20	4.4	3.9	2.1	2.4	1.2	0.749	0.04	0.146	0.50	1.278	2.71
130	124	0.307	18	4.4	3.8	2.0	2.2	1.2	0.720	0.04	0.140	0.49	1.208	2.59
120	114	0.271	16	4.3	3.6	1.9	2.1	1.2	0.699	0.04	0.134	0.48	1.149	2.50
110	105	0.244	14	4.3	3.5	1.8	2.0	1.1	0.681	0.04	0.130	0.47	1.097	2.41
100	95	0.222	12	4.2	3.3	1.7	2.0	1.1	0.666	0.03	0.126	0.46	1.051	2.34

		FLOW	EFF	INSUL		DIAMETER		VEL	PIPE	PUMP	INS	HEAT	RET	TOTAL
250		0.039	31	5.0	2.1	2.4	0.8	4.4	0.809	0.05	0.186	0.63	0.638	2.32
240	242	2.826	31	6.1	5.8	5.7	4.9	1.4	1.483	0.12	0.359	0.90	2.683	5.55
220	215	0.613	29	5.2	4.8	2.7	2.6	1.3	0.879	0.06	0.204	0.66	1.661	3.46
200	190	0.364	27	4.9	4.4	2.1	2.1	1.3	0.756	0.04	0.171	0.60	1.401	2.97
180	167	0.267	25	4.7	4.0	1.8	1.8	1.2	0.697	0.04	0.155	0.57	1.251	2.71
160	145	0.215	22	4.6	3.7	1.7	1.7	1.2	0.661	0.03	0.145	0.55	1.143	2.53
140	126	0.182	20	4.5	3.5	1.6	1.6	1.2	0.636	0.03	0.138	0.54	1.057	2.40

		FLOW	EFF	INSUL		DIAMETER		VEL	PIPE	PUMP	INS	HEAT	RET	TOTAL
300		0.040	34	5.0	2.0	1.8	0.7	3.3	0.685	0.04	0.171	0.66	0.621	2.17
290	291	2.063	34	6.3	6.0	5.0	4.0	1.5	1.349	0.10	0.363	0.98	2.604	5.41
270	259	0.467	32	5.4	4.9	2.5	2.1	1.4	0.824	0.05	0.214	0.74	1.629	3.45
250	231	0.287	31	5.1	4.5	2.0	1.7	1.3	0.720	0.04	0.182	0.68	1.386	3.01
230	206	0.216	30	5.0	4.2	1.7	1.5	1.3	0.670	0.04	0.167	0.65	1.246	2.76
210	184	0.178	28	4.9	3.9	1.6	1.4	1.3	0.639	0.03	0.157	0.63	1.146	2.60
190	163	0.153	26	4.8	3.7	1.5	1.3	1.3	0.618	0.03	0.150	0.61	1.067	2.43
170	143	0.136	24	4.7	3.5	1.4	1.2	1.3	0.603	0.03	0.145	0.60	1.001	2.38
150	125	0.123	21	4.7	3.3	1.3	1.2	1.3	0.591	0.03	0.141	0.59	0.943	2.30

		FLOW	EFF	INSUL		DIAMETER		VEL	PIPE	PUMP	INS	HEAT	RET	TOTAL
350		0.043	36	5.0	2.0	1.4	0.7	2.5	0.603	0.03	0.161	0.69	0.636	2.11
340	338	1.224	35	6.5	6.0	4.2	3.2	1.6	1.170	0.09	0.345	1.02	2.509	5.13
320	300	0.315	35	5.6	4.9	2.2	1.6	1.5	0.762	0.04	0.216	0.80	1.617	3.44
300	269	0.206	34	5.3	4.5	1.8	1.4	1.5	0.681	0.04	0.189	0.74	1.392	3.04
280	241	0.161	33	5.2	4.2	1.6	1.2	1.4	0.642	0.03	0.175	0.71	1.261	2.82
260	217	0.136	32	5.1	4.0	1.5	1.1	1.4	0.617	0.03	0.166	0.70	1.167	2.68
240	195	0.120	31	5.0	3.8	1.4	1.1	1.4	0.601	0.03	0.160	0.68	1.093	2.57
220	175	0.109	29	5.0	3.6	1.3	1.0	1.4	0.588	0.03	0.156	0.67	1.032	2.48
200	156	0.100	27	4.9	3.4	1.3	1.0	1.4	0.579	0.03	0.153	0.67	0.979	2.40
180	139	0.093	25	4.9	3.2	1.2	1.0	1.4	0.571	0.03	0.150	0.66	0.932	2.34

TABLE 7-2

Heat Transport Optimization Printout for a Thermal Power Level of 1.0 MW

THE FOLLOWING DATA ARE COMPUTED AT A TRANSFERRED POWER OF 1.00MW

STM TMP DEG C	RET TMP DEG C	FLOW RATE KG/ SEC	ENG EFF %	INS THCK CM OUT	INS THCK CM RET	PIPE DIA CM OUT	PIPE DIA CM RET	OPT VEL M/ SEC	PIPE COST $/YR /M	PUMP COST $/YR /M	INS COST $/YR /M	HEAT COST $/YR /M	RET TOTAL COST $/YR /M
100		0.412	12	5.4	2.7	25.2	2.6	14.2	5.465	0.63	0.825	1.16	1.065
90	94	43.461	10	5.3	5.1	21.4	18.6	1.3	4.694	0.45	0.705	1.03	6.07412.
80	84	14.770	8	4.9	4.5	12.6	11.2	1.2	2.930	0.27	0.437	0.72	3.799
70	74	9.038	5	4.7	4.1	10.1	9.2	1.2	2.388	0.21	0.352	0.63	3.080
60	64	6.585	2	4.6	3.8	8.7	8.1	1.1	2.103	0.18	0.308	0.57	2.684
		FLOW	EFF	INSUL		DIAMETER		VEL	PIPE	PUMP	INS	HEAT	RET TOTA
150		0.400	21	6.0	2.7	14.8	2.5	8.9	3.333	0.35	0.620	1.05	1.048
140	144	39.413	20	6.3	6.0	20.1	17.1	1.4	4.425	0.42	0.828	1.28	6.15013.
130	132	13.397	18	5.7	5.3	12.0	10.6	1.3	2.767	0.25	0.512	0.92	3.902
120	121	8.193	16	5.5	5.0	9.5	8.7	1.3	2.257	0.20	0.414	0.80	3.190
110	110	5.963	14	5.3	4.7	8.2	7.6	1.2	1.987	0.17	0.363	0.74	2.797
100	100	4.726	12	5.2	4.4	7.3	6.9	1.2	1.816	0.15	0.330	0.70	2.534
90	90	3.940	10	5.1	4.2	6.7	6.5	1.2	1.695	0.14	0.307	0.67	2.339
80	81	3.398	8	5.1	3.9	6.3	6.1	1.2	1.605	0.13	0.290	0.65	2.185
		FLOW	EFF	INSUL		DIAMETER		VEL	PIPE	PUMP	INS	HEAT	RET TOTAL
200		0.392	27	6.2	2.7	9.9	2.5	6.4	2.351	0.23	0.507	1.02	1.037
190	193	34.708	26	7.0	6.7	18.9	15.9	1.4	4.176	0.39	0.909	1.49	6.16613.
180	180	11.286	25	6.4	6.0	11.3	10.0	1.4	2.625	0.23	0.568	1.09	3.975
170	168	7.312	24	6.1	5.6	9.0	8.2	1.3	2.148	0.19	0.462	0.96	3.277
160	157	5.346	22	5.9	5.3	7.7	7.2	1.3	1.896	0.16	0.406	0.89	2.889
150	145	4.250	21	5.8	5.1	6.9	6.6	1.3	1.734	0.14	0.371	0.84	2.628
140	135	3.551	20	5.7	4.8	6.4	6.1	1.3	1.620	0.13	0.345	0.81	2.433
130	124	3.066	18	5.6	4.6	6.0	5.8	1.3	1.535	0.12	0.326	0.78	2.279
120	114	2.710	16	5.5	4.4	5.6	5.5	1.3	1.468	0.12	0.311	0.76	2.152
110	105	2.438	14	5.5	4.2	5.4	5.3	1.2	1.415	0.11	0.299	0.74	2.045
100	95	2.223	12	5.4	4.1	5.1	5.1	1.2	1.371	0.11	0.289	0.73	1.951
		FLOW	EFF	INSUL		DIAMETER		VEL	PIPE	PUMP	INS	HEAT	RET TOTA
250		0.391	31	6.4	2.6	7.3	2.1	4.8	1.804	0.16	0.439	1.02	1.029
240	242	28.255	31	7.6	7.2	17.3	14.3	1.5	3.850	0.36	0.944	1.64	6.30013.
220	215	6.129	29	6.6	5.9	8.3	6.8	1.4	2.015	0.17	0.492	1.09	3.364
200	190	3.643	27	6.2	5.4	6.5	5.4	1.4	1.644	0.13	0.399	0.96	2.699
180	167	2.671	25	6.0	5.0	5.6	4.7	1.4	1.465	0.12	0.354	0.90	2.349
160	145	2.146	22	5.9	4.6	5.1	4.3	1.3	1.355	0.10	0.327	0.86	2.114
140	126	1.817	20	5.8	4.3	4.7	4.1	1.3	1.280	0.10	0.308	0.83	1.940
		FLOW	EFF	INSUL		DIAMETER		VEL	PIPE	PUMP	INS	HEAT	RET TOTA
300		0.400	34	6.4	2.5	5.4	1.9	3.6	1.426	0.12	0.385	1.02	1.004
290	291	20.628	34	7.5	7.4	10.9	10.8	3.1	3.703	1.61	0.691	1.44	7.29918.
270	259	4.674	32	6.9	6.2	7.5	5.9	1.5	1.850	0.16	0.501	1.18	3.260
250	231	2.873	31	6.6	5.6	5.9	4.7	1.5	1.533	0.12	0.414	1.06	2.648
230	206	2.165	30	6.4	5.2	5.2	4.1	1.4	1.381	0.11	0.372	1.00	2.323
210	184	1.779	28	6.3	4.9	4.7	3.7	1.4	1.289	0.10	0.346	0.96	2.104
190	163	1.532	26	6.2	4.6	4.4	3.5	1.4	1.225	0.09	0.329	0.93	1.940
170	143	1.358	24	6.1	4.3	4.2	3.3	1.4	1.178	0.09	0.315	0.91	1.808
150	125	1.229	21	6.0	4.1	4.0	3.1	1.4	1.141	0.08	0.305	0.89	1.700
		FLOW	EFF	INSUL		DIAMETER		VEL	PIPE	PUMP	INS	HEAT	RET TOTA
350		0.432	36	6.5	2.5	4.2	1.9	2.7	1.178	0.09	0.347	1.01	1.076
340	338	12.237	35	7.6	7.4	8.5	8.4	3.7	4.200	1.73	0.612	1.42	7.66913.
320	300	3.145	35	6.7	6.2	4.8	4.5	3.0	1.545	0.62	0.384	1.09	3.234
300	269	2.056	34	6.8	5.8	5.4	3.9	1.6	1.416	0.11	0.419	1.14	2.624
280	241	1.610	33	6.7	5.4	4.8	3.5	1.6	1.296	0.10	0.383	1.09	2.328
260	217	1.362	32	6.5	5.0	4.4	3.2	1.6	1.222	0.09	0.360	1.05	2.125
240	195	1.201	31	6.5	4.8	4.2	3.0	1.5	1.171	0.09	0.345	1.02	1.978
220	175	1.087	29	6.4	4.5	4.0	2.9	1.5	1.134	0.08	0.333	1.01	1.858
200	156	1.000	27	6.3	4.3	3.8	2.7	1.5	1.105	0.08	0.324	0.99	1.758
180	139	0.931	25	6.3	4.1	3.7	2.7	1.5	1.081	0.08	0.317	0.98	1.672

TABLE 7-3

Heat Transport Optimization Printout for a Thermal Power Level of 10.0 MW

THE FOLLOWING DATA ARE COMPUTED AT A TRANSFERRED POWER OF 10.00MW

STM IMP DEG C	RET TMP DEG C	FLOW RATE KG/ SEC	ENG EFF %	INS THCK CM OUT	INS THCK CM RET	PIPE DIA CM OUT	PIPE DIA CM RET	OPT VEL M/ SEC	PIPE COST $/YR /M	PUMP COST $/YR /M	INS COST $/YR /M	HEAT COST $/YR /M	RET COST $/YR /M	TOTAL COST $/YR /M
100		4.118	12	5.8	3.3	57.6	6.6	27.2	17.069	7.47	1.858	2.24	2.15	830.80
90	94	434.611	10	5.7	5.6	48.9	48.9	2.4	12.370	5.38	1.579	1.95	21.15	142.43
80	84	147.700	8	5.6	5.1	38.8	33.8	1.3	8.238	0.81	1.257	1.62	10.34	622.27
70	74	90.376	5	5.5	4.7	30.7	26.8	1.3	6.594	0.64	1.001	1.35	8.19	917.79
60	64	65.850	2	5.4	4.4	26.5	23.2	1.2	5.728	0.55	0.866	1.21	7.03	715.39

	FLOW	EFF	INSUL	DIAMETER	VEL	PIPE	PUMP	INS	HEAT	RET	TOTAL
150	3.999	21	6.7 3.3	36.0 6.4	15.0	6.840	3.10	1.436	1.96	2.11	215.44
140	144394.128	20	6.9 6.8	46.3 46.3	2.6	11.131	4.83	1.839	2.38	20.07	440.25
130	132133.968	18	6.7 6.2	36.4 31.1	1.4	7.745	0.76	1.452	1.97	10.36	322.30
120	121 81.929	16	6.5 5.8	28.8 24.8	1.4	6.196	0.60	1.157	1.66	8.24	017.85
110	110 59.634	14	6.4 5.5	24.8 21.2	1.3	5.378	0.52	1.001	1.49	7.08	615.47
100	100 47.262	12	6.3 5.2	22.2 19.2	1.3	4.857	0.46	0.911	1.37	6.33	313.94
90	90 39.404	10	6.3 5.0	20.4 17.7	1.3	4.491	0.43	0.841	1.29	5.78	812.84
80	81 33.979	8	6.2 4.7	19.1 16.6	1.3	4.219	0.40	0.789	1.24	5.36	812.01

	FLOW	EFF	INSUL	DIAMETER	VEL	PIPE	PUMP	INS	HEAT	RET	TOTAL
200	3.924	27	7.4 3.3	30.2 6.3	6.9	6.481	0.71	1.405	2.06	2.08	012.74
190	193347.075	26	7.8 7.7	43.5 43.5	2.7	9.860	4.53	2.004	2.70	18.97	138.07
180	180118.865	25	7.6 7.1	34.3 28.9	1.5	7.314	0.72	1.588	2.26	10.30	022.18
170	168 73.123	24	7.4 6.7	27.2 23.1	1.5	5.866	0.57	1.276	1.91	8.22	517.84
160	157 53.461	22	7.2 6.4	23.4 19.7	1.4	5.101	0.49	1.113	1.72	7.09	315.51
150	145 42.503	21	7.1 6.1	21.0 17.8	1.4	4.611	0.44	1.006	1.60	6.35	214.01
140	135 35.510	20	7.0 5.8	19.3 16.4	1.4	4.266	0.40	0.930	1.51	5.81	512.92
130	124 30.659	18	6.9 5.5	18.1 15.3	1.4	4.006	0.38	0.872	1.45	5.39	912.10
120	114 27.098	16	6.9 5.3	17.1 14.5	1.4	3.804	0.36	0.827	1.40	5.06	611.45
110	105 24.377	14	6.8 5.1	16.3 13.9	1.4	3.641	0.34	0.792	1.36	4.79	110.92
100	95 22.234	12	6.8 4.9	15.6 13.3	1.3	3.508	0.32	0.762	1.32	4.55	710.47

	FLOW	EFF	INSUL	DIAMETER	VEL	PIPE	PUMP	INS	HEAT	RET	TOTAL
250	3.912	31	7.5 3.2	16.9 5.6	8.9	3.913	1.82	0.924	1.62	2.13	810.41
240	242282.552	31	8.4 8.3	35.6 35.5	3.6	16.277	7.12	1.849	2.68	27.71	155.64
220	215 61.291	29	7.7 7.2	18.8 18.6	2.7	4.795	2.13	1.022	1.73	9.24	618.92
200	190 36.429	27	7.7 6.7	19.7 16.1	1.5	4.337	0.41	1.064	1.78	6.59	114.18
180	167 26.705	25	7.5 6.2	17.0 13.9	1.5	3.792	0.35	0.930	1.63	5.62	912.33
160	145 21.462	22	7.4 5.7	15.4 12.6	1.4	3.460	0.32	0.843	1.53	5.01	911.18
140	126 18.167	20	7.3 5.3	14.3 11.7	1.4	3.232	0.30	0.792	1.46	4.58	010.36

	FLOW	EFF	INSUL	DIAMETER	VEL	PIPE	PUMP	INS	HEAT	RET	TOTAL
300	4.003	34	7.6 3.2	11.7 5.6	7.8	4.220	1.85	0.736	1.49	2.16	110.46
290	291206.279	34	8.9 8.7	28.7 28.5	4.5	23.687	9.61	1.672	2.58	37.08	074.82
270	259 46.744	32	8.0 7.5	15.5 15.1	3.5	7.103	3.03	0.941	1.75	12.03	924.86
250	231 28.734	31	7.7 6.9	12.7 12.2	3.2	4.883	2.04	0.788	1.56	8.37	917.65
230	206 21.648	30	7.5 6.4	11.2 10.8	3.1	3.886	1.69	0.707	1.46	6.77	114.51
210	184 17.787	28	7.4 6.0	10.4 10.0	3.0	3.371	1.45	0.661	1.40	5.82	612.70
190	163 15.318	26	7.3 5.7	9.8 9.4	2.9	3.035	1.29	0.628	1.36	5.18	611.49
170	143 13.583	24	7.2 5.3	9.3 8.9	2.8	2.798	1.18	0.604	1.32	4.71	710.62
150	125 12.292	21	7.2 5.0	8.9 8.6	2.8	2.579	1.14	0.581	1.29	4.35	6 9.95

	FLOW	EFF	INSUL	DIAMETER	VEL	PIPE	PUMP	INS	HEAT	RET	TOTAL
350	4.316	36	7.6 3.1	8.7 5.0	6.4	4.303	1.78	0.618	1.43	2.62	510.75
340	338122.368	35	9.1 8.9	22.3 21.8	5.5	26.637	11.04	1.428	2.42	39.91	861.45
320	300 31.450	35	8.2 7.6	12.7 12.0	4.3	8.937	3.62	0.862	1.75	13.46	328.63
300	269 20.564	34	7.9 7.0	10.6 9.8	4.1	6.301	2.67	0.735	1.58	9.57	020.86
280	241 16.103	33	7.7 6.6	9.6 8.8	3.9	5.227	2.19	0.675	1.51	7.84	917.45
260	217 13.619	32	7.6 6.2	9.0 8.1	3.7	4.612	1.92	0.638	1.46	6.83	815.44
240	195 12.012	31	7.6 5.9	8.6 7.7	3.6	4.208	1.74	0.612	1.42	6.15	814.13
220	175 10.870	29	7.5 5.6	8.2 7.4	3.6	3.920	1.61	0.593	1.39	5.66	113.17
200	156 10.002	27	7.4 5.3	8.0 7.1	3.5	3.702	1.51	0.578	1.37	5.27	612.44
180	139 9.312	25	7.4 5.0	7.7 6.9	3.5	3.473	1.50	0.561	1.35	4.97	111.85

region of Figure 7-4. In this small pipe regime, steam is superior only above 175 °C. In the large pipe regime (10 MW), on the other hand, steam is superior above 150 °C and the differential is much larger at higher temperatures.

The above results were necessary for the consideration of preliminary systems designs. They are also important data for the verification of results of the more complex total system optimization. Many of the formulations developed for this heat transport subsystem optimization have been included in the overall system optimization.

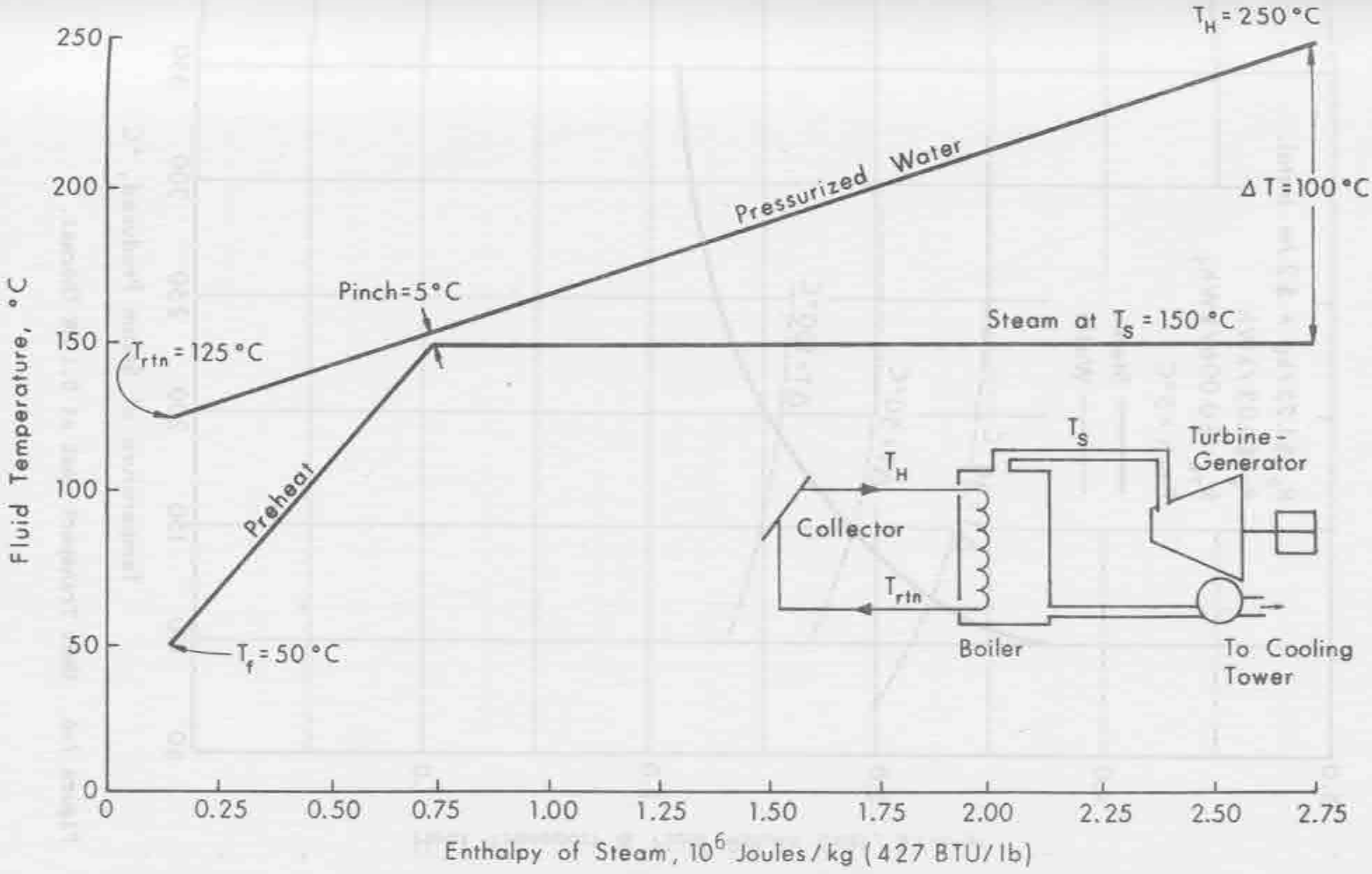

Figure 7-5. Heat Exchanger Performance is Presented as the Hot Water Input (upper line) at T_H Heating Feed Water from 50 °C to T_S and Boiling it (lower line). Lower Scale Applies only to Lower Trace. Upper Trace is Superimposed.

Increasing the flow rate in the transport loop decreases the slope of this upper line, rotating it about the pinch point.

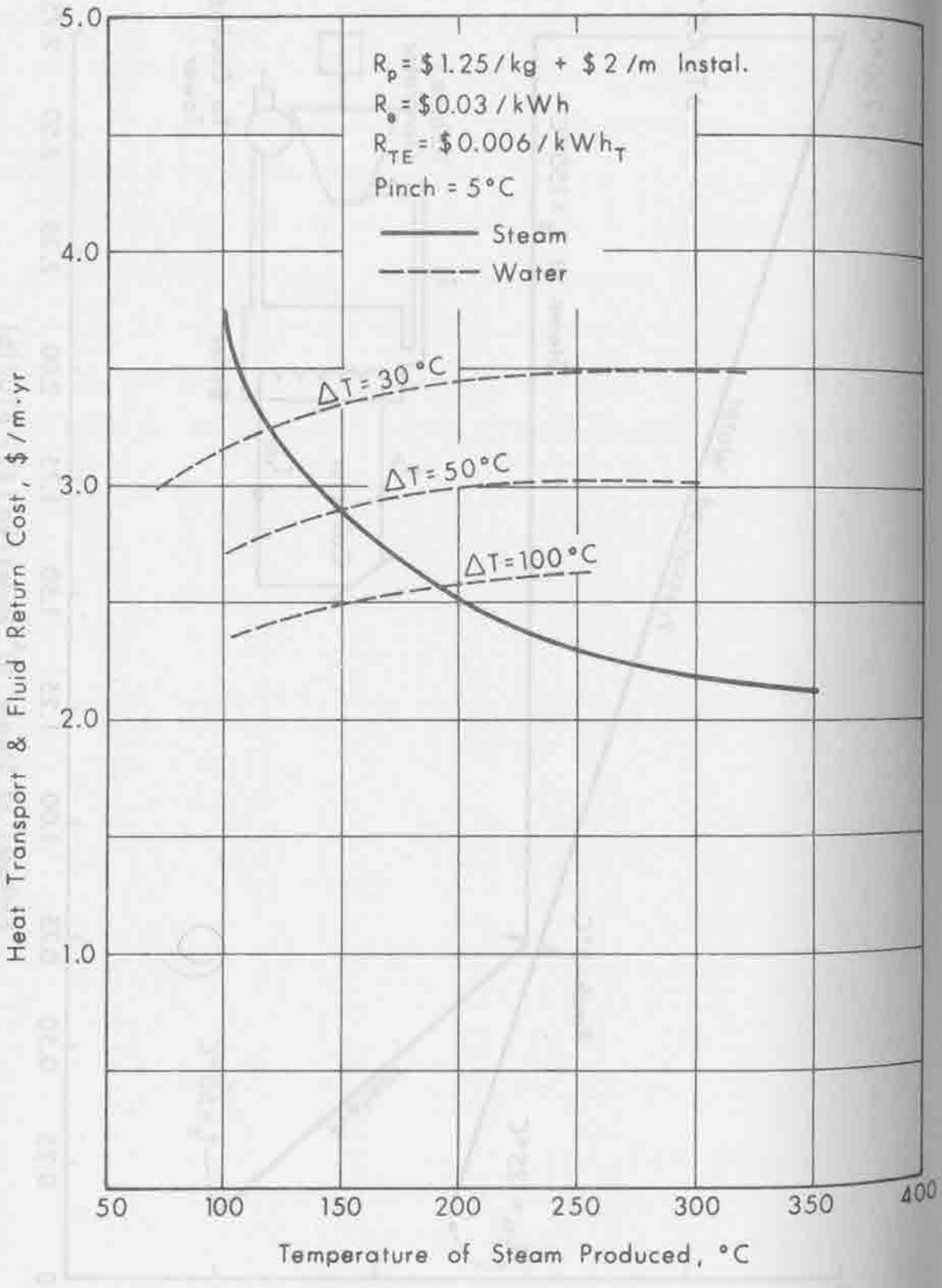

Figure 7-6. Heat Transport Cost at 0.1 MW Thermal.

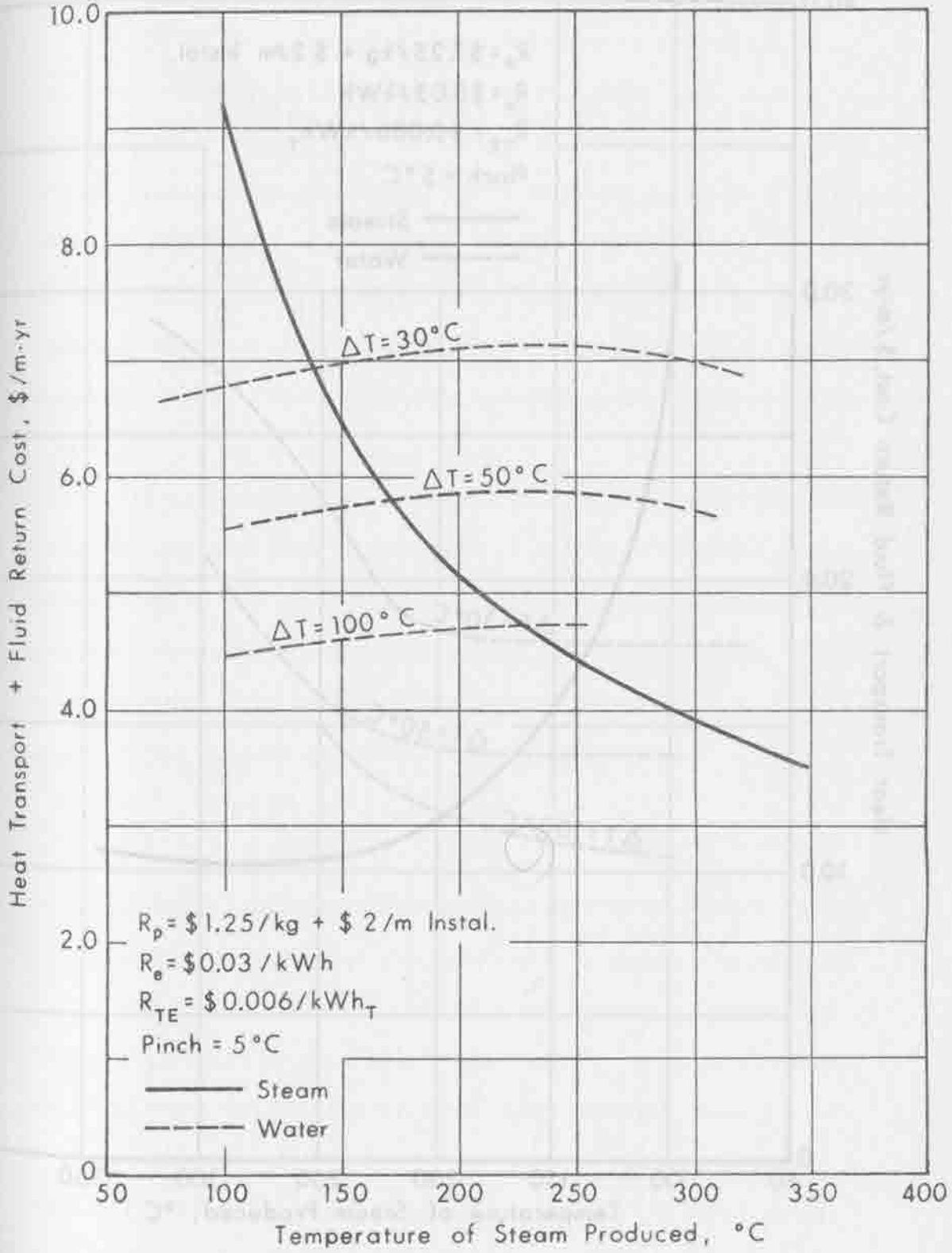

Figure 7-7. Heat Transport Cost for 1.0 MW Thermal.

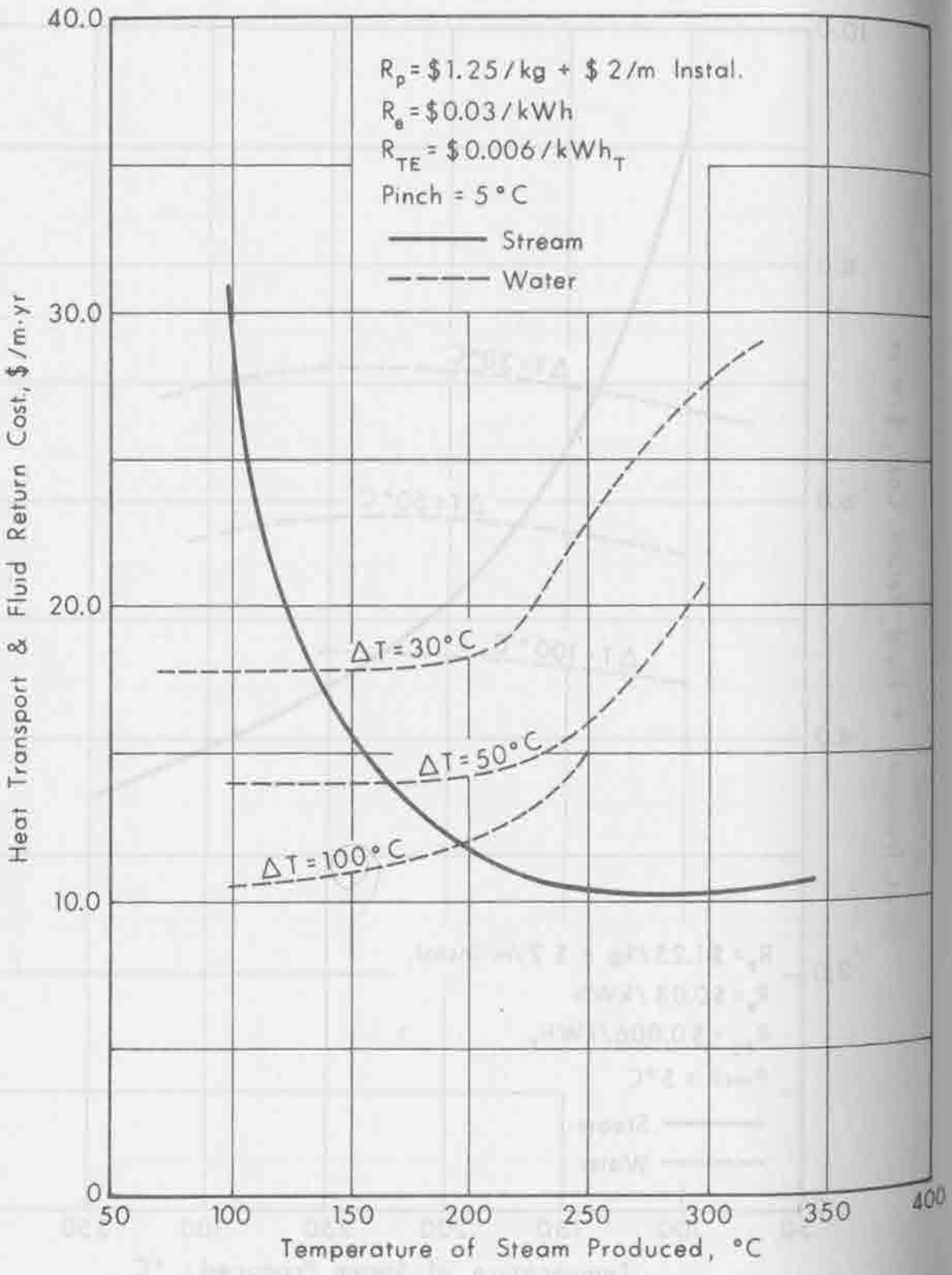

Figure 7-8. Heat Transport Cost for 10.0 MW Thermal.

8.0 HEAT TRANSPORT JUNCTIONS

One of the important factors involved in the layout of a solar collector field is to know how to optimally join several heat sources into a single pipe. In Section 6.0 it was shown that the cost of heat transport by pressurized water or steam varies as the transfer power level raised to the exponent 0.48 or 0.8, depending upon whether the pipe costs are vaying directly as the diameter of the pipe or as the square of the pipe diameter. The ranges of pipe sizes and saturated steam temperatures where these two conditions occur were shown in Figure 7-4.

When pipe diameters are small and the pressures are not too high, the cost per unit length tends to increase directly with diameter. When either pipe diameter increases or the pressure increases, a region is reached, as shown in Figure 7-4, where the cost per unit length varies as the square of the pipe diameter.

Starting with the basic relationships:

$$\$/m = kP^{0.48} \text{ and } \$/m = kP^{0.82}$$

we will examine pipe costs for combining heat from various sources by manifolding arrangements for transfer to a central location.

Figure 8-1 shows the general configuration in which heat is flowing from right to left at a power transfer level of rP up to the point where two additional pipes, each carrying power at a level P, join the main trunk. To the left of the junction the trunkline is carrying power at a rate (r + 2)P. It is possible to solve for a minimum cost, by noting the differential pipe configurations shown in Figure 8-2, where the differential trunk length is

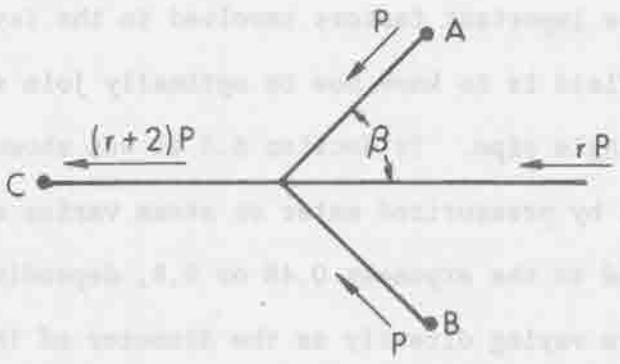

Figure 8-1. Pipe Junctions in Heat Transport System.

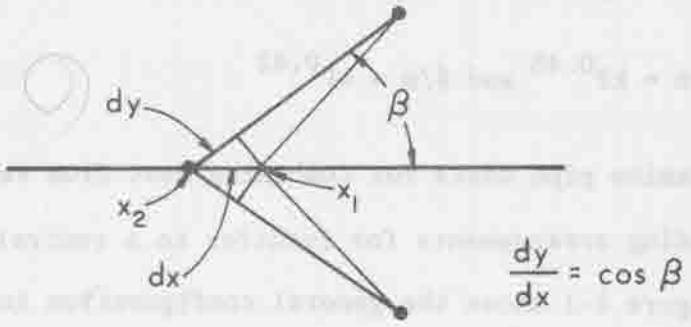

Figure 8-2. Differential Pipe Lengths.

dx and the differential spur pipe lengths are dy. The junction angle, as shown, is defined as β, and from the configuration it can be seen that $dy/dx = \cos \beta$.

If the junction is located at x_1, the cost of transporting heat from point x_1 to point x_2 is equal to

$$\left[(r + 2)P\right]^k dx \tag{8-1}$$

If, on the other hand, the junction were at point x_2, the variable cost portion would be a reduced cost for dx and the additional cost of two dy sections which is given as

$$(rP)^k dx + 2P^k dy \tag{8-2}$$

It can be seen that the minimum cost solution occurs when the cost of transporting heat from a junction at x_1 and then to x_2 is equal to transporting to point x_2 as dx becomes differentially small. Equating Equation (8-1) and (8-2) we obtain

$$\left((r + 2)^k - r^k\right) dx = 2\, dy. \tag{8-3}$$

Solving for the cosine β yields

$$\frac{dy}{dx} = \cos \beta = \frac{(r + 2)^k - r^k}{2}. \tag{8-4}$$

It is instructive to examine a range of numerical examples where the power ratio varies from r = 0 to 1,000, as shown in Table 8-1. When r = 0 there is no trunkline and we are merely dealing with the combining of two spur power sources into a single powerline. Under these conditions, if the large pipe relations are obtaining where the cost of pipe is varying as the square of the diameter, the optimum

TABLE 8-1

Optimum Junction Angles

Power ratio r	Optimum Junction angle, β, degrees (large pipe) k = 0.82	(small pipe) k = 0.48
0	28	45.8
1	43	69.6
2	47.5	74.0
4	52	77.9
10	57.8	83.6
100	69.1	88
1000	76.3	89.6

junction angle is 28°. If the small pipe relations are holding such that the power constant is equal to 0.48, the optimum angle is seen to be 45.8°. When the junction is to a large trunkline, the optimum junction angle increases considerably as shown, and in particular for the small pipe, it approaches very close to a 90° junction angle.

In applying these optimum junction angles to the field layout optimization, it will be necessary to apply feasibility restrictions. The actual fabrication of pipe junctions on a large scale will require the selection of several standard junction angles (e.g., 30, 45, 60, 75, 90°). The selection of a given angle can be made on the basis of the relative power levels involved.

APPENDIX G

HEAT STORAGE

BY

T. B. JONES

1.0 INTRODUCTION

The purpose of this aspect of the STEPS study has been to consider heat storage systems for solar-thermal electric power applications. The significant results reviewed below include a review of thermal storage concepts, and detailed performance and cost calculations for the two prime candidate systems, steam accumulators and hot water displacement storage tanks.

As in solar home heating, there is good reason to consider energy storage for solar-thermal electric power plants. Numerous energy storage concepts might be realistically considered, including thermal, mechanical (kinetic or potential), chemical, and electrical methods. However, of these, only thermal energy storage can be reasonably thought of as an integral part of a solar-thermal electric power plant. Other systems, for example pumped storage, might be compatible with a solar-thermal plant, but consideration of these hybrid systems is not within the scope of the STEPS project. Thus this study is limited to thermal energy storage systems.

1.1 Rationale for Considering Integral Thermal Storage

Numerous attractive features about thermal storage can be cited as evidence that storage should be an important system component. For example, the nature of insolation suggests storage as a means of gaining generation system flexibility. Storage can be used to extend the generation of electricity from the sun beyond sunset, and it can also be used to smooth out the unpredictability of insolation. Such arguments are attractive to the layman but not necessarily to the power company

engineer, who wants to know if storage can cut the costs of solar-thermal power. If the conservative assumption is made that solar-thermal power plants are never going to produce a significant portion of the nation's total electrical energy needs, then it may be argued that the small amount of energy generated by solar plants will always be "useful", obviating storage. Hence, another more easily verified rationale for the consideration of storage is presented here. Figure 1-1 shows a representative solar-thermal power generation curve. With no storage, a plant designed to use all the thermal energy supplied by a collector field must have a turbine which has a capacity equal to the maximum occurring at solar noon. This capacity is utilized for only a short time each day, and the turbine is operated off-design at lower efficiency during the remainder of the day. With storage, it is possible to use a smaller turbine which runs at capacity for a much more extended period, as the Figure 1-1 shows. Initial calculations reviewed in an earlier report [CSU/Westinghouse, (1973)] show that such a turbine/storage capacity trade-off may be cost effective.

1.2 Preliminary Decisions on Design and Optimization Strategy for Storage

The investigative procedure for this part of the STEPS project was based in part on the three decisions reviewed below:

(i) Electrical power generated from a solar-thermal power plant is assumed to be useful whenever it is generated; thus, thermal storage is to be considered as a possibly cost-effective trade-off for turbine capacity.

(ii) The costs per kWh_e stored per day for thermal storage systems are calculated for various system parameters such as temperature, etc.

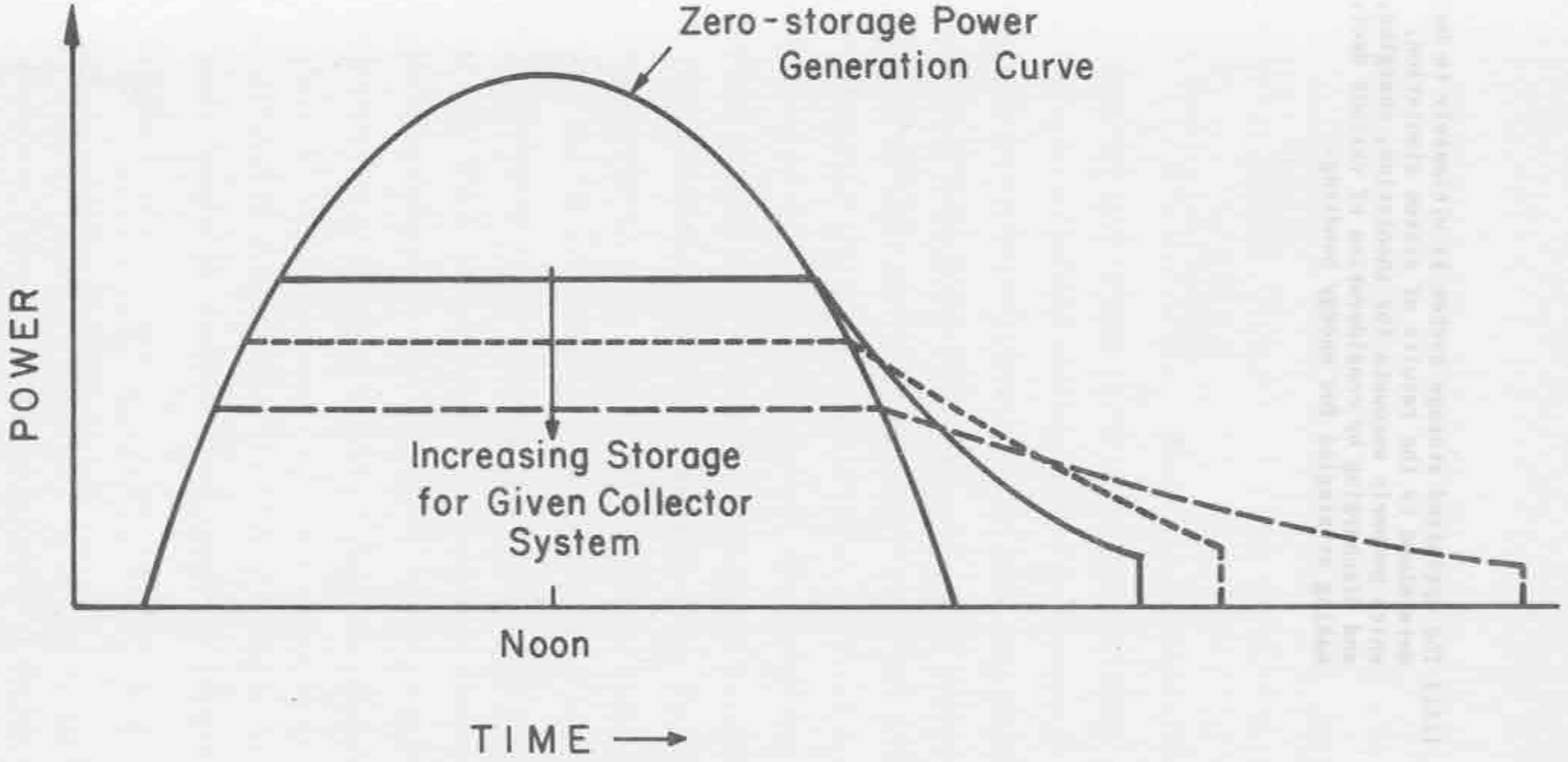

TYPICAL UTILIZATION OF THERMAL STORAGE

Figure 1-1. Typical Utilization of Thermal Storage.

(iii) The optimized storage system is ultimately to be determined by the results of system simulation, which properly accounts for insolation, charging, and discharging by consideration of various decision-making strategies for energy handling.

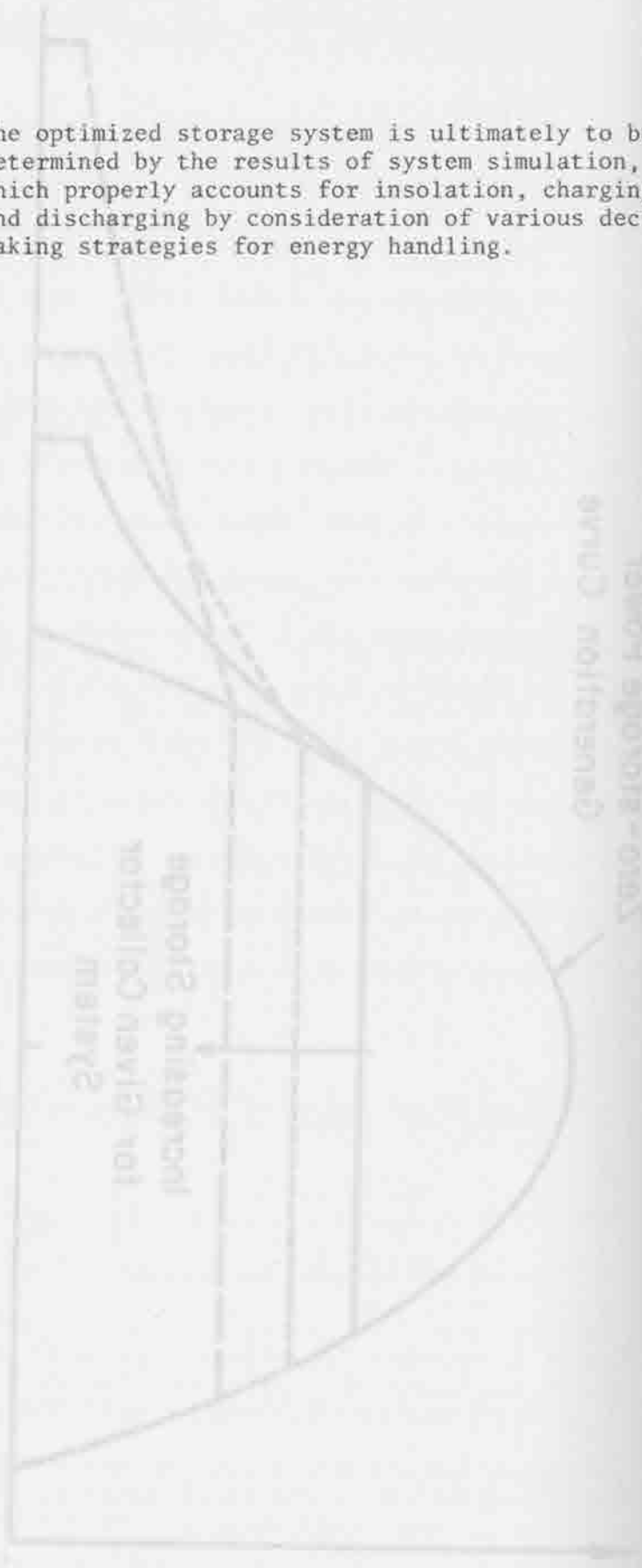

2.0 PRELIMINARY THERMAL STORAGE SYSTEM SELECTION

2.1 Review of Systems Considered

Thermal storage systems may be divided conveniently into two fundamentally different categories, sensible and phase change schemes.

2.1.1 Sensible Heat Storage

Sensible heat storage is the easiest to implement, partly because of the existence of conventional heat exchanger technology. The temperature variability required in sensible heat storage is a disadvantage, but not necessarily a severe one if condensing turbines are used. Practical sensible heat storage schemes are naturally divided into (i) fluid and (ii) solid schemes. Often the fluid is also the working fluid of the system (e.g., water), which makes the heat exchange problem less significant. Principal among working fluid heat storage schemes are the steam accumulator, where the working fluid is steam and the storage medium is water (steam, condensed under pressure and then re-boiled), and the stratified hot water displacement tank, where pressurized water serves as both working fluid and storage medium. One sensible heat storage scheme using a solid material (iron) is the superheat accumulator [Marguerre, F., (1933) and Dolezal, R., (1962)], but the relatively low temperature of solar-thermal systems precludes serious consideration of superheated steam. Iron can be placed directly in hot water sensible heat storage tanks, but it is not attractive on a tank volume (cost) basis. No other practical solid heat storage medium has been located.

2.1.2 Change of Phase Heat Storage

Because material phase transitions occur isothermally, usually with the release or absorption of significant latent heats, change of

phase heat storage is a concept with great potential. Many different phase change concepts have been considered.

Solid-Liquid Phase Changes--The heat of fusion of some solids such as salt-hydrates, alloys, and eutectics [Locklin, D. W., Droege, J. W., Ward, J. J. and Eibling, J. A., (1958); Goldstein, M., (1961); University of Pennsylvania, (1971); Aerospace Corp., (1972)] make them attractive as potential heat storage media. There is some experience with salt hydrates in solar home heating storage systems [Telkes, M., (1964); Telkes, M., and Raymond, E., (1949)], but problems of phase separation and cumulative material degradation are significant [Hodgins, J. W., and Hoffman, T. W., (1955)]. Also, their temperature range is generally below the range of solar-thermal plants.

Work with eutectics has produced a number of new potential storage media, such as LiOH-LiF which melts at 420 ^{o}C [Aerospace Corp., (1972)], but their temperatures are generally above the realistic range of solar-thermal plants. Further, problems in the design of heat exchangers and sub-cooling effects exist.

Solid-Solid Phase Changes--Certain phase transitions from one solid state to another have been considered for heat storage [Goldstein, M., (1961)], but the latent heats of these transitions are smaller than those of fusion. They are not actively being considered at this time.

Heat of Vaporization--The utilization of the heat of vaporization in storing thermal energy is not in itself attractive because of the requirement of a huge costly vapor containment vessel. However, Goldstein (1961) has proposed a vaporization-distillation scheme which uses two liquid tanks, one of which absorbs water vapor into solution, (e.g., sulphuric acid absorbs water into solution without too large a heat of solution) boiled away from the other tank. With the vapor volume proble

thus solved, this scheme looks attractive. Unfortunately no effort has been devoted to development of this potentially attractive heat storage scheme past the conceptual stage, and there is no basis for engineering feasibility studies.

Others--Heats of solution have been proposed [Goldstein, M., (1961)] but problems of material segregation are likely to be encountered.

2.1.3 Hybrid Systems

The Minnesota-Honeywell research team has discussed the possibility of placing a matrix of capsules of a eutectic material into a steam accumulator [University of Minnesota/Honeywell, (1972)]. Presumably the water is displaced by a eutectic or salt-hydrate with an increased thermal energy storage density. Further, the small capsules insure good heat transfer. Whether incongruent melting and sub-cooling problems can be avoided by encapsulation is completely unknown.

2.2 Discussion of Heat Storage Systems

2.2.1 Materials

Liquids--Liquids considered for working fluid/storage media include water, organic liquids, such as the insulating dielectrics, alcohol, etc., and inorganics, such as fluorocarbons, and ammonia. By any measure (storage and heat transfer properties, cost, availability of engineering data, etc.) water is the best possible fluid in the expected operating range of a solar-thermal electric power plant. Thus, water is the only sensible heat storage material seriously considered here.

Solids--On a per volume basis, iron is not as attractive as water. Other metals with good heat transfer properties are either too

scarce, too expensive, or, in the case of sodium, too dangerous. Sensible heat in solids has been eliminated from consideration.

2.2.2 Systems

Reference has been made above to numerous heat storage systems, some of which have been extensively developed (e.g., the steam accumulator [Goldstern, W., (1970); Lamb, W., (1962-3)], some of which have been tested experimentally (e.g., the salt-hydrate fusion systems [Telkes, M., (1964); Telkes, M., and Raymond, E., (1949); Hodgins, J. W. and Hoffman, T. W., (1955)]), and some of which are strictly conceptual (e.g., the vaporization-distillation scheme [Goldstein, M., (1961)]). In this study, data covering the physical properties of a large number of possible heat storage materials have been collected, but, aside from the steam accumulator and the salt-hydrate heat storage system used in the Dover house [Telkes, M., and Raymond, E., (1949)], no useful engineering data on systems have been obtained.

For many of the systems or concepts discussed above, it is only possible at this point to state problems already encountered or anticipated by engineers. For heat of fusion systems, these problems include degradation of materials, incongruent melting, heat exchanger problems, toxicity and/or fire hazards of certain materials. To this list should be added the pragmatic matter of unknown materials cost and availability. The vaporization-distillation concept is untested experimentally, as is the encapsulation of eutectics in hot heat transfer fluids. Major uncertainties in the design and cost of all these systems cannot be denied.

2.3 Result of Initial Screening of Thermal Storage Systems

The predictable result of the initial screening and data collection process is the choice of two sensible heat storage systems, both of which use water: the steam accumulator (see Section 3.0) and the stratified hot water displacement system (see Section 4.0). In the following two sections, these two storage schemes are considered in detail. Performance and cost data are presented. The good reliability of these figures should provide useful benchmarks for comparison to new heat storage systems as more useful engineering and cost data on these new systems become available. One might reasonably expect a breakthrough in intermediate temperature eutectics (100 ^{o}C - 300 ^{o}C) to make an immediate impact on heat storage technology for solar-thermal electric power system applications.

3.0 STEAM ACCUMULATOR HEAT STORAGE: DESIGN, PERFORMANCE, COSTING

3.1 Operation of Steam Accumulators

Refer to Figure 3-1 which shows a cut-away view of a steam accumulator. The steam accumulator is essentially a pressure vessel filled to about 90 percent with water at elevated temperature and pressure. It accepts and delivers steam, while storing the thermal energy as sensible heat in the water. To store heat, live steam is bubbled into the vessel through a special nozzle shown in the figure. The nozzle is located axially (with vertical steam accumulators) inside a circulation pipe. When steam is introduced through the nozzle, it rises in the circulation pipe, drawing water with it. The circulation thereby set up mixes the water and helps to maintain near-equilibrium conditions in the water mass. As the steam flows in, the water temperature rises, while the water mass increases slightly.

The accumulator is discharged by valving off the steam volume above the water to drop the pressure slightly. Boiling results, and, if the accumulator is not discharged too quickly, dry saturated steam is delivered to the turbine. An internal network of tapered discharge structures is usually used to maximize mixing and minimize local superheating of the water, to avoid explosive boiling. See Figure 3-1.

Typically, the water volume of a steam accumulator varies from ∿60-70 percent uncharged to ∿90 percent fully charged. Larger accumulators exhibit considerable expansion and contraction during the charge-discharge cycle and so must be specially designed to account for this. The maximum rate of discharge for dry steam generation in a steam accumulator is proportional to the steam volume, and is also dependent

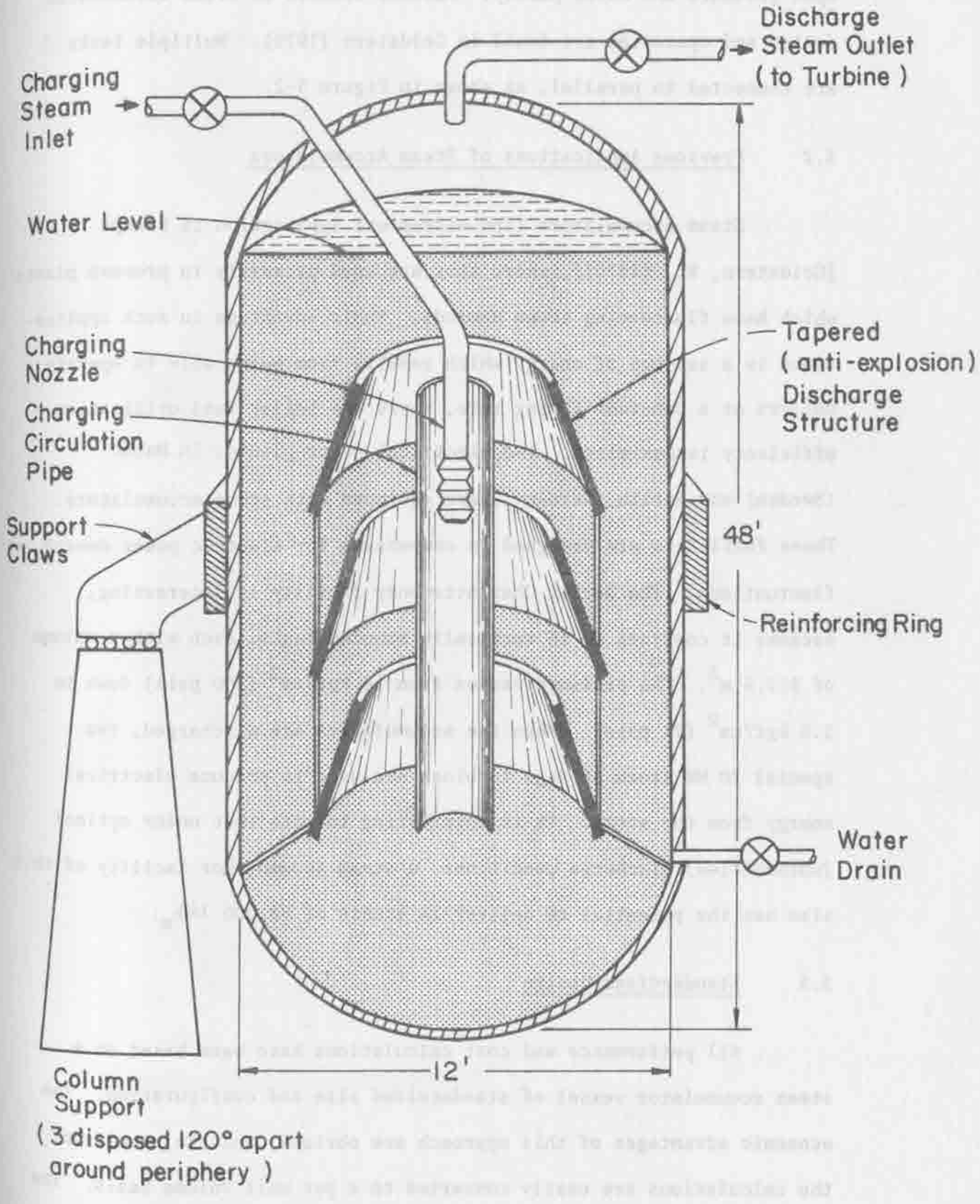

Figure 3-1. Cut-Away View of Vertically Mounted Steam Accumulator Thermal Storage Tank.

upon pressure and water purity. Further details of steam accumulator design and operation are found in Goldstern (1970). Multiple tanks are connected in parallel, as shown in Figure 3-2.

3.2 Previous Applications of Steam Accumulators

Steam accumulators find widespread application in Europe [Goldstern, W., (1970)], where they are used primarily in process plants which have fluctuating steam demands. Their advantage in such applications is a savings of energy which results from being able to operate boilers at a constant firing rate, where the boiler fuel utilization efficiency is maximized. Two electrical power plants, in Malmö (Sweden) and Berlin (Germany), are equipped with steam accumulators. These facilities are designed to compensate for electric power demand fluctuations. The Berlin-Charlottenburg facility is interesting, because it consists of 16 vertically mounted tanks, each with a volume of 312.5 m^3. The pressure varies from 14 kgf/cm^2 (200 psia) down to 1.5 kgf/cm^2 (21 psia). When the accumulators are discharged, two special 20 MW steam storage turbines are used to produce electrical energy from the steam. It is interesting to note that under optimal (unthrottled) discharge conditions, a steam accumulator facility of this size has the potential to deliver in excess of 88,000 kWh_e.

3.3 Standardized Design

All performance and cost calculations have been based on a steam accumulator vessel of standardized size and configuration. The economic advantages of this approach are obvious, and the results of the calculations are easily converted to a per unit volume basis. The

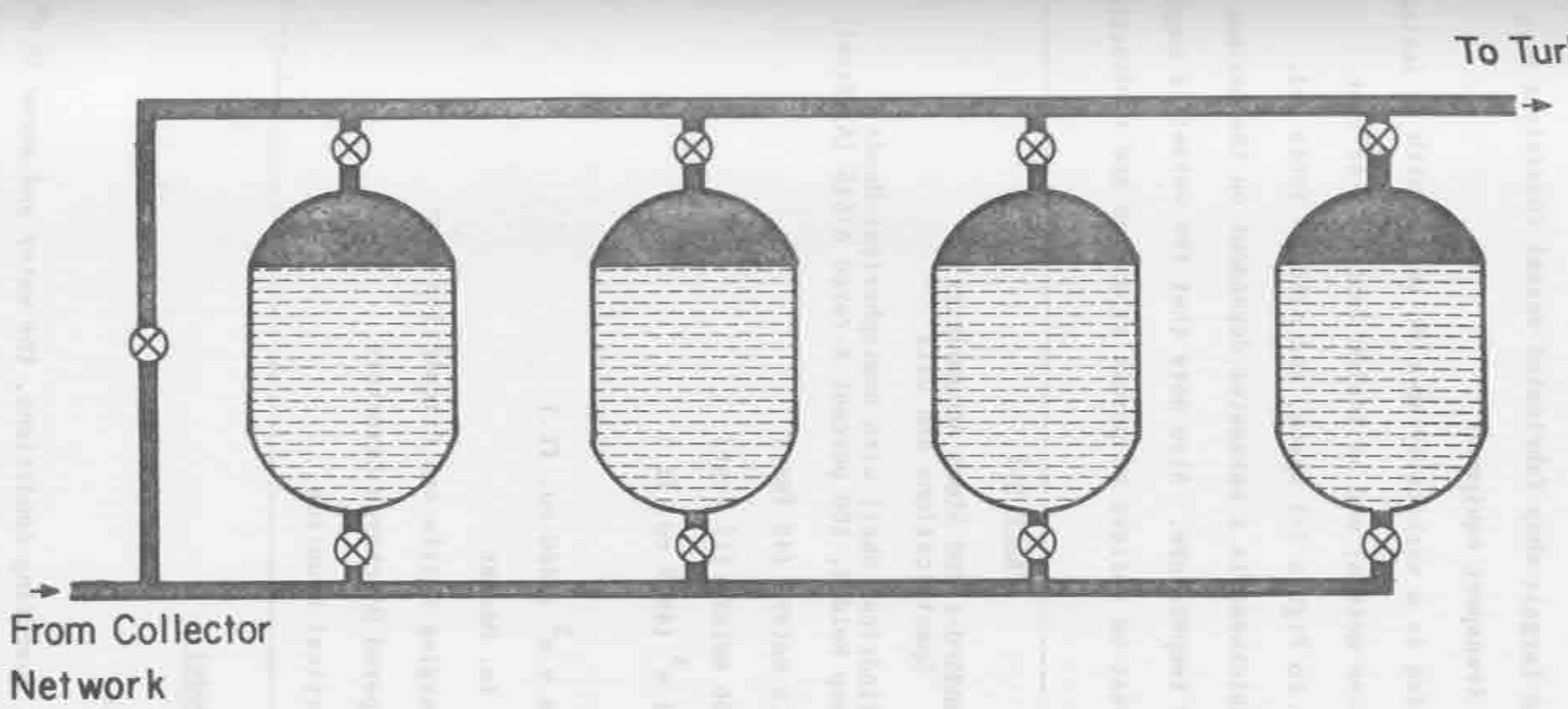

Figure 3-2. Proposed Steam Accumulator Heat Storage Network Allowing Charging/Discharging of Accumulators Individually.

tank size chosen is the largest shop fabricated vessel consistent with readily available rail transport equipment.

The configuration is a vertically mounted vessel with an inside diameter of 12 feet (3.66 meters) and an inside length of 48 feet (14.63 meters). Refer to Figure 3-1 again, and also to Table 3-1. Note that the vessel thickness is a parameter dependent on the maximum operating pressure and temperature. Also note that the vessel is supported by three claws which rest on rollers to permit expansion and contraction.

TABLE 3-1

Standard-sized Steam Accumulator
Specifications and Data

*	CONFIGURATION:	Cylindrical Shell with Hemispherical Heads (Shop Welded, 100 percent X-rayed A-515 (A) Steel)
*	INSIDE LENGTH:	14.6 meters (48 feet)
*	INSIDE DIAMETER:	3.66 meters (12 feet)
*	VOLUME:	141 m^3 (4977 cu. ft.)
*	WATER FILL VOLUME AT FULL CHARGE:	126.9 m^3 (4480 cu. ft.)
*	FEATURES:	24 in. Manway
		Charging Nozzle and Circulation Pipe
		Tapered Discharge Structure
		Vertical Mounting

3.4 Performance Model

3.4.1 Thermodynamics

Under typical operating conditions, the water and steam in an accumulator are essentially in equilibrium, that is, they are saturated.

Thus, the thermodynamic state of the accumulator is completely determined by a specification of either temperature or pressure. If certain conditions are maintained on the rate of discharge (not too rapid, with good mixing), the evolved steam is dry and saturated, and the discharge is a reversible process. Typically, the accumulator and all inter-connecting piping are well-insulated, so the adiabatic condition may be assumed. Thermodynamic irreversibility is introduced if the accumulator is charged with steam at a higher temperature than that of the accumulator. The attendant lose in energy availability is measured by means of the efficiency of storage, $\eta_{storage}$.

$$\eta_{storage} = \frac{E_{electric}}{E_{electric,o}}, \qquad (3\text{-}1)$$

where $E_{electric,o} = \eta_{cycle} E_{thermal}$ is the electric energy provided directly from the thermal energy $E_{thermal}$, at constant temperature T_2, and $E_{electric}$ is the electric energy produced from the discharge of a storage system which has been charged with the same thermal energy $E_{thermal}$ at the same temperature T_2. It is easy to show that

$$\eta_{storage}(T_2,T_1,T_c) = \frac{\frac{1}{T_2-T_1}\int_{T_1}^{T_2} \eta_{cycle}(T,T_c)\, dT}{\eta_{cycle}(T_2,T_c)} \qquad (3\text{-}2)$$

where T_2 = maximum temperature of storage (same as design operating temperature),

T_1 = minimum temperature of storage, and

T_c = heat sink (condenser) temperature.

If the cycle efficiency is a constant fraction of Carnot efficiency, then the constant fraction cancels out of Equation (3-2) and

$$\eta_{storage}\ (T_2,T_1,T_c) = \frac{\frac{1}{T_2-T_1}\int_{T_1}^{T_2} \eta_{carnot}\ (T,T_c)\ dT}{\eta_{carnot}\ (T_2,T_c)} \qquad (3\text{-}3)$$

But

$$\eta_{carnot}\ (T,T_c) = \frac{T - T_c}{T} \qquad (3\text{-}4)$$

and so the storage efficiency may be shown to be [Hottel, H. C., (1974)]:

$$\eta_{storage}\ (T_2,T_1,T_c) = \frac{(T_{lm} - T_c)/T_{lm}}{(T_2 - T_c)/T_2} \qquad (3\text{-}5)$$

where $T_{lm} = (T_2-T_1)/\ln(T_2/T_1)$ is the log-mean temperature difference. Equation (3-5) clearly shows the loss in energy availability suffered by the cyclic process of storing thermal energy supplied at constant temperature in an accumulator and then withdrawing and delivering it under conditions of decreasing temperature to a turbine/generator.

The relevance of the result, Equation (3-5), to the real accumulator-turbine/generator subsystem considered here hinges on the validity of the assumption that cycle efficiency is a constant fraction of Carnot efficiency. This assumption may be checked by reference to the calculated off-design condensing turbine performance data provided by Westinghouse (Section 11.0 [CSU/Westinghouse,(1973)]). The fraction

of Carnot efficiency is constant within ∿5% for a given turbine with a given design operating temperature and capacity, but this fraction varies significantly with respect to these parameters. Thus, the simplified efficiency of storage expression, Equation (3-5), is of limited use in parametric studies, such as the one undertaken here.

3.4.2 Dynamics

The dynamics of charging and discharging a steam accumulator are more relevant to simulation studies than to the performance calculations, but the constant steam volumetric flow rate condition, which is maintained over a wide range of saturated steam inlet temperature conditions in condensing turbines [CSU/Westinghouse, (1973)], makes the discharge dynamics trivial. The only problem is to check that the maximum discharge rate condition of the accumulator itself is not exceeded. This condition is empirically described by the equation below [Goldstern, W., (1970)]:

$$d = (2.35 + .014\ p)\ D_W^{-.715} \qquad (3\text{-}6)$$

where $d = \dfrac{\text{metric tons steam/hour}}{m^3 \text{ steam volume}}$,

p = pressure (atmospheres), and

D_W = density of water (degree of purity), ^{o}Baume.

For typical conditions, and 90% maximum water fill, this maximum flow rate is not exceeded except when a very small storage installation is coupled with a very large turbine.

The dynamics of charging can only be dealt with in simulation studies, where various power generation strategies can be tested. Therefore, this aspect of the dynamics problem is not considered here.

3.4.3 Discharge Equations

The choice of turbine capacity and maximum operating temperature determines the total amount of electrical energy available in the discharge of an accumulator between two temperatures T_2 and T_1. Because of the nature of the turbine data, a numerical approach using tabular efficiency and flow data is used. The condition of constant volumetric steam flow rate is assumed to hold over the entire discharge temperature range (from T_2 down to T_1). The differential equations are:

$$dE_{thermal} \simeq -m(T)\ d\ h_f - h_f(T)\ dm \tag{3-7}$$

$$dm = -\frac{dE_{thermal}}{h_{fg}(T)}, \tag{3-8}$$

where the heat content of the steam in the accumulator has been neglected in Equation (3-7). Combining Equation (3-7) and (3-8),

$$dE_{thermal} = -\left[h_{fg}(T)\ m(T)\ \frac{dh_f}{dT} / (h_{fg} - h_f)\right] dT \tag{3-9}$$

The dynamics of the accumulator discharge are constrained by the condensing turbine to a constant volumetric flow of steam. Thus,

$$dE_{thermal} = \{[h_g(T) - h_f(T_c)]\ \dot{v}/v_g(T)\}dt \tag{3-10}$$

and, from the cycle efficiency, we can calculate the electric energy.

$$dE_{electric} = \eta_{cycle}\ (T_2, T, T_c)\ dE_{thermal} \tag{3-11}$$

The time interval associated with a temperature drop dT is then

$$dt = - \frac{h_{fg}(T) \frac{dh_f}{dT} V(T) v_g(T)}{\dot{v} v_f [h_{fg}(T) - h_f(T)][h_g(T) - h_f(T_c)]} dT \qquad (3\text{-}12)$$

The Equations (3-10), (3-11), and (3-12) can be numerically integrated quite conveniently using small temperature increments to calculate important performance quantities such as the available electric energy, the thermal charging energy, the discharge time, and the water mass and volume remaining in the tank.

Note that the thermal energy $E_{thermal}$ refers to the heat content of steam, not water. The results of these calculations may be used directly if it is assumed that the heat transport medium is steam, produced directly in the absorber. However, if hot water is the working fluid in the collector system and if the water is used to produce steam in a heat exchanger-boiler, then additional energy availability is lost and the cycle and storage efficiency functions cannot be used as a complete description of the conversion efficiency from heated water to electric power.

All the data are presented for a condenser temperature (T_c) of 40 ^{o}C. The results can be altered to any different condenser temperature T_c' by accounting for the cycle efficiency transformation provided below.

$$\eta_{cycle}(T,T_c') \approx \frac{1-T_c'/T}{1-T_c/T} \cdot \eta_{cycle}(T,T_c) \qquad (3\text{-}13)$$

3.4.4 Summary of Performance Calculation Results

All the performance results are obtained on a per tank basis for turbines of various design temperatures and capacities. The computer program used to make the numerical calculations provides data on various discharge parameters at temperature intervals during the discharge. In so doing, we gain knowledge of the dynamics of the discharge cycle under the assumed constant steam volume flow rate conditions. A typical normalized plot of the thermal and electrical energies and powers is shown in Figure 3-3. Note the times of 90% and 95% electrical energy discharge are marked on the curves. These times give a measure of the time dependence of the electric power, which starts at the full power level and decreases rapidly with time as the accumulator temperature drops.

Other more useful performance data are plotted in Figures 3-4 and 3-5. Figure 3-4 shows the thermal charging energy and the available electrical energy per standard tank (as specified in Table 3-1) as a function of the design maximum storage temperature (turbine design temperature). The turbine data used for these calculations is a 10 $MW_{electric}$ capacity unit, the important specifications of which are reviewed in Table 3-2. The table shows the lower limit T_1 on the discharge of the accumulator, which is somewhat arbitrarily limited to the lowest temperature at which valid turbine data has been supplied [CSU/Westinghouse,(1973)]. Figure 3-5 shows the times required for 90%, 95% and 100% discharge of the electrical energy available in the accumulator.

The data supplied in Figures 3-4 and 3-5 is actually of general validity and can be used with other size accumulators and condensing

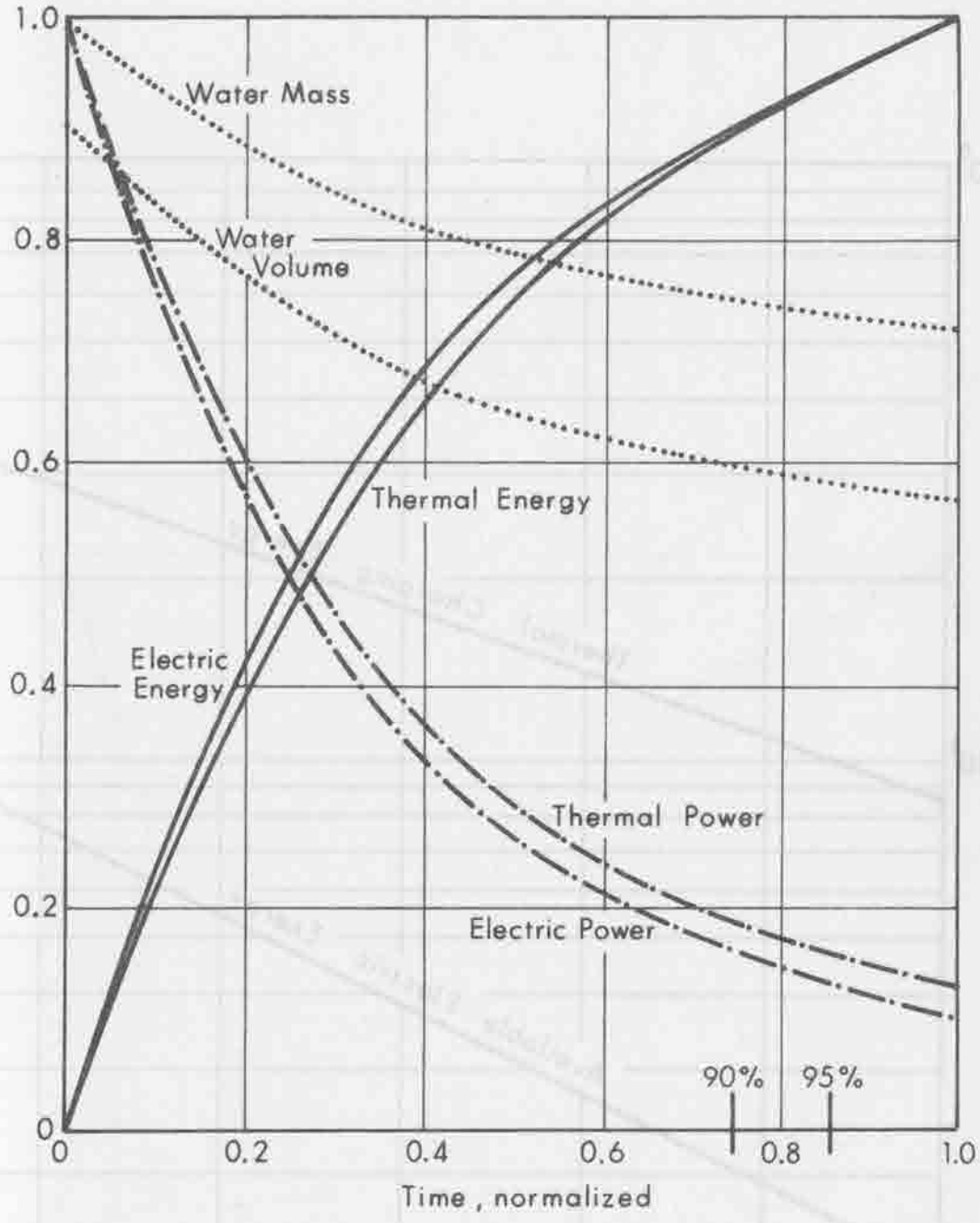

Figure 3-3. Normalized Plot of Time Dependence of Important Parameters in Steam Accumulator Discharge. (Basis: 10 MW Turbine, T_c = 40 °C, T_1 = 170 °C, T_2 = 250 °C).

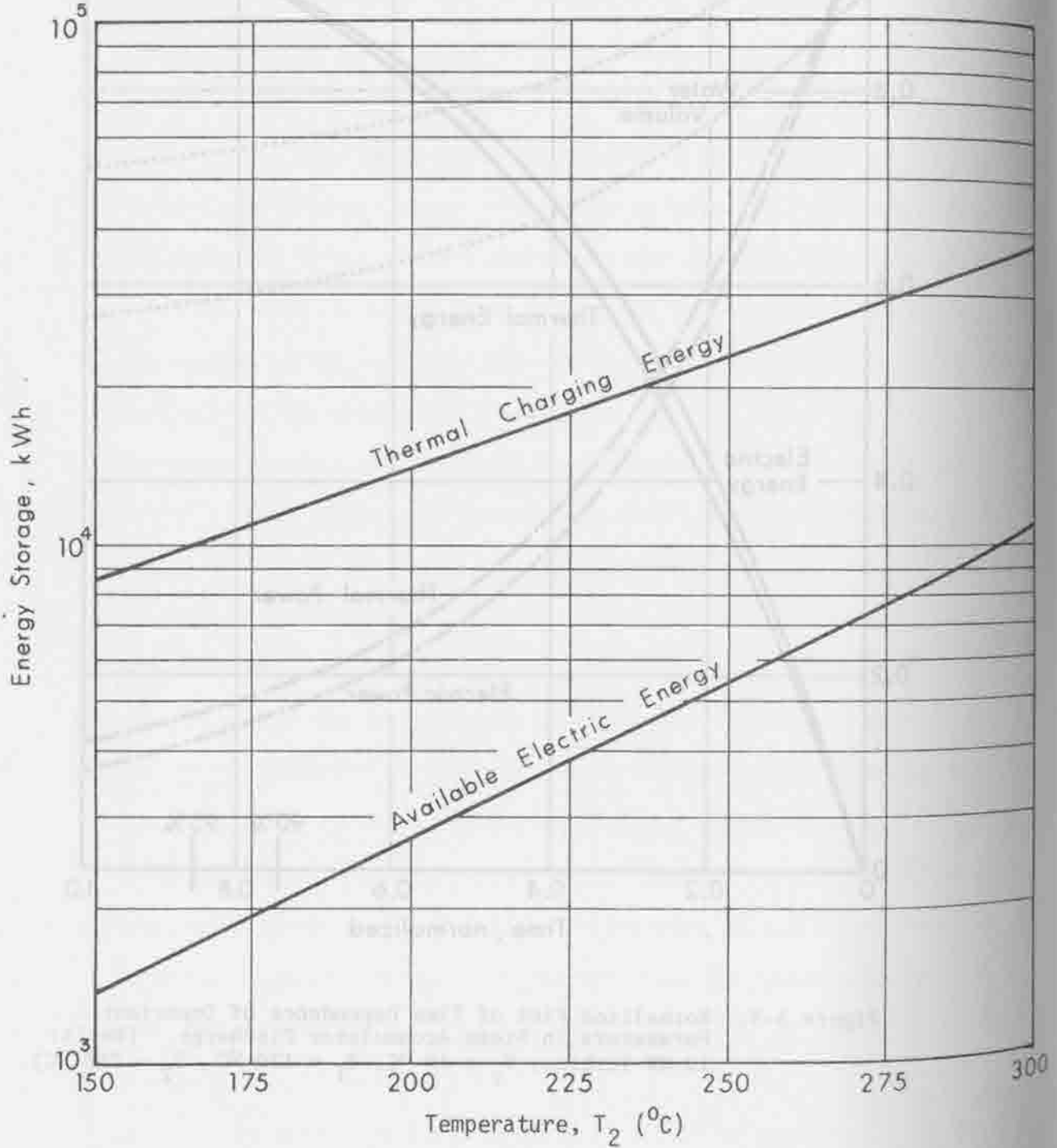

Figure 3-4. Steam Accumulator Thermal and Electrical Energy Storage per Standard Tank (Basis: 10 MW Turbine, T_c = 40 ^oC).

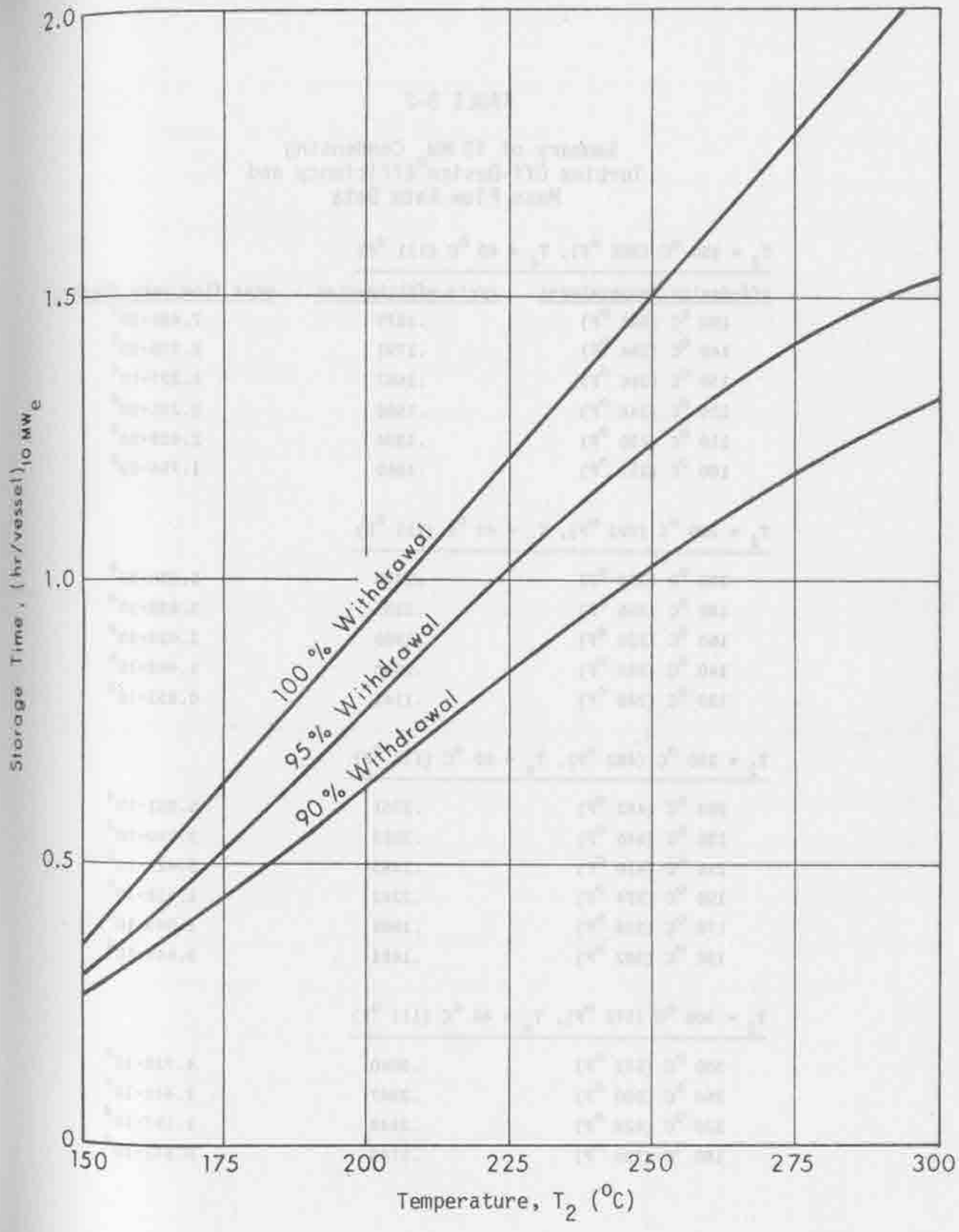

Figure 3-5. Steam Accumulator Storage Time per Standard Vessel. (Basis: 10 MW Turbine, T_c = 40 °C).

TABLE 3-2

Summary of 10 MW_e Condensing Turbine Off-Design Efficiency and Mass Flow Rate Data

off-design temperatures	cycle efficiencies	mass flow rate (kg/hr)*
T_2 = 150 °C (302 °F), T_c = 40 °C (111 °F)		
150 °C (302 °F)	.1877	$7.486 \cdot 10^4$
140 °C (284 °F)	.1791	$5.778 \cdot 10^4$
130 °C (266 °F)	.1667	$4.397 \cdot 10^4$
120 °C (248 °F)	.1506	$3.295 \cdot 10^4$
110 °C (230 °F)	.1304	$2.428 \cdot 10^4$
100 °C (212 °F)	.1060	$1.756 \cdot 10^4$
T_2 = 200 °C (392 °F), T_c = 40 °C (111 °F)		
200 °C (392 °F)	.2379	$5.836 \cdot 10^4$
180 °C (356 °F)	.2231	$3.830 \cdot 10^4$
160 °C (320 °F)	.1989	$2.420 \cdot 10^4$
140 °C (284 °F)	.1648	$1.460 \cdot 10^4$
120 °C (248 °F)	.1142	$0.833 \cdot 10^4$
T_2 = 250 °C (482 °F), T_c = 40 °C (111 °F)		
250 °C (482 °F)	.2761	$5.051 \cdot 10^4$
230 °C (446 °F)	.2653	$3.540 \cdot 10^4$
210 °C (410 °F)	.2483	$2.427 \cdot 10^4$
190 °C (374 °F)	.2242	$1.618 \cdot 10^4$
170 °C (338 °F)	.1909	$1.043 \cdot 10^4$
150 °C (302 °F)	.1481	$0.645 \cdot 10^4$
T_2 = 300 °C (572 °F), T_c = 40 °C (111 °F)		
300 °C (572 °F)	.3040	$4.738 \cdot 10^4$
260 °C (500 °F)	.2847	$2.441 \cdot 10^4$
220 °C (428 °F)	.2448	$1.197 \cdot 10^4$
180 °C (356 °F)	.1744	$0.532 \cdot 10^4$

* mass flow rate assuming constant volumetric flow condition.

turbines, if the appropriate multipliers are employed. To calculate the thermal energy or electrical energy in a vessel of a different volume V', use the multiplier V'/141 on data from Figure 3-4, where V' is in cubic meters. The data in Figure 3-4 is roughly independent of turbine capacity for turbines in the size range 3 MW to 300 MW. To calculate the discharge time for 90%, 95% or 100% withdrawal of an accumulator of volume $V'(m^3)$ through a turbine of capacity P'(MW), use the multiplier (V'/141)/(P'/10) on data from Figure 3-5.

3.5 Cost Model

A very detailed approach to the costing of installed steam accumulators is possible. The results of this calculation are reviewed in this section.

3.5.1 Breakdown of Costs and Assumptions

The breakdown of cost items in steam accumulators is shown in the Table 3-3. Two obvious omissions from this table are off-loading and hauling to the plant site. These costs are actually expected to be quite small, and have been neglected. Another cost item not considered is maintenance. Steam accumulators of this size would presumably be subject to yearly internal inspection [Garver, W. L. (1974)]. (For this reason, a manway is included in the vessel design.)

TABLE 3-3

Steam Accumulator Costing Breakdown

I VESSEL FABRICATION & TESTING

- A. Shell and Heat Costs
- B. Shop Preparation, Stress Relief
- C. Manways

II CONTROLS & PERIPHERALS

- A. Valves and Actuators (Inlet, Outlet, Safety, etc.)
- B. Liquid Level Gauge
- C. Nozzle and Charging Pipe
- D. Painting
- E. Discharge Structure
- F. Insulation

III SUPPORT STRUCTURE

- A. Reinforcing Ring
- B. Support Claws
- C. Concrete Columns and Foundation

IV TRANSPORT & SITE WORK

- A. Rail Transportation
- B. Erection of Vessel
- C. Installation of Valves and Fittings

V CONTINGENCY (5%)

The cost of such maintenance/inspection would be largely accrued in the down-time essential to such inspection. This type of cost is most easily accounted for by considering the value of steam accumulators when temporarily shut down. This matter is not considered here, because of the far greater uncertainties in the costs of collector system maintenance.

It is assumed that pressure shop fabricated vessel costing procedures are applicable to steam accumulators. The inclusion of 1/16" (.16 cm)

corrosion safety factor in wall thickness calculations is intended to account for corrosion due to the presence of pressurized water in the vessel [Brinkman, W. H. (1973)]. Several sources on pressure vessel costing have been located [Clark, F. C., and Terni, S. P., (1972); Reilly, A. J. (1960)], but the easiest to use and the most complete are the Richardson Engineering Services documents [Richardson Engineering Services, Inc. (1973)]. These documents contain not only pressure vessel cost data, but also information on much of the peripheral equipment needed for the steam accumulators, plus installation and erection costs.

Note that all costs are in mid-1972 dollars. A standard $\pm$ 10% cost accuracy [Richardson Engineering Services, Inc. (1973)] must be assumed to apply to all results given here.

3.5.2 Cost Calculation Results

The costs are per standard vessel unless otherwise specified. Cost per volume can be obtained by dividing the tank cost by 141 m^3 to get the cost per unit volume.

The maximum charging temperature of a steam accumulator, T_2, is equal or almost equal to the design operating temperature of the steam turbine. Thus, this maximum accumulator temperature is a very important system parameter. The cost of a standard vessel is a strong function of T_2 because the vessel thickness is proportional to the maximum pressure associated with the maximum temperature. Figure 3-6 shows a plot of vessel weight and total installed cost versus T_2. Another very useful cost function is the cost per unit of electrical energy available from a full accumulator charge. Since an accumulator will undoubtedly be designed on the basis of a daily charge/discharge

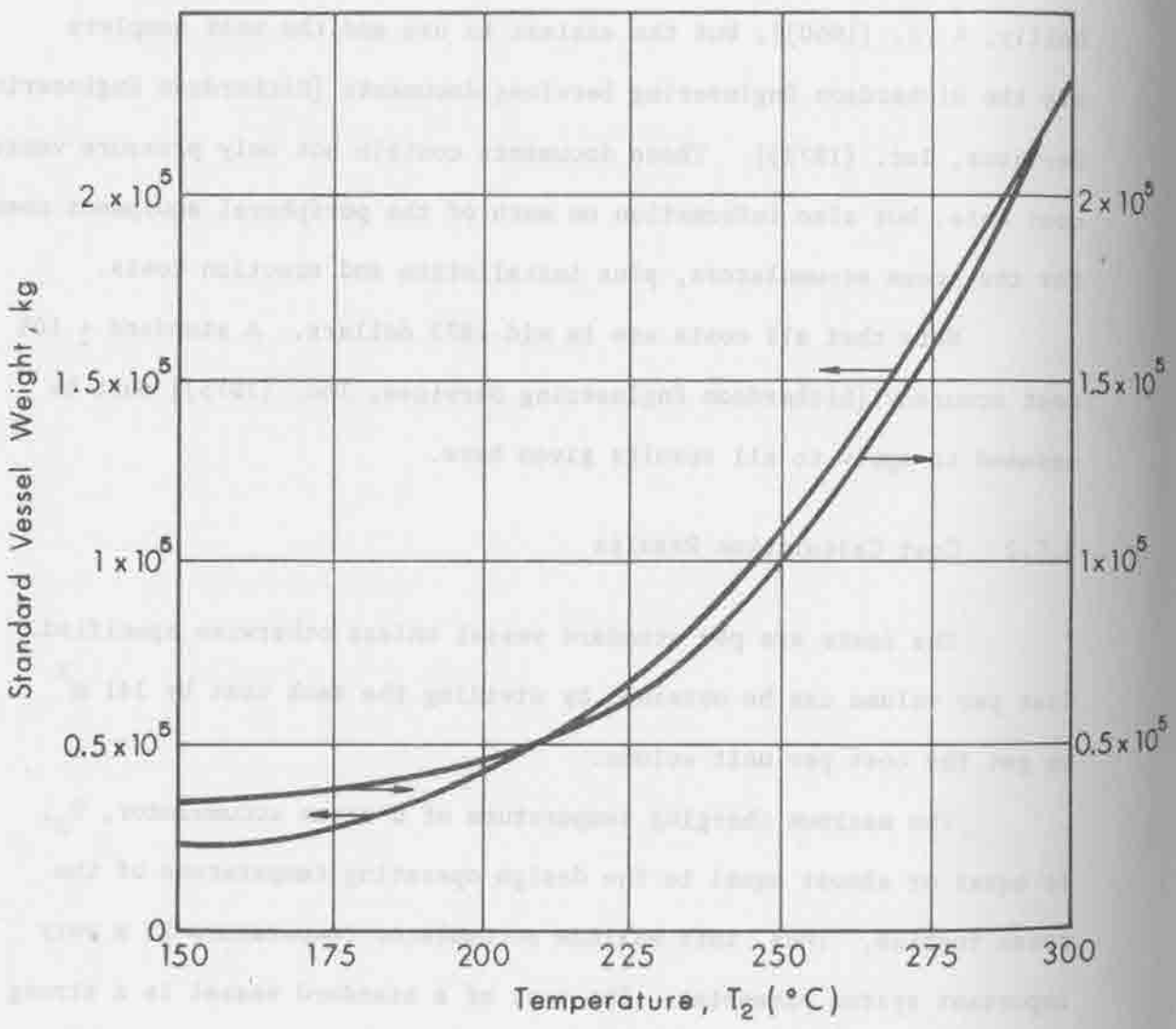

Figure 3-6. Steam Accumulator Storage Standard Vessel Weight and Cost (installed).

cycle, the available electric energy is considered as kilowatt-hours per day. This cost function is not too easily used in comparing accumulator and turbine costs, because information on insolation is needed, but it is a very useful function for (i) comparisons amongst storage schemes, and (ii), sub-optimal choices of system parameters such as operating temperatures. This cost function is plotted in Figure 3-7. Also plotted in Figure 3-7 is the cost per unit thermal charging energy. This plot shows that the cost per unit useful energy is minimized at around 210 ^{o}C. This minimum is not too sharp, indicating that steam accumulator storage may be cost effective over a rather broad range of operating temperatures.

The thickness of a standard vessel is over 15 cm. at 300 ^{o}C operating temperature. Such vessels are not easily fabricated in shops, and, because Richardson (1973) does not consider thick-walled vessels, an approximate vessel cost multiplier, [F. D. Clark and S. P. Terni (1972)], has been used to account for this factor. Thus, an additional $\pm$ 10% uncertainty exists for the 300 ^{o}C cost data in Figures 3-6 and 3-7.

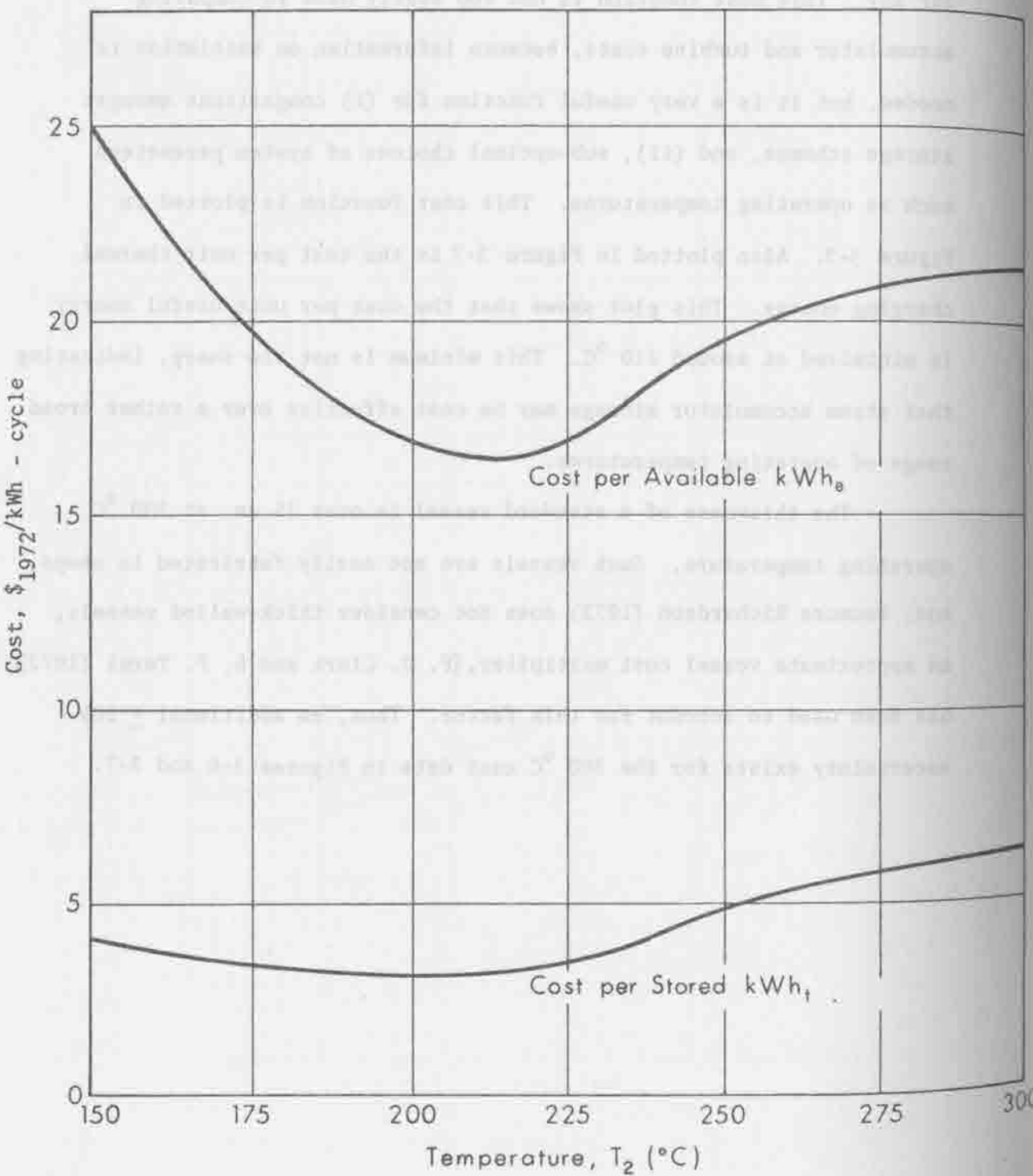

Figure 3-7. Steam Accumulator Cost per kWh (thermal and electrical). (Basis: 10 MW Turbine, T_c = 40 °C).

4.0 STRATIFIED HOT WATER DISPLACEMENT HEAT STORAGE: DESIGN, PERFORMANCE, COSTING

4.1 Operation of Hot Water Storage

Refer to Figure 4-1, which shows the essential features of a stratified hot water displacement heat storage tank. The vessel used must be mounted vertically with a large enough aspect ratio to allow a stable stratification layer to prevent mixing of hot and cold water during withdrawal. The heat from the collector field is stored by pumping hot water into the tank from the top, displacing cold water which drains out the bottom and flows into the collector. When the stored hot water is to be used, it is drawn off the top and fed into a heat exchanger-boiler. The water returning from the heat exchanger is pumped into the storage tank at the bottom. The energy is stored as sensible heat in the tank, and usually it is advantageous to discharge the tank by a series of cyclic passes through the heat exchanger, each cycle producing steam at a lower (off-design) temperature than the previous cycle. As a result, the hot water displacement storage system requires a more complex energy control system than the steam accumulator. Figure 4-2 shows the arrangement of several hot water storage tanks connected in series.

4.2 Other Applications of Hot Water Storage

Hot water storage has been proposed for use in central heating plants for large apartment complexes [Schönholzer, E. (1969)]. Common hot water heater systems rely on thermal stratification to maintain constant hot water temperatures until all the heated water has been

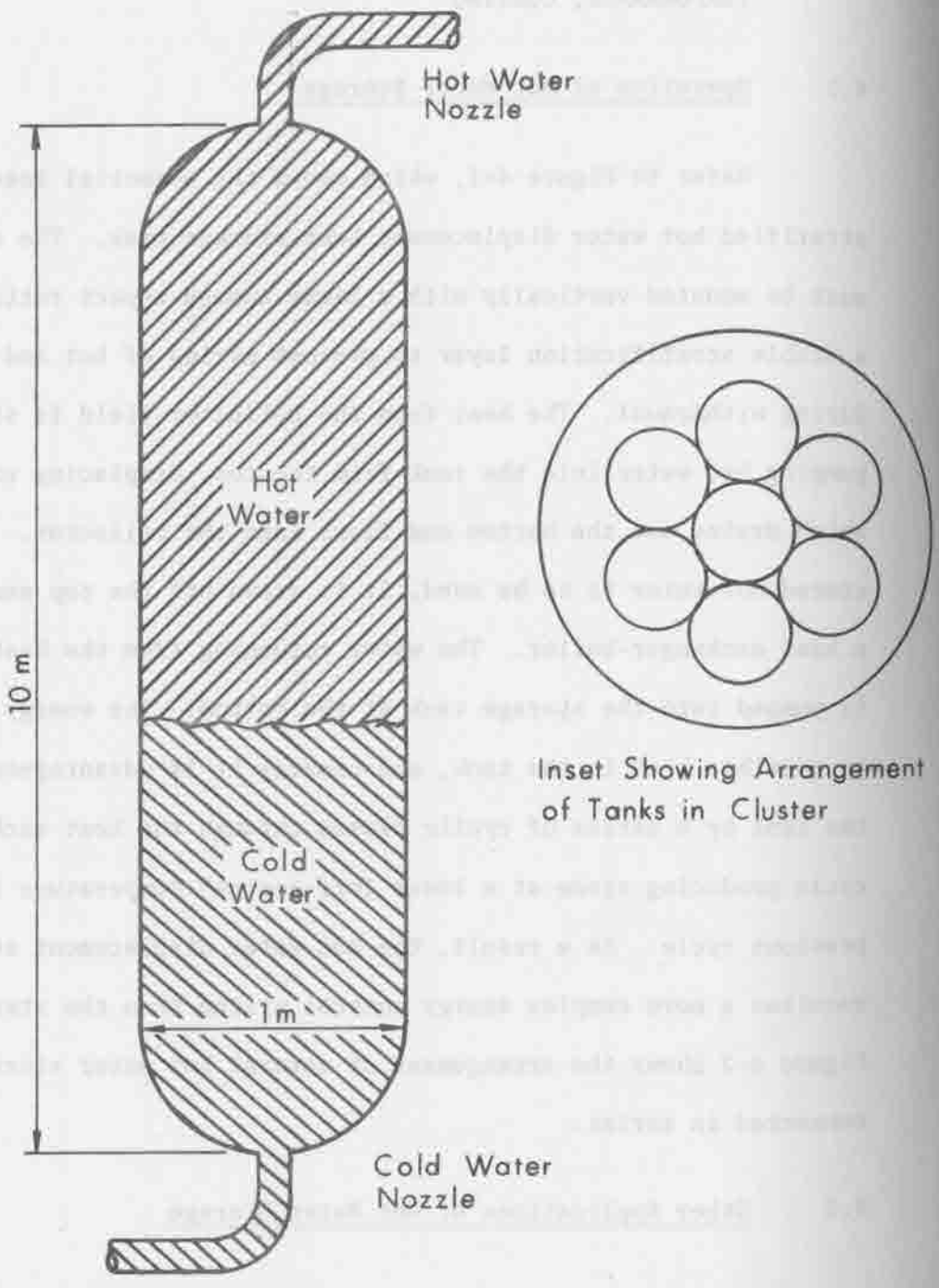

Figure 4-1. Stratified Hot Water Displacement Storage Tank.

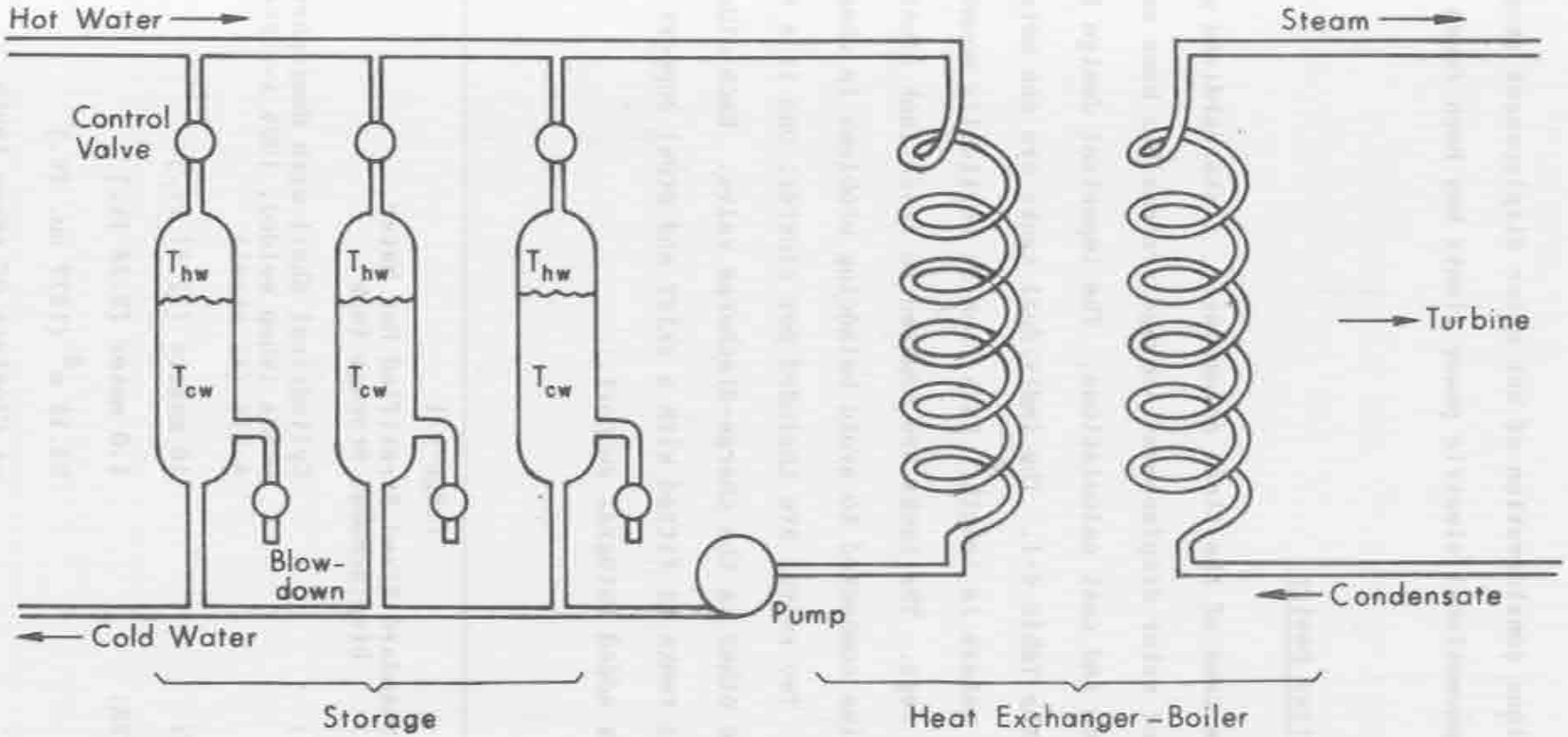

Note: Each Vessel Represents A Cluster of Seven Individual Tanks Connected in Series.

Figure 4-2. Arrangement of Hot Water Storage Tanks.

used up. No serious consideration of hot water displacement storage utilization in conventional electric power plants has been found in the literature.

4.3 Standardized Design

As in the case of the steam accumulator, a standardized design for stratified hot water displacement storage systems has been employed in all performance and cost calculations. The important design features are reviewed in the Table 4-1. The individual tanks are one meter in diameter and ten meters in length. Each tank is vertically mounted on three support legs. The tanks are mounted in seven tank clusters and they are series connected to avoid balancing problems in charging and discharging. Two valves are included per cluster; one is a safety blow-down and the other is the charge-discharge valve. Each cluster of seven vertical tanks is fitted with a skirt and steel support hoops to give the tanks added integral support.

TABLE 4-1

Standard Sized Stratified Hot Water Displacement Storage Tank

• CONFIGURATION:	Cylindrical Shell with Hemispherical Heads (shop welded, 100% x-rayed A-515 (A) steel)
• INSIDE LENGTH:	10 meters (32.81 ft.)
• INSIDE DIAMETER:	1.0 meter (3.28 ft.)
• VOLUME:	53.15 m^3 (1877 cu. ft.)
• FEATURES:	-- Clusters of seven tanks -- Vertical Mounting -- One skirt per cluster

4.4 Performance Model

4.4.1 Thermodynamics

The heat extracted from a displacement hot water tank operated between temperatures T_{hw} and T_{cw} is

$$E_{thermal} = V \left[\frac{h_f(T_{hw})}{v_f(T_{hw})} - \frac{h_f(T_{cw})}{v_f(T_{cw})} \right], \qquad (4\text{-}1)$$

The tank does not have to be completely discharged all at once, but can be discharged through several intermediate temperatures until eventually the lower operating temperature limit of the turbine is reached. During each step of the discharge cycle, the hot water is delivered at a constant temperature which is lower than the previous step. Thus, the turbine operates in a step-wise fashion, with steam at successively lower operating temperatures, much like the turbine run from an accumulator. The total electrical energy available from storage is

$$E_{electric} = \sum_{i=1}^{N-1} \eta_{cycle}\,(T_{i,steam})\, V \left[\frac{h_f(T_{i,water})}{v_f(T_{i,water})} - \frac{h_f(T_{i+1,water})}{v_f(T_{i+1,water})} \right], \qquad (4\text{-}2)$$

where $T_{1,steam}$ is the design operating steam temperature of the turbine/collector system, and $T_{N-1,steam}$ is the minimum operating steam temperature of the turbine as defined in Section 3.4.4. Because turbines cannot be operated safely under rapidly varying steam temperature conditions, the water temperature drops, $T_{i,water} - T_{i+1,water}$, must be kept small so that the steam temperature drop, $T_{i,steam} - T_{i+1,steam}$, is not too large.

It should be noted that the discharge process, and not the charging process, is irreversible in hot water displacement storage. This is just opposite to the situation in steam accumulator storage. Further, the energy storage density is somewhat lower for hot water displacement storage than for accumulators. This is because of the significantly greater net mass change in an accumulator from a fully charged to fully discharged state. These differences show up in the performance and cost figures for the two systems.

4.4.2 Dynamics and Heat Transfer

To consider the dynamics, the operating characteristics of the turbine and the heat exchanger-boiler must be taken into account. The constant volumetric flow condition for the condensing turbine is employed to calculate the steam mass flow rate. Then the heat exchanger-boiler relations are used to calculate the temperatures.

For a given hot water temperature T_{hw}, condenser temperature T_c, the steam temperature $T_{steam} < T_{hw}$, and the pinch point $T_{steam} < T_{pinch} < T_{hw}$ are chosen. If it is assumed that the heat exchanger boiler produces dry saturated steam and that the process is adiabatic, then the following relations hold amongst the operating parameters.

$$T_{cw} = T_{pinch} - \frac{[h_f(T_{steam}) - h_f(T_c)]}{h_{fg}(T_{steam})} \cdot (T_{hw} - T_{steam}) \qquad (4\text{-}3)$$

$$\dot{m}_{hw} \simeq \frac{h_g(T_{steam}) - h_f(T_c)}{h_f(T_{hw}) - \frac{v_f(T_{hw})}{v_f(T_{cw})}\, h_f(T_{cw})} \cdot \dot{m}_{steam} \qquad (4\text{-}4)$$

Using Equations 4-3 and 4-4, with the appropriate turbine data and Equation 4-2, the stored thermal and available electric energies can be calculated, as well as the discharge times, etc.

4.4.3 Summary of Performance Calculation Results

Using the formalism reviewed above, Equations 4-1 through 4-4, plus the same turbine data, Table 3-2, the performance of the stratified hot water displacement storage system has been studied parametrically. The data presented here are for the standardized seven tank cluster described in Table 4-1. A pinch point of T_{steam} + 5 ^{o}C was considered to be an adequate choice regarding the operating characteristic of the heat exchanger-boiler. The range of temperature drops $T_{hw} - T_{steam}$ = 10, 20, 30, 40, 50 ^{o}C was chosen for parametric study initially, though it was decided that the larger values (30, 40, 50 ^{o}C) might be unacceptable for safe turbine operating practice. Table 4-2 shows a typical step-wise discharge of a tank cluster into a 10 MW turbine with a design operating temperature of 200 ^{o}C. Note that the initial hot water temperature is 210 ^{o}C, and that it drops in 13 temperature steps of ~ 7 ^{o}C each down to a final value of 123 ^{o}C, delivering steam at a final temperature of 119 ^{o}C. The initial few steps occur in very short time intervals, suggesting the possibility of combining the first few into a somewhat bigger temperature step, which would take longer and require less sophisticated controls. Actually, one cluster represents very little storage capacity (~ 19 minutes) for a 200 ^{o}C steam, 10 MW plant, and so one would reasonably expect several of these clusters per 10 MW to provide a more realistic amount of storage capacity. Operated in

TABLE 4-2

Performance Data for Discharge of Standard Hot Water Storage Tank Through 10 MW Condensing Turbine, T_c = 40 °C, ΔT_{pinch} = 5 °C.

Temperatures (°C)									
Steam	Hot Water	Cold Water	Steam Flow (kg/hr)	Hot Water Flow (kg/hr)	Thermal Power (kW)	Thermal Energy (kWh)	Electrical Power (kW)	Electrical Energy (kWh)	Discharge Time Intervals (hr)
200/210/203			5.83E+04	6.78E+06	4.25E+04	284	1.01E+04	6.76E+01	6.68E-03
193/203/197			5.08E+04	5.90E+06	3.69E+04	287	8.60E+03	6.68E+01	7.76E-03
187/197/190			4.41E+04	5.12E+06	3.20E+04	289	7.30E+03	6.59E+01	9.02E-03
180/190/184			3.83E+04	4.44E+06	2.77E+04	291	6.19E+03	6.49E+01	1.05E-02
174/184/177			3.31E+04	3.84E+06	2.39E+04	293	5.16E+03	6.30E+01	1.22E-02
167/177/171			2.86E+04	3.32E+06	2.06E+04	294	4.28E+03	6.11E+01	1.43E-02
161/171/165			2.47E+04	2.86E+06	1.77E+04	296	3.55E+03	5.91E+01	1.67E-02
155/165/158			2.12E+04	2.46E+06	1.52E+04	297	2.88E+03	5.63E+01	1.95E-02
148/158/152			1.82E+04	2.11E+06	1.30E+04	298	2.33E+03	5.34E+01	2.29E-02
142/152/146			1.55E+04	1.80E+06	1.11E+04	299	1.87E+03	5.05E+01	2.70E-02
136/146/140			1.32E+04	1.53E+06	9.41E+03	300	1.46E+03	4.67E+01	3.19E-02
130/140/135			1.12E+04	1.30E+06	7.96E+03	301	1.12E+03	4.23E+01	3.78E-02
125/135/129			9.50E+03	1.10E+06	6.71E+03	301	8.44E+02	3.79E+01	4.49E-02
119/129/123			8.01E+03	9.30E+05	5.64E+03	302	6.26E+02	3.35E+01	5.35E-02
						4132. kWh		769.	.315 hr

Final Steam Temperature

Final Water Temperature

Total Thermal Energy

Total Electrical Energy (kWh)

Total Discharge Time

parallel, they would increase the time per step linearly with the number of tanks. Thus, this issue is not a real problem for real hot water storage systems.

The performance data is plotted in a more useable form in Figure 4-3 and 4-4. Figure 4-3 plots the thermal charging energy and available electric energy (per standard cluster) for $T_{hw} - T_{steam} =$ 10, 20 ^{o}C against the design operating temperature of the steam turbine. Note that this temperature, $T_{1,steam}$, is not equal to the maximum hot water temperature, $T_{1,water}$. Figure 4-4 plots the storage time for the same parameters versus the same temperature, $T_{1,steam}$. The data in Figures 4-3 and 4-4 can be generalized by the same multipliers described in Section 3.4.4.

4.5 Cost Model

The similarity of the components in hot water displacement tanks and steam accumulators means that essentially the same detailed methods as those reviewed in Section 3.5 can be applied here. The tank costs are computed using pressure vessel cost data [Richardson Engineering Services, Inc. (1973)]. A breakdown of the important cost items is outlined in Table 4-3. Comparison of Table 4-3 to Table 3-3 shows that the necessary costing information for hot water storage tanks is quite similar to that for steam accumulators. One important difference exists, however, in relation to valve costs, and, as a result, stratified hot water displacement storage costing presents a much more complex problem.

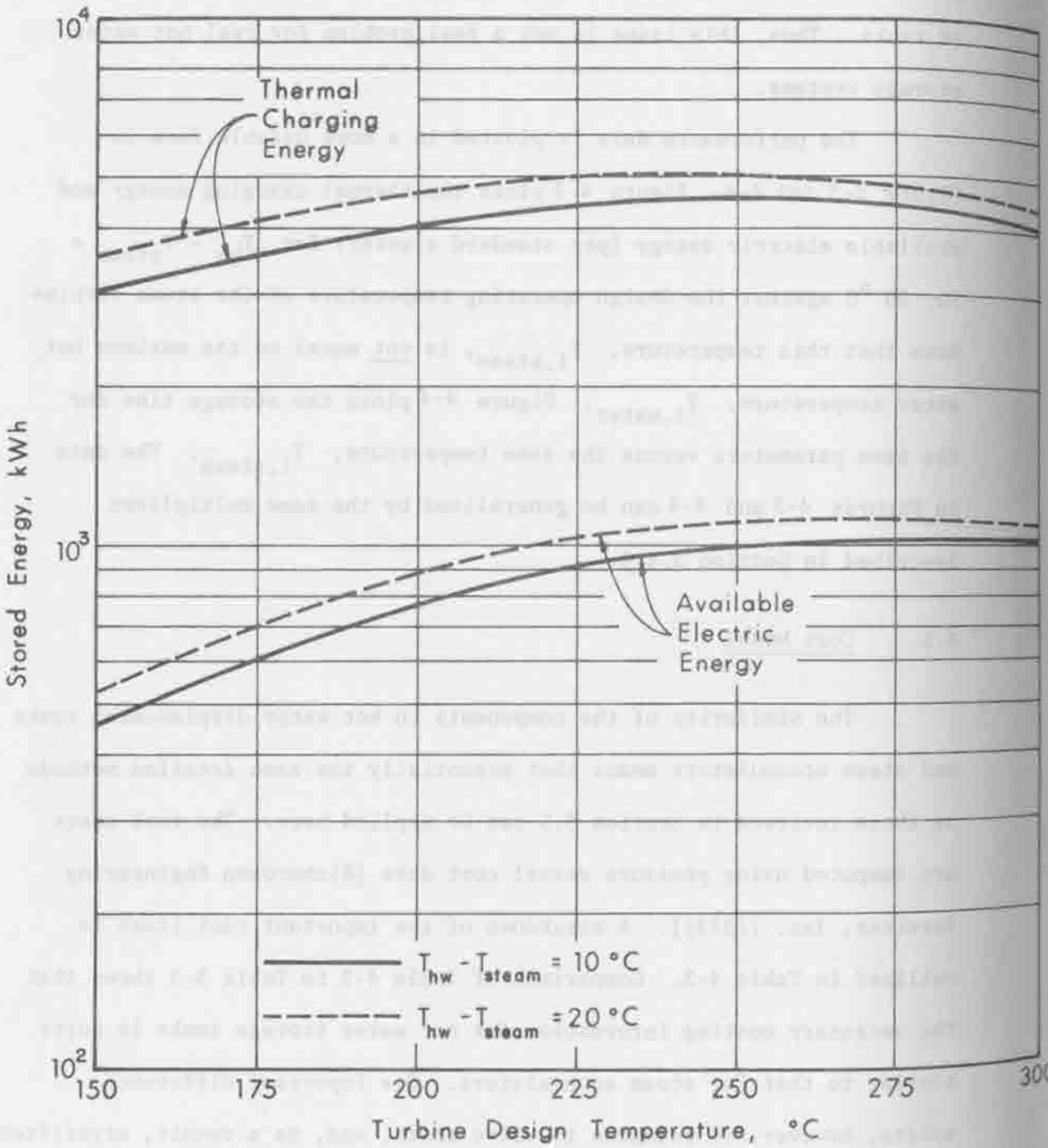

Figure 4-3. Hot Water Thermal and Electrical Storage per Standard Tank Cluster. (Basis: 10 MW Turbine, T_c = 40 °C, ΔT_{pinch} = 5°C).

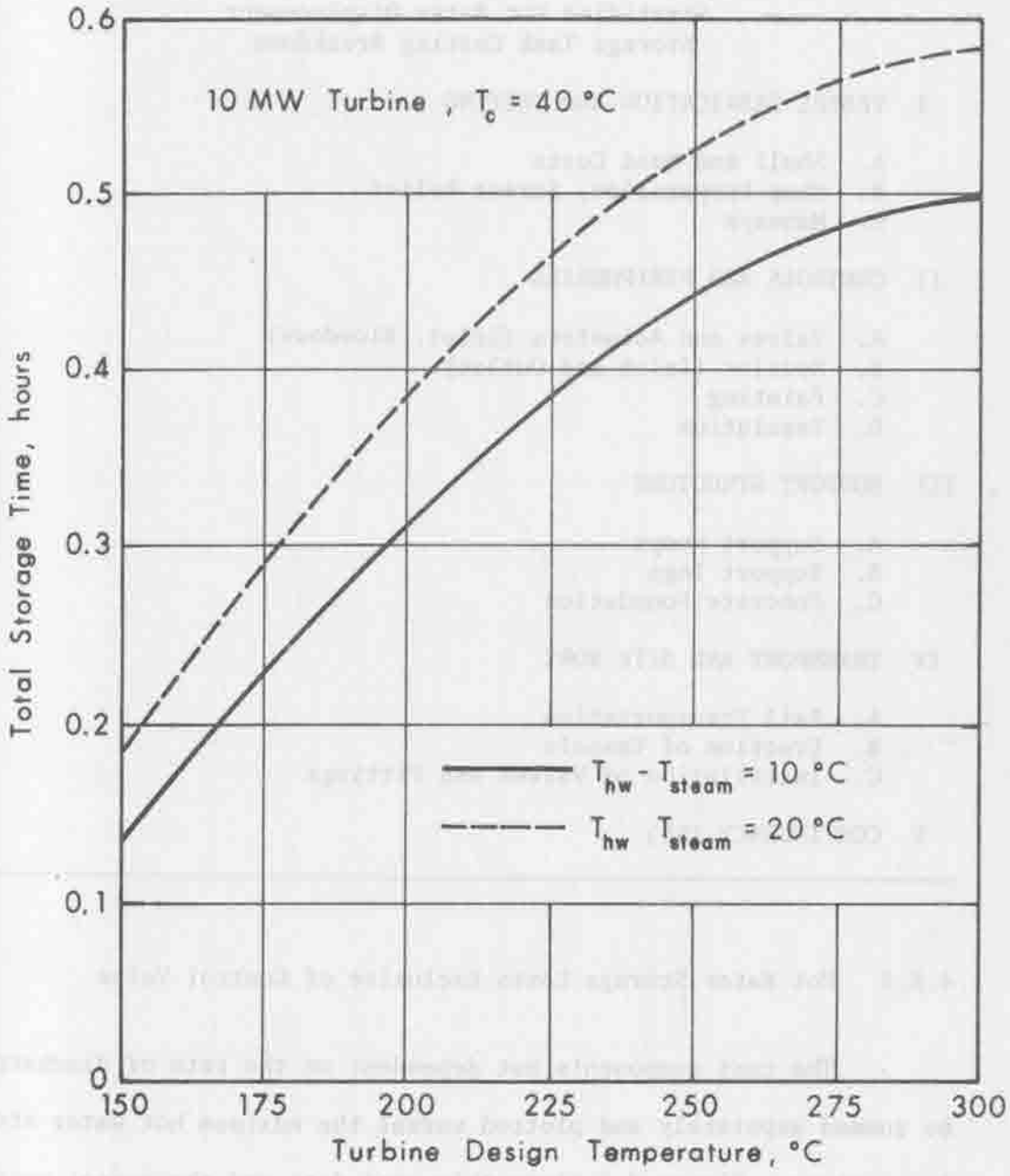

Figure 4-4. Hot Water Storage Discharge Time per Standard Cluster. (Basis: 10 MW Turbine, T_c = 40°C, ΔT_{pinch} = 5°C).

TABLE 4-3

Stratified Hot Water Displacement
Storage Tank Costing Breakdown

I VESSEL FABRICATION AND TESTING

- A. Shell and Head Costs
- B. Shop Preparation, Stress Relief
- C. Manways

II CONTROLS AND PERIPHERALS

- A. Valves and Actuators (Inlet, Blowdown)
- B. Nozzles (Inlet and Outlet)
- C. Painting
- D. Insulation

III SUPPORT STRUCTURE

- A. Support Hoops
- B. Support Legs
- C. Concrete Foundation

IV TRANSPORT AND SITE WORK

- A. Rail Transportation
- B. Erection of Vessels
- C. Installation of Valves and Fittings

V CONTINGENCY (5%)

4.5.1 Hot Water Storage Costs Exclusive of Control Valve

The cost components not dependent on the rate of discharge can be summed separately and plotted versus the maximum hot water storage temperature. Figure 4-5 plots this cost data and the vessel weight together. In Figure 4-6, the cost per available kWh_e and per kWh_t, are plotted versus the design operating turbine temperature to show the dependence of cost on this parameter. For $T_{hw} - T_{steam} =$

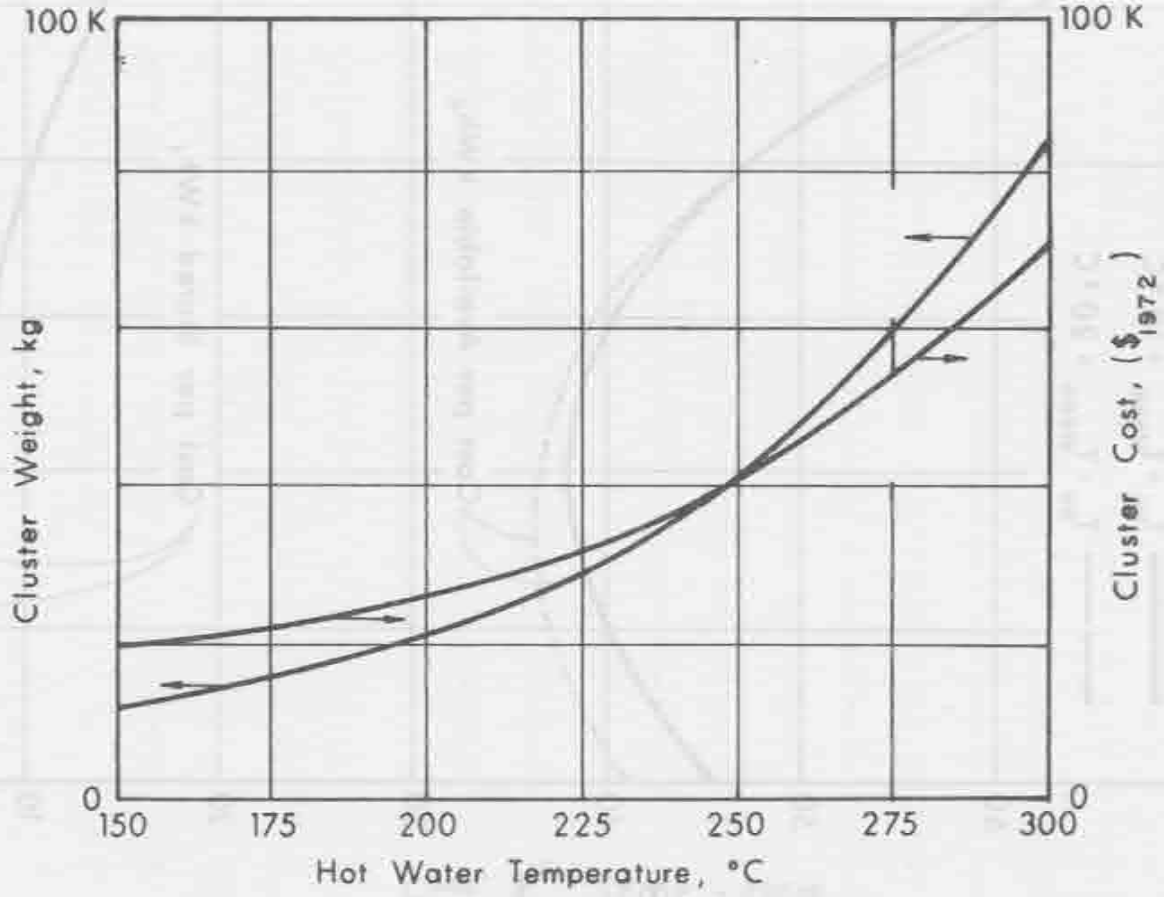

Figure 4-5. Hot Water Storage Weight and Cost (installed) per Standard Cluster.

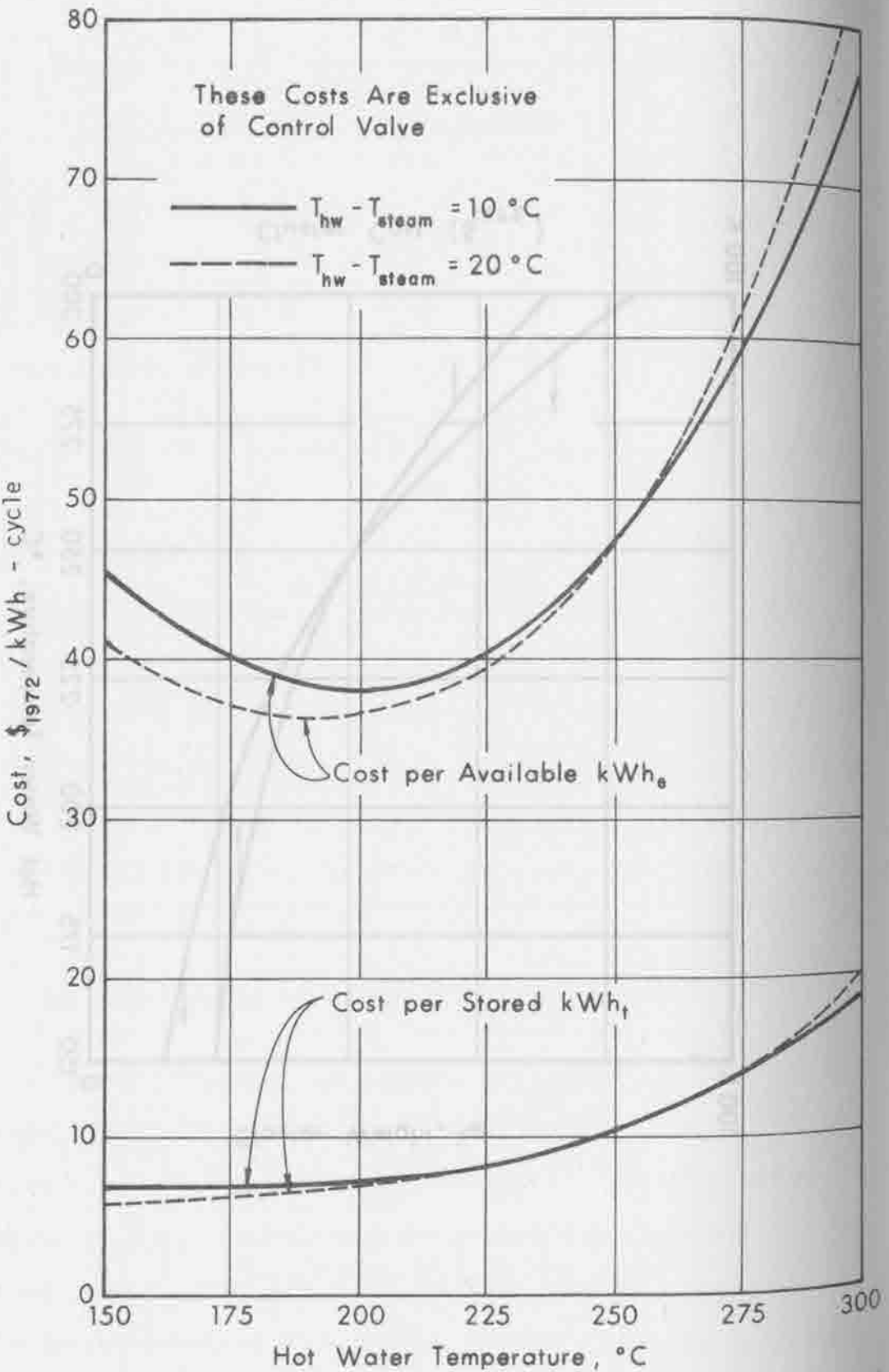

Figure 4-6. Hot Water Storage per kWh (electric and thermal) Exclusive of Control Valve. (Basis: 10 MW Turbine $T_c = 40^{o}C$, $\Delta T_{pinch} = 5^{o}C$).

10 and 20 °C, optima occur near $T_{i,steam}$ = 200 °C, but the case of $T_{hw} - T_{steam}$ = 20 °C is somewhat cheaper per kWh_e.

4.5.2 Valve Costing for Hot Water Storage

As opposed to steam accumulators, the cost of valves for stratified hot water displacement storage tanks is a significant fraction of the total system cost. This is because the energy flow per unit mass during discharge is from one to two orders of magnitude lower for hot water storage than for steam accumulators. Further, the energy availability is lower due to the irreversibility of the heat exchanger stage. The valve cost for a storage system will depend on the required rate of withdrawal (the turbine capacity). For purposes of this parametric cost study, the storage time is chosen as the additional parameter. (Note that for steam accumulators, the storage time is not a significant storage parameter except for impractically short storage times.)

If annualized valve costs are traded off against pumping head costs (i.e., cost of the power required to overcome the frictional losses of the valve), a reasonably well optimized choice of valve sizes may be made for a given maximum mass flow rate [Watt, A. D. and Wilcox, G. L. (1974)]. The simple relation

$$C_{valve} = .001244\ \dot{m}_{hw} \qquad (4\text{-}5)$$

where C_{valve} is in dollars (1972) and $\dot{m}$ is the hot water mass flow rate in kg/hr, may be used to calculate the cost of the optimum valve for this application. In Figure 4-7, C_{valve} is plotted versus design

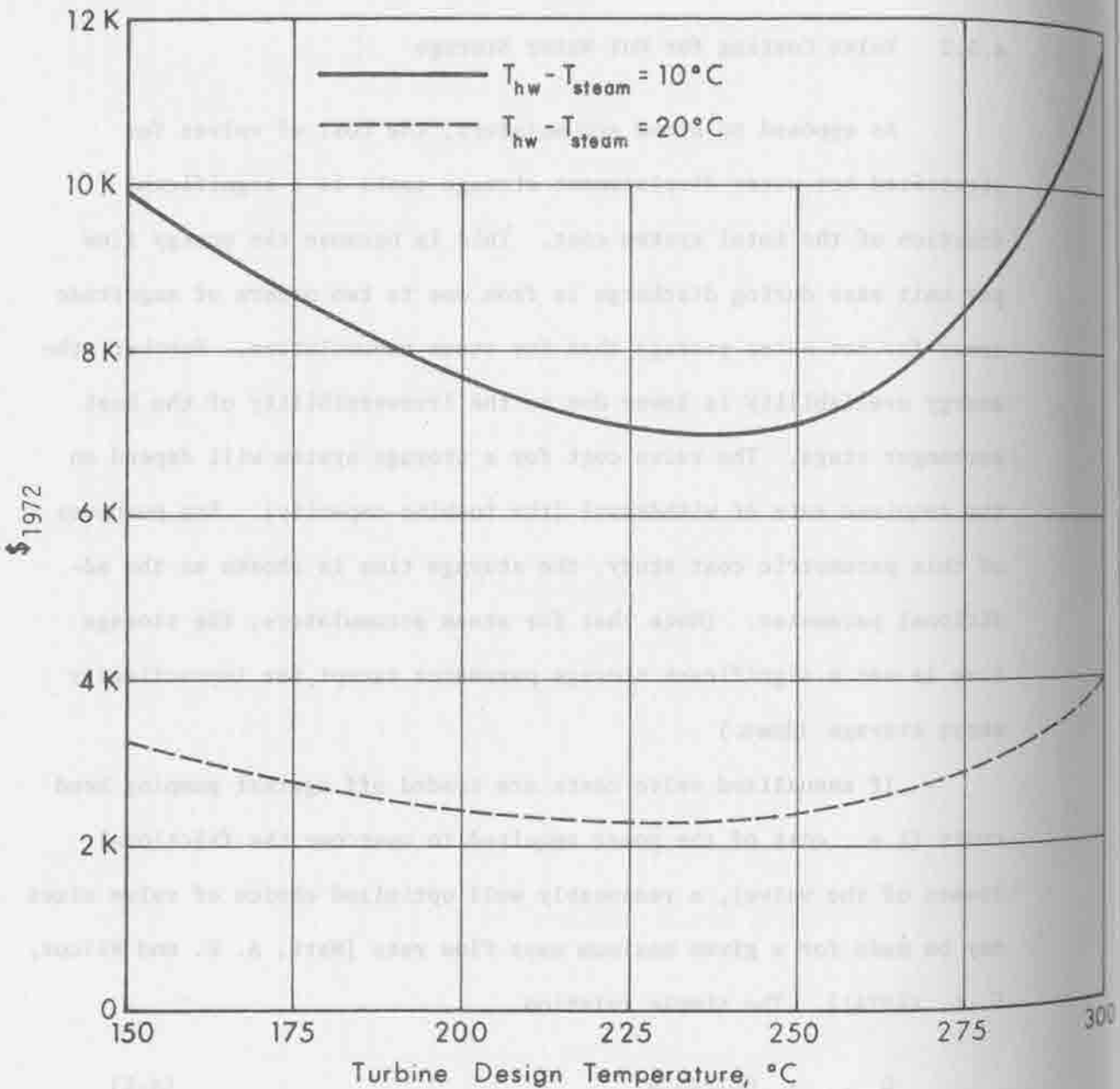

Figure 4-7. Control Valve Cost per Hot Water Storage Facility, (Basis: 10 MW_e Turbine T_c = 40 ^oC, ΔT_{pinch} = 5 ^oC).

operating steam turbine temperature for a standard tank cluster used with a 10 MW turbine operated with T_c = 40 °C. The multiplier P/10n may be used to adjust the valve cost per cluster to an n cluster system used with a turbine capacity of P (in MW).

4.5.3 Results

Typical results of hot water storage costs are plotted in Figures 4-8a and b. The plots are of cost per kWh_e versus design steam temperature, with the total storage time as a parameter. The parametric studies show that as the storage time is increased, the cost per kWh_e approaches the cost function of Figure 4-6. This is because, as the amount of storage increases, the valve cost per tank decreases until it becomes a negligible fraction of the total.

The general observations can be made that for realistic storage times (>.5 hours), the valve cost becomes insignificant rather rapidly. Further, the cost per available electrical energy unit is minimized for design steam temperatures around 200 °C. Also, somewhat cheaper storage is obtained for larger temperature drop discharge steps (i.e., $T_{hw} - T_{steam}$ = 20 °C). Finally, it appears that hot water storage is roughly twice as expensive as steam accumulator storage over the realistic operating temperature range of solar-thermal electric power systems.

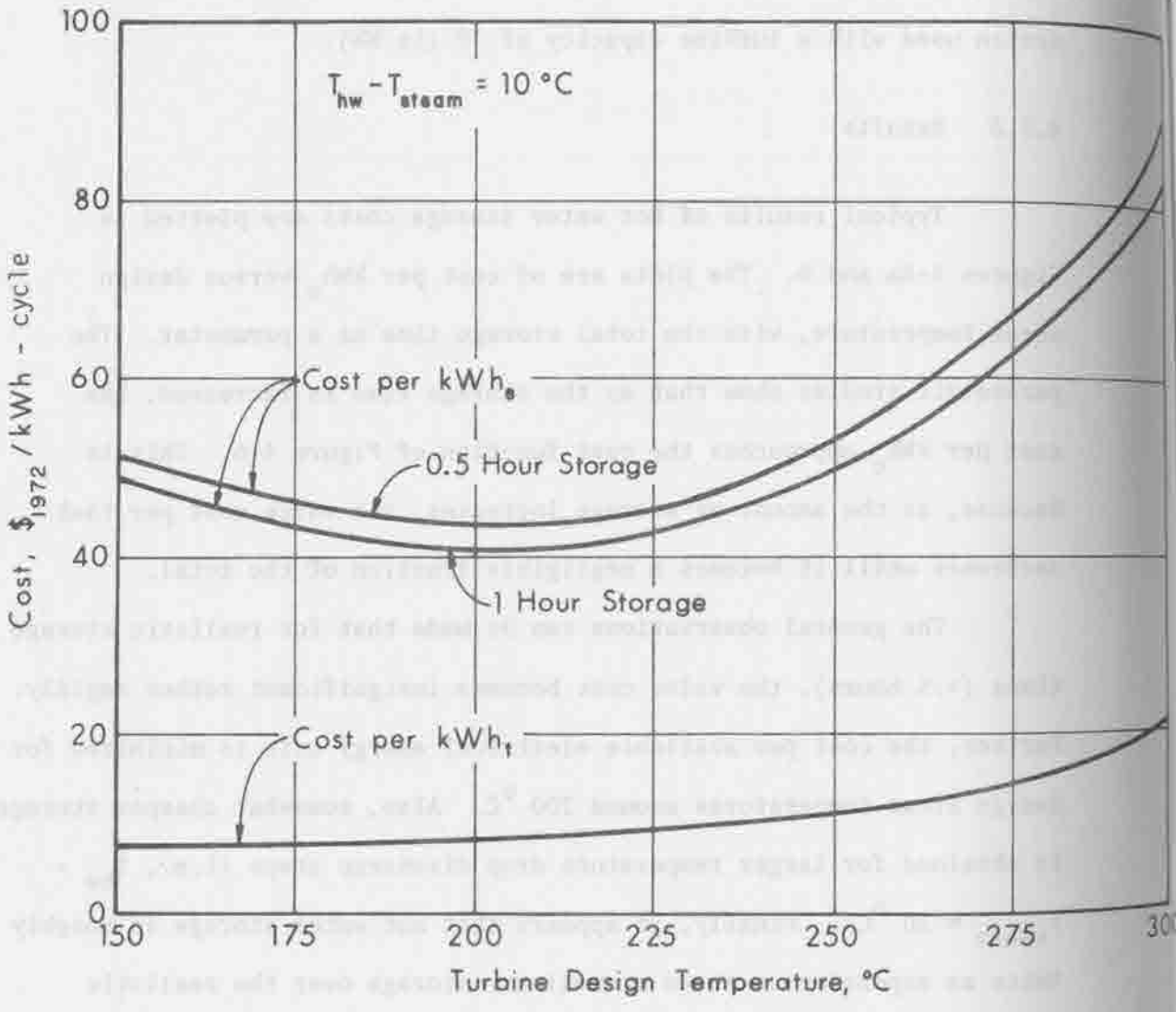

Figure 4-8a. Total Hot Water Storage Cost per kWh (thermal and electric) (Basis: 10 MW Turbine, $T_c = 40^{o}C$, $\Delta T_{pinch} = 5^{o}C$).

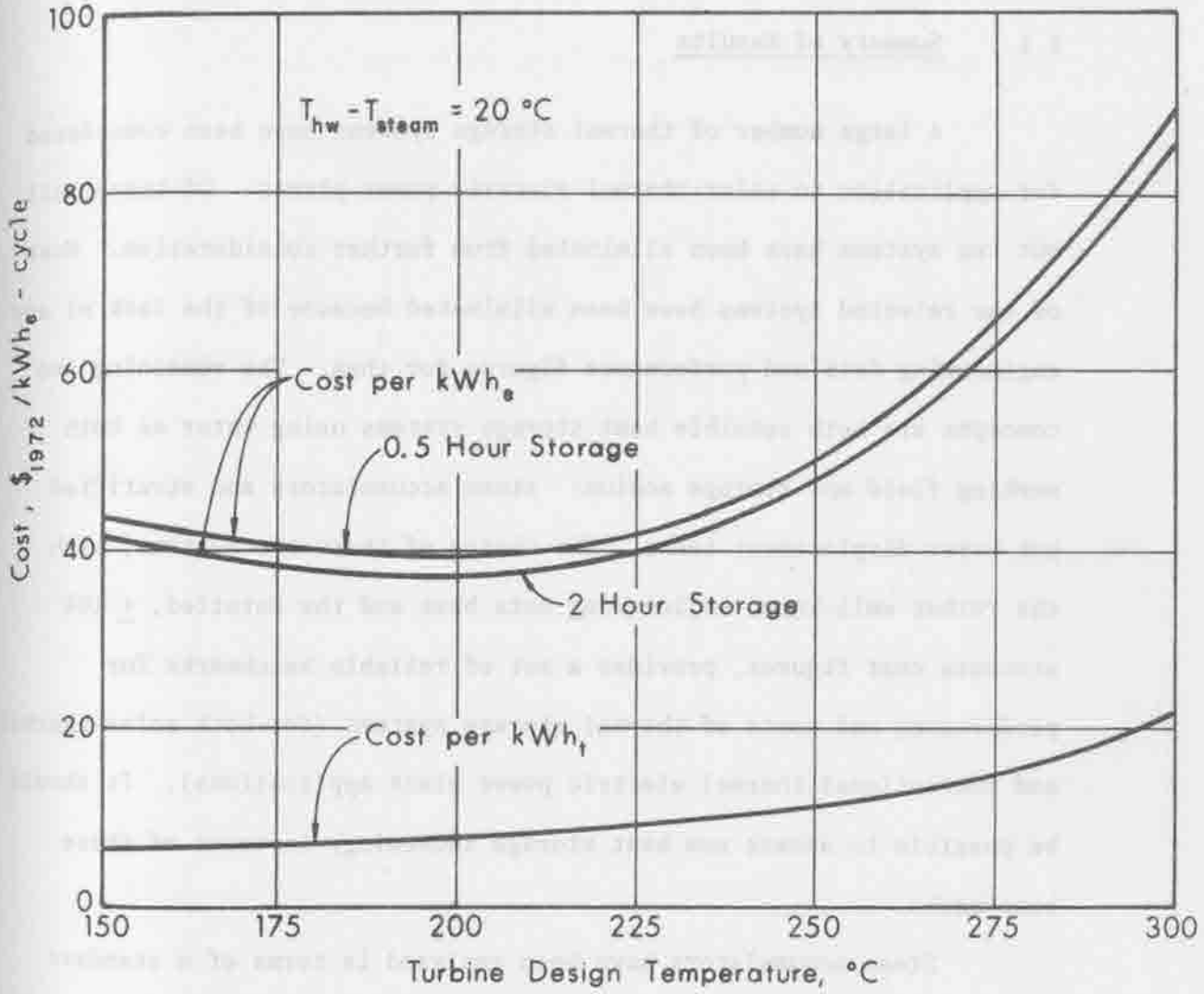

Figure 4-8b. Total Hot Water Storage Cost per kWh (thermal and electric). (Basis: 10 MW Turbine, $T_c = 40^{\circ}C$, $\Delta T_{pinch} = 5^{\circ}C$).

5.0 CONCLUSION

5.1 Summary of Results

A large number of thermal storage systems have been considered for application to solar-thermal electric power plants. Of these, all but two systems have been eliminated from further consideration. Most of the rejected systems have been eliminated because of the lack of any engineering data and performance figures for them. The remaining two concepts are both sensible heat storage systems using water as both working fluid and storage medium: steam accumulators and stratified hot water displacement tanks. The choice of these two systems, with the rather well-known engineering data base and the detailed, $\pm$ 10% accurate cost figures, provides a set of reliable benchmarks for performance and costs of thermal storage systems (for both solar-thermal and conventional thermal electric power plant applications). It should be possible to assess new heat storage technology in terms of these benchmarks.

Steam accumulators have been analyzed in terms of a standard accumulator design unit, the specifications of which are detailed in Table 3-1. These units are capable of storing in excess of 35 kWh_e of available electrical energy per cubic meter of vessel volume depending on temperature. The accumulator delivers dry saturated steam at a temperature and pressure which decrease with time. The condensing turbine used is designed to handle such variable steam inlet conditions. The costs of storage depend on the maximum storage temperature, which is the same as the turbine design temperature. At around 210 ^{o}C this

cost is minimized at ∿ \$16/kWh$_e$ * which coincides with ∿ \$3/kWh$_t$ as a cost of storing delivered steam.

Stratified hot water displacement storage tanks have been analyzed in terms of a standard tank cluster of seven individual units connected in series (see Table 4-1). These units are capable of storing in excess of 19 kWh$_e$ of available electrical energy per cubic meter of vessel volume depending on temperature. Hot water is pumped from the displacement storage tanks through a heat exchanger-boiler which produces dry saturated steam to run the condensing turbine. The cold water coming out of the heat exchanger is run into the bottom of the storage tank to replace the hot water removed at the top. Again, storage costs depend on temperature parameters, but they further depend somewhat on the storage time. For reasonable storage times, costs of ∿\$38/kWh$_e$, or ∿\$7/kWh$_t$ for storing delivered hot water, are achieved.

These cost figures are high enough to raise the question of whether or not hot water storage can really be used to trade off against turbine capacity. Still, the figures are presented here because of their possible value in assessing and optimizing total solar-thermal electric power systems.

Earlier calculations (CSU/Westinghouse, 1973) indicated that the steam accumulator presented a possible cost effective trade-off with peak heat engine capacity. The definitive answer to the question of whether and under what conditions such a trade-off would decrease the cost of solar thermal electric power must await a considerable extension of the simulation studies. Still, some simple calculations reported here reflect continued optimism about steam accumulator storage at lower operating temperatures in smaller sized plants. To compare heat

---

* 1972 dollars used throughout this report

engine costs, which are commonly given per unit of generating or heat rejection capacity, and steam accumulator costs, which are given per unit of deliverable electric energy, a common basis must be established. This common basis is conveniently provided by converting the heat engine/generator costs to dollars per kWh_e generated per day. Using the turbine generator cost figures from Appendix H (Figure 4-2) and the condenser and cooling tower cost data from Appendix I (Figures 2-2, 2-3, 3-4), approximate total capital costs per unit electrical power can be calculated. These figures are tabulated in the third column of Table 5-1. These cost figures may be converted to capital costs per unit electric energy per day by division by the average time per day which a plant operates effectively at capacity. The limited simulation results in Appendix J, Table 4-1, provide us with simulated performance of a 12 MW distributed collector plant at Albuquerque, New Mexico, El Paso, Texas, and Inyokern, California. The effective times at capacity for the four runs are tabulated below:

Albuquerque, N.M.	1962	6.1 hours;
Albuquerque, N.W.	1959	6.0 hours;
El Paso, Texas	1962	6.4 hours;
Inyokern, California	1962	6.9 hours

The fourth column in Table 5-1 is obtained by dividing the figures in column three by 6.0 hours, which is appropriate to the 1959 Albuquerque data. A direct comparison of these cost figures to the steam accumulator cost figures of Figure 3-7 is misleading, because Figure 3-7 does not account for storage efficiency (see Figure 5-1). The cost data from Figure 3-7 are divided by the storage efficiency figures, and tabulated in column five of Table 5-1.

Comparisons of the heat engine/generator and steam accumulator costs shows that, at least in certain operating conditions, storage can

TABLE 5-1

Comparison of Steam Accumulator and Heat Engine Costs for Various Plant Sizes and Design Operating Temperatures

		Installed Heat Engine Cost, including Turbine Generator, Condenser, Cooling Tower		Installed Steam Accum. Cost
Turbine Size MW	Design Operating Temp. (°C)	Per Unit Capacity ($/kW$_e$)	Per Unit Energy Per Day*	Per Unit Energy Per Day ($/kWh$_e$)
10	150	160.	27.	29.
10	200	140.	23.	21.
10	250	138.	22.	21.
10	300	128.	21.	23.
30	200	112.	19.	21.
10	200	88.	15.	21.

* Based on 6 hours of "effective capacity" operation per day (Albuquerque, New Mexico, 1959).

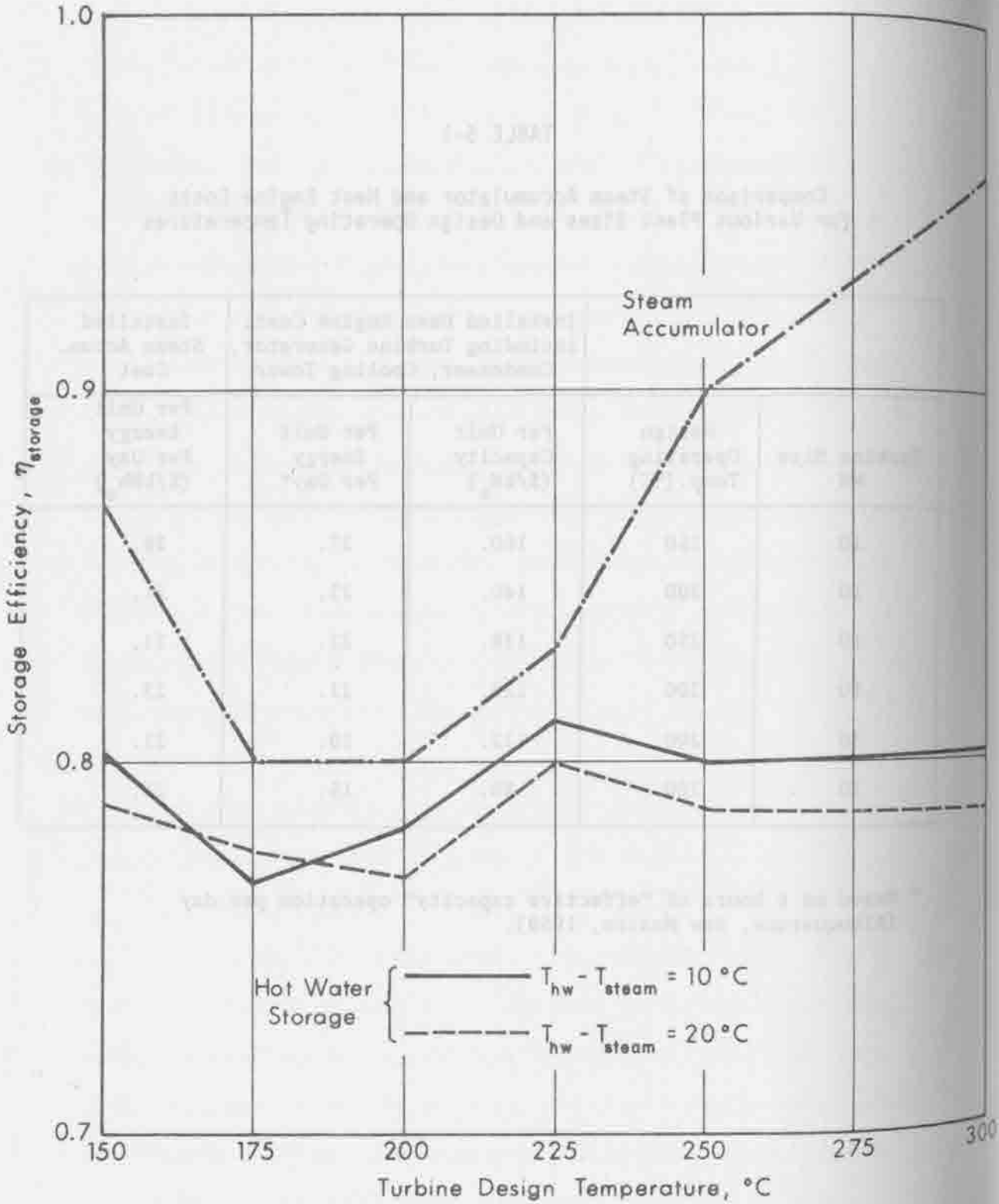

Figure 5-1. Storage Efficiencies for Steam Accumulator and Hot Water Displacement. (Basis: 10 MW Turbine T_c = 40 °C).

be used cost effectively to trade off against turbine peak capacity. The small amount of data in Table 5-1 show that the trade-off will be more cost effective for temperatures from -200 °C to -250 °C and for plant capacities of ∿30 MW or smaller. Parallel calculations with El Paso or Inyoker data show storage to be less feasible economically at such sites than at Albuquerque or other less favorable locations. The figures in Table 5-1 must be qualified by several factors, principally the choice of the effective hours at capacity. The most important thin to be learned from these calculations is that steam accumulator storage, besides being an attractive means to gain power generation flexibility, improved performance, and reliability, still promises to provide a cost effective trade-off for turbine generator capacity in small plants operated at low temperatures. A more precise statement of these limits on temperature, capacity, and other factors, including storage time, will await more extensive simulation results with a variety of solar plant types.

5.2 Comparison of Systems

The steam accumulator system indeed appears as the cheapest thermal storage system, if Figures 3-7 and 4-8a,b are compared. Accumulator storage is essentially half as expensive per kWh_e as hot water displacement storage. On this basis, hot water storage might be eliminated from further consideration. However, such subsystem optimization is neither really justifiable nor in the spirit of this study. The main reason for the cheaper cost of steam accumulator storage is the greater effective storage density of accumulators. Even though both accumulators and displacement tanks are sensible heat systems, the accumulator turns

out to be more attractive because of the fact that an accumulator actually loses mass as it is discharged, whereas the hot water storage tanks gain mass. The loss of mass in an accumulator contributes to a more complete exhaustion of useable thermal energy per unit volume during discharge. The performance figures of Figures 3-4 and 4-3, when converted to a per unit volume basis, confirm this point.

There is a further advantage to the steam accumulator, which is shown in the plots of storage efficiency in Figure 5-1. The plots clearly show the improved availability of energy stored in a steam accumulator, versus the availability of the same energy stored in a stratified hot water displacement tank. Note further that, overall, the larger temperature drop heat exchanger system ($20^{\circ}C$) reflects lower efficiency than the $10^{\circ}C$ system. The storage efficiency calculation of Figure 5-1 for steam accumulators is based on the delivery of thermal energy to the accumulator as steam. It therefore does not take into account any loss in availability due to a heat exchanger-boiler somewhere between the collector and the accumulator. Still the curve does relate directly to the efficiency of the storage cycle itself, because the same loss of energy availability occurs for the steam used to run the turbine as that used to charge the accumulator.

The curve for the steam accumulator in Figure 5-1 represents the worst case thermodynamically (that of charging steam at the turbine design temperature). It might be possible to charge an accumulator with lower temperature steam at the beginning of the day as the collector system is heating up. In this way, further improvements in the storage efficiency might be effected. It would not appear possible to achieve a similar effect in hot water storage, due to the presence of the heat exchanger/boiler.

5.3 Recommended Future Work

Further refinements in the design of steam accumulators and stratified hot water displacement storage could be of some use, but experimental work with turbine/thermal storage systems would be of greater benefit. The study of potential heat storage materials, such as eutectics, and systems, such as fusion heat exchangers, will be very important to solar energy exploitation in particular, and energy resource conservation in general.

ACKNOWLEDGMENT

The author acknowledges the support and assistance of many who made this work possible. J. R. Campbell (CSU) wrote and executed all the computer programs. A. D. Watt and G. L. Wilcox (WGL) provided considerable assistance on valve and pressure vessel costing. L. Ball (WGL) compiled a considerable amount of data on heat storage fluids. W. H. Brinkman and W. L. Garver (Stearns-Roger, Inc., Denver, Colorado) provided very helpful general consultation on the costing of pressure vessels, and the application of these techniques to steam accumulators.

REFERENCES

Aerospace Corporation (1972): Task Reports, NSF Contract #NSF-C716, task reports #1 through #5.

Brinkman, W. H., (1974): Stearns-Roger, Inc., Private Communication, (March).

Clark, F. D., and Terni, S. P., (1972): Thick-Wall Pressure Vessels, Chemical Engineering, pp. 112-116, (April).

CSU/Westinghouse, (1973): First Progress Report, NSF/RANN/SE/GI-37815/PR/73/2, (July).

CSU/Westinghouse, (1973): Annual Progress Report, NSF/RANN/SE/GI-37815/PR/73/4.

Dolezal, R., (1962): Output-Spray in Steam Generators with Frequency Control, Combustion, pp. 25-29.

Garver, W. L., (1974): Stearns-Roger, Inc., Private Communication, (August).

Goldstein, M., (1961): Some Physical-Chemical Aspects of Heat Storage, paper #S/7, U.N. Conference on New Energy Sources, Rome, Vol. 5, p. 411.

Goldstern, W., (1970): Steam Storage Accumulators, (Pergamon Press, London).

Hodgins, J. W., and Hoffman, T. W., (1955): The Storage and Transfer of Low Potential Heat, Canadian Journal of Technology, Vol. 33, pp. 293-302.

Hottell, H. C., (1974): Massachusetts Institute of Technology, Private Communication, (June).

Lamb, W. (1962-3): Steam Accumulators, Heating and Vent. Eng., Vol. 36, pp. 199-202, 263-265, 323-325, 382-384, 445-447.

Locklin, D. W., Droege, J. W., Ward, J. J., and Eibling, J. A., (1958): Summary Report of Methods of Heat Storage for the Heat Pump, Battelle Memorial Institute, (September).

Marguerre, F., (1933): New Heat Storage System, Power Plant Engineering, pp. 426-7, (October).

Reilly, A. J., (1960): Rapid Estimating for Pressure Vessels, Chemical Engineering, Vol.67, pp. 146-148.

Richardson Engineering Services, Inc. (1973): Process Plant Construction Estimating and Engineering Standards, Vol. 5, Division 15, Downey, California.

Schönholzer, E., (1969): Hygienic Clean Winter Space Heating with Solar and Hydroelectric Energy Accumulated During the Summer and Stored in Insulated Reservoirs, Solar Energy, Vol. 12, pp. 379-385.

Telkes, M., (1964): Solar-Heat Storage, ASME Winter Annual Meeting, ASME Paper #64-WA/SOL-9, (November).

Telkes, M., and Raymond, E., (1949): Storing Solar Heat in Chemicals - A Report on the Dover House, Heating and Ventilating, Vol. 46, pp. 80-86.

University of Minnesota/Honeywell, (1972): The Minnesota/Honeywell Solar Power Concept, (October).

University of Pennsylvania, (1971): Conservation and Better Utilization of Electric Power By Means of Thermal Energy Storage and Solar Heating, NSF Grant #GI-27976, (October).

Watt, A. D., and Wilcox, G. L., (1974): Westinghouse Georesearch Laboratory, Private Communication, (July).

APPENDIX H

HEAT ENGINES

BY

F. A. BELDECOS,
R. J. BUDENHOLZER,
D. Q. HOOVER,
C. D. BEACH,
A. D. WATT,
AND
G. WILCOX

1.0 INTRODUCTION

The choice of an engine for converting heat into work depends on the temperature and the rate at which heat is supplied. In internal combustion engines the source of the heat is important, but in engines for which the working fluid is heated outside of the engine, the source of the heat is immaterial as long as the characteristics of the heat supplied are identical.

When solar energy is used as a heat source in place of a fuel, the principal difference in the character of the supplied heat is its time variability. Thus in solar energy use the temperature may be chosen, but the rate of heat is dependent on collector and storage subsystem design, and the variable nature of the sunshine that reaches the earth.

Many technical areas can be immediately defined which require intensive investigation in order to develop a solar operated heat engine having the characteristics and capability to operate reliably, and in many instances, in parallel with existing large generating systems. Only three technical areas will be identified and reviewed in this appendix.

The first area is the problem of choice of thermodynamic heat cycle. This includes the choice of working fluids and consideration of the cycle limitations. The second is the power conversion system, particularly the principles and problems of heat engines. The third and final area of consideration is the heat rejection system of the heat cycle and its characteristics.

In addition, it could be noted that an operating fluid in any heat cycle is subjected to the same four sequences of events--namely,

(1) compression, (2) heating, (3) expansion, and (4) cooling. What man has been able to invent are merely ingenious ways of utilizing those fundamental principles to ultimately produce machines that extract more useful work.

2.0 PRACTICAL HEAT CYCLES

Few areas of modern technology have benefited from more consistent and fruitful development than the design of cycles and equipment for the conversion of heat into work. Clearly, there is no unique choice of cycle or equipment which provides the best source of power for all applications. Rather, several very different classes of prime movers have enjoyed parallel development because of their marked advantages in dissimilar applications.

2.1 Commonly Used Cycles

The reciprocating Otto and Diesel Cycles use air as a working fluid and find wide application as inexpensive, small scale power sources, but by no means do they approach Carnot efficiency. They are inherently limited in power output by large size requirements for a given fluid mass flow rate.

The gas turbine is finding greater and greater use as a power sources for moderate to high output and moderate efficiency. The design is well adapted to handling very high working fluid mass flow rates, and in fact its use at low output levels requires small, highly toleranced, and expensive engine components. Attainment of reasonable efficiency has been historically tied to attainment of very high turbine inlet temperatures, which are generally available only with direct internal combustion. Many enhancements to the simple gas turbine cycle are possible which can significantly improve efficiency. Their application, however, requires extensive heat transfer apparatus which is capable of transferring heat with low losses to very large volumes of working fluid per unit of power output.

For large central station power generation, a modified Rankine cycle has dominated the market due to its unexcelled efficiency, reliability, and adaptability to large output designs. Because practical embodiments of the Rankine cycle have most closely approached the ideal Carnot efficiency, this cycle must be very attractive for solar power applications, where collection of input heat, especially at high temperatures, is very difficult. The discussions which follow are most specifically directed toward Rankine cycle engines; not to the exclusion of other alternatives, but to provide a logical background to the state of the art in central station cycle development.

An interesting candidate for solar power applications is the Stirling cycle, which promises theoretical efficiencies approaching the ideal. For this reason alone, it merits considerable attention. But since practical embodiments of the cycle involve reciprocating machinery similar to that of the Otto and Diesel Cycles, application seems best suited to small power outputs. The fact that heat input requires convective heat transfer to large volumes of low density gas reinforces the same conclusion.

2.2 The Rankine Cycle

Although the Carnot cycle provides a theoretical means of obtaining maximum conversion efficiency, its practical application leaves much to be desired. For instance, application of the Carnot cycle to steam could involve compression and expansion of excessively moist fluids, which lead to erosion problems in engines, as well as high aerodynamic losses. In addition, the work required to compress a vapor or gas is a rather high fraction of that which is extracted through

expansion. This not only involves large compressors, but reduces the net work output from the cycle.

A more practical cycle is achieved by modifying the Carnot cycle to accomplish the compression process in the liquid phase. In this way the work of compression is minimized by the low fluid volume. Such a cycle is shown in Figure 2-1 and is known as an ideal Rankine cycle. The isentropic compression of the Carnot cycle is replaced by three processes which include condensation of the vapor at constant pressure along the path AA', isentropic compression of the fluid along the path A'B', and isobaric heating of the fluid to the point B. State B' is drawn off scale simply to illustrate the compression process which would not otherwise be visible.

The efficiency of this cycle is lower than that of the Carnot cycle operating with the same upper and lower temperature limits. This can be recognized by dividing the overall cycle into a large number of arbitrarily narrow Carnot cycles as shown in Figure 2-2. The cycle is now approximated by many smaller cycles, some of which operate with the original Carnot efficiency, but many of which convert a portion of the input heat to useful work with efficiency somewhat below that of the parent cycle.

Theoretically, this net degradation of efficiency can be completely eliminated through the use of regenerative feedwater heating. The T-S diagram of a regenerative Rankine cycle is shown in Figure 2-3. Almost all of the heat is added to the fluid at the maximum cycle temperature along the path AB, before passing into the engine. At some point C during the expansion process, a small fraction of the fluid is

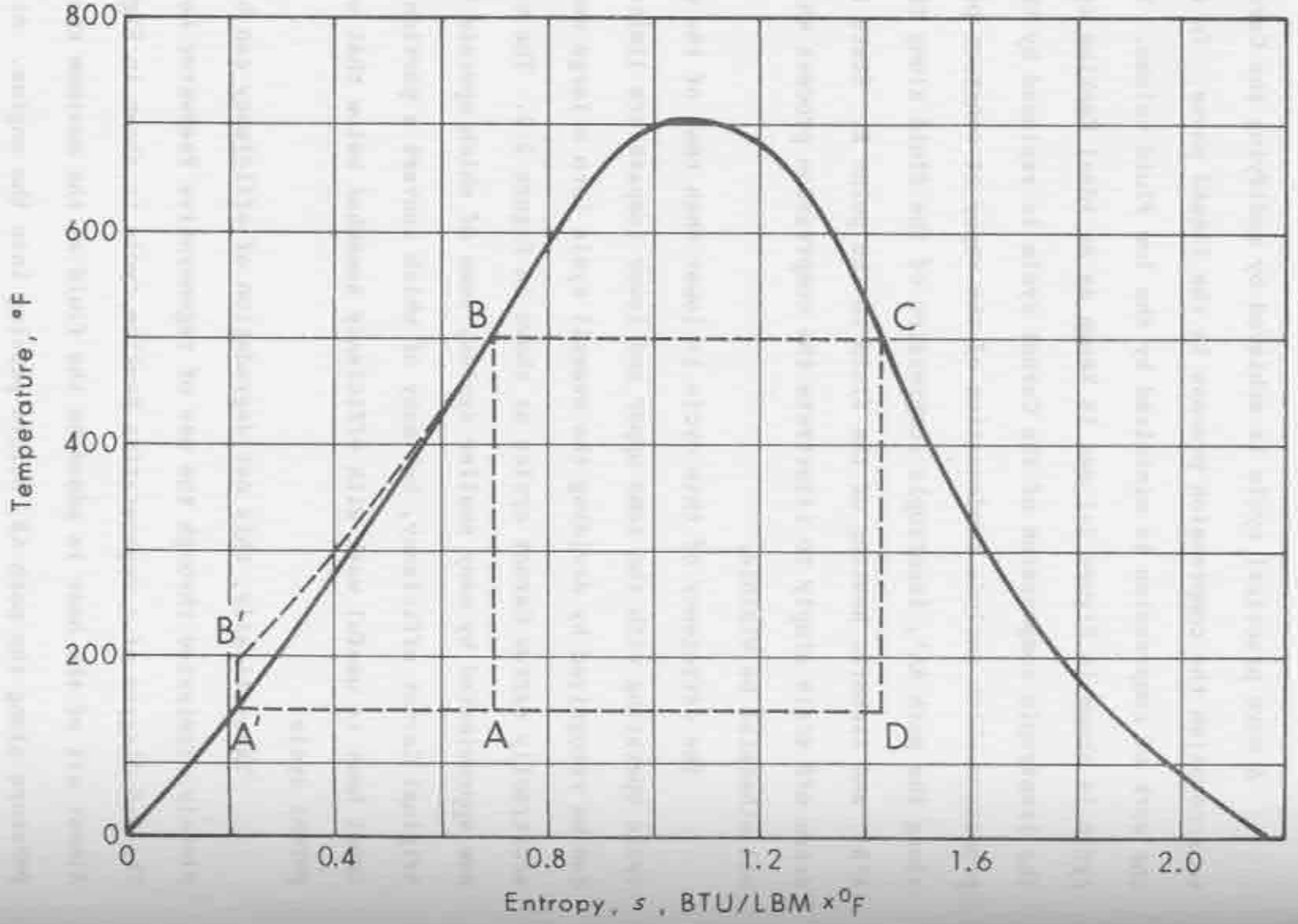

Figure 2-1. Idealized Rankine Cycle Using Water. The Isentropic Compression A'B' is exagerated. The Cycle A B C D would be a Carnot Cycle.

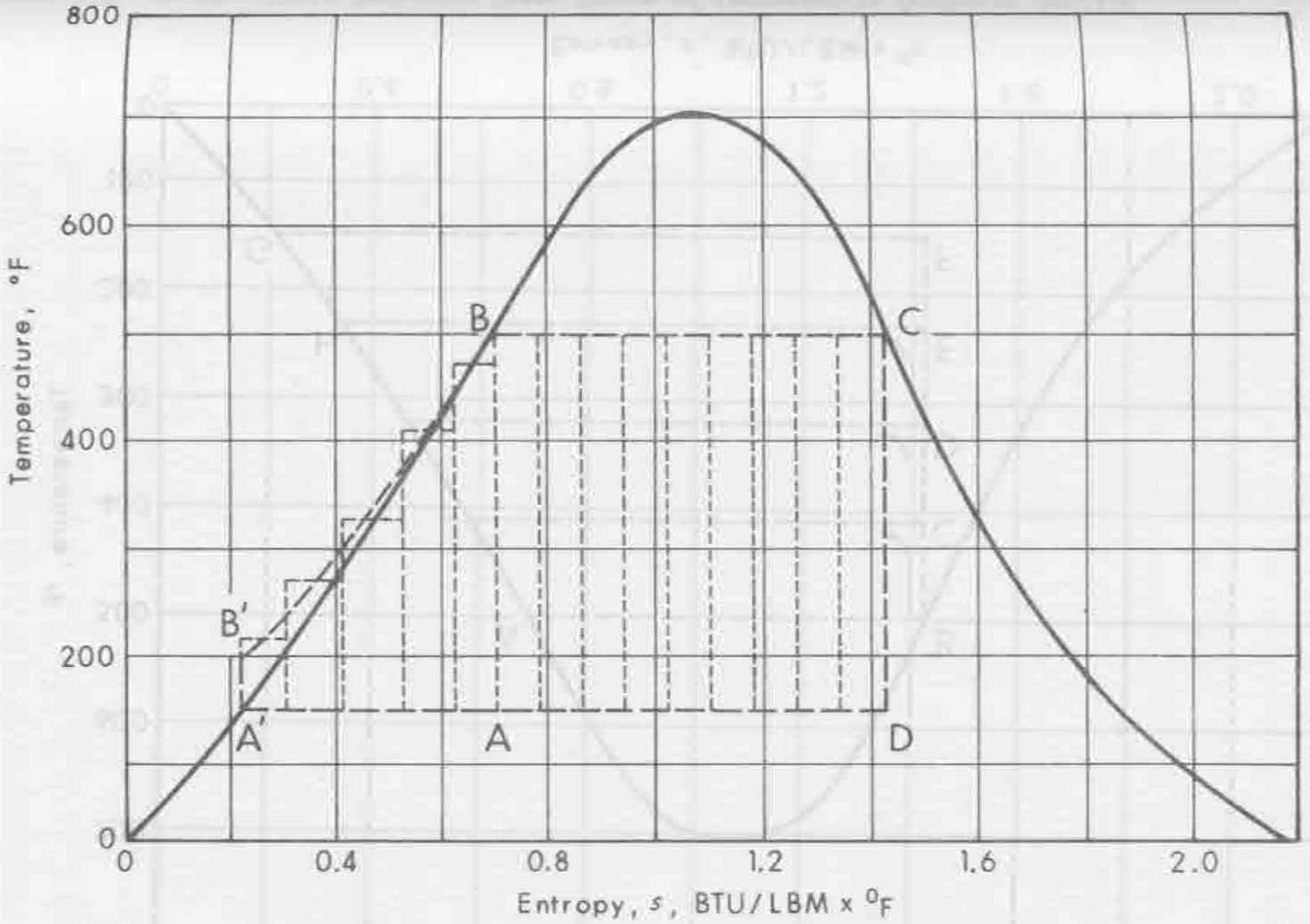

Figure 2-2. Idealized Rankine Cycle Approximated by Several Carnot Cycles.

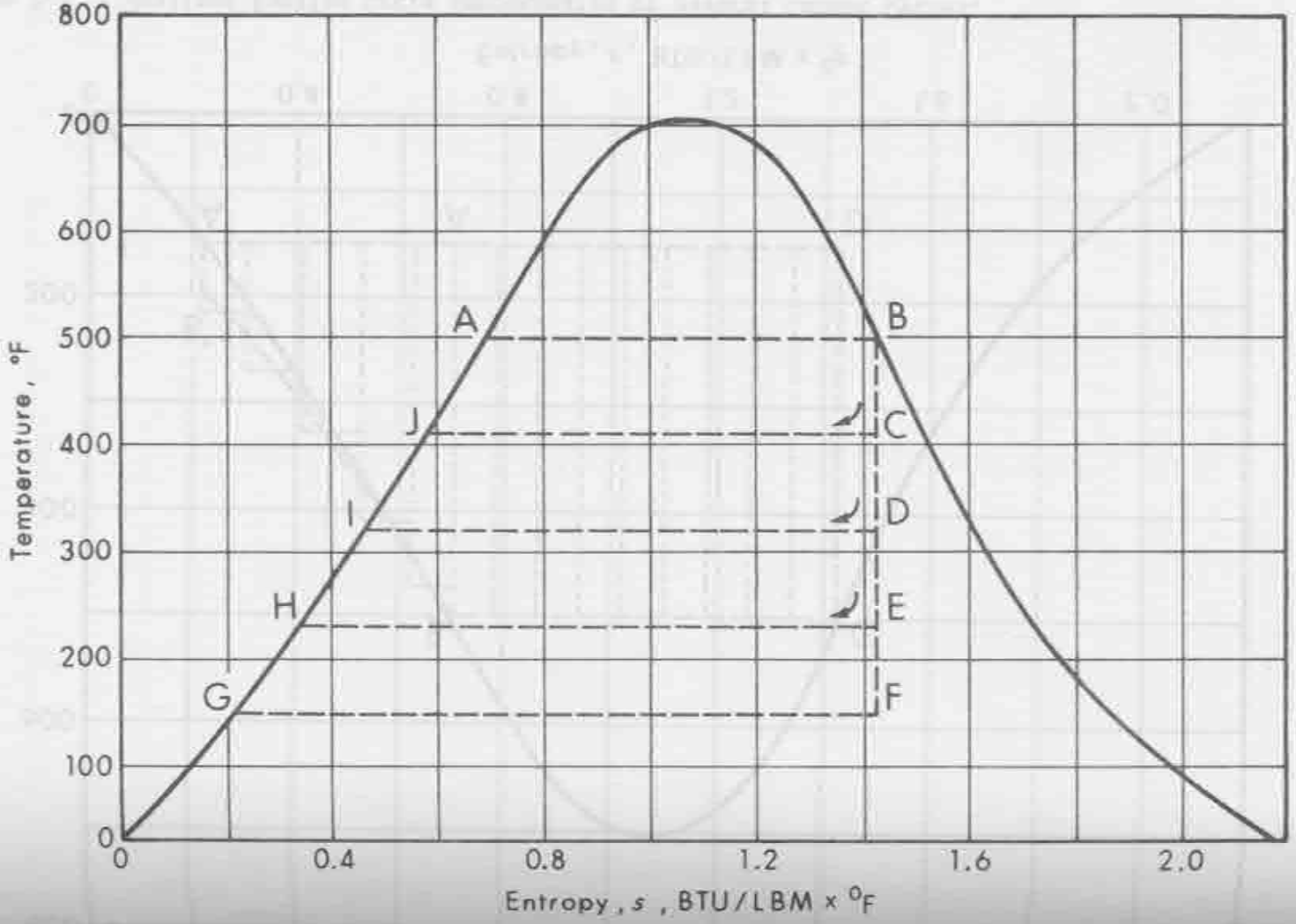

Figure 2-3. Rankine Cycle Employing Three Stages of Regenerative Feedwater Heating.

extracted from the turbine and condensed at nearly constant pressure. Its latent heat is used to supply the heat requirements of the isobaric feedwater heating process IJ, and the condensate is itself mixed with the feedwater. Only a small quantity of heat is required below the maximum cycle temperature to raise the feedwater temperature from state I to state A. Several similar stages of steam extraction and feedwater heating are encountered during the expansion, and perhaps only 65 percent of the engine inlet mass flow reaches the condenser.

If a cycle could be constructed with an infinite number of feedwater heaters with infinitesimal resistance to heat transfer, then the cycle could be made entirely reversible and thus equal the ideal Carnot efficiency. Practically speaking, modern steam cycles use five to seven heaters to minimize irreversibilities in the regenerative feedheating process.

Two important benefits accrue from the use of regenerative feedwater heating in the conventional steam Rankine cycles. First, a larger portion of the cycle work is obtained from steam at the highest cycle pressures. This allows the use of more compact machinery. The engine condensing end, which is large due to the very low exhaust steam density, must be made only large enough to handle the inlet steam flow minus the steam extracted for feedheating.

Secondly, there is potential for moisture removal during extraction. Engines can be designed so that the extracted steam contains a higher than average fraction of moisture, leaving higher quality steam to continue expansion. Such designs, especially applicable to today's nuclear plant low pressure turbines, can significantly reduce blade erosion damage due to moisture.

Modern steam power cycles embody two additional features which surprisingly decrease the theoretical efficiency of the cycle relative to the Carnot cycle. These are superheat and resuperheating. This anomally requires some explanation.

The critical point for steam occurs at 705.4 ^{o}F and a pressure of 3206.2 psia. The Rankine cycles which have been illustrated thus far involve evaporative heat input which is both isothermal and isobaric, so that most heat input occurs at the maximum cycle temperature. This is a sound theoretical objective only insofar as it does not place a limit on the maximum cycle temperature. This indeed is the case with water in conventional steam plants. Metallurgically, heat engines and steam generators can be designed to operate continuously at temperatures exceeding 1100 ^{o}F, so that more efficient cycles are indeed possible. It is not, however, practical to add all of the heat at such a temperature because this would require a complex process of heating with a well controlled decrease in pressure. But several means are available for approaching a goal of maximum heat input at the highest cycle temperatures.

First, the fluid is superheated to raise the maximum temperature to perhaps 1100 ^{o}F. Introducing the concept of replacing a cycle by an arbitrarily large number of hypothetical Carnot cycles, it is evident that the addition of superheat, as illustrated by the cycle ABCDE in Figure 2-4, will increase the overall cycle efficiency. However, a majority of the heat is still added at lower temperatures during the evaporative process.

A greater proportion of heat may be added above the saturation temperature by introducing one stage of resuperheating by the cycle ABCDEFG as shown in Figure 2-5. By expanding the superheated steam

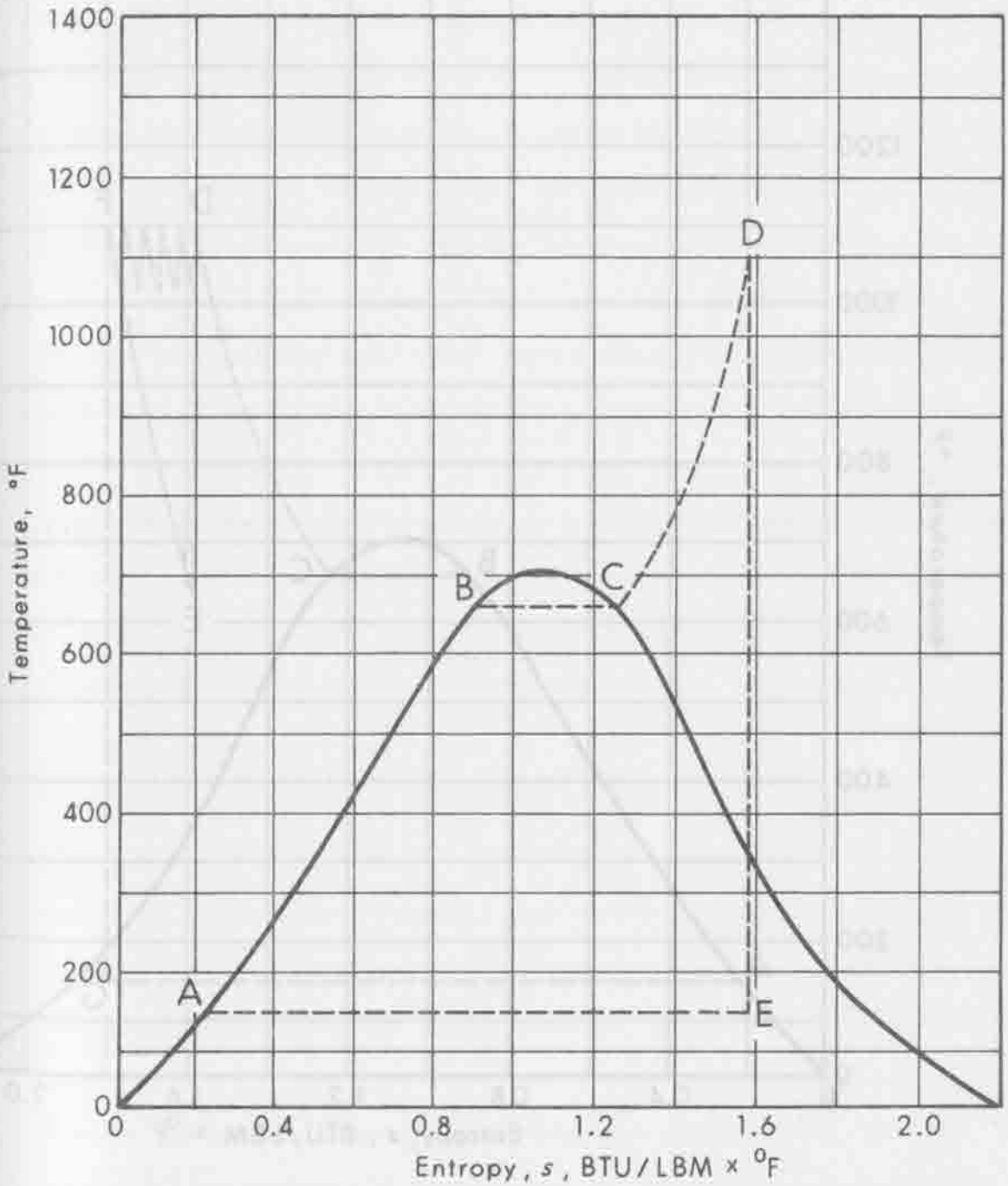

Figure 2-4. Rankine Cycle with Superheat.

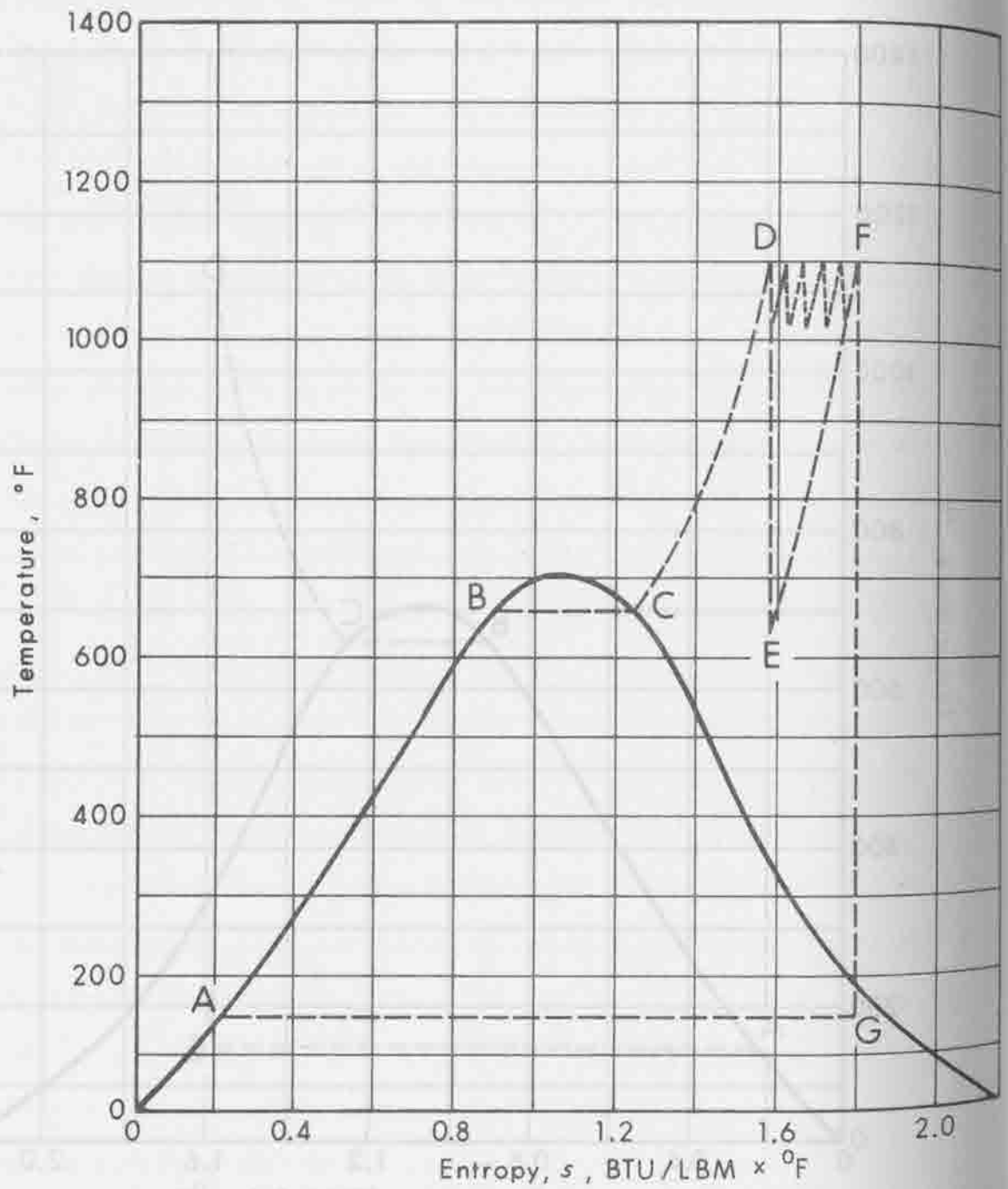

Figure 2-5. Rankine Cycle with Single and Multiple Resuperheating Stages.

to lower pressures, then resuperheating it to the maximum cycle temperature, and repeating this process for an arbitrarily large number of cycles, one can approach the controlled pressure decrease which is necessary for isothermal heat input from states D to F. Actually the practical limit to such an ideal strategy is in the cost of moving fluids to and from the engine from the heat source, but an ultimate limit results from irreversible pressure losses which degrade the cycle performance. Aside from the benefits of superheat and resuperheating to theoretical cycle efficiency, they are necessary to limit moisture formation in the low pressure end of the engine, thus greatly reducing erosion of critical engine components.

An alternative method of increasing the average temperature of heat input to the engine is to add heat at supercritical pressures. This results in a modest improvement in efficiency but is primarily justified by providing higher heat transfer rates in the heat input portion of the cycle, and thus more economical equipment.

2.3 The Ideal Working Fluid

From the preceding discussion of conventional Rankine cycle adaptation to steam power plants, various problems become evident. First, it is seen that regenerative feedwater heating is necessary to minimize the amount of heat addition to the fluid at low temperature. Second, both superheat and one or more resuperheating stages serve to increase the average temperature of heat input, while reducing the fraction of moisture which will develop in the expansion process. It is recognized that all of these additional processes are invented to avoid certain undesirable properties of water, namely, the specific heat at constant pressure of the liquid phase, the critical temperature

and pressure of the fluid, and the slope of the saturation line in the vicinity of the engine expansion line. Knowing the motivations for the various enhancements to the ideal Rankine cycle, it becomes possible to characterize properties of some hypothetical fluid which might allow a return to a more basic Rankine vapor cycle. The incentives for doing this include a reduction in the cost and complexity of the cycle equipment, and an increase in the efficiency of the cycle.

From strictly thermodynamic considerations, it is recognized that an ideal fluid should have the following properties:

1) The critical temperature should be well in excess of the maximum cycle temperature, so that isothermal heat input may be accomplished at the maximum temperature while at constant pressure.

2) The specific heat at constant pressure of the liquid phase should be low in order to minimize the requirement for costly, and somewhat irreversible regenerative feedwater heating, or alternatively to minimize direct heat input at temperatures below the maximum.

3) The saturation line in the vicinity of the turbine expansion line should be nearly isentropic. A negative slope, such as that of water, results in excessive moisture. A positive slope, on the other hand, results in superheat of the turbine exhaust. Desuperheating, obviously required prior to condensation, makes heat available at a temperature somewhat higher than that of condensation. If this heat is rejected in the condenser, it represents a loss to the cycle efficiency. Alternatively it may be applied to feedwater heating, but only at considerable expense.

In addition to these strictly thermodynamic considerations, several practical design considerations present themselves as follows:

4) The fluid must be chemically stable at the maximum cycle temperature.

5) The isentropic enthalpy drop which is available during expansion should be high, resulting in lower mass requirements and reduced equipment size.

6) The vapor pressure of the fluid at the maximum cycle temperature should be low enough so that material stress levels can be decreased.

7) The vapor pressure of the fluid at the condensing temperature should be high enough to minimize equipment size and problems of ejection of non-condensible gases.

8) The heat transfer properties of the fluid should be good, to minimize the cost of steam generators, condensers, and feedwater heaters.

9) The freezing point of the fluid should be low to eliminate handling difficulties as well as freeze damage to equipment.

10) The cost of the fluid should be low.

The challenge of obtaining useful work from solar energy presents a framework for heat cycle optimization which is quite different from that in which today's steam power cycles have evolved. The maximum temperature limits which are common to conventional steam plants due to metallurgical limitations are undercut by economic considerations which recognize a high cost for solar heat collection at high temperatures. The well known increase in heat cycle efficiency with temperature must be optimally reconciled with the reverse characteristic for solar collector efficiency. The inevitable decrease in cycle temperature levels, combined with a high cost of heat collection, provide great incentive for the closest possible approach to ideal heat engine efficiency levels.

2.4 Heat Engine Design Variables

In reviewing the previous discussion it is apparent that present day power cycles are designed to manage the complex task of converting various energy forms by processes that are both economical and socially acceptable. So that conventional power cycles can perform their function they first require a source of heat energy that must be transferred to some motive fluid. Next, and most importantly, the power cycles must be

designed to produce useful mechanical work that can be transformed (electrically), transmitted, distributed, and utilized by the end users. Finally, power cycles must reject energy in a controlled manner to cooler environments such as the earth's waters, the earth's atmosphere, or in rarer instances, to outer space. Each of the three elements of a power cycle (heat supply, work output, and heat rejection) possess singular and unique problems in addition to those important problems they share because of their interdependence or relationship within a given power cycle.

From the point of view of one subsystem within the heat cycle such as an engine that produces useful work ... and in particular prime movers and electric generators .... The concept of useful work is important because it can reveal what design freedoms will exist for the machine builders of the future to harness solar energy systems.

The most direct manner of conceptualizing the problem areas that the future designers of these systems will face is to combine the simple physical definitions of useful work, of mechanical shaft torque, and of electrical torque. These elementary manipulations are developed in such a manner that from these physical concepts the basic engineering design parameters for prime movers or heat engines can be delineated.

These parameters are expressed in terms of the major prime mover and generator terminal characteristics and appear in Table 2-1.

TABLE 2-1

Prime Mover and Generator System Design Parameters

Prime Mover	Generator
1. Flow Rate (Fluid)	1. Current Flow
2. Inlet State Point (Fluid)	2. Voltage
3. Pressure Ratio (Fluid)	3. *
4. Speed of Shaft	4. Speed of Shaft
5. Efficiency of Conversion	5. Efficiency of Conversion

* The analogy here might be viewed as "ground potential."

The most obvious conclusion drawn from Table 2-1 is that all prime movers can be completely described in a most elementary manner by means of only five system design parameters. The same conclusion holds for electrical machines. However, in this instance the technology of electrical machines is well developed and may undergo only minor impact. The primary emphasis in this analysis will naturally be directed to the problems of the prime mover, where the state of the art may require the development of corrolary technologies in the application of solar energies.

Since the prime mover will remain the focal point of this study, it is appropriate to define more fully the five system design parameters relating to the prime mover and demonstrate their importance to the engineering design functions.

1. Mass Flow Rate (Fluid) -- $\dot{m}$. The production of prime movers with large power capabilities is critically dependent on large fluid mass flow rates (water, steam, air, ammonia, etc.). Consequently, the primary heat source (input) to the fluid mass must be potentially capable of extrapolation to the large sizes which are necessary for economic power generation.

2. Inlet State Point (Fluid) -- P,T. Traditionally, the thermodynamic conditions or state of a particular fluid (enthalpy, H) determined the energy level (above some reference level) of the fluid. Within the context of this study, the concept has been enlarged to include the totality of physical fluid properties to which a prime mover designer must relate. Pressure (P) and temperature (T), although embodied in the notation (P,T), are intended to include among other properties - the purity of fluid, the chemistry of the fluid and other such factors as fluid radioactivity within which a reference frame can be defined for the fluid entering the prime mover.

3. Pressure Ratio (Fluid) -- ρ. The notion of a pressure ratio relates to the total energy available (H) to the prime mover for conversion to useful work. In an analogous manner, the notion could relate to the condition of the heat sink (i.e.; condenser pressure) to which level the prime mover must reject the unused energy of its motive fluid. It clearly follows that the ideal state is to strive to develop engines with reasonably large pressure ratios (ρ) although this is by no means a limiting consideration to any prime mover design. It is nevertheless an important impediment to most engines if not obtainable.

4. Speed of Shaft -- σ_s. For commercial power productions in the United States, alternating electricity must be generated at some established frequency, consequently the shaft speeds of both prime movers and the electric generators must be carefully controlled. The discrete acceptable speeds of the electrical machines can be developed according to the following formula.

$$\text{Shaft Rpm} = \frac{120 \times \text{system frequency}}{\text{Number of generator poles}} \qquad (2\text{-}1)$$

For the 60 Hz generation systems of the United States this works out to be as shown in Table 2-2 below for up to ten generator poles.

TABLE 2-2

Acceptable Speeds for Prime Mover and Generator Shafts

No. of Poles	Rpm
2	3600
4	1800
6	1200
8	900
10	720

For 50 Hz generation systems, the shaft speeds would be 5/6 of those shown.

5. Efficiency of Conversion -- η. The usefulness of any machine, particularly those for power generation, is in large measure determined by the degree that energy inputs can be converted to satisfactory levels of useful work. Consequently, the efficiency of

conversion (η) embodies not only the basic efficiency of the heat cycle but the efficiency of the engine (and generator) components through a wide spectrum of loads or operating modes.

In summary, a prime mover viewed as a subsystem of a power network incorporates each of the five system design parameters described above. It must be understood that all prime movers are designed only after making a descrete choice for each of the design parameters ($\dot{m}$, P,T, ρ, σ, η). This does not imply that prime movers cannot be "operated" within different ranges of $\dot{m}$'s, ρ's, σ's, etc. -- it implies that only <u>one</u> discrete choice from each parameter is permitted in the "design" process.

Since the "design" process may be viewed as a process that translates the design parameters to physical dimensions (drawings, hardware, etc.) the following relationship must hold:

$$\text{Physical Dimensions of Prime Mover} = f(\dot{m}, P, T, \rho, \sigma, \eta) \tag{2-3}$$

A somewhat clearer understanding could be developed if the prime mover were restricted to a turbine possessing n stages. Each turbine stage would be designed to its unique set of design parameters so that the equation would be restructured as follows:

$$\text{Physical Dimensions of Turbine} = \sum_{i = \text{Stage 1}}^{\text{Stage n}} f(\gamma, PT, \rho, \sigma, \eta) \tag{2-4}$$

The above equation should leave no doubt that turbine stage No. 1 and the last turbine stage, No. n, must be designed for two widely

differing environments. But the sum, comprising stage No. 1 to n, will actually control the basic dimensional requirements of the turbine.

The usefulness of the above concept is not restricted to heat engines and holds even if applied to pumps, compressors, or other rotating machine employing fluids. This factor will be true as long as the equations shown allow for both positive and negative values of the design parameters. For example, a turbo-compressor could be viewed as having a "negative" pressure ratio ($-\rho$), flow rates ($-\dot{m}$), and perhaps efficiency ($-\eta$). Similar analogies could be developed for pumps and hydro-electric turbines with little difficulty.

The major usefulness of the concept embodied in the notation $f(\dot{m}, PT, \rho, \sigma, \eta)$ is that product life and product costs also fall within this conceptual framework and are clearly related to the choices required by the system.

Since the prime mover will be subjected to a wide range of forces and stresses during its operation, i.e.; centrifugal, thermal, pressure, vibratory, etc., the physical dimension of the equipment will be physically strained to accommodate the new equilibrium state of the forces acting. This change in physical dimensions could be expressed as:

$$\Delta f(\dot{m}, PT, \rho, \sigma, \eta) = \text{equivalent strain} \qquad (2\text{-}4)$$

Since these strains must occur or must exist over some finite time periods ($\Delta\theta$), it is more proper to introduce time (θ) into the above equation so that it can be expressed as:

$$\frac{\Delta f}{\Delta\theta}\ (\dot{m}, PT, \rho, \sigma, \eta) = \text{strain/time interval} \qquad (2\text{-}5)$$

The concept of equipment lifetimes can be viewed as the frequency (number of cycles) with which a particular component has been subjected to certain levels of strain. This process is usually referred to as the "duty cycle" of the equipment but poses the most severe problem to the designer. First, he must make an estimate (at best) on how the equipment will be operated and second, after estimating the "duty cycle", make a decision on the economic life-cycle of the particular equipment (should it last 120 seconds as a space rocket or 30 years as a nuclear turbine).

The last decision enumerated is crucial to the entire design process as it will have a most profound effect on material selection. Ultimately, the product cost and the economic viability of the power generation system (energy cost) must be affected.

If, for the sake of simplicity, (N) is assumed to be the number of starts and stops the prime mover (neglecting load changes) will be subjected to during its lifetime, then we can view the equipment duty cycle as follows:

$$\frac{N}{\Delta\theta} \quad \Delta f(\dot{m},\ PT,\ \rho,\ \sigma,\ \eta) = \text{duty cycle} \qquad (2\text{-}6)$$

Finally, and most important, the relative economic costs can be related to any prime mover (for a given duty cycle) by returning to the original equation for the physical dimension of the prime mover, but assuming the cost function of the engine related to some exponential function of the engineering constraints as follows:

$$\text{Cost} = K \cdot f(\dot{m}^a,\ PT^b,\ \rho^c,\ \sigma^d,\ \eta^e) \qquad (2\text{-}7)$$

where K is an arbitrary constant.

A clear understanding of the above short discussion is crucial to a review of solar energy applications for electrical generation. Although the theoretical principles of mechanics and thermodynamics must be rigorously observed, the above practical philosophical and conceptual framework within which all heat engines or prime movers must ultimately be measured must be fully appreciated.

Unfortunately it is not enough to describe ideal cycles, ideal fluids, perfect engines, etc.--real cycles, real fluids and practical engines will eventually be required to perform the work.

3.0 HEAT ENGINE DESIGN

A comprehensive review of heat cycle and working fluid applications has led to the view that a conventional axial flow turbine operating in a Rankine cycle with water as the working fluid represents the best choice for initial investigations of the collector types and temperature levels which are most economic. The experience of many investigators over the past years has shown that water is the most practical working fluid for application in all but the smallest or largest scale turbines which might be designed. It seems clear that detailed consideration of other fluids should not precede initial design choices of collector type, collector field configuration, and operating temperature levels based on use of water.

A small-scale computer program was written to provide design and performance data for steam turbine-generators as a function of initial steam conditions (temperature and pressure) turbine capacity, and exhaust pressure. This program provided the necessary performance data as well as physical dimensions needed for turbine cost estimating routines.

In the design phase, the computer program accepts input of inlet steam conditions (temperature and pressure), condenser temperature, and the desired electrical output at the generator terminals. An iterative procedure is then used to determine the required steam flow rate. Rather than assuming a constant level of engine efficiency which seems representative of modern steam turbines, separate factors are used to account for the effects of inlet throttle valve losses, inlet volume flow rate, moisture production during expansion, exhaust losses, mechanical losses, and generator electrical losses.

3.1 Cycle Performance Calculations

The basic cycle evaluated by this program is a straight condensing or non-regenerative cycle. Dry saturated conditions are regarded by the power generation task group as the most promising class of steam conditions because of the simplicity of the individual collectors and the overall collector field, the rather inconsequential effect of small amounts of superheat, the expense of obtaining significant amounts of superheat, and the high density of input steam which yields economies in heat transport equipment.

Similarly, regenerative feedwater heating has been neglected because although it increases cycle efficiency the effect is not great at the modest operating temperatures anticipated. The low temperature heat required for feedwater heating will be the least expensive to collect in the field, and by pumping cool condensate from the condenser to the collector field, the need for insulating this line is reduced or eliminated. Furthermore, the size of heat transport equipment is reduced because the inlet steam mass flow required to generate a given power output is higher with regenerative heating than without it.

3.1.1 Control Strategy

An assumption of constant inlet volume flow is made for design calculations, approximating the actual steam swallowing capacity of the turbine at valves wide open conditions.

This assumption is significant, as it reflects the current thinking of the power generation group, regarding control of the turbine-generator equipment. It is hoped that the turbine can be designed without a control stage and with a very simple control system which will allow its load to "float" with the supply of heat from the collector field, relying on stiff electrical ties with a much larger power system to maintain synchronism. In this way, slight inefficiencies inherent with control stages are eliminated, the turbine-generator equipment becomes simpler and less expensive, and hopefully a near-optimum operating characteristic will be achieved more or less automatically.

An optimum control scheme requires that at each instant collector temperatures are maintained at a level such that the product of collector efficiency and power cycle efficiency is maximized. This is the point at which electrical power output will be the highest. As insolation declines below the value for which the system is designed, it is reasonable to believe that the optimum operating temperature will fall, along with the total electrical output. Such a characteristic is inherent with the constant volume flow assumption, at least qualitatively.

3.1.2 Cycle Without Moisture Removal

Performance calculations were made for turbine-generators of 3000 to 100,000 kilowatts output with inlet steam temperature from 302 ^{o}F (150 ^{o}C) to 482 ^{o}F (250 ^{o}C) dry and saturated. It is evident from the design calculations that high levels of moisture will be produced in the turbine in the absence of some form of moisture separation.

Current practice in nuclear steam turbines limits condenser moisture to approximately 12 percent, as higher levels cause excessive blade erosion. However, several factors indicate that the limit might be a little higher for a turbine associated with a solar plant.

First, the erosive behavior of moisture droplets depends on the impact velocity of droplets on the rotating turbine blades. Small turbines with relatively short low pressure blading will have relatively low tip speeds, and less erosion.

Second, the maximum moisture occurs only at the indicated design condition. Solar turbines might run at maximum output only for short durations annually, while the bulk of operation will be at lower than design inlet temperatures and pressures, with a consequent reduction in moisture.

Lastly, techniques have been developed in nuclear turbine design which allow moisture extraction within the turbine by means of centrifugal force with only modest levels of steam extraction.

The prudent limit for moisture in solar plant turbines is arguable, but it would be unwise to assume that values over 18 percent would be tolerable in any case.

Figure 3-1 summarizes the design calculations by means of a graph of cycle efficiency as a function of inlet steam temperature for turbine-generator ratings of 3 MW, 10 MW, 30 MW and 100 MW. The most startling feature of these curves is the poor performance of the smaller turbines at the higher temperatures. This is directly related to the low volume flow rate of inlet steam, which leads to high leakage flows in proportion to the main steam flow through the inlet stages of the turbine.

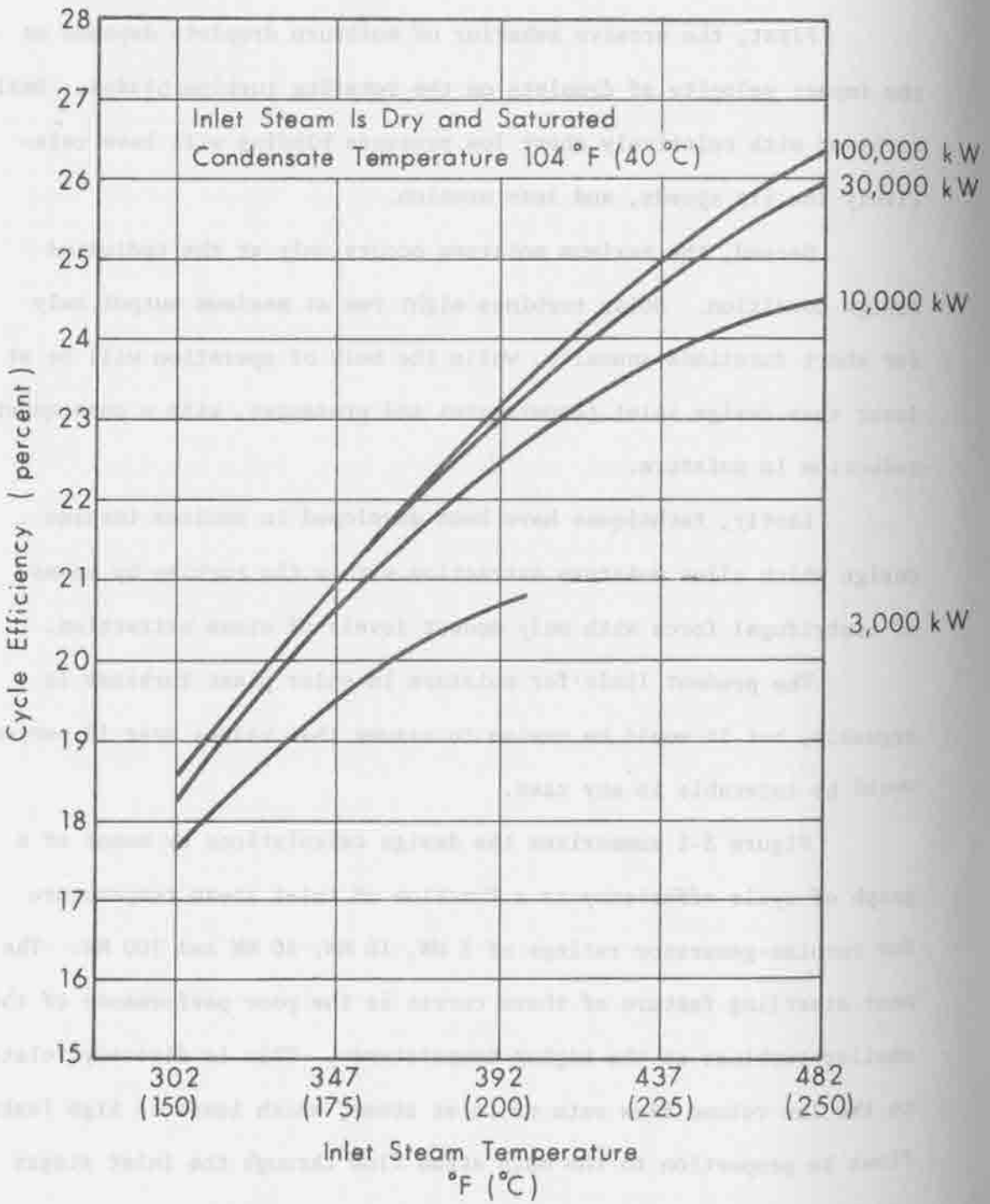

Figure 3-1. Turbine Design Point Cycle Efficiency vs. Unit Size and Inlet Steam Temperature. No Moisture Separation.

3.1.3 Off Design Performance - No Moisture Separation

The computer program was used to calculate turbine-generator performance for conditions of partial load on the 10 MW machine; that is, at reduced steam temperatures but constant volumetric flow. The computation was made for design condenser temperature, and an array of dry and saturated inlet steam conditions at design temperature and below. This information is summarized in Figure 3-2, which shows turbine-generator output in kilowatts as a function of the inlet conditions.

3.2 Turbine With Moisture Separation

To overcome the disadvantage of high moisture in low-pressure stages, the steam may be removed at an intermediate point in the expansion and the moisture removed before reintroducing the steam into the lower-pressure stages of the turbine. A design advantage ensues from this separation, because the high-pressure and low-pressure sections of the turbine are uncoupled aerodynamically. The two parts can then be optimized individually.

The turbine design program was used to compute the cycle efficiency and off-design performance for the turbine with constant volumetric flow but with moisture separation between stages. In Figure 3-3 is shown the cycle efficiency, and in Figure 3-4 is shown the off-design performance. Specific steam mass flow rate is shown in Figure 3-5 as a function of inlet steam temperature for the same turbine design.

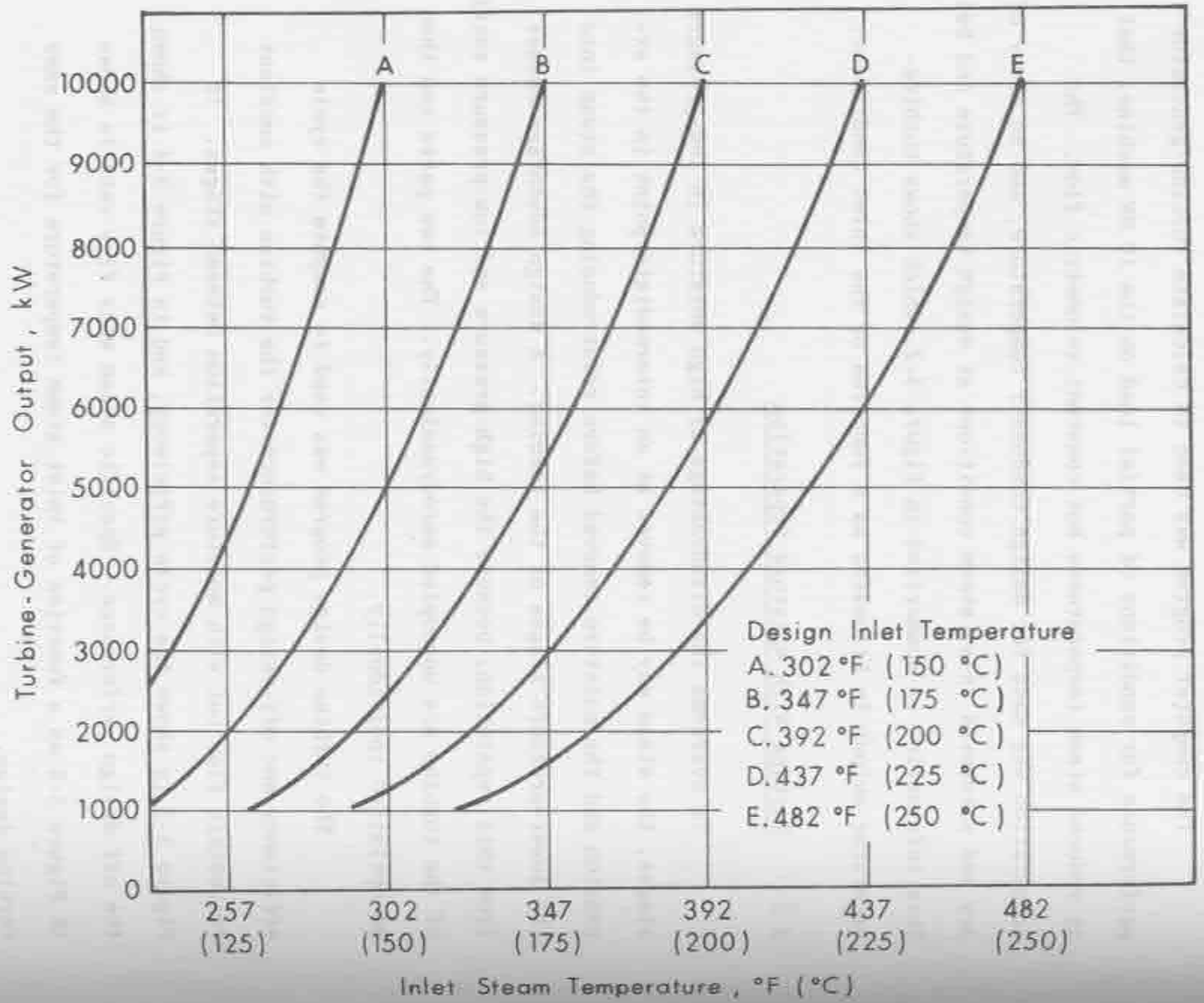

Figure 3-2. Turbine Output Below Design Temperature, Cycle with Constant Volumetric Flow, No Moisture Separation. 10 MW Rating, Dry, Saturated Steam

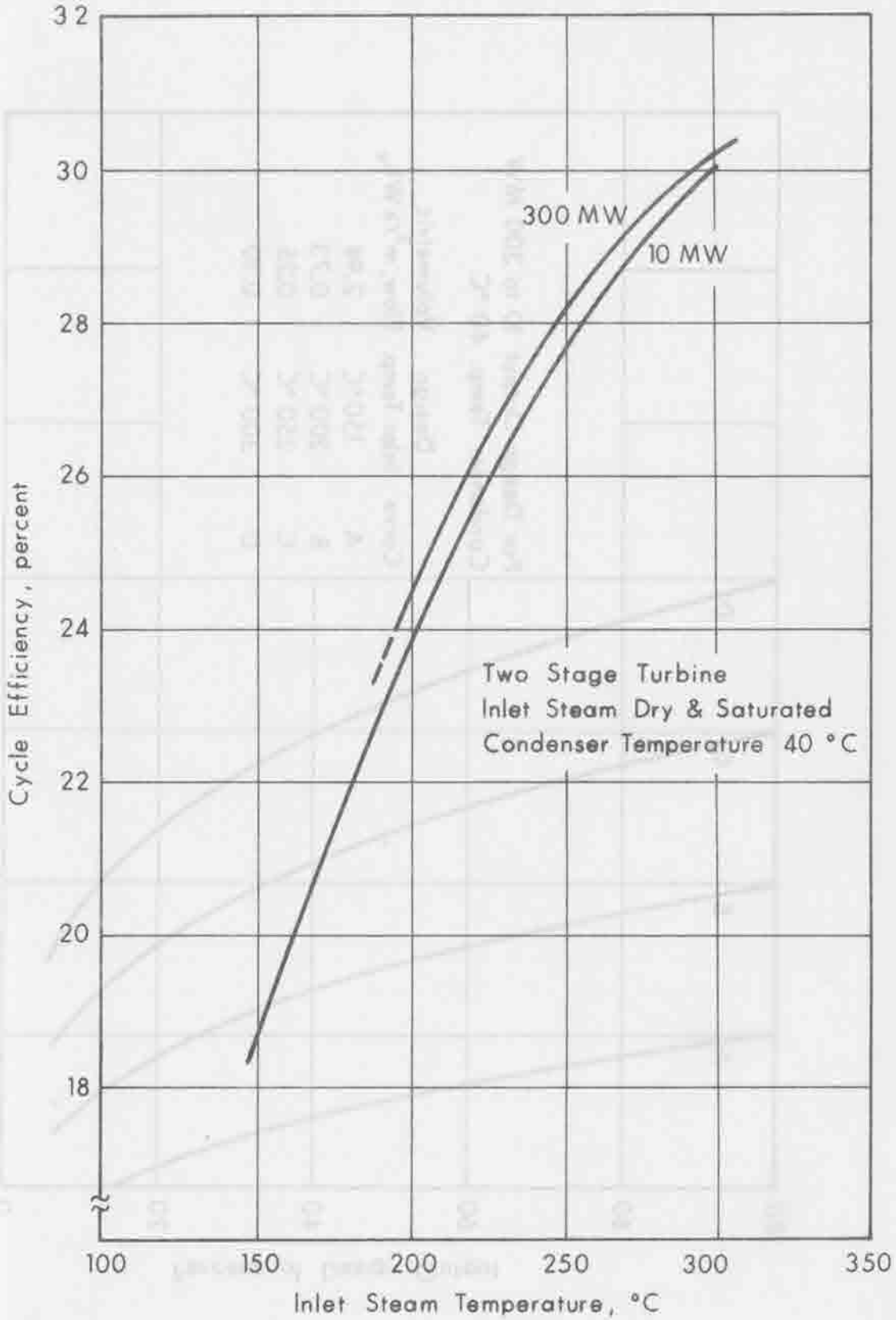

Figure 3-3. Cycle Design Point Efficiency; Moisture Separation Between Stages.

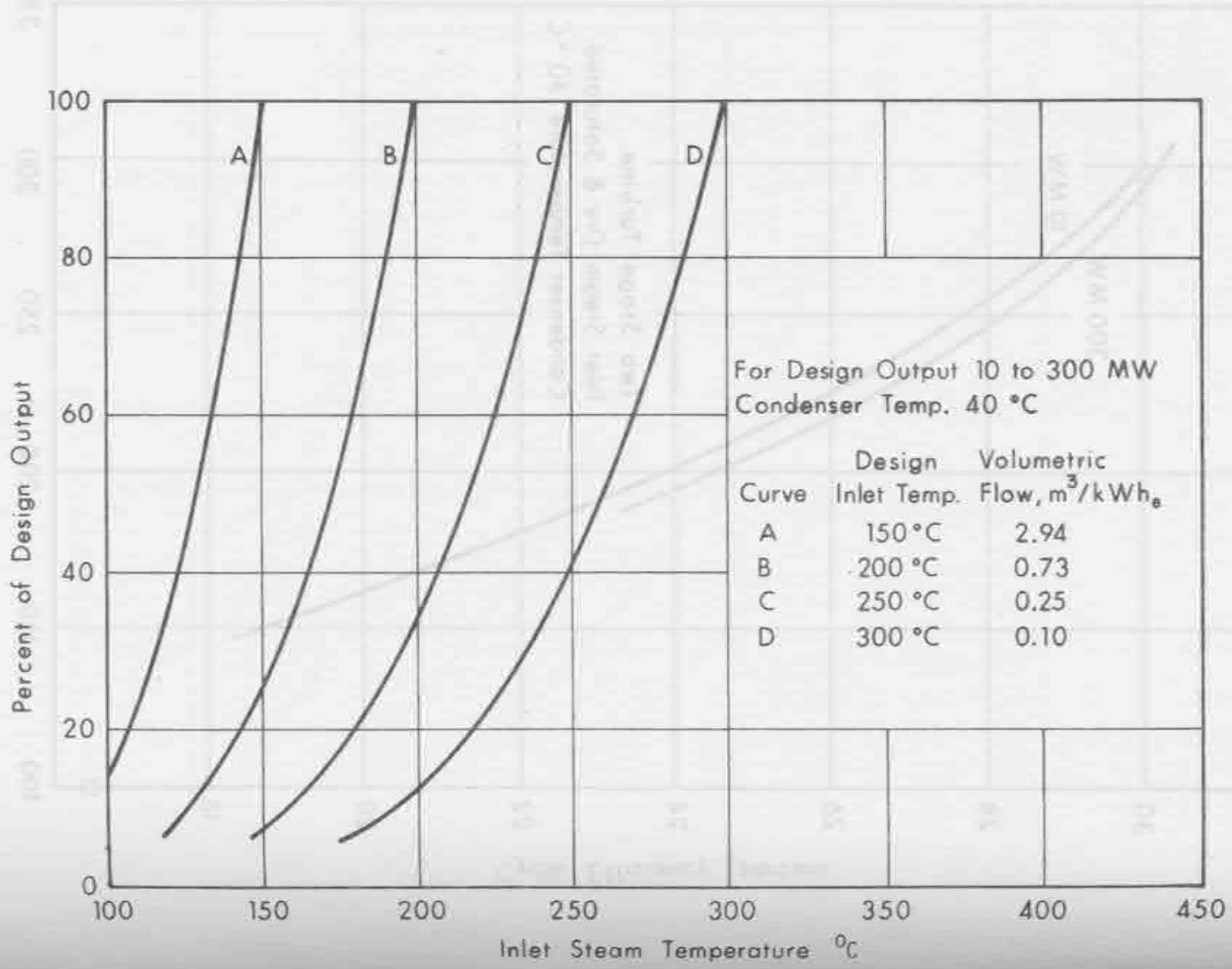

Figure 3-4. Calculated Turbine Generator Output Below Design Temperatures, Constant Volumetric Flow, Moisture Separation Between Stages.

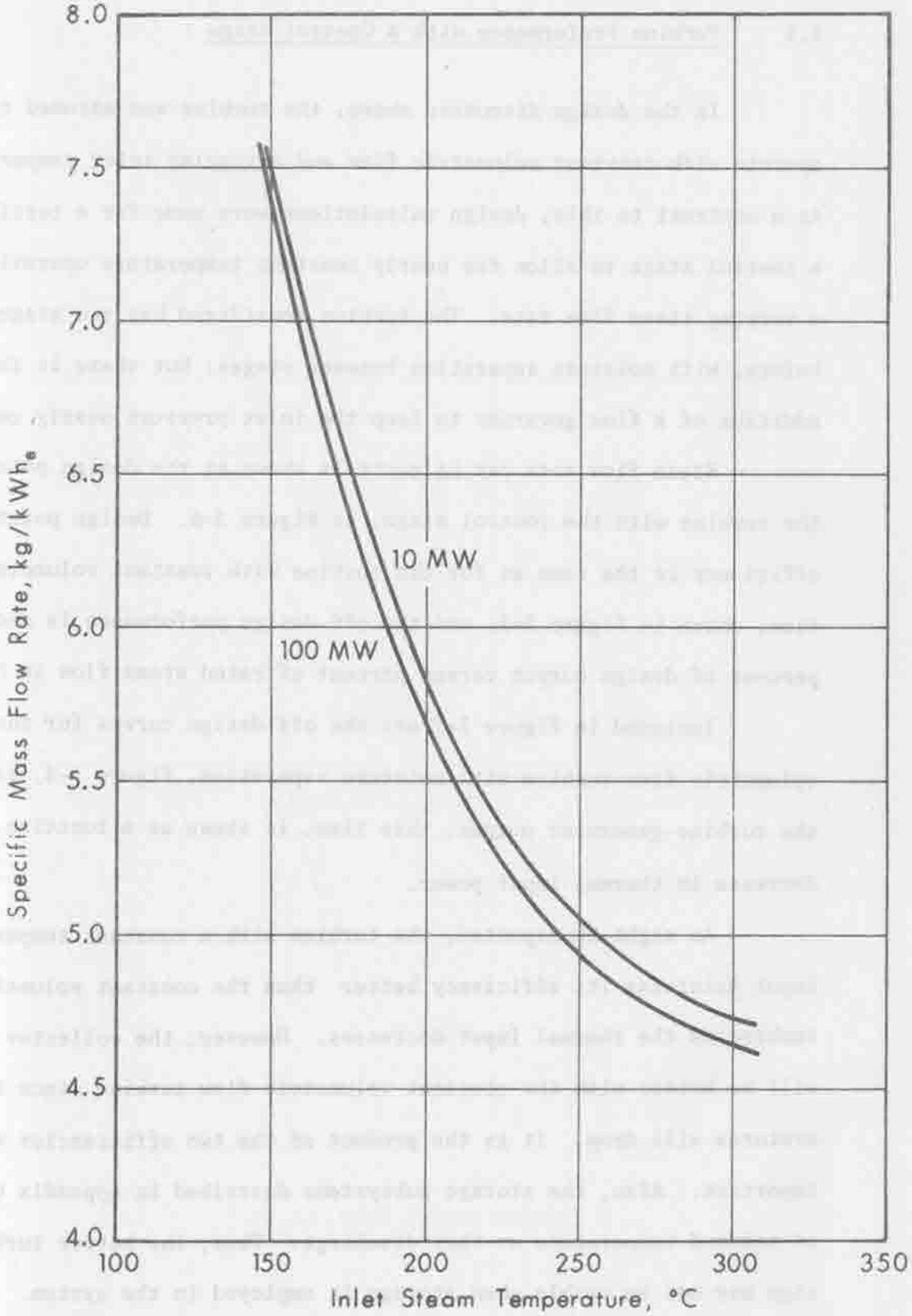

Figure 3-5. Design Point Steam Flow Rate, Two-Stage Turbine with Moisture Separation Between Stages.

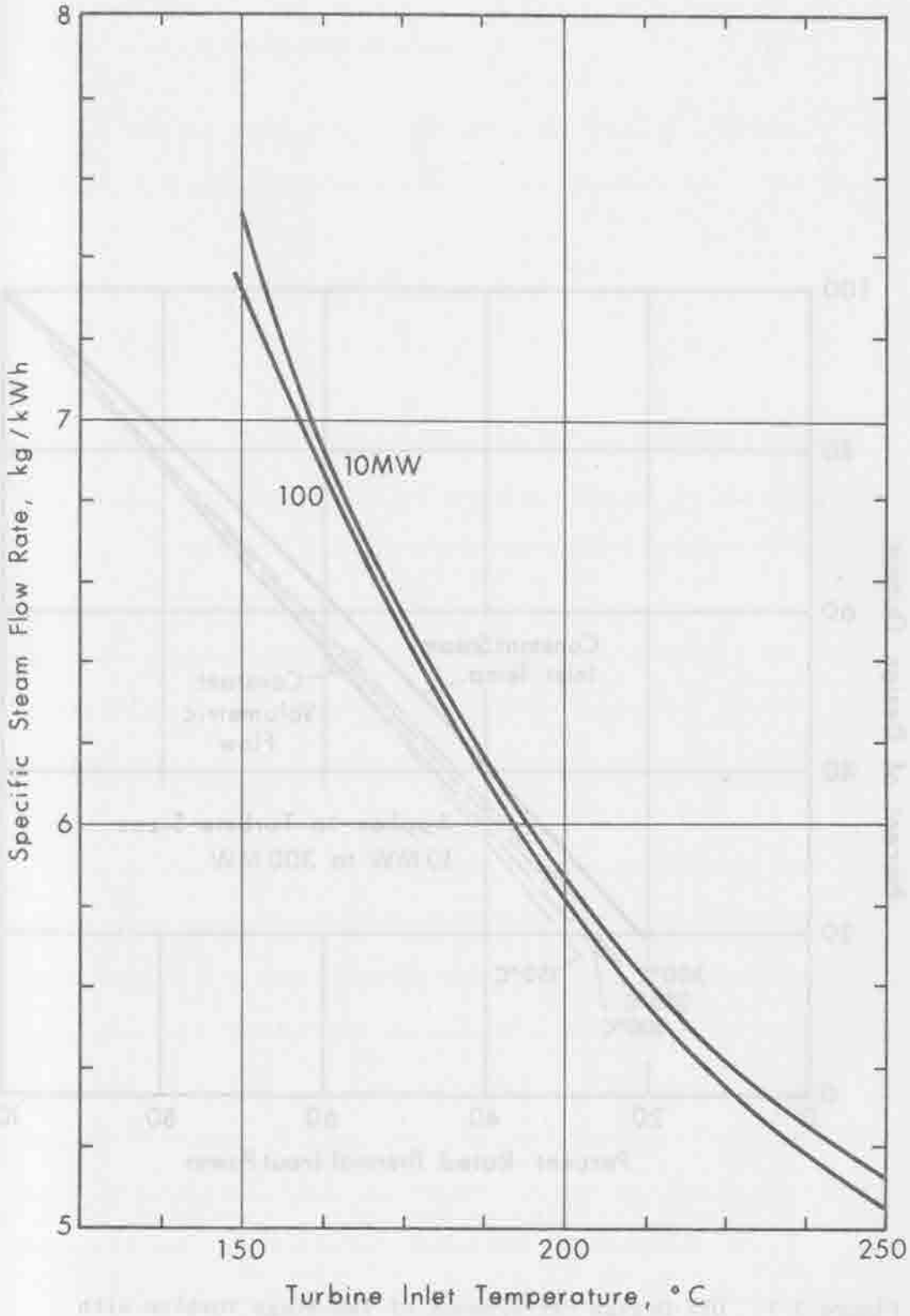

Figure 3-6. Design Point Conditions with Moisture Separation and One Control Stage.

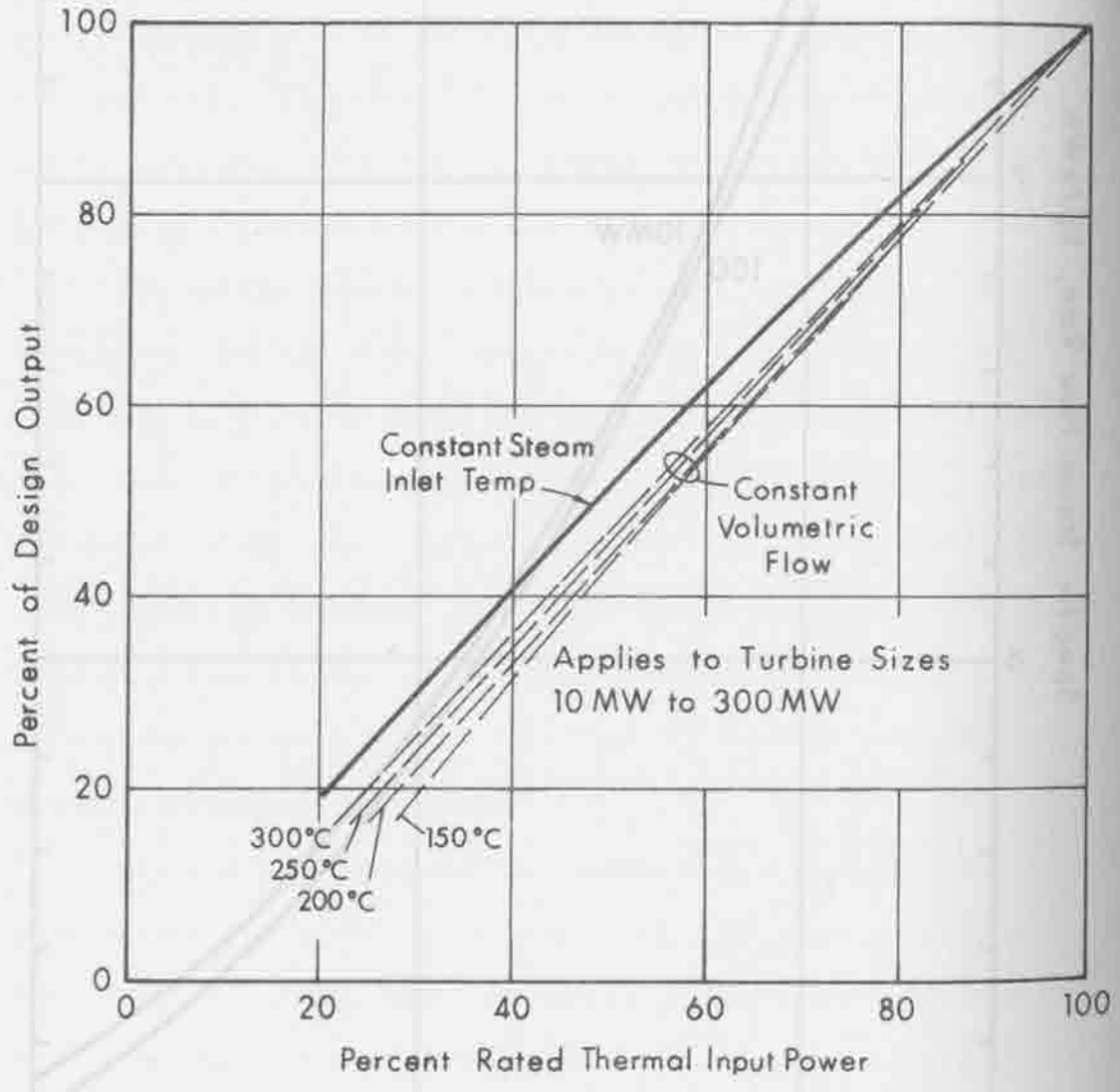

Figure 3-7. Off-Design Performance of Two-Stage Turbine with Moisture Separation.

4.0 TURBINE-GENERATOR PRICING

For the steam conditions and power ratings considered by this project, the selling price for a turbine generator is approximated by:

$$C_{TG} = 710\ P^{0.75} + 140{,}000\ E_A \qquad (4\text{-}1)$$

where

P is the generator rated output in kilowatts, and

E_A is the exhaust end annulus area of the turbine in square meters. Figure 4-1 shows exhaust annulus for the turbine designs considered.

The price equation above does not include installation cost which is estimated to be 30 percent of the turbine-generator selling price. No distinction in cost is made between the two types of turbines evaluated above.

Prices for the turbine-generator were developed from actual prices of delivered equipment and the two principal factors affecting cost. Figure 4-2 shows the turbine-generator installed cost, from Equation (4-1), in dollars per kilowatt of capacity over the temperature range 150 ^{o}C to 300 ^{o}C. The selection of a condensing temperature other than 40 ^{o}C changes the required E_A and thereby affects the turbine cost. The cost multiplier shown in Figure 4-3 may be used to adjust the turbine-generator cost for condenser temperatures other than 40 ^{o}C.

It was also desired to have the option of varying the turbine generator efficiency. No dependable cost data existed for extension of turbine efficiency above normal design levels. The maximum conceivable engine efficiency was assumed to be 90 percent and the cost of achieving

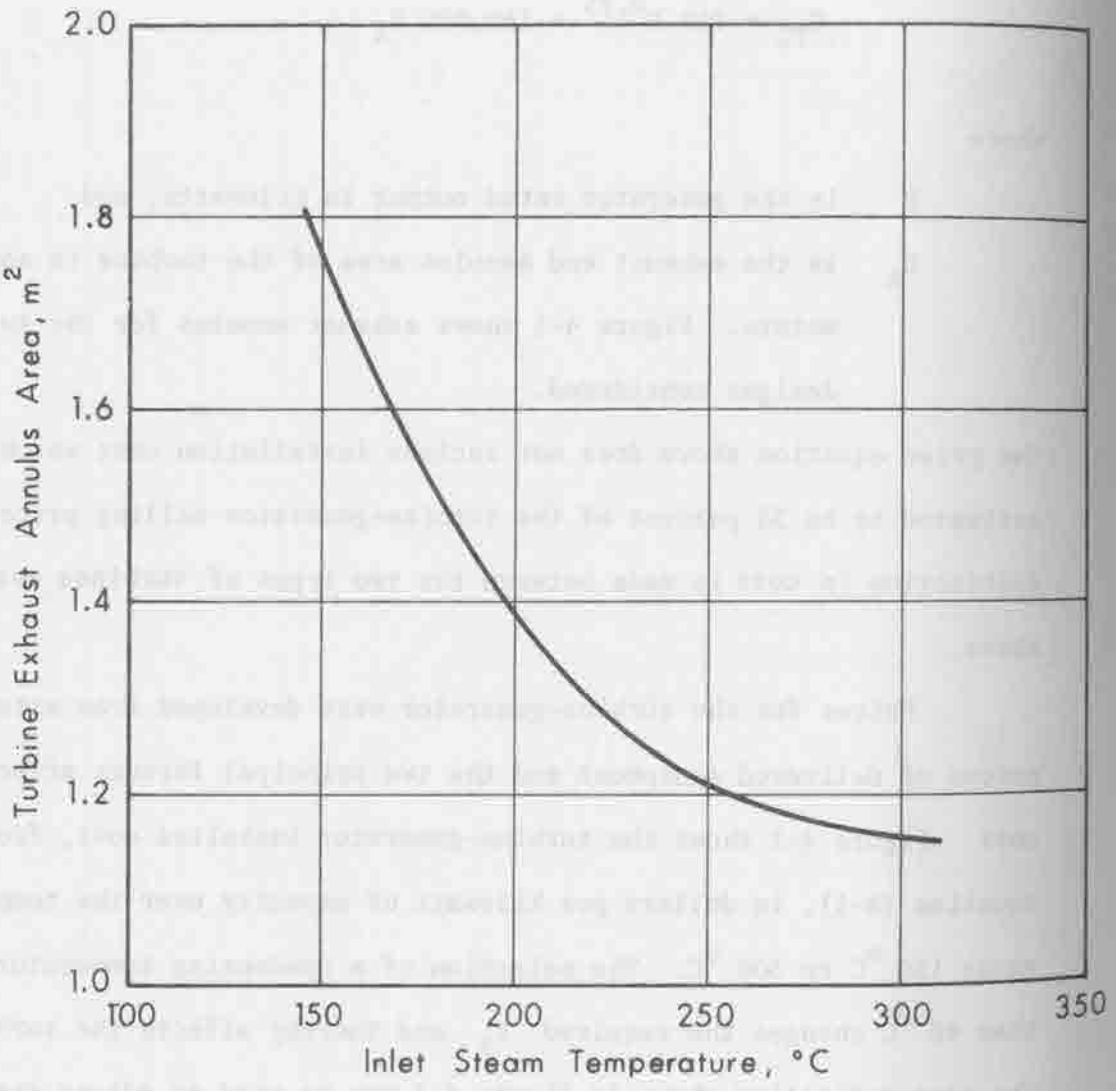

Figure 4-1. Turbine Exhaust End Annulus Area for Two-Stage Turbine Design Condensing Temperature 40 °C.

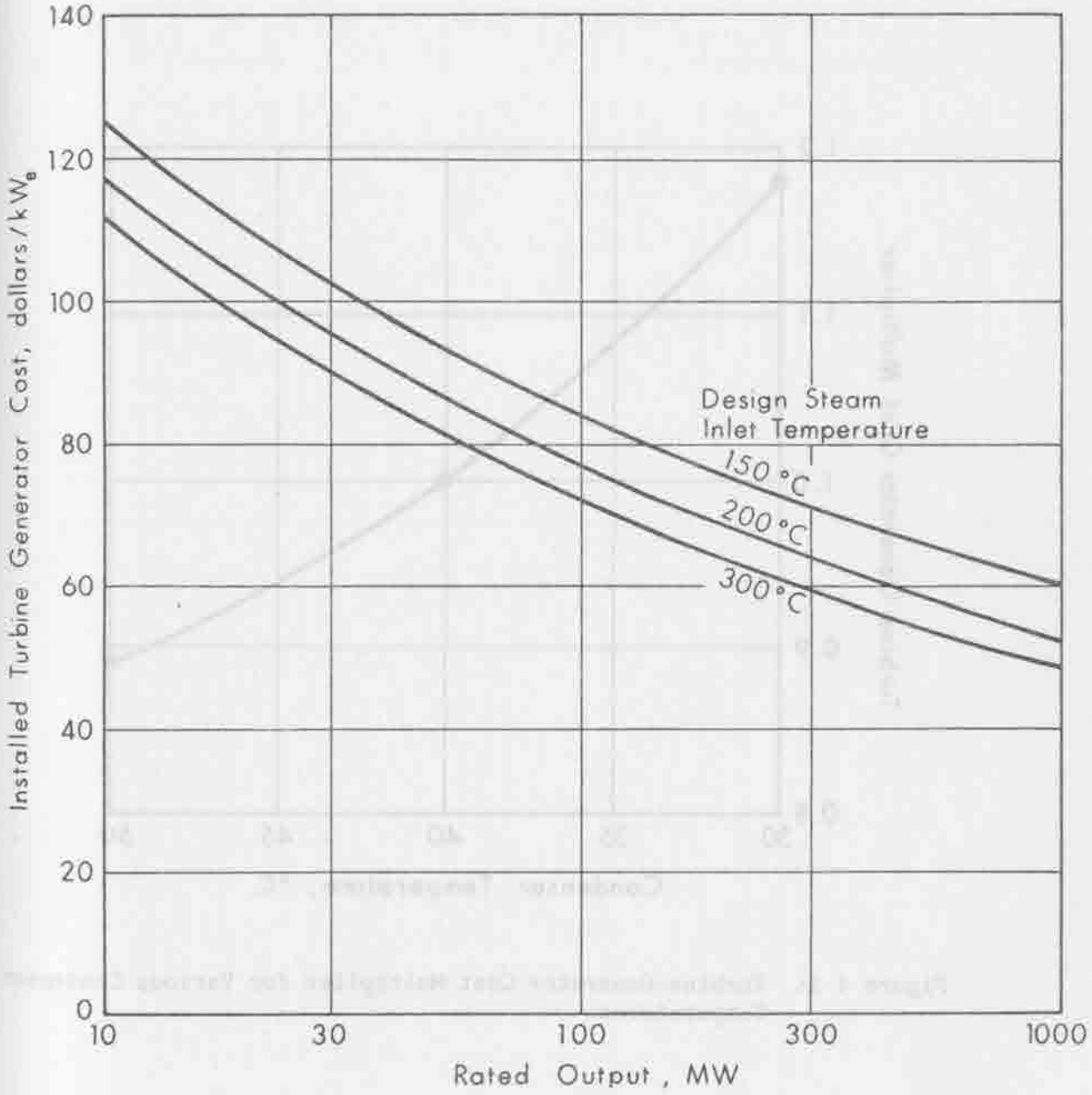

Figure 4-2. Installed Turbine Generator Cost Model for Condensing Temperature 40 °C.

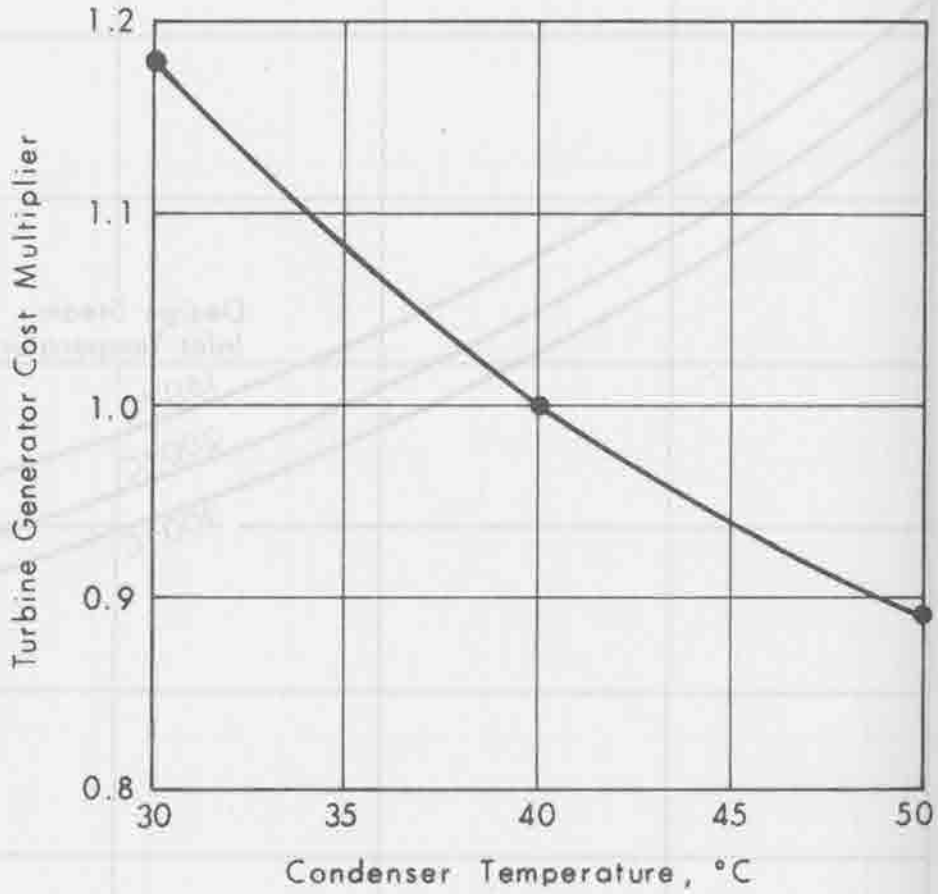

Figure 4-3. Turbine-Generator Cost Multiplier for Various Condenser Temperatures.

this was estimated to be obtainable at ten times the base cost. The curve describing this relationship is shown in Figure 4-4. The validity of this cost multiplier is open to question, but it can be modified if more satisfactory cost data becomes available.

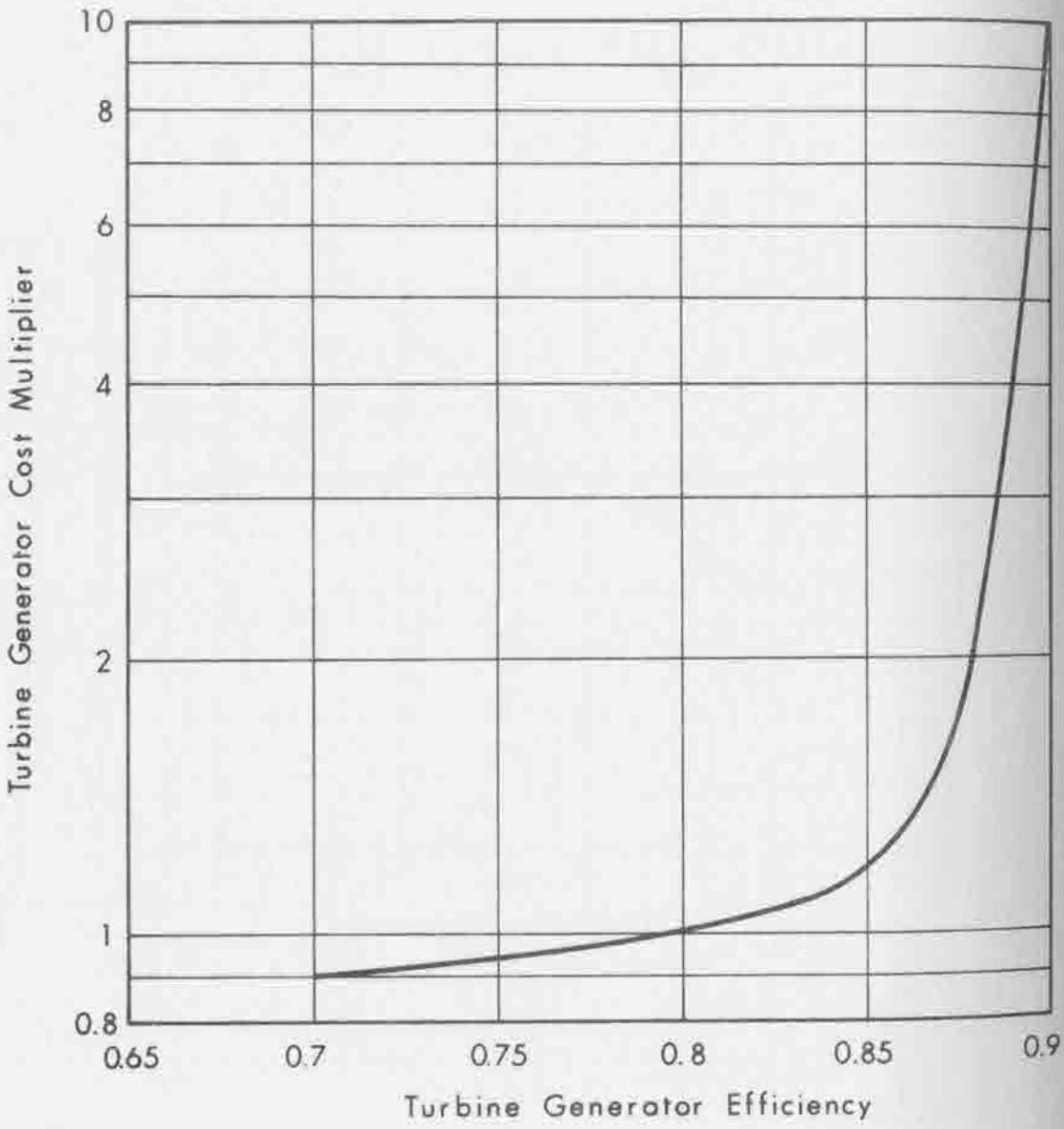

Figure 4-4. Cost Multiplier Used for Variable Turbine Efficiency.

APPENDIX I

HEAT REJECTION

BY

R. J. BUDENHOLZER,

D. Q. HOOVER,

C. D. BEACH,

AND

A. D. WATT

1.0 INTRODUCTION

There is such a high degree of interaction between the performance of the turbine, the condenser and the cooling system that separate design of these components is impossible if the optimum system is desired. To correctly design the turbine and heat rejection subsystems requires consideration of the annual heat rejection load profile as well as the profile of relevant ambient weather conditions.

Design conditions for turbines are described in Appendix H, but a comparison of the performance of two different turbines with variation in exhaust pressure illustrates the interdependence of design choice for turbine and heat rejection systems.

A reduction in condensing temperature (and pressure) will increase the power output of a turbine, provided that it is designed to utilize the increased available energy. This point is brought out clearly in Figure 1-1 which shows the maximum capability of two different turbines as a function of exhaust pressure. Both turbines are operating at the same constant throttle flow but have different size low-pressure ends. As the exhaust pressure decreases, both units produce more power because of more complete expansion of steam through the turbine. However, at about 2.5 In. Hg. exhaust pressure, the power output of one turbine levels off and even experiences a slight decline. The same holds true for the other turbine, which has a larger annulus area, when the exhaust pressure is reduced to 2 In. Hg. This leveling off is characteristic of a "choked" condition in the turbine exhaust hood when steam approaches accoustic velocity. Further reductions in the condenser pressure do

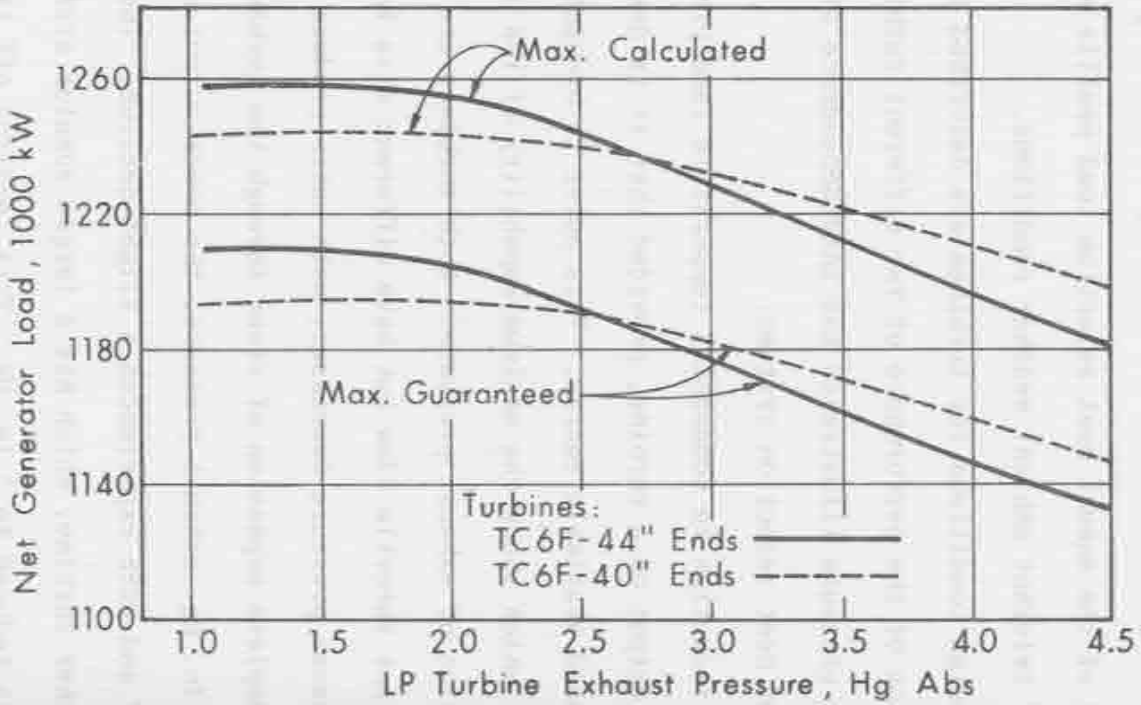

Figure 1-1. Turbine Output Variation with Exhaust Pressure.

not allow greater pressure drops through the last row of low pressure blades, and no further work is obtained. The turbine with the larger annulus area is able to generate more power at low exhaust pressures because its choke point is at a lower pressure.

As exhaust pressures increase, however, the situation is reversed. Exhaust steam volume and velocity decrease with a parallel decline of low pressure blade efficiencies. The larger low pressure end meets this effect more rapidly and has lower capability at high exhaust pressures than the end with the smaller annulus area. This lower capability is likely to occur at times of maximum system demand during the hottest summer days, when heat rejection is the most difficult.

A trade-off appears between higher output during hot summer days with the smaller size low pressure ends, and higher output and efficiency during the winter months if the larger size low pressure ends are chosen. The selection of turbine low pressure end sizes is an integral part of the cooling system optimization.

2.0 CONDENSER PERFORMANCE AND COST

The simplified diagram of Figure 2-1 shows the temperature relationships involved in the heat rejection system design when a wet cooling tower is used. With regard to the condenser design the two important temperature differences are the range, and the terminal temperature difference (TTD). The range is the temperature rise in the cooling water as it passes through the condenser and depends upon the heat rejection requirements and the flow rate of the water. That is, the range in degrees Celsius is

$$T_O - T_I = 14.3\ Q_R/F \quad {}^{o}C \qquad (2\text{-}1)$$

where Q_R is the heat rejection rate in kilowatts (thermal) and F is the water flow rate in kg/min (1 gallon/min = 3.785 kg/min). The range is also the temperature drop required in the cooling water as it goes through the cooling tower.

Since a practical heat exchanger cannot transfer heat without a temperature difference, the condensing temperature is higher than the exit temperature of the cooling water. This difference is the terminal temperature difference, expressed by

$$TTD = T_C - T_O = \Delta T_R/[\exp\ (3.4\ S_A \Delta T_R/Q_R) - 1] \quad {}^{o}C \qquad (2\text{-}2)$$

where T_R is the range, $T_O - T_I$ above, and S_A is the effective condenser surface area in square meters. The effective surface area of the condenser to be used is chosen from the desired TTD and range by solving Equation (2-2) for S_A. This gives

$$S_A = \frac{Q_R}{3.4\ \Delta T_R} \ln \left[\frac{TTD + \Delta T_R}{TTD} \right] m^2 \qquad (2\text{-}3)$$

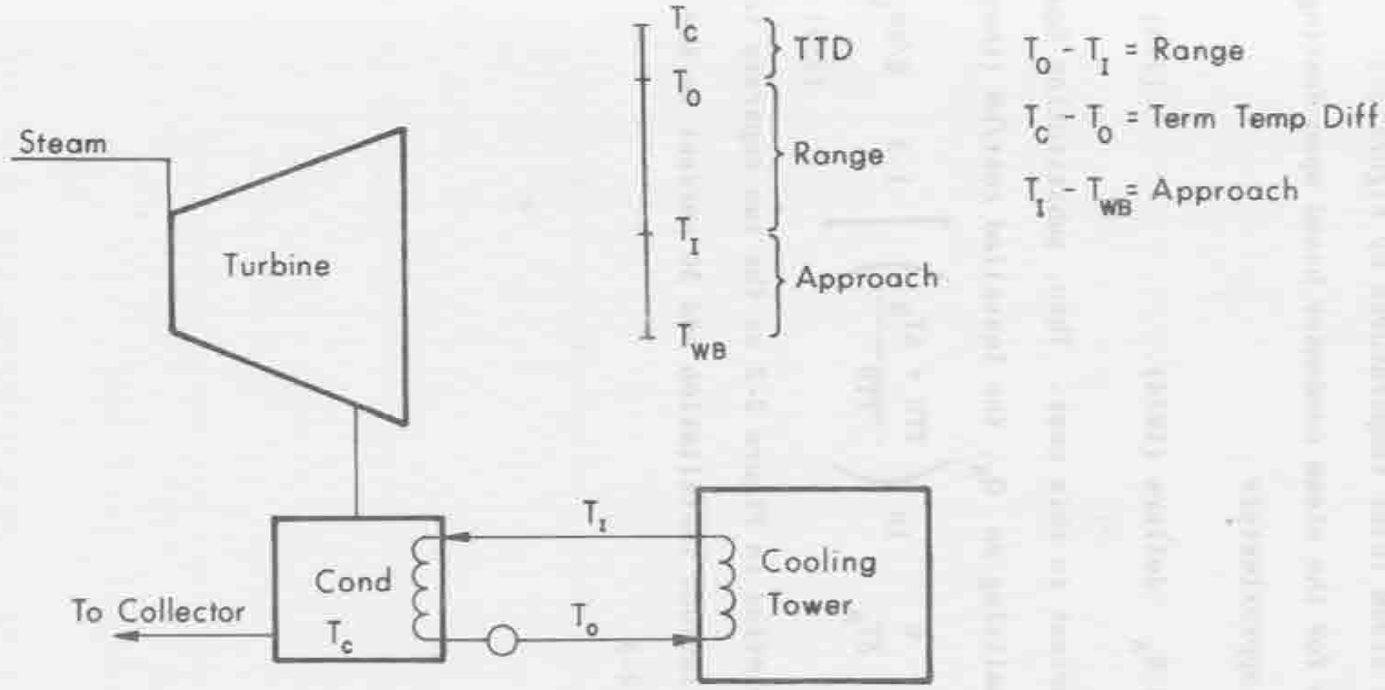

Figure 2-1. Diagram to Relate Approach, Range and Terminal Temperature Difference in Heat Rejection Subsystem.

Required heat rejection per kilowatt of electrical output is shown for the different steam inlet temperatures by Figure 2-2.

A selling price for the steam condenser based upon Westinghouse catalog information is approximately

$$C_c = 10^5 + 20.4\ S_A \quad \text{dollars (1974).} \tag{2-4}$$

Installation adds 30 percent to this cost. Then, substituting Equation (2-3) in (2-4) and normalizing on Q_R, the installed cost/kW (thermal) is

$$C_c/Q_R = \left[\frac{10^5}{Q_R} + \frac{6}{\Delta T_R} \ln \left(\frac{TTD + \Delta T_R}{TTD} \right) \right] 1.3 \quad \$/kW_t \tag{2-5}$$

This cost function is plotted in Figure 2-3 as the two separate terms in brackets above. To include installation add 30 percent to the cost determined from Figure 2-3.

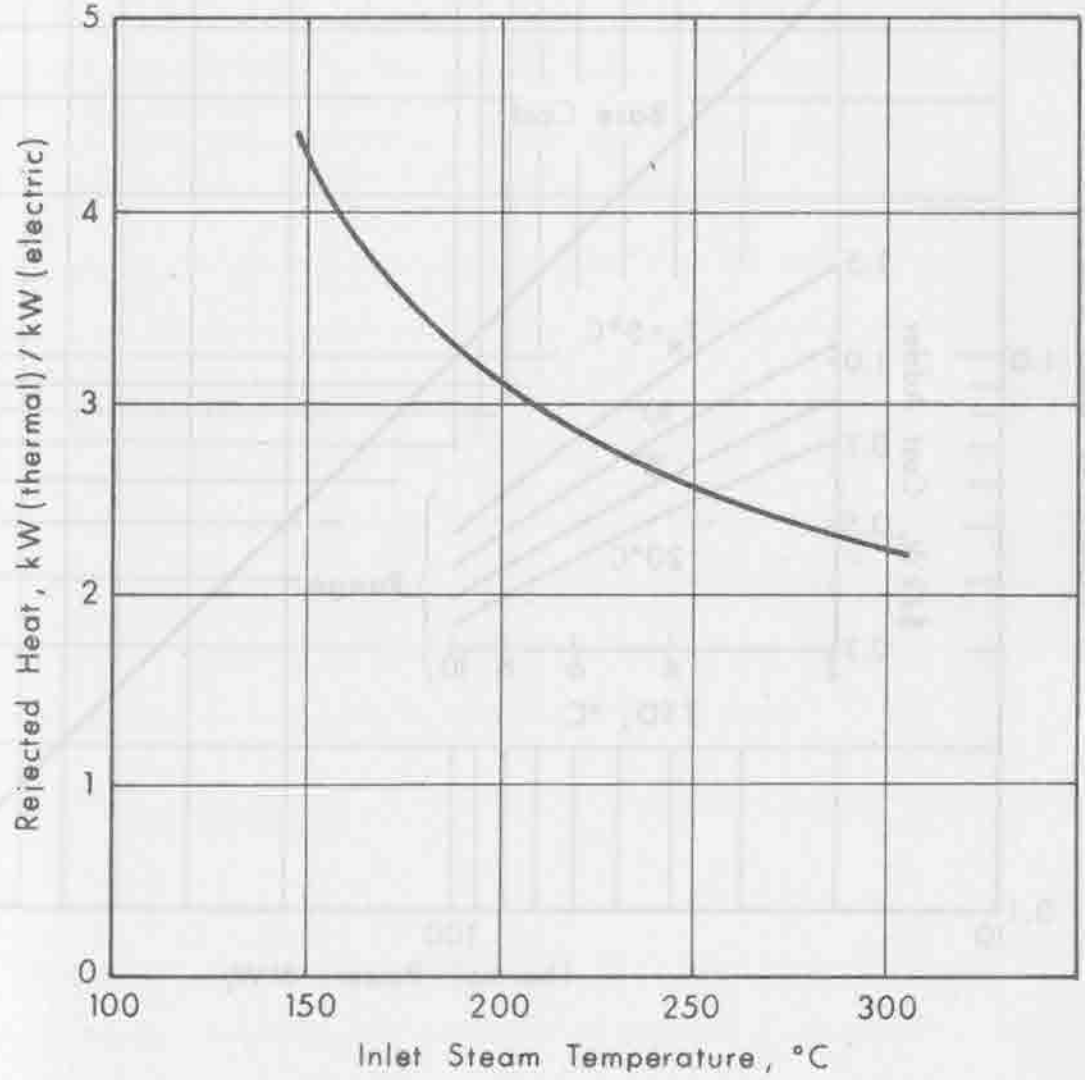

Figure 2-2. Heat Rejection Requirement for Turbine with Condenser Temperature 40 °C Operating at Rated Load.

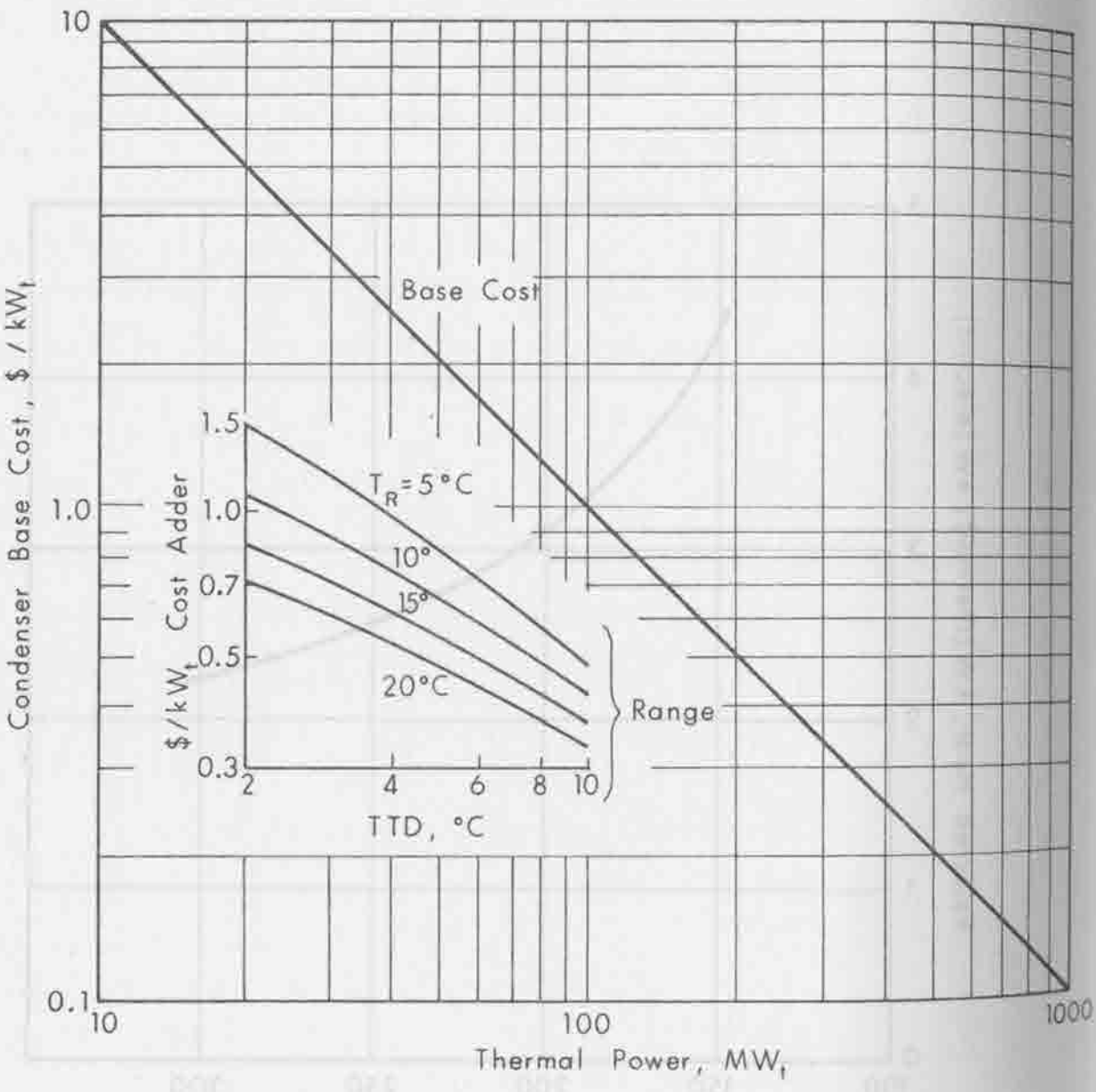

Figure 2-3. Steam Condenser Cost Versus Heat Rejection Rate. Total Cost is Base Cost Plus Cost Adder. For Installation, add 30 percent.

3.0 COOLING SYSTEM

There are five basic types of cooling systems typically useful for large steam electric power plants. These include once-thru cooling, cooling lakes, spray ponds, wet (evaporative) cooling towers, and dry cooling towers. In addition to these basic systems, combinations are often proposed such as the use of "helper" cooling towers or tempering canals with spray systems on basically once-thru systems. A variation of the dry cooling tower, the air cooled condenser, has received much attention for small plant applications, but its use on large units has met with little enthusiasm thus far. It shares many operating characteristics with the dry cooling tower.

Cooling systems designs which have the ability to reject waste heat at low condensing temperatures and consequent low turbine exhaust pressures allow the maximum utilization of available energy by the steam turbine. The result is increased turbine output and efficiency if the turbine is designed to make use of this energy.

3.1 Cooling Types

The basic environmental factors which influence cooling system performance are shown in Figure 3-1, with dots representing major variables and circles representing variables of secondary importance. With once-thru cooling systems, performance is dictated by the water temperature at the cooling water intake. This temperature, however, is a complex function of the ambient wet bulb temperature, dry bulb temperature, wind speed, cloud cover, day of the year, and various stream flow effects. The steam condensing temperature with this system is the sum of the intake cooling water temperature, the temperature rise or range through

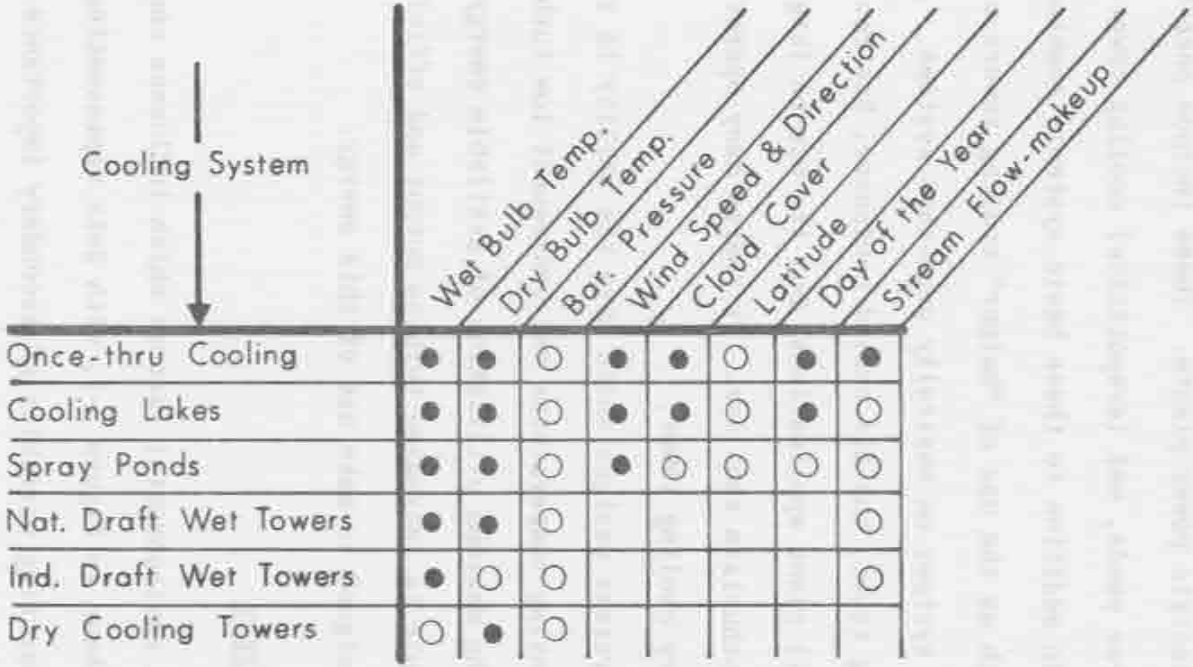

Figure 3-1. Environmental Influence on Cooling System Performance.

the condenser, and the terminal temperature difference. The latter is the difference between the steam saturation temperature and the temperature of the warm water leaving the condenser, and is indicative of the temperature differential required for heat transfer.

Cooling lakes are influenced by the environment in the same ways as once-thru systems. However, cooling lakes usually operate at higher intake temperatures, because the water is continuously recirculated and does not cool to the natural equilibrium temperature of once-thru systems.

Spray ponds are like miniature cooling lakes, except that evaporative heat transfer is promoted by spraying the water into the air. The enhancement of evaporative heat transfer, controlled, primarily by the wet bulb temperature and wind speed, makes cloud cover and day of the year of secondary importance. Thus, the performance of a spray pond should correspond more closely to an evaporative cooling tower than a cooling lake.

Performance of natural draft wet cooling towers is affected by both dry bulb and wet bulb temperatures. The wet bulb temperature controls the heat transfer process in the tower, but the dry bulb temperature or relative humidity becomes important in determining the air flow rate. Induced draft wet cooling towers rely on fans to produce air flow and thus, are sensitive only to the ambient wet bulb temperature. The steam saturation temperature with evaporative cooling towers and spray systems is the sum of the wet bulb temperature, the approach, the condenser or tower range, and the terminal temperature difference in the condenser. The approach measures how closely the cold water temperature "approaches"

the ambient wet bulb temperature, and would be zero degrees for a tower of infinite size.

Dry cooling towers rely totally on convective heat transfer which is controlled by the ambient dry bulb temperature, and the "approach" of dry cooling systems is measured with reference to this temperature.

Figure 3-2 shows the general relationships between cooling system temperatures and turbine exhaust pressure for once-thru cooling and wet and dry cooling towers. During typical summer operation, once-thru cooling systems generally operate with turbine exhaust pressures of 1.5 to 2.25 In. Hg. Wet cooling tower systems will yield exhaust pressures of 2.5 to 4.5 In. Hg. while dry cooling towers will result in turbine exhaust pressures in excess of 6 In. Hg. Exhaust pressures with cooling lakes and spray ponds are in the same general range as wet cooling towers.

For the purposes of this study, where moderate steam temperatures may be the most desirable operating conditions, it was felt that a wet cooling tower is the best candidate cooling subsystem. Many suitable sites are available with adequate water and sunshine for pilot or even larger scale demonstration solar thermal electric power plants. Design and siting considerations may ultimately suggest the use of dry cooling towers, but only wet cooling towers are included in analysis and optimization of STEPS systems for this study.

3.2 Wet Cooling Tower Performance and Cost

Cooling tower inlet temperature depends on the approach and range temperature differences and the water flow rate and ambient wet bulb temperature. The design point wet bulb temperature was chosen as 25 ^{o}C (77 ^{o}F). The temperature of the cooling water from the condenser

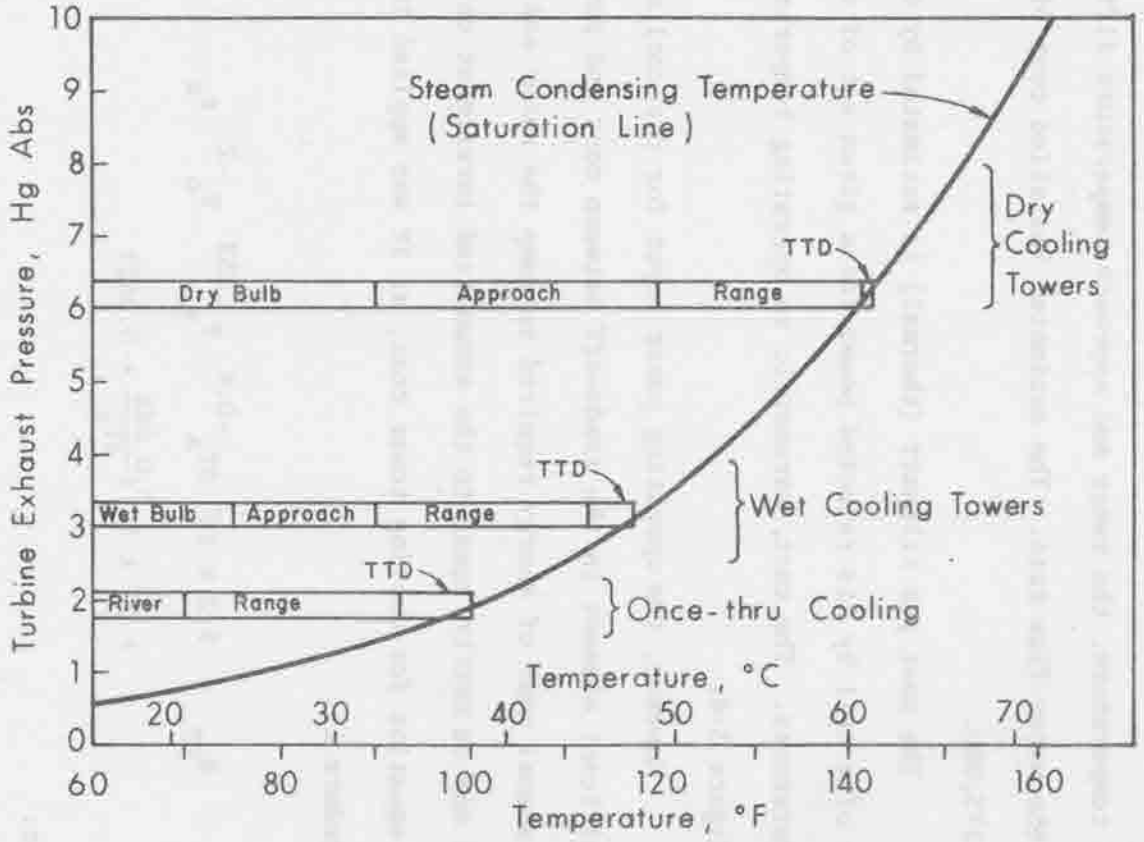

Figure 3-2. Cooling System Temperature-Exhaust Pressure Relationships.

is plotted for different flow rates and heat rejection rates against the wet bulb temperature in Figure 3-3.

Costing for cooling towers was done on the basis of individual cells, with each cell rejecting 40 to 90 MW_t depending on the wet bulb temperature, the range and approach temperature differences and the water flow rate. The estimated installed cost of each cell is $175,000.

The cost per kilowatt (thermal) is estimated by dividing the cost of a cell by its rejected power for a given set of operating temperatures. The cost, parametric in operating temperatures, is presented in Figure 3-4.

However, the operating power input for the cooling tower is a significant element in the trade-off between cost and performance. The annual cost of energy required to pump the water and drive the fans may be nearly equal to the annualized investment cost. Therefore, the equation for cooling tower cost, as it was applied to the optimization procedure is:

$$R_{CT} = 5.2 \times 10^3 \, \Delta T_A^{-0.4} \, T_w^{.233} \, T_o^{-2} \, r_a + 97 \times 10^3 \left(\frac{0.048}{\Delta T_R} + 0.002\right) \quad (3\text{-}1)$$

where:

R_{CT} is the annualized cooling tower cost in $\$/kW_t$ - yr

ΔT_A is the cooling tower approach to wet bulb temperature, ^oC

ΔT_R is the condenser range, ^oC

T_w is the design wet bulb temperature, ^oC

T_o is the condenser outlet temperature, ^oC

r_a is the rate of amortization.

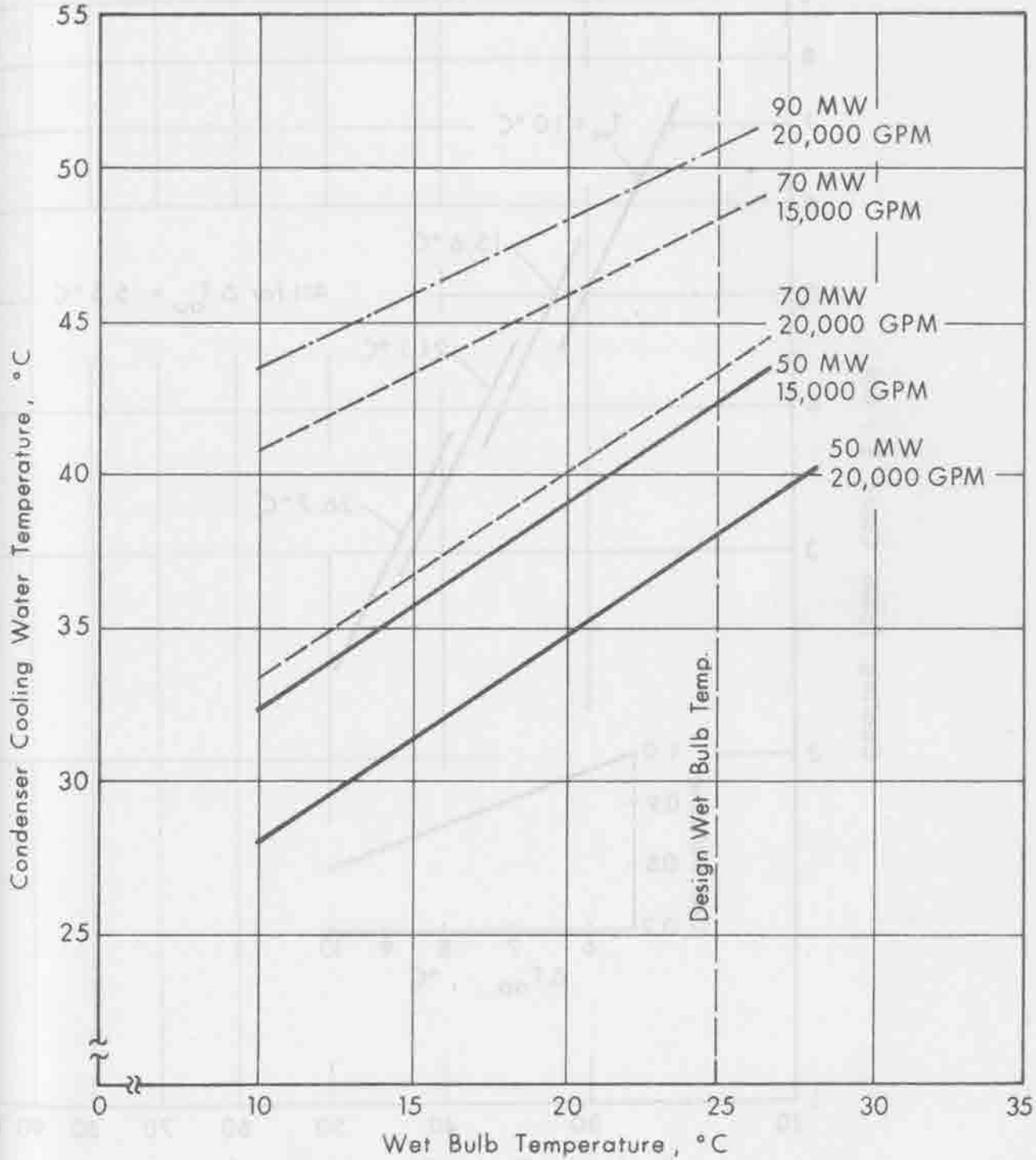

Figure 3-3. Condenser Cooling Water Temperature, vs. Wet Bulb Temperature.

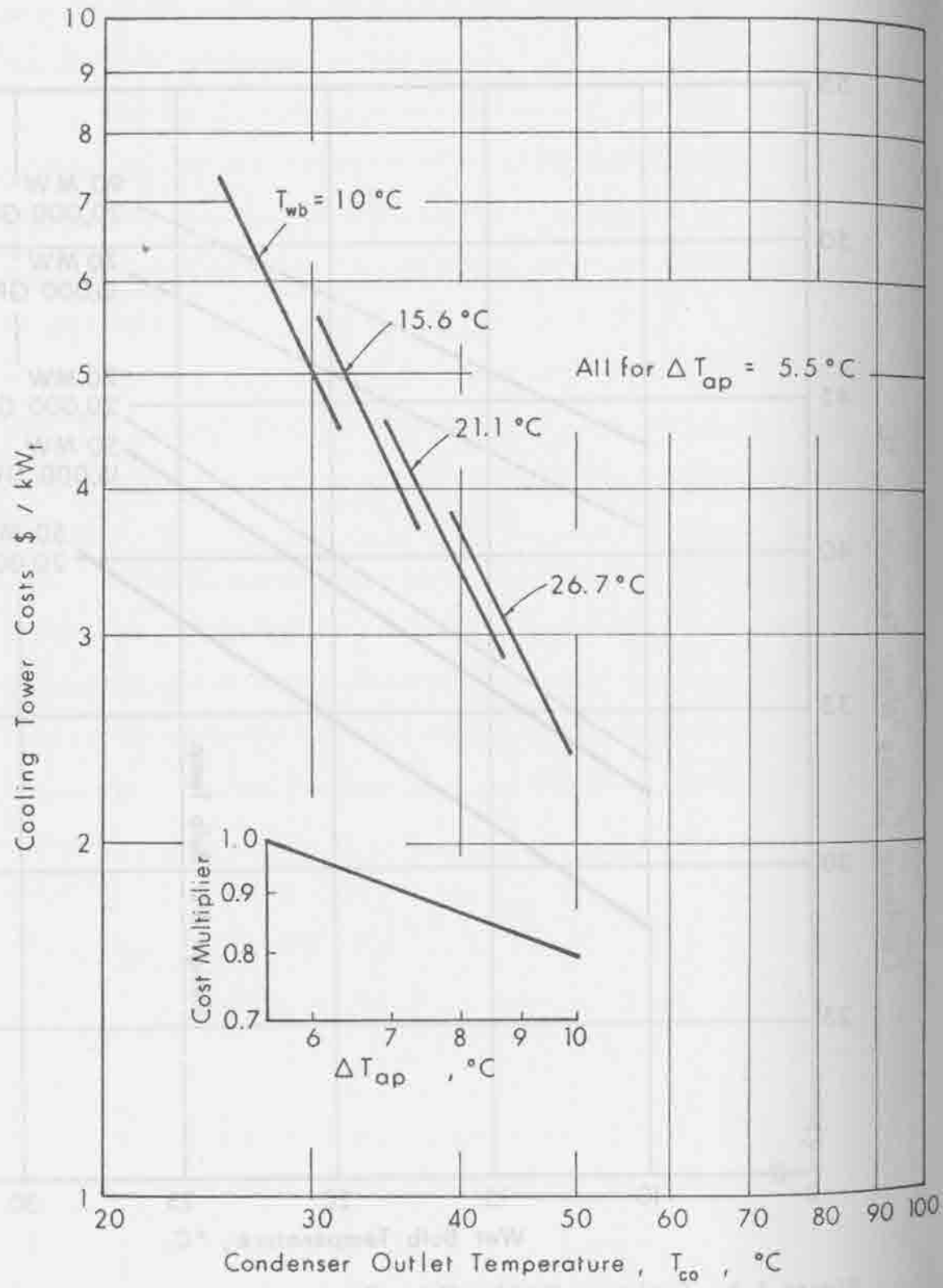

Figure 3-4. Installed Cooling Tower Cost per Kilowatt of Heat Rejected.

In Equation (3-1) the first term is the annualized investment cost, expressing the cost relationship shown in Figure 3-4. The second term in the cost equation expresses the annual cost of pumping and fan power.

For the design conditions, a total pressure drop of 20 metres was assumed in the condenser and cooling tower water lines, and a 200-hp fan was used. The cost of circulating pumps and piping are not included in cooling subsystem cost. They are included, instead, in other plant costs. The 3 ^{o}C approach which was indicated in Figure 2-22 of Appendix B may have used the cost equation (3-1) beyond its normal limits. In future developments an increase in cost of fan power with decreasing approach may be required.

APPENDIX J

DYNAMIC SIMULATIONS

BY

G. R. JOHNSON

AND

N. EL GABALAWI

1.0 INTRODUCTION

The satisfactory development of solar thermal electric power systems requires a thorough understanding of the interaction of the system components. There are, at present, many different types of collectors being proposed along with many different absorbers (heat exchangers), storage system, turbine systems, etc. Each of these subsystems has different characteristics that affect the overall system performance and the cost of the complete system. For example, it is not sufficient to do simple heat balances because the operation of some components are not only heat sensitive but also temperature sensitive. The computer can play an extremely important role in aiding the design because of the inordinate amount of bookkeeping required even for the simplest system. This section of the report deals with the development of a computer program written for determining the performance of viable solar thermal electric power systems.

If solar power systems are to be effectively designed, it would appear that a general simulation model can be effectively utilized. Such a model should be capable of simulating general system configurations with arbitrary control policies. The interest in solar thermal electric power systems has taken a marked upturn and the state-of-the-art is changing rapidly; therefore, as new and more sophisticated subsystem models become available they should be easily incorporated into the model. For these reasons coupled with the need to provide detailed system performance as a back-up to the overall performance and cost optimization, the development of a generalized computer simulation model for the dynamic performance analysis of solar thermal electric power systems was undertaken during this investigation.

2.0 PROGRAM STRUCTURE

A dynamic simulation model for use in the performance analysis of specific designs of solar thermal electric power systems has been developed. The program is called SIMSTEPS, an acronym for SImulation Model for Solar Thermal Electric Power Systems. The objectives for the development of SIMSTEPS were to:

1. Develop a general model, that is, one that can be used for any specified system configuration for solar thermal electric power plants.
2. Modularize the program so that subsystems can be introduced or replaced as more sophisticated subsystems become available.
3. Develop a model that is simple in terms of the knowledge required by the system designer, and hence easy to use.
4. Develop a dynamic model because the primary problem being modeled is a dynamics problem and therefore the dependence on time is required.
5. Develop a dynamic point design performance analysis model with an specifiable level of simulation complexity such that a very simple module can be used for sensitivity analyses, and more complex simulation subsystems can be used for detailed time-step-by-time-step analysis of the overall system.
6. Develop a control driven model so that the total system responds to the decisions and actions of the control subsystem.

The program is executor and library file oriented. The library file contains all of the subsystem modules. To use the program the user specifies the components included in the system and the manner in which they are connected. The executor program in SIMSTEPS will then write the computer program for the specific system to be analyzed.

In short, program SIMSTEPS is a program to write a program. It is open-ended in terms of the number of subsystems allowable in a given system. Each specific system as defined by the user will be analyzed by the executor overlay. Systems are considered like electrical networks and any configuration can be treated. This does not mean the electrical analogy approach is followed, rather the program treats the system like an electrical circuit with flow variables (temperature, pressure and mass flow rate) used as the system state variables.

One of the interesting features of the program is that it is "control driven." These controllers can take advantage of as much information as the system designer deems necessary for successful operation of the system. These include, but are not limited to, absorber fluid temperature, incident insolation, storage tank temperature, and turbine inlet and outlet conditions.

The overall schematic for the program structure is shown in Figure 2-1. There are four overlay levels. The first level is the input overlay, the second is the executor overlay, the third is the output overlay and the fourth is for reading weather data from magnetic tape. The primary function of the input overlay is to read in the system description and input-output connections as well as state variable initial conditions. The role of the output overlay is to produce step-by-step outputs for the system variables as well as plots (either flat-

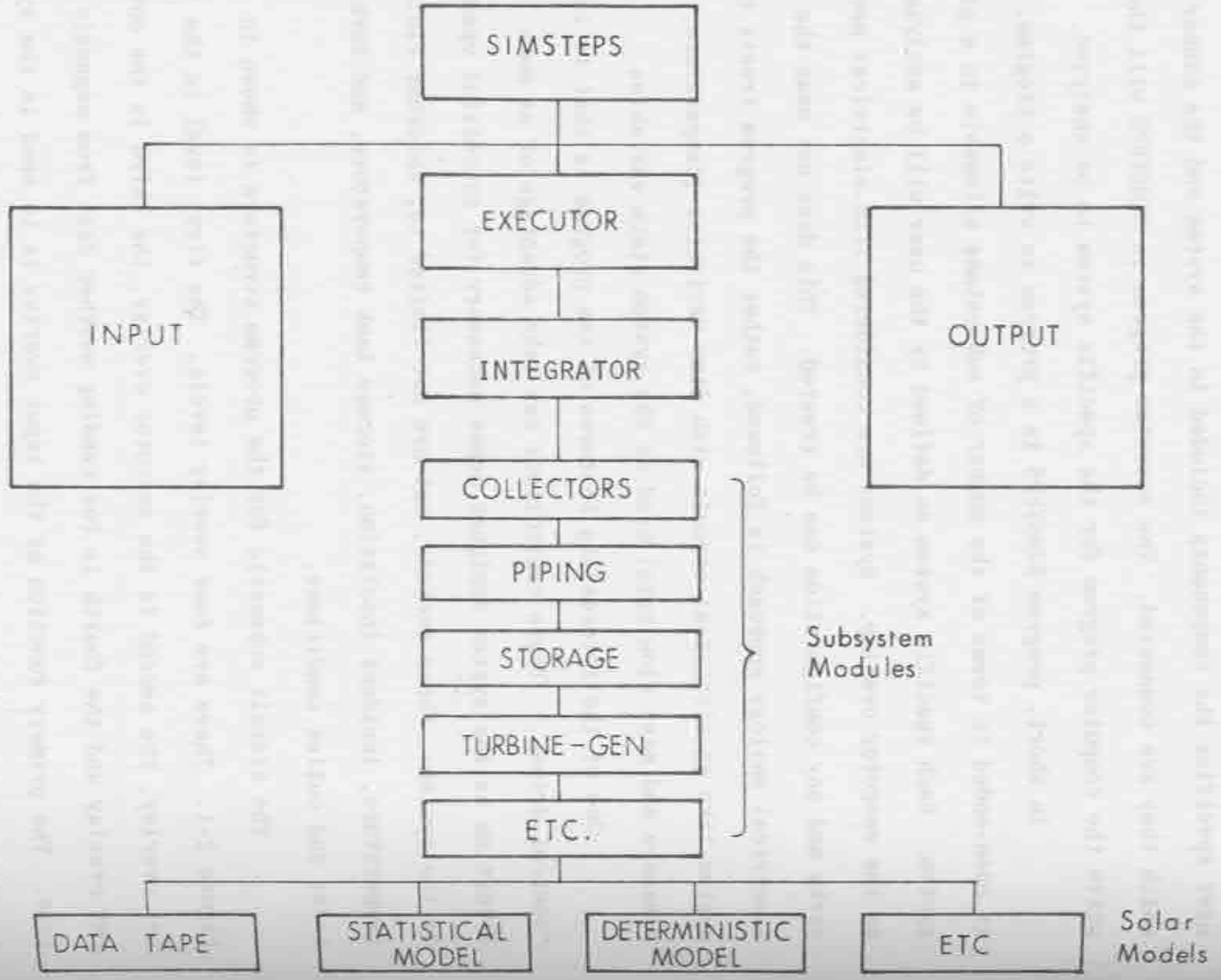

Figure 2-1. Schematic Representation of SIMSTEPS Structure.

bed or microfilm) of any of the system variables as a function of time. Information contained on the weather data tapes includes hour-by-hour data for a specified geographic location. These data are:

- Wet and dry bulb temperatures
- Wind Speed
- Diffuse and direct components of insolation
- Atmospheric pressure
- Relative humidity
- Sun position (azimuth and eleration angles)

The executor overlay is the heart of the program and it is where the description of the program is turned into an executable program. The specific solar thermal electric power system to be analyzed can consist of any given collection of components. For example, Figure 2-2 is a schematic representation of a hot water system using parabaloid collectors, cavity absorber and a hot water storage system. The inputs and outputs of each subsystem are labeled (arbitrarily) as shown in Figure 2-2 and it is this labeling that enables the executor program to construct the system mode.

The number of modules or subsystems allowable in the subsystem library is virtually unlimited. At the present time the following subsystems have been modeled and are included in the library: collector subsystems (both flat-plate and focusing), absorbers, plumbing, valves, pumps, heat storage subsystems, turbine, cooling tower, heat exchangers, and the control units. Where necessary, subsystems are described by a set of time dependent differential equations. System state variables are

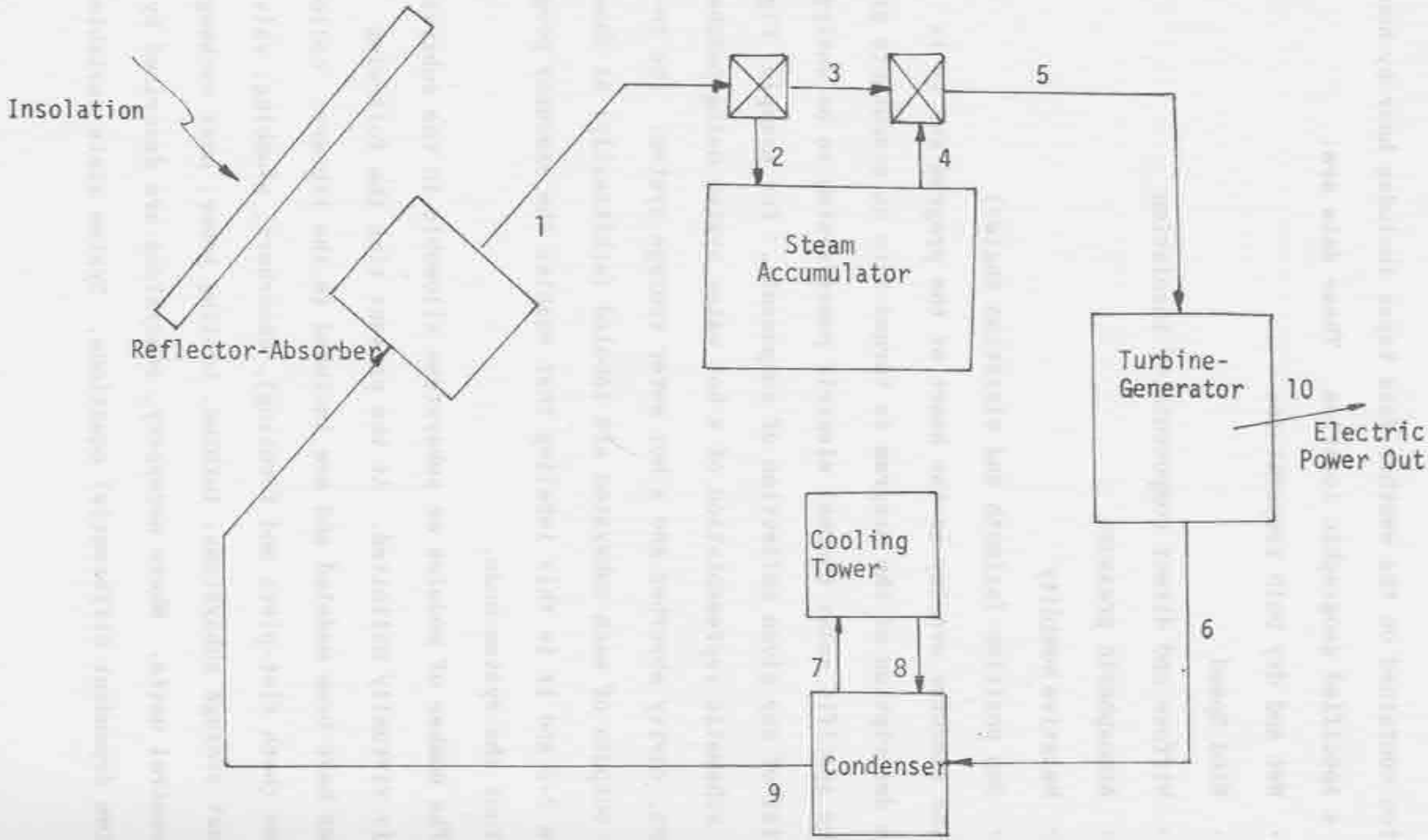

FIGURE 2-2. SYSTEM DESCRIPTION FOR PROGRAM INPUT

temperature, pressure and mass flow rate. Additional or new subsystem modules will be included in the system design program as they become available. The library contains: presently a flat-plate collector module based on the work of Hottel and Whillier, (1958) and Duffie and Beckman, (1974), paraboloidal and parabolic cylinder concentrator models; a cylindrical receiver-coil steam generator absorber model, a pancake-helix steam generator and a straight line pipe steam generator model; two heat storage models, a dynamic steam accumulator model and a stratified (or well mixed) hot water storage model; a model for mixer valves; a model for splitter valves; a model for pumps; a model for the pipes; a model for a counter flow heat exchanger; a generalized solar tracking model for full equatorial, elevation-azimuth, roll about a single axis, etc.; and a turbine-generator model based upon a Westinghouse Electric Corporation model used extensively for turbine design. These models are described in more detail in the following section.

The program has been developed so that any type of incident solar radiation data or model can be used. These include: 1) deterministic (an algebraic equation) sun model; 2) random simulation model based upon cloud cover statistics; and 3) actual tabulated input information based upon collected data. The integrator model is a second-order predictor-corrector routine.

The program is written in EXTENDED FORTRAN for a Control Data Corporation 6400 computer. Run time for the simulation of a 24 hour day in 6 minute time increments is in the 4-30 second range, depending on the system configuration and the complexity of the control strategy.

3.0 SUBSYSTEM MODEL DESCRIPTIONS

A dynamic model was developed for each subsystem in the STEP system selected for simulation. Each of the subsystems is described in detail in the following section.

3.1 Concentrator Models

Two types of concentrators were modeled: (1) Paraboloidal mirror and (2) Fresnel reflector. Both are double curvature concentrators. The paraboloid is considered as a reference since it has the best performance. The solar radiation incident on the concentrator is considered normal to the reflector plane.

3.1.1 The Paraboloidal Mirror

The model used is based on the formula

$$E = E_{max}\, e^{-Cr^2}$$

$$E = \left(\frac{180}{\pi}\right)^2 h^2 \sin^2 \theta_{max}\; R\, E_{sun}$$

and

$$C = \left(\frac{180}{\pi}\right)^2 \left(\frac{h}{2f}\right)^2 (1 + \cos \theta_{max})^2$$

where (see Figure 3-1);

θ_{max} is the concentrator rim angle

f is the concentrator focal length

r is the radius of the circle whose center is the focal point and is completely in the focal plane

R is the reflectivity of the reflecting surface (dimensionless)

h is a dimensionelss parameter characterizing the accurach of the reflecting surface and is related to the reflected beam deviation angle

E_{sun} is the direct normal solar radiation falling on the reflector plane, in kWh_t/m^2-hr.

Figure 3-2 shows the distribution of E over the focal plane which has its maximum value E at r=o (focal point). If E_{max} is constant, then the distribution curve of E will drop-off more rapidly with increasing C, i.e., if the value of C is small, then the distribution will be spread over a larger area.

Integrating E over a circle of radius r inthe focal plane results in the amount of energy per unit time falling on the circle:

$$\Phi_r = \int_o^r E\, 2\pi r\, dr = 2\pi E_{max} \int_o^r re^{-Cr^2} dr = \frac{\pi E_{max}}{C} (1-e^{-Cr^2})$$

which can be rewritten in the following form:

$$\Phi_r = \Phi_{max} (1-e^{-Cr^2})$$

where Φ_{max} is the total amount of solar energy per unit time falling on the focal plane, i.e., when $r = \infty$.

If the cavity absorber is placed with its opening circle in the focal plane and its axis coincident with the concentrator axis, where the opening radius is r_o, then the amount of energy per unit time entering the cavity opening is:

$$\Phi_{r_o} = \frac{\pi E_{max}}{C}\left(1-e^{-Cr_o^2}\right) = \pi(2f)^2 \frac{\sin^2\theta_{max}}{(1+\cos\theta_{max})^2} R E_{sun}\left(1-e^{-Cr_o^2}\right) \quad (3\text{-}1)$$

The ratio of the energy entering the cavity opening to the energy falling on the concentrator plane is

$$\frac{\Phi_{r_o}}{\frac{\pi}{4} D^2_{reflector} E_{sun}} = R\left(1-e^{-Cr_o^2}\right)$$

3.1.2 Fresnel Reflectors (see Figure 3-3)

The model considers the Fresnel reflector to be a number of coaxial paraboloidal rings. Each paraboloid has a different focal length but they all have the same focal plane. The model is also based on the paraboloidal mirror formula, Equation (3-1). This equation is applied to each ring, for example, the i^{th} ring has rim angle θ^i_{max} and focal length f^i, and is shaded by the $i+1$ st ring which has rim angle θ^{i+1}_{max}, then:

$$\Phi^i_{r_o} = \pi R E_{sun} (2f^i)^2 \left[\frac{\sin^2\theta^i_{max}}{(1+\cos\theta^i_{max})^2} - \frac{\sin^2\theta^{i+1}_{max}}{(1+\cos\theta^{i+1}_{max})^2}\right] \cdot$$

$$\left(1-e^{-C^i r_o^2}\right)$$

or

$$\Phi^i_{r_o} = \pi R E_{sun} K^i$$

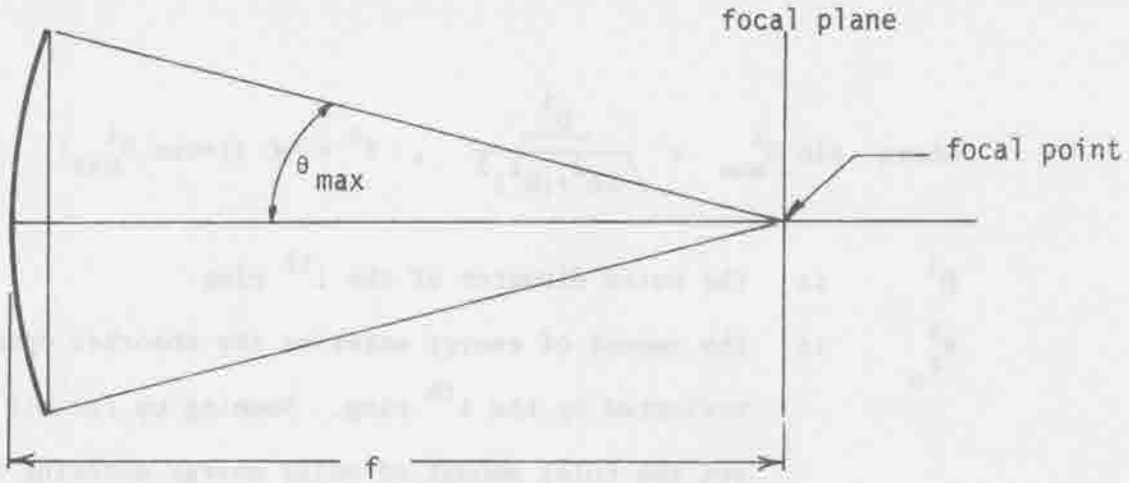

FIGURE 3-1. PARABOLOIDAL MIRROR GEOMETRY

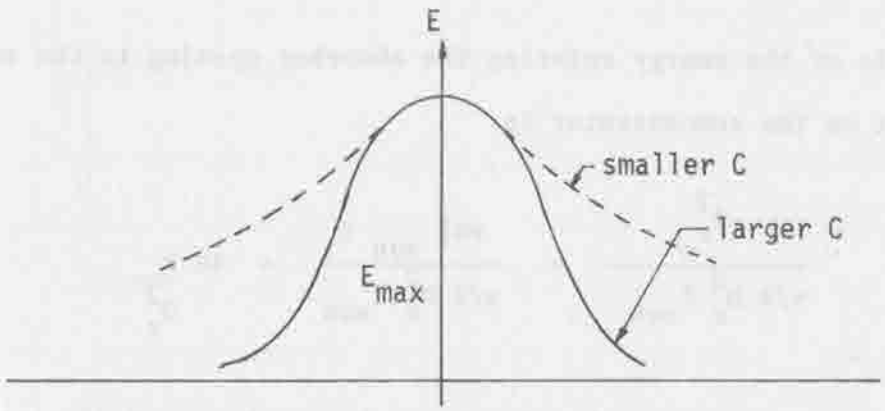

FIGURE 3-2. ENERGY DISTRIBUTION AT FOCAL PLANE

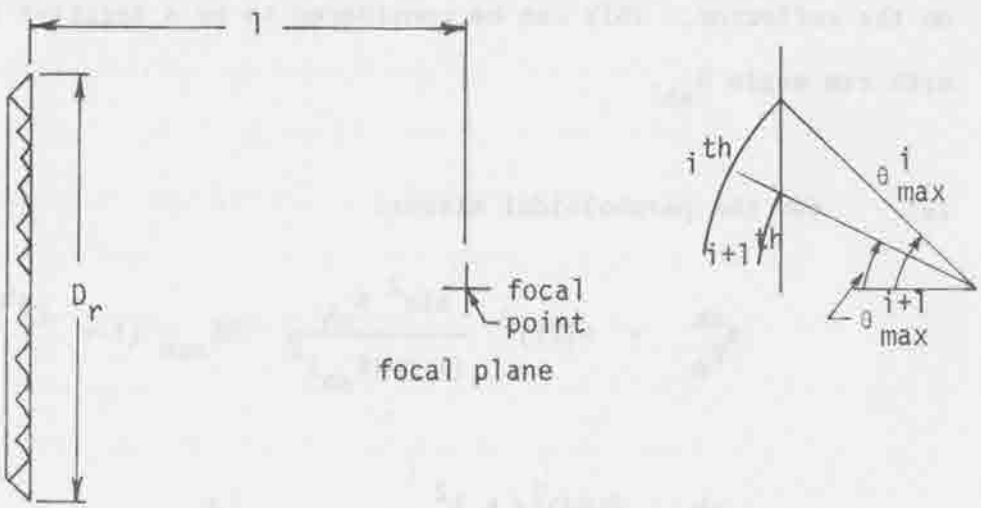

FIGURE 3-3. FRESNEL REFLECTOR GEOMETRY

where $\sin \theta^i_{max} = \frac{D^i}{\sqrt{4\ell^2+(D^i)^2}}$, $f^i = \frac{1}{2}\ell\ (1+\cos\ \theta^i_{max})$, and

D^i is the outer diameter of the i^{th} ring

$\phi^i_{r_o}$ is the amount of energy entering the absorber opening and reflected by the i^{th} ring. Summing up for all rings we get the total amount of solar energy entering the absorber opening and reflected by all rings, i.e., the whole reflector.

$$\Phi_{r_o} = \sum_{i=1}^{n} \phi^i_{r_o} = \pi R E_{sun} \sum_{i=1}^{n} K^i = \pi R E_{sun}\ K$$

The ratio of the energy entering the absorber opening to the energy incident on the concentrator is:

$$\frac{\phi^T_{r_o}}{\pi/4\ D_r^2\ E_{sun}} = \frac{\pi R E_{sun}\ K}{\pi/4\ D_r^2\ E_{sun}} = 4R\ \frac{K}{D_r^2}$$

As shown in Figure 3-4, the absorber makes a shadow of diameter D_{abs} on the reflector. This can be considered to be a negative reflector with rim angle θ_{sh}.

(a) for the paraboloidal mirror:

$$\phi^{sh}_{r_o} = \pi(2f)^2\ \frac{\sin^2\theta_{sh}}{(1+\cos\theta_{sh})^2}\ RE_{sun}\ (1-e^{-C^{sh} r_o^2}) \quad \text{and}$$

$$C^{sh} = \left(\frac{180}{n}\right)^2 \left(\frac{h}{2f}\right)^2\ (1+\cos\ \theta_{sh})^2$$

Therefore,

$$\Phi_{r_o}^{net} = \Phi_{r_o} - \Phi_{r_o}^{sh}$$

(b) for the Fresnel reflector the summation over the i^{th} ring stops if $D_{abs} \geq D_i$, then:

$$\Phi_{r_o}^{T} = \sum_{i=1} \Phi_{r_o}^{i}$$

where n is the number of rings with $D^i > D_{abs}$.

3.2 Absorber Model

The mathematical model was developed for a cylindrical cavity-type absorber with a coil forming the wall of the absorber. The model consists of two parts: (1) the cavity absorber and (2) the heat transfer process through the pipe for one or two phase flow.

The cavity absorber model (see Figure 3-5) is based on the work of Rubanovich (1965). The cavity absorber approximates a black body. We will first condiser an expression for the heat flux absorbed by the cavity wall. The first simple model assumes that the internal cavity surface temperature is uniform and the interior surface is gray and emits and reflects diffusely. Consider the cavity interior surface and the cavity opening as two surfaces radiating at each other, where A_1 is the area of the opening and A_2 is the surface area of the cavity interior as shown in Figure 3-6. The shape factor relationship is:

$$F_{11} + F_{12} = 1 \quad .$$

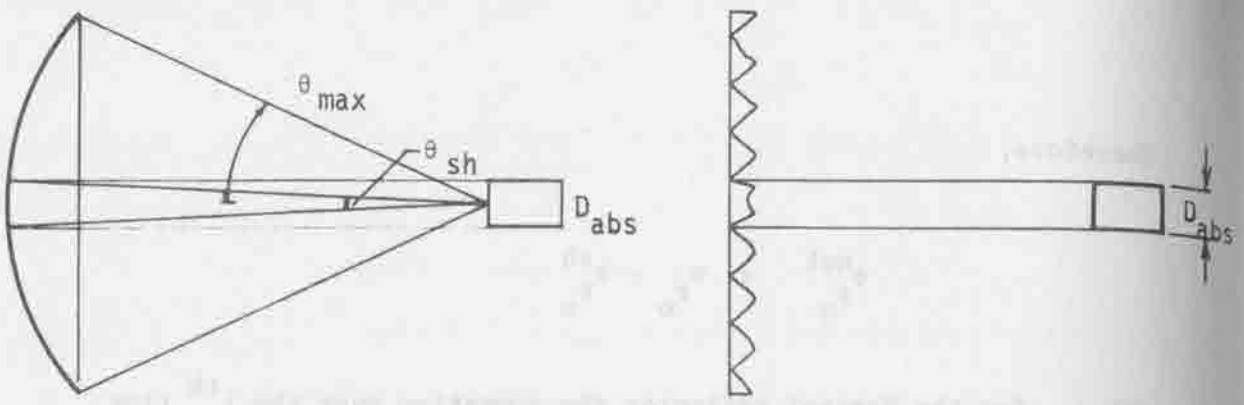

FIGURE 3-4. ABSORBER SHADING

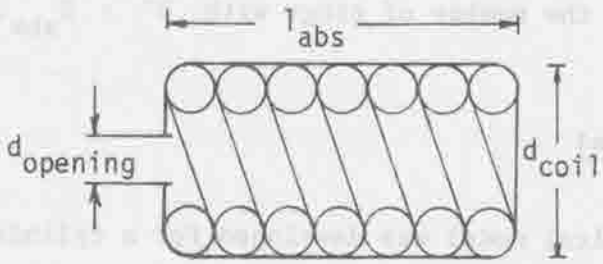

FIGURE 3-5. ABSORBER GEOMETRY

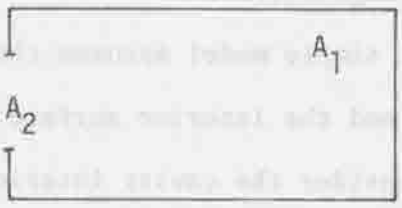

FIGURE 3-6. ABSORBER SHAPE FACTORS

The reradiation shape factor of the cavity wall is:

$$F_{11} = 1 - F_{12}$$

where F_{12} is the shape factor from the interior to the opening.

The absorption factor B_{12}, which is the fraction of the radiation emitted by surface 1 and absorbed by surface 2 can be expressed as:

$$B_{12} = F_{12}\, e_2 + F_{11}\, (1-e_1)\, B_{12}$$

where e is emissivity of the surface. Therefore,

$$B_{12} = \frac{F_{12}\, e_2}{1-(1-F_{12})\, (1-e_1)} \quad .$$

In this case, B_{12} is the fraction of radiation emitted by the cavity interior surface that is lost through the cavity opening. The radiation emitted from the cavity wall per unit time is $e_1 A_1 \sigma T_1^4$. The radiation lost through the cavity opening is

$$Q_{loss} = e_1 A_1 \sigma T_1^4\, B_{12} = \frac{F_{12} e_1}{1-(1-F_{12})\, (1-e_1)}\, A_1\, \sigma T_1^4$$

where σ is the Stephen- Boltzman constant.

Similarly, the fraction of the entering solar radiation absorbed by the cavity interior wall can be calculated as follows:

$$B_{11} = F_{11}\, e_1 + F_{12}\, (1-e_1)\, B_{11}$$

$$B_{21} = F_{21}\, e_1 + F_{21}\, (1-e_1)\, B_{11}$$

Therefore,

$$B_{21} = \frac{e_1}{1-(1-F_{12})\ (1-e_1)}$$

The radiation absorbed by the cavity wall per unit time is

$$Q_{abs} = A_2\, \Phi^T_{r_o} \quad B_{21} = \frac{e_1}{1-(1-F_{12})\ (1-e_1)} \quad A_2\, \Phi^T_{r_o}$$

and the efficiency of the absorber is

$$\eta_{abs} = (Q_{abs} - Q_{loss})/(A_2\, \Phi^T_{r_o}) = B_{21} - \frac{Q_{loss}}{A_2\, \Phi^T_r} \quad .$$

The following formulas are used for calculation of the shape factor F_{12}. They pertain to the interchange between an infinitesimal element and a finite surface. The interior surface of the cavity is divided into small elements, and the interchange between these elements and the cavity opening (as a finite surface) is considered. The result is then integrated over the entire cavity interior surface A_1, which consists of the cylindrical wall and the back disk wall.

$$F_{12}\, A_1 = \int_{A_1} F_{d\, A_1 - A_2} \, dA_1$$

where $F_{dA_1-A_2}$ is the shape factor between the infinitesimal element dA_1 and A_2. Changing the integration sign to a summation by taking small finite elements instead of infinitesimal elements, yields

$$F_{12} = \frac{1}{A_1} \sum_{n=1}^{N} F_{\Delta A_1-A_2} \Delta A_1$$

$$= \frac{1}{A_1} \left[\sum_{n_1=1}^{N_1} F_{\Delta A_1-A_2} \Delta A_1 + \sum_{n_2=1}^{N_2} F_{\Delta A_1-A_2} \Delta A_1 \right]$$

where N_1 and N_2 are the total number of elements on the cylindrical wall and the back disk wall, respectively. $F_{dA_1-A_2}$, the shape factor between the infinitesimal element on a cylindrical surface and a disk is given by

$$F_{dA_1-A_2} = \frac{X}{2} \left[\frac{1 + Y^2 + X^2}{\sqrt{1 + Y^2 + X^2 - 4Y^2}} - 1 \right]$$

where $X = a/c$ and $Y = b/c$ as shown in Figure 3-7.

$F_{dA_1-A_2}$, the shape factor between an infinitesimal element on the disk and another disk is given by

$$F_{dA_1-A_2} = \tfrac{1}{2} \left(1 - \frac{Z - 2Y^2X^2}{\sqrt{Z^2 - 4Y^2X^2}} \right)$$

where $X = c/a$, $Y = b/c$ and $Z = 1 + (1+Y^2)X^2$ as shown in Figure 3-8.

It is clear that the ratio A_2/A_1 changes the shape factor F_{12}, the heat flux absorbed q_{abs} and the absorber efficiency η_{abs}. Also the dimensions of the cavity, i.e., l_{abs}/d_{coil} affect F_{12}. This indicates that the performance of the cavity absorber can be optimized by finding the best combination of $d_{opening}$, d_{coil} and l_{abs}.

The above model was a simplified model which used the assumption that the internal cavity surface temperature is uniform. This model is accurate enough since the temperatures are not very high -- in the range of 250 ^{o}C in the case of boiling in the absorber, and up to 350 ^{o}C in the case of pressurized water heating. A more rigourous model has been developed by Grilikhes, et.al., (1972 a) in which they obtained the interesting results shown in Figure 3-9.

If the reflectivity ρ of the interior surface is low, then the radiation flux distribution along the length of the cylindrical wall has a high peak, which means a hot spot. By increasing ρ the distribution becomes more and more uniform. In the simplified model, the radiation flux density is constant along the cylindrical wall of the cavity where the coil is located.

The heat transfer model used for the pipe analysis is based upon a simple one-dimensional heat transfer model. The helical pipe is divided into small segments (normally, the pipe was made up of more than 100 segments). The heat balance equation was written for each segment as shown in Figure 3-10 and it was assumed that the heat flux q_{abs} was uniform around the pipe. Although this assumption does not appear to be satisfactory, according to the experimental results by I. A. Grilikhes, et.al., (1969 and 1972 b), this assumption can be used if we consider that the assumed uniform heat flux density q_{abs} equals,

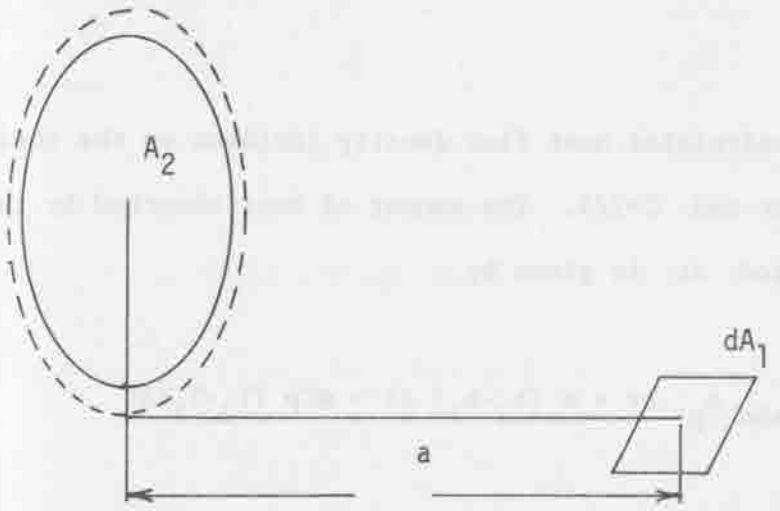

FIGURE 3-7. SHAPE FACTOR FOR INFINITESIMAL AREA

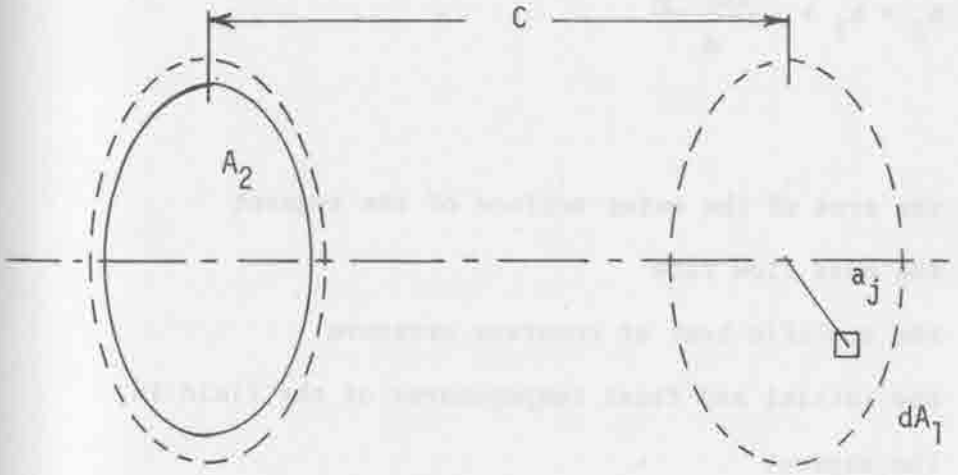

FIGURE 3-8. SHAPE FACTOR BETWEEN DISKS

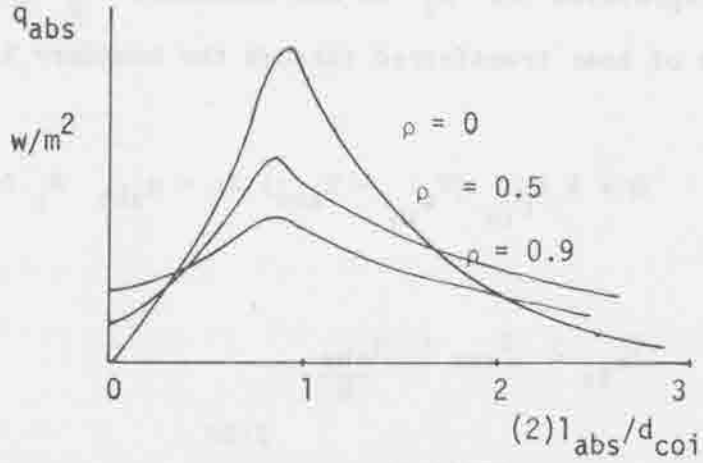

FIGURE 3-9. BOILING IN ABSORBER

$$q_{abs} = Cq_w$$

where q_w is the calculated heat flux density incident on the inside wall of the cylinder and C=2/3. The amount of heat absorbed by the pipe in a time period Δt is given by

$$Q = q_{abs} A_p \Delta t = \dot{m} (h_2-h_1) \Delta t = \dot{m}Cp (T_2-T_1)\Delta t$$

or

$$h_2 = h_1 + \frac{q_{abs} A_p}{\dot{m}}$$

where

A_p is the area of the outer surface of the segment

$\dot{m}$ is the mass flow rate

C_p is the specific heat at constant pressure;

T_1, T_2 are the initial and final temperatures of the fluid in the segment

h_1, h_2 are the initial and final enthalpies of the fluid in the segment.

From the expression for h_2 we can determine T_2 for a given pressure. The amount of heat transferred through the boundary layer is:

$$Q = h A_{p_{in}} (T_{w_{in}} - T_{ave}) \Delta t = q_{abs} A_p \Delta t$$

or

$$T_{w_{in}} \approx T_{ave} + \frac{q_{abs}}{h}$$

(if we consider that A_p equals $A_{p_{in}}$ approximately)

where

h is the heat transfer coefficient

$T_{w_{in}}$ is the inside wall temperature and

T_{ave} is the average fluid temperature in each segment = $\frac{T_1+T_2}{2}$.

The amount of heat transferred through the pipe wall is

$$Q = \frac{2\pi \quad T_{w_{out}} - T_{w_{in}} \quad \ell\Delta t}{\ell n \ (d_{out}/d_{in})/k_p} = q_{abs} \quad A_p \quad \Delta t$$

or

$$T_{w_{out}} = T_{w_{in}} + q_{abs} \quad \frac{\ell n \quad (d_{out}/d_{in}) \ d_{out}}{k_p}$$

where

k_p is the thermal conductivity of the pipe wall

$T_{w_{out}}$ is the outer surface all temperature and

l is the length of the pipe segment.

The relationship for the flow-stream pressure drop in the absence of an abrupt enterance and exit and for an incompressible flow is

$$P = \tfrac{1}{2}\rho \ V^2 \quad \frac{L}{d} \quad (4f)$$

where

f is the pressure drop coefficient.

The formulas for evaluating the pressure drop coefficient "f" are as follows:

Straight pipe

(a) Laminar Flow

$$f = 16/R_e$$

(b) Turbulent Flow

$$f = 0.079\ Re^{-0.25} \quad \text{for } 5{,}000 < Re < 30{,}000$$

$$f = 0.046\ Re^{-0.2} \quad \text{for } 30{,}000 < Re < 1{,}000{,}000$$

Coils

(a) Laminar Flow

$$\frac{f_c}{f_s} = \frac{21.5\ K}{(1.56+\log_{10} K)^{5.73}} \quad \text{for } 13.5 < K < 2000$$

(b) Turbulent Flow

$$f_c = 1/4\left(\frac{r}{R}\right)^{\frac{1}{2}} \left\{0.029 + 0.034\ \left[Re\left(\frac{r}{R}\right)^2\right]^{-0.25}\right\}$$

where the subscripts c and s refer to coil and straight pipe, respectively. The heat transfer coefficient h_ℓ, for liquid flow and the heat flux at the wall of the pipe can be calculated from

$$q_w = h_\ell\ (T_w - T_b)$$

where

T_w is the temperature at the wall, and

T_b is the bulk or mixed mean temperature.

The heat transfer coefficient is:

$$h_1 = Nu \left(\frac{k}{d}\right)$$

where

Nu is the Nusselt Number,

k is the thermal conductivity of the fluid and

d is the tube inner diameter.

In order to calculate the heat transfer coefficient correlations the Nu for inner flow in circular tubes are required. For Reynolds numbers below 2,200, the flow is considered laminar. For Reynolds numbers between 2,200 and 10,000, the flow is considered transient, and it is difficult to predict the Nusselt number in this region because of insufficient information in literature except for some very specific situations.

For the simulation purposes, a Reynolds number of 5,000 was selected as the separation between the laminar and turbulent regimes and a transient flow region was not considered. This approximation appeared acceptable for preliminary design studies. The correlations for straight pipes and for coils are usually presented in terms of the Reynolds Number:

$$Re = \frac{Vd\rho}{\mu} = \frac{\dot{m}}{\frac{\pi d^2}{4}} \quad \frac{d}{\mu}$$

where

$\dot{m}$ is the fluid mass flow rate

μ is the fluid dynamic viscosity

ρ is the fluid density

V is the mean flow velocity.

3.3 Inner Flow in Straight Pipes

The flow either laminar or turbulent, is considered to be fully developed in both the velocity and temperature profiles since the thermal entry length is very small compared to the length of the pipe. Expressions for the Nusselt number are as follows:

(a) Laminar Flow ($Re < 5,000$)

For a constant heat rate, the Nu is constant

$Nu = 4.364$

(b) Turbulent Flow ($Re > 5,000$)

For a constant heat rate, $Nu = 0.022\ Re^{0.8}\ Pr^{0.6}$

for $0.7 < Pr < 120$, $Re < 120,000$, and $L/d > 60$

where

Pr is the Prandtl number $\frac{\mu C_p}{k}$

L is the length of the pipe.

The flow in the coil is also considered to have fully developed velocity and temperature profiles. The difference between straight pipes and coils is that the transition Reynolds number is not considered 5,000, but rather

$$Re_{crit} = 2\left(\frac{r}{R}\right)^{0.32} \quad (10^4)$$

where

r is the inner radius of the pipe, and

R is the radius of curvatureof the coil.

For $R/r > 860$, the Re_{crit} for a curved pipe is equal to that of a straight pipe

(a) Laminar Flow

The Nu for curved pipes is related to that of straight pipes through the following two approximations from Sparrow, (1973).

First Approximation:

$$\left(\frac{Nu_{coil}}{Nu_{straight}}\right)_I = 0.1979 \quad \frac{\sqrt{K}}{\xi}$$

where

$$\xi = \frac{2}{11}\left(1 + \sqrt{1+\frac{77}{4}\ \frac{1}{P_r^{\ 2}}}\right) \quad \text{for} \quad P_r \geq 1$$

and

$$\xi = \frac{1}{5}\left(2 + \sqrt{\frac{10}{P_r^{\ 2}} - 1}\right) \quad \text{for} \quad P_r \leq 1$$

where

K is the Dean number = $Re\ \sqrt{r/R}$

Second Approximation:

$$\left(\frac{Nu_c}{Nu_s}\right)_{II} = \left(\frac{Nu_c}{Nu_s}\right) \frac{1}{1 + \frac{37.05}{\xi}\left[\frac{1}{40} - \frac{17}{120}\xi + \left(\frac{1}{10\xi} + \frac{13}{30}\right)\frac{1}{10P_r}\right]K^{-\frac{1}{2}}}$$

for $P_r \geq 1$

$$\left(\frac{Nu_c}{Nu_s}\right)_{II} = \left(\frac{Nu_c}{Nu_s}\right)_{I} \frac{1}{1 - \frac{37.05}{\xi}\left[\frac{\xi^7}{12} + \frac{1}{24} - \frac{1}{120\xi} - \left(\frac{4}{3}\xi - \frac{1}{3\xi} + \frac{1}{15\xi^2}\right)\frac{1}{20P_r}\right]K^{-\frac{1}{2}}}$$

for $P_r \leq 1$

(b) Turbulent Flow

The following correlations are given (6)

$$Nu = 0.021\ P_r^{0.4}\ Re^{0.85}\ \left(\frac{r}{R}\right)^{0.1}$$

For both flows, laminar and turbulent, the Nusselt number is the average of the peripheral values.

3.4 Two-Phase Heat Transfer Coefficient, h_{TP}

The two-phase flow considered here is a flow of a liquid and its vapor. We are considering forced convection heat transfer processes inside the tubes. Unfortunately, boiling heat transfer is not well known, especially for the case under consideration. There is very little information about forced convection boiling heat transfer as compared to pool boiling heat transfer, for example. And, there is even

less information about inner flow boiling for flows inside coils with small curvatures. The correlations available are for coils of large curvature with high temperature flows such as used in atomic reactors. One study was found that used smaller coils for steam-powered cars, but still the diameter of the coil was larger than those considered for solar cavity absorbers. There is certainly need for additional data for forced convection boiling in small coils.

Isbin, et.al., (1961), developed the following correlation for the ratio of the two-phase heat transfer coefficient to that of liquid only flow

$$\frac{h_{TP}}{h_{\ell}} = a \left[\frac{(1-x)}{(1-\alpha)} \right]^{0.8}$$

where

x is the weight fraction of steam in the steam-water flow mixture

α is the void fraction

a equals 1.5 to fit their experimental results.

By using the thermodynamic relations for boiling, which give the properties of the boiling substance in terms of the saturated (liquid and vapor) properties

$$v = (1-x)\, v_f + x\, v_g$$

$$\rho = (1-\alpha)\, \rho_f + \alpha_g \quad \rho$$

where v and ρ are the specific volume and density of the boiling substance, respectively, and subscripts f and g refer to saturated liquid and saturated vapor, respectively.

Noting that $\rho = 1/v$, the following expression results:

$$\frac{1-x}{1-\alpha}\,\frac{\alpha}{x} = \frac{\rho_f v_g - 1}{1 - \rho_g v_f} = \frac{v_g/v_f - 1}{1 - v_f/v_g}$$

which after some algebraic manipulation becomes

$$\frac{1-x}{1-\alpha} = 1 + x \left(\frac{v_g/v_f - 1}{1-v_f/v_g} - 1\right) \quad .$$

Substituting this value into the heat transfer coefficient ratio yields

$$\frac{h_{TP}}{h_\ell} = a \left[1 + x \left(\frac{v_g/v_f - 1}{1 - v_f/v_g} - 1\right)\right]^{0.8}$$

which is a function only of x since v_f and v_g are constants at the given boiling pressure.

The authors (Isbin, et.al., (1961) claim that the heat transfer coefficient "h_{TP}" increases with the steam quality x, to high values of x. The model used here utilized the above correlation up to values of x = 1.0. Above that single phase flow correlations were used with the pure steam properties.

3.5 Heat Exchanger Model

Heat exchangers were modeled for systems using pressurized hot water. The modeling of the steam generation in the heat exchangers was divided into the following two processes, where a heat exchanger was designed for each: (1) heating the water from the condenser temperature up to the boiling temperature; (2) evaporation at constant temperature. Figure 3-11 shows the changes in temperature

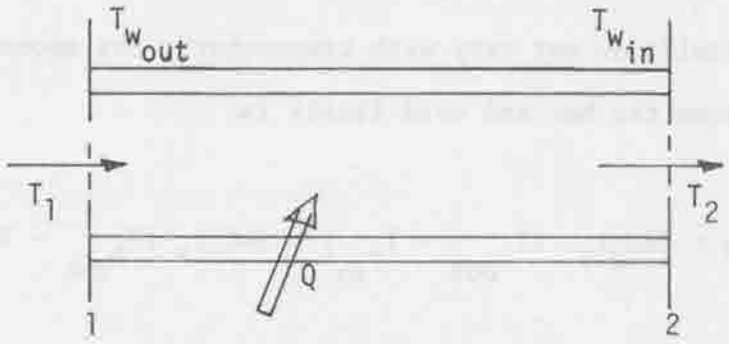

FIGURE 3-10. HEAT TRANSFER IN PIPES

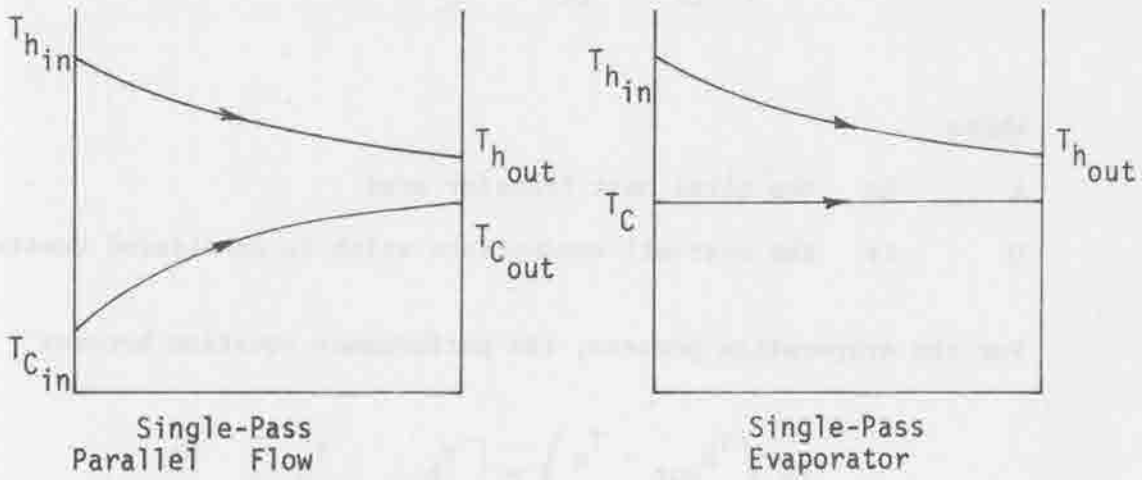

FIGURE 3-11. HEAT EXCHANGERS

that occurs in each heat exchanger. Considering that the specific heats of the fluids do not vary with temperature, the amount of heat exchanged between the hot and cold fluids is:

$$q = (\dot{m}C_p)_c \quad (T_{c_{out}} - T_{c_{in}}) = (\dot{m}C_p)_h \quad (T_{h_{out}} - T_{h_{in}})$$

where

$\dot{m}$ is the mass flow rate of the fluid

C_p is the specific heat of the fluid,

c and h are subscripts which refer to the cold and hot fluids respectively.

The equation for the performance of the heat exchangers is

$$\ell n \left(\frac{T_{h_{out}} - T_{c_{out}}}{T_{h_{in}} - T_{c_{in}}} \right) = \left[\left(T_{h_{out}} - T_{c_{out}} \right) - \left(T_{h_{in}} - T_{c_{in}} \right) \right] \frac{UA}{q}$$

where

A is the total heat transfer area

U is the over-all conductance which is considered constant.

For the evaporation process, the performance equation becomes

$$\ell n \left(\frac{T_{h_{out}} - T_c}{T_{h_{in}} - T_c} \right) = \left[T_{h_{out}} - T_{h_{in}} \right] \quad \frac{UA}{q} \quad .$$

The above equations are for single-pass flow. A correction factor F is used to consider the counter flow in a multiple pass, where F is less than or equal to one.

The correction factor F can be found from curves for the different designs as a function of two variables P and Z, where

$$P = \frac{T_{c_{out}} - T_{c_{in}}}{T_{h_{in}} - T_{c_{in}}} \quad \text{and} \quad Z = \frac{T_{h_{in}} - T_{h_{out}}}{T_{c_{out}} - T_{c_{in}}} .$$

The performance equation becomes

$$\ell n \left(\frac{T_{h_{out}} - T_{c_{out}}}{T_{h_{in}} - T_{c_{in}}} \right) = \left[\left(T_{h_{out}} - T_{c_{out}} \right) - \left(T_{h_{in}} - T_{c_{in}} \right) \right] \frac{UAF}{q}$$

For the evaporation process, F = 1. In solar energy applications, the heat exchangers do not work under the design point conditions because the hot water temperatures depend on the insolation. This means that in order to evaluate the off-design performance and generate steam which matches the turbine performance, an iterative procedure is required.

A different approach to heat exchanger modeling uses an exchanger effectiveness

$$\varepsilon = \frac{(\dot{m}C_p)_h \left(T_{h_{in}} - T_{h_{out}} \right)}{C_{min} \left(T_{h_{in}} - T_{c_{in}} \right)}$$

or

$$\varepsilon = \frac{(\dot{m}C_p)_c \left(T_{c_{out}} - T_{c_{in}} \right)}{C_{min} \left(T_{h_{in}} - T_{c_{in}} \right)}$$

where C_{min} is the smaller of the $(\dot{m}C_p)_h$ and $(\dot{m}C_p)_c$ values. The rate of heat transfer between the hot and cold fluids is

$$q = \varepsilon C_{min} \left(T_{h_{in}} - T_{c_{in}} \right) .$$

3.6 Heat Storage - Steam Accumulator Model

The modeling of the steam accumulators is based on the first law of thermodynamics. Considering the storage tanks as a control volume, with charging steam flowing in, discharging steam flowing out, and Q the rate of heat loss through the wall of the tank, then

$$dE = (\dot{m}h)_{in}\, dt - (\dot{m}h)_{out}\, dt + dQ - dW$$

where

E is the internal energy of the water in the tank

h is the specific enthalpy of the steam

$\dot{m}$ is the steam mass flow rate

dQ is the amount of heat exchanged between the tank and the environment in time dt

dW is the amount of work exchanged between the tank and the environment in time dt.

Now, $dW = 0$ and $dQ = Qdt$, then

$$\Delta E \{ (\dot{m}h)_{in} - (\dot{m}h)_{out} + \dot{Q} \} \Delta t \quad .$$

The dynamics of the charging or discharging processes are considered as if the change of the property of water in the tank is along the saturated liquid line. This is a very good approximation since the steam in the tank is negligible compared to the mass of liquid. This means that all of the charging steam will condense after it enters the tank and the temperature and the pressure of the tank will rise. In discharging, the steam discharged will be saturated steam at the

temperature and the pressure of the tank. In actual use of steam accumulators there is a limit on the rate of discharge as discussed by Goldstern (1970).

$$(\dot{m}_{out})_{max} = (2.35 + 0.014\ p)\ D_W^{-0.715} \quad \text{ton/hour-m}^3$$

where

P is the tank pressure in bars and

D_W is the density of the storage water in (^oB), a measure of water purity.

Notice that the maximum rate of steam discharge is per m^3 of the steam space, which is the volume occupied by steam. This puts limits on the minimum steam space for a given maximum pressure and for a specific water density D_W.

3.7 Steam Turbine Model

The steam turbine modeled here is based on a Westinghouse constant volume turbine design. The performance curves of the turbine were constructed using a Westinghouse turbine design computer program (TURDES). The information used consisted of the output in Megawatts as a function of the steam temperature, and the steam mass flow rate required as a function of the steam temperature. Then, knowing the steam temperature, the required steam mass flow rate and the turbine output in Megawatts can be calculated.

3.8 System Description and Control Model

In the present study two distributed systems were simulated. The first system utilized steam generation in the absorber. The second

system was a pressurized hot water system, where no boiling takes place in the absorber and heat exchangers are used to generate steam, one for direct supply to the turbine and the other for storage.

In the distributed system, the concentrator-absorber pairs are arranged in rows, each row is connected with a pair of transport pipes, one to deliver the feed water and the other to collect the hot water or steam. Three concepts were considered in the design of distributed systems: (1) considering that all the absorbers in the field work under the same conditions, i-e., all have the same mass flow rate, inlet temperature and consequently outlet temperature. In this case, the mass flow rate is very small. The controls for this system are the simplest and the simulation computations are the shortest. (2) considering that the absorbers are divided into two gropus, one for heating the water to the boiling temperature, and a second group for boiling the water. For this case, the controls and computations are more complex, expecially for the off-design cases. Since solar systems do not work at the design point most of the time because the solar insolation varies continuously, the complexity of the computation is always there. The primary reason for this complexity in the off-design case is that the number of absorbers in the field has to be divided so that the amount of water brought to the boiling temperature in the first group can become saturated steam in the second. Otherwise some of the reflector-absorbers will be idle. Practically, this division might not be feasible. Notice that concepts (1) and (2) are the same for pressurized hot water systems. (3) the water is heated up successively in each group to the boiling temperature, then boiling takes place, also successively until saturation. The mass flow rate in this case is much larger than it is in the first two concepts, but the controls and

computations for this case are also much more complex. It is impractical to run the simulation model over a whole year to evaluate a full year's performance for this concept because of the large number of calculations involved in treating hundreds of individual collectors and their interconnecting pipes. To save computation time, the collectors in each row were modeled as a single large collector having the total losses and the net gain of all the collectors and piping in the row. The concentrators were considered to be sun tracking, i.e., solar radiation was always perpendicular to the concentrator plane. The absorber shadow was always in the center of the concentrator. The turbine was constant volume type, in which the power output as well as the steam mass flow rate required decrease with a decrease in the steam temperature. Steam accumulators were used as thermal storage units.

3.8.1 System 1: Steam Generation in the Absorber (see Figure 3-12)

(1) If the solar insolation is more than the design level, the mass flow rate $\dot{m}_{w_d}$ to the absorber will be more than the design value $\dot{m}_{w_d}$ to produce saturated steam. The extra steam generated will be proportional to the difference between the insolation and the insolation design level.

(2) If the solar insolation is less than the design level, then $\dot{m}_w$ will be reduced to match the turbine performance requirement because the temperature will be lower than the design temperature.

3.8.2 System 2: Pressurized Hot Water Figure (see Figure 3-13)

In this system pressurized hot water is fed to the absorber where it is heated to the boiling temperature at constant pressure. Similarly,

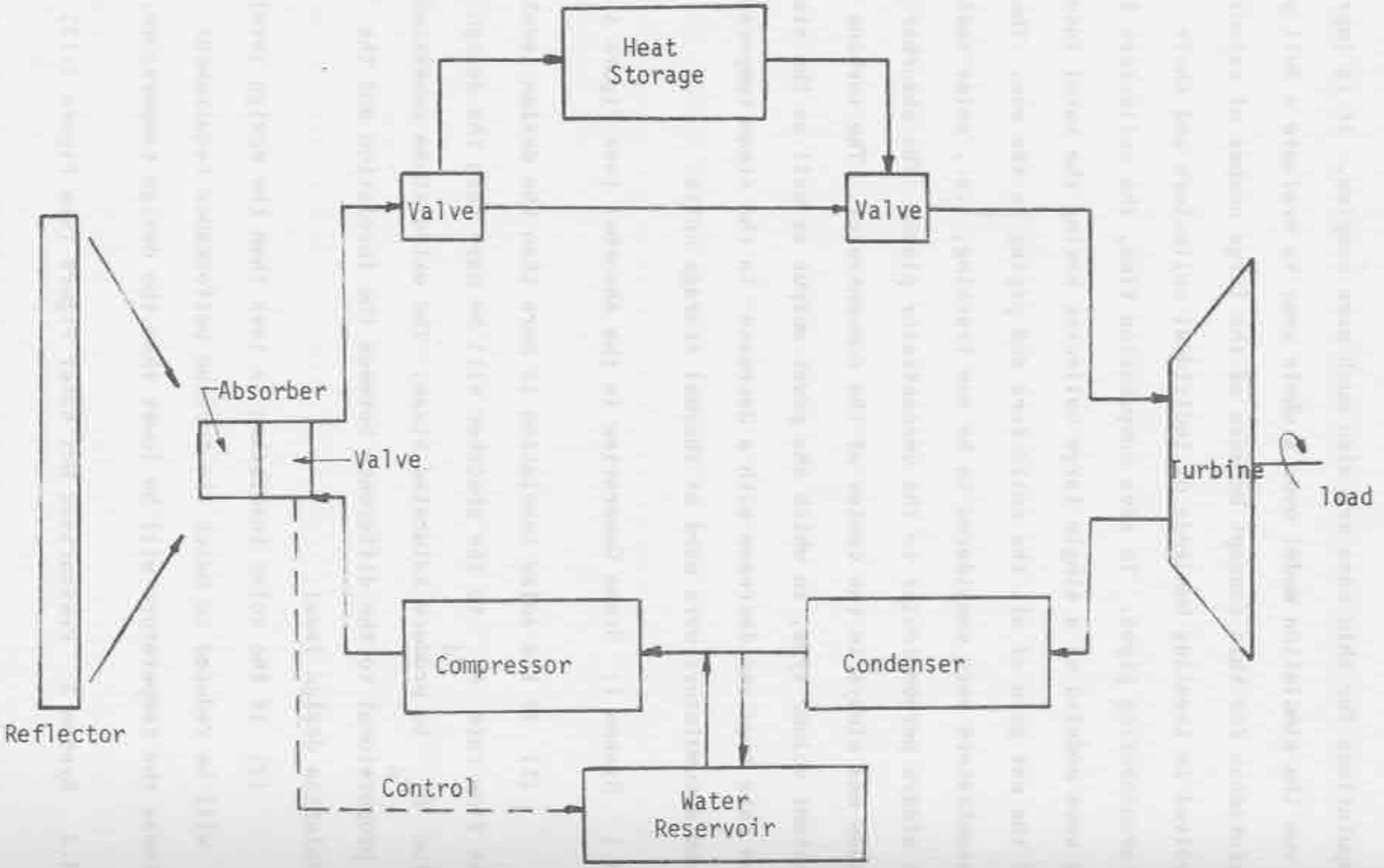

FIGURE 3-12. SYSTEM CONFIGURATION - STEAM GENERATION IN ABSORBER

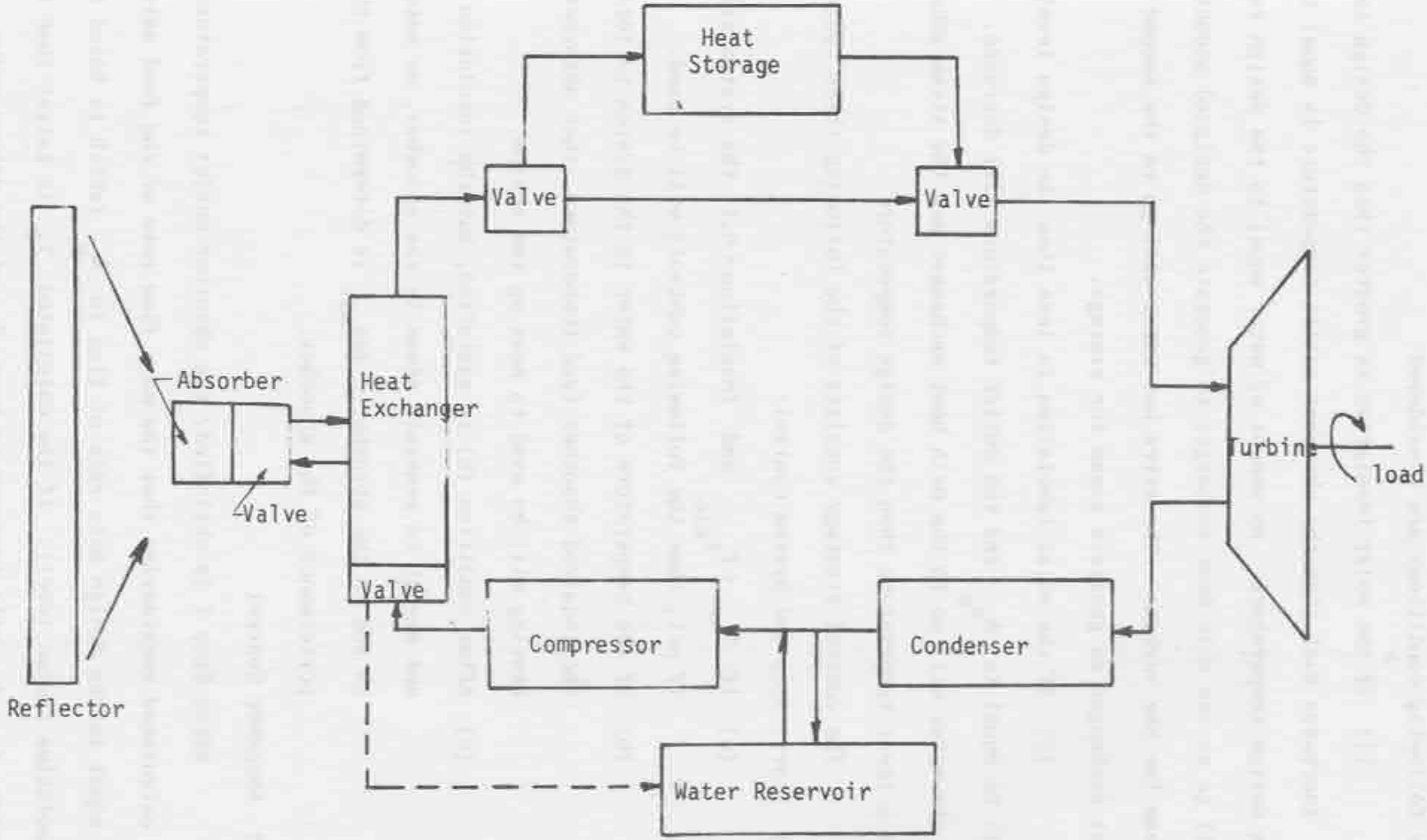

FIGURE 3-13. SYSTEM CONFIGURATION - PRESSURIZED HOT WATER

the following conditions are considered:

(1) If the solar insolation is greater than the design level, $\dot{m}_w$ increases such that the absorber outlet temperature is equal to the design temperature. An amount of water equal to the design value will go to the main heat exchanger to generate the designed amount of steam for the turbine. The extra hot water will go to the second heat exchanger to generate steam for storage.

(2) If the solar insolation is less than the design level, $\dot{m}_w$ will be equal to $\dot{m}_{w_d}$ and the outlet temperature will decrease. All of the water will go to the main heat exchanger and the steam generated has a lower temperature than the design temperature.

The control strategy consists of the following three controls:

(1) Start, Stop and System Control:

(a) If $T_{acc} < T_{t_{min}}$ and Insolation < 0.1 the system will stop if not, then the following controls will be used.

(b) If the temperature of the water in the system is less than the required absorber feed temperature, then absorber heating will be used to heat up the system.

(c) After condition (b) is satisfied, but the insolation is still not enough to generate steam in the absorber, no water will be fed to the absorber. Ins_{min} is determined from the performance of the absorber.

(2) Absorber Control

After Step 1 is satisfied, the absorber outlet temperature T_2 is calculated considering that the mass flow rate of the feed water $\dot{m}_w$ is equal to the design mass rate of flow in $\dot{m}_w$ (which is based on the insolation design level). If the calculated T_2 is larger than the design T_2, $\dot{m}_w$ will increase to keep T_2 at the design value. However,

if T_2 is less than T_{abs_d}, $\dot{m}_w$ will remain equal to $\dot{m}_{w_d}$, and T_2 will be greater than T_{abs_d}.

(3) Storage Control

(a) After satisfying step 2, if the steam delivered is the required amount for the turbine according to the turbine performance characteristics it will go directly to the turbine.

(b) If there is steam in excess of the turbine requirement, a check on the temperature of the excess steam is made to determine if the storage tank can be charged. If the storage unit can be charged, it is, otherwise the excess steam is vented.

(c) If the $T_{acc} > T_{t_{min}}$ and Insolation < Insolation_{min} the accumulator will be discharged.

The program control algorithm described above is shown in flow diagram form, Figure 3-14 with the symbols defined as follows:

T_{acc} is the steam accumulator (storage) temperature

T_{min} is the minimum operating temperature

T_w is the temperature of the water in the entire system

T_{out} is the absorber outlet temperature

T_{abs_d} is the design value of T_{out}

T_{ES_a} is the temperature of the excess steam for charging the accumulators

Ins is the solar insolation

Ins_d is the design level insolation

Ins_{min} is the minimum level insolation for the absorber to generate steam

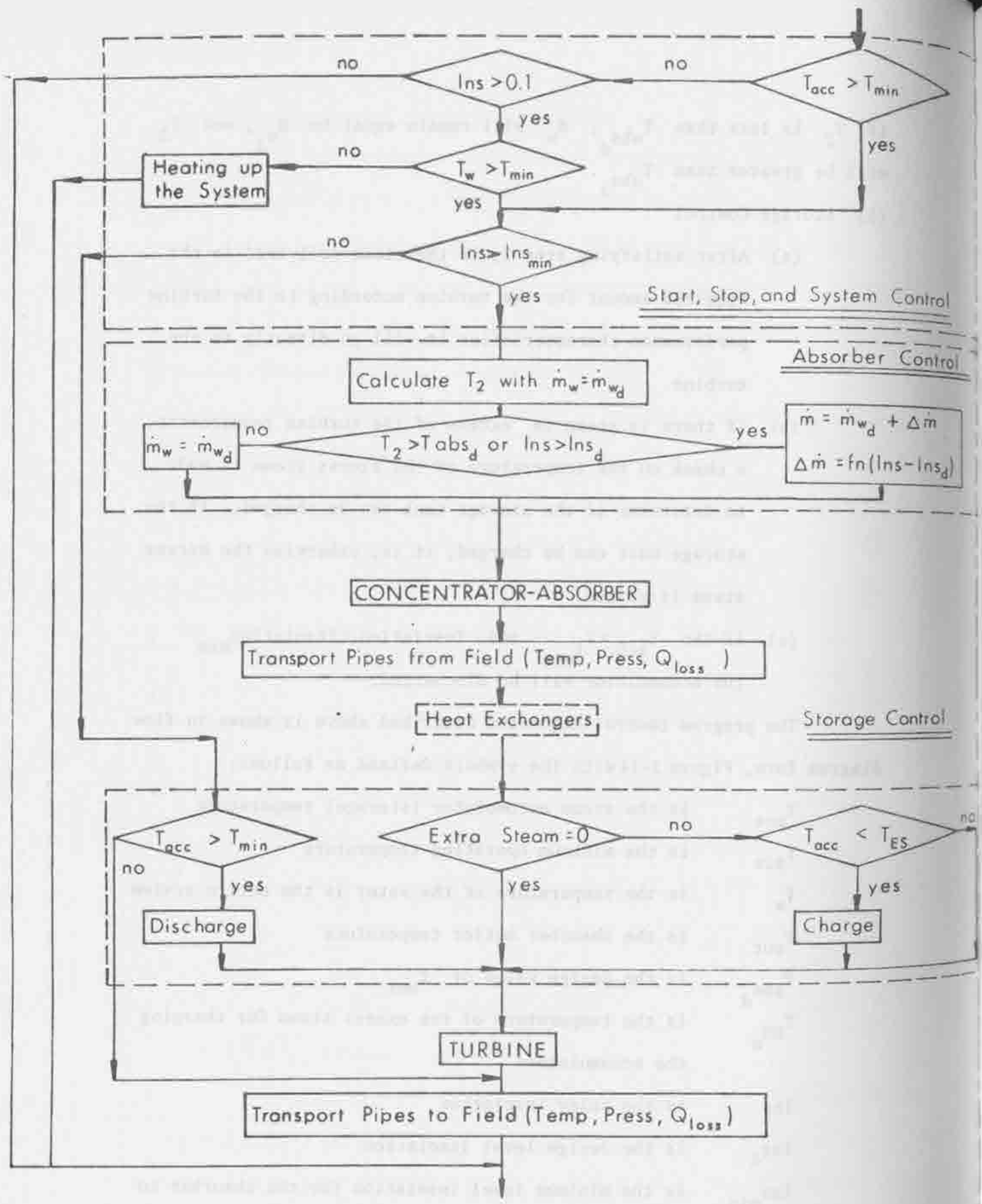

Figure 3-14. Simulation Program Structure and Control Algorithm.

$\dot{m}_w$ is the mass flow rate of feed water to the absorber

$\dot{m}_{w_d}$ is the design mass flow rate of feedwater

$\Delta\dot{m}$ is a function of the difference (ins-Ins_d) which is determined from the absorber performance

4.0 SIMULATION RESULTS

The simulation model was used to simulate a distributed system in three geographic locations. The distributed system that was selected was a 12 megawatt plant using Fresnel reflectors and cavity absorbers. Thermal storage was also used in the system. The power plant was designed for 250 ^{o}C operation and used a constant volumetric flow rate turbine. The field configuration consisted of 33 reflectors in each row. Each quadrant was made up of 13 rows. The reflectors are 6.9 meters in diameter with a 25 degree rim angle. The nominal flow rate was 16.5 kilograms/second of steam and was based upon an insolation value of one kilowatt per square meter. The flow in each line was controlled so that with design insolation conditions, the water entering the outer end of each line, at the condensing temperature (40 ^{o}C), would be 100 percent saturated steam at 250 ^{o}C when it reached the other end of the row of 33 collectors. This permitted the main steam return lines to deliver high quality steam to the accumulator and turbine.

System operation for the simulation runs was based upon delivering steam either from the collectors or from storage but not a mixture of the two. This meant that the turbo-generator operated when the sun provided enough heat to the collectors to produce a flow of steam sufficient to drive the turbine, which was approximately 15 to 20 percent of rated thermal input. As mid-day approached, the collectors produced more steam than the required capacity of the turbine, and some of the steam was diverted to storage. During four to eight hours, the turbo-gnerator operated at peak capacity and the storage was charged.

At low sun angles, less than 30 degrees from horizontal, there was some shading of the collectors by neighboring collectors and the

output of steam was quickly reduced. When the steam flow rate reduced below the minimum required for operating the turbine, the fluid flow to the collector was stopped and the heat stored in the steam accumulator was used to operate the turbine until all the useful stored heat was released.

The diurnal cycle is illustrated by Figures 4-1 through 4-3, which show the time-history of typical clear-day insolation along with the thermal power delivered to the turbine and the cycle efficiency for a summer day, a winter day, and a spring day.

Because the system design was based on steam returned from the collectors, the thermal storage was provided by a steam accumulator, composed of as many modules as required to provide the design storage capacity. The 12-MW_e generating station was simulated with nominal storage (about one hour on a clear spring or fall day), and then with about four times as much storage as shown in Figure 4-4.

As the storage discharged the steam temperature and pressure in the accumulator were reduced, and as a result, the turbine-generator output fell off by approximately and exponential decay. The time constant of the decay, on the discharge time, was governed by the total thermal energy stored and the rate of use by the turbine. The storage vessels were operated in parallel during discharge.

Many days of the year will not be as clear as these particular examples. Cloudiness can turn the direct insolation on and off abruptly. During such days the heat supplied to the turbines must come alternately from the collectors and from storage. Whether the storage can supply enough heat when a cloud passes to keep the system running depends on the stored solar energy available at the time of cloud cover, the duration

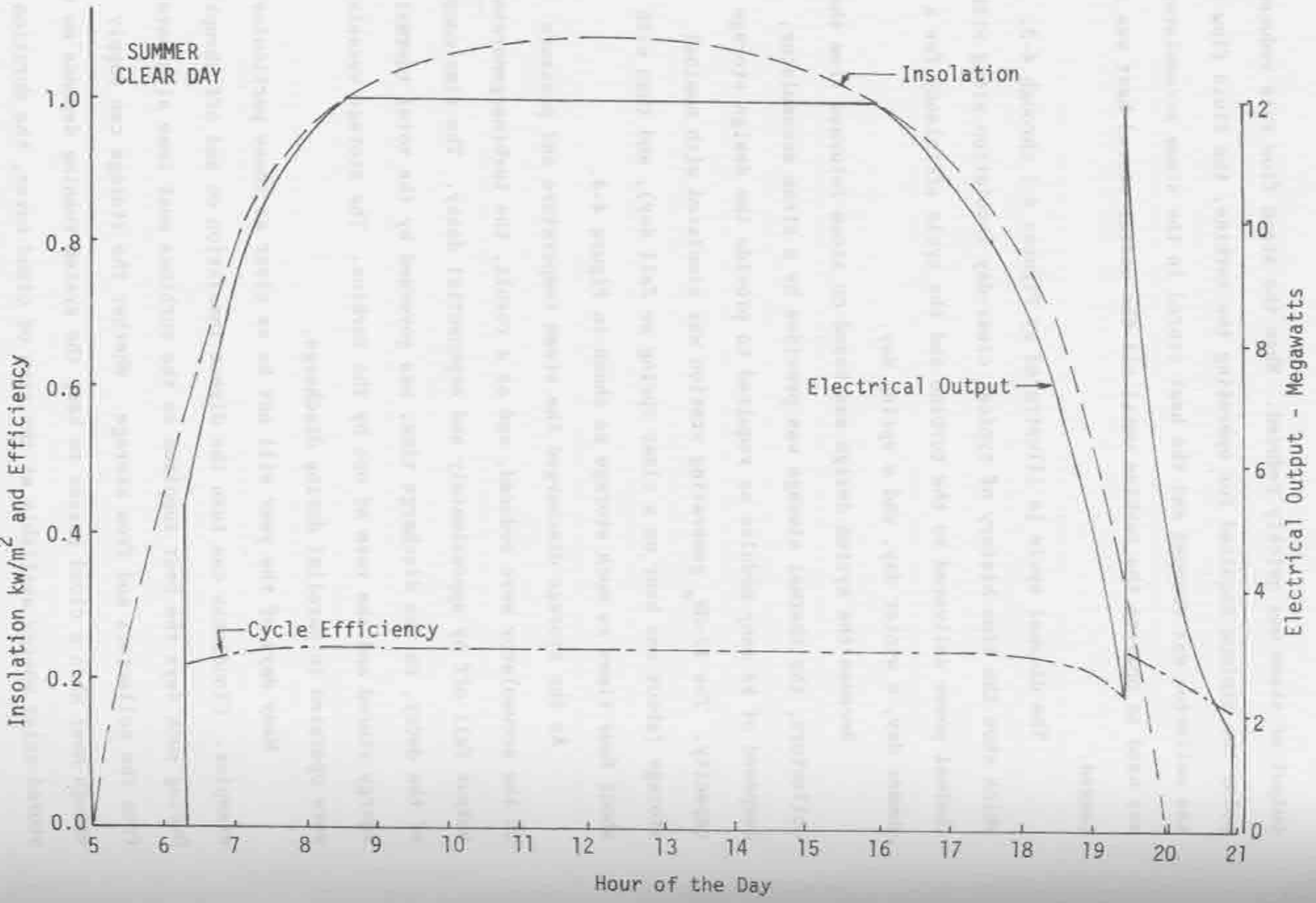

FIGURE 4-1. SIMULATION RESULTS - DISTRIBUTED POWER PLANT WITH STORAGE

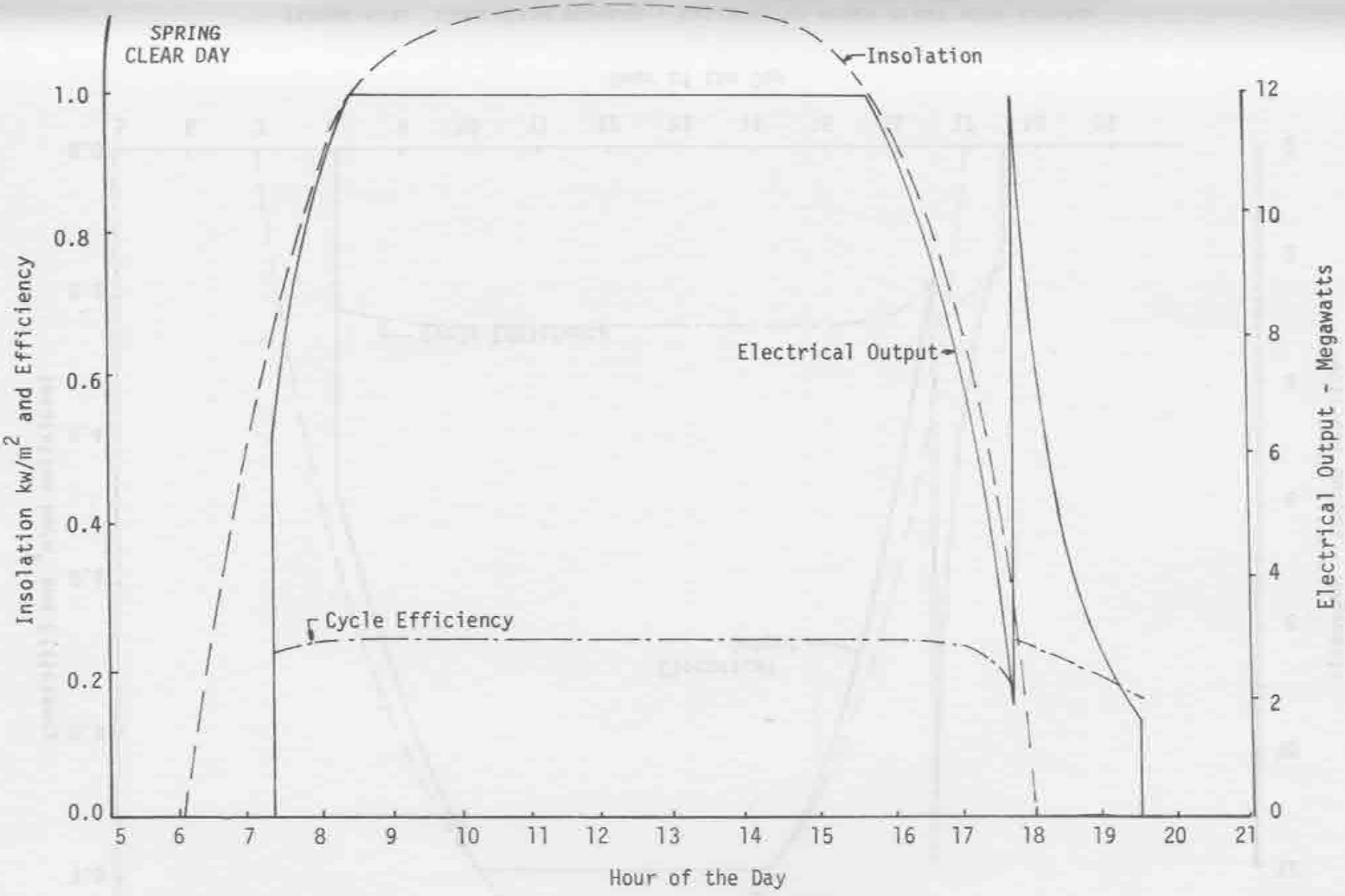

FIGURE 4-2. SIMULATION RESULTS - DISTRIBUTED POWER PLANT WITH STORAGE

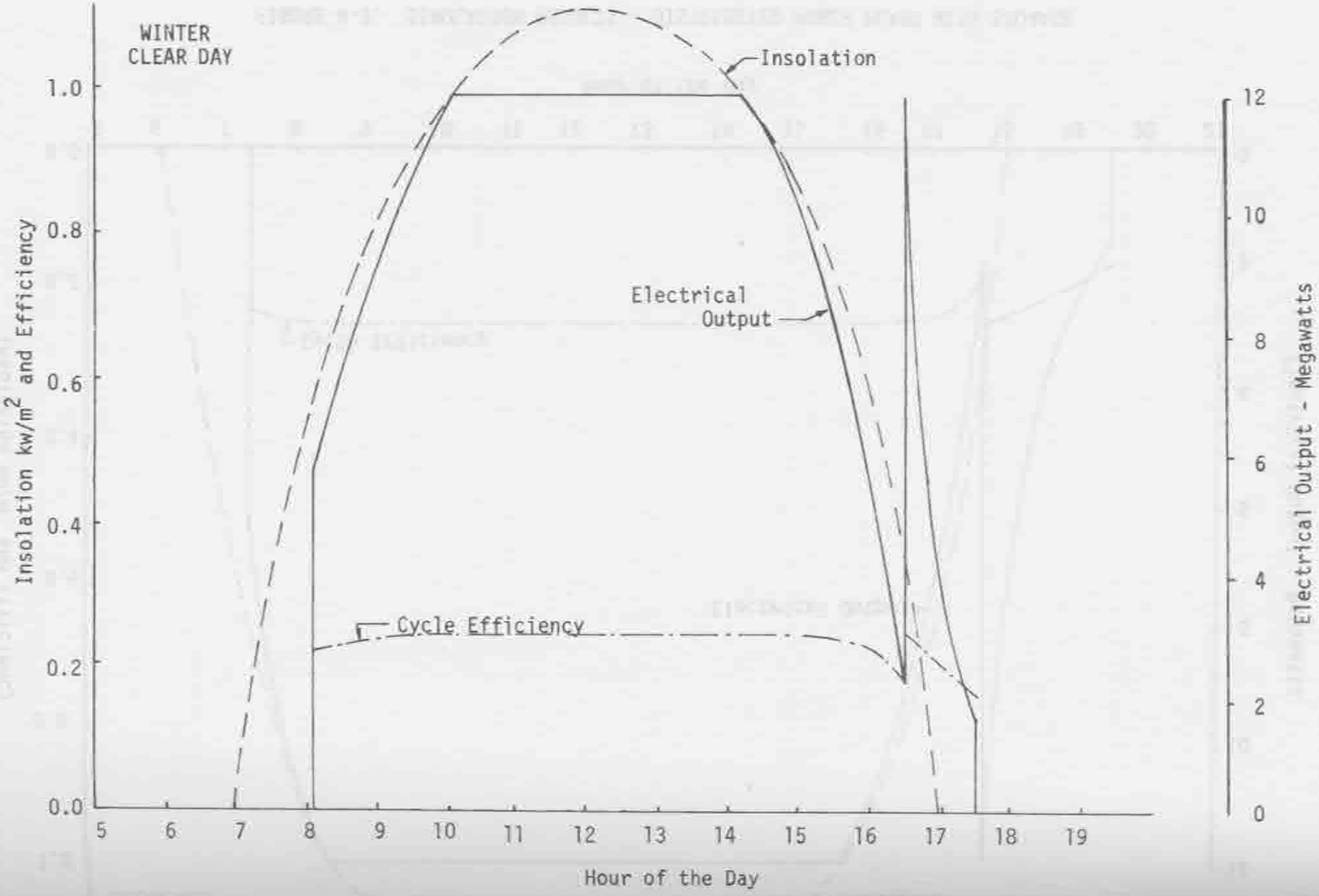

FIGURE 4-3. SIMULATION RESULTS - DISTRIBUTED POWER PLANT WITH STORAGE

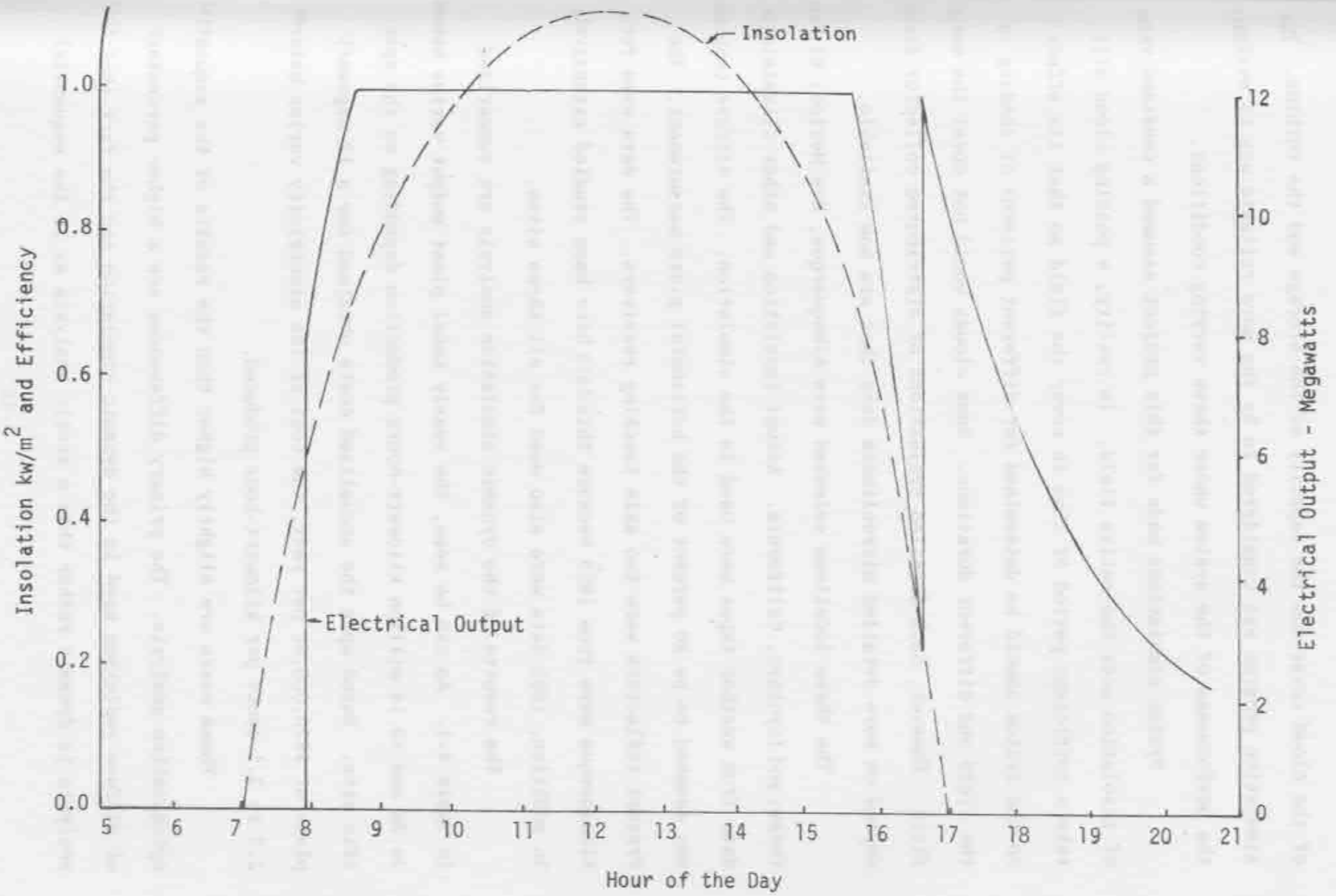

FIGURE 4-4. SIMULATION RESULTS - DISTRIBUTED PLANT WITH FOUR HOURS OF STORAGE

of the cloud cover and the capacity of the storage and the turbine. The simulation program was considered to be the more reliable way to evaluate the performance of the system under these varying conditions.

System simulations made for this project assumed a constant value of insolation over the entire field. In reality, a passing cloud will take a sufficient period of time to cover the field so that its effect on the system should be determined for different patterns of shading in the field and different durations. Some clouds would not cover the entire field. However, such detailed evaluations of distributed collector fields depend on more detailed microclimate data than are now available.

The three locations selected were Albuquerque, New Mexico; El Paso, Texas; and Inyokern, California. Actual insolation and other climatologic data from weather tapes were used in the simulation. The diffuse component was assumed to be 20 percent of the horizontal plate measurement. The Fresnel reflectors were two axis tracking receivers. The data used for Albuquerque were from 1959 because this data have been studied extensively. In addition, 1962 data were also used for all three sites.

The results of the dynamic simulation analysis are summarized in Table 4-1. As can be seen, the yearly total plant output varies between 26.76 and 30.14 million kilowatt-hours production depending on the specific site. Based upon the annualized costs obtained for a 12 megawatt plant of $820,000.00 per year, the cost of the electricity varies between 2.7 to 3.1 cents per kilowatt-hour produced.

These costs are slightly higher than the results of the sequential optimization analysis. The primary differences are a higher percentage of diffuse radiation used in the dynamic simulation and the fact that this analysis is dynamic rather than a static analysis as is the sequential

TABLE 4-1
12 Megawatt Distributed Plant

Site	Data Used	Output (Kilowatt-Hours)	Annualized Cost (Dollars)	Cost ($/Kilowatt-Hour)
Albuquerque, N.M.	1962	26,760,000	820,000	0.031
El Paso, Texas	1962	28,160,000	820,000	0.029
Inyokern, Calif.	1962	30,140,000	820,000	0.027
Albuquerque, N. M.	1959	26,290,000	820,000	0.031

Capacity Factor ∿ 0.25 - 0.29, Pricing Base (1972-1973)
No Adders for A&E, IDC, O&M.

optimization procedure.

Figures 4-5 through 4-10 present more detailed information about each of the simulated plants. Figures 4-5 through 4-7 show the monthly total kilowatt-hour production for each of the three sites. In addition, Figures 4-8 through 4-10 present histograms of the daily electrical production for each of the sites.

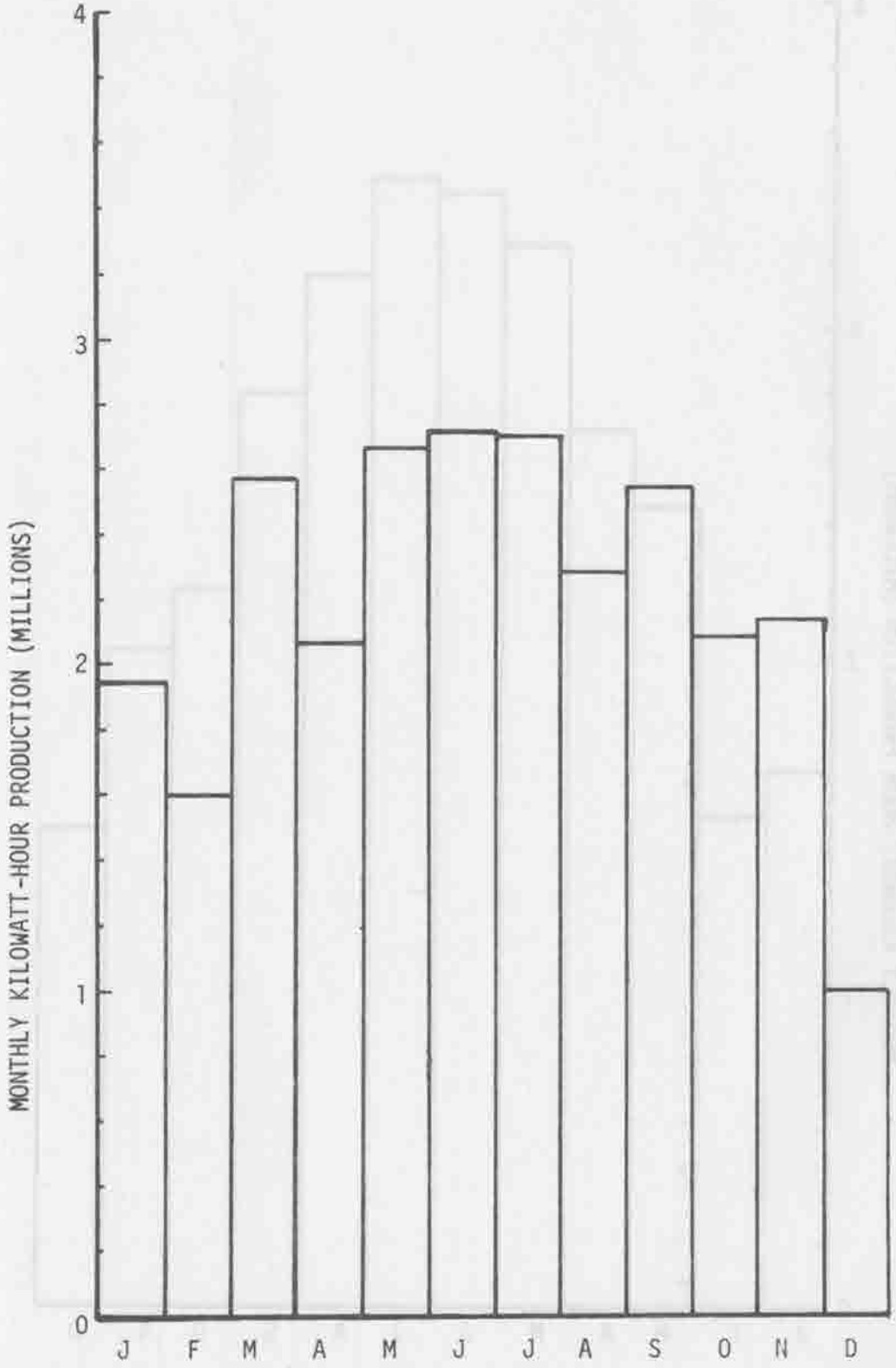

FIGURE 4-5. MONTHLY ELECTRICAL OUTPUT - ALBUQUERQUE (1959)

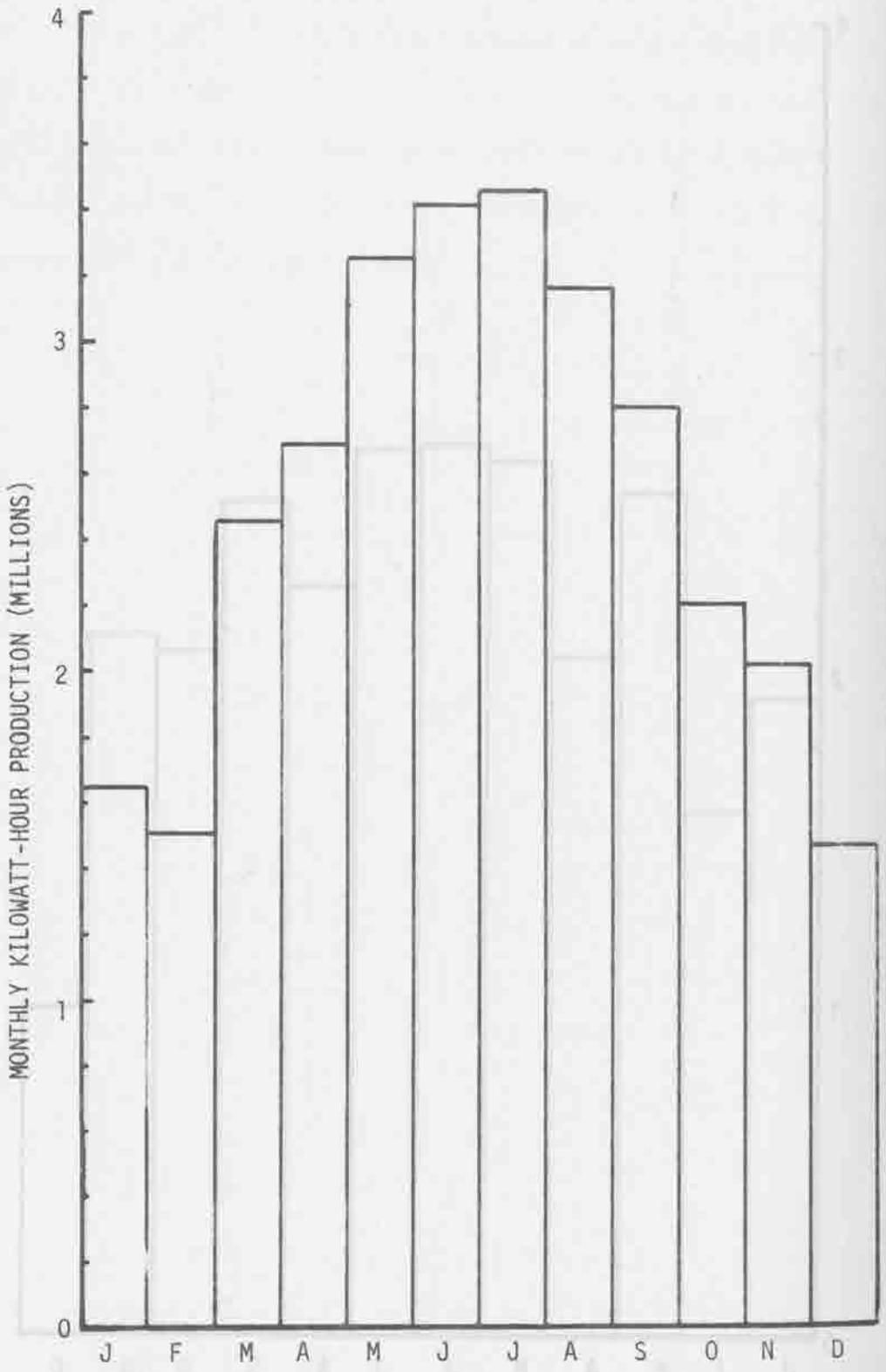

FIGURE 4-6. MONTHLY ELECTRICAL OUTPUT - INYOKERN (1962)

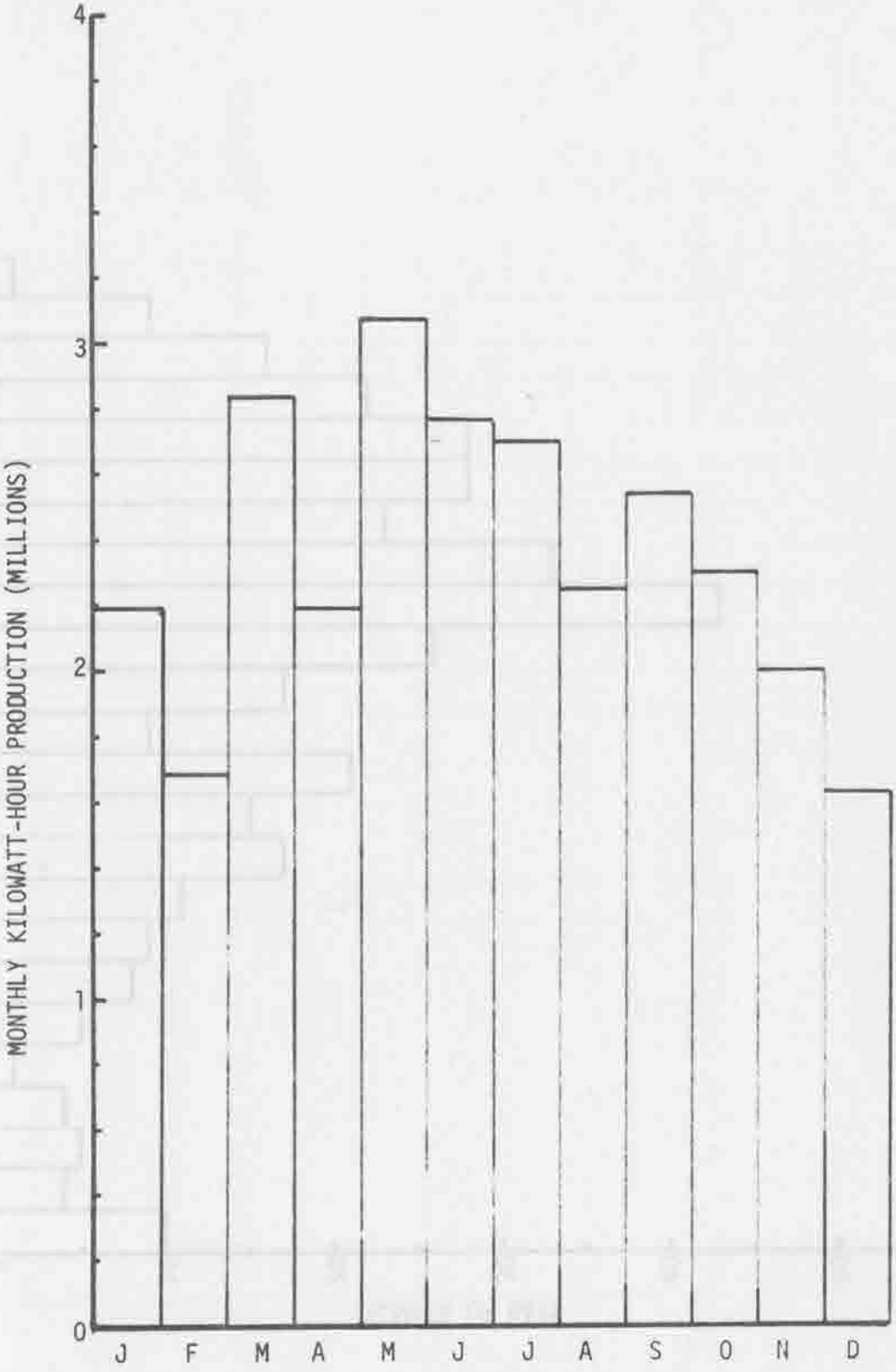

FIGURE 4-7. MONTHLY ELECTRICAL OUTPUT - EL PASO (1962)

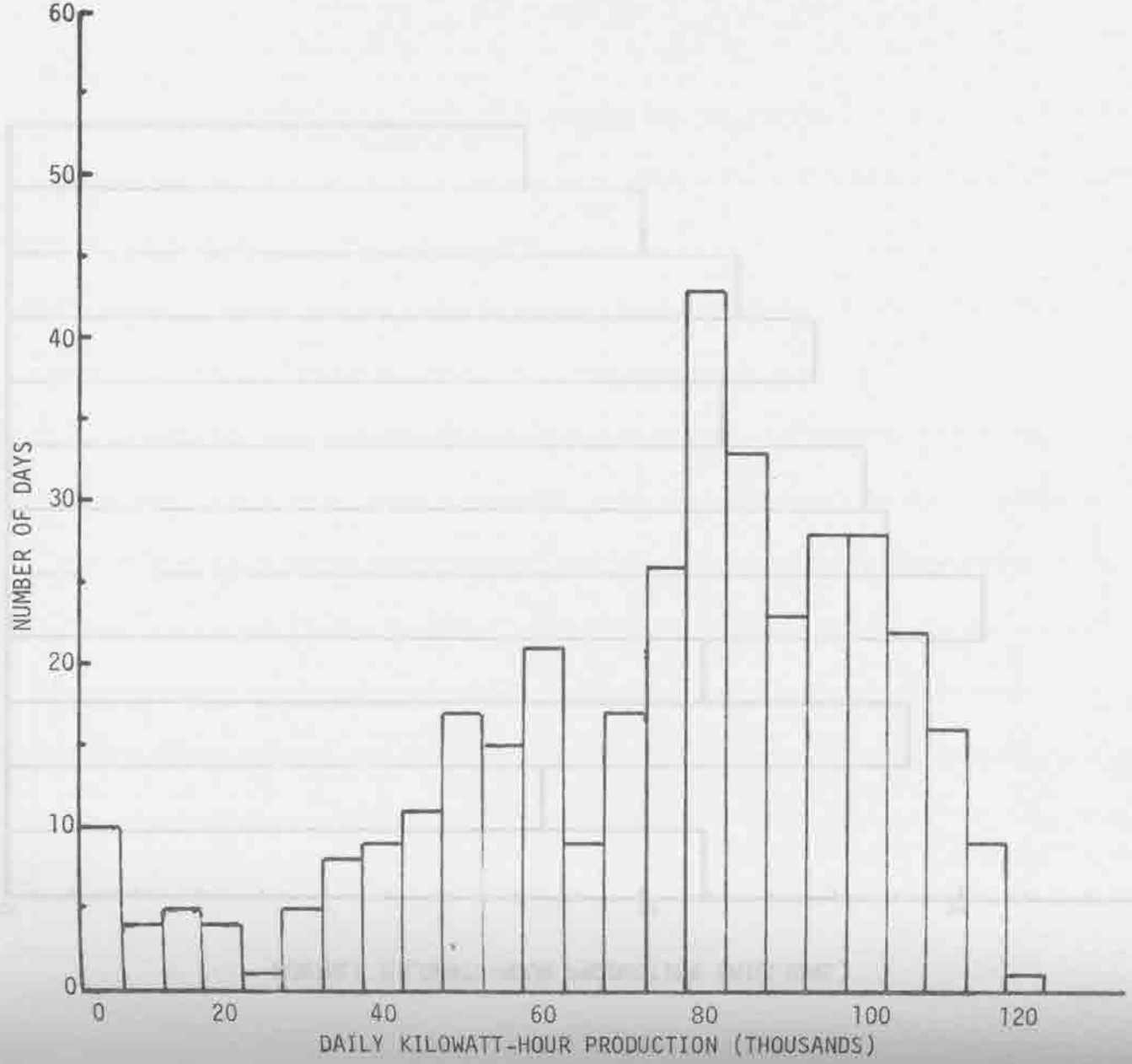

FIGURE A-6 HISTOGRAM OF DAILY ELECTRICAL ENERGY - ALBUQUERQUE (1959)

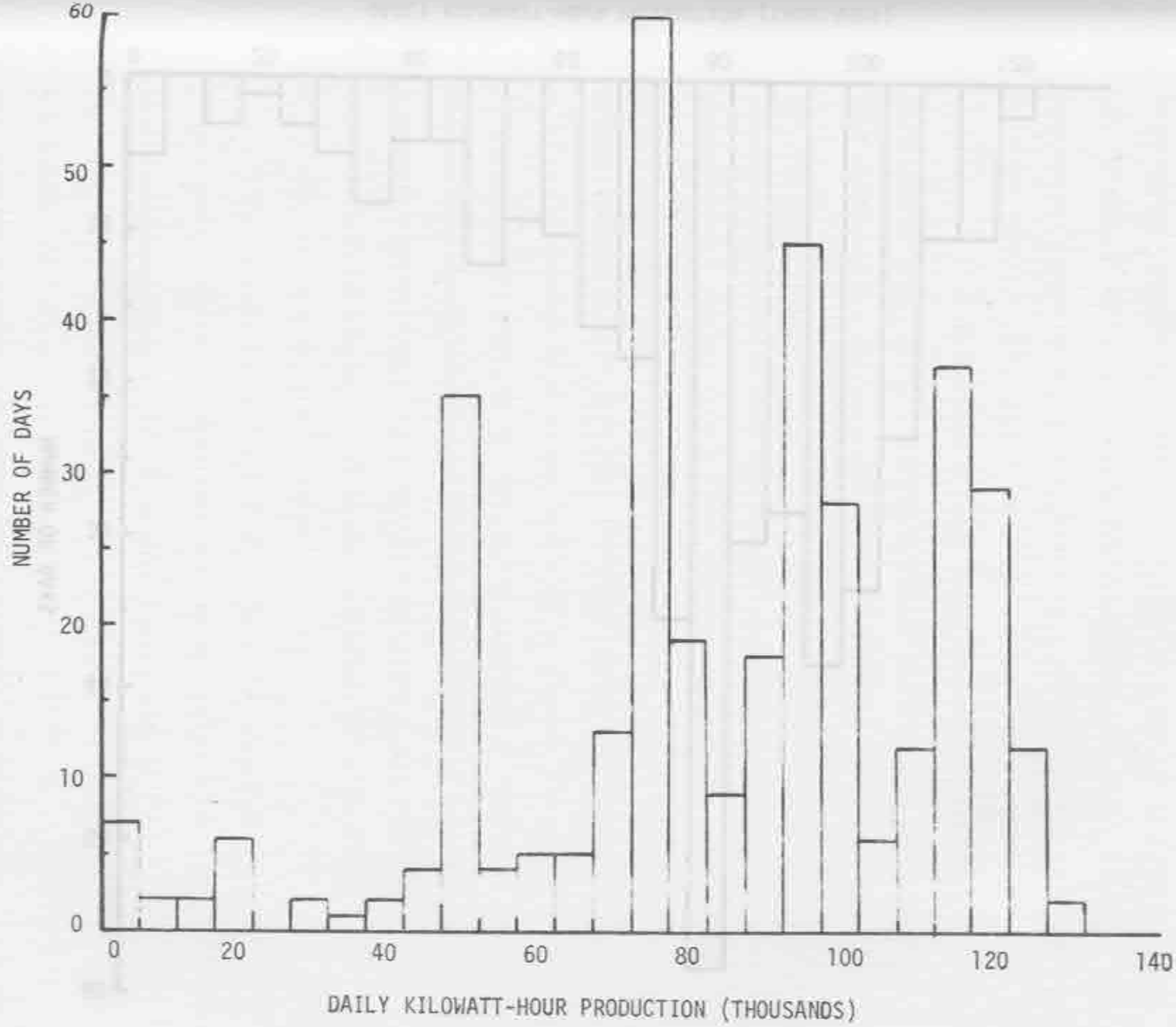

FIGURE 4-9. HISTOGRAM OF DAILY ELECTRICAL OUTPUT - INYOKERN (1962)

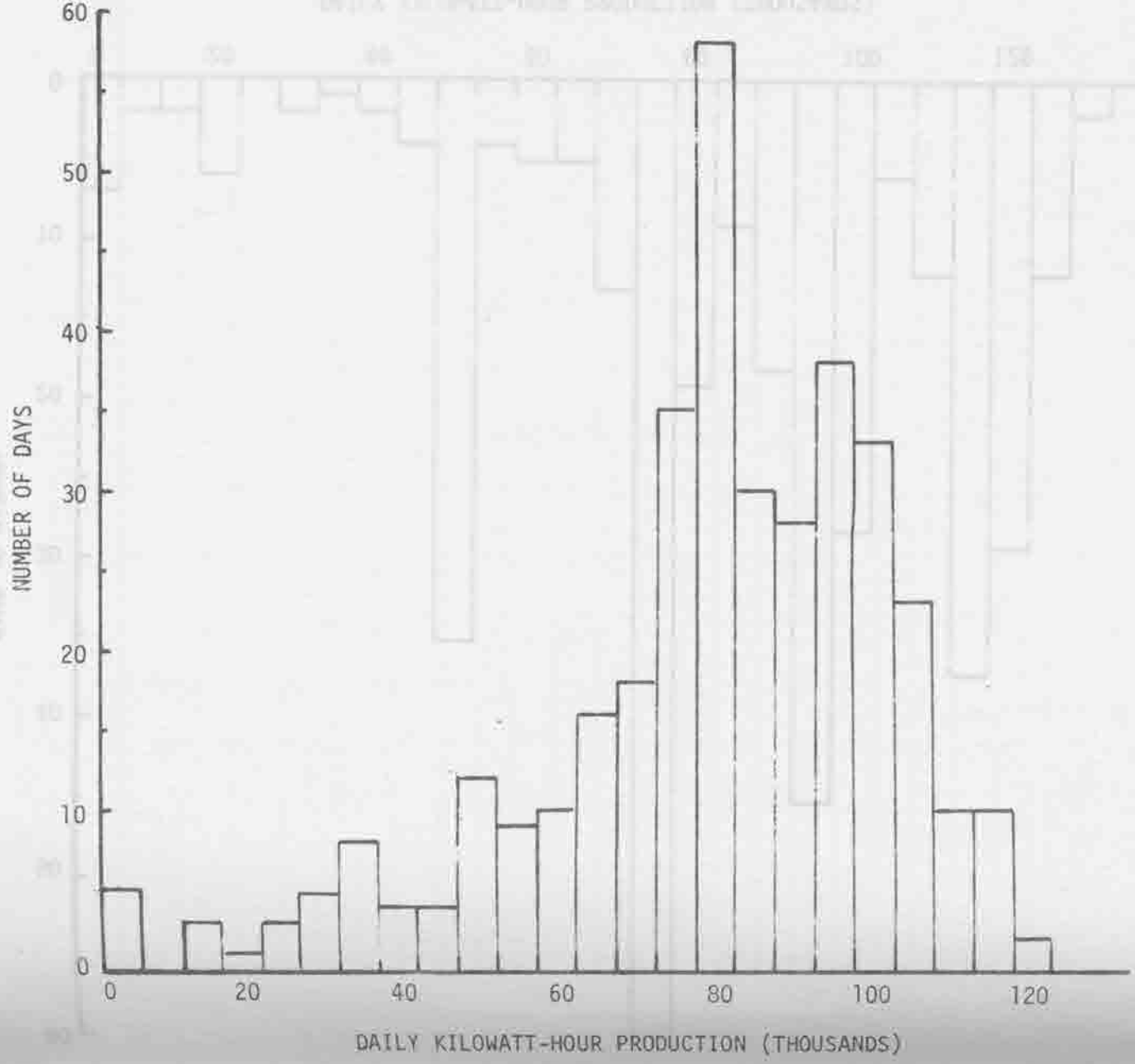

FIGURE A-10. HISTOGRAM OF DAILY ELECTRICAL OUTPUT - EL PASO (1962)

5.0 CONCLUSIONS

Systems analysis involves repetitious searches for practical engineering compromises. The final result of a design is usually based not so much on achieving a sharp-peaked optimum with respect to any one particular subsystem as it is on reaching a plateau of compromise on which all of the system elements behave acceptably within prescribed constraints. In attempting to reach these engineering compromises, the analyst must continually trade off different combinations of parameters that influence the system response. By far the greatest part of the analyst's time is devoted to performing the many routine and tedious operations involved in such repetitious trade off calculations and then presenting the results in a compact and meaningful form. The use of a computer aided design program can be an immense aid in reducing the tedium associated with this most important aspect of systems analysis.

The present program has been used to analyze the performance of different system concepts as well as the distributed configuration that emerged from the sequential optimization procedure. The results compare favorably with the sequential optimization results and indicate that a dynamic simulation model can be used effectively in the design of solar thermal electric power plants.

Two recommendations for further work did emerge during this investigation. First, control schemes for operating solar power plants to provide reliable generation of electric energy need to be developed and included in the design analysis. The strategy of controls in the field, for unequal heating of the collectors, and for efficient and effective heat storage discharge are deserving of detailed investigation. Second,

in order to perform detailed control and performance simulations of solar thermal electric power plants with thermal storage, solar radiation data that approximates instantaneous values is required. The integrated data (which is normally available) is insufficient for a study of this type because of the lack of the short term details which are the necessary inputs for the control decisions in the storage discharging mode.

REFERENCES

Duffie, J. A., and Beckman, W. A., (1974), Solar Energy Thermal Processes, Wiley Interscience, New York.

Goldstern, W., (1970), Steam Storage Accumulators, Pergamon Press, London.

Grilikhes, V. A., and Oblemperanskii, F. V., (1969), "Analysis of Radiative Heat Exchanger Process in Cylindrical Cavity-Type Collectors of Solar Power Plants", Geliotekhnika, Vol. 5, No. 2, pp. 40-48.

Grilikhes, V. A., et.al., (1972 a) "Thermal Regime Studies of a Coil-Type Solar Receiver Vapor Generator," Geliotekhnika, Vol. 8, No. 2, pp. 52-59.

Grilikhes, V. A., Grshutin, M. M., and Syrtsov, L. A., (1972 b) "Thermo-hydraulic Calculation of a Coil-Type Solar Receiver and Steam Generator", Geliotekhnika, Vol.8, No. 1, pp. 8-18.

Hottel, H. C., and Whillier, A., (1958) "Evaluation of Flat-Plate Collector Performance", Trans. Conference on the Use of Solar Energy, Tucson, Vol. 2, Part I, p. 74, University of Arizona Press.

Isbin, H. S., et.al., (1961), "Heat Transfer to Steam-Water Flows", Proceedings of the 1961 Heat Transfer and Fluid Mechanics Institute, Stanford University Press, pp. 70-78.

Rosenow, J. P., and Hartnett, editors, (1973), Handbook of Heat Transfer McGraw-Hill, New York.

Rubanovich, I. M., (1965) "Determining Optimum Dimensions of High Temperature Cylindrical Solar Energy Cavity Receivers", Geliotekhnika, Vol. 1, No. 4, pp. 11-22.

APPENDIX K

OPTIMIZATION RESULTS

BY

W. S. DUFF

1.0 INTRODUCTION

This appendix consists of detailed examples of outputs from the sequential optimization computer runs. These runs contain much information of which only a small fraction has been condensed in the tables and figures in this report. The purpose of this appendix is to describe the details of these outputs and to indicate how the information can be retrieved.

With the exception of the series boiling feeder lines, each data line on a computer output is for a minimum-cost system. The screening of hundreds or thousands of designs delivering the same performance has been done by the computer and is not shown.

There is an in-house report, which is an expanded version of this appendix, containing a much larger set of computer outputs from the optimization runs. For details of optimized designs and costs of all concentrating collectors and other subsystems that were investigated, readers should refer to the in-house report "Solar Thermal Electric Power Systems Final Report, Supplementary Volume, Optimization Computer Output, November 1974. The report may be obtained by writing to Solar Energy Applications Laboratory, Colorado State University, Fort Collins, Colorado, 80521.

2.0 CONCENTRATOR OPTIMIZATION RUNS

Examples of concentrator optimization runs are given in this section. In order of their appearance they are:

C1G1 - Paraboloid with spherical target individually mounted

C1G3 - Paraboloid with pancake target individually mounted

C5G2 - Fresnel circular reflector with spherical target

C5G4 - Fresnel circular reflector with pancake target

C7G2 - Fresnel lens with spherical target

C7G4 - Fresnel lens with pancake target

C12G15 - Fresnel strip reflector with flat target

C12G15 - Fresnel strip reflector with flat target and ρ_{ave} degraded to .85

D1G3M - Paraboloid with pancake target individually mounted with ρ_{ave} degraded by 8%

C11G11 - Parabolic trough with cylindrical target

C9G2A - Tower-heliostat system with spherical target, 5000 - 9600 m^2 effective aperture

C9G2D - Tower-heliostat system with spherical target, 150,000 - 288,30 m^2 effective aperture

The column headings on the printouts are:

EAP - Effective aperture, E (m^2 or m^2/m)

G - g (m^2 or m^2/m)

N - Number of concentrators on a module

WP - Dimension of square heliostat (m)

SCOS - Not used

NW - Number of heliostats in a field

TH - Rim angle, θ_{max} (degrees)

RHO - Average reflectivity or transmissivity, ρ_{ave}

AP - Aperture, A_p (m^2 or m^2/m)

SIGMA - Contour and pointing accuracy, $\sigma_{\phi,\lambda,\delta}$ (^{o})

TWR - Tower height (m)

COST, TWR - Tower cost ($)

COST, HELI - Heliostat cost ($)

COST, HT - Heat transport cost ($)

As shown in Appendix E, the parameter g is the parameter of a normal distribution for line-focus concentrators and of an exponential distribution for point-focus concentrators. Both these distributions can be normalized so that the fraction of radiation intercepted for a given target dimension a and a given g can be read from a single curve. These curves are given in Figure 2-1. Performance analyses of concentrators can be carried out directly from this figure and the detailed outputs in this section. The procedure is as follows:

1. Select a concentrator type and values of E and g.
2. Determine f_c from the computer outputs.
3. Use appropriate curve in Figure 2-1 to determine Φ, the fraction of radiation intercepted by a target of the appropriate type and required size, a.
4. Compute the cost per unit of power intercepted by $f_c/I_D \eta E \Phi$.
5. Compute the average intensity of the concentrated radiation intercepted by $I_D \eta E \Phi / a$.

For example, consider a paraboloid with a pancake target having average reflectivity of .78, an effective aperture of 8.15 m^2 and a g of .00348 m^2. Looking at the D1G3M computer output, the optimum design is found to be $\theta_{max} = 60^o$, $A_p = 10.4\ m^2$ and $\sigma_{\phi,\lambda,\delta} = .311^o$. This design has a cost of $785 which is a minimum cost for the specified performance

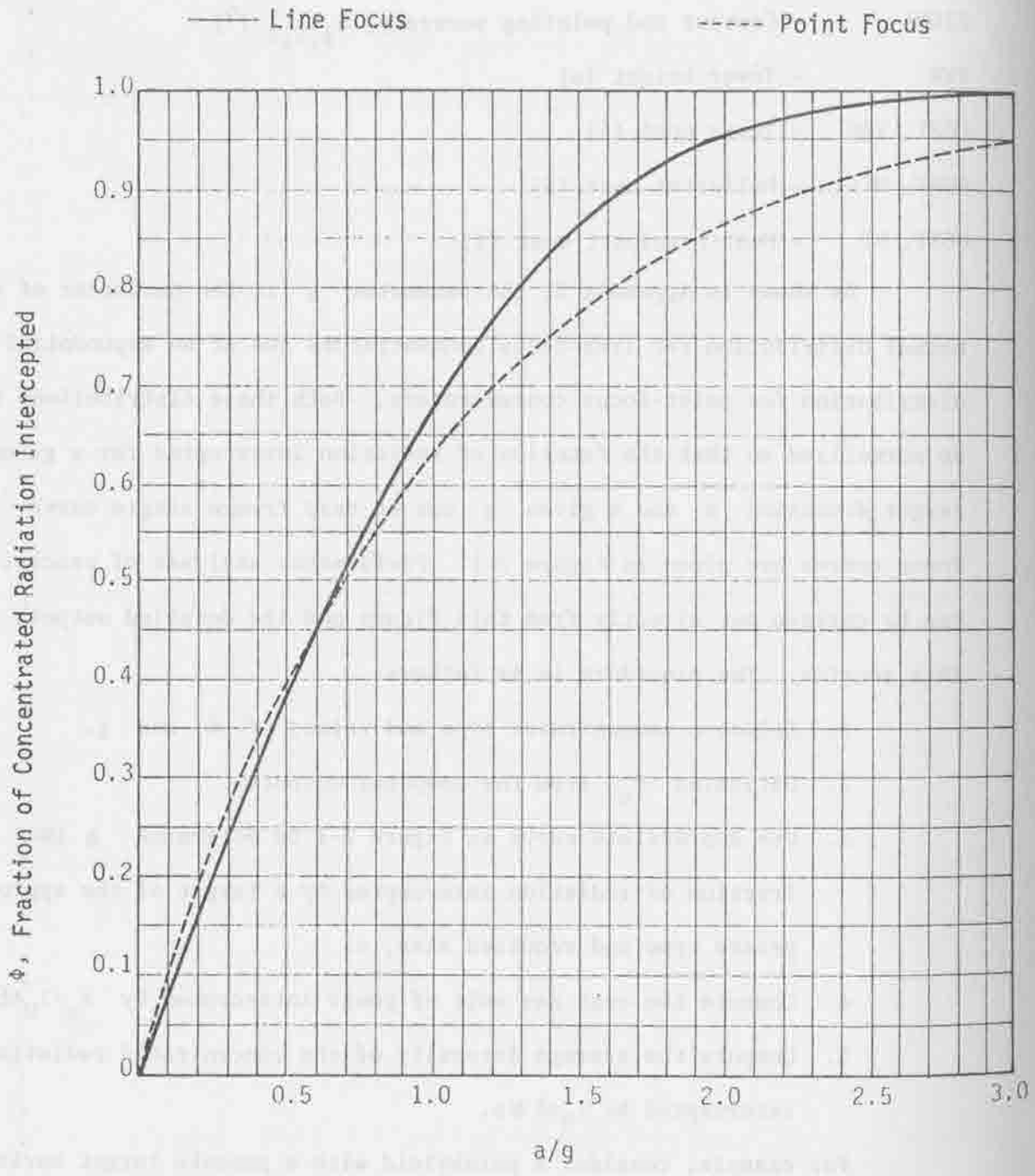

Figure 2-1. Normalized Distribution Functions, G (1, a/g), Giving the Fraction of Concentrated Radiation Intercepted.

and target shape. Suppose a target that intercepted 90% of the radiation is required. From Figure 2-1, using the dotted line, this corresponds to an a/g ratio of 2.3. Since g = .00348, the area of one side of the pancake target, a = 2.3 (.00348) = .00800 m^2. At an insolation level of 1 kW_t per m^2 the cost per unit of power intercepted is \$785/(1 x 8.15 x .9) = \$107 per kW_t. The average intensity of the radiation intercepted is 1 x 8.15 x .9/.00800 = 917 kW_t per m^2.

The results of all the concentrator runs were stored on disk for use in the next step in the sequential optimization.

PER MODULE COST FOR POINTING AND SURFACE ACCURACY 1.0
PER SQUARE METER COST FOR POINTING AND SURFACE ACCURACY 1.0

----PARAMETERS----		----------OPTIMUM DESIGNS----------								MINIMUM
EAP	G	N	WP	SCOS	NW	TH	RHO	AP	SIGMA	COST
5.52E+00	6.13E-04	1	1	.80	1	75	.75	7.35E+00	.227	6.37E+02
5.52E+00	8.58E-04	1	1	.80	1	75	.75	7.35E+00	.273	6.36E+02
5.52E+00	1.20E-03	1	1	.80	1	75	.75	7.35E+00	.327	6.35E+02
5.52E+00	1.68E-03	1	1	.80	1	75	.75	7.35E+00	.389	6.35E+02
5.52E+00	2.35E-03	1	1	.80	1	75	.75	7.35E+00	.463	6.34E+02
5.52E+00	3.30E-03	1	1	.80	1	75	.75	7.35E+00	.550	6.34E+02
5.52E+00	4.61E-03	1	1	.80	1	70	.75	7.35E+00	.611	6.34E+02
5.52E+00	6.46E-03	1	1	.80	1	70	.75	7.35E+00	.724	6.33E+02
5.79E+00	6.44E-04	1	1	.80	1	75	.75	7.72E+00	.227	6.50E+02
5.79E+00	9.01E-04	1	1	.80	1	75	.75	7.72E+00	.273	6.49E+02
5.79E+00	1.26E-03	1	1	.80	1	75	.75	7.72E+00	.327	6.49E+02
5.79E+00	1.77E-03	1	1	.80	1	75	.75	7.72E+00	.389	6.48E+02
5.79E+00	2.47E-03	1	1	.80	1	75	.75	7.72E+00	.463	6.48E+02
5.79E+00	3.46E-03	1	1	.80	1	75	.75	7.72E+00	.550	6.47E+02
5.79E+00	4.85E-03	1	1	.80	1	75	.75	7.72E+00	.653	6.47E+02
5.79E+00	6.78E-03	1	1	.80	1	70	.75	7.72E+00	.724	6.46E+02
6.08E+00	6.76E-04	1	1	.80	1	65	.85	7.15E+00	.208	6.52E+02
6.08E+00	9.46E-04	1	1	.80	1	65	.85	7.15E+00	.251	6.51E+02
6.08E+00	1.32E-03	1	1	.80	1	60	.85	7.15E+00	.277	6.50E+02
6.08E+00	1.85E-03	1	1	.80	1	60	.85	7.15E+00	.331	6.50E+02
6.08E+00	2.60E-03	1	1	.80	1	60	.85	7.15E+00	.395	6.49E+02
6.08E+00	3.63E-03	1	1	.80	1	60	.85	7.15E+00	.470	6.49E+02
6.08E+00	5.09E-03	1	1	.80	1	60	.85	7.15E+00	.558	6.48E+02
6.08E+00	7.12E-03	1	1	.80	1	60	.85	7.15E+00	.662	6.48E+02
6.39E+00	7.09E-04	1	1	.80	1	65	.85	7.51E+00	.208	6.66E+02
6.39E+00	9.93E-04	1	1	.80	1	65	.85	7.51E+00	.251	6.65E+02
6.39E+00	1.39E-03	1	1	.80	1	60	.85	7.51E+00	.277	6.64E+02
6.39E+00	1.95E-03	1	1	.80	1	60	.85	7.51E+00	.331	6.64E+02
6.39E+00	2.73E-03	1	1	.80	1	60	.85	7.51E+00	.395	6.63E+02
6.39E+00	3.82E-03	1	1	.80	1	60	.85	7.51E+00	.470	6.63E+02
6.39E+00	5.34E-03	1	1	.80	1	60	.85	7.51E+00	.558	6.62E+02
6.39E+00	7.48E-03	1	1	.80	1	60	.85	7.51E+00	.662	6.62E+02
6.70E+00	7.45E-04	1	1	.80	1	65	.85	7.89E+00	.208	6.81E+02
6.70E+00	1.04E-03	1	1	.80	1	65	.85	7.89E+00	.251	6.80E+02
6.70E+00	1.46E-03	1	1	.80	1	60	.85	7.89E+00	.277	6.80E+02
6.70E+00	2.04E-03	1	1	.80	1	60	.85	7.89E+00	.331	6.79E+02
6.70E+00	2.86E-03	1	1	.80	1	60	.85	7.89E+00	.395	6.78E+02
6.70E+00	4.01E-03	1	1	.80	1	60	.85	7.89E+00	.470	6.78E+02
6.70E+00	5.61E-03	1	1	.80	1	60	.85	7.89E+00	.558	6.77E+02
6.70E+00	7.85E-03	1	1	.80	1	60	.85	7.89E+00	.662	6.77E+02
7.04E+00	7.82E-04	1	1	.80	1	65	.85	8.28E+00	.208	6.97E+02
7.04E+00	1.10E-03	1	1	.80	1	65	.85	8.28E+00	.251	6.96E+02
7.04E+00	1.53E-03	1	1	.80	1	65	.85	8.28E+00	.301	6.96E+02
7.04E+00	2.15E-03	1	1	.80	1	60	.85	8.28E+00	.331	6.95E+02
7.04E+00	3.00E-03	1	1	.80	1	60	.85	8.28E+00	.395	6.94E+02
7.04E+00	4.21E-03	1	1	.80	1	60	.85	8.28E+00	.470	6.94E+02
7.04E+00	5.89E-03	1	1	.80	1	60	.85	8.28E+00	.558	6.93E+02
7.04E+00	8.25E-03	1	1	.80	1	60	.85	8.28E+00	.662	6.93E+02
7.39E+00	8.21E-04	1	1	.80	1	70	.85	8.70E+00	.226	7.15E+02
7.39E+00	1.15E-03	1	1	.80	1	65	.85	8.70E+00	.251	7.13E+02
7.39E+00	1.61E-03	1	1	.80	1	65	.85	8.70E+00	.301	7.13E+02
7.39E+00	2.25E-03	1	1	.80	1	60	.85	8.70E+00	.331	7.12E+02
7.39E+00	3.16E-03	1	1	.80	1	60	.85	8.70E+00	.395	7.11E+02

ER MODULE COST FOR POINTING AND SURFACE ACCURACY 1.0
ER SQUARE METER COST FOR POINTING AND SURFACE ACCURACY 1.0

---PARAMETERS----		----------OPTIMUM DESIGNS----------								MINIMUM
EAP	G	N	WP	SCOS	NW	TH	RHO	AP	SIGMA	COST
5.52E+00	6.13E-04	1	1	.80	1	75	.75	7.35E+00	.161	6.39E+02
5.52E+00	8.58E-04	1	1	.80	1	75	.75	7.35E+00	.197	6.38E+02
5.52E+00	1.20E-03	1	1	.80	1	75	.75	7.35E+00	.238	6.37E+02
5.52E+00	1.68E-03	1	1	.80	1	70	.75	7.35E+00	.277	6.36E+02
5.52E+00	2.35E-03	1	1	.80	1	70	.75	7.35E+00	.332	6.35E+02
5.52E+00	3.30E-03	1	1	.80	1	70	.75	7.35E+00	.396	6.35E+02
5.52E+00	4.61E-03	1	1	.80	1	70	.75	7.35E+00	.471	6.34E+02
5.52E+00	6.46E-03	1	1	.80	1	70	.75	7.35E+00	.559	6.34E+02
5.79E+00	6.44E-04	1	1	.80	1	75	.75	7.72E+00	.161	6.53E+02
5.79E+00	9.01E-04	1	1	.80	1	75	.75	7.72E+00	.197	6.51E+02
5.79E+00	1.26E-03	1	1	.80	1	75	.75	7.72E+00	.238	6.50E+02
5.79E+00	1.77E-03	1	1	.80	1	75	.75	7.72E+00	.286	6.49E+02
5.79E+00	2.47E-03	1	1	.80	1	70	.75	7.72E+00	.332	6.48E+02
5.79E+00	3.46E-03	1	1	.80	1	70	.75	7.72E+00	.396	6.48E+02
5.79E+00	4.85E-03	1	1	.80	1	70	.75	7.72E+00	.471	6.47E+02
5.79E+00	6.78E-03	1	1	.80	1	70	.75	7.72E+00	.559	6.47E+02
6.08E+00	6.76E-04	1	1	.80	1	65	.85	7.15E+00	.161	6.54E+02
6.08E+00	9.46E-04	1	1	.80	1	60	.85	7.15E+00	.187	6.52E+02
6.08E+00	1.32E-03	1	1	.80	1	60	.85	7.15E+00	.226	6.51E+02
6.08E+00	1.85E-03	1	1	.80	1	60	.85	7.15E+00	.272	6.50E+02
6.08E+00	2.60E-03	1	1	.80	1	60	.85	7.15E+00	.325	6.50E+02
6.08E+00	3.63E-03	1	1	.80	1	60	.85	7.15E+00	.388	6.49E+02
6.08E+00	5.09E-03	1	1	.80	1	60	.85	7.15E+00	.461	6.49E+02
6.08E+00	7.12E-03	1	1	.80	1	60	.85	7.15E+00	.548	6.48E+02
6.39E+00	7.09E-04	1	1	.80	1	65	.85	7.51E+00	.161	6.68E+02
6.39E+00	9.93E-04	1	1	.80	1	60	.85	7.51E+00	.187	6.67E+02
6.39E+00	1.39E-03	1	1	.80	1	60	.85	7.51E+00	.226	6.65E+02
6.39E+00	1.95E-03	1	1	.80	1	60	.85	7.51E+00	.272	6.65E+02
6.39E+00	2.73E-03	1	1	.80	1	60	.85	7.51E+00	.325	6.64E+02
6.39E+00	3.82E-03	1	1	.80	1	60	.85	7.51E+00	.388	6.63E+02
6.39E+00	5.34E-03	1	1	.80	1	60	.85	7.51E+00	.461	6.63E+02
6.39E+00	7.48E-03	1	1	.80	1	60	.85	7.51E+00	.548	6.62E+02
6.70E+00	7.45E-04	1	1	.80	1	65	.85	7.89E+00	.161	6.83E+02
6.70E+00	1.04E-03	1	1	.80	1	60	.85	7.89E+00	.187	6.82E+02
6.70E+00	1.46E-03	1	1	.80	1	60	.85	7.89E+00	.226	6.81E+02
6.70E+00	2.04E-03	1	1	.80	1	60	.85	7.89E+00	.272	6.80E+02
6.70E+00	2.86E-03	1	1	.80	1	60	.85	7.89E+00	.325	6.79E+02
6.70E+00	4.01E-03	1	1	.80	1	60	.85	7.89E+00	.388	6.78E+02
6.70E+00	5.61E-03	1	1	.80	1	60	.85	7.89E+00	.461	6.78E+02
6.70E+00	7.85E-03	1	1	.80	1	60	.85	7.89E+00	.548	6.77E+02
7.04E+00	7.82E-04	1	1	.80	1	65	.85	8.28E+00	.161	6.99E+02
7.04E+00	1.10E-03	1	1	.80	1	65	.85	8.28E+00	.197	6.98E+02
7.04E+00	1.53E-03	1	1	.80	1	60	.85	8.28E+00	.226	6.97E+02
7.04E+00	2.15E-03	1	1	.80	1	60	.85	8.28E+00	.272	6.96E+02
7.04E+00	3.00E-03	1	1	.80	1	60	.85	8.28E+00	.325	6.95E+02
7.04E+00	4.21E-03	1	1	.80	1	60	.85	8.28E+00	.388	6.94E+02
7.04E+00	5.89E-03	1	1	.80	1	60	.85	8.28E+00	.461	6.94E+02
7.04E+00	8.25E-03	1	1	.80	1	60	.85	8.28E+00	.548	6.93E+02
7.39E+00	8.21E-04	1	1	.80	1	65	.85	8.70E+00	.161	7.16E+02
7.39E+00	1.15E-03	1	1	.80	1	65	.85	8.70E+00	.197	7.15E+02
7.39E+00	1.61E-03	1	1	.80	1	60	.85	8.70E+00	.226	7.14E+02
7.39E+00	2.25E-03	1	1	.80	1	60	.85	8.70E+00	.272	7.13E+02
7.39E+00	3.16E-03	1	1	.80	1	60	.85	8.70E+00	.325	7.12E+02

7.39E+00	4.42E-03	1	1	.80	1	60	.85	8.70E+00	.388	7.11E+02
7.39E+00	6.18E-03	1	1	.80	1	60	.85	8.70E+00	.461	7.11E+02
7.39E+00	8.66E-03	1	1	.80	1	60	.85	8.70E+00	.548	7.10E+02
7.76E+00	8.62E-04	1	1	.80	1	65	.85	9.13E+00	.161	7.35E+02
7.76E+00	1.21E-03	1	1	.80	1	65	.85	9.13E+00	.197	7.33E+02
7.76E+00	1.69E-03	1	1	.80	1	60	.85	9.13E+00	.226	7.32E+02
7.76E+00	2.37E-03	1	1	.80	1	60	.85	9.13E+00	.272	7.31E+02
7.76E+00	3.31E-03	1	1	.80	1	60	.85	9.13E+00	.325	7.30E+02
7.76E+00	4.64E-03	1	1	.80	1	60	.85	9.13E+00	.388	7.29E+02
7.76E+00	6.49E-03	1	1	.80	1	60	.85	9.13E+00	.461	7.29E+02
7.76E+00	9.09E-03	1	1	.80	1	60	.85	9.13E+00	.548	7.28E+02
8.15E+00	9.06E-04	1	1	.80	1	65	.85	9.59E+00	.161	7.54E+02
8.15E+00	1.27E-03	1	1	.80	1	65	.85	9.59E+00	.197	7.52E+02
8.15E+00	1.77E-03	1	1	.80	1	65	.85	9.59E+00	.238	7.51E+02
8.15E+00	2.48E-03	1	1	.80	1	60	.85	9.59E+00	.272	7.50E+02
8.15E+00	3.48E-03	1	1	.80	1	60	.85	9.59E+00	.325	7.49E+02
8.15E+00	4.87E-03	1	1	.80	1	60	.85	9.59E+00	.388	7.48E+02
8.15E+00	6.82E-03	1	1	.80	1	60	.85	9.59E+00	.461	7.48E+02
8.15E+00	9.55E-03	1	1	.80	1	60	.85	9.59E+00	.548	7.47E+02
8.56E+00	9.51E-04	1	1	.80	1	65	.85	1.01E+01	.161	7.75E+02
8.56E+00	1.33E-03	1	1	.80	1	65	.85	1.01E+01	.197	7.73E+02
8.56E+00	1.86E-03	1	1	.80	1	65	.85	1.01E+01	.238	7.71E+02
8.56E+00	2.61E-03	1	1	.80	1	60	.85	1.01E+01	.272	7.70E+02
8.56E+00	3.65E-03	1	1	.80	1	60	.85	1.01E+01	.325	7.69E+02
8.56E+00	5.11E-03	1	1	.80	1	60	.85	1.01E+01	.388	7.69E+02
8.56E+00	7.16E-03	1	1	.80	1	60	.85	1.01E+01	.461	7.68E+02
8.56E+00	1.00E-02	1	1	.80	1	60	.85	1.01E+01	.548	7.67E+02
8.99E+00	9.98E-04	1	1	.80	1	65	.85	1.06E+01	.161	7.96E+02
8.99E+00	1.40E-03	1	1	.80	1	65	.85	1.06E+01	.197	7.95E+02
8.99E+00	1.96E-03	1	1	.80	1	65	.85	1.06E+01	.238	7.93E+02
8.99E+00	2.74E-03	1	1	.80	1	65	.85	1.06E+01	.285	7.92E+02
8.99E+00	3.84E-03	1	1	.80	1	60	.85	1.06E+01	.325	7.91E+02
8.99E+00	5.37E-03	1	1	.80	1	60	.85	1.06E+01	.388	7.90E+02
8.99E+00	7.52E-03	1	1	.80	1	60	.85	1.06E+01	.461	7.90E+02
8.99E+00	1.05E-02	1	1	.80	1	60	.85	1.06E+01	.548	7.89E+02
9.43E+00	1.05E-03	1	1	.80	1	70	.85	1.11E+01	.168	8.20E+02
9.43E+00	1.47E-03	1	1	.80	1	65	.85	1.11E+01	.197	8.18E+02
9.43E+00	2.05E-03	1	1	.80	1	65	.85	1.11E+01	.238	8.16E+02
9.43E+00	2.88E-03	1	1	.80	1	65	.85	1.11E+01	.285	8.15E+02
9.43E+00	4.03E-03	1	1	.80	1	65	.85	1.11E+01	.341	8.14E+02
9.43E+00	5.64E-03	1	1	.80	1	60	.85	1.11E+01	.388	8.13E+02
9.43E+00	7.89E-03	1	1	.80	1	60	.85	1.11E+01	.461	8.12E+02
9.43E+00	1.10E-02	1	1	.80	1	60	.85	1.11E+01	.548	8.12E+02
9.91E+00	1.10E-03	1	1	.80	1	70	.85	1.17E+01	.168	8.44E+02
9.91E+00	1.54E-03	1	1	.80	1	65	.85	1.17E+01	.197	8.42E+02
9.91E+00	2.16E-03	1	1	.80	1	65	.85	1.17E+01	.238	8.41E+02
9.91E+00	3.02E-03	1	1	.80	1	65	.85	1.17E+01	.285	8.39E+02
9.91E+00	4.23E-03	1	1	.80	1	65	.85	1.17E+01	.341	8.38E+02
9.91E+00	5.92E-03	1	1	.80	1	65	.85	1.17E+01	.407	8.38E+02
9.91E+00	8.29E-03	1	1	.80	1	60	.85	1.17E+01	.461	8.37E+02
9.91E+00	1.16E-02	1	1	.80	1	60	.85	1.17E+01	.548	8.36E+02
1.04E+01	1.16E-03	1	1	.80	1	70	.85	1.22E+01	.168	8.70E+02
1.04E+01	1.62E-03	1	1	.80	1	70	.85	1.22E+01	.205	8.68E+02
1.04E+01	2.27E-03	1	1	.80	1	65	.85	1.22E+01	.238	8.67E+02
1.04E+01	3.17E-03	1	1	.80	1	65	.85	1.22E+01	.285	8.65E+02
1.04E+01	4.44E-03	1	1	.80	1	65	.85	1.22E+01	.341	8.64E+02
1.04E+01	6.22E-03	1	1	.80	1	65	.85	1.22E+01	.407	8.63E+02
1.04E+01	8.70E-03	1	1	.80	1	65	.85	1.22E+01	.484	8.63E+02
1.04E+01	1.22E-02	1	1	.80	1	65	.85	1.22E+01	.574	8.62E+02

FLR MODULE COST FOR POINTING AND SURFACE ACCURACY 1.0
PER SQUARE METER COST FOR POINTING AND SURFACE ACCURACY 1.0

----PARAMETERS----					----------OPTIMUM DESIGNS----------					MINIMUM
EAP	G	I	P	SCOS	NW	TH	RHO	AP	SIGMA	COST
7.04E+00	7.32E-04	1	1	.80	1	45	.95	7.41E+00	.168	7.12E+02
7.04E+00	1.10E-03	1	1	.80	1	40	.95	7.41E+00	.172	6.91E+02
7.04E+00	1.57E-03	1	1	.80	1	35	.95	7.41E+00	.174	6.65E+02
7.04E+00	2.15E-03	1	1	.80	1	30	.95	7.41E+00	.173	6.50E+02
7.04E+00	3.00E-03	1	1	.80	1	25	.95	7.41E+00	.167	6.38E+02
7.04E+00	4.21E-03	1	1	.80	1	25	.95	7.41E+00	.204	6.36E+02
7.04E+00	5.89E-03	1	1	.80	1	25	.95	7.41E+00	.246	6.35E+02
7.04E+00	8.25E-03	1	1	.80	1	25	.95	7.41E+00	.295	6.35E+02
7.39E+00	8.21E-04	1	1	.80	1	45	.95	7.78E+00	.168	7.30E+02
7.39E+00	1.15E-03	1	1	.80	1	40	.95	7.78E+00	.172	7.09E+02
7.39E+00	1.61E-03	1	1	.80	1	35	.95	7.78E+00	.174	6.82E+02
7.39E+00	2.25E-03	1	1	.80	1	30	.95	7.78E+00	.173	6.66E+02
7.39E+00	3.15E-03	1	1	.80	1	25	.95	7.78E+00	.167	6.54E+02
7.39E+00	4.42E-03	1	1	.80	1	25	.95	7.78E+00	.204	6.52E+02
7.39E+00	6.19E-03	1	1	.80	1	25	.95	7.78E+00	.246	6.51E+02
7.39E+00	8.66E-03	1	1	.80	1	25	.95	7.78E+00	.295	6.51E+02
7.76E+00	8.62E-04	1	1	.80	1	45	.95	8.17E+00	.168	7.48E+02
7.76E+00	1.21E-03	1	1	.80	1	40	.95	8.17E+00	.172	7.26E+02
7.76E+00	1.69E-03	1	1	.80	1	35	.95	8.17E+00	.174	6.99E+02
7.76E+00	2.37E-03	1	1	.80	1	30	.95	8.17E+00	.173	6.83E+02
7.76E+00	3.31E-03	1	1	.80	1	25	.95	8.17E+00	.167	6.70E+02
7.76E+00	4.64E-03	1	1	.80	1	25	.95	8.17E+00	.204	6.69E+02
7.76E+00	6.49E-03	1	1	.80	1	25	.95	8.17E+00	.246	6.67E+02
7.76E+00	9.09E-03	1	1	.80	1	25	.95	8.17E+00	.295	6.67E+02
8.15E+00	9.06E-04	1	1	.80	1	45	.95	8.58E+00	.168	7.66E+02
8.15E+00	1.27E-03	1	1	.80	1	40	.95	8.58E+00	.172	7.44E+02
8.15E+00	1.77E-03	1	1	.80	1	35	.95	8.58E+00	.174	7.16E+02
8.15E+00	2.49E-03	1	1	.80	1	30	.95	8.58E+00	.173	6.99E+02
8.15E+00	3.48E-03	1	1	.80	1	25	.95	8.58E+00	.167	6.86E+02
8.15E+00	4.87E-03	1	1	.80	1	25	.95	8.58E+00	.204	6.84E+02
8.15E+00	6.82E-03	1	1	.80	1	25	.95	8.58E+00	.246	6.83E+02
8.15E+00	9.55E-03	1	1	.80	1	25	.95	8.58E+00	.295	6.82E+02
8.56E+00	9.51E-04	1	1	.80	1	45	.95	9.01E+00	.168	7.84E+02
8.56E+00	1.33E-03	1	1	.80	1	40	.95	9.01E+00	.172	7.61E+02
8.56E+00	1.86E-03	1	1	.80	1	35	.95	9.01E+00	.174	7.32E+02
8.56E+00	2.61E-03	1	1	.80	1	30	.95	9.01E+00	.173	7.15E+02
8.56E+00	3.65E-03	1	1	.80	1	25	.95	9.01E+00	.167	7.02E+02
8.56E+00	5.11E-03	1	1	.80	1	25	.95	9.01E+00	.204	7.00E+02
8.56E+00	7.16E-03	1	1	.80	1	25	.95	9.01E+00	.246	6.99E+02
8.56E+00	1.00E-02	1	1	.80	1	25	.95	9.01E+00	.295	6.98E+02
8.99E+00	9.98E-04	1	1	.80	1	45	.95	9.46E+00	.168	8.01E+02
8.99E+00	1.40E-03	1	1	.80	1	40	.95	9.46E+00	.172	7.77E+02
8.99E+00	1.96E-03	1	1	.80	1	35	.95	9.46E+00	.174	7.49E+02
8.99E+00	2.74E-03	1	1	.80	1	30	.95	9.46E+00	.173	7.31E+02
8.99E+00	3.84E-03	1	1	.80	1	25	.95	9.46E+00	.167	7.17E+02
8.99E+00	5.37E-03	1	1	.80	1	25	.95	9.46E+00	.204	7.15E+02
8.99E+00	7.52E-03	1	1	.80	1	25	.95	9.46E+00	.246	7.14E+02
8.99E+00	1.05E-02	1	1	.80	1	25	.95	9.46E+00	.295	7.13E+02
9.43E+00	1.05E-03	1	1	.80	1	45	.95	9.93E+00	.168	8.18E+02
9.43E+00	1.47E-03	1	1	.80	1	40	.95	9.93E+00	.172	7.94E+02
9.43E+00	2.05E-03	1	1	.80	1	35	.95	9.93E+00	.174	7.64E+02
9.43E+00	2.86E-03	1	1	.80	1	30	.95	9.93E+00	.173	7.46E+02
9.43E+00	4.03E-03	1	1	.80	1	25	.95	9.93E+00	.167	7.32E+02

PER MODULE COST FOR POINTING AND SURFACE ACCURACY 1.0
PER SQUARE METER COST FOR POINTING AND SURFACE ACCURACY 1.0

----PARAMETERS----		----------OPTIMUM DESIGNS----------								MINIMUM
EAP	G	N	WP	SCOS	NW	TH	RHO	AP	SIGMA	COST
7.04E+00	7.82E-04	1	1	.80	1	30	.95	7.41E+00	.077	7.58E+04
7.04E+00	1.10E-03	1	1	.80	1	40	.95	7.41E+00	.151	7.92E+02
7.04E+00	1.53E-03	1	1	.80	1	35	.95	7.41E+00	.159	7.66E+02
7.04E+00	2.15E-03	1	1	.80	1	30	.95	7.41E+00	.163	7.50E+02
7.04E+00	3.00E-03	1	1	.80	1	25	.95	7.41E+00	.160	7.38E+02
7.04E+00	4.21E-03	1	1	.80	1	25	.95	7.41E+00	.196	7.37E+02
7.04E+00	5.89E-03	1	1	.80	1	25	.95	7.41E+00	.237	7.36E+02
7.04E+00	8.25E-03	1	1	.80	1	25	.95	7.41E+00	.284	7.35E+02
7.39E+00	8.21E-04	1	1	.80	1	30	.95	7.78E+00	.077	7.75E+04
7.39E+00	1.15E-03	1	1	.80	1	40	.95	7.78E+00	.151	7.10E+02
7.39E+00	1.61E-03	1	1	.80	1	35	.95	7.78E+00	.159	6.83E+02
7.39E+00	2.25E-03	1	1	.80	1	30	.95	7.78E+00	.163	6.67E+02
7.39E+00	3.16E-03	1	1	.80	1	25	.95	7.78E+00	.160	6.54E+02
7.39E+00	4.42E-03	1	1	.80	1	25	.95	7.78E+00	.196	6.53E+02
7.39E+00	6.18E-03	1	1	.80	1	25	.95	7.78E+00	.237	6.52E+02
7.39E+00	8.66E-03	1	1	.80	1	25	.95	7.78E+00	.284	6.51E+02
7.76E+00	8.62E-04	1	1	.80	1	30	.95	8.17E+00	.077	7.92E+04
7.76E+00	1.21E-03	1	1	.80	1	40	.95	8.17E+00	.151	7.27E+02
7.76E+00	1.69E-03	1	1	.80	1	35	.95	8.17E+00	.159	7.00E+02
7.76E+00	2.37E-03	1	1	.80	1	30	.95	8.17E+00	.163	6.83E+02
7.76E+00	3.31E-03	1	1	.80	1	25	.95	8.17E+00	.160	6.70E+02
7.76E+00	4.64E-03	1	1	.80	1	25	.95	8.17E+00	.196	6.69E+02
7.76E+00	6.49E-03	1	1	.80	1	25	.95	8.17E+00	.237	6.68E+02
7.76E+00	9.09E-03	1	1	.80	1	25	.95	8.17E+00	.284	6.67E+02
8.15E+00	9.06E-04	1	1	.80	1	30	.95	8.58E+00	.077	7.09E+04
8.15E+00	1.27E-03	1	1	.80	1	40	.95	8.58E+00	.151	7.45E+02
8.15E+00	1.77E-03	1	1	.80	1	35	.95	8.58E+00	.159	7.17E+02
8.15E+00	2.48E-03	1	1	.80	1	30	.95	8.58E+00	.163	6.99E+02
8.15E+00	3.48E-03	1	1	.80	1	25	.95	8.58E+00	.160	6.86E+02
8.15E+00	4.87E-03	1	1	.80	1	25	.95	8.58E+00	.196	6.85E+02
8.15E+00	6.82E-03	1	1	.80	1	25	.95	8.58E+00	.237	6.83E+02
8.15E+00	9.55E-03	1	1	.80	1	25	.95	8.58E+00	.284	6.83E+02
8.56E+00	9.51E-04	1	1	.80	1	30	.95	9.01E+00	.077	7.25E+04
8.56E+00	1.33E-03	1	1	.80	1	40	.95	9.01E+00	.151	7.62E+02
8.56E+00	1.86E-03	1	1	.80	1	35	.95	9.01E+00	.159	7.33E+02
8.56E+00	2.61E-03	1	1	.80	1	30	.95	9.01E+00	.163	7.16E+02
8.56E+00	3.65E-03	1	1	.80	1	25	.95	9.01E+00	.160	7.02E+02
8.56E+00	5.11E-03	1	1	.80	1	25	.95	9.01E+00	.196	7.00E+02
8.56E+00	7.16E-03	1	1	.80	1	25	.95	9.01E+00	.237	6.99E+02
8.56E+00	1.00E-02	1	1	.80	1	25	.95	9.01E+00	.284	6.98E+02
8.99E+00	9.98E-04	1	1	.80	1	30	.95	9.46E+00	.077	7.41E+04
8.99E+00	1.40E-03	1	1	.80	1	40	.95	9.46E+00	.151	7.79E+02
8.99E+00	1.96E-03	1	1	.80	1	35	.95	9.46E+00	.159	7.49E+02
8.99E+00	2.74E-03	1	1	.80	1	30	.95	9.46E+00	.163	7.31E+02
8.99E+00	3.84E-03	1	1	.80	1	25	.95	9.46E+00	.160	7.17E+02
8.99E+00	5.37E-03	1	1	.80	1	25	.95	9.46E+00	.196	7.16E+02
8.99E+00	7.52E-03	1	1	.80	1	25	.95	9.46E+00	.237	7.14E+02
8.99E+00	1.05E-02	1	1	.80	1	25	.95	9.46E+00	.284	7.13E+02
9.43E+00	1.05E-03	1	1	.80	1	30	.95	9.93E+00	.077	7.57E+04
9.43E+00	1.47E-03	1	1	.80	1	40	.95	9.93E+00	.151	7.95E+02
9.43E+00	2.05E-03	1	1	.80	1	35	.95	9.93E+00	.159	7.65E+02
9.43E+00	2.88E-03	1	1	.80	1	30	.95	9.93E+00	.163	7.46E+02
9.43E+00	4.03E-03	1	1	.80	1	25	.95	9.93E+00	.160	7.32E+02

PER MODULE COST FOR POINTING AND SURFACE ACCURACY 1.0
PER SQUARE METER COST FOR POINTING AND SURFACE ACCURACY 1.0

----PARAMETERS----		----------OPTIMUM DESIGNS----------								MINIMUM
EAP	G	N	WP	SCOS	NW	TH	RHO	AP	SIGMA	COST
1.00E+00	1.11E-04	1	1	.80	1	45	.90	1.11E+00	.162	7.44E+01
1.00E+00	1.56E-04	1	1	.80	1	45	.90	1.11E+00	.198	7.40E+01
1.00E+00	2.18E-04	1	1	.80	1	45	.90	1.11E+00	.239	7.38E+01
1.00E+00	3.05E-04	1	1	.80	1	45	.90	1.11E+00	.287	7.36E+01
1.00E+00	4.27E-04	1	1	.80	1	45	.90	1.11E+00	.343	7.34E+01
1.00E+00	5.98E-04	1	1	.80	1	45	.90	1.11E+00	.409	7.33E+01
1.00E+00	8.37E-04	1	1	.80	1	45	.90	1.11E+00	.487	7.32E+01
1.00E+00	1.17E-03	1	1	.80	1	45	.90	1.11E+00	.578	7.31E+01
1.05E+00	1.17E-04	1	1	.80	1	45	.90	1.17E+00	.162	7.47E+01
1.05E+00	1.63E-04	1	1	.80	1	45	.90	1.17E+00	.198	7.43E+01
1.05E+00	2.29E-04	1	1	.80	1	45	.90	1.17E+00	.239	7.41E+01
1.05E+00	3.20E-04	1	1	.80	1	45	.90	1.17E+00	.287	7.38E+01
1.05E+00	4.48E-04	1	1	.80	1	45	.90	1.17E+00	.343	7.37E+01
1.05E+00	6.27E-04	1	1	.80	1	45	.90	1.17E+00	.409	7.35E+01
1.05E+00	8.78E-04	1	1	.80	1	45	.90	1.17E+00	.487	7.34E+01
1.05E+00	1.23E-03	1	1	.80	1	45	.90	1.17E+00	.578	7.33E+01
1.10E+00	1.22E-04	1	1	.80	1	45	.90	1.22E+00	.162	7.50E+01
1.10E+00	1.71E-04	1	1	.80	1	45	.90	1.22E+00	.198	7.46E+01
1.10E+00	2.40E-04	1	1	.80	1	45	.90	1.22E+00	.239	7.43E+01
1.10E+00	3.36E-04	1	1	.80	1	45	.90	1.22E+00	.287	7.41E+01
1.10E+00	4.71E-04	1	1	.80	1	45	.90	1.22E+00	.343	7.39E+01
1.10E+00	6.59E-04	1	1	.80	1	45	.90	1.22E+00	.409	7.38E+01
1.10E+00	9.22E-04	1	1	.80	1	45	.90	1.22E+00	.487	7.37E+01
1.10E+00	1.29E-03	1	1	.80	1	45	.90	1.22E+00	.578	7.36E+01
1.16E+00	1.29E-04	1	1	.80	1	45	.90	1.29E+00	.162	7.53E+01
1.16E+00	1.80E-04	1	1	.80	1	45	.90	1.29E+00	.198	7.49E+01
1.16E+00	2.52E-04	1	1	.80	1	45	.90	1.29E+00	.239	7.46E+01
1.16E+00	3.53E-04	1	1	.80	1	45	.90	1.29E+00	.287	7.44E+01
1.16E+00	4.94E-04	1	1	.80	1	45	.90	1.29E+00	.343	7.42E+01
1.16E+00	6.92E-04	1	1	.80	1	45	.90	1.29E+00	.409	7.41E+01
1.16E+00	9.68E-04	1	1	.80	1	45	.90	1.29E+00	.487	7.39E+01
1.16E+00	1.36E-03	1	1	.80	1	45	.90	1.29E+00	.578	7.38E+01
1.22E+00	1.35E-04	1	1	.80	1	45	.90	1.35E+00	.162	7.56E+01
1.22E+00	1.89E-04	1	1	.80	1	45	.90	1.35E+00	.198	7.52E+01
1.22E+00	2.65E-04	1	1	.80	1	45	.90	1.35E+00	.239	7.49E+01
1.22E+00	3.71E-04	1	1	.80	1	45	.90	1.35E+00	.287	7.47E+01
1.22E+00	5.19E-04	1	1	.80	1	45	.90	1.35E+00	.343	7.45E+01
1.22E+00	7.26E-04	1	1	.80	1	45	.90	1.35E+00	.409	7.44E+01
1.22E+00	1.02E-03	1	1	.80	1	45	.90	1.35E+00	.487	7.42E+01
1.22E+00	1.42E-03	1	1	.80	1	45	.90	1.35E+00	.578	7.41E+01
1.28E+00	1.42E-04	1	1	.80	1	45	.90	1.42E+00	.162	7.59E+01
1.28E+00	1.99E-04	1	1	.80	1	45	.90	1.42E+00	.198	7.56E+01
1.28E+00	2.78E-04	1	1	.80	1	45	.90	1.42E+00	.239	7.53E+01
1.28E+00	3.89E-04	1	1	.80	1	45	.90	1.42E+00	.287	7.50E+01
1.28E+00	5.45E-04	1	1	.80	1	45	.90	1.42E+00	.343	7.48E+01
1.28E+00	7.63E-04	1	1	.80	1	45	.90	1.42E+00	.409	7.47E+01
1.28E+00	1.07E-03	1	1	.80	1	45	.90	1.42E+00	.487	7.45E+01
1.28E+00	1.49E-03	1	1	.80	1	45	.90	1.42E+00	.578	7.44E+01
1.34E+00	1.49E-04	1	1	.80	1	45	.90	1.49E+00	.162	7.63E+01
1.34E+00	2.08E-04	1	1	.80	1	45	.90	1.49E+00	.198	7.59E+01
1.34E+00	2.92E-04	1	1	.80	1	45	.90	1.49E+00	.239	7.56E+01
1.34E+00	4.09E-04	1	1	.80	1	45	.90	1.49E+00	.287	7.53E+01
1.34E+00	5.72E-04	1	1	.80	1	45	.90	1.49E+00	.343	7.51E+01

PER MODULE COST FOR POINTING AND SURFACE ACCURACY 1.0
PER SQUARE METER COST FOR POINTING AND SURFACE ACCURACY 1.0

----PARAMETERS----			----------OPTIMUM DESIGNS----------							MINIMUM
EAP	G	N	WP	SCOS	NW	TH	RHO	AP	SIGMA	COST
1.00E+00	1.11E-04	1	1	.80	1	40	.90	1.11E+00	.116	7.45E+03
1.00E+00	1.56E-04	1	1	.80	1	45	.90	1.11E+00	.167	7.43E+01
1.00E+00	2.18E-04	1	1	.80	1	45	.90	1.11E+00	.204	7.40E+01
1.00E+00	3.05E-04	1	1	.80	1	45	.90	1.11E+00	.246	7.38E+01
1.00E+00	4.27E-04	1	1	.80	1	45	.90	1.11E+00	.295	7.36E+01
1.00E+00	5.98E-04	1	1	.80	1	45	.90	1.11E+00	.352	7.34E+01
1.00E+00	8.37E-04	1	1	.80	1	45	.90	1.11E+00	.420	7.33E+01
1.00E+00	1.17E-03	1	1	.80	1	45	.90	1.11E+00	.499	7.31E+01
1.05E+00	1.17E-04	1	1	.80	1	45	.90	1.17E+00	.135	7.50E+03
1.05E+00	1.63E-04	1	1	.80	1	45	.90	1.17E+00	.167	7.46E+01
1.05E+00	2.29E-04	1	1	.80	1	45	.90	1.17E+00	.204	7.43E+01
1.05E+00	3.20E-04	1	1	.80	1	45	.90	1.17E+00	.246	7.40E+01
1.05E+00	4.48E-04	1	1	.80	1	45	.90	1.17E+00	.295	7.38E+01
1.05E+00	6.27E-04	1	1	.80	1	45	.90	1.17E+00	.352	7.36E+01
1.05E+00	8.78E-04	1	1	.80	1	45	.90	1.17E+00	.420	7.35E+01
1.05E+00	1.23E-03	1	1	.80	1	45	.90	1.17E+00	.499	7.34E+01
1.10E+00	1.22E-04	1	1	.80	1	45	.90	1.22E+00	.135	7.53E+03
1.10E+00	1.71E-04	1	1	.80	1	45	.90	1.22E+00	.167	7.49E+01
1.10E+00	2.40E-04	1	1	.80	1	45	.90	1.22E+00	.204	7.46E+01
1.10E+00	3.36E-04	1	1	.80	1	45	.90	1.22E+00	.246	7.43E+01
1.10E+00	4.71E-04	1	1	.80	1	45	.90	1.22E+00	.295	7.41E+01
1.10E+00	6.59E-04	1	1	.80	1	45	.90	1.22E+00	.352	7.39E+01
1.10E+00	9.22E-04	1	1	.80	1	45	.90	1.22E+00	.420	7.38E+01
1.10E+00	1.29E-03	1	1	.80	1	45	.90	1.22E+00	.499	7.36E+01
1.16E+00	1.29E-04	1	1	.80	1	45	.90	1.29E+00	.135	7.57E+03
1.16E+00	1.80E-04	1	1	.80	1	45	.90	1.29E+00	.167	7.52E+01
1.16E+00	2.52E-04	1	1	.80	1	45	.90	1.29E+00	.204	7.49E+01
1.16E+00	3.53E-04	1	1	.80	1	45	.90	1.29E+00	.246	7.46E+01
1.16E+00	4.94E-04	1	1	.80	1	45	.90	1.29E+00	.295	7.44E+01
1.16E+00	6.92E-04	1	1	.80	1	45	.90	1.29E+00	.352	7.42E+01
1.16E+00	9.68E-04	1	1	.80	1	45	.90	1.29E+00	.420	7.40E+01
1.16E+00	1.36E-03	1	1	.80	1	45	.90	1.29E+00	.499	7.39E+01
1.22E+00	1.35E-04	1	1	.80	1	45	.90	1.35E+00	.135	7.60E+03
1.22E+00	1.89E-04	1	1	.80	1	45	.90	1.35E+00	.167	7.55E+01
1.22E+00	2.65E-04	1	1	.80	1	45	.90	1.35E+00	.204	7.52E+01
1.22E+00	3.71E-04	1	1	.80	1	45	.90	1.35E+00	.246	7.49E+01
1.22E+00	5.19E-04	1	1	.80	1	45	.90	1.35E+00	.295	7.47E+01
1.22E+00	7.26E-04	1	1	.80	1	45	.90	1.35E+00	.352	7.45E+01
1.22E+00	1.02E-03	1	1	.80	1	45	.90	1.35E+00	.420	7.43E+01
1.22E+00	1.42E-03	1	1	.80	1	45	.90	1.35E+00	.499	7.42E+01
1.28E+00	1.42E-04	1	1	.80	1	45	.90	1.42E+00	.135	7.64E+03
1.28E+00	1.99E-04	1	1	.80	1	45	.90	1.42E+00	.167	7.59E+01
1.28E+00	2.78E-04	1	1	.80	1	45	.90	1.42E+00	.204	7.55E+01
1.28E+00	3.89E-04	1	1	.80	1	45	.90	1.42E+00	.246	7.52E+01
1.28E+00	5.45E-04	1	1	.80	1	45	.90	1.42E+00	.295	7.50E+01
1.28E+00	7.63E-04	1	1	.80	1	45	.90	1.42E+00	.352	7.48E+01
1.28E+00	1.07E-03	1	1	.80	1	45	.90	1.42E+00	.420	7.46E+01
1.28E+00	1.49E-03	1	1	.80	1	45	.90	1.42E+00	.499	7.45E+01
1.34E+00	1.49E-04	1	1	.80	1	45	.90	1.49E+00	.135	7.67E+03
1.34E+00	2.08E-04	1	1	.80	1	45	.90	1.49E+00	.167	7.62E+01
1.34E+00	2.92E-04	1	1	.80	1	45	.90	1.49E+00	.204	7.59E+01
1.34E+00	4.09E-04	1	1	.80	1	45	.90	1.49E+00	.246	7.56E+01
1.34E+00	5.72E-04	1	1	.80	1	45	.90	1.49E+00	.295	7.53E+01

PER MODULE COST FOR POINTING AND SURFACE ACCURACY 1.0
PER SQUARE METER COST FOR POINTING AND SURFACE ACCURACY 1.0

----PARAMETERS----					----------OPTIMUM DESIGNS----------					MINIMUM
EAP	C	N	NP	SCOS	NW	TH	RHO	AP	SIGMA	COST
1.00E+00	3.05E-03	1	1	.80	1	35	.95	1.05E+00	.065	5.69E+03
1.00E+00	4.27E-03	1	1	.80	1	45	.95	1.05E+00	.161	5.73E+01
1.00E+00	5.98E-03	1	1	.80	1	30	.95	1.05E+00	.151	5.32E+01
1.00E+00	8.37E-03	1	1	.80	1	25	.95	1.05E+00	.183	5.19E+01
1.00E+00	1.17E-02	1	1	.80	1	25	.95	1.05E+00	.267	5.14E+01
1.05E+00	3.20E-03	1	1	.80	1	35	.95	1.11E+00	.065	5.93E+03
1.05E+00	4.48E-03	1	1	.80	1	45	.95	1.11E+00	.161	5.98E+01
1.05E+00	6.27E-03	1	1	.80	1	30	.95	1.11E+00	.151	5.55E+01
1.05E+00	8.78E-03	1	1	.80	1	25	.95	1.11E+00	.183	5.42E+01
1.05E+00	1.23E-02	1	1	.80	1	25	.95	1.11E+00	.267	5.37E+01
1.10E+00	3.36E-03	1	1	.80	1	35	.95	1.16E+00	.065	6.16E+03
1.10E+00	4.71E-03	1	1	.80	1	45	.95	1.16E+00	.161	6.23E+01
1.10E+00	6.59E-03	1	1	.80	1	30	.95	1.16E+00	.151	5.79E+01
1.10E+00	9.22E-03	1	1	.80	1	25	.95	1.16E+00	.183	5.65E+01
1.10E+00	1.29E-02	1	1	.80	1	25	.95	1.16E+00	.267	5.60E+01
1.16E+00	3.53E-03	1	1	.80	1	35	.95	1.22E+00	.065	6.44E+03
1.16E+00	4.94E-03	1	1	.80	1	45	.95	1.22E+00	.161	6.50E+01
1.16E+00	6.92E-03	1	1	.80	1	30	.95	1.22E+00	.151	6.04E+01
1.16E+00	9.68E-03	1	1	.80	1	25	.95	1.22E+00	.183	5.89E+01
1.16E+00	1.36E-02	1	1	.80	1	25	.95	1.22E+00	.267	5.84E+01
1.22E+00	3.71E-03	1	1	.80	1	35	.95	1.28E+00	.065	6.71E+03
1.22E+00	5.19E-03	1	1	.80	1	45	.95	1.28E+00	.161	6.77E+01
1.22E+00	7.26E-03	1	1	.80	1	30	.95	1.28E+00	.151	6.29E+01
1.22E+00	1.02E-02	1	1	.80	1	25	.95	1.28E+00	.183	6.14E+01
1.22E+00	1.42E-02	1	1	.80	1	25	.95	1.28E+00	.267	6.09E+01
1.28E+00	3.89E-03	1	1	.80	1	35	.95	1.34E+00	.065	6.99E+03
1.28E+00	5.45E-03	1	1	.80	1	45	.95	1.34E+00	.161	7.06E+01
1.28E+00	7.63E-03	1	1	.80	1	30	.95	1.34E+00	.151	6.55E+01
1.28E+00	1.07E-02	1	1	.80	1	25	.95	1.34E+00	.183	6.40E+01
1.28E+00	1.49E-02	1	1	.80	1	25	.95	1.34E+00	.267	6.34E+01
1.34E+00	4.09E-03	1	1	.80	1	35	.95	1.41E+00	.065	7.27E+03
1.34E+00	5.72E-03	1	1	.80	1	45	.95	1.41E+00	.161	7.35E+01
1.34E+00	8.01E-03	1	1	.80	1	30	.95	1.41E+00	.151	6.83E+01
1.34E+00	1.12E-02	1	1	.80	1	25	.95	1.41E+00	.183	6.67E+01
1.34E+00	1.57E-02	1	1	.80	1	25	.95	1.41E+00	.267	6.61E+01
1.41E+00	4.29E-03	1	1	.80	1	35	.95	1.48E+00	.065	7.57E+03
1.41E+00	6.01E-03	1	1	.80	1	45	.95	1.48E+00	.161	7.65E+01
1.41E+00	8.41E-03	1	1	.80	1	30	.95	1.48E+00	.151	7.11E+01
1.41E+00	1.18E-02	1	1	.80	1	25	.95	1.48E+00	.183	6.94E+01
1.41E+00	1.65E-02	1	1	.80	1	25	.95	1.48E+00	.267	6.88E+01
1.48E+00	4.50E-03	1	1	.80	1	35	.95	1.56E+00	.065	7.88E+03
1.48E+00	6.31E-03	1	1	.80	1	45	.95	1.56E+00	.161	7.97E+01
1.48E+00	8.83E-03	1	1	.80	1	30	.95	1.56E+00	.151	7.40E+01
1.48E+00	1.24E-02	1	1	.80	1	25	.95	1.56E+00	.183	7.22E+01
1.48E+00	1.73E-02	1	1	.80	1	25	.95	1.56E+00	.267	7.16E+01
1.55E+00	4.73E-03	1	1	.80	1	35	.95	1.63E+00	.065	8.19E+03
1.55E+00	6.62E-03	1	1	.80	1	45	.95	1.63E+00	.161	8.29E+01
1.55E+00	9.27E-03	1	1	.80	1	30	.95	1.63E+00	.151	7.69E+01
1.55E+00	1.30E-02	1	1	.80	1	25	.95	1.63E+00	.183	7.51E+01
1.55E+00	1.82E-02	1	1	.80	1	25	.95	1.63E+00	.267	7.45E+01
1.63E+00	4.97E-03	1	1	.80	1	35	.95	1.71E+00	.065	8.51E+03
1.63E+00	6.95E-03	1	1	.80	1	45	.95	1.71E+00	.161	8.62E+01
1.63E+00	9.73E-03	1	1	.80	1	30	.95	1.71E+00	.151	8.00E+01

PER MODULE COST FOR POINTING AND SURFACE ACCURACY 1.0
PER SQUARE METER COST FOR POINTING AND SURFACE ACCURACY 1.0

----PARAMETERS----		----------OPTIMUM DESIGNS----------								MINIMUM
EAP	G	N	WP	SCOS	NW	TH	RHO	AP	SIGMA	COST
1.00E+00	3.05E-03	1	1	.80	1	40	.85	1.18E+00	.067	6.42E+03
1.00E+00	4.27E-03	1	1	.80	1	30	.85	1.18E+00	.076	6.06E+03
1.00E+00	5.98E-03	1	1	.80	1	35	.85	1.18E+00	.159	5.97E+01
1.00E+00	8.37E-03	1	1	.80	1	25	.85	1.18E+00	.160	5.74E+01
1.00E+00	1.17E-02	1	1	.80	1	25	.85	1.18E+00	.236	5.68E+01
1.05E+00	3.20E-03	1	1	.80	1	40	.85	1.24E+00	.067	6.69E+03
1.05E+00	4.48E-03	1	1	.80	1	30	.85	1.24E+00	.076	6.31E+03
1.05E+00	6.27E-03	1	1	.80	1	35	.85	1.24E+00	.159	6.23E+01
1.05E+00	8.78E-03	1	1	.80	1	25	.85	1.24E+00	.160	5.99E+01
1.05E+00	1.23E-02	1	1	.80	1	25	.85	1.24E+00	.236	5.92E+01
1.10E+00	3.36E-03	1	1	.80	1	40	.85	1.30E+00	.067	6.97E+03
1.10E+00	4.71E-03	1	1	.80	1	30	.85	1.30E+00	.076	6.57E+03
1.10E+00	6.59E-03	1	1	.80	1	35	.85	1.30E+00	.159	6.49E+01
1.10E+00	9.22E-03	1	1	.80	1	25	.85	1.30E+00	.160	6.24E+01
1.10E+00	1.29E-02	1	1	.80	1	25	.85	1.30E+00	.236	6.17E+01
1.16E+00	3.53E-03	1	1	.80	1	40	.85	1.36E+00	.067	7.26E+03
1.16E+00	4.94E-03	1	1	.80	1	30	.85	1.36E+00	.076	6.85E+03
1.16E+00	6.92E-03	1	1	.80	1	35	.85	1.36E+00	.159	6.76E+01
1.16E+00	9.68E-03	1	1	.80	1	25	.85	1.36E+00	.160	6.50E+01
1.16E+00	1.36E-02	1	1	.80	1	25	.85	1.36E+00	.236	6.43E+01
1.22E+00	3.71E-03	1	1	.80	1	40	.85	1.43E+00	.067	7.56E+03
1.22E+00	5.19E-03	1	1	.80	1	30	.85	1.43E+00	.076	7.13E+03
1.22E+00	7.26E-03	1	1	.80	1	35	.85	1.43E+00	.159	7.04E+01
1.22E+00	1.02E-02	1	1	.80	1	25	.85	1.43E+00	.160	6.77E+01
1.22E+00	1.42E-02	1	1	.80	1	25	.85	1.43E+00	.236	6.70E+01
1.28E+00	3.89E-03	1	1	.80	1	40	.85	1.50E+00	.067	7.86E+03
1.28E+00	5.45E-03	1	1	.80	1	30	.85	1.50E+00	.076	7.42E+03
1.28E+00	7.63E-03	1	1	.80	1	35	.85	1.50E+00	.159	7.33E+01
1.28E+00	1.07E-02	1	1	.80	1	25	.85	1.50E+00	.160	7.05E+01
1.28E+00	1.49E-02	1	1	.80	1	25	.85	1.50E+00	.236	6.97E+01
1.34E+00	4.09E-03	1	1	.80	1	40	.85	1.58E+00	.067	8.18E+03
1.34E+00	5.72E-03	1	1	.80	1	30	.85	1.58E+00	.076	7.71E+03
1.34E+00	8.01E-03	1	1	.80	1	35	.85	1.58E+00	.159	7.63E+01
1.34E+00	1.12E-02	1	1	.80	1	25	.85	1.58E+00	.160	7.33E+01
1.34E+00	1.57E-02	1	1	.80	1	25	.85	1.58E+00	.236	7.26E+01
1.41E+00	4.29E-03	1	1	.80	1	40	.85	1.66E+00	.067	8.50E+03
1.41E+00	6.01E-03	1	1	.80	1	30	.85	1.66E+00	.076	8.02E+03
1.41E+00	8.41E-03	1	1	.80	1	35	.85	1.66E+00	.159	7.94E+01
1.41E+00	1.18E-02	1	1	.80	1	25	.85	1.66E+00	.160	7.63E+01
1.41E+00	1.65E-02	1	1	.80	1	25	.85	1.66E+00	.236	7.55E+01
1.48E+00	4.50E-03	1	1	.80	1	40	.85	1.74E+00	.067	8.84E+03
1.48E+00	6.31E-03	1	1	.80	1	30	.85	1.74E+00	.076	8.34E+03
1.48E+00	8.83E-03	1	1	.80	1	35	.85	1.74E+00	.159	8.25E+01
1.48E+00	1.24E-02	1	1	.80	1	25	.85	1.74E+00	.160	7.93E+01
1.48E+00	1.73E-02	1	1	.80	1	25	.85	1.74E+00	.236	7.85E+01
1.55E+00	4.73E-03	1	1	.80	1	40	.85	1.83E+00	.067	9.18E+03
1.55E+00	6.62E-03	1	1	.80	1	30	.85	1.83E+00	.076	8.66E+03
1.55E+00	9.27E-03	1	1	.80	1	35	.85	1.83E+00	.159	8.57E+01
1.55E+00	1.30E-02	1	1	.80	1	25	.85	1.83E+00	.160	8.23E+01
1.55E+00	1.82E-02	1	1	.80	1	25	.85	1.83E+00	.236	8.15E+01
1.63E+00	4.97E-03	1	1	.80	1	40	.85	1.92E+00	.067	9.53E+03
1.63E+00	6.95E-03	1	1	.80	1	30	.85	1.92E+00	.076	8.99E+03
1.63E+00	9.73E-03	1	1	.80	1	35	.85	1.92E+00	.159	8.90E+01

PER MODULE COST FOR POINTING AND SURFACE ACCURACY 1.0
PER SQUARE METER COST FOR POINTING AND SURFACE ACCURACY 1.0

----PARAMETERS----					----------OPTIMUM DESIGN----------					MINIMUM
EAP	G	M	UP	COS	NW	TH	RHO	AP	SIGMA	COST
5.00E+00	5.56E-04	1	1	.80	1	75	.69	7.25E+00	.153	6.36E+02
5.00E+00	7.73E-04	1	1	.80	1	75	.69	7.25E+00	.183	6.34E+02
5.00E+00	1.09E-03	1	1	.80	1	75	.69	7.25E+00	.227	6.33E+02
5.00E+00	1.53E-03	1	1	.80	1	70	.69	7.25E+00	.265	6.32E+02
5.00E+00	2.14E-03	1	1	.80	1	70	.69	7.25E+00	.316	6.32E+02
5.00E+00	2.99E-03	1	1	.80	1	70	.69	7.25E+00	.379	6.31E+02
5.00E+00	4.19E-03	1	1	.80	1	70	.69	7.25E+00	.451	6.31E+02
5.00E+00	5.86E-03	1	1	.80	1	70	.69	7.25E+00	.536	6.30E+02
5.25E+00	5.84E-04	1	1	.80	1	75	.69	7.61E+00	.153	6.49E+02
5.25E+00	8.17E-04	1	1	.80	1	75	.69	7.61E+00	.183	6.47E+02
5.25E+00	1.14E-03	1	1	.80	1	75	.69	7.61E+00	.227	6.46E+02
5.25E+00	1.60E-03	1	1	.80	1	75	.69	7.61E+00	.273	6.45E+02
5.25E+00	2.24E-03	1	1	.80	1	70	.69	7.61E+00	.316	6.45E+02
5.25E+00	3.14E-03	1	1	.80	1	70	.69	7.61E+00	.379	6.44E+02
5.25E+00	4.40E-03	1	1	.80	1	70	.69	7.61E+00	.451	6.44E+02
5.25E+00	6.15E-03	1	1	.80	1	70	.69	7.61E+00	.536	6.43E+02
5.52E+00	6.13E-04	1	1	.80	1	75	.69	7.99E+00	.153	6.63E+02
5.52E+00	8.58E-04	1	1	.80	1	75	.69	7.99E+00	.183	6.61E+02
5.52E+00	1.20E-03	1	1	.80	1	75	.69	7.99E+00	.227	6.60E+02
5.52E+00	1.68E-03	1	1	.80	1	75	.69	7.99E+00	.273	6.59E+02
5.52E+00	2.35E-03	1	1	.80	1	75	.69	7.99E+00	.327	6.59E+02
5.52E+00	3.30E-03	1	1	.80	1	70	.69	7.99E+00	.379	6.58E+02
5.52E+00	4.61E-03	1	1	.80	1	70	.69	7.99E+00	.451	6.57E+02
5.52E+00	6.46E-03	1	1	.80	1	70	.69	7.99E+00	.536	6.57E+02
5.79E+00	6.44E-04	1	1	.80	1	65	.73	7.41E+00	.153	6.64E+02
5.79E+00	9.01E-04	1	1	.80	1	60	.73	7.41E+00	.173	6.63E+02
5.79E+00	1.26E-03	1	1	.80	1	60	.73	7.41E+00	.216	6.61E+02
5.79E+00	1.77E-03	1	1	.80	1	60	.73	7.41E+00	.260	6.61E+02
5.79E+00	2.47E-03	1	1	.80	1	60	.73	7.41E+00	.311	6.60E+02
5.79E+00	3.46E-03	1	1	.80	1	60	.73	7.41E+00	.371	6.59E+02
5.79E+00	4.85E-03	1	1	.80	1	60	.73	7.41E+00	.442	6.59E+02
5.79E+00	6.78E-03	1	1	.80	1	60	.73	7.41E+00	.529	6.58E+02
6.05E+00	6.76E-04	1	1	.80	1	65	.73	7.76E+00	.153	6.79E+02
6.05E+00	9.46E-04	1	1	.80	1	60	.73	7.76E+00	.173	6.79E+02
6.05E+00	1.32E-03	1	1	.80	1	60	.73	7.76E+00	.216	6.78E+02
6.05E+00	1.85E-03	1	1	.80	1	60	.73	7.76E+00	.260	6.78E+02
6.05E+00	2.60E-03	1	1	.80	1	60	.73	7.76E+00	.311	6.78E+02
6.05E+00	3.63E-03	1	1	.80	1	60	.73	7.76E+00	.371	6.77E+02
6.05E+00	5.09E-03	1	1	.80	1	60	.73	7.76E+00	.442	6.77E+02
6.05E+00	7.12E-03	1	1	.80	1	60	.73	7.76E+00	.529	6.76E+02
6.32E+00	7.09E-04	1	1	.80	1	65	.73	8.12E+00	.153	6.95E+02
6.32E+00	9.90E-04	1	1	.80	1	65	.73	8.12E+00	.183	6.93E+02
6.32E+00	1.39E-03	1	1	.80	1	60	.73	8.12E+00	.216	6.92E+02
6.32E+00	1.95E-03	1	1	.80	1	60	.73	8.12E+00	.260	6.91E+02
6.32E+00	2.73E-03	1	1	.80	1	60	.73	8.12E+00	.311	6.90E+02
6.32E+00	3.82E-03	1	1	.80	1	60	.73	8.12E+00	.371	6.90E+02
6.32E+00	5.34E-03	1	1	.80	1	60	.73	8.12E+00	.442	6.89E+02
6.32E+00	7.45E-03	1	1	.80	1	60	.73	8.12E+00	.529	6.88E+02
6.59E+00	7.43E-04	1	1	.80	1	65	.73	8.47E+00	.153	7.12E+02
6.59E+00	1.04E-03	1	1	.80	1	65	.73	8.47E+00	.183	7.10E+02
6.59E+00	1.46E-03	1	1	.80	1	60	.73	8.47E+00	.216	7.09E+02
6.59E+00	2.04E-03	1	1	.80	1	60	.73	8.47E+00	.260	7.08E+02
6.59E+00	2.86E-03	1	1	.80	1	60	.73	8.47E+00	.311	7.07E+02

[illegible]								
[illegible]								
[illegible]								
[illegible]								
[illegible]		1	1	.80	1	65	.73	9.00E+00	.197	7.23E+02
7.04E+00	1.53E-03	1	1	.80	1	60	.73	9.00E+00	.216	7.27E+02
7.04E+00	2.15E-03	1	1	.80	1	60	.73	9.00E+00	.260	7.26E+02
7.04E+00	3.00E-03	1	1	.80	1	60	.73	9.00E+00	.311	7.25E+02
7.04E+00	4.21E-03	1	1	.80	1	60	.73	9.00E+00	.371	7.24E+02
7.04E+00	5.89E-03	1	1	.80	1	60	.73	9.00E+00	.442	7.23E+02
7.04E+00	8.25E-03	1	1	.80	1	60	.73	9.00E+00	.525	7.23E+02
7.39E+00	8.21E-04	1	1	.80	1	65	.73	9.45E+00	.153	7.49E+02
7.39E+00	1.15E-03	1	1	.80	1	65	.73	9.45E+00	.197	7.47E+02
7.39E+00	1.61E-03	1	1	.80	1	65	.73	9.45E+00	.227	7.46E+02
7.39E+00	2.25E-03	1	1	.80	1	60	.73	9.45E+00	.260	7.45E+02
7.39E+00	3.16E-03	1	1	.80	1	60	.73	9.45E+00	.311	7.44E+02
7.39E+00	4.42E-03	1	1	.80	1	60	.73	9.45E+00	.371	7.43E+02
7.39E+00	6.19E-03	1	1	.80	1	60	.73	9.45E+00	.442	7.42E+02
7.39E+00	8.66E-03	1	1	.80	1	60	.73	9.45E+00	.525	7.42E+02
7.76E+00	8.62E-04	1	1	.80	1	65	.73	9.93E+00	.153	7.69E+02
7.76E+00	1.21E-03	1	1	.80	1	65	.73	9.93E+00	.197	7.67E+02
7.76E+00	1.69E-03	1	1	.80	1	65	.73	9.93E+00	.227	7.66E+02
7.76E+00	2.37E-03	1	1	.80	1	60	.73	9.93E+00	.260	7.65E+02
7.76E+00	3.31E-03	1	1	.80	1	60	.73	9.93E+00	.311	7.64E+02
7.76E+00	4.64E-03	1	1	.80	1	60	.73	9.93E+00	.371	7.63E+02
7.76E+00	6.49E-03	1	1	.80	1	60	.73	9.93E+00	.442	7.63E+02
7.76E+00	9.09E-03	1	1	.80	1	60	.73	9.93E+00	.525	7.62E+02
8.15E+00	9.06E-04	1	1	.80	1	70	.73	1.09E+01	.160	7.91E+02
8.15E+00	1.27E-03	1	1	.80	1	65	.73	1.04E+01	.197	7.89E+02
8.15E+00	1.77E-03	1	1	.80	1	65	.73	1.04E+01	.227	7.87E+02
8.15E+00	2.48E-03	1	1	.80	1	65	.73	1.04E+01	.273	7.86E+02
8.15E+00	3.48E-03	1	1	.80	1	60	.73	1.04E+01	.311	7.85E+02
8.15E+00	4.87E-03	1	1	.80	1	60	.73	1.04E+01	.371	7.84E+02
8.15E+00	6.82E-03	1	1	.80	1	60	.73	1.04E+01	.442	7.83E+02
8.15E+00	9.55E-03	1	1	.80	1	60	.73	1.04E+01	.525	7.83E+02
8.56E+00	9.51E-04	1	1	.80	1	70	.73	1.09E+01	.160	8.13E+02
8.56E+00	1.33E-03	1	1	.80	1	65	.73	1.09E+01	.197	8.11E+02
8.56E+00	1.86E-03	1	1	.80	1	65	.73	1.09E+01	.227	8.10E+02
8.56E+00	2.61E-03	1	1	.80	1	65	.73	1.09E+01	.273	8.09E+02
8.56E+00	3.65E-03	1	1	.80	1	65	.73	1.09E+01	.326	8.07E+02
8.56E+00	5.11E-03	1	1	.80	1	60	.73	1.09E+01	.371	8.07E+02
8.56E+00	7.16E-03	1	1	.80	1	60	.73	1.09E+01	.442	8.06E+02
8.56E+00	1.00E-02	1	1	.80	1	60	.73	1.09E+01	.525	8.05E+02
8.99E+00	9.93E-04	1	1	.80	1	70	.73	1.15E+01	.160	8.37E+02
8.99E+00	1.40E-03	1	1	.80	1	65	.73	1.15E+01	.197	8.35E+02
8.99E+00	1.96E-03	1	1	.80	1	65	.73	1.15E+01	.227	8.34E+02
8.99E+00	2.74E-03	1	1	.80	1	65	.73	1.15E+01	.273	8.33E+02
8.99E+00	3.84E-03	1	1	.80	1	65	.73	1.15E+01	.326	8.31E+02
8.99E+00	5.37E-03	1	1	.80	1	65	.73	1.15E+01	.389	8.31E+02
8.99E+00	7.52E-03	1	1	.80	1	60	.73	1.15E+01	.442	8.30E+02
8.99E+00	1.05E-02	1	1	.80	1	60	.73	1.15E+01	.525	8.29E+02
9.43E+00	1.05E-03	1	1	.80	1	70	.73	1.21E+01	.160	8.63E+02
9.43E+00	1.47E-03	1	1	.80	1	70	.73	1.21E+01	.195	8.61E+02
9.43E+00	2.05E-03	1	1	.80	1	65	.73	1.21E+01	.227	8.59E+02
9.43E+00	2.88E-03	1	1	.80	1	65	.73	1.21E+01	.273	8.58E+02
9.43E+00	4.03E-03	1	1	.80	1	65	.73	1.21E+01	.326	8.57E+02
9.43E+00	5.64E-03	1	1	.80	1	65	.73	1.21E+01	.389	8.56E+02
9.43E+00	7.89E-03	1	1	.80	1	65	.73	1.21E+01	.453	8.55E+02
9.43E+00	1.10E-02	1	1	.80	1	60	.73	1.21E+01	.525	8.54E+02

PER MODULE COST FOR PAINTING AND SURFACE ACCURACY 1.0
PER SQUARE METER COST FOR PAINTING AND SURFACE ACCURACY 1.0

----PARAMETERS----					----------OPTIMUM DESIGN----------				MINIMUM
EAP	C	U	UP	SOLS	NU	TH	PHO	AP SIGMA	COST
1.00E+00	1.11E-03	1	1	.80	1110	.85	1.13E+00	.060	6.96E+03
1.00E+00	1.56E-03	1	1	.80	1 80	.85	1.13E+00	.079	6.51E+03
1.00E+00	2.18E-03	1	1	.80	1 90	.85	1.13E+00	.144	6.37E+01
1.00E+00	3.05E-03	1	1	.80	1 65	.85	1.13E+00	.149	6.17E+01
1.00E+00	4.27E-03	1	1	.80	1 60	.85	1.13E+00	.202	6.09E+01
1.00E+00	5.93E-03	1	1	.80	1 60	.85	1.13E+00	.294	6.05E+01
1.00E+00	8.37E-03	1	1	.80	1 60	.85	1.13E+00	.414	6.03E+01
1.00E+00	1.17E-02	1	1	.80	1 60	.85	1.13E+00	.580	6.09E+01
1.05E+00	1.17E-03	1	1	.80	1110	.85	1.07E+00	.060	7.15E+03
1.05E+00	1.63E-03	1	1	.80	1 80	.85	1.06E+00	.071	6.78E+03
1.05E+00	2.29E-03	1	1	.80	1 90	.85	1.06E+00	.101	6.65E+01
1.05E+00	3.20E-03	1	1	.80	1 65	.85	1.06E+00	.149	6.44E+01
1.05E+00	4.47E-03	1	1	.80	1 60	.85	1.06E+00	.205	6.36E+01
1.05E+00	6.27E-03	1	1	.80	1 60	.85	1.06E+00	.294	6.31E+01
1.05E+00	8.76E-03	1	1	.80	1 60	.85	1.06E+00	.414	6.27E+01
1.05E+00	1.22E-02	1	1	.80	1 60	.85	1.06E+00	.580	6.28E+01
1.10E+00	1.22E-03	1	1	.80	1110	.85	1.00E+00	.060	7.46E+03
1.10E+00	1.71E-03	1	1	.80	1 80	.85	1.00E+00	.071	7.07E+03
1.10E+00	2.40E-03	1	1	.80	1 90	.85	1.00E+00	.101	6.93E+01
1.10E+00	3.36E-03	1	1	.80	1 65	.85	1.00E+00	.149	6.71E+01
1.10E+00	4.71E-03	1	1	.80	1 60	.85	1.00E+00	.205	6.62E+01
1.10E+00	6.59E-03	1	1	.80	1 60	.85	1.00E+00	.294	6.57E+01
1.10E+00	9.22E-03	1	1	.80	1 60	.85	1.00E+00	.414	6.54E+01
1.10E+00	1.29E-02	1	1	.80	1 60	.85	1.00E+00	.580	6.59E+01
1.16E+00	1.29E-03	1	1	.80	1110	.85	1.06E+00	.060	7.77E+03
1.16E+00	1.80E-03	1	1	.80	1 80	.85	1.06E+00	.071	7.36E+03
1.16E+00	2.52E-03	1	1	.80	1 90	.85	1.06E+00	.101	7.23E+01
1.16E+00	3.53E-03	1	1	.80	1 65	.85	1.06E+00	.149	6.99E+01
1.16E+00	4.94E-03	1	1	.80	1 60	.85	1.06E+00	.205	6.90E+01
1.16E+00	6.93E-03	1	1	.80	1 60	.85	1.06E+00	.294	6.85E+01
1.16E+00	9.69E-03	1	1	.80	1 60	.85	1.06E+00	.414	6.82E+01
1.16E+00	1.35E-02	1	1	.80	1 60	.85	1.06E+00	.580	6.87E+01
1.22E+00	1.35E-03	1	1	.80	1110	.85	1.13E+00	.060	8.00E+03
1.22E+00	1.89E-03	1	1	.80	1 80	.85	1.13E+00	.071	7.66E+03
1.22E+00	2.65E-03	1	1	.80	1 90	.85	1.13E+00	.144	7.53E+01
1.22E+00	3.71E-03	1	1	.80	1 65	.85	1.13E+00	.149	7.33E+01
1.22E+00	5.19E-03	1	1	.80	1 60	.85	1.13E+00	.202	7.19E+01
1.22E+00	7.26E-03	1	1	.80	1 60	.85	1.13E+00	.294	7.14E+01
1.22E+00	1.02E-02	1	1	.80	1 60	.85	1.13E+00	.414	7.10E+01
1.22E+00	1.42E-02	1	1	.80	1 60	.85	1.13E+00	.580	7.08E+01
1.28E+00	1.42E-03	1	1	.80	1110	.85	1.19E+00	.060	8.23E+03
1.28E+00	1.99E-03	1	1	.80	1 80	.85	1.19E+00	.071	7.97E+03
1.28E+00	2.79E-03	1	1	.80	1 90	.85	1.19E+00	.144	7.84E+01
1.28E+00	3.91E-03	1	1	.80	1 65	.85	1.19E+00	.149	7.59E+01
1.28E+00	5.45E-03	1	1	.80	1 60	.85	1.19E+00	.202	7.49E+01
1.28E+00	7.63E-03	1	1	.80	1 60	.85	1.19E+00	.294	7.43E+01
1.28E+00	1.07E-02	1	1	.80	1 60	.85	1.19E+00	.414	7.40E+01
1.28E+00	1.49E-02	1	1	.80	1 60	.85	1.19E+00	.580	7.37E+01
1.34E+00	1.49E-03	1	1	.80	1110	.85	1.25E+00	.060	8.77E+03
1.34E+00	2.07E-03	1	1	.80	1 80	.85	1.25E+00	.071	8.36E+03
1.34E+00	2.92E-03	1	1	.80	1 90	.85	1.25E+00	.144	8.16E+01
1.34E+00	4.09E-03	1	1	.80	1 65	.85	1.25E+00	.149	7.90E+01
1.34E+00	5.72E-03	1	1	.80	1 60	.85	1.25E+00	.202	7.79E+01

PER MODULE COST FOR POINTING AND SURFACE ACCURACY 1.0
PER SQUARE METER COST FOR POINTING AND SURFACE ACCURACY 1.0

--PARAMETERS--			--------OPTIMUM DESIGNS--------						--------COST/1000------			
EX100	1000	FO	AP	TA	RHO	AP/100	TUR	STRIA	MIN	TUR	MEAN	HT
50	137	1	6943	65	.90	139	31	.101	66950	231	427	2
50	192	1	6943	65	.90	139	31	.166	666	231	427	2
50	269	1	6943	65	.90	139	31	.232	664	231	427	2
50	376	1	6943	65	.90	139	31	.304	663	231	427	2
50	527	2	1735	65	.90	139	31	.229	635	231	400	2
50	738	2	1735	65	.90	139	31	.344	634	231	400	2
51	140	1	7052	65	.90	141	31	.104	67237	231	435	2
51	196	1	7052	65	.90	141	31	.168	675	231	435	2
51	274	1	7052	65	.90	141	31	.243	673	231	435	2
51	384	1	7052	65	.90	141	31	.305	672	231	435	2
51	538	2	1770	65	.90	141	31	.233	643	231	409	2
51	753	2	1770	65	.90	141	31	.347	643	231	409	2
52	143	1	7203	65	.90	144	32	.106	68736	232	444	2
52	200	1	7203	65	.90	144	32	.170	684	232	444	2
52	280	1	7203	65	.90	144	32	.235	682	232	444	2
52	392	1	7203	65	.90	144	32	.306	681	232	444	2
52	548	2	1786	65	.90	144	32	.237	650	232	417	2
52	768	2	1786	75	.90	203	22	.144	638	232	407	2
53	146	1	7359	65	.90	147	32	.108	69666	232	453	2
53	204	1	7359	65	.90	147	32	.171	693	232	453	2
53	285	1	7359	65	.90	147	32	.236	691	232	453	2
53	400	1	7359	65	.90	147	32	.307	690	232	453	2
53	559	2	1949	65	.90	147	32	.241	656	232	425	2
53	783	3	1109	70	.90	165	26	.147	636	226	407	2
54	149	1	7515	65	.90	150	32	.110	70606	232	462	2
54	208	1	7515	65	.90	150	32	.173	703	232	462	2
54	291	1	7515	65	.90	150	32	.237	701	232	462	2
54	408	2	1951	75	.90	211	22	.149	676	222	450	2
54	571	2	1951	65	.90	150	32	.245	669	232	433	2
54	799	3	835	65	.90	150	30	.142	644	232	403	2
55	151	1	7665	65	.90	153	33	.113	71557	233	471	2
55	212	1	7665	65	.90	153	33	.175	712	233	471	2
55	297	1	7665	65	.90	153	33	.239	711	233	471	2
55	416	2	1947	70	.90	172	27	.145	630	227	449	2
55	532	2	1916	65	.90	153	33	.248	678	232	442	2
55	815	3	951	65	.90	153	33	.151	652	233	416	2
56	155	1	7819	65	.90	156	33	.115	72554	233	480	3
56	216	1	7819	65	.90	156	33	.176	722	233	480	3
56	303	1	7819	65	.90	156	33	.240	720	233	480	3
56	424	2	1954	65	.90	156	33	.142	691	233	451	3
56	594	2	1954	65	.90	156	33	.252	687	233	451	3
56	831	3	989	65	.90	156	33	.140	661	233	425	3
57	158	1	7975	65	.90	159	33	.117	73553	233	490	3
57	221	1	7975	65	.90	159	33	.179	732	233	490	3
57	309	1	7975	65	.90	159	33	.242	731	233	490	3
57	432	2	1993	65	.90	159	33	.147	698	233	460	3
57	605	2	1993	65	.90	159	33	.256	697	233	460	3
57	849	3	946	65	.90	159	33	.143	670	233	433	3
59	161	1	8135	65	.90	162	34	.119	74570	234	500	3
59	225	1	8135	65	.90	162	34	.179	743	234	500	3
59	315	1	8135	65	.90	162	34	.243	741	234	500	3
59	441	2	2033	65	.90	162	34	.152	707	234	469	3
59	613	2	2033	65	.90	162	34	.259	707	234	469	3

PER MODULE COST FOR POINTING AND SURFACE ACCURACY 1.0
PER SQUARE METER COST FOR POINTING AND SURFACE ACCURACY 1.0

--PARAMETERS--						--------OPTIMUM DESIGNS---------				--------COST/1000------		
F/100	DOG	VP	NV	TH	DIØ	AP/100	TUR	SIGMA	MIS	TUR	HELI	HT
1500	1500	2	52074	65	.90	4159	170	.0541876947		489	12019	175
1500	2100	1211717		70	.90	4668	140	.145	13716	340	13010	158
1500	2940	2	52074	65	.90	4159	170	.159	12729	489	12019	175
1500	4116	4	13015	65	.90	4159	170	.154	11319	489	10644	175
1500	5762	6	5331	70	.90	4668	140	.155	9963	340	9464	158
1500	8067	7	4329	70	.90	4668	140	.193	9291	340	8789	158
1500	11294	7	4329	70	.90	4668	140	.273	9290	340	8789	158
1500	15812	7	4329	70	.90	4668	140	.360	9290	340	8789	158
1500	20137	7	4329	70	.90	4668	140	.453	9289	340	8789	158
1530	1530	2	53115	65	.90	4243	171	.0351303010		503	12259	179
1530	2142	1215952		70	.90	4762	142	.145	13955	342	13270	162
1530	2999	2	53115	65	.90	4243	171	.159	12989	503	12259	179
1530	4193	4	13273	65	.90	4243	171	.155	11551	503	10856	179
1530	5878	6	5998	70	.90	4762	142	.157	10162	342	9652	162
1530	8229	7	4407	70	.90	4762	142	.195	9474	342	8966	162
1530	11520	7	4407	70	.90	4762	142	.275	9473	342	8966	162
1530	16128	7	4407	70	.90	4762	142	.362	9472	342	8966	162
1530	22580	7	4407	70	.90	4762	142	.460	9472	342	8966	162
1561	1561	2	54177	65	.90	4327	173	.0351329617		519	12504	184
1561	2185	1220871		70	.90	4857	143	.145	14260	343	13536	167
1561	3059	2	54177	65	.90	4327	173	.159	13255	519	12504	184
1561	4282	4	13766	70	.90	4857	143	.162	11777	343	11255	167
1561	5995	6	6117	70	.90	4857	143	.159	10550	343	9845	167
1561	8383	7	4495	70	.90	4857	143	.199	9658	343	9145	167
1561	11751	7	4495	70	.90	4857	143	.277	9657	343	9145	167
1561	16451	7	4495	70	.90	4857	143	.384	9657	343	9145	167
1561	23031	7	4495	70	.90	4857	143	.461	9656	343	9145	167
1592	1592	2	56169	70	.90	4954	145	.0901356761		545	12964	171
1592	2229	1223373		70	.90	4954	145	.145	14541	345	13806	171
1592	3129	2	24064	70	.90	4954	145	.142	12752	345	12211	171
1592	4383	4	14043	70	.90	4954	145	.163	12003	345	11481	171
1592	6115	6	6241	70	.90	4954	145	.161	10564	345	10043	171
1592	8561	7	4595	70	.90	4954	145	.200	9847	345	9328	171
1592	11986	7	4595	70	.90	4954	145	.279	9846	345	9328	171
1592	16780	7	4595	70	.90	4954	145	.365	9846	345	9328	171
1592	23492	7	4595	70	.90	4954	145	.463	9845	345	9328	171
1624	1624	2	57398	70	.90	5053	146	.0911383383		346	13283	175
1624	2273	1225466		65	.90	4533	177	.142	14324	550	13355	194
1624	3182	3	25463	70	.90	5053	146	.143	13002	346	12455	175
1624	4455	4	14358	70	.90	5053	146	.164	12244	346	11710	175
1624	6237	6	6369	70	.90	5053	146	.163	10769	346	10248	175
1624	8732	7	4673	70	.90	5053	146	.202	10033	346	9514	175
1624	12225	7	4673	70	.90	5053	146	.281	10032	346	9514	175
1624	17115	7	4676	70	.90	5052	146	.367	10037	346	9514	175
1624	23962	7	4676	70	.90	5053	146	.464	10036	346	9514	175
1656	1656	2	58438	70	.90	5154	147	.0911410561		347	13437	180
1656	2319	1233753		70	.90	5154	147	.145	15119	347	14364	180
1656	3246	3	25979	70	.90	5154	147	.143	13257	347	12704	180
1656	4544	4	14609	70	.90	5154	147	.165	12484	347	11844	180
1656	6362	6	6483	70	.90	5154	147	.165	10969	347	10449	180
1656	8907	7	4770	70	.90	5154	147	.204	10236	347	9705	180
1656	12470	7	4770	70	.90	5154	147	.283	10235	347	9705	180
1656	17458	7	4770	70	.90	5154	147	.385	10234	347	9705	180

3.0 COLLECTOR OPTIMIZATION

In this section examples of the absorber-heat exchanger optimization runs are presented. As explained in Appendix B, E and g are now design variables and their associated minimum costs are included as costs in the absorber-heat exchanger optimization. Thus the computed outputs in this section show optimum collector designs providing thermal power at specific $\dot{m}$, T_{in} and T_{out} conditions at minimum cost. The trace-back information on the minimum cost concentrator designs associated with the E and g selected as part of an optimum collector design has been accessed from the disk file and is shown on the computer outputs. This was simply a matter of convenience, since the minimum cost concentrator designs could be looked up in the outputs generated from the concentrator optimization.

The Fresnel strip reflector and the Fresnel circular reflector were the minimum cost, line- and point-focus concentrators, respectively, regardless of the values of E and g or the target shape. Thus the runs to determine minimum-cost movable collectors used these concentrator type disk files. Therefore, most of the movable collector runs in this section show C12G12, C12G15, C5G2 or C5G4 disk file inputs. However, for purposes of sensitivity analysis, other concentrator type disk file inputs were used.

The terminal queries and user responses (underlined) for these computer runs are shown below:

AHX5 - Pressurized water runs

AHXBL - Boiling runs

CXGX FILE NAME - Name of the disk file where the desired concentrator optimization run information input is located. Typical response is C5G4 meaning Fresnel circular reflectors with pancake targets.

TYPE - 0 for pancake, 1 for spherical, 2 for cylindrical and 3 for flat rectangular absorber-heat exchangers.

COST MODEL - 1 except 9 for the tower heliostat system, 6 for Meinel type absorber-heat exchangers, 5 for evacuated covered cylinders, 4 for non-evacuated covered cylinders and 3 for bare cylinders.

DELTA T - The extent to which a collector must be designed to produce a higher output temperature above a base temperature in pressurized water systems. Typical response is 10.

CAVITY - 0 pancake absorber-heat exchanger and 1 cavity absorber heat exchanger. Available only when a TYPE 0 response is made.

The column headings on the printouts are:

TOUT - The collector outlet temperature, T_{out} (^{o}C)

TIN - The collector inlet temperature, T_{in} (^{o}C)

MDOT - The collector mass flow rate $\dot{m}$ (kg/sec)

D - Heat exchanger tube internal diameter, d (m)

L - Heat exchanger tube length, ℓ (m)

LA - Absorber length, L (m)

AL - Absorber area for losses, A_L (m^2 or m^2/m)

PWR - Power output of collector (W)

CR - Concentration ratio based on a/A_p

ETA - Collector efficiency, $PWR/(I_D A_p)$

FC - Concentrator minimum cost

TBOIL - Boiling temperature (^{o}C)

QF - Fraction of latent heat added per collector

TW - Heat exchanger tube wall temperature, T_W (^oC)

C. TYPE - Concentrator disk file name

CONC. FILE - Same as C. TYPE

$/kW - Minimum cost of thermal power from the collector ($/kW$_t$)

kW - Power output of collector (kW_t)

As an example of how to use these computer outputs, suppose the optimum design and minimum cost of a collector having a spherical absorber-heat exchanger and producing pressurized water with an inlet temperature of 200 ^oC, an outlet temperature of 260 ^oC and a mass flow rate of .05 kg/sec was needed. The required computer output is one with the following information:

AHX5

CXGX FILE NAME - C5G2

TYPE, COST MODEL, DELTA T - 1, 1, 10

The optimum design is found on the line with TOUT of 260, TIN of 200 and MDOT of .050 and is $d = .027$ m, $\ell = 2.01$ m, $A_L = .05622$ m^2, $g = .003514$ m^2, $E = 16.14$ m^2, $\theta_{max} = 35^o$, $\rho_{ave} = .95$, $A_p = 17.0$ m^2 and $\sigma_{\$,\lambda,\delta} = .174^o$. It is a circular Fresnel reflector type. It produces 13.672 kW_t at 1000 w/m^2 insolation level at a cost of $1032 or $75.5 per kW_t and has a concentration ratio (A_p/a) of 1208 to 1 (or, in terms of A_p/A_L, 302 to 1) and an efficiency (P_{out}/P_{in}) of 80.5 percent.

09/05/74. 23.32.11.
PROGRAM AIRS

CKGX FILE NAME
? C5G2
TYPE, COST MODEL, DELTA T
? 1,1,10

KFIN= 211, EPSILON= .9, ALPHA= .95, TAU= 1.00, TAMB= 30.
SMACDL= 1.00, VELOCITY= 5.0, TYPE= 1, COST MODEL= CAI

--PARAMETERS--						--OPTIMUM DESIGNS--			MINIMUM	--------TRACE BACK--------												
TBUT	TIN	HDOT	D	L	LA	AL	G	E	COST	PWR	N	V	CR	NV	TH	RHO	AP	SIGMA	C.	TYPE	FC	ETA*	E/KV
ID= 1000																							
160	150	.200	.031	2.40	1	7.459E-02	6.216E-03	1.040E+01	7.584E+02	8549	1	1	537	1	25	.95	1.09E+01	.204	C5G2		7.580E+02	.781	8.67E+01
160	150	.500	.040	3.15	1	1.268E-01	1.066E-02	2.503E+01	1.354E+03	1374	1	1	822	1	25	.95	2.62E+01	.167	C5G2		1.353E+03	.811	6.33E+01
160	125	.050	.026	2.04	1	5.369E-02	3.833E-03	8.703E+00	7.171E+02	7845	1	1	705	1	20	.95	9.46E+00	.167	C5G2		7.169E+02	.787	9.63E+01
160	125	.100	.027	2.37	1	1.068E-01	7.893E-03	1.739E+01	1.426E+03	3589	1	1	705	1	25	.95	1.87E+01	.167	C5G2		1.056E+03	.795	7.09E+01
160	125	.200	.052	4.06	1	2.105E-01	1.503E-02	3.503E+01	2.777E+03	29379	1	1	705	1	35	.95	3.71E+01	.167	C5G2		1.778E+03	.903	5.97E+01
160	100	.020	.022	2.15	1	4.059E-02	5.390E-03	7.040E+00	6.256E+02	5080	1	1	610	1	25	.95	7.41E+00	.246	C5G2		6.254E+02	.695	1.25E+02
160	100	.050	.033	2.47	1	7.371E-02	6.539E-03	1.537E+01	9.510E+02	12699	1	1	822	1	25	.95	1.62E+01	.167	C5G2		9.506E+02	.765	7.49E+01
160	100	.100	.046	3.62	1	1.688E-01	1.279E-02	3.063E+01	1.553E+03	3255	1	1	759	1	25	.95	3.70E+01	.167	C5G2		1.552E+03	.793	6.23E+01
160	75	.020	.021	1.97	1	3.392E-02	2.609E-03	3.551E+00	7.153E+02	7163	1	1	1062	1	30	.95	9.01E+00	.173	C5G2		7.150E+02	.795	9.98E+01
160	75	.050	.041	3.17	1	1.292E-01	9.230E-03	2.160E+01	1.210E+03	7908	1	1	705	1	35	.95	2.23E+01	.167	C5G2		1.209E+03	.797	6.75E+01
160	50	.010	.011	1.70	1	5.356E-02	5.246E-03	7.060E+00	6.348E+02	4621	1	1	553	1	25	.95	7.41E+00	.295	C5G2		6.346E+02	.628	1.37E+02
160	50	.020	.022	3.94	1	8.909E-02	8.693E-03	1.147E+01	7.330E+02	9243	1	1	542	1	25	.95	1.21E+01	.204	C5G2		7.326E+02	.706	8.47E+01
160	50	.050	.036	2.53	1	1.031E-01	8.418E-03	2.760E+01	1.494E+03	3107	1	1	1127	1	30	.95	2.91E+01	.173	C5G2		1.493E+03	.795	6.40E+01
160	40	.010	.011	6.89	1	7.827E-02	5.246E-03	7.040E+00	6.309E+02	5036	1	1	359	1	25	.95	7.41E+00	.295	C5G2		6.306E+02	.670	1.26E+02
160	40	.020	.022	2.11	1	4.772E-02	3.671E-03	1.204E+01	8.141E+02	10071	1	1	1062	1	30	.95	1.27E+01	.173	C5G2		8.139E+02	.795	8.03E+01
160	40	.050	.036	2.85	1	1.084E-01	8.277E-03	3.043E+01	1.615E+03	5178	1	1	1225	1	30	.95	3.20E+01	.173	C5G2		1.614E+03	.716	6.41E+01
210	200	.030	.027	2.06	1	5.594E-02	6.662E-03	1.092E+01	7.734E+02	8878	1	1	822	1	25	.95	1.15E+01	.167	C5G2		7.729E+02	.772	8.71E+01
210	200	.500	.065	3.45	1	1.571E-01	1.122E-02	2.622E+01	1.410E+03	29195	1	1	705	1	25	.95	2.77E+01	.167	C5G2		1.407E+03	.502	6.35E+01
210	175	.050	.030	2.32	1	7.104E-02	5.226E-03	8.004E+00	7.454E+02	7681	1	1	587	1	25	.95	1.04E+01	.204	C5G2		7.444E+02	.737	9.70E+01
210	175	.100	.038	2.91	1	1.416E-01	1.033E-02	2.067E+01	1.098E+03	5361	1	1	705	1	25	.95	1.97E+01	.167	C5G2		1.092E+03	.731	7.12E+01
210	175	.200	.040	3.05	1	1.033E-01	7.671E-03	3.560E+01	1.662E+03	30782	1	1	1208	1	35	.95	3.71E+01	.174	C5G2		1.660E+03	.522	6.00E+01
210	150	.020	.022	1.72	1	3.891E-02	4.207E-03	7.060E+00	6.303E+02	5310	1	1	762	1	25	.95	7.41E+00	.204	C5G2		6.251E+02	.703	1.27E+02
210	150	.050	.032	2.50	1	9.066E-02	6.837E-03	1.614E+01	9.851E+02	13026	1	1	822	1	25	.95	1.77E+01	.167	C5G2		9.846E+02	.757	7.52E+01
210	150	.100	.046	3.52	1	1.636E-01	1.254E-02	3.175E+01	1.643E+03	6052	1	1	822	1	25	.95	3.36E+01	.167	C5G2		1.644E+03	.775	6.33E+01
210	125	.020	.020	1.54	1	3.150E-02	3.739E-03	8.003E+00	7.309E+02	7319	1	1	1201	1	30	.95	9.46E+00	.173	C5G2		7.307E+02	.774	9.98E+01
210	125	.050	.038	2.97	1	1.162E-01	9.671E-03	2.270E+01	1.252E+03	8297	1	1	822	1	25	.95	2.43E+01	.167	C5G2		1.250E+03	.765	6.54E+01
210	100	.010	.015	2.75	1	6.123E-02	5.670E-03	7.040E+00	6.356E+02	4702	1	1	719	1	25	.95	7.41E+00	.246	C5G2		6.354E+02	.635	1.30E+02
210	100	.020	.026	2.00	1	5.063E-02	5.140E-03	1.704E+01	7.991E+02	9404	1	1	962	1	25	.95	1.27E+01	.167	C5G2		7.989E+02	.782	8.27E+01
210	100	.050	.047	3.62	1	1.702E-01	1.237E-02	3.040E+01	1.525E+03	3511	1	1	705	1	25	.95	3.05E+01	.167	C5G2		1.523E+03	.771	6.49E+01
210	40	.010	.015	2.94	1	4.410E-02	3.339E-03	8.703E+00	7.172E+02	7182	1	1	858	1	25	.95	9.46E+00	.167	C5G2		7.169E+02	.759	9.93E+01
210	40	.020	.029	3.55	1	1.063E-01	7.593E-03	1.778E+01	1.057E+03	10364	1	1	705	1	25	.95	1.27E+01	.167	C5G2		1.056E+03	.767	7.12E+01
260	250	.100	.024	1.84	1	4.712E-03	5.090E-03	7.040E+00	6.366E+02	4719	1	1	629	1	25	.95	7.41E+00	.246	C5G2		6.354E+02	.637	1.30E+02
260	250	.200	.026	1.92	1	5.140E-02	5.140E-03	1.204E+01	7.999E+02	9439	1	1	986	1	25	.95	1.27E+01	.167	C5G2		7.993E+02	.765	8.47E+01
260	250	.500	.043	3.28	1	1.404E-01	1.237E-02	2.897E+01	1.529E+03	3597	1	1	822	1	25	.95	3.01E+01	.167	C5G2		1.527E+03	.774	6.47E+01
260	225	.050	.026	1.95	1	5.328E-02	4.440E-03	1.040E+01	7.613E+02	8099	1	1	822	1	25	.95	1.09E+01	.167	C5G2		7.599E+02	.740	9.40E+01
260	225	.100	.033	2.45	1	8.372E-02	5.910E-03	1.961E+01	1.156E+03	8199	1	1	986	1	30	.95	2.06E+01	.173	C5G2		1.155E+03	.775	7.14E+01
260	200	.020	.016	1.21	1	2.039E-02	2.140E-03	7.040E+00	6.501E+02	5469	1	1	1454	1	30	.95	7.41E+00	.173	C5G2		6.497E+02	.733	1.17E+02
260	200	.050	.027	2.01	1	5.603E-02	3.514E-03	1.614E+01	1.033E+03	8372	1	1	1208	1	35	.95	1.70E+01	.174	C5G2		1.031E+03	.805	7.55E+01
260	200	.100	.038	2.84	1	1.125E-01	1.003E-02	3.353E+01	1.749E+03	3237	1	1	1255	1	30	.95	3.53E+01	.173	C5G2		1.744E+03	.774	6.23E+01
260	175	.020	.025	1.91	1	5.074E-02	4.228E-03	9.906E+00	7.476E+02	7680	1	1	822	1	25	.95	1.04E+01	.167	C5G2		7.465E+02	.733	9.77E+01
260	175	.050	.029	2.15	1	6.428E-02	4.945E-03	2.270E+01	1.310E+03	9099	1	1	1487	1	35	.95	2.39E+01	.174	C5G2		1.308E+03	.799	6.85E+01
260	150	.010	.010	1.77	1	3.366E-02	4.207E-03	7.040E+00	6.370E+02	4883	1	1	881	1	25	.95	7.41E+00	.204	C5G2		6.364E+02	.659	1.30E+02
260	150	.020	.029	2.15	1	6.436E-02	5.397E-03	1.204E+01	8.259E+02	9766	1	1	822	1	25	.95	1.33E+01	.167	C5G2		8.269E+02	.734	8.49E+01
260	150	.050	.032	2.42	1	8.204E-02	6.311E-03	2.897E+01	1.536E+03	28414	1	1	1487	1	35	.95	3.05E+01	.174	C5G2		1.593E+03	.800	6.54E+01
260	40	.005	.009	4.71	1	4.491E-02	5.890E-03	7.040E+00	6.358E+02	4693	1	1	660	1	25	.95	7.41E+00	.246	C5G2		6.354E+02	.633	1.25E+02
260	40	.010	.018	2.97	1	5.653E-02	5.140E-03	1.204E+01	7.996E+02	9286	1	1	897	1	25	.95	1.27E+01	.167	C5G2		7.985E+02	.741	8.52E+01
260	40	.020	.036	4.27	1	1.625E-01	1.019E-02	2.574E+01	1.307E+03	18775	1	1	617	1	25	.95	2.51E+01	.167	C5G2		1.301E+03	.745	6.96E+01
310	275	.050	.026	1.83	1	5.140E-02	5.140E-03	1.204E+01	8.013E+02	8948	1	1	986	1	25	.95	1.27E+01	.167	C5G2		7.985E+02	.706	8.96E+01
310	275	.100	.027	1.92	1	5.851E-02	4.709E-03	2.162E+01	1.269E+03	17688	1	1	1611	1	35	.95	2.28E+01	.174	C5G2		1.265E+03	.736	7.09E+01
310	250	.020	.015	1.10	1	1.051E-02	1.610E-03	7.072E+00	6.331E+02	5939	1	1	1681	1	35	.95	7.78E+00	.173	C5G2		6.329E+02	.763	1.18E+02
310	250	.050	.029	2.11	1	6.834E-02	5.695E-03	1.568E+01	1.119E+03	14947	1	1	1151	1	30	.95	1.97E+01	.173	C5G2		1.115E+03	.755	7.54E+01
310	250	.100	.029	2.07	1	6.575E-02	5.479E-03	3.502E+01	1.943E+03	29694	1	1	2256	1	40	.95	3.71E+01	.173	C5G2		1.933E+03	.801	6.54E+01
310	225	.020	.023	1.63	1	4.099E-02	4.695E-03	1.147E+01	7.866E+02	8208	1	1	1178	1	25	.95	1.21E+01	.167	C5G2		7.846E+02	.610	9.95E+01
310	225	.050	.029	2.06	1	6.582E-02	5.451E-03	2.503E+01	1.480E+03	20521	1	1	1611	1	35	.95	2.62E+01	.174	C5G2		1.476E+03	.779	6.93E+01
310	200	.010	.015	1.09	1	1.824E-02	2.140E-03	7.040E+00	6.503E+02	5191	1	1	1625	1	30	.95	7.41E+00	.173	C5G2		6.497E+02	.701	1.25E+02
310	200	.020	.024	1.74	1	4.654E-02	4.047E-03	1.027E+01	8.755E+02	10383	1	1	1201	1	30	.95	1.40E+01	.173	C5G2		8.730E+02	.743	9.43E+01
310	200	.050	.031	2.21	1	7.419E-02	6.955E-03	3.195E+01	1.727E+03	25957	1	1	1799	1	35	.95	3.36E+01	.174	C5G2		1.720E+03	.772	6.65E+01
310	40	.005	.011	2.22	1	2.648E-02	2.254E-03	7.392E+00	6.663E+02	5842	1	1	1175	1	30	.95	7.78E+00	.173	C5G2		6.661E+02	.751	1.14E+02
310	40	.010	.022	2.99	1	7.140E-02	6.462E-03	1.868E+01	9.394E+02	11684	1	1	863	1	30	.95	1.96E+01	.173	C5G2		9.360E+02	.755	8.00E+01
310	40	.020	.030	2.15	1	7.099E-02	6.311E-03	2.895E+01	1.598E+03	23367	1	1	1719	1	35	.95	3.05E+01	.174	C5G2		1.592E+03	.786	6.85E+01
360	40	.005	.013	1.50	1	2.697E-02	2.878E-03	9.438E+00	7.477E+02	7067	1	1	1473	1	30	.95	9.93E+00	.173	C5G2		7.459E+02	.712	1.06E+02
360	40	.010	.025	1.81	1	5.824E-02	3.878E-03	1.779E+01	1.110E+03	14134	1	1	1381	1	35	.95	1.87E+01	.174	C5G2		1.105E+03	.755	7.85E+01
360	40	.020	.025	1.63	1	4.752E-02	3.727E-03	3.355E+01	1.931E+03	28269	1	1	2972	1	45	.95	3.53E+01	.155	C5G2		1.927E+03	.801	6.83E+01

END.

332.873 / 7665.826 / 157210

```
 09/05/78. 22.59.47.
PROGRAM   AMS5

CKGK FILE NAME
 ? C5GA
TYPE, COST MODEL, DELTA T
 ? 0.1,10
CAVITY
 ? 0

KFIN= 211, EPSILON= .9, ALPHA= .95, TAU= 1.00, TAND= 20.
FRACDL= 1.00, VELOCITY= 5.0, TYPE= 0, COST MODEL= CAI

--PARAMETERS-- -------------OPTIMUM DESIGNS-------------  MINIMUM
TBUT TIN MDBT    D     L  LA       AL          G          E          COST      PWR  --------TRACE BACK--------
                                                                                    N  V   CR      HV TH RHO       AP SIGMA C. TYPE          FC  ETA   E/M

 ID= 1000

160 150  .200 .024  1.49  | 3.552E-02 7.593E-03 9.436E+00 7.293E+02 8549     |  1  1  280     | 25 .95 9.93E+00  .237 C5GA    7.291E+02 .861 8.53E+01
160 150  .500 .023  1.47  | 3.461E-02 8.955E-03 2.270E+01 1.277E+03 21374    |  1  1  691     | 30 .95 2.39E+01  .163 C5GA    1.277E+03 .894 5.97E+01
160 125  .050 .016  .99   | 1.565E-02 3.479E-03 8.150E+00 6.863E+02 7445     |  1  1  548     | 25 .95 8.52E+00  .160 C5GA    6.862E+02 .858 8.61E+01
160 125  .100 .019  1.17  | 2.014E-02 4.976E-03 1.614E+01 1.006E+03 8899     |  1  1  767     | 30 .95 1.70E+01  .163 C5GA    1.005E+03 .877 6.71E+01
160 125  .200 .029  1.83  | 5.057E-02 9.734E-03 3.195E+01 1.680E+03 20779    |  1  1  629     | 30 .95 3.36E+01  .163 C5GA    1.680E+03 .886 5.84E+01
160 100  .020 .014  .90   | 1.314E-02 3.246E-03 7.040E+00 6.343E+02 5080     |  1  1  564     | 25 .95 7.41E+00  .234 C5GA    6.347E+02 .685 1.25E+02
160 100  .050 .021  1.29  | 2.677E-02 5.950E-03 1.394E+01 8.870E+02 12699    |  1  1  548     | 25 .95 1.47E+01  .160 C5GA    8.869E+02 .806 6.91E+01
160 100  .100 .024  1.54  | 3.734E-02 8.414E-03 2.760E+01 1.495E+03 25398    |  1  1  767     | 30 .95 2.91E+01  .163 C5GA    1.495E+03 .874 5.88E+01
160  75  .020 .016  1.03  | 1.705E-02 4.270E-03 3.150E+00 6.955E+02 7183     |  1  1  503     | 25 .95 8.52E+00  .196 C5GA    6.867E+02 .835 9.58E+01
160  75  .050 .021  1.30  | 2.691E-02 5.970E-03 1.961E+01 1.154E+03 21908    |  1  1  767     | 30 .95 2.08E+01  .163 C5GA    1.154E+03 .861 6.65E+01
160  50  .010 .011  .94   | 1.076E-02 2.246E-03 7.040E+00 6.348E+02 8621     |  1  1  689     | 25 .95 7.41E+00  .234 C5GA    6.347E+02 .634 1.27E+02
160  50  .020 .016  1.02  | 1.665E-02 4.480E-03 1.040E+01 7.608E+02 9243     |  1  1  658     | 25 .95 1.09E+01  .160 C5GA    7.603E+02 .848 8.23E+01
160  50  .050 .029  1.36  | 5.637E-02 1.171E-02 2.978E+01 1.405E+03 23107    |  1  1  503     | 25 .95 2.79E+01  .154 C5GA    1.404E+03 .835 6.69E+01
160  40  .010 .011  1.26  | 1.266E-02 2.246E-03 7.040E+00 6.348E+02 5036     |  1  1  479     | 25 .95 7.41E+00  .234 C5GA    6.347E+02 .630 1.26E+02
160  40  .020 .016  1.01  | 1.652E-02 4.093E-03 1.147E+01 7.852E+02 10071    |  1  1  731     | 25 .95 1.21E+01  .160 C5GA    7.551E+02 .824 7.85E+01
160  40  .050 .039  2.47  | 9.697E-02 2.474E-02 2.898E+01 1.514E+03 25178    |  1  1  515     | 25 .95 3.05E+01  .237 C5GA    1.514E+03 .825 6.01E+01
210 200  .200 .018  1.13  | 2.072E-02 5.930E-03 9.906E+00 7.449E+02 8878     |  1  1  503     | 25 .95 1.04E+01  .196 C5GA    7.447E+02 .931 8.39E+01
210 200  .500 .023  1.42  | 3.571E-02 7.269E-03 2.384E+01 1.329E+03 22195    |  1  1  767     | 30 .95 2.51E+01  .163 C5GA    1.328E+03 .924 5.99E+01
210 175  .050 .019  1.19  | 2.301E-02 5.114E-03 8.557E+00 7.005E+02 7681     |  1  1  391     | 25 .95 9.01E+00  .196 C5GA    7.003E+02 .853 9.12E+01
210 175  .100 .021  1.33  | 2.593E-02 7.232E-03 1.698E+01 1.021E+03 21361    |  1  1  617     | 25 .95 1.79E+01  .160 C5GA    1.020E+03 .861 6.66E+01
210 175  .200 .030  1.89  | 6.483E-02 1.483E-02 3.315E+01 1.711E+03 20702    |  1  1  548     | 25 .95 3.53E+01  .160 C5GA    1.710E+03 .870 5.57E+01
210 150  .020 .015  .94   | 1.483E-02 8.246E-03 7.040E+00 6.383E+02 5210     |  1  1  518     | 25 .95 7.41E+00  .234 C5GA    6.347E+02 .703 1.11E+02
210 150  .050 .022  1.37  | 3.061E-02 8.746E-03 1.468E+01 9.159E+02 9213026  |  1  1  503     | 25 .95 1.54E+01  .196 C5GA    9.155E+02 .826 7.03E+01
210 150  .100 .033  2.06  | 6.903E-02 1.703E-02 2.897E+01 1.519E+03 26052    |  1  1  440     | 25 .95 3.05E+01  .196 C5GA    1.518E+03 .854 5.81E+01
210 125  .020 .015  .92   | 1.391E-02 3.479E-03 8.150E+00 6.863E+02 7319     |  1  1  617     | 25 .95 8.52E+00  .160 C5GA    6.862E+02 .850 9.33E+01
210 125  .050 .026  1.62  | 4.307E-02 1.031E-02 2.027E+01 1.161E+03 8218297  |  1  1  503     | 25 .95 2.17E+01  .196 C5GA    1.160E+03 .834 6.44E+01
210 100  .010 .013  .83   | 1.134E-02 5.246E-03 7.040E+00 6.285E+02 4702     |  1  1  654     | 25 .95 7.41E+00  .234 C5GA    6.347E+02 .635 1.35E+02
210 100  .020 .018  1.11  | 1.998E-02 6.440E-03 1.040E+01 7.604E+02 9404     |  1  1  548     | 25 .95 1.09E+01  .160 C5GA    7.600E+02 .859 8.47E+01
210 100  .050 .031  1.96  | 6.283E-02 1.571E-02 2.628E+01 1.405E+03 25511    |  1  1  440     | 25 .95 2.77E+01  .196 C5GA    1.404E+03 .850 5.99E+01
210  40  .010 .015  .98   | 1.461E-02 3.653E-03 8.557E+00 7.020E+02 7182     |  1  1  617     | 25 .95 9.01E+00  .160 C5GA    7.019E+02 .737 9.75E+01
210  40  .020 .016  1.03  | 1.722E-02 4.920E-03 1.614E+01 1.006E+03 10364    |  1  1  986     | 30 .95 1.70E+01  .163 C5GA    1.005E+03 .846 5.90E+01
260 250  .100 .013  .61   | 1.134E-02 8.246E-03 7.040E+00 6.349E+02 4719     |  1  1  654     | 25 .95 7.41E+00  .234 C5GA    6.347E+02 .637 1.34E+02
260 250  .200 .017  1.02  | 1.776E-02 8.480E-03 1.080E+01 7.606E+02 9439     |  1  1  617     | 25 .95 1.09E+01  .160 C5GA    7.603E+02 .860 8.47E+01
260 250  .500 .029  1.79  | 5.497E-02 1.571E-02 2.627E+01 1.405E+03 25507    |  1  1  503     | 25 .95 2.77E+01  .196 C5GA    1.404E+03 .859 5.99E+01
260 225  .050 .016  1.00  | 1.726E-02 3.835E-03 8.955E+00 7.176E+02 8099     |  1  1  548     | 25 .95 9.46E+00  .160 C5GA    7.173E+02 .856 8.89E+01
260 225  .100 .024  1.48  | 3.797E-02 7.592E-03 1.779E+01 1.057E+03 21316    |  1  1  493     | 25 .95 1.87E+01  .163 C5GA    1.056E+03 .864 5.93E+01
260 225  .200 .026  1.55  | 4.296E-02 1.078E-02 3.522E+01 1.815E+03 8332398  |  1  1  863     | 30 .95 3.71E+01  .163 C5GA    1.814E+03 .874 5.60E+01
260 200  .020 .017  1.01  | 1.752E-02 8.246E-03 7.040E+00 6.350E+02 5469     |  1  1  403     | 25 .95 7.41E+00  .234 C5GA    6.347E+02 .737 1.16E+02
260 200  .050 .024  1.46  | 3.673E-02 9.133E-03 1.537E+01 9.494E+02 8413672  |  1  1  440     | 25 .95 1.62E+01  .196 C5GA    9.435E+02 .840 6.44E+01
260 200  .100 .034  2.05  | 7.273E-02 1.815E-02 3.063E+01 1.581E+03 27345    |  1  1  440     | 25 .95 3.20E+01  .196 C5GA    1.573E+03 .854 5.81E+01
260 175  .020 .014  .86   | 1.078E-02 3.653E-03 8.557E+00 7.021E+02 7640     |  1  1  705     | 25 .95 9.01E+00  .160 C5GA    7.019E+02 .843 9.18E+01
260 175  .050 .022  1.35  | 3.139E-02 8.277E-03 2.059E+01 1.195E+03 8319009  |  1  1  691     | 30 .95 2.17E+01  .163 C5GA    1.194E+03 .851 6.71E+01
260 150  .010 .014  .85   | 1.250E-02 8.246E-03 7.040E+00 6.349E+02 4883     |  1  1  593     | 25 .95 7.41E+00  .234 C5GA    6.347E+02 .633 1.33E+02
260 150  .020 .021  1.31  | 2.937E-02 6.506E-03 1.032E+01 7.716E+02 9766     |  1  1  391     | 25 .95 1.15E+01  .196 C5GA    7.712E+02 .539 7.90E+01
260 150  .050 .024  1.45  | 3.606E-02 9.014E-03 2.627E+01 1.403E+03 8324414  |  1  1  767     | 30 .95 2.77E+01  .163 C5GA    1.403E+03 .812 5.07E+01
260  40  .005 .009  1.19  | 1.134E-02 5.246E-03 7.040E+00 6.348E+02 4693     |  1  1  654     | 25 .95 7.41E+00  .234 C5GA    6.347E+02 .633 1.33E+02
260  40  .010 .016  1.35  | 2.570E-02 6.353E-03 1.141E+01 7.835E+02 9386     |  1  1  470     | 25 .95 1.21E+01  .196 C5GA    7.830E+02 .770 8.25E+01
260  40  .020 .021  1.27  | 2.769E-02 9.230E-03 2.162E+01 1.210E+03 8318773  |  1  1  822     | 25 .95 2.28E+01  .160 C5GA    1.210E+03 .825 6.46E+01
310 275  .050 .017  1.00  | 1.903E-02 4.273E-03 9.906E+00 7.473E+02 8944     |  1  1  548     | 25 .95 1.04E+01  .160 C5GA    7.469E+02 .857 8.89E+01
310 275  .100 .026  1.41  | 3.767E-02 8.372E-03 1.961E+01 1.132E+03 8317886  |  1  1  548     | 25 .95 2.06E+01  .160 C5GA    1.131E+03 .856 6.03E+01
310 250  .020 .017  .98   | 1.841E-02 5.798E-03 7.040E+00 6.362E+02 5939     |  1  1  403     | 25 .95 7.41E+00  .237 C5GA    6.358E+02 .801 1.01E+02
310 250  .050 .018  1.02  | 1.968E-02 4.920E-03 1.614E+01 1.006E+03 8318847  |  1  1  863     | 30 .95 1.70E+01  .163 C5GA    1.005E+03 .874 6.71E+01
310 250  .100 .026  1.52  | 4.383E-02 9.741E-03 3.195E+01 1.672E+03 8329694  |  1  1  767     | 30 .95 3.36E+01  .163 C5GA    1.669E+03 .883 5.33E+01
310 225  .020 .016  .95   | 1.726E-02 3.835E-03 8.955E+00 7.179E+02 8708     |  1  1  548     | 25 .95 9.46E+00  .160 C5GA    7.173E+02 .859 8.89E+01
310 225  .050 .029  1.69  | 5.427E-02 1.353E-02 2.278E+01 1.251E+03 8320591  |  1  1  440     | 25 .95 2.39E+01  .196 C5GA    1.247E+03 .830 5.97E+01
310 200  .010 .015  .89   | 1.507E-02 8.246E-03 7.040E+00 6.350E+02 5191     |  1  1  492     | 25 .95 7.41E+00  .234 C5GA    6.347E+02 .761 1.09E+02
310 200  .050 .017  .98   | 1.836E-02 3.792E-03 1.149E+01 7.858E+02 8318283  |  1  1  658     | 25 .95 1.21E+01  .160 C5GA    7.851E+02 .890 7.76E+01
310 200  .050 .026  1.49  | 4.207E-02 8.414E-03 2.760E+01 1.497E+03 8329957  |  1  1  691     | 30 .95 2.91E+01  .163 C5GA    1.495E+03 .874 5.88E+01
310  40  .005 .011  1.37  | 1.630E-02 4.207E-03 7.040E+00 6.370E+02 5842     |  1  1  455     | 25 .95 7.41E+00  .234 C5GA    6.366E+02 .787 1.04E+02
310  40  .010 .014  .00   | 1.227E-02 6.043E-03 1.327E+01 8.742E+02 8311634  |  1  1 1139     | 30 .95 1.40E+01  .163 C5GA    8.739E+02 .836 6.69E+01
310  40  .020 .026  1.49  | 4.227E-02 1.122E-02 2.628E+01 1.411E+03 8323367  |  1  1  658     | 25 .95 2.77E+01  .160 C5GA    1.409E+03 .845 9.39E+01
360  40  .005 .013  1.22  | 1.822E-02 5.114E-03 8.557E+00 7.012E+02 7067     |  1  1  994     | 25 .95 9.01E+00  .196 C5GA    7.008E+02 .874 7.00E+01
360  40  .010 .014  .76   | 1.297E-02 3.347E-03 1.537E+01 9.969E+02 8314134  |  1  1 1247     | 35 .95 1.62E+01  .163 C5GA    9.963E+02 .874 5.83E+01
360  40  .020 .026  1.40  | 4.347E-02 1.364E-02 3.195E+01 1.650E+03 8325269  |  1  1  774     | 25 .95 3.36E+01  .160 C5GA    1.646E+03 .841 5.49E+01
                                                                              END.

                                                                    276.254 /  6027.122 /    175068
```

08/29/74. 17:46:09.
PROGRAM ANXRL

CKGX FILE NAME
 1 C5G2
TYPE. COST MODEL
 1 S,2+--1,1

BOILING HEAT TRANSFER VERSION
KFIN= 211, EPSILON= .90, ALPHA= .95, TAU= 1.00, TAMB= 20,
FRACOL= 1.00, VELOCITY= 5.0, TYPE= 1, COST MODEL= CA1

--PARAMETERS--				--------OPTIMUM DESIGNS--------			MINIMUM	------TRACE BACK------										
TBAIL	QF	MDOT	D	L	LA	AL	G	E	COST	TV	R	V	CR	HV	TH	TUB	AP	SIGMA	C.	TYPE
ID= 1000																				
150	.075	.040	.021	1.63		3.327E-02	3.213E-03	7.740E-00	6.791E-02	156			956		25	.95	7.41E+00	.167	C5G2	6.699E+02	.775	1.06E+07
150	.100	.040	.031	2.40		3.409E-02	6.216E-03	1.040E+01	7.184E+02	160			592		25	.95	1.03E+01	.208	C5G2	7.580E+02	.771	8.99E+01
150	.025	.050	.023	1.75		3.942E-02	3.005E-03	7.040E+00	6.378E+02	154			748		25	.95	7.41E+00	.167	C5G2	6.376E+02	.793	1.08E+07
150	.050	.080	.030	2.35		7.109E-02	6.216E-03	1.040E+01	7.554E+02	156			614		25	.95	1.09E+01	.208	C5G2	7.580E+02	.771	8.99E+01
150	.075	.090	.039	3.05		1.194E-01	9.182E-03	1.537E+01	9.486E+02	158			542		25	.95	1.60E+01	.208	C5G2	9.480E+02	.783	7.49E+01
150	.100	.090	.043	3.35		1.440E-01	1.231E-02	2.059E+01	1.166E+03	161			602		25	.95	2.17E+01	.208	C5G2	1.166E+03	.779	6.91E+01
150	.015	.160	.030	2.35		7.135E-02	6.216E-03	1.040E+01	6.349E+02	152			415		25	.95	7.41E+00	.295	C5G2	6.346E+02	.653	1.35E+07
150	.020	.160	.032	1.74		3.903E-02	3.479E-03	8.150E+00	6.864E+02	153			879		25	.95	8.53E+00	.167	C5G2	6.859E+02	.787	1.02E+07
150	.025	.160	.030	2.33		7.002E-02	6.216E-03	1.040E+01	7.574E+02	153			625		25	.95	1.09E+01	.208	C5G2	7.580E+02	.771	8.99E+01
150	.035	.160	.032	2.48		7.902E-02	5.950E-03	1.394E+01	8.867E+02	154			743		25	.95	1.47E+01	.167	C5G2	8.863E+02	.805	7.50E+01
150	.050	.160	.042	3.30		1.395E-01	1.231E-02	2.059E+01	1.166E+03	156			620		25	.95	2.17E+01	.208	C5G2	1.166E+03	.779	6.91E+01
150	.075	.160	.054	4.25		2.321E-01	1.912E-02	3.040E+01	1.578E+03	159			552		25	.95	3.20E+01	.208	C5G2	1.577E+03	.790	6.23E+01
150	.010	.320	.032	1.73		3.998E-02	3.479E-03	8.150E+00	6.861E+02	151			883		25	.95	8.53E+00	.167	C5G2	6.859E+02	.787	1.02E+07
150	.015	.320	.028	2.21		6.250E-02	5.190E-03	1.204E+01	7.995E+02	152			807		25	.95	1.27E+01	.167	C5G2	7.985E+02	.795	7.83E+01
150	.020	.320	.032	2.48		7.824E-02	6.797E-03	1.614E+01	9.550E+02	153			868		25	.95	1.70E+01	.167	C5G2	9.546E+02	.795	7.29E+01
150	.025	.320	.047	3.27		1.377E-01	1.231E-02	2.059E+01	1.166E+03	153			630		25	.95	2.17E+01	.208	C5G2	1.166E+03	.779	6.91E+01
150	.035	.320	.045	3.53		1.599E-01	1.376E-02	2.760E+01	1.464E+03	155			727		25	.95	2.91E+01	.167	C5G2	1.463E+03	.813	6.20E+01
150	.005	.640	.022	1.73		3.875E-02	3.479E-03	8.150E+00	6.862E+02	151			865		25	.95	8.53E+00	.167	C5G2	6.859E+02	.787	1.02E+07
150	.010	.640	.031	2.46		7.781E-02	6.897E-03	1.614E+01	9.550E+02	152			873		25	.95	1.70E+01	.167	C5G2	9.546E+02	.795	7.30E+01
150	.015	.640	.040	3.14		1.226E-01	1.031E-02	2.398E+01	1.301E+03	152			794		25	.95	2.51E+01	.167	C5G2	1.301E+03	.807	6.43E+01
150	.020	.640	.045	3.51		1.553E-01	1.366E-02	3.195E+01	1.645E+03	153			851		25	.95	3.30E+01	.167	C5G2	1.644E+03	.803	6.09E+01
200	.075	.040	.020	1.53		3.096E-02	3.155E-03	7.392E+00	6.541E+02	207			1008		25	.95	7.78E+00	.167	C5G2	6.538E+02	.746	1.10E+07
200	.100	.040	.022	1.73		3.935E-02	4.227E-03	9.906E+00	7.465E+02	209			1059		25	.95	1.04E+01	.167	C5G2	7.462E+02	.742	9.68E+01
200	.035	.080	.024	1.86		4.569E-02	4.207E-03	9.906E+00	6.369E+02	203			652		25	.95	7.41E+00	.208	C5G2	6.366E+02	.731	1.18E+07
200	.050	.080	.030	2.32		7.087E-02	5.920E-03	9.906E+00	7.452E+02	205			590		25	.95	1.04E+01	.208	C5G2	7.448E+02	.742	9.63E+01
200	.075	.080	.038	2.15		6.087E-02	6.247E-03	1.464E+01	9.182E+02	207			1016		25	.95	1.54E+01	.167	C5G2	9.175E+02	.754	7.91E+01
200	.100	.080	.041	3.20		1.341E-01	1.177E-02	1.961E+01	1.129E+03	209			614		25	.95	2.06E+01	.208	C5G2	1.127E+03	.750	7.29E+01
200	.015	.160	.029	2.21		6.290E-02	8.246E-03	7.040E+00	6.353E+02	202			464		25	.95	7.41E+00	.295	C5G2	6.346E+02	.627	1.37E+07
200	.020	.160	.021	1.63		3.510E-02	3.313E-03	7.740E+00	6.702E+02	203			931		25	.95	8.17E+00	.167	C5G2	6.699E+02	.758	1.08E+07
200	.025	.160	.030	2.29		6.882E-02	5.920E-03	9.906E+00	7.452E+02	203			606		25	.95	1.04E+01	.208	C5G2	7.448E+02	.742	9.63E+01
200	.035	.160	.030	2.29		6.835E-02	5.696E-03	1.327E+01	9.569E+02	204			815		25	.95	1.40E+01	.167	C5G2	9.562E+02	.776	7.91E+01
200	.050	.160	.041	3.15		1.300E-01	1.132E-02	1.961E+01	1.129E+03	205			635		25	.95	2.06E+01	.208	C5G2	1.127E+03	.750	7.29E+01
200	.075	.160	.052	4.03		2.138E-01	1.737E-02	2.898E+01	1.521E+03	207			571		25	.95	3.05E+01	.208	C5G2	1.517E+03	.761	6.55E+01
200	.010	.320	.021	1.63		3.499E-02	3.313E-03	7.740E+00	6.702E+02	201			934		25	.95	8.17E+00	.167	C5G2	6.699E+02	.758	1.08E+07
200	.015	.320	.027	2.09		5.530E-02	4.895E-03	1.143E+01	7.852E+02	202			673		25	.95	1.21E+01	.167	C5G2	7.846E+02	.770	8.45E+01
200	.020	.320	.030	2.29		6.877E-02	6.559E-03	1.537E+01	9.514E+02	202			961		25	.95	1.67E+01	.167	C5G2	9.506E+02	.788	7.68E+01
200	.025	.320	.038	2.92		1.121E-01	7.977E-03	1.869E+01	1.094E+03	203			701		25	.95	1.93E+01	.167	C5G2	1.092E+03	.793	7.07E+01
200	.035	.320	.041	3.19		1.335E-01	1.122E-02	2.602E+01	1.409E+03	204			829		25	.95	2.77E+01	.167	C5G2	1.407E+03	.733	6.50E+01
200	.005	.640	.021	1.63		3.479E-02	3.313E-03	7.740E+00	6.705E+02	201			937		25	.95	8.17E+00	.167	C5G2	6.699E+02	.758	1.03E+07
200	.010	.640	.030	2.29		6.853E-02	6.559E-03	1.537E+01	9.514E+02	201			944		25	.95	1.67E+01	.167	C5G2	9.506E+02	.788	7.67E+01
200	.015	.640	.037	2.88		1.086E-01	9.691E-03	2.270E+01	1.252E+03	202			880		25	.95	2.39E+01	.167	C5G2	1.250E+03	.777	6.74E+01
200	.020	.640	.042	3.22		1.384E-01	1.299E-02	3.043E+01	1.554E+03	203			939		25	.95	3.20E+01	.167	C5G2	1.552E+03	.771	6.39E+01
250	.075	.040	.023	1.73		4.102E-02	4.207E-03	7.040E+00	6.372E+02	255			723		25	.95	7.41E+00	.208	C5G2	6.364E+02	.691	1.24E+07
250	.100	.040	.021	1.61		3.590E-02	3.835E-03	8.985E+00	7.176E+02	257			1054		25	.95	9.46E+00	.167	C5G2	7.169E+02	.722	1.05E+07
250	.035	.080	.026	1.96		5.280E-02	5.890E-03	7.040E+00	6.366E+02	253			561		25	.95	7.41E+00	.584	C5G2	6.354E+02	.645	1.30E+07
250	.050	.080	.021	1.61		3.554E-02	3.835E-03	8.985E+00	7.176E+02	256			1065		25	.95	9.46E+00	.167	C5G2	7.169E+02	.722	1.05E+07
250	.075	.080	.036	2.80		5.503E-02	5.866E-03	1.327E+01	8.575E+02	256			1016		25	.95	1.40E+01	.167	C5G2	8.562E+02	.733	8.37E+01
250	.100	.080	.030	2.25		6.936E-02	7.552E-03	1.779E+01	1.057E+03	257			1078		25	.95	1.87E+01	.167	C5G2	1.056E+03	.709	7.74E+01
250	.020	.160	.021	1.56		3.538E-02	3.835E-03	8.985E+00	7.176E+02	252			1070		25	.95	9.46E+00	.167	C5G2	7.169E+02	.722	1.05E+07
250	.025	.160	.021	1.60		3.536E-02	3.835E-03	8.985E+00	7.176E+02	252			1070		25	.95	9.46E+00	.167	C5G2	7.169E+02	.722	1.05E+07
250	.035	.160	.024	1.85		4.697E-02	5.397E-03	1.264E+01	8.280E+02	253			1103		25	.95	1.33E+01	.167	C5G2	8.269E+02	.718	8.66E+01
250	.050	.160	.030	2.24		6.917E-02	7.593E-03	1.779E+01	1.057E+03	254			1083		25	.95	1.87E+01	.167	C5G2	1.056E+03	.709	7.74E+01
250	.075	.160	.037	2.79		1.010E-01	1.122E-02	2.627E+01	1.411E+03	256			1031		25	.95	2.77E+01	.167	C5G2	1.407E+03	.740	6.99E+01
250	.100	.160	.042	3.16		1.371E-01	1.503E-02	3.520E+01	1.781E+03	258			1084		25	.95	3.71E+01	.167	C5G2	1.776E+03	.737	6.52E+01
250	.010	.320	.021	1.56		2.383E-02	3.005E-03	7.040E+00	6.382E+02	251			867		25	.95	7.41E+00	.167	C5G2	6.376E+02	.737	1.17E+07
250	.015	.320	.026	1.98		5.383E-02	6.442E-03	1.040E+01	7.612E+02	251			814		25	.95	1.09E+01	.167	C5G2	7.595E+02	.707	9.29E+01
250	.020	.320	.025	2.14		6.272E-02	5.950E-03	1.394E+01	8.880E+02	252			928		25	.95	1.47E+01	.167	C5G2	8.863E+02	.745	8.13E+01
250	.025	.320	.030	2.24		6.890E-02	7.593E-03	1.779E+01	1.057E+03	252			1088		25	.95	1.87E+01	.167	C5G2	1.056E+03	.709	7.74E+01
250	.035	.320	.040	3.00		1.239E-01	1.019E-02	2.384E+01	1.295E+03	253			810		25	.95	2.51E+01	.167	C5G2	1.301E+03	.762	6.83E+01
250	.050	.320	.042	3.14		1.361E-01	1.503E-02	3.520E+01	1.781E+03	254			1090		25	.95	3.71E+01	.167	C5G2	1.776E+03	.737	6.52E+01
250	.005	.640	.021	1.56		3.343E-02	3.005E-03	7.040E+00	6.396E+02	251			887		25	.95	7.41E+00	.167	C5G2	6.376E+02	.737	1.17E+07
250	.010	.640	.028	2.14		6.294E-02	5.950E-03	1.394E+01	8.880E+02	25			933		25	.95	1.47E+01	.167	C5G2	8.863E+02	.745	8.13E+01
250	.015	.640	.036	2.69		9.955E-02	8.790E-03	2.052E+01	1.172E+03	251			871		25	.95	2.17E+01	.167	C5G2	1.169E+03	.756	7.15E+01
250	.020	.640	.039	2.98		1.282E-01	1.175E-02	2.760E+01	1.468E+03	252			951		25	.95	2.91E+01	.167	C5G2	1.463E+03	.758	6.72E+01
250	.025	.640	.042	3.14		1.355E-01	1.503E-02	3.520E+01	1.781E+03	252			1095		25	.95	3.71E+01	.167	C5G2	1.776E+03	.737	6.52E+01

END.

09/04/74. 20.10.23.
PROGRAM AXXEL

CXGX FILE NAME
? CXGX
TYPE. COST MODEL
? 0.1
CAVITY
? 1

BOILING HEAT TRANSFER VERSION
NFIN= 211, EPSILON= .90, ALPHA= .95, TAU= 1.00, TAMB= 20.
FRACDL= 1.00, VELOCITY= 5.0, TYPE= 0, COST MODEL= CAI

--PARAMETERS-- TOTAL GF	MDOT	D	L	LA	OPTIMUM DESIGNS AL	G	E	MINIMUM COST	IV	TRACE BACK N	M	CR	NV	TH	TUB	AP	SIGMA	C. TYPE	FC	ETA	E/XX

ID= 1000

150	.075	.040	.020	1.25	2.525E-02	8.246E-03	7.040E+00	6.350E+02	161	1	1	293	1	25	.95	7.41E+00	.294	CSGA	6.347E+02	.854	1.00E+00
150	.100	.040	.021	1.33	2.519E-02	8.249E-03	5.285E+00	7.159E+02	164	1	1	336	1	25	.95	9.46E+00	.194	CSGA	7.156E+02	.892	8.44E+01
150	.035	.090	.017	1.06	1.506E-02	8.246E-03	7.040E+00	6.349E+02	156	1	1	411	1	25	.95	7.41E+00	.294	CSGA	6.347E+02	.797	1.00E+00
150	.050	.090	.021	1.32	2.795E-02	5.369E-03	8.985E+00	7.159E+02	158	1	1	340	1	25	.95	9.66E+00	.194	CSGA	7.156E+02	.892	8.44E+01
150	.075	.090	.039	1.34	5.462E-02	1.633E-02	1.394E+01	8.013E+02	161	1	1	272	1	25	.95	1.42E+01	.234	CSGA	8.008E+02	.863	9.06E+01
150	.100	.030	.033	2.09	6.361E-02	7.117E-02	1.069E+01	8.015E+02	165	1	1	202	1	25	.95	1.93E+01	.294	CSGA	1.008E+03	.858	8.83E+01
150	.015	.160	.018	.85	1.127E-02	8.246E-03	7.040E+00	6.349E+02	153	1	1	429	1	25	.95	7.41E+00	.294	CSGA	6.347E+02	.803	1.00E+00
150	.020	.160	.022	1.37	2.995E-02	8.493E-03	7.392E+00	6.511E+02	156	1	1	260	1	25	.95	7.75E+00	.294	CSGA	6.509E+02	.868	9.66E+01
150	.025	.160	.028	1.75	4.784E-02	7.547E-03	8.985E+00	7.160E+02	159	1	1	194	1	25	.95	9.46E+00	.237	CSGA	7.149E+02	.892	8.44E+01
150	.035	.160	.025	2.02	4.067E-02	1.451E-02	1.254E+01	8.227E+02	156	1	1	169	1	25	.95	1.23E+01	.294	CSGA	8.219E+02	.839	8.96E+01
150	.050	.160	.033	2.09	6.939E-02	2.131E-02	1.807E+01	1.086E+03	158	1	1	283	1	25	.95	1.93E+01	.294	CSGA	1.085E+03	.853	8.83E+01
150	.075	.160	.042	2.72	1.172E-01	3.232E-02	2.760E+01	1.464E+03	162	1	1	247	1	25	.95	2.91E+01	.294	CSGA	1.463E+03	.839	8.74E+01
150	.010	.320	.022	1.37	2.990E-02	2.627E-03	7.392E+00	6.511E+02	152	1	1	260	1	25	.95	7.75E+00	.294	CSGA	6.509E+02	.868	9.66E+01
150	.015	.320	.029	1.83	5.257E-02	4.227E-03	1.693E+01	9.447E+02	153	1	1	215	1	25	.95	1.15E+01	.294	CSGA	9.445E+02	.871	9.39E+01
150	.020	.320	.038	2.04	6.663E-02	3.714E-03	1.464E+01	9.125E+02	154	1	1	232	1	25	.95	1.06E+01	.294	CSGA	9.113E+02	.875	9.76E+01
150	.025	.320	.033	2.09	6.937E-02	2.189E-02	1.807E+01	1.086E+03	155	1	1	284	1	25	.95	1.93E+01	.294	CSGA	1.085E+03	.853	8.83E+01
150	.035	.320	.034	2.17	9.479E-02	1.961E-02	2.503E+01	1.315E+03	156	1	1	352	1	25	.95	2.63E+01	.160	CSGA	1.314E+03	.897	9.32E+01
150	.005	.640	.029	1.37	2.995E-02	5.627E-03	7.392E+00	6.511E+02	151	1	1	260	1	25	.95	7.75E+00	.294	CSGA	6.509E+02	.868	9.66E+01
150	.010	.640	.032	2.04	6.629E-02	3.714E-02	1.464E+01	9.125E+02	152	1	1	232	1	25	.95	1.54E+01	.294	CSGA	9.113E+02	.876	9.76E+01
150	.015	.640	.035	2.39	9.087E-02	1.809E-02	2.162E+01	1.204E+03	153	1	1	251	1	25	.95	2.27E+01	.237	CSGA	1.203E+03	.890	9.96E+01
150	.020	.640	.050	3.17	1.591E-01	3.394E-02	2.893E+01	1.513E+03	154	1	1	192	1	25	.95	3.05E+01	.294	CSGA	1.511E+03	.905	9.60E+01
200	.075	.040	.015	1.03	1.717E-02	2.246E-03	7.040E+00	6.349E+02	209	1	1	432	1	25	.95	7.41E+00	.294	CSGA	6.347E+02	.784	1.00E+00
200	.100	.040	.023	1.43	3.321E-02	1.002E-02	8.557E+00	6.936E+02	211	1	1	271	1	25	.95	9.01E+00	.234	CSGA	6.980E+02	.859	9.02E+01
200	.035	.090	.015	.93	1.395E-02	8.246E-03	7.040E+00	6.349E+02	205	1	1	531	1	25	.95	7.41E+00	.294	CSGA	6.347E+02	.731	1.00E+00
200	.050	.090	.023	1.43	3.310E-02	1.002E-02	8.557E+00	6.936E+02	206	1	1	272	1	25	.95	9.01E+00	.234	CSGA	6.980E+02	.859	9.02E+01
200	.075	.090	.030	1.89	5.003E-02	1.431E-02	1.254E+01	8.032E+02	209	1	1	299	1	25	.95	1.33E+01	.234	CSGA	8.219E+02	.873	9.09E+01
200	.100	.030	.034	2.12	7.020E-02	1.959E-02	1.694E+01	1.015E+03	212	1	1	244	1	25	.95	1.72E+01	.234	CSGA	1.013E+03	.868	8.55E+01
200	.015	.160	.012	.78	9.490E-03	8.246E-03	7.040E+00	6.349E+02	202	1	1	750	1	25	.95	7.41E+00	.294	CSGA	6.347E+02	.627	1.27E+00
200	.020	.160	.019	1.18	2.251E-02	8.246E-03	7.040E+00	6.350E+02	203	1	1	329	1	25	.95	7.41E+00	.294	CSGA	6.347E+02	.836	1.00E+00
200	.025	.160	.023	1.43	3.304E-02	1.002E-02	8.557E+00	6.936E+02	203	1	1	273	1	25	.95	9.01E+00	.294	CSGA	6.980E+02	.859	9.02E+01
200	.035	.160	.027	1.66	4.465E-02	1.410E-02	1.204E+01	7.964E+02	205	1	1	284	1	25	.95	1.23E+01	.294	CSGA	7.937E+02	.855	9.32E+01
200	.050	.160	.034	2.12	7.256E-02	1.954E-02	1.694E+01	1.015E+03	206	1	1	246	1	25	.95	1.72E+01	.294	CSGA	1.013E+03	.857	8.55E+01
200	.075	.160	.033	2.30	9.146E-02	2.094E-02	2.503E+01	1.389E+03	210	1	1	289	1	25	.95	2.62E+01	.237	CSGA	1.386E+03	.891	9.41E+01
200	.100	.160	.052	3.24	1.701E-01	3.929E-02	3.355E+01	1.703E+03	212	1	1	208	1	25	.95	3.53E+01	.234	CSGA	1.696E+03	.877	9.50E+01
200	.010	.320	.019	1.19	2.251E-02	8.246E-03	7.040E+00	6.351E+02	202	1	1	329	1	25	.95	7.41E+00	.294	CSGA	6.347E+02	.836	1.00E+00
200	.015	.320	.023	1.43	3.330E-02	5.920E-03	9.906E+00	7.452E+02	202	1	1	313	1	25	.95	1.04E+01	.194	CSGA	7.447E+02	.891	9.00E+01
200	.020	.320	.030	1.87	5.693E-02	1.111E-02	1.327E+01	8.537E+02	203	1	1	246	1	25	.95	1.40E+01	.237	CSGA	8.525E+02	.856	8.99E+01
200	.025	.320	.034	2.11	7.225E-02	1.954E-02	1.694E+01	1.015E+03	204	1	1	247	1	25	.95	1.72E+01	.264	CSGA	1.013E+03	.868	8.85E+01
200	.035	.320	.039	2.44	9.463E-02	2.292E-02	2.254E+01	1.294E+03	205	1	1	260	1	25	.95	2.51E+01	.264	CSGA	1.292E+03	.866	9.01E+01
200	.050	.320	.051	3.22	1.676E-01	3.929E-02	3.355E+01	1.703E+03	207	1	1	211	1	25	.95	3.53E+01	.234	CSGA	1.696E+03	.877	9.50E+01
200	.009	.640	.019	1.18	2.048E-02	5.246E-03	7.040E+00	6.354E+02	201	1	1	330	1	25	.95	7.41E+00	.294	CSGA	6.347E+02	.836	1.00E+00
200	.010	.640	.030	1.87	5.657E-02	1.111E-02	1.327E+01	8.537E+02	202	1	1	247	1	25	.95	1.40E+01	.237	CSGA	8.525E+02	.856	8.99E+01
200	.015	.640	.035	2.19	7.769E-02	2.412E-03	2.059E+01	1.163E+03	202	1	1	279	1	25	.95	2.17E+01	.220	CSGA	1.161E+03	.857	8.71E+01
200	.020	.640	.040	2.49	1.002E-01	3.237E-02	2.760E+01	1.456E+03	203	1	1	290	1	25	.95	2.91E+01	.234	CSGA	1.453E+03	.893	9.23E+01
200	.025	.640	.051	3.20	1.664E-01	3.929E-02	3.355E+01	1.703E+03	204	1	1	212	1	25	.95	3.53E+01	.234	CSGA	1.696E+03	.877	9.50E+01
250	.075	.040	.014	.95	1.222E-02	8.246E-03	7.040E+00	6.350E+02	257	1	1	606	1	25	.95	7.41E+00	.294	CSGA	6.347E+02	.691	1.00E+00
250	.100	.040	.021	1.27	2.748E-02	6.184E-03	7.392E+00	6.527E+02	259	1	1	284	1	25	.95	7.78E+00	.237	CSGA	6.516E+02	.877	9.55E+01
250	.035	.080	.013	.99	1.052E-02	8.246E-03	7.040E+00	6.350E+02	254	1	1	705	1	25	.95	7.41E+00	.294	CSGA	6.347E+02	.645	1.00E+00
250	.050	.080	.021	1.27	2.725E-02	6.184E-03	7.392E+00	6.527E+02	255	1	1	286	1	25	.95	7.78E+00	.237	CSGA	6.516E+02	.877	9.55E+01
250	.075	.080	.026	1.57	4.185E-02	1.349E-02	1.147E+01	7.820E+02	257	1	1	288	1	25	.95	1.21E+01	.294	CSGA	7.800E+02	.727	1.14E+00
250	.100	.080	.021	1.31	2.870E-02	6.247E-03	1.464E+01	9.193E+02	260	1	1	506	1	25	.95	1.56E+01	.160	CSGA	9.180E+02	.886	8.72E+01
250	.020	.160	.015	.92	1.438E-02	8.246E-03	7.040E+00	6.351E+02	252	1	1	515	1	25	.95	7.41E+00	.294	CSGA	6.347E+02	.727	1.14E+00
250	.025	.160	.021	1.26	2.706E-02	6.184E-03	7.392E+00	6.527E+02	253	1	1	288	1	25	.95	7.78E+00	.237	CSGA	6.516E+02	.877	9.55E+01
250	.035	.160	.023	1.43	3.454E-02	5.702E-03	1.040E+01	7.584E+02	254	1	1	317	1	25	.95	1.09E+01	.237	CSGA	7.562E+02	.873	9.31E+01
250	.050	.160	.027	1.68	4.810E-02	8.786E-03	1.464E+01	9.180E+02	255	1	1	300	1	25	.95	1.56E+01	.196	CSGA	9.155E+02	.896	8.72E+01
250	.075	.160	.031	1.91	6.173E-02	1.900E-02	2.270E+01	1.248E+03	258	1	1	287	1	25	.95	2.09E+01	.237	CSGA	1.246E+03	.857	8.70E+01
250	.100	.160	.035	2.16	7.965E-02	2.546E-02	3.043E+01	1.579E+03	260	1	1	402	1	25	.95	2.70E+01	.237	CSGA	1.576E+03	.853	9.15E+01
250	.010	.320	.015	.92	1.437E-02	5.246E-03	7.040E+00	6.352E+02	251	1	1	516	1	25	.95	7.41E+00	.294	CSGA	6.347E+02	.727	1.14E+00
250	.015	.320	.025	1.54	4.029E-02	1.092E-02	8.985E+00	7.151E+02	252	1	1	235	1	25	.95	9.66E+00	.220	CSGA	7.132E+02	.886	1.00E+00
250	.020	.320	.023	1.32	5.037E-02	1.410E-02	1.204E+01	7.963E+02	252	1	1	251	1	25	.95	1.23E+01	.234	CSGA	7.937E+02	.867	9.32E+01
250	.025	.320	.027	1.66	4.701E-02	8.786E-03	1.464E+01	9.179E+02	253	1	1	328	1	25	.95	1.56E+01	.196	CSGA	9.155E+02	.896	8.72E+01
250	.035	.320	.029	1.79	5.461E-02	1.231E-02	2.059E+01	1.169E+03	254	1	1	397	1	25	.95	2.17E+01	.196	CSGA	1.166E+03	.855	8.70E+01
250	.050	.320	.035	2.16	7.965E-02	2.546E-02	3.043E+01	1.579E+03	256	1	1	403	1	25	.95	2.70E+01	.237	CSGA	1.576E+03	.853	9.15E+01
250	.005	.640	.015	.92	1.437E-02	8.246E-03	7.040E+00	6.352E+02	251	1	1	516	1	25	.95	7.41E+00	.294	CSGA	6.347E+02	.727	1.14E+00
250	.010	.640	.028	1.72	5.068E-02	1.410E-02	1.204E+01	7.964E+02	251	1	1	251	1	25	.95	1.23E+01	.234	CSGA	7.937E+02	.867	9.32E+01
250	.015	.640	.031	1.90	4.116E-02	1.493E-02	1.779E+01	1.054E+03	252	1	1	306	1	25	.95	1.87E+01	.237	CSGA	1.051E+03	.878	8.77E+01
250	.020	.640	.035	2.11	7.578E-02	1.994E-02	2.384E+01	1.299E+03	253	1	1	331	1	25	.95	2.51E+01	.237	CSGA	1.296E+03	.871	9.14E+01
250	.025	.640	.035	2.16	7.925E-02	2.546E-02	3.043E+01	1.579E+03	253	1	1	404	1	25	.95	3.20E+01	.237	CSGA	1.576E+03	.853	9.15E+01

END.

175.037 / 1379.662 / 81324

STOP

RUN TERMINATED.

```
COST FILE NAME
T C12G15
TYPE, COST MODEL, DELTA T
T 2.5.10

XFIN= 211, EPSILON= .0, ALPHA= .95, TAU= .95, TYMO= 20,
FRACDL= 1.00, VELOCITY= 5.0, TYPE= 2, COST MODEL= CAS
```

--PARAMETERS-- TOUT	TIN	MDOT	D	L	LA	OPTIMUM DESIGNS AL	G	E	MINIMUM COST	PWR	N	M	GR	TRACE BACK NU	TH	PHI	AP	SIGMA	C.	TYPE	FC	ETA	S/R
ID= 1000																							
160	150	.200	.029	8.00	8	7.397E-01	8.409E-03	1.407E+00	8.537E+02	8549	1	1	50	1	30	.95	1.48E+00	.151	C12G15	7.108E+01	.722	9.98E+01
160	150	1.000	.055	16.00	16	2.906E+00	1.445E-02	3.236E+00	3.262E+02	8747	1	1	62	1	45	.95	3.36E+00	.161	C12G15	1.910E+02	.750	7.82E+01
160	125	.050	.025	8.00	8	6.309E-01	7.264E-03	1.216E+00	7.882E+02	7445	1	1	50	1	30	.95	1.22E+00	.151	C12G15	6.391E+01	.727	1.06E+02
160	125	.200	.065	16.00	16	3.233E+00	1.433E-02	3.407E+00	3.474E+02	8779	1	1	39	1	30	.95	2.53E+00	.151	C12G15	1.181E+02	.735	7.30E+01
160	125	.500	.090	24.00	24	6.810E+00	2.523E-02	8.352E+00	6.020E+02	8744	1	1	50	1	30	.95	4.55E+00	.151	C12G15	2.397E+02	.682	5.11E+01
160	125	1.000	.095	32.00	32	9.539E+00	2.726E-02	8.375E+00	1.077E+03	8894	1	1	70	1	45	.95	6.72E+00	.161	C12G15	3.725E+02	.693	6.20E+01
160	100	.050	.033	8.00	8	8.251E-01	9.451E-03	1.939E+00	1.098E+02	8912	1	1	64	1	45	.95	2.01E+00	.164	C12G15	1.017E+02	.768	8.65E+01
160	100	.100	.043	16.00	16	2.116E+00	1.242E-02	2.079E+00	2.131E+02	8398	1	1	50	1	30	.95	2.19E+00	.151	C12G15	9.977E+01	.725	7.41E+01
160	100	.200	.030	24.00	24	8.055E+00	2.570E-02	3.072E+00	3.979E+02	8350	1	1	40	1	25	.95	3.03E+00	.163	C12G15	1.539E+02	.685	7.83E+01
160	100	.500	.078	32.00	32	7.890E+00	2.242E-02	5.253E+00	1.045E+03	8991	1	1	70	1	45	.95	5.53E+00	.161	C12G15	3.177E+02	.718	6.23E+01
160	75	.020	.030	8.00	8	7.651E-01	6.502E-03	1.100E+00	7.481E+02	8163	1	1	39	1	30	.95	1.16E+00	.151	C12G15	5.709E+01	.772	1.04E+02
160	75	.100	.043	16.00	16	2.155E+00	1.241E-02	2.058E+00	2.641E+02	8315	1	1	49	1	30	.95	3.08E+00	.151	C12G15	1.415E+02	.727	7.43E+01
160	75	.200	.064	24.00	24	4.906E+00	1.594E-02	3.733E+00	5.456E+02	8316	1	1	62	1	45	.95	3.93E+00	.164	C12G15	2.154E+02	.752	7.61E+01
160	50	.020	.036	8.00	8	9.153E-01	8.529E-03	1.477E+00	8.749E+02	9243	1	1	43	1	30	.95	1.56E+00	.151	C12G15	7.397E+01	.743	9.49E+01
160	50	.050	.048	16.00	16	2.604E+00	1.739E-02	2.079E+00	1.884E+02	8107	1	1	46	1	25	.95	2.19E+00	.163	C12G15	9.744E+01	.660	7.98E+01
160	50	.100	.065	16.00	16	3.433E+00	1.538E-02	3.556E+00	3.530E+02	8215	1	1	55	1	45	.95	3.74E+00	.161	C12G15	2.029E+02	.718	7.68E+01
160	50	.200	.121	32.00	32	1.212E+01	2.441E-02	4.116E+00	7.341E+02	8029	1	1	36	1	25	.95	4.33E+00	.163	C12G15	2.205E+02	.667	7.94E+01
160	40	.020	.037	8.00	8	9.327E-01	9.734E-03	1.629E+00	9.750E+02	8210	1	1	46	1	30	.95	1.71E+00	.151	C12G15	7.999E+01	.724	9.19E+01
160	40	.050	.055	16.00	16	3.115E+00	1.739E-02	2.079E+00	1.844E+02	8178	1	1	35	1	25	.95	2.19E+00	.163	C12G15	9.744E+01	.719	7.32E+01
160	40	.100	.067	16.00	16	3.344E+00	1.473E-02	3.920E+00	3.946E+02	8357	1	1	62	1	45	.95	4.12E+00	.161	C12G15	2.289E+02	.763	7.84E+01
160	40	.200	.092	32.00	32	9.270E+00	2.460E-02	4.116E+00	7.499E+02	8714	1	1	47	1	30	.95	4.33E+00	.151	C12G15	2.554E+02	.726	7.45E+01
210	200	.200	.037	8.00	8	9.390E-01	9.210E-03	1.551E+00	9.006E+02	8815	1	1	44	1	30	.95	1.63E+00	.151	C12G15	7.998E+01	.620	1.01E+02
210	200	.500	.037	16.00	16	1.273E+00	1.242E-02	2.079E+00	1.324E+02	8195	1	1	59	1	30	.95	2.19E+00	.151	C12G15	9.977E+01	.606	8.43E+01
210	200	1.000	.059	16.00	16	2.944E+00	1.473E-02	3.920E+00	3.946E+02	8390	1	1	70	1	45	.95	4.12E+00	.161	C12G15	2.288E+02	.672	6.89E+01
210	175	.050	.032	8.00	8	8.051E-01	8.008E-03	1.340E+00	8.312E+02	7681	1	1	44	1	30	.95	1.41E+00	.151	C12G15	6.829E+01	.654	1.09E+02
210	175	.200	.053	16.00	16	2.279E+00	1.465E-02	2.786E+00	2.525E+02	8328	1	1	50	1	30	.95	2.93E+00	.151	C12G15	1.402E+02	.655	8.23E+01
210	175	.500	.063	24.00	24	5.112E+00	1.937E-02	4.530E+00	6.539E+02	8376	1	1	70	1	45	.95	4.71E+00	.161	C12G15	2.752E+02	.670	6.97E+01
210	175	1.000	.066	32.00	32	9.679E+00	2.044E-02	6.705E+00	1.204E+03	8611	1	1	106	1	35	.95	7.06E+00	.065	C12G15	3.767E+04	.880	7.85E+01
210	150	.100	.050	16.00	16	2.896E+00	1.370E-02	2.022E+00	2.078E+02	8252	1	1	49	1	30	.95	2.41E+00	.151	C12G15	1.114E+02	.625	7.93E+01
210	150	.200	.059	24.00	24	4.450E+00	1.927E-02	3.225E+00	4.297E+02	8104	1	1	58	1	30	.95	3.37E+00	.151	C12G15	1.670E+02	.638	8.24E+01
210	150	.500	.099	32.00	32	9.961E+00	2.470E-02	5.780E+00	1.120E+03	8260	1	1	62	1	45	.95	6.10E+00	.161	C12G15	3.443E+02	.668	3.68E+01
210	125	.020	.022	8.00	8	5.553E-01	4.941E-03	1.155E+00	6.049E+02	7319	1	1	55	1	45	.95	1.22E+00	.161	C12G15	6.499E+01	.751	1.10E+02
210	125	.100	.045	16.00	16	2.065E+00	1.311E-02	2.072E+00	2.001E+02	8336	1	1	72	1	45	.95	2.23E+00	.161	C12G15	1.695E+02	.707	8.20E+01
210	125	.200	.061	24.00	24	4.702E+00	1.737E-02	4.116E+00	5.122E+02	8357	1	1	68	1	45	.95	4.33E+00	.161	C12G15	3.432E+02	.704	8.37E+01
210	100	.020	.020	8.00	8	7.122E-01	6.306E-03	1.477E+00	9.229E+02	9404	1	1	55	1	45	.95	1.56E+00	.161	C12G15	7.967E+01	.756	9.81E+01
210	100	.050	.028	16.00	16	1.993E+00	1.242E-02	2.079E+00	1.861E+02	8511	1	1	58	1	30	.95	2.19E+00	.151	C12G15	9.977E+01	.671	8.00E+01
210	100	.100	.041	16.00	16	2.043E+00	1.473E-02	2.920E+00	2.946E+02	8347	1	1	68	1	45	.95	4.12E+00	.161	C12G15	2.288E+02	.712	8.39E+01
210	100	.200	.084	32.00	32	8.114E+00	2.583E-02	4.322E+00	7.956E+02	8404	1	1	56	1	30	.95	4.55E+00	.151	C12G15	2.237E+02	.666	5.48E+01
210	40	.010	.025	8.00	8	6.161E-01	7.064E-03	1.210E+00	7.093E+02	7182	1	1	52	1	30	.95	1.27E+00	.151	C12G15	6.291E+01	.702	1.10E+02
210	40	.050	.041	16.00	16	3.556E+00	1.825E-02	3.072E+00	2.504E+02	8309	1	1	53	1	30	.95	3.73E+00	.151	C12G15	1.574E+02	.694	7.91E+01
210	40	.100	.092	24.00	24	6.955E+00	2.460E-02	4.116E+00	5.696E+02	8318	1	1	67	1	30	.95	4.33E+00	.151	C12G15	2.258E+02	.691	7.93E+01
210	40	.200	.091	32.00	32	9.134E+00	2.594E-02	6.081E+00	1.175E+04	3636	1	1	70	1	45	.95	6.42E+00	.161	C12G15	3.532E+02	.701	6.18E+01
260	250	.200	.026	8.00	8	6.402E-01	7.300E-03	1.710E+00	1.001E+03	9439	1	1	70	1	45	.95	1.80E+00	.161	C12G15	8.955E+01	.655	1.05E+02
260	250	.500	.033	16.00	16	1.639E+00	9.347E-03	2.183E+00	2.104E+02	9293	1	1	70	1	45	.95	2.33E+00	.161	C12G15	1.137E+02	.682	8.91E+01
260	225	.050	.020	8.00	8	5.151E-01	6.306E-03	1.477E+00	9.203E+02	8099	1	1	76	1	45	.95	1.56E+00	.161	C12G15	7.967E+01	.651	1.14E+02
260	225	.200	.041	16.00	16	2.059E+00	1.311E-02	2.072E+00	2.001E+02	8298	1	1	79	1	45	.95	2.23E+00	.161	C12G15	1.695E+02	.626	9.25E+01
260	225	.500	.053	24.00	24	3.838E+00	1.450E-02	4.765E+00	6.831E+02	8294	1	1	99	1	35	.95	5.02E+00	.065	C12G15	2.965E+04	.673	5.63E+01
260	200	.020	.020	8.00	8	5.195E-01	6.215E-03	1.050E+00	7.070E+02	8.69	1	1	54	1	30	.95	1.11E+00	.151	C12G15	5.553E+01	.617	1.33E+02
260	200	.100	.039	16.00	16	1.603E+00	1.079E-02	2.537E+00	2.440E+02	8327	1	1	79	1	45	.95	2.66E+00	.161	C12G15	1.347E+02	.663	9.07E+01
260	200	.200	.064	24.00	24	3.478E+00	1.445E-02	3.268E+00	4.870E+02	8298	1	1	77	1	45	.95	3.56E+00	.161	C12G15	1.810E+02	.638	7.20E+01
260	200	.500	.065	32.00	32	8.278E+00	1.850E-02	6.081E+00	1.115E+04	6725	1	1	99	1	35	.95	6.80E+00	.065	C12G15	3.435E+04	.647	8.16E+01
260	175	.020	.019	8.00	8	4.352E-01	5.700E-03	1.340E+00	8.733E+02	7640	1	1	73	1	45	.95	1.41E+00	.161	C12G15	7.352E+01	.577	1.10E+02
260	175	.100	.046	16.00	16	2.238E+00	1.510E-02	2.556E+00	2.630E+02	8199	1	1	81	1	45	.95	2.76E+00	.161	C12G15	2.029E+02	.633	9.04E+01
260	175	.200	.066	24.00	24	4.954E+00	2.014E-02	4.765E+00	7.306E+02	8298	1	1	76	1	45	.95	5.07E+00	.161	C12G15	2.926E+02	.635	9.56E+01
260	150	.020	.024	8.00	8	6.023E-01	7.300E-03	1.710E+00	1.001E+03	9766	1	1	74	1	45	.95	1.80E+00	.161	C12G15	8.955E+01	.678	1.02E+02
260	150	.050	.034	16.00	16	1.729E+00	9.814E-03	2.079E+00	2.078E+02	8414	1	1	64	1	45	.95	2.41E+00	.161	C12G15	1.073E+02	.697	7.21E+01
260	150	.100	.026	24.00	24	2.313E+00	1.311E-02	3.072E+00	4.352E+02	8029	1	1	90	1	45	.95	3.23E+00	.161	C12G15	1.695E+02	.609	8.93E+01
260	150	.200	.059	32.00	32	5.964E+00	1.937E-02	4.530E+00	9.092E+02	7658	1	1	81	1	45	.95	4.71E+00	.161	C12G15	2.752E+02	.537	9.31E+01
260	40	.010	.022	8.00	8	5.617E-01	6.607E-03	1.551E+00	9.650E+02	9386	1	1	73	1	45	.95	1.63E+00	.161	C12G15	8.285E+01	.715	1.01E+02
260	40	.050	.067	16.00	16	3.368E+00	1.473E-02	3.920E+00	3.946E+02	8931	1	1	62	1	45	.95	4.12E+00	.161	C12G15	2.288E+02	.711	8.41E+01
260	40	.100	.082	32.00	32	8.276E+00	2.583E-02	4.322E+00	7.956E+02	8404	1	1	55	1	30	.95	4.55E+00	.151	C12G15	2.237E+02	.665	5.48E+01
310	275	.050	.017	8.00	8	4.399E-01	4.944E-03	1.629E+00	6.837E+04	8944	1	1	99	1	35	.95	1.71E+00	.065	C12G15	8.511E+03	.657	7.66E+01
310	275	.200	.032	16.00	16	1.622E+00	1.032E-02	2.386E+00	2.990E+03	9776	1	1	110	1	35	.95	3.56E+00	.065	C12G15	1.843E+04	.607	8.26E+01
310	275	.500	.050	32.00	32	5.047E+00	1.255E-02	4.116E+00	7.357E+03	9440	1	1	86	1	35	.95	4.33E+00	.065	C12G15	2.370E+04	.665	7.48E+01
310	250	.020	.012	8.00	8	2.917E-01	3.904E-03	1.050E+00	4.774E+04	5939	1	1	95	1	35	.95	1.11E+00	.065	C12G15	5.321E+03	.672	3.01E+01
310	250	.100	.030	16.00	16	1.125E+00	5.990E-03	2.653E+00	2.262E+03	9894	1	1	92	1	35	.95	2.73E+00	.065	C12G15	1.249E+04	.684	7.51E+01
310	250	.200	.043	24.00	24	2.770E+00	1.008E-02	3.556E+00	6.726E+03	9388	1	1	86	1	35	.95	3.74E+00	.065	C12G15	1.858E+04	.661	7.01E+01
310	225	.020	.026	8.00	8	6.857E-01	6.607E-03	1.551E+00	9.650E+02	8206	1	1	62	1	45	.95	1.63E+00	.161	C12G15	8.285E+01	.678	1.15E+02
310	225	.100	.033	16.00	16	1.931E+00	1.139E-02	2.920E+00	3.065E+02	8181	1	1	102	1	35	.95	3.02E+00	.065	C12G15	2.102E+04	.693	3.20E+01
310	225	.200	.061	24.00	24	4.660E+00	1.527E-02	5.003E+00	7.129E+03	8083	1	1	86	1	35	.95	5.27E+00	.065	C12G15	2.765E+04	.649	8.67E+01
310	200	.020	.027	8.00	8	6.993E-01	8.451E-03	1.980E+00	1.098E+03	8383	1	1	76	1	45	.95	2.01E+00	.161	C12G15	1.017E+02	.653	1.06E+02
310	200	.050	.053	16.00	16	1.164E+00	6.088E-03	2.592E+00	2.292E+03	9757	1	1	104	1	35	.95	2.41E+00	.065	C12G15	1.173E+04	.678	7.30E+01
310	200	.100	.032	24.00	24	2.772E+00	9.306E-03	3.072E+00	3.991E+03	9154	1	1	102	1	35	.95	3.23E+00	.065	C12G15	1.662E+04	.669	7.69E+01
310	200	.200	.066	32.00	32	4.655E+00	1.445E-02	4.765E+00	9.107E+03	9479	1	1	108	1	35	.95	5.07E+00	.065	C12G15	2.345E+04	.647	8.77E+01
310	40	.005	.020	8.00	8	5.031E-01	6.588E-03	1.180E+00	7.481E+02	5862	1	1	58	1	30	.95	1.16E+00	.151	C12G15	5.709E+01	.609	1.08E+02
310	40	.010	.021	8.00	8	5.277E-01	5.749E-03	1.066E+00	7.042E+02	6614	1	1	94	1	35	.95	1.07E+00	.065	C12G15	9.452E+03	.726	6.55E+01
310	40	.020	.040	16.00	16	1.939E+00	1.308E-02	2.183E+00	1.973E+02	8367	1	1	58	1	30	.95	2.30E+00	.151	C12G15	1.056E+02	.636	8.44E+01
310	40	.050	.049	24.00	24	3.661E+00	1.445E-02	3.268E+00	4.870E+02	8298	1	1	73	1	45	.95	3.56E+00	.161	C12G15	1.810E+02	.653	8.33E+01
310	40	.100	.077	32.00	32	7.789E+00	2.242E-02	5.253E+00	1.045E+04	8836	1	1	72	1	45	.95	5.53E+00	.161	C12G15	3.177E+02	.690	8.90E+01
360	40	.005	.023	8.00	8	4.963E-01	5.041E-03	1.276E+00	8.897E+02	7067	1	1	68	1	45	.95	1.52E+00	.161	C12G15	7.757E+01	.551	1.20E+02
360	40	.010	.037	16.00	16	1.756E+00	1.078E-02	2.527E+00	2.448E+03	9269	1	1	72	1	45	.95	2.66E+00	.161	C12G15	1.347E+02	.668	8.63E+01
360	40	.050	.040	24.00	24	3.031E+00	1.255E-02	4.116E+00	5.691E+03	9672	1	1	109	1	35	.95	4.33E+00	.065	C12G15	2.370E+04	.617	8.05E+01
360	40	.100	.061	32.00	32	6.116E+00	1.947E-02	6.385E+00	1.160E+04	1344	1	1	110	1	35	.95	6.72E+00	.065	C12G15	3.604E+04	.657	8.21E+01

```
END.

  809.720 /  8415.766 /     72692
STOP

 PIN TERMINATED.
```

09/30/74. 16.34.50.

CYCLE FILE NAME
 * CIICII
TYPE, COST MODEL
 T 2.5

BOILING HEAT TRANSFER VERSION
KFIN= 211, EPSILON= .90, ALPHA= .95, TAU= .95, TAMB= 20,
PMACOL= 1.00, VELOCITY= 5.0, TYPE= 2, COST MODEL= CAS

--PARAMETERS-- TOTAL OF	HOST	D	L	LA	AL	G	E	OPTIMUM DESIGNS- MINIMUM COST	TV	TRACE BACK N	W	CR	HV	TH	RHA	AP	SIGMA	G.	TYPE	FC	ETA
ID= 1000																					
150 .075	.040	.026	8.00	8	9.663E-01	1.200E-02	1.015E+00	7.853E+02	161	1	1	34		1	60	.95	1.04E+00		.590	C11C11	6.253E+01	.680
150 .100	.040	.052	8.00	8	1.565E+00	1.426E-02	1.218E+00	7.518E+02	173	1	1	23		1	60	.95	1.03E+00		.590	C11C11	7.079E-01	.777
150 .035	.050	.030	8.00	8	7.629E-01	1.020E-02	1.050E+00	7.853E+02	155	1	1	41		1	60	.95	1.04E+00		.590	C11C11	6.253E+01	.596
150 .050	.030	.041	8.00	8	1.540E+00	1.404E-02	1.715E+00	8.516E+02	163	1	1	23		1	60	.95	1.02E+00		.590	C11C11	7.079E-01	.778
150 .075	.080	.105	8.00	8	2.631E+00	2.103E-02	2.795E+00	1.073E+03	179	1	1	20		1	60	.95	2.11E+00		.590	C11C11	9.850E+01	.769
150 .020	.160	.030	8.00	8	1.003E+00	1.722E-02	1.050E+00	7.853E+02	154	1	1	31		1	60	.95	1.24E+00		.590	C11C11	6.253E+01	.693
150 .035	.160	.061	8.00	8	1.539E+00	1.671E-02	2.715E+00	8.516E+02	157	1	1	23		1	60	.95	1.02E+00		.590	C11C11	7.079E-01	.777
150 .025	.160	.093	8.00	8	2.719E+00	2.000E-02	1.710E+00	1.020E+03	163	1	1	24		1	60	.95	1.71E+00		.590	C11C11	9.016E+01	.776
150 .075	.160	.030	16.00	16	3.512E+00	2.403E-02	2.079E+00	2.155E+03	182	1	1	35		1	60	.95	2.12E+00		.590	C11C11	1.167E+02	.687
150 .100	.160	.124	16.00	16	4.933E+00	2.719E-02	2.407E+00	2.409E+03	176	1	1	21		1	60	.95	2.82E+00		.590	C11C11	1.396E+02	.765
150 .010	.320	.042	8.00	8	1.003E+00	1.228E-02	1.055E+00	7.853E+02	152	1	1	31		1	60	.95	1.24E+00		.590	C11C11	6.253E+01	.693
150 .015	.320	.632	8.00	8	7.534E-01	4.090E-02	1.407E+00	9.413E+02	153	1	1	55		1	60	.95	1.66E+00		.197	C11C11	6.203E+01	.755
150 .020	.320	.069	8.00	8	1.699E+00	1.823E-02	1.396E+00	1.175E+03	157	1	1	33		1	60	.95	1.65E+00		.394	C11C11	1.052E+02	.761
150 .035	.320	.061	16.00	16	2.079E+00	2.403E-02	2.079E+00	2.155E+03	156	1	1	40		1	60	.95	2.65E+00		.590	C11C11	1.167E+02	.684
150 .050	.320	.135	16.00	16	4.776E+00	2.819E-02	2.407E+00	2.569E+03	164	1	1	21		1	60	.95	3.77E+00		.590	C11C11	1.396E+02	.765
150 .075	.320	.118	16.00	16	5.912E+00	3.105E-02	3.736E+00	3.777E+03	169	1	1	36		1	60	.95	4.15E+00		.394	C11C11	2.062E+02	.757
150 .100	.320	.170	24.00	24	1.355E+01	3.777E-02	3.225E+00	5.076E+03	174	1	1	21		1	60	.95	3.39E+00		.590	C11C11	1.975E+02	.741
150 .005	.640	.040	8.00	8	1.003E+00	1.850E-02	1.050E+00	7.853E+02	151	1	1	31		1	60	.95	1.24E+00		.590	C11C11	6.253E+01	.693
150 .010	.640	.091	8.00	8	1.680E+00	1.977E-02	1.715E+00	1.175E+03	156	1	1	33		1	60	.95	2.07E+00		.394	C11C11	1.052E+02	.761
150 .020	.640	.041	16.00	16	4.026E+00	2.403E-02	2.077E+00	2.155E+03	154	1	1	20		1	60	.95	2.65E+00		.590	C11C11	1.167E+02	.684
150 .025	.640	.135	16.00	16	6.762E+00	2.819E-02	2.407E+00	2.569E+03	168	1	1	21		1	60	.95	3.43E+00		.590	C11C11	1.396E+02	.765
150 .035	.640	.130	16.00	16	9.553E+00	3.986E-02	3.376E+00	3.643E+03	164	1	1	21		1	60	.95	3.99E+00		.590	C11C11	2.089E+02	.741
150 .050	.640	.177	24.00	24	1.350E+01	3.777E-02	3.225E+00	5.076E+03	163	1	1	21		1	60	.95	3.39E+00		.590	C11C11	1.975E+02	.741
150 .075	.640	.153	24.00	24	1.132E+01	3.783E-02	4.765E+00	7.727E+03	167	1	1	37		1	60	.95	5.61E+00		.394	C11C11	3.101E+02	.753
150 .100	.640	.150	32.00	32	1.509E+01	5.847E-02	4.765E+00	1.021E+04	167	1	1	37		1	60	.95	5.61E+00		.394	C11C11	3.101E+02	.753
200 .075	.040	.000	8.00	8	7.425E-01	1.023E-02	1.050E+00	7.853E+02	208	1	1	42		1	60	.95	1.24E+00		.590	C11C11	6.253E+01	.680
200 .100	.040	.067	8.00	8	1.487E+00	1.291E-02	1.407E+00	8.046E+02	219	1	1	21		1	60	.95	1.30E+00		.590	C11C11	6.519E+01	.746
200 .050	.080	.061	8.00	8	1.582E+00	1.291E-02	1.410E+00	8.046E+02	210	1	1	21		1	60	.95	1.30E+00		.590	C11C11	6.519E+01	.746
200 .075	.080	.089	8.00	8	2.375E+00	1.543E-02	1.407E+00	1.024E+03	220	1	1	22		1	60	.95	1.62E+00		.418	C11C11	8.091E+01	.757
200 .020	.160	.033	8.00	8	8.025E-01	1.200E-02	1.050E+00	7.853E+02	203	1	1	37		1	60	.95	1.24E+00		.590	C11C11	6.253E+01	.693
200 .035	.160	.061	8.00	8	1.539E+00	1.291E-02	1.407E+00	8.046E+02	206	1	1	21		1	60	.95	1.30E+00		.590	C11C11	6.519E+01	.746
200 .035	.160	.093	8.00	8	2.078E+00	1.811E-02	1.551E+00	9.750E+02	210	1	1	22		1	60	.95	1.83E+00		.590	C11C11	9.479E+01	.747
200 .075	.160	.060	16.00	16	2.096E+00	2.425E-02	2.079E+00	2.155E+03	208	1	1	41		1	60	.95	2.65E+00		.590	C11C11	1.167E+02	.693
200 .100	.160	.039	16.00	16	4.913E+00	3.809E-02	2.415E+00	2.247E+03	216	1	1	26		1	60	.95	2.57E+00		.418	C11C11	1.223E+02	.754
200 .010	.320	.033	8.00	8	9.325E-01	1.230E-02	1.050E+00	7.853E+02	202	1	1	37		1	60	.95	1.24E+00		.590	C11C11	6.253E+01	.693
200 .015	.320	.064	8.00	8	1.760E+00	1.537E-02	1.040E+00	8.039E+02	204	1	1	23		1	60	.95	1.58E+00		.590	C11C11	7.677E+01	.735
200 .020	.320	.099	8.00	8	2.332E+00	2.103E-02	1.796E+00	1.073E+03	207	1	1	24		1	60	.95	2.11E+00		.590	C11C11	9.850E+01	.730
200 .035	.320	.053	16.00	16	2.681E+00	2.403E-02	2.079E+00	2.155E+03	204	1	1	45		1	60	.95	2.65E+00		.590	C11C11	1.167E+02	.684
200 .050	.320	.097	16.00	16	4.334E+00	3.809E-02	2.415E+00	2.247E+03	209	1	1	26		1	60	.95	2.57E+00		.418	C11C11	1.223E+02	.754
200 .075	.320	.165	16.00	16	6.961E+00	3.965E-02	3.376E+00	3.663E+03	220	1	1	24		1	60	.95	4.09E+00		.590	C11C11	2.032E+02	.729
200 .100	.320	.137	24.00	24	1.003E+01	3.777E-02	3.072E+00	4.750E+03	215	1	1	26		1	60	.95	3.81E+00		.590	C11C11	1.850E+02	.744
200 .005	.640	.033	8.00	8	9.325E-01	1.230E-02	1.050E+00	7.853E+02	201	1	1	37		1	60	.95	1.24E+00		.590	C11C11	6.253E+01	.693
200 .010	.640	.099	8.00	8	2.230E+00	2.103E-02	1.796E+00	1.073E+03	204	1	1	24		1	60	.95	2.11E+00		.590	C11C11	9.850E+01	.730
200 .020	.640	.067	16.00	16	3.369E+00	2.425E-02	2.079E+00	2.155E+03	203	1	1	36		1	60	.95	2.65E+00		.590	C11C11	1.167E+02	.693
200 .025	.640	.097	16.00	16	4.870E+00	3.809E-02	2.415E+00	2.247E+03	205	1	1	27		1	60	.95	2.57E+00		.418	C11C11	1.223E+02	.754
200 .035	.640	.131	16.00	16	6.579E+00	3.965E-02	3.072E+00	3.289E+03	209	1	1	28		1	60	.95	3.61E+00		.418	C11C11	1.965E+02	.750
200 .050	.640	.137	24.00	24	1.003E+01	3.777E-02	3.072E+00	4.750E+03	219	1	1	23		1	60	.95	3.81E+00		.590	C11C11	2.981E+02	.725
200 .075	.640	.229	24.00	24	1.717E+01	5.315E-02	4.537E+00	7.391E+03	219	1	1	23		1	60	.95	5.34E+00		.590	C11C11	2.981E+02	.725
200 .100	.640	.278	32.00	32	2.290E+01	5.315E-02	4.537E+00	9.760E+03	219	1	1	23		1	60	.95	5.34E+00		.590	C11C11	2.981E+02	.725
250 .100	.040	.042	8.00	8	1.045E+00	1.222E-02	1.050E+00	7.853E+02	261	1	1	30		1	60	.95	1.24E+00		.590	C11C11	6.253E+01	.693
250 .050	.080	.042	8.00	8	1.044E+00	1.200E-02	1.050E+00	7.853E+02	256	1	1	30		1	60	.95	1.24E+00		.590	C11C11	6.253E+01	.693
250 .075	.080	.076	8.00	8	1.915E+00	1.730E-02	1.477E+00	9.689E+02	265	1	1	23		1	60	.95	1.76E+00		.590	C11C11	8.897E+01	.737
250 .100	.080	.100	8.00	8	2.511E+00	2.317E-02	1.477E+00	1.187E+03	274	1	1	23		1	60	.95	2.33E+00		.590	C11C11	1.167E+02	.684
250 .020	.160	.027	8.00	8	8.755E-01	1.030E-02	1.050E+00	7.853E+02	252	1	1	46		1	60	.95	1.24E+00		.590	C11C11	6.253E+01	.693
250 .025	.160	.042	8.00	8	1.044E+00	1.222E-02	1.050E+00	7.853E+02	253	1	1	30		1	60	.95	1.24E+00		.590	C11C11	6.253E+01	.693
250 .035	.160	.065	8.00	8	1.102E+00	1.508E-02	1.341E+00	9.020E+02	255	1	1	35		1	60	.95	1.58E+00		.590	C11C11	7.979E+01	.737
250 .050	.160	.100	8.00	8	2.824E+00	2.319E-02	1.477E+00	1.187E+03	263	1	1	23		1	60	.95	2.33E+00		.590	C11C11	1.167E+02	.684
250 .100	.160	.025	16.00	16	4.074E+00	2.425E-02	2.079E+00	2.155E+03	262	1	1	29		1	60	.95	2.65E+00		.590	C11C11	1.167E+02	.684
250 .010	.320	.027	8.00	8	8.755E-01	1.030E-02	1.050E+00	7.853E+02	251	1	1	46		1	60	.95	1.24E+00		.590	C11C11	6.253E+01	.693
250 .015	.320	.075	8.00	8	1.826E+00	1.356E-02	1.150E+00	8.971E+02	254	1	1	18		1	60	.95	1.38E+00		.590	C11C11	8.755E+01	.744
250 .020	.320	.093	8.00	8	2.340E+00	1.811E-02	1.551E+00	9.750E+02	256	1	1	20		1	60	.95	1.83E+00		.590	C11C11	8.624E+01	.747
250 .025	.320	.099	8.00	8	2.500E+00	2.319E-02	1.477E+00	1.187E+03	257	1	1	23		1	60	.95	2.33E+00		.590	C11C11	1.167E+02	.684
250 .050	.320	.035	16.00	16	4.283E+00	2.425E-02	2.079E+00	2.155E+03	253	1	1	29		1	60	.95	2.65E+00		.590	C11C11	1.167E+02	.684
250 .075	.320	.132	16.00	16	9.163E+00	3.809E-02	2.415E+00	3.289E+03	267	1	1	19		1	60	.95	3.61E+00		.418	C11C11	1.965E+02	.750
250 .100	.320	.152	16.00	16	7.447E+00	3.965E-02	3.072E+00	4.332E+03	270	1	1	30		1	60	.95	4.61E+00		.418	C11C11	2.589E+02	.738
250 .005	.640	.027	8.00	8	6.755E-01	1.200E-02	1.050E+00	7.853E+02	254	1	1	46		1	60	.95	1.24E+00		.590	C11C11	6.253E+01	.693
250 .010	.640	.093	8.00	8	2.340E+00	1.811E-02	1.551E+00	9.750E+02	253	1	1	20		1	60	.95	1.83E+00		.590	C11C11	8.624E+01	.747
250 .020	.640	.058	16.00	16	3.720E+00	2.403E-02	2.079E+00	2.155E+03	252	1	1	35		1	60	.95	2.65E+00		.590	C11C11	1.167E+02	.684
250 .025	.640	.095	16.00	16	4.991E+00	3.809E-02	2.415E+00	2.247E+03	254	1	1	29		1	60	.95	2.65E+00		.590	C11C11	1.167E+02	.684
250 .035	.640	.131	16.00	16	6.939E+00	3.965E-02	3.072E+00	3.289E+03	257	1	1	24		1	60	.95	3.23E+00		.590	C11C11	1.651E+02	.750
250 .050	.640	.197	16.00	16	7.623E+00	3.780E-02	3.072E+00	4.332E+03	261	1	1	30		1	60	.95	4.61E+00		.418	C11C11	2.589E+02	.738
250 .075	.640	.152	24.00	24	1.144E+01	3.809E-02	3.072E+00	6.356E+03	261	1	1	30		1	60	.95	4.61E+00		.418	C11C11	3.593E+02	.738
250 .100	.640	.804	24.00	24	1.541E+01	6.091E-02	5.253E+00	7.333E+03	269	1	1	30		1	60	.95	6.18E+00		.418	C11C11	3.593E+02	.738

END.

379.624 / 3015.079 / 65529

10/ 0/ 74. 17.14.31.
PROGRAM: MAIN

ENTER FILE NAME
? plude
TYPE: COST MODEL, DELTA T
? 0,1,5
CAVITY
? 0

BRINE 211, SALINITY .9, ALPHA .93, TAUW 1.00, TDOWN 20,
PRANDLE 1.00, VELOCITY= 5.0, TYPE= 0, COST MODEL= CM1

--PARAMETERS--					--EFFICIENCY--			MINIMUM															
NOT	TIN	MDOT	D	L	LM	NU	U	A	COST	PWR													

IWP 1000																							
155	150	.200	.011	1.04	1	1.755E-04	5.860E+03	5.003E+00	6.302E-04	4320	1	1	412	1	70	.69	7.25E+00	.536	DIGM	6.301E+03	.596	1.40E+03	
155	150	.500	.020	1.04	1	3.064E-04	8.453E+03	1.14?E+01	9.741E-04	10800	1	1	876	1	70	.72	1.07E+01	.468	DIGM	9.720E+03	.736	9.03E+03	
155	150	1.000	.040	1.04	1	9.[illegible]E-04	[illegible]	[illegible]	[illegible]	[illegible]	1	1	312	1	75	.77	3.05E+01	.317	DIGM	1.760E+03	.709	8.15E+01	
155	150	.050	.015	.91	1	1.352E-02	4.065E-02	7.040E+00	7.249E-02	8424	1	1	666	1	60	.70	9.00E+00	.311	WIGM	7.247E-02	.716	1.13E-02	
155	150	.100	.020	1.00	1	1.[illegible]E-04	[illegible]	[illegible]	[illegible]	[illegible]	1	1	509	1	75	.70	1.77E+01	.249	DIGM	1.174E+03	.721	8.76E+01	
155	125	.200	.026	1.62	1	4.[illegible]E-04	1.[illegible]E-03	2.760E+01	9.[illegible]E-04	[illegible]	1	1	839	1	75	.78	3.63E+01	.293	WIGM	2.[illegible]E-03	.798	7.23E+01	
155	100	.020	.007	.41	1	2.[illegible]E-03	5.[illegible]E-04	5.003E+00	6.357E-03	4639	1	1	2609	1	75	.69	7.25E+00	.152	DIGM	6.357E+03	.887	1.36E+03	
155	100	.050	.015	1.15	1	2.[illegible]E-03	5.[illegible]E-03	1.[illegible]E+01	1.[illegible]E-03	[illegible]	1	1	763	1	70	.78	1.67E+01	.278	DIGM	1.[illegible]E-03	.725	3.93E+01	
155	100	.100	.023	1.42	1	3.[illegible]E-03	5.[illegible]E-03	2.[illegible]E+01	1.[illegible]E-03	[illegible]	1	1	979	1	75	.78	3.20E+01	.263	WIGM	1.652E+03	.732	7.00E+01	
155	75	.010	.011	.73	1	8.[illegible]E-03	5.[illegible]E-03	5.003E+00	6.[illegible]E-03	3393	1	1	900	1	70	.69	7.25E+00	.526	DIGM	6.[illegible]E-03	.668	1.26E+03	
155	75	.020	.013	.79	1	1.[illegible]E-02	2.[illegible]E-03	7.993E+00	7.[illegible]E-02	5786	1	1	932	1	60	.78	9.45E+00	.260	WIGM	7.[illegible]E-02	.719	1.40E+02	
155	75	.050	.030	1.87	1	5.[illegible]E-03	1.[illegible]E-02	1.[illegible]E+01	1.[illegible]E-03	[illegible]	1	1	425	1	75	.76	1.39E+01	.416	WIGM	1.[illegible]E-03	.710	8.38E+01	
155	50	.010	.011	2.63	1	2.[illegible]E-02	5.[illegible]E-03	5.[illegible]E+00	6.[illegible]E-03	4431	1	1	297	1	70	.69	7.25E+00	.226	DIGM	6.[illegible]E-03	.611	1.45E+03	
155	50	.020	.020	1.39	1	2.[illegible]E-02	5.[illegible]E-03	7.[illegible]E+00	7.[illegible]E-02	8363	1	1	876	1	65	.72	1.07E+01	.389	WIGM	8.[illegible]E-02	.700	9.96E+01	
155	50	.050	.016	1.02	1	1.[illegible]E-03	2.[illegible]E-03	2.[illegible]E+01	1.[illegible]E-03	[illegible]	1	1	1337	1	75	.77	3.07E+01	.202	DIGM	1.[illegible]E-03	.727	9.01E+01	
155	40	.010	.003	.50	1	4.[illegible]E-03	8.[illegible]E-04	5.[illegible]E+00	6.[illegible]E-03	4546	1	1	1663	1	75	.69	7.61E+00	.138	WIGM	6.[illegible]E-03	.638	1.24E+03	
155	40	.020	.010	.59	1	5.[illegible]E-03	1.[illegible]E-03	1.[illegible]E+01	9.[illegible]E-03	9691	1	1	2303	1	70	.77	1.33E+01	.160	WIGM	9.[illegible]E-03	.728	9.48E+01	
155	40	.050	.020	1.27	1	2.[illegible]E-02	5.[illegible]E-03	7.[illegible]E+01	1.[illegible]E-03	[illegible]	1	1	1305	1	75	.78	3.26E+01	.243	DIGM	1.[illegible]E-03	.721	9.02E+01	
205	200	.200	.017	1.03	1	1.[illegible]E-03	6.[illegible]E-03	5.003E+00	6.[illegible]E-03	4518	1	1	385	1	70	.69	7.25E+00	.651	WIGM	6.[illegible]E-03	.673	1.40E+03	
205	200	.500	.023	1.43	1	3.[illegible]E-03	5.[illegible]E-03	1.[illegible]E+01	1.[illegible]E-03	[illegible]	1	1	981	1	70	.73	1.53E+01	.339	WIGM	1.[illegible]E-03	.734	8.49E+01	
205	200	1.000	.032	1.62	1	8.[illegible]E-03	1.[illegible]E-02	2.[illegible]E+01	1.[illegible]E-03	[illegible]	1	1	666	1	75	.78	3.05E+01	.369	WIGM	1.[illegible]E-03	.741	7.57E+01	
205	175	.050	.014	.79	1	1.[illegible]E-03	3.[illegible]E-03	1.[illegible]E+00	7.[illegible]E-03	6691	1	1	749	1	60	.78	9.45E+00	.311	WIGM	7.[illegible]E-03	.705	1.11E+03	
205	175	.100	.021	1.31	1	2.[illegible]E-03	6.[illegible]E-03	1.[illegible]E+01	1.[illegible]E-03	[illegible]	1	1	886	1	75	.78	1.07E+01	.369	WIGM	1.[illegible]E-03	.715	9.73E+01	
205	175	.200	.033	2.05	1	6.[illegible]E-03	1.[illegible]E-02	2.[illegible]E+01	2.[illegible]E-03	[illegible]	1	1	565	1	75	.78	3.63E+01	.269	DIGM	2.[illegible]E-03	.722	7.92E+01	
205	150	.020	.009	.56	1	5.[illegible]E-03	1.[illegible]E-03	5.[illegible]E+00	6.[illegible]E-03	4548	1	1	1479	1	75	.69	7.61E+00	.227	DIGM	6.[illegible]E-03	.637	1.23E+03	
205	150	.050	.020	1.05	1	2.[illegible]E-03	5.[illegible]E-03	1.[illegible]E+01	1.[illegible]E-03	[illegible]	1	1	666	1	70	.78	1.67E+01	.339	WIGM	1.[illegible]E-03	.718	9.49E+01	
205	150	.100	.030	1.65	1	5.[illegible]E-03	1.[illegible]E-02	2.[illegible]E+01	1.[illegible]E-03	[illegible]	1	1	599	1	75	.78	3.26E+01	.349	WIGM	1.[illegible]E-03	.731	7.99E+01	
205	125	.010	.012	.74	1	8.[illegible]E-03	5.[illegible]E-03	5.003E+00	6.[illegible]E-03	3489	1	1	825	1	70	.69	7.25E+00	.536	WIGM	6.[illegible]E-03	.671	1.41E+03	
205	125	.020	.009	.50	1	8.[illegible]E-03	8.[illegible]E-04	7.[illegible]E+00	7.[illegible]E-03	6917	1	1	930?	1	65	.78	9.45E+00	.193	WIGM	7.[illegible]E-03	.722	1.04E+03	
205	125	.050	.017	1.04	1	1.[illegible]E-02	4.[illegible]E-03	1.[illegible]E+01	1.[illegible]E-03	[illegible]	1	1	1305	1	75	.78	3.20E+01	.263	DIGM	1.[illegible]E-03	.730	8.11E+01	
205	100	.010	.009	.59	1	5.[illegible]E-03	1.[illegible]E-03	5.[illegible]E+00	6.[illegible]E-03	4536	1	1	1259	1	70	.69	7.25E+00	.269	WIGM	6.[illegible]E-03	.676	1.29E+03	
205	100	.020	.014	.89	1	1.[illegible]E-02	2.[illegible]E-03	9.[illegible]E+00	8.[illegible]E-03	9072	1	1	957	1	65	.78	1.07E+01	.273	DIGM	8.[illegible]E-03	.718	8.76E+01	
205	100	.050	.033	2.03	1	6.[illegible]E-03	1.[illegible]E-02	2.[illegible]E+01	1.[illegible]E-03	[illegible]	1	1	976	1	75	.78	3.05E+01	.416	WIGM	1.[illegible]E-03	.709	7.32E+01	
205	80	.005	.007	1.19	1	8.[illegible]E-03	5.[illegible]E-03	5.003E+00	6.[illegible]E-03	3510	1	1	825	1	70	.69	7.25E+00	.536	DIGM	6.[illegible]E-03	.674	1.40E+03	
205	80	.010	.012	.76	1	9.[illegible]E-03	2.[illegible]E-03	7.[illegible]E+00	7.[illegible]E-03	7019	1	1	1049	1	60	.74	9.93E+00	.260	WIGM	7.[illegible]E-03	.707	1.01E+03	
205	40	.020	.019	1.20	1	2.[illegible]E-03	6.[illegible]E-03	1.[illegible]E+01	1.[illegible]E-03	[illegible]	1	1	939	1	75	.77	1.97E+01	.292	WIGM	1.[illegible]E-03	.714	8.92E+01	
255	250	.200	.013	.79	1	1.[illegible]E-02	1.[illegible]E-03	5.[illegible]E+00	6.[illegible]E-03	4977	1	1	731	1	75	.69	7.61E+00	.273	DIGM	6.[illegible]E-03	.661	1.23E+03	
255	250	.500	.028	1.68	1	3.[illegible]E-03	7.[illegible]E-03	1.[illegible]E+01	1.[illegible]E-03	[illegible]	1	1	476	1	70	.78	1.70E+01	.404	DIGM	1.[illegible]E-03	.710	8.04E+01	
255	250	1.000	.025	1.51	1	3.[illegible]E-03	1.[illegible]E-02	2.[illegible]E+01	1.[illegible]E-03	[illegible]	1	1	856	1	75	.78	3.26E+01	.349	DIGM	1.[illegible]E-03	.725	7.93E+01	
255	225	.050	.010	.63	1	6.[illegible]E-03	1.[illegible]E-03	7.[illegible]E+00	7.[illegible]E-03	7134	1	1	1469	1	65	.83	9.93E+00	.213	WIGM	7.[illegible]E-03	.718	1.01E+03	
255	225	.100	.015	.94	1	1.[illegible]E-03	3.[illegible]E-03	1.[illegible]E+01	1.[illegible]E-03	[illegible]	1	1	1305	1	75	.78	1.97E+01	.263	WIGM	1.[illegible]E-03	.776	8.52E+01	
255	225	.200	.024	1.46	1	3.[illegible]E-03	6.[illegible]E-03	3.[illegible]E+01	2.[illegible]E-03	[illegible]	1	1	1068	1	75	.78	3.89E+01	.303	WIGM	2.[illegible]E-03	.739	7.81E+01	
255	200	.020	.015	.90	1	1.[illegible]E-02	3.[illegible]E-03	5.[illegible]E+00	6.[illegible]E-03	5133	1	1	535	1	60	.78	9.45E+00	.311	WIGM	6.[illegible]E-03	.693	1.21E+03	
255	200	.050	.017	1.06	1	1.[illegible]E-02	4.[illegible]E-03	1.[illegible]E+01	1.[illegible]E-03	[illegible]	1	1	930	1	75	.78	1.33E+01	.288	WIGM	1.[illegible]E-03	.770	9.30E+01	
255	200	.100	.024	1.49	1	2.[illegible]E-03	8.[illegible]E-03	2.[illegible]E+01	2.[illegible]E-03	[illegible]	1	1	932	1	75	.78	3.63E+01	.292	WIGM	2.[illegible]E-03	.737	7.99E+01	
255	175	.010	.013	.78	1	1.[illegible]E-03	5.[illegible]E-03	5.[illegible]E+00	6.[illegible]E-03	3567	1	1	701	1	70	.69	7.25E+00	.526	WIGM	6.[illegible]E-03	.668	1.26E+03	
255	175	.020	.010	.62	1	6.[illegible]E-03	1.[illegible]E-03	1.[illegible]E+00	7.[illegible]E-03	7334	1	1	1405	1	65	.78	9.93E+00	.187	WIGM	7.[illegible]E-03	.739	1.05E+03	
255	175	.050	.017	1.06	1	1.[illegible]E-02	4.[illegible]E-03	1.[illegible]E+01	1.[illegible]E-03	[illegible]	1	1	1305	1	75	.78	3.26E+01	.243	WIGM	1.[illegible]E-03	.724	8.17E+01	
255	150	.010	.007	.40	1	2.[illegible]E-03	5.[illegible]E-04	5.[illegible]E+00	6.[illegible]E-03	4744	1	1	2609	1	75	.69	7.25E+00	.152	DIGM	6.[illegible]E-03	.684	1.34E+03	
255	150	.020	.013	1.05	1	1.[illegible]E-02	3.[illegible]E-03	1.[illegible]E+00	9.[illegible]E-03	9488	1	1	705	1	65	.78	1.33E+01	.325	WIGM	9.[illegible]E-03	.712	9.54E+01	
255	150	.050	.023	1.34	1	3.[illegible]E-03	5.[illegible]E-03	1.[illegible]E+01	1.[illegible]E-03	[illegible]	1	1	939	1	75	.77	3.07E+01	.263	WIGM	1.[illegible]E-03	.741	7.91E+01	
255	80	.005	.007	.45	1	2.[illegible]E-03	7.[illegible]E-04	5.[illegible]E+00	6.[illegible]E-03	4698	1	1	2070	1	75	.69	7.25E+00	.185	DIGM	6.[illegible]E-03	.647	1.32E+03	
255	80	.010	.009	.52	1	4.[illegible]E-03	1.[illegible]E-03	9.[illegible]E+00	8.[illegible]E-03	9256	1	1	1708	1	70	.78	1.67E+01	.180	WIGM	8.[illegible]E-03	.721	9.49E+01	
255	80	.020	.013	1.41	1	3.[illegible]E-03	8.[illegible]E-03	2.[illegible]E+01	1.[illegible]E-03	[illegible]	1	1	773	1	75	.78	3.63E+01	.349	WIGM	1.[illegible]E-03	.709	7.39E+01	
305	275	.020	.011	.68	1	8.[illegible]E-03	5.[illegible]E-03	5.[illegible]E+00	6.[illegible]E-03	3681	1	1	900	1	70	.69	7.25E+00	.536	DIGM	6.[illegible]E-03	.652	1.29E+03	
305	275	.050	.018	.90	1	1.[illegible]E-02	2.[illegible]E-03	8.[illegible]E+00	8.[illegible]E-03	8208	1	1	749	1	65	.78	1.13E+01	.326	WIGM	8.[illegible]E-03	.718	9.61E+01	
305	275	.100	.023	1.27	1	3.[illegible]E-03	7.[illegible]E-03	2.[illegible]E+01	1.[illegible]E-03	[illegible]	1	1	749	1	75	.78	3.07E+01	.349	WIGM	1.[illegible]E-03	.736	7.98E+01	
305	250	.050	.010	.66	1	9.[illegible]E-03	1.[illegible]E-03	6.[illegible]E+00	6.[illegible]E-03	5693	1	1	1305	1	60	.78	7.73E+00	.216	WIGM	6.[illegible]E-03	.732	1.47E+03	
305	250	.050	.017	1.00	1	1.[illegible]E-02	4.[illegible]E-03	1.[illegible]E+01	1.[illegible]E-03	[illegible]	1	1	1049	1	75	.78	1.97E+01	.292	WIGM	1.[illegible]E-03	.724	8.25E+01	
305	250	.100	.026	1.49	1	4.[illegible]E-03	9.[illegible]E-03	3.[illegible]E+01	2.[illegible]E-03	[illegible]	1	1	933	1	75	.78	3.89E+01	.292	WIGM	2.[illegible]E-03	.737	7.99E+01	
305	225	.010	.010	.64	1	1.[illegible]E-02	5.[illegible]E-03	5.[illegible]E+00	6.[illegible]E-03	4681	1	1	963	1	70	.69	7.25E+00	.526	WIGM	6.[illegible]E-03	.663	1.29E+03	
305	225	.020	.014	.83	1	1.[illegible]E-02	2.[illegible]E-03	8.[illegible]E+00	8.[illegible]E-03	8429	1	1	839	1	65	.78	1.09E+01	.312	WIGM	8.[illegible]E-03	.724	9.61E+01	
305	225	.050	.023	1.45	1	3.[illegible]E-03	7.[illegible]E-03	2.[illegible]E+01	1.[illegible]E-03	[illegible]	1	1	705	1	75	.78	3.11E+01	.349	WIGM	1.[illegible]E-03	.729	7.98E+01	
305	200	.010	.010	.60	1	9.[illegible]E-03	1.[illegible]E-03	6.[illegible]E+00	6.[illegible]E-03	5140	1	1	1178	1	75	.69	7.99E+00	.273	WIGM	6.[illegible]E-03	.641	1.26E+03	
305	200	.020	.015	.83	1	1.[illegible]E-02	3.[illegible]E-03	1.[illegible]E+01	9.[illegible]E-03	9267	1	1	967	1	70	.78	1.40E+01	.234	WIGM	9.[illegible]E-03	.724	9.49E+01	
305	200	.050	.027	1.58	1	3.[illegible]E-03	1.[illegible]E-02	2.[illegible]E+01	2.[illegible]E-03	[illegible]	1	1	749	1	75	.78	3.63E+01	.349	WIGM	2.[illegible]E-03	.725	7.99E+01	
305	40	.005	.007	.50	1	4.[illegible]E-03	1.[illegible]E-03	1.[illegible]E+01	1.[illegible]E-03	[illegible]	1	1	1708	1	60	.74	9.61E+00	.216	WIGM	1.[illegible]E-03	.714	1.01E+03	
305	40	.010	.013	.73	1	9.[illegible]E-03	2.[illegible]E-03	1.[illegible]E+01	1.[illegible]E-03	[illegible]	1	1	1049	1	70	.74	1.09E+01	.260	DIGM	1.[illegible]E-03	.719	9.61E+01	
305	40	.020	.024	1.47	1	2.[illegible]E-03	5.[illegible]E-03	3.[illegible]E+01	2.[illegible]E-03	[illegible]	1	1	1401	1	75	.78	3.70E+01	.243	DIGM	2.[illegible]E-03	.727	7.92E+01	
305	40	.050	.044	.97	1	3.[illegible]E-03	1.[illegible]E-02	7.[illegible]E+01	7.[illegible]E-03	[illegible]	1	1	1860	1	65	.78	9.93E+00	.207	DIGM	7.[illegible]E-03	.713	1.01E+03	
305	40	.100	.057	.80	1	1.[illegible]E-02	4.[illegible]E-03	1.[illegible]E+02	1.[illegible]E-02	[illegible]	1	1	1115	1	75	.78	1.93E+01	.292	DIGM	1.[illegible]E-03	.770	8.11E+01	
305	40	.050	.024	1.30	1	4.[illegible]E-03	9.[illegible]E-03	3.[illegible]E+01	2.[illegible]E-03	[illegible]	1	1	1049	1	75	.78	3.89E+01	.292	DIGM	2.[illegible]E-03	.729	7.93E+01	

END.

317.218 / 2514.722 / 83083

10/04/74. 14.01.37.
MWSTAT MRYDL

COST FILE NAME
? CIG3
TYPE, COST MODEL
? 0.1
CAVITY
? 0

HEELING HEAT TRANSFER VERSION
XPIN= 231, EPSILON= .90, ALPHA= .95, TAU= 1.00, TANB= 20.
TRACDL= 1.00, VELOCITY= 5.0, TYPE= 0, COST MODEL= CAI

--PARAMETERS-- TWIL OF	HDOT	--------------OPTIMUM DESIGNS-------------- D	L	LA	AL	Q	E	MINIMUM COST	TW	---------TRACE BACK--------- N	V	CR	UV	TH	RHR	AP	SIGMA	C.	TYPE	PE	ETA	e/KV
IP= 1000																							
150 .100	.070	.014	.86	1 1.193E-02	6.861E-03	5.516E+00	6.338E+02	163	1	1	615	1 70	.75	7.35E+00	.359	CIG3	6.337E+02	.574	1.50E-02
150 .050	.040	.014	.86	1 1.189E-02	6.841E-03	5.516E+00	6.338E+02	157	1	1	619	1 70	.75	7.35E+00	.359	CIG3	6.337E+02	.574	1.50E-02
150 .075	.040	.017	1.05	1 1.775E-02	6.903E-03	3.048E+00	6.940E+02	169	1	1	463	1 60	.85	9.75E+00	.385	CIG3	6.943E+02	.764	1.10E-02
150 .100	.040	.018	1.14	1 2.077E-02	6.838E-03	9.482E+00	7.133E+02	184	1	1	529	1 60	.85	1.11E+01	.385	CIG3	8.133E+02	.760	9.66E-01
150 .025	.090	.018	.86	1 1.194E-02	6.841E-03	5.516E+00	6.339E+02	154	1	1	621	1 70	.75	7.35E+00	.359	CIG3	6.337E+02	.574	1.50E-02
150 .025	.060	.018	1.13	1 1.961E-02	6.842E-03	6.370E+00	6.978E+02	155	1	1	398	1 60	.85	7.89E+00	.381	CIG3	6.777E+02	.749	1.15E-02
150 .050	.020	.015	1.13	1 2.055E-02	6.837E-03	9.482E+00	8.133E+02	158	1	1	541	1 60	.85	1.11E+01	.385	CIG3	8.133E+02	.760	9.66E-01
150 .075	.020	.019	1.01	1 2.353E-02	6.870E-03	4.274E+01	1.026E+03	161	1	1	697	1 70	.85	1.64E+01	.354	CIG3	1.055E+03	.772	5.36E-01
150 .100	.010	.017	1.07	1 4.743E-02	7.116E-03	1.867E+01	1.355E+03	164	1	1	806	1 75	.85	2.20E+01	.403	CIG3	1.325E+03	.767	7.85E-01
150 .015	.160	.022	1.38	1 3.053E-02	6.787E-03	5.737E+00	6.471E+02	152	1	1	253	1 70	.75	7.72E+00	.359	CIG3	6.469E+02	.658	1.28E-02
150 .020	.160	.022	1.40	1 3.122E-02	6.811E-03	7.767E+00	7.287E+02	153	1	1	291	1 60	.85	9.13E+00	.365	CIG3	7.271E+02	.729	1.03E-02
150 .025	.160	.018	1.12	1 2.025E-02	6.837E-03	9.482E+00	8.133E+02	154	1	1	548	1 60	.85	1.11E+01	.385	CIG3	8.133E+02	.760	9.66E+01
150 .033	.160	.025	1.61	1 4.130E-02	6.811E-03	1.327E+01	1.017E+03	154	1	1	378	1 70	.85	1.56E+01	.357	CIG3	1.017E+03	.757	8.61E+01
150 .050	.160	.024	1.56	1 4.012E-02	6.811E-03	1.327E+01	1.017E+03	154	1	1	408	1 75	.85	2.20E+01	.404	CIG3	1.325E+03	.769	7.85E+01
150 .075	.160	.023	1.51	1 3.911E-02	6.811E-03	1.327E+01	1.017E+03	152	1	1	440	1 75	.85	2.20E+01	.403	CIG3	1.325E+03	.768	7.85E+01
150 .100	.160	.021	1.47	1 3.811E-02	6.811E-03	1.327E+01	1.017E+03	152	1	1	501	1 80	.85	2.20E+01	.403	CIG3	1.325E+03	.768	7.85E+01
150 .015	.320	.031	2.01	1 4.711E-02	6.811E-03	1.327E+01	1.017E+03	153	1	1	202	1 60	.75	9.67E+00	.378	CIG3	9.675E+02	.751	9.03E+01
150 .020	.320	.029	1.89	1 4.511E-02	6.811E-03	1.327E+01	1.017E+03	153	1	1	247	1 70	.75	1.14E+01	.396	CIG3	1.125E+03	.747	7.13E+01
150 .025	.320	.026	1.69	1 4.311E-02	6.811E-03	1.327E+01	1.017E+03	154	1	1	305	1 75	.85	2.20E+01	.404	CIG3	1.325E+03	.769	7.85E+01
150 .033	.320	.023	1.51	1 4.111E-02	6.811E-03	1.327E+01	1.017E+03	156	1	1	368	1 75	.85	2.09E+01	.396	CIG3	1.256E+03	.764	7.55E+01
150 .050	.320	.021	1.36	1 3.911E-02	6.811E-03	1.327E+01	1.017E+03	157	1	1	479	1 80	.75	9.67E+00	.378	CIG3	9.675E+02	.776	9.03E+01
150 .075	.320	.020	2.00	1 4.0	6.811E-03	1.327E+01	1.017E+03	152	1	1	636	1 80	.75	1.14E+01	.41	CIG3	1.125E+03	.785	7.02E+01
150 .015	.640	.033	2.07	1 4.7	6.811E-03	1.327E+01	1.017E+03	153	1	1	365	1 75	.85	2.67E+01	.431	CIG3	1.595E+03	.751	9.57E+01
150 .020	.640	.046	2.90	1 5.9E+01	6.811E-03	1.327E+01	1.017E+03	154	1	1	267	1 80	.85	2.67E+01	.432	CIG3	1.595E+03	.774	9.57E+01
200 .100	.020	.012	.74	1 9.851E-03	6.861E-03	5.516E+00	6.339E+02	211	1	1	346	1 70	.75	7.35E+00	.359	CIG3	6.337E+02	.574	1.50E+02
200 .010	.040	.012	.78	1 9.761E-03	6.861E-03	5.516E+00	6.339E+02	206	1	1	749	1 70	.75	7.35E+00	.359	CIG3	6.337E+02	.576	1.50E+02
200 .075	.040	.018	1.13	1 2.064E-02	6.861E-03	6.370E+00	6.977E+02	208	1	1	351	1 80	.75	7.89E+00	.381	CIG3	6.777E+02	.736	1.15E+02
200 .100	.040	.020	1.23	1 2.451E-02	7.517E-03	8.985E+00	7.899E+02	211	1	1	431	1 90	.85	1.06E+01	.481	CIG3	7.899E+02	.732	1.07E+02
200 .025	.080	.012	.78	1 9.792E-03	6.861E-03	5.516E+00	6.339E+02	203	1	1	751	1 70	.75	7.35E+00	.359	CIG3	6.337E+02	.576	1.50E+02
200 .035	.080	.012	.77	1 9.653E-03	6.598E-03	6.041E+00	6.697E+02	205	1	1	741	1 60	.85	7.15E+00	.325	CIG3	6.697E+02	.753	1.20E+02
200 .050	.080	.019	1.22	1 2.441E-02	7.517E-03	8.985E+00	7.899E+02	206	1	1	436	1 80	.75	1.06E+01	.451	CIG3	7.899E+02	.732	1.07E+02
200 .075	.080	.020	1.60	1 3.165E-02	7.113E-03	1.327E+01	1.017E+03	204	1	1	375	1 70	.85	1.55E+01	.502	CIG3	1.017E+03	.744	8.78E+01
200 .100	.080	.025	1.75	1 4.911E-02	6.898E-03	1.178E+01	1.072E+03	211	1	1	471	1 75	.85	2.09E+01	.416	CIG3	1.225E+03	.748	9.27E+01
200 .015	.160	.018	1.14	1 2.410E-02	6.661E-03	5.516E+00	6.339E+02	202	1	1	349	1 70	.75	7.35E+00	.359	CIG3	6.337E+02	.630	1.50E+02
200 .020	.160	.015	.96	1 1.897E-02	6.787E-03	1.068E+00	6.943E+02	203	1	1	555	1 80	.85	8.21E+00	.366	CIG3	6.943E+02	.745	1.12E+02
200 .025	.160	.019	1.21	1 2.390E-02	7.517E-03	8.985E+00	7.899E+02	203	1	1	442	1 80	.85	1.06E+01	.481	CIG3	7.899E+02	.732	1.07E+02
200 .033	.160	.018	1.13	1 2.064E-02	6.840E-03	1.226E+01	9.515E+02	205	1	1	686	1 85	.85	1.42E+01	.341	CIG3	9.515E+02	.765	8.76E+01
200 .050	.160	.025	1.76	1 4.895E-02	1.457E-02	1.179E+01	1.027E+03	206	1	1	428	1 75	.85	2.09E+01	.516	CIG3	1.227E+03	.740	9.27E+01
200 .075	.160	.027	2.31	1 8.858E-02	2.637E-02	1.179E+01	1.027E+03	209	1	1	357	1 75	.85	2.09E+01	.518	CIG3	1.178E+03	.751	7.98E+01
200 .100	.160	.040	2.52	1 1.023E+01	2.943E-02	3.322E+01	2.315E+03	218	1	1	408	1 75	.85	4.18E+01	.516	CIG3	2.315E+03	.747	7.82E+01
300 .010	.320	.015	.96	1 1.897E-02	6.787E-03	1.068E+00	6.943E+02	202	1	1	559	1 80	.85	8.21E+00	.366	CIG3	6.943E+02	.748	1.12E+02
300 .015	.320	.016	.99	1 1.592E-02	6.840E-03	1.068E+01	8.643E+02	203	1	1	369	1 85	.85	1.27E+01	.341	CIG3	8.643E+02	.759	9.31E+01
300 .020	.320	.017	1.09	1 2.111E-02	6.837E-03	1.179E+01	1.055E+03	203	1	1	527	1 90	.85	1.64E+01	.422	CIG3	1.055E+03	.735	8.52E+01
300 .025	.320	.024	1.53	1 4.858E-02	1.458E-02	1.179E+01	1.027E+03	204	1	1	431	1 75	.85	2.09E+01	.516	CIG3	1.227E+03	.740	9.27E+01
300 .033	.320	.027	1.72	1 4.707E-02	1.017E-02	2.394E+01	1.837E+03	205	1	1	558	1 75	.85	2.97E+01	.365	CIG3	1.836E+03	.773	7.35E+01
300 .050	.320	.040	2.49	1 1.004E+01	2.967E-02	3.322E+01	2.359E+03	207	1	1	411	1 75	.85	4.18E+01	.516	CIG3	2.357E+03	.747	7.82E+01
300 .010	.640	.015	.96	1 1.889E-02	6.787E-03	1.068E+00	6.953E+02	201	1	1	558	1 80	.85	8.24E+00	.368	CIG3	6.940E+02	.748	1.12E+02
300 .010	.640	.022	1.38	1 3.009E-02	6.930E-03	1.179E+01	1.055E+03	202	1	1	529	1 90	.85	1.64E+01	.422	CIG3	1.055E+03	.755	8.52E+01
300 .015	.640	.023	1.45	1 3.406E-02	6.740E-03	1.024E+01	1.940E+03	202	1	1	711	1 75	.85	2.97E+01	.365	CIG3	1.440E+03	.767	7.35E+01
300 .020	.640	.032	2.03	1 4.674E-02	1.049E-02	2.740E+01	1.669E+03	203	1	1	606	1 75	.85	4.18E+01	.516	CIG3	1.669E+03	.763	7.50E+01
300 .025	.640	.040	2.48	1 9.986E-02	2.967E-02	3.322E+01	2.358E+03	208	1	1	419	1 75	.85	4.18E+01	.516	CIG3	2.357E+03	.747	7.82E+01
450 .015	.640	.016	1.00	1 1.885E-02	6.787E-03	1.068E+00	6.989E+02	257	1	1	565	1 80	.85	8.24E+00	.368	CIG3	6.976E+02	.748	1.12E+02
450 .100	.040	.014	.84	1 1.191E-02	6.811E-03	7.767E+00	7.300E+02	260	1	1	767	1 60	.85	9.13E+00	.365	CIG3	7.299E+02	.743	1.07E+02
450 .050	.040	.014	.83	1 1.187E-02	6.811E-03	7.767E+00	7.300E+02	258	1	1	776	1 70	.75	9.13E+00	.365	CIG3	7.299E+02	.743	1.07E+02
450 .075	.040	.014	.83	1 1.183E-02	6.811E-03	7.767E+00	7.300E+02	257	1	1	777	1 80	.85	9.13E+00	.365	CIG3	7.299E+02	.743	1.07E+02
450 .100	.040	.014	.83	1 1.179E-02	6.811E-03	7.767E+00	7.300E+02	257	1	1	776	1 90	.85	9.13E+00	.365	CIG3	7.299E+02	.743	1.07E+02
450 .015	.080	.014	.84	1 1.191E-02	6.811E-03	7.767E+00	7.300E+02	260	1	1	767	1 60	.85	9.13E+00	.365	CIG3	7.299E+02	.743	1.07E+02
450 .020	.080	.014	.83	1 1.187E-02	6.811E-03	7.767E+00	7.300E+02	258	1	1	776	1 70	.75	9.13E+00	.365	CIG3	7.299E+02	.743	1.07E+02
450 .025	.080	.014	.83	1 1.183E-02	6.811E-03	7.767E+00	7.300E+02	257	1	1	777	1 80	.85	9.13E+00	.365	CIG3	7.299E+02	.743	1.07E+02
450 .033	.080	.014	.83	1 1.179E-02	6.811E-03	7.767E+00	7.300E+02	257	1	1	776	1 90	.85	9.13E+00	.365	CIG3	7.299E+02	.743	1.07E+02
450 .050	.080	.014	.84	1 1.191E-02	6.811E-03	7.767E+00	7.300E+02	260	1	1	767	1 60	.85	9.13E+00	.365	CIG3	7.299E+02	.743	1.07E+02
450 .075	.080	.014	.83	1 1.187E-02	6.811E-03	7.767E+00	7.300E+02	258	1	1	776	1 70	.75	9.13E+00	.365	CIG3	7.299E+02	.743	1.07E+02
450 .100	.080	.014	.83	1 1.183E-02	6.811E-03	7.767E+00	7.300E+02	257	1	1	777	1 80	.85	9.13E+00	.365	CIG3	7.299E+02	.743	1.07E+02
450 .015	.160	.018	.96	1 1.885E-02	6.787E-03	1.068E+00	6.989E+02	257	1	1	565	1 80	.85	8.24E+00	.368	CIG3	6.976E+02	.748	1.12E+02
450 .020	.160	.014	.84	1 1.191E-02	6.811E-03	7.767E+00	7.300E+02	260	1	1	767	1 60	.85	9.13E+00	.365	CIG3	7.299E+02	.743	1.07E+02
450 .025	.160	.014	.83	1 1.187E-02	6.811E-03	7.767E+00	7.300E+02	258	1	1	776	1 70	.75	9.13E+00	.365	CIG3	7.299E+02	.743	1.07E+02
450 .033	.160	.014	.83	1 1.183E-02	6.811E-03	7.767E+00	7.300E+02	257	1	1	777	1 80	.85	9.13E+00	.365	CIG3	7.299E+02	.743	1.07E+02
450 .050	.160	.014	.84	1 1.191E-02	6.811E-03	7.767E+00	7.300E+02	260	1	1	767	1 60	.85	9.13E+00	.365	CIG3	7.299E+02	.743	1.07E+02
450 .075	.160	.014	.83	1 1.187E-02	6.811E-03	7.767E+00	7.300E+02	258	1	1	776	1 70	.75	9.13E+00	.365	CIG3	7.299E+02	.743	1.07E+02
450 .100	.160	.014	.83	1 1.183E-02	6.811E-03	7.767E+00	7.300E+02	257	1	1	777	1 80	.85	9.13E+00	.365	CIG3	7.299E+02	.743	1.07E+02
450 .015	.320	.018	.96	1 1.885E-02	6.787E-03	1.068E+00	6.989E+02	257	1	1	565	1 80	.85	8.24E+00	.368	CIG3	6.976E+02	.748	1.12E+02
450 .020	.320	.016	.84	1 1.191E-02	6.811E-03	7.767E+00	7.300E+02	260	1	1	767	1 60	.85	9.13E+00	.365	CIG3	7.299E+02	.743	1.07E+02
450 .025	.320	.016	.83	1 1.187E-02	6.811E-03	7.767E+00	7.300E+02	258	1	1	776	1 70	.75	9.13E+00	.365	CIG3	7.299E+02	.743	1.07E+02
450 .033	.320	.016	.83	1 1.183E-02	6.811E-03	7.767E+00	7.300E+02	257	1	1	777	1 80	.85	9.13E+00	.365	CIG3	7.299E+02	.743	1.07E+02
450 .050	.320	.016	.84	1 1.191E-02	6.811E-03	7.767E+00	7.300E+02	260	1	1	767	1 60	.85	9.13E+00	.365	CIG3	7.299E+02	.743	1.07E+02
450 .075	.320	.016	.83	1 1.187E-02	6.811E-03	7.767E+00	7.300E+02	258	1	1	776	1 70	.75	9.13E+00	.365	CIG3	7.299E+02	.743	1.07E+02
450 .100	.320	.016	.83	1 1.183E-02	6.811E-03	7.767E+00	7.300E+02	257	1	1	777	1 80	.85	9.13E+00	.365	CIG3	7.299E+02	.743	1.07E+02
450 .015	.640	.018	.96	1 1.885E-02	6.787E-03	1.068E+00	6.989E+02	257	1	1	565	1 80	.85	8.24E+00	.368	CIG3	6.976E+02	.748	1.12E+02
450 .020	.640	.014	.84	1 1.191E-02	6.811E-03	7.767E+00	7.300E+02	260	1	1	767	1 60	.85	9.13E+00	.365	CIG3	7.299E+02	.743	1.07E+02
450 .025	.640	.014	.83	1 1.187E-02	6.811E-03	7.767E+00	7.300E+02	258	1	1	776	1 70	.75	9.13E+00	.365	CIG3	7.299E+02	.743	1.07E+02
450 .033	.640	.014	.83	1 1.183E-02	6.811E-03	7.767E+00	7.300E+02	257	1	1	777	1 80	.85	9.13E+00	.365	CIG3	7.299E+02	.743	1.07E+02
450 .050	.640	.014	.84	1 1.191E-02	6.811E-03	7.767E+00	7.300E+02	260	1	1	767	1 60	.85	9.13E+00	.365	CIG3	7.299E+02	.743	1.07E+02
450 .075	.640	.014	.83	1 1.187E-02	6.811E-03	7.767E+00	7.300E+02	258	1	1	776	1 70	.75	9.13E+00	.365	CIG3	7.299E+02	.743	1.07E+02
450 .100	.640	.014	.83	1 1.183E-02	6.811E-03	7.767E+00	7.300E+02	257	1	1	777	1 80	.85	9.13E+00	.365	CIG3	7.299E+02	.743	1.07E+02
450 .015	.640	.020	1.22	1 2.549E-02	6.926E-03	1.033E+01	6.912E+02	254	1	1	504	1 65	.75	1.27E+01	.407	CIG3	6.907E+02	.744	9.35E+01
450 .020	.640	.020	1.20	1 2.485E-02	6.559E-03	1.327E+01	1.136E+03	256	1	1	738	1 75	.75	1.81E+01	.365	CIG3	1.135E+03	.755	8.37E+01
450 .025	.640	.022	1.36	1 3.364E-02	6.944E-03	2.354E+01	1.835E+03	258	1	1	629	1 75	.85	2.80E+01	.516	CIG3	1.693E+03	.730	7.90E+01
450 .033	.640	.029	1.73	1 5.406E-02	6.789E-03	3.643E+01	2.351E+03	260	1	1	662	1 75	.85	3.97E+01	.365	CIG3	2.350E+03	.763	7.34E+01
450 .050	.640	.034	.83	1 1.178E-02	6.811E-03	6.381E+00	6.635E+02	251	1	1	638	1 60	.85	7.21E+00	.388	CIG3	6.633E+02	.727	1.01E+02
450 .075	.640	.018	1.07	1 1.951E-02	6.839E-03	9.439E+00	8.138E+02	252	1	1	569	1 60	.85	1.11E+01	.378	CIG3	8.138E+02	.738	9.92E+01
450 .100	.640	.023	1.48	1 2.382E-02	7.565E-03	1.268E+01	9.839E+02	252	1	1	825	1 70	.85	1.48E+01	.402	CIG3	9.823E+02	.734	9.01E+01
450 .015	.640	.025	1.53	1 2.429E-02	6.929E-03	1.327E+01	1.136E+03	253	1	1	744	1 75	.85	1.81E+01	.365	CIG3	1.135E+03	.755	8.37E+01
450 .020	.640	.029	1.77	1 3.350E-02	6.927E-02	2.354E+01	1.501E+03	254	1	1	675	1 75	.85	2.58E+01	.438	CIG3	1.500E+03	.751	7.69E+01
450 .025	.640	.029	1.76	1 5.266E-02	6.789E-02	3.643E+01	2.351E+03	256	1	1	680	1 75	.85	3.97E+01	.365	CIG3	2.350E+03	.763	7.34E+01
450 .033	.640	.034	.83	1 1.178E-02	6.811E-03	6.381E+00	6.635E+02	251	1	1	638	1 60	.85	7.21E+00	.388	CIG3	6.633E+02	.727	1.01E+02
450 .050	.640	.019	1.19	1 2.393E-02	7.565E-03	1.268E+01	9.839E+02	252	1	1	827	1 70	.85	1.48E+01	.402	CIG3	9.823E+02	.734	9.01E+01
450 .075	.640	.023	1.48	1 2.382E-02	7.565E-03	1.268E+01	9.839E+02	252	1	1	825	1 70	.85	1.48E+01	.402	CIG3	9.823E+02	.734	9.01E+01
450 .100	.640	.025	1.53	1 2.429E-02	6.929E-03	1.327E+01	1.136E+03	253	1	1	744	1 75	.85	1.81E+01	.365	CIG3	1.135E+03	.755	8.37E+01
450 .020	.640	.029	1.69	1 4.787E-02	1.476E-02	7.562E+01	1.700E+03	253	1	1	606	1 75	.85	2.94E+01	.414	CIG3	1.700E+03	.762	7.87E+01
450 .025	.640	.029	1.75	1 5.205E-02	1.799E-02	3.043E+01	2.051E+03	253	1	1	658	1 75	.85	3.57E+01	.365	CIG3	2.050E+03	.763	7.51E+01

END.

206.244 / 1607.017 / 83944

```
CXGN FILE NAME
 ? C9G2D
TYPE, CØST MØDEL
 ? 9,1 *DEL*
1,9
MDØTL
 ? 50

BØILING HEAT TRANSFER VERSIØN
KFIN= 211, EPSILØN= .90, ALPHA= .95, TAU= 1.00, TAMD= 20,
FRACDL= 1.00, VELØCITY=  5.0, TYPE= 1, CØST MØDEL= CA9
```

PARAMETERS			-------ØPTIMUM DESIGNS------				MINIMUM			--------TRACE BACK--------									
TBØIL	MDØT	D	L	AL	1000	E/100	CØST	$/KW	KW	VP	NV	CR	TH	DHØ	AP/100	TWR	SIGMA	FC/1000	ETA	CØNC.	FILE
ID= 1000																					
150	50.0	.160	10106	1625	17115	1624	10074470	78	128719	7	4676	1244	70	.90	5053	145	.367	10037	.255	C9G2D	
150	51.0	.240	6120	1476	17807	1689	10474818	80	131293	7	4865	1425	70	.90	5257	149	.370	10433	.250	C9G2D	
150	52.0	.120	5595	675	9452	1757	10876123	81	133568	7	5062	3240	70	.90	5470	152	.211	10847	.245	C9G2D	
150	53.0	.200	2834	569	10858	2019	12512331	92	136442	7	5815	4414	70	.90	6283	163	.224	12498	.217	C9G2D	
150	54.0	.240	7470	1801	18163	1723	10679517	77	139017	7	4963	1191	70	.90	5363	150	.371	10629	.259	C9G2D	
150	55.0	.120	20047	2417	28075	1902	11872454	84	141591	7	5479	980	70	.90	5921	159	.475	11759	.239	C9G2D	
150	56.0	.220	7744	1712	19275	1828	11337251	79	144165	7	5266	1330	70	.90	5691	155	.376	11292	.253	C9G2D	
150	57.0	.160	6090	979	15201	2019	12522368	85	146740	7	5815	2567	70	.90	6283	163	.299	12497	.234	C9G2D	
150	58.0	.200	9508	1911	19660	1865	11572134	78	149314	7	5372	1215	70	.90	5805	156	.377	11524	.257	C9G2D	
150	59.0	.220	4141	915	16783	2229	13853494	91	151888	7	6420	3031	70	.90	6937	171	.306	13829	.219	C9G2D	
150	60.0	.240	4848	1169	14903	1979	12280026	80	154463	7	5701	2108	70	.90	6160	161	.297	12247	.251	C9G2D	
200	50.0	.240	2552	622	9641	1793	11123731	85	131001	7	5163	3538	70	.90	5579	153	.213	11068	.235	C9G2D	
200	51.0	.220	3866	864	8732	1624	10109336	76	133621	7	4676	2340	70	.90	5053	146	.202	10035	.254	C9G2D	
200	52.0	.240	5942	1449	12470	1656	10364144	76	136241	7	4770	1424	70	.90	5154	147	.203	10235	.264	C9G2D	
200	53.0	.240	7316	1733	16397	1793	11226182	81	138861	7	5163	1252	70	.90	5579	153	.274	11067	.249	C9G2D	
200	54.0	.200	5429	1226	8907	1656	10336669	73	141481	7	4770	1621	70	.90	5154	147	.204	10230	.274	C9G2D	
200	55.0	.200	7953	1615	20455	1940	12132976	84	144101	7	5539	1495	70	.90	6039	160	.350	12000	.239	C9G2D	
200	56.0	.220	3645	814	10021	1865	11593230	79	146722	7	5372	2351	70	.90	5805	156	.216	11526	.253	C9G2D	
200	57.0	.160	6539	1071	9641	1793	11139130	75	149342	7	5163	2074	70	.90	5579	153	.213	11068	.268	C9G2D	
200	58.0	.240	9742	2375	31617	2142	13492299	89	151962	7	6171	1103	70	.90	6666	163	.402	13079	.223	C9G2D	
200	59.0	.200	14755	2997	30997	2100	13241479	86	154582	7	6050	872	70	.90	6537	166	.481	13013	.236	C9G2D	
200	60.0	.180	6623	1211	10031	1865	11611683	74	157202	7	5372	1918	70	.90	5805	156	.216	11526	.271	C9G2D	
250	50.0	.240	2604	650	9641	1793	11212758	85	131271	7	5163	3434	70	.90	5579	153	.213	11068	.235	C9G2D	
250	51.0	.220	5061	1226	12974	1723	10880186	81	133936	7	4963	1749	70	.90	5363	150	.206	10629	.250	C9G2D	
250	52.0	.120	7901	986	14610	1940	12139242	89	136602	7	5599	2450	70	.90	6039	160	.296	12001	.226	C9G2D	
250	53.0	.100	8979	934	9452	1757	11010598	79	139267	7	5062	2340	70	.90	5470	152	.211	10847	.254	C9G2D	
250	54.0	.140	7580	1104	14610	1940	12158157	86	141932	7	5559	2139	70	.90	6039	160	.296	12001	.235	C9G2D	
250	55.0	.240	3731	931	9641	1793	11275526	78	144598	7	5163	3397	70	.90	5579	153	.213	11068	.259	C9G2D	
250	56.0	.180	7260	1359	14324	1902	11990620	82	147263	7	5479	1740	70	.90	5921	158	.294	11760	.243	C9G2D	
250	57.0	.100	9370	974	17118	2273	14303367	96	149649	7	6543	2905	70	.90	7076	173	.307	14112	.211	C9G2D	
250	58.0	.160	4931	820	10858	2019	12625825	83	152274	7	5615	3064	70	.90	6283	163	.224	12498	.242	C9G2D	
250	59.0	.120	4677	584	14613	2717	17030246	110	154899	7	7826	5796	70	.90	8456	189	.247	16941	.183	C9G2D	
250	60.0	.100	8825	918	11075	2059	12948809	82	157525	7	5931	2794	70	.90	6409	164	.226	12753	.246	C9G2D	

```
END.

3653.078 / 29204.370 /     32752
```

[illegible]

OLD FILE NAME
? C902A
TYPE COST MODEL
? 1,9
RATE
? 1.66667
READY
USED IN EXECUTION,
ACCUM. CPU SECONDS = 787.656

BOILING HEAT TRANSFER VERSION
[illegible]= 211, EPSILON= .90, ALPHA= .95, TAU= 1.00, TAUB= 20,
[illegible]= 1.90, VELOCITY= 5.0, TYPE= 1, COST MODEL= [illegible]

PARAMETERS --------OPTIMUM DESIGNS------ ANNUAL ----------PRICE PAGE---------

II = 1000

ROOT	D		L	NL	100C	×100	COST	[illegible]	AW	LP	[illegible]	CT	TI	[illegible]	AP/100	T	SIGMA	FC/1000	ETA	CONC. FILE
150	1.7	.240	390	92	799	54	646434	151	4291	3	635	655	65	.90	150	33	.142	644	.206	C932A
155	1.7	.240	393	94	815	55	656657	150	4376	3	851	655	65	.90	153	33	.151	652	.236	C902A
152	1.7	.240	393	95	831	56	663370	149	4462	3	865	659	65	.92	156	33	.160	661	.256	C902A
150	1.8	.220	459	101	[illegible]	57	678093	143	4548	3	856	625	65	.98	157	33	.158	670	[illegible]	[illegible]
150	1.8	.220	367	58	403	54	677122	145	4634	2	1951	[illegible]	75	[illegible]	211	[illegible]	.142	676	.220	C902A
150	1.8	.180	444	54	424	56	[illegible]	146	4709	2	1954	1163	65	[illegible]	[illegible]	33	.142	[illegible]	.302	C902A
[illegible]	1.9	.200	296	59	454	56	689706	140	4806	2	1954	1051	65	[illegible]	156	33	.142	[illegible]	.325	[illegible]
150	1.9	.200	258	55	432	57	[illegible]	145	4891	2	1993	[illegible]	65	[illegible]	159	33	.147	[illegible]	.297	[illegible]
150	1.9	.180	[illegible]	59	441	59	[illegible]	142	4977	2	2033	1017	65	.40	162	34	.152	707	.306	[illegible]
[illegible]	2.0	[illegible]	197	47	459	51	723221	144	5063	2	2115	[illegible]	65	[illegible]	[illegible]	34	.161	[illegible]	.330	[illegible]
150	2.0	.140	441	52	437	51	723911	141	5149	2	2115	1070	65	.30	169	34	.161	727	.285	C902A
[illegible]	1.7	[illegible]	154	43	274	51	675236	155	4357	1	[illegible]	1362	[illegible]	[illegible]	141	31	.232	673	.309	C902A
200	1.7	.200	252	51	497	54	650150	153	4454	2	1931	1265	75	[illegible]	211	32	.142	678	.211	[illegible]
200	1.7	.120	410	50	424	56	696306	152	4531	2	1954	1030	65	[illegible]	151	33	.142	[illegible]	.201	[illegible]
[illegible]	1.8	.130	309	56	414	58	692977	150	4697	2	1954	[illegible]	[illegible]	.00	156	33	.142	[illegible]	.295	[illegible]
200	1.8	.140	338	48	441	59	[illegible]	151	4716	2	[illegible]	[illegible]	[illegible]	.70	[illegible]	34	.152	707	.270	[illegible]
[illegible]	1.7	.150	300	55	441	59	711370	145	[illegible]	2	[illegible]	[illegible]	[illegible]	.00	[illegible]	34	.152	707	[illegible]	[illegible]
[illegible]	1.9	.130	361	59	450	60	[illegible]	147	[illegible]	2	[illegible]	[illegible]	[illegible]	.10	[illegible]	[illegible]	.155	717	.275	[illegible]
[illegible]	1.7	.110	395	54	[illegible]	61	735667	147	[illegible]	2	2115	[illegible]	65	[illegible]	[illegible]	34	.161	727	[illegible]	[illegible]
[illegible]	1.9	.140	432	61	[illegible]	62	[illegible]	140	5063	2	[illegible]	[illegible]	[illegible]	[illegible]	[illegible]	35	.155	727	.294	[illegible]
[illegible]	2.0	[illegible]	251	[illegible]	435	52	[illegible]	146	5153	2	2157	[illegible]	[illegible]	[illegible]	172	35	.155	[illegible]	[illegible]	[illegible]
[illegible]	[illegible]	[illegible]	275	52	477	53	752792	144	5240	2	2201	[illegible]	[illegible]	.20	178	35	.169	[illegible]	.298	C902A
250	1.7	.220	202	40	412	55	[illegible]	153	4376	2	1947	[illegible]	[illegible]	[illegible]	172	27	.146	670	.255	C902A
250	1.7	.180	[illegible]	59	424	56	[illegible]	[illegible]	[illegible]	2	1958	[illegible]	65	[illegible]	[illegible]	33	.142	[illegible]	.236	C902A
250	1.7	[illegible]	241	50	412	57	[illegible]	[illegible]	4551	2	1995	[illegible]	[illegible]	[illegible]	159	33	.147	695	.235	[illegible]
300	[illegible]	.200	240	51	441	57	716573	155	4635	2	2032	[illegible]	65	.30	162	34	.152	707	.296	C902A
250	[illegible]	.260	191	43	457	60	727741	154	4725	2	2074	[illegible]	65	.90	156	24	.155	717	.275	[illegible]
250	[illegible]	.200	244	51	[illegible]	61	736416	153	4813	2	2115	1321	65	.90	159	34	.161	727	.285	C902A
[illegible]	[illegible]	[illegible]	[illegible]	[illegible]	[illegible]	62	[illegible]	152	[illegible]	2	2157	[illegible]	65	[illegible]	[illegible]	[illegible]	.165	727	[illegible]	C902A
[illegible]	[illegible]	.150	341	57	477	63	756061	152	[illegible]	2	2201	[illegible]	65	[illegible]	[illegible]	35	.169	766	.254	C902A
250	1.9	.160	[illegible]	55	[illegible]	65	765410	151	5076	2	[illegible]	1290	[illegible]	.90	[illegible]	35	.173	758	.293	C902A
[illegible]	2.0	.100	326	54	477	66	[illegible]	151	5163	2	[illegible]	1300	[illegible]	.40	172	35	.177	769	.292	C902A
250	2.0	.220	215	[illegible]	507	57	769107	150	5251	2	2326	1510	[illegible]	[illegible]	187	36	.181	*770	.231	C902A

END.

2 [illegible] 15577

4.0 FIELD OPTIMIZATION RUNS

Section 2.3.9 of Appendix B contains sample results along with a discussion of how to interpret the runs. Two different basic kinds of optimization runs were conducted, feeder line and trunk line optimization. The difference between the two kinds is shown in Figure 4-1.

4.1 Series Boiling Feeder Lines

These computer runs are for a feeder line where a fraction of latent heat is added in each collector and the collectors are in series. The return line parallels the line with the collectors and is the input to the outermost collector in the feeder line. In these runs the minimum cost numbers of feeder line subsystems (see Figure 4-1) is indicated by an X. The associated optimum high and low temperature side insulation thicknesses and pipe diameters are the entries on the indicated line.

As can be seen from the computer runs, it was evident after a number of runs that the largest collectors were going to produce minimum cost feeder lines for a given steam mass flow output requirement. Because of the discrete nature of the optimization, many combinations of QF and $\dot{m}$ that would result in the largest collectors were not examined. Figures 4-2 to 4-4 illustrate the manner in which existing collector optimization results were extrapolated to yield the performance characteristics, QF and $\dot{m}$, of the largest collector. Examples of these computer runs appear at the end of this section.

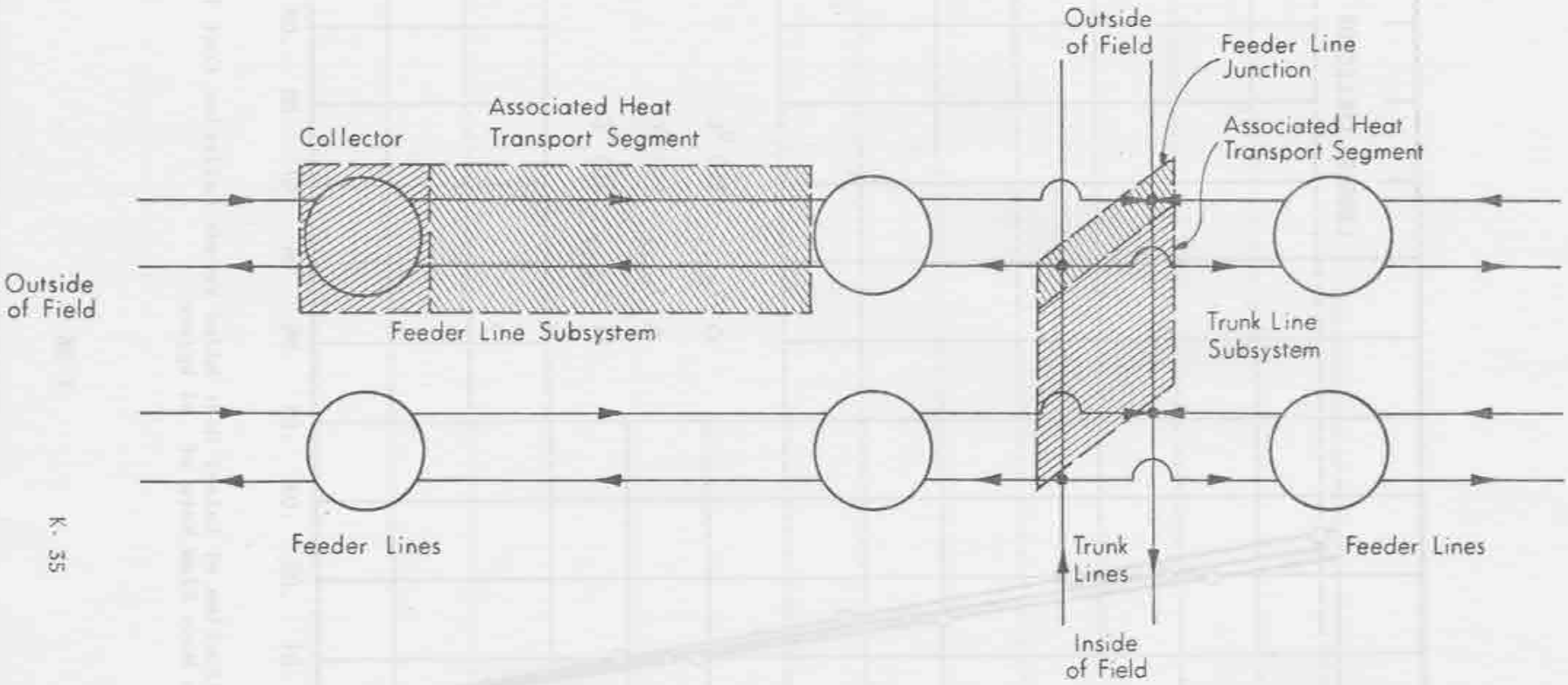

Figure 4-1. Feeder Line and Trunk Line Components for the Optimization Runs.

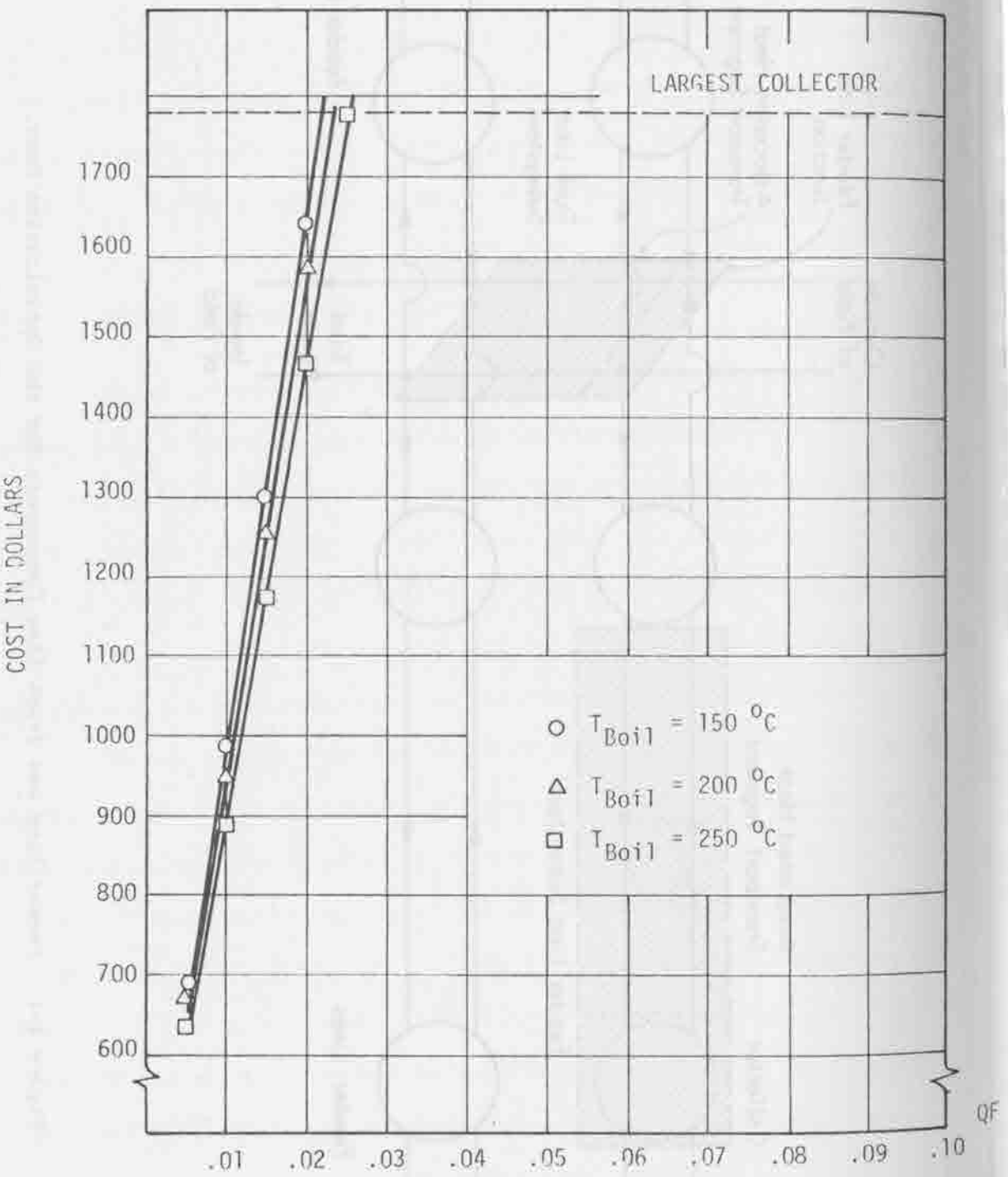

Figure 4-2. Fraction of Latent Heat Added Versus Collector Cost for a Mass Flow Rate of .64 kg/sec.

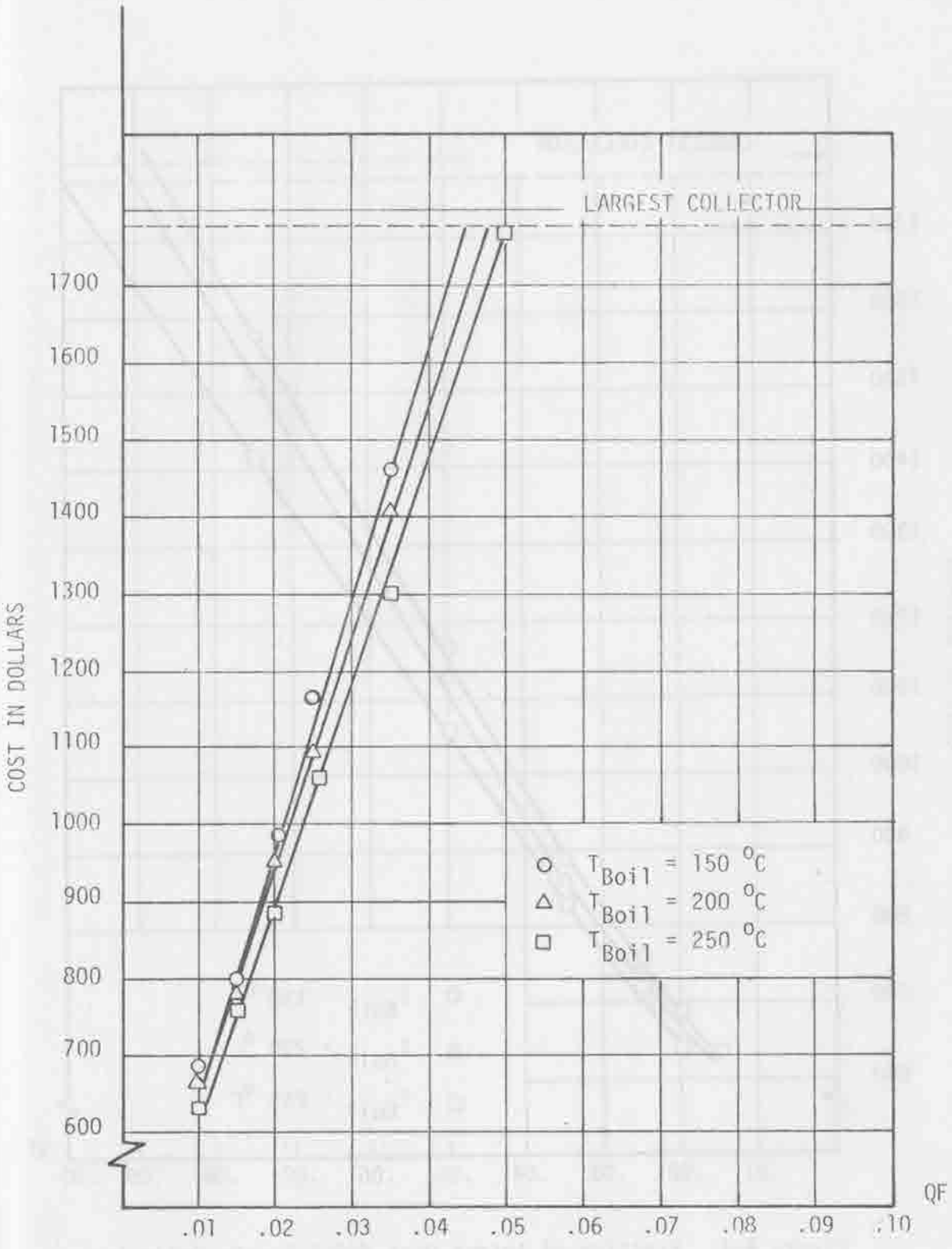

Figure 4-3. Fraction of Latent Heat Added Versus Collector Cost for a Mass Flow Rate of .32 kg/sec.

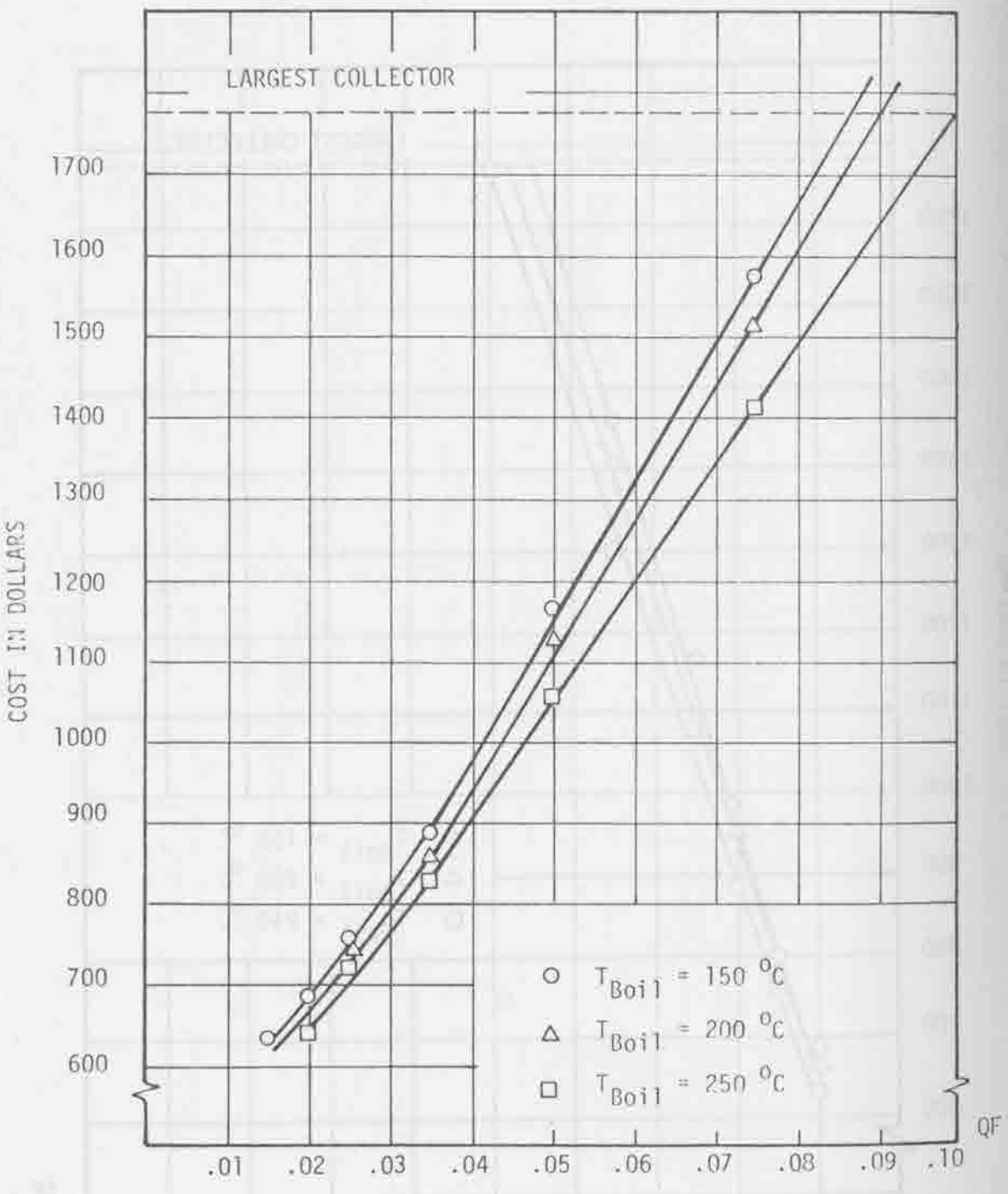

Figure 4-4. Fraction of Latent Heat Added Versus Collector Cost for a Mass Flow Rate of .16 kg/sec.

COLLECTOR DIAMETER 6.03

0 ADDED PER COLLECTOR 25317, 0 TO BOIL 227145, 0 PER T PIPE 74336

LENGTH BTW COLLECTORS 12.5, LENGTH BTW PIPES 12.5

N	0 ADDED	LOSS PER HT SEGMENT	--HIGH SIDE-- DIA- METER	INSUL. THICK.	--LOW SIDE-- DIA- METER	INSUL. THICK.	MINIMUM COST
17	437393	1209	.1758	.0497	.0135	.0111	31782 X
18	455782	2304	.1579	.0078	.0135	.0111	31743
19	473172	3419	.1717	.0143	.0135	.0111	31915
20	490562	4555	.1715	.0137	.0134	.0111	31891
21	507952	5714	.1707	.0131	.0133	.0111	31869
22	525343	6896	.1707	.0131	.0133	.0111	31869
23	542733	8102	.1707	.0131	.0133	.0111	31869
24	560123	9332	.1707	.0131	.0133	.0111	31869
25	577513	10586	.1707	.0131	.0133	.0111	31869
26	594903	11865	.1707	.0131	.0133	.0111	31869
27	612293	13169	.1707	.0131	.0133	.0111	31869
28	629683	14498	.1707	.0131	.0133	.0111	31869
29	647073	15853	.1707	.0131	.0133	.0111	31869
30	664463	17234	.1707	.0131	.0133	.0111	31869
31	681853	18641	.1707	.0131	.0133	.0111	31869
32	699243	20074	.1707	.0131	.0133	.0111	31869
33	716633	21534	.1707	.0131	.0133	.0111	31869

COLLECTOR DIAMETER 6.03

0 ADDED PER COLLECTOR 22025, 0 TO BOIL 203647, 0 PER T PIPE 67787

LENGTH BTW COLLECTORS 12.5, LENGTH BTW PIPES 12.5

N	0 ADDED	LOSS PER HT SEGMENT	--HIGH SIDE-- DIA- METER	INSUL. THICK.	--LOW SIDE-- DIA- METER	INSUL. THICK.	MINIMUM COST
19	441877	1091	.1760	.0596	.0131	.0104	31071 X
20	454502	2165	.1599	.0394	.0135	.0101	30177
21	477795	3136	.1541	.0307	.0145	.0083	30367
22	519953	4017	.1715	.0161	.0137	.0091	31760
23	534173	4754	.1778	.0131	.0130	.0091	31919
24	557403	5619	.1715	.0121	.0140	.0086	31111
25	575623	6323	.1753	.0139	.0147	.0089	31727
26	603853	6913	.1771	.0100	.0140	.0091	31981
27	627073	7525	.1903	.0093	.0144	.0094	34159
28	650303	8134	.1909	.0077	.0143	.0088	34158
29	673529	8655	.1945	.0083	.0142	.0089	34778
30	696754	9140	.1965	.0079	.0142	.0092	35132
31	719979	9595	.1930	.0075	.0139	.0094	34884
32	743204	10021	.1994	.0073	.0133	.0097	35937
33	766429	10421	.2006	.0070	.0137	.0090	36111
34	789654	10797	.2017	.0068	.0135	.0093	36279
35	812879	11152	.2027	.0066	.0134	.0095	36431
36	836104	11488	.2037	.0064	.0132	.0097	36577

COLLECTOR DIAMETER 5.74

0 ADDED PER COLLECTOR 21833, 0 TO BOIL 273106, 0 PER T PIPE 140960

LENGTH BTW COLLECTORS 11.9, LENGTH BTW PIPES 11.9

N	0 ADDED	LOSS PER HT SEGMENT	--HIGH SIDE-- DIA- METER	INSUL. THICK.	--LOW SIDE-- DIA- METER	INSUL. THICK.	MINIMUM COST
21	427153	617	.1778	.0578	.0133	.0110	42677
22	449043	1301	.1399	.0111	.0117	.0141	33174 X
23	470933	2011	.1491	.0071	.0133	.0116	34150
24	492823	2745	.1581	.0077	.0149	.0093	35143
25	514713	3503	.1672	.0083	.0165	.0069	36152
26	536603	4287	.1757	.0089	.0179	.0046	37175
27	558493	5095	.1749	.0071	.0136	.0091	38119
28	580383	5931	.1793	.0055	.0138	.0069	41117
29	602273	6792	.1717	.0107	.0143	.0056	42756
30	624163	7680	.1731	.0107	.0147	.0033	44379
31	646053	8595	.1759	.0104	.0161	.0029	45933
32	667943	9536	.1776	.0111	.0163	.0032	47488
33	689833	10503	.1793	.0117	.0167	.0035	49037
34	711723	11496	.1903	.0133	.0137	.0073	50115
35	733613	12516	.1921	.0134	.0135	.0071	51578
36	755503	13562	.1933	.0107	.0135	.0033	53034
37	777393	14634	.1945	.0097	.0134	.0035	54495
38	799283	15731	.1955	.0094	.0133	.0039	55957

COLLECTOR DIAMETER 6.27

0 ADDED PER COLLECTOR 27311, 0 TO BOIL 273106, 0 PER T PIPE 111[illegible]

LENGTH BTW COLLECTORS 12.7, LENGTH BTW PIPES 12.7

N	0 ADDED	LOSS PER HT SEGMENT	--HIGH SIDE-- DIA- METER	INSUL. THICK.	--LOW SIDE-- DIA- METER	INSUL. THICK.	MINIMUM COST
16	403970	994	.1776	.1010	.0111	.0105	35113
17	464231	2902	.1909	.0346	.0131	.0095	35107 X
18	491991	3705	.1825	.0240	.0147	.0084	35151
19	519902	5036	.1719	.0103	.0134	.0049	35419
20	546212	6140	.1750	.0156	.0132	.0011	35117
21	573523	7147	.1937	.0126	.0135	.0054	36173
22	600834	8065	.1764	.0102	.0147	.0037	40119
23	628144	8902	.1894	.0112	.0147	.0063	42174
24	655455	9667	.1930	.0106	.0148	.0088	44179
25	682766	10374	.1942	.0095	.0144	.0095	46224
26	710076	11026	.1961	.0092	.0142	.0101	48142
27	737387	11629	.1978	.0070	.0141	.0071	48414
28	764697	12139	.1993	.0055	.0139	.0074	51119
29	792003	12710	.2006	.0053	.0137	.0077	52152
30	819319	13197	.2017	.0079	.0136	.0080	53179
31	846629	13652	.2029	.0077	.0135	.0083	53241
32	873940	14079	.2039	.0075	.0134	.0086	59154
33	901251	14480	.2049	.0073	.0133	.0089	61057

```
HDOT,TRAIL,OF
 ? .32,250,.05
L,AD,FUS,FD",CC
 ? 1,27.1,.5,.5,1731
COLLECTOR DIAMETER              6.37

0 ADDED PER COLLECTOR   27311, 0 TO TRAIL  545210, 0 FWD 0 FUSE  993920

LENGTH BTWN COLLECTORS  13.7, LENGTH BTWN PIPES  13.7
```

N	ADDED	LOSS PER HT SEGMENT	--HIGH SIDE-- DIA- METER	INSUL. THICK.	--LOW SIDE--- DIA- METER	INSUL. THICK.	MINIMUM COST
31	740989	159	.7435	4.7579	.0110	.7104	4407591
32	872940	994	.1565	.1313	.0143	.0829	63511
33	901351	1771	.1747	.0695	.0104	.0156	65165
34	951561	2512	.1937	.0417	.0175	.0103	65664
35	985979	3178	.2170	.0277	.0132	.0103	66137
36	1003128	3758	.2375	.0201	.0171	.0077	67071
37	1016493	4442	.2526	.0137	.0309	.0070	67370
38	1027704	5015	.2715	.0115	.0204	.0055	71451
39	1035816	5527	.2830	.0096	.0192	.0066	73350
40	1040105	6140	.2928	.0063	.0232	.0063	75134
41	1112726	6037	.2481	.0193	.0001	.0070	76906
42	1170[illegible]	7187	.2480	.0171	.0173	.0070	77072
43	1174387	7617	.2455	.0171	.0137	.0074	30491
44	1201067	7965	.2472	.0101	.0137	.0075	52697
45	1207377	7332	.2501	.0123	.0154	.0077	54112
46	1236379	7939	.2585	.0139	.0125	.0079	55929
47	1270279	7893	.2530	.0132	.0135	.0081	57751
48	1310210	9669	.2554	.0103	.0190	.0083	59570

```
HDOT,TRAIL,OF
 ? .32,130,.045
L,AD,FUS,FD",CC
 ? 1,27.1
 ? .5,.5,1731
COLLECTOR DIAMETER              6.37

0 ADDED PER COLLECTOR   30331, 0 TO TRAIL  675100, 0 FWD 0 FUSE  [illegible]

LENGTH BTWN COLLECTORS  13.7, LENGTH BTWN PIPES  13.7
```

N	ADDED	LOSS PER HT SEGMENT	--HIGH SIDE-- DIA- METER	INSUL. THICK.	--LOW SIDE--- DIA- METER	INSUL. THICK.	MINIMUM COST
28	859640	881	.1709	.0750	.0157	.0170	63314
29	881044	1659	.2015	.0255	.0103	.0128	65077
30	911435	2765	.2170	.0515	.0197	.0073	65971
31	941206	3604	.2275	.0177	.0203	.0123	67021
32	972127	4403	.2353	.0139	.0212	.0151	67710
33	1002537	5215	.2417	.0137	.0211	.0159	71051
34	1032945	5956	.2470	.0105	.0221	.0157	73577
35	1063333	6653	.2514	.0111	.0223	.0159	75570
36	1070713	7012	.2552	.0105	.0207	.0071	69779
37	1104021	7935	.2558	.0095	.0205	.0073	62280
38	1134472	8503	.2615	.0093	.0208	.0075	70017
39	1134352	9005	.2641	.0074	.0203	.0066	72741
40	1215003	9419	.2665	.0090	.0202	.0070	76165
41	1245514	10125	.2686	.0077	.0201	.0070	77587
42	1272995	10607	.2706	.0074	.0199	.0072	77752
43	1300376	11067	.2724	.0071	.0191	.0074	78134
44	1303757	11506	.2740	.0063	.0197	.0073	78577
45	1307107	11926	.2755	.0060	.0193	.0077	79227

```
HDOT,TRAIL,OF
 ? .32,200,.0475
L,AD,FUS,FD",CC
 ? 1,27.1,.5,.5,1731
COLLECTOR DIAMETER              6.37

0 ADDED PER COLLECTOR   29417, 0 TO TRAIL  [illegible]  0 FWD 0 FUSE  817072

LENGTH BTWN COLLECTORS  13.7, LENGTH BTWN PIPES  13.7
```

N	ADDED	LOSS PER HT SEGMENT	--HIGH SIDE-- DIA- METER	INSUL. THICK.	--LOW SIDE--- DIA- METER	INSUL. THICK.	MINIMUM COST
30	733106	435	.1431	.9369	.0187	.0021	77114
31	770557	1097	.1711	.0722	.0158	.0031	59250
32	811073	1915	.1915	.0431	.0110	.0110	59392
33	851695	2670	.2102	.0297	.0145	.0079	60410
34	877340	3230	.2215	.0249	.0200	.0070	58191
35	1[illegible]	4038	.2332	.0110	.0204	.0066	63352
36	1[illegible]	4673	.2451	.0127	.0200	.0069	65370
37	1[illegible]	5046	.2509	.0100	.0207	.0061	67335
38	1[illegible]	5820	.2660	.0100	.0205	.0060	69170
39	1[illegible]	7175	.2675	.0110	.0206	.0065	70729
40	1147261	7740	.2703	.0102	.0200	.0069	72697
41	1178740	8291	.2823	.0105	.0202	.0040	74023
42	1178[illegible]	8763	.2827	.0117	.0201	.0070	76225
43	1225589	9297	.2910	.0110	.0199	.0072	78147
44	1264935	9795	.2981	.0107	.0197	.0074	79973
45	1294414	10212	.2917	.0106	.0197	.0073	81702
46	1[illegible]	10683	.3029	.0100	.0195	.0077	83533
47	1[illegible]	11067	.3032	.0097	.0195	.0077	85452

```
[illegible],TRAIL,OF
 ? .32,250,.04
L,AD,FUS,FD",CC
 ? 1,29.1,.5,.5,4-1470
COLLECTOR DIAMETER              6.09

0 ADDED PER COLLECTOR   21540, 0 TO TRAIL  546910, 0 FWD 0 FUSE  [illegible]

LENGTH BTWN COLLECTORS  13.8, LENGTH BTWN PIPES  13.8
```

N	ADDED	LOSS PER HT SEGMENT	--HIGH SIDE-- DIA- METER	INSUL. THICK.	--LOW SIDE--- DIA- METER	INSUL. THICK.	MINIMUM COST
35	852091	259	.3041	.9360	.0080	.0407	878413
36	870940	798	.1510	.1585	.0142	.0155	77351
37	895743	1292	.1737	.0357	.0153	.0177	61[illegible]
38	917637	1766	.1870	.0313	.0170	.0137	61[illegible]
39	939405	2217	.1995	.0407	.0173	.0113	64021
40	961334	2645	.2073	.0303	.0185	.0090	67251
41	975112	3040	.2133	.0355	.0191	.0082	71854
42	1005031	3454	.2193	.0317	.0196	.0079	74[illegible]
43	1026279	3831	.2235	.0293	.0200	.0071	76[illegible]
44	1043725	4206	.2293	.0253	.0199	.0073	77731
45	1070576	4567	.2327	.0244	.0198	.0074	77477
46	1092425	4912	.2326	.0208	.0197	.0076	78[illegible]
47	1114273	5244	.2353	.0215	.0196	.0073	81477
48	1136122	5564	.2377	.0204	.0195	.0079	82[illegible]
49	1157970	5871	.2399	.0194	.0194	.0081	84[illegible]
50	1179819	6167	.2419	.0185	.0193	.0083	85[illegible]
51	1201667	6452	.2433	.0173	.0192	.0084	87[illegible]
52	1223516	6727	.2455	.0171	.0191	.0086	87[illegible]

```
:ROOT,TRAIL,OF
 ? .32,250,.05
L,AP,FIS,FE',CC
 ? 1,37.1,.5,.5,1731
COLLECTOR DIAMETER              6.37

0 ADDED PER COLLECTOR   27381, 0 TO DATA  545210, 0 FOR T RISE  993920

LENGTH BTWN COLLECTORS  13.7, LENGTH BTWN PIPES  13.7
```

N	ADDED	0 PER HT SEGMENT	LOSS DIA- METER	--HIGH SIDE-- INSUL. THICK.	DIA- METER	--LOW SIDE--- INSUL. THICK.	NETWORK COST
31	748997	196	.0439	4.0979	.0020	.0154	4407591
32	872940	894	.1355	.1243	.0141	.0323	63511
33	904731	1771	.1947	.0973	.0184	.0156	65167
34	927451	2502	.1979	.0917	.0175	.0103	66564
35	948772	3193	.1970	.0773	.0173	.0103	66737
36	970115	3885	.2015	.0765	.0171	.0027	68274
37	1147423	4442	.2002	.0710	.0203	.0029	69370
38	1277704	5026	.2015	.0755	.0204	.0155	71659
39	1334134	5597	.2730	.0776	.0203	.0056	73320
40	1377423	6146	.2767	.0753	.0203	.0063	75104
41	1419736	6697	.2781	.0197	.0201	.0070	76906
42	1.7.5	7197	.2811	.0171	.0172	.0035	77633
43	1454357	7617	.2845	.0171	.0197	.0074	80491
44	1501169	8085	.2879	.0197	.0197	.0075	82097
45	1537377	8492	.2931	.0193	.0196	.0077	84110
46	1576779	8903	.2955	.0197	.0193	.0039	85939
47	1620291	9293	.2930	.0193	.0195	.0071	87751
48	1310515	9669	.2959	.0197	.0195	.0053	89573

```
:ROOT,TRAIL,OF
 ? .32,150,.045
L,AP,FIS,FE',CC
 ? 1,37.1
 ? .5,.5,1731
COLLECTOR DIAMETER              6.37

0 ADDED PER COLLECTOR   30331, 0 TO DATA  675103, 0 FOR T RISE  1.1 ??

LENGTH BTWN COLLECTORS  13.7, LENGTH BTWN PIPES  13.7
```

N	ADDED	0 PER HT SEGMENT	LOSS DIA- METER	--HIGH SIDE-- INSUL. THICK.	DIA- METER	--LOW SIDE--- INSUL. THICK.	NETWORK COST
23	859033	577	.1709	.0758	.0157	.0173	55514
29	901044	1659	.2515	.0235	.0122	.0102	58157
30	911405	2745	.2170	.0231	.0197	.0070	59[illegible]
31	941506	3624	.2273	.0121	.0203	.0033	60[illegible]
32	972137	4407	.2353	.0159	.0212	.0054	62[illegible]
33	1002507	5215	.2317	.0137	.0211	.0132	63[illegible]
34	1032945	5955	.2370	.0171	.0227	.0055	65[illegible]
35	1033379	6653	.2514	.0111	.0233	.0139	65[illegible]
36	1070710	7210	.2556	.0102	.0207	.0091	69[illegible]
37	1104021	7935	.2596	.0005	.0205	.0033	67[illegible]
38	1154472	8525	.2615	.0037	.0224	.0235	75[illegible]
39	1154852	9005	.2641	.0078	.0203	.0006	72[illegible]
40	1215033	9613	.2663	.0238	.0201	.0035	74[illegible]
41	1245314	10125	.2686	.0077	.0201	.0270	75[illegible]
42	1275995	10607	.2706	.0074	.0199	.0072	77[illegible]
43	1306376	11067	.2724	.0071	.0191	.0274	78[illegible]
44	1333757	11506	.2740	.0033	.0197	.0075	81[illegible]
45	1367137	11920	.2755	.0099	.0193	.0077	83[illegible]

```
:ROOT,TRAIL,OF
 ? .32,250,.04
L,AP,FIS,FE',CC
 ? 1,37.1,.5,.5,1731
COLLECTOR DIAMETER              6.37

0 ADDED PER COLLECTOR   27381, 0 TO DATA  545210, 0 FOR T RISE  993920

LENGTH BTWN COLLECTORS  13.7, LENGTH BTWN PIPES  13.7
```

N	ADDED	0 PER HT SEGMENT	LOSS DIA- METER	--HIGH SIDE-- INSUL. THICK.	DIA- METER	--LOW SIDE--- INSUL. THICK.	NETWORK COST
31	748997	196	.0439	4.0979	.0020	.0154	4407591
32	872940	894	.1355	.1243	.0141	.0323	63511
33	904731	1771	.1947	.0973	.0184	.0156	65167
34	927451	2502	.1979	.0917	.0175	.0103	66564
35	948772	3193	.1970	.0773	.0173	.0103	66737
36	970115	3885	.2015	.0765	.0171	.0027	68274
37	1147423	4442	.2002	.0710	.0203	.0029	69370
38	1277704	5026	.2015	.0755	.0204	.0155	71659
39	1334134	5597	.2730	.0776	.0203	.0056	73320
40	1377423	6146	.2767	.0753	.0203	.0063	75104
41	1419736	6697	.2781	.0197	.0201	.0070	76906
42	1454357	7197	.2811	.0171	.0172	.0035	77633
43	1501169	7617	.2845	.0171	.0197	.0074	80491
44	1537377	8085	.2879	.0197	.0197	.0075	82097
45	1576779	8492	.2931	.0193	.0196	.0077	84110
46	1620291	8903	.2955	.0197	.0193	.0039	85939
47	1670811	9293	.2930	.0193	.0195	.0071	87751
48	1310515	9669	.2959	.0197	.0195	.0053	89573

```
:ROOT,TRAIL,OF
 ? .32,250,.04
L,AP,FIS,FE',CC
 ? 1,37.1,.5,.5,1731
COLLECTOR DIAMETER              6.37

0 ADDED PER COLLECTOR   21845, 0 TO DATA  546210, 0 FOR T RISE  1.0277

LENGTH BTWN COLLECTORS  13.7, LENGTH BTWN PIPES  13.7
```

N	ADDED	0 PER HT SEGMENT	LOSS DIA- METER	--HIGH SIDE-- INSUL. THICK.	DIA- METER	--LOW SIDE--- INSUL. THICK.	NETWORK COST
39	892091	259	.0741	.3500	.0220	.0127	275417
40	870940	795	.1510	.1525	.0142	.0255	62[illegible]
41	895733	1292	.1757	.0957	.0153	.0107	64[illegible]
42	917637	1784	.1900	.0913	.0193	.0107	64[illegible]
43	934405	2217	.1993	.0427	.0179	.0113	67[illegible]
44	951034	2643	.2073	.0301	.0185	.0090	68[illegible]
45	953152	3050	.2133	.0355	.0191	.0024	71[illegible]
46	1005031	3454	.2183	.0317	.0195	.0073	73[illegible]
47	1026379	3831	.2225	.0287	.0200	.0071	75[illegible]
48	1040725	4205	.2293	.0293	.0199	.0079	77031
49	1070576	4567	.2337	.0244	.0193	.0074	78[illegible]
50	1092425	4912	.2336	.0224	.0197	.0076	79[illegible]
51	1114273	5244	.2353	.0215	.0196	.0073	81[illegible]
52	1136122	5564	.2377	.0204	.0195	.0079	82[illegible]
53	1157970	5871	.2399	.0194	.0194	.0031	84[illegible]
54	1179819	6167	.2419	.0185	.0193	.0033	85[illegible]
55	1201667	6452	.2433	.0173	.0192	.0054	87[illegible]
56	1223516	6727	.2455	.0171	.0191	.0056	88[illegible]

4.2 Boiling Trunk Lines

Computer runs were made for trunk line optimization where saturated steam is being delivered to the trunk line by feeder lines. Example printouts are included. Refer to Figure 4-1 for an explanation of the terms used, in these runs. The minimum cost and its associated optimum pipe diameters and insulation thicknesses for the high or low-temperature sides are given for each trunk line subsystem and for a fixed number of subsystems in a trunk line. Various numbers of subsystems in a trunk line were traced back.

The headings on these runs are for the purpose of identifying unique disk files that are required for the dynamic programming trace backs. All the information contained in the headings, either directly or indirectly, are in subsequent query-response lines. One item of information that is not direction available is the fraction of latent heat added per collector in the feeder lines. This can be found from the first two or three alpha-numerics in the header line as follows:

First alpha-numeric

Q - Target 10 MW_e plant

R - Target 30 MW_e plant

S - Target 100 MW_e plant

Second entry

Smallest integer not greater than (fraction of latent heat added x 100).

Third entry (if required)

F - Add .0025 to the fraction of latent heat as indicated by the second entry

H - Add .0050 to the fraction of latent heat as indicated by the second entry

T - Add .0075 to the fraction of latent heat as indicated by the second entry

The first query-response line is:

KMX - The number of points in the high temperature side grid

NMX - The maximum number of feeder line intersections on a trunk line. That is, 2 KMX is the number of feeder lines to a trunk line. There are 4 KMX trunk lines to a plant since a plant has a trunk line on each side of the trubine-generator.

SM - The collector mass flow rate, $\dot{m}$ (kg/sec)

TO - The boiling temperature (^{o}C)

III - The collector side temperature grid increment (see Appendix B, Section 2.3.9 for an explanation) (^{o}C)

DTL - The return side temperature loss per subsystem (^{o}C)

The second query-response line is:

L - Collector length (1 indicates point focus collectors are used) (m)

A_p - Collector aperture (m^2 or m^2/m)

FNS - North to South fill factor

FEW - East to West fill factor

CSIDE - One feeder line's minimum cost. This is from the runs in Section 4.1.

FILE NAME ? DSN471

NEW EXPERIMENT ? 1

IGM,NMX,SM,TM,TII,DTL ? 201,17,,64,150,,1,,1

L,AP,FNS,FEV,CSIDE ? 1,33.6,,5,,5,118243

LENGTH BETWEEN BRANCHES 13.08

TRACE BACK STAGE ? 17

DESIGN T AND DTL ? 130,,1

COST 8046620

	---HIGH SIDE----			----LOW SIDE----		
STAGE	DT	DIA.	TI	DT	DIA.	TI
17	-1.10	2.0445	.0096	.10	.2330	.0011
16	-1.10	1.9742	.0099	.10	.2253	.0011
15	-1.10	1.9021	.0103	.10	.2173	.0011
14	-1.10	1.8231	.0109	.10	.2090	.0012
13	-1.10	1.7519	.0113	.10	.2005	.0012
12	-1.20	1.6953	.0109	.10	.1917	.0012
11	-1.20	1.6139	.0114	.10	.1826	.0013
10	-1.20	1.5273	.0120	.10	.1731	.0013
9	-1.20	1.4381	.0127	.10	.1632	.0014
8	-1.20	1.3447	.0136	.10	.1527	.0015
7	-1.30	1.2463	.0145	.10	.1417	.0016
6	-1.20	1.1416	.0157	.10	.1299	.0017
5	-1.20	1.0292	.0172	.10	.1172	.0018
4	-1.20	.9065	.0193	.10	.1034	.0020
3	-1.20	.7696	.0222	.10	.0879	.0023
2	-1.20	.6104	.0270	.10	.0693	.0028
1	-1.30	.4143	.0355	.10	.0468	.0039

FRACTION OF LATENT HEAT LOST .0066

MASS FLOW RATE OUT OF SEPARATORS 43.2343

TRACE BACK STAGE ? 17

DESIGN T AND DTL ? 132.5,,1

COST 8047109

	---HIGH SIDE----			----LOW SIDE----		
STAGE	DT	DIA.	TI	DT	DIA.	TI
17	-1.00	1.9482	.0103	.10	.2330	.0011
16	-1.00	1.9419	.0110	.10	.2253	.0011
15	-1.00	1.8718	.0114	.10	.2173	.0011
14	-1.00	1.7986	.0119	.10	.2090	.0012
13	-1.00	1.7239	.0124	.10	.2005	.0012
12	-1.00	1.6467	.0129	.10	.1917	.0012
11	-1.00	1.5669	.0136	.10	.1826	.0013
10	-1.00	1.4840	.0143	.10	.1731	.0013
9	-1.00	1.3975	.0151	.10	.1632	.0014
8	-1.00	1.3069	.0160	.10	.1527	.0015
7	-1.00	1.2113	.0172	.10	.1417	.0016
6	-1.00	1.1097	.0185	.10	.1299	.0017
5	-1.10	1.0015	.0197	.10	.1172	.0018
4	-1.10	.8841	.0209	.10	.1034	.0020
3	-1.10	.7589	.0240	.10	.0879	.0023
2	-1.10	.6017	.0293	.10	.0698	.0028
1	-1.10	.4023	.0415	.10	.0463	.0039

FRACTION OF LATENT HEAT LOST .0053

MASS FLOW RATE OUT OF SEPARATORS 43.2874

TRACE BACK STAGE ? 17

DESIGN T AND DTL ? 135-35,,1

COST 8047739

	---HIGH SIDE----			----LOW SIDE----		
STAGE	DT	DIA.	TI	DT	DIA.	TI
17	-.80	1.8743	.0127	.10	.2330	.0011
16	-.80	1.8743	.0136	.10	.2253	.0011
15	-.80	1.8064	.0141	.10	.2173	.0011
14	-.80	1.7343	.0146	.10	.2090	.0012
13	-.80	1.6744	.0134	.10	.2005	.0012
12	-.80	1.6157	.0144	.10	.1917	.0012
11	-.80	1.5503	.0150	.10	.1826	.0013
10	-.80	1.4859	.0157	.10	.1731	.0013
9	-.80	1.3748	.0167	.10	.1632	.0014
8	-.80	1.2950	.0177	.10	.1527	.0015
7	-.80	1.1910	.0190	.10	.1417	.0016
6	-.80	1.0811	.0205	.10	.1299	.0017
5	-.80	.9636	.0224	.10	.1172	.0018
4	-.80	.8407	.0250	.10	.1034	.0020
3	-.80	.7070	.0287	.10	.0879	.0023
2	-.80	.5523	.0351	.10	.0698	.0028
1	-1.00	.3954	.0453	.10	.0468	.0039

FRACTION OF LATENT HEAT LOST .0041

MASS FLOW RATE OUT OF SEPARATORS 43.3433

TRACE BACK STAGE ? 17

DESIGN T AND DTL ? 140,,1

COST 8049807

	---HIGH SIDE----			----LOW SIDE----		
STAGE	DT	DIA.	TI	DT	DIA.	TI
17	-.50	1.7391	.0128	.10	.2330	.0011
16	-.50	1.7395	.0212	.10	.2253	.0011
15	-.50	1.6768	.0219	.10	.2173	.0011
14	-.60	1.6573	.0124	.10	.2090	.0012
13	-.60	1.5889	.0201	.10	.2005	.0012
12	-.60	1.5132	.0210	.10	.1917	.0012
11	-.60	1.4449	.0219	.10	.1826	.0013
10	-.60	1.3637	.0230	.10	.1731	.0013
9	-.60	1.2791	.0242	.10	.1632	.0014
8	-.60	1.2056	.0257	.10	.1527	.0015
7	-.60	1.1174	.0274	.10	.1417	.0016
6	-.60	1.0234	.0296	.10	.1299	.0017
5	-.60	.9223	.0323	.10	.1172	.0018
4	-.60	.8117	.0360	.10	.1034	.0020
3	-.60	.6775	.0415	.10	.0879	.0023
2	-.60	.5433	.0509	.10	.0698	.0028
1	-.70	.3693	.0637	.10	.0468	.0039

FRACTION OF LATENT HEAT LOST .0016

MASS FLOW RATE OUT OF SEPARATORS 43.4518

FILE NAME ? [redacted]

NEW EXPERIMENT ? 1

KMX,NMX,SM,T3,T11,DTL ? 201,17,.64,250,.1,.1

L,AP,FNS,FEV,CSIDE ? 1,39,1,.5,.5,143227

LENGTH BETWEEN BRANCHES 12.17

TRACE BACK STAGE ? 17

DESIGN T AND DTL ? 230
? .1

COST 9747706

	---HIGH SIDE----			----LOW SIDE----		
STAGE	DT	DIA.	TI	DT	DIA.	TI
17	-1.10	1.9640	.0167	.10	.2352	.0010
16	-1.10	1.8978	.0172	.10	.2274	.0010
15	-1.10	1.8293	.0178	.10	.2193	.0010
14	-1.10	1.7597	.0185	.10	.2110	.0011
13	-1.10	1.6875	.0192	.10	.2025	.0011
12	-1.20	1.6341	.0185	.10	.1936	.0012
11	-1.20	1.5556	.0194	.10	.1844	.0012
10	-1.20	1.4740	.0203	.10	.1748	.0013
9	-1.20	1.3883	.0214	.10	.1648	.0013
8	-1.20	1.2992	.0227	.10	.1543	.0014
7	-1.20	1.2046	.0243	.10	.1431	.0015
6	-1.20	1.1038	.0262	.10	.1313	.0016
5	-1.20	.9953	.0286	.10	.1185	.0017
4	-1.20	.8765	.0319	.10	.1045	.0019
3	-1.20	.7435	.0367	.10	.0883	.0022
2	-1.20	.5884	.0449	.10	.0706	.0026
1	-1.30	.3964	.0597	.10	.0474	.0036

FRACTION OF LATENT HEAT LOST .0080

MASS FLOW RATE OUT OF SEPARATORS 43.1740

TRACE BACK STAGE ? 17

DESIGN T AND DTL ? 240,.1

COST 9752583

	---HIGH SIDE----			----LOW SIDE----		
STAGE	DT	DIA.	TI	DT	DIA.	TI
17	-.50	1.6619	.0329	.10	.2352	.0010
16	-.50	1.6706	.0355	.10	.2274	.0010
15	-.50	1.6702	.0366	.10	.2193	.0010
14	-.60	1.6622	.0323	.10	.2110	.0011
13	-.60	1.5963	.0335	.10	.2025	.0011
12	-.60	1.5832	.0340	.10	.1936	.0012
11	-.60	1.5074	.0364	.10	.1844	.0012
10	-.60	1.4239	.0381	.10	.1748	.0013
9	-.60	1.3468	.0401	.10	.1648	.0013
8	-.60	1.1658	.0425	.10	.1543	.0014
7	-.60	1.0702	.0453	.10	.1431	.0015
6	-.60	.9689	.0489	.10	.1313	.0016
5	-.60	.8604	.0535	.10	.1185	.0017
4	-.60	.7435	.0594	.10	.1045	.0019
3	-.60	.6013	.0686	.10	.0883	.0022
2	-.60	.5108	.0839	.10	.0706	.0026
1	-.70	.3485	.1105	.10	.0474	.0036

FRACTION OF LATENT HEAT LOST .0019

MASS FLOW RATE OUT OF SEPARATORS 43.4393

TRACE BACK STAGE ? 17

DESIGN T AND DTL ? 232,-.5,.1

COST 9748437

	---HIGH SIDE----			----LOW SIDE----		
STAGE	DT	DIA.	TI	DT	DIA.	TI
17	-1.00	1.8403	.0175	.10	.2352	.0010
16	-1.00	1.7697	.0189	.10	.2274	.0010
15	-1.00	1.6927	.0195	.10	.2193	.0010
14	-1.00	1.7337	.0203	.10	.2110	.0011
13	-1.00	1.6626	.0210	.10	.2025	.0011
12	-1.00	1.5990	.0219	.10	.1936	.0012
11	-1.00	1.5187	.0229	.10	.1844	.0012
10	-1.00	1.4333	.0240	.10	.1748	.0013
9	-1.00	1.3503	.0253	.10	.1647	.0013
8	-1.00	1.2612	.0268	.10	.1543	.0014
7	-1.00	1.1711	.0278	.10	.1431	.0015
6	-1.00	1.0709	.0291	.10	.1313	.0016
5	-1.00	.9672	.0307	.10	.1185	.0017
4	-1.10	.8685	.0335	.10	.1045	.0019
3	-1.10	.7230	.0387	.10	.0883	.0022
2	-1.10	.5787	.0479	.10	.0706	.0026
1	-1.20	.3984	.0648	.10	.0474	.0036

FRACTION OF LATENT HEAT LOST .0064

MASS FLOW RATE OUT OF SEPARATORS 43.3398

TRACE BACK STAGE ? 17

DESIGN T AND DTL ? 235,.1

COST 9749394

	---HIGH SIDE----			----LOW SIDE----		
STAGE	DT	DIA.	TI	DT	DIA.	TI
17	-.90	1.7368	.0215	.10	.2352	.0010
16	-.80	1.8070	.0202	.10	.2274	.0010
15	-.80	1.7322	.0209	.10	.2193	.0010
14	-.80	1.6755	.0218	.10	.2110	.0011
13	-.90	1.6357	.0222	.10	.2025	.0011
12	-.90	1.5633	.0242	.10	.1936	.0012
11	-.90	1.4882	.0252	.10	.1844	.0012
10	-.90	1.4100	.0264	.10	.1748	.0013
9	-.90	1.3283	.0278	.10	.1648	.0013
8	-.90	1.2425	.0295	.10	.1543	.0014
7	-.90	1.1518	.0315	.10	.1431	.0015
6	-.90	1.0552	.0339	.10	.1313	.0016
5	-.90	.9510	.0371	.10	.1185	.0017
4	-.90	.8369	.0413	.10	.1045	.0019
3	-.90	.7091	.0477	.10	.0883	.0022
2	-.90	.5597	.0595	.10	.0706	.0026
1	-1.00	.3765	.0770	.10	.0474	.0036

FRACTION OF LATENT HEAT LOST .0049

MASS FLOW RATE OUT OF SEPARATORS 43.3067

FILE NAME ? [illegible]TI

NEW EXPERIMENT ? 1

NMX,NMY,SM,T0,TII,DTL ? 201,13,.16,150,.1,.1

L,AP,FNS,FEU,CSIDE ? 1,17.8,.5,.5,.69951

LENGTH BETWEEN BRANCHES 9.30

TRACE BACK STAGE ? 13

DESIGN T AND DTL ? 130,.1

COST 3639711

STAGE	---HIGH SIDE--- DT	DIA.	TI	----LOW SIDE---- DT	DIA.	TI
13	-1.40	.8414	.0122	.10	.0969	.0017
12	-1.40	.8414	.0123	.10	.0926	.0017
11	-1.40	.8081	.0135	.10	.0891	.0018
10	-1.50	.7652	.0134	.10	.0835	.0019
9	-1.50	.7200	.0142	.10	.0787	.0020
8	-1.50	.6723	.0152	.10	.0736	.0021
7	-1.50	.6229	.0163	.10	.0683	.0022
6	-1.50	.5700	.0178	.10	.0625	.0024
5	-1.50	.5132	.0196	.10	.0563	.0026
4	-1.60	.4559	.0203	.10	.0496	.0029
3	-1.60	.3859	.0241	.10	.0420	.0033
2	-1.70	.3077	.0293	.10	.0331	.0040
1	-1.90	.2075	.0371	.10	.0217	.0059

FRACTION OF LATENT HEAT LOST .0063

MASS FLOW RATE OUT OF SEPARATORS 8.2470

TRACE BACK STAGE ? 13

DESIGN T AND DTL ? 132.5,.1

COST 3639867

STAGE	---HIGH SIDE--- DT	DIA.	TI	----LOW SIDE---- DT	DIA.	TI
13	-1.30	.8225	.0137	.10	.0969	.0017
12	-1.30	.8203	.0143	.10	.0926	.0017
11	-1.30	.7895	.0145	.10	.0891	.0018
10	-1.30	.7472	.0154	.10	.0835	.0019
9	-1.30	.7032	.0164	.10	.0787	.0020
8	-1.30	.6576	.0174	.10	.0736	.0021
7	-1.30	.6104	.0187	.10	.0683	.0022
6	-1.30	.5567	.0204	.10	.0625	.0024
5	-1.30	.5011	.0224	.10	.0563	.0026
4	-1.40	.4453	.0234	.10	.0496	.0029
3	-1.40	.3772	.0276	.10	.0420	.0033
2	-1.50	.3000	.0335	.10	.0331	.0040
1	-1.70	.2029	.0414	.10	.0217	.0059

FRACTION OF LATENT HEAT LOST .0075

MASS FLOW RATE OUT OF SEPARATORS 8.2575

TRACE BACK STAGE ? 13

DESIGN T AND DTL ? 135,.1

COST 3640072

STAGE	---HIGH SIDE--- DT	DIA.	TI	----LOW SIDE---- DT	DIA.	TI
13	-1.10	.8166	.0151	.10	.0969	.0017
12	-1.10	.8073	.0160	.10	.0926	.0017
11	-1.10	.7870	.0172	.10	.0891	.0018
10	-1.10	.7563	.0188	.10	.0835	.0019
9	-1.10	.7180	.0199	.10	.0787	.0020
8	-1.10	.6691	.0219	.10	.0736	.0021
7	-1.10	.6119	.0240	.10	.0683	.0022
6	-1.10	.5414	.0263	.10	.0625	.0024
5	-1.10	.4673	.0288	.10	.0563	.0026
4	-1.20	.4383	.0272	.10	.0496	.0029
3	-1.20	.3671	.0317	.10	.0420	.0033
2	-1.30	.2930	.0385	.10	.0331	.0040
1	-1.40	.1946	.0504	.10	.0217	.0059

FRACTION OF LATENT HEAT LOST .0064

MASS FLOW RATE OUT OF SEPARATORS 8.2672

TRACE BACK STAGE ? 13

DESIGN T AND DTL ? 140,.1

COST 3640769

STAGE	---HIGH SIDE--- DT	DIA.	TI	----LOW SIDE---- DT	DIA.	TI
13	-.70	.7590	.0236	.10	.0969	.0017
12	-.70	.7494	.0253	.10	.0926	.0017
11	-.70	.7128	.0265	.10	.0891	.0018
10	-.70	.6747	.0278	.10	.0835	.0019
9	-.70	.6349	.0294	.10	.0787	.0020
8	-.70	.5930	.0313	.10	.0736	.0021
7	-.70	.5488	.0336	.10	.0683	.0022
6	-.70	.5017	.0364	.10	.0625	.0024
5	-.80	.4614	.0358	.10	.0563	.0026
4	-.80	.4047	.0399	.10	.0496	.0029
3	-.80	.3411	.0465	.10	.0420	.0033
2	-.90	.2729	.0522	.10	.0331	.0040
1	-1.10	.1841	.0646	.10	.0217	.0059

FRACTION OF LATENT HEAT LOST .0037

MASS FLOW RATE OUT OF SEPARATORS 8.2890

TRACE BACK STAGE ? 13

DESIGN T AND DTL ? 145,.1

COST 3642918

STAGE	---HIGH SIDE--- DT	DIA.	TI	----LOW SIDE---- DT	DIA.	TI
13	-.30	.6576	.0517	.10	.0969	.0017
12	-.30	.6498	.0559	.10	.0926	.0017
11	-.30	.6174	.0585	.10	.0891	.0018
10	-.30	.5836	.0615	.10	.0835	.0019
9	-.30	.5483	.0651	.10	.0787	.0020
8	-.40	.5090	.0691	.10	.0736	.0021
7	-.40	.4673	.0741	.10	.0683	.0022
6	-.40	.4236	.0801	.10	.0625	.0024
5	-.40	.4043	.0887	.10	.0563	.0026
4	-.40	.3543	.0731	.10	.0496	.0029
3	-.40	.2954	.0850	.10	.0420	.0033
2	-.50	.2302	.0957	.10	.0331	.0040
1	-.60	.1550	.1297	.10	.0217	.0059

FRACTION OF LATENT HEAT LOST .0019

MASS FLOW RATE OUT OF SEPARATORS 8.3099

4.3 Parallel Pressurized Water Feeder Lines

Computer runs were made for feeder line optimization where pressurized water is being heated in a single parallel collector piping arrangement. Examples are included to illustrate the general feeder-line optimization case whereas the runs in Section 4.1 are a special case because of simplifications that were possible. Refer to Figure 4-1 for an explanation of the terms used in these runs. The minimum cost and its associated high and low temperature side optimum ΔT's, pipe diameters and insulation thicknesses are given for feeder lines comprised of different numbers of subsystems.

The runs are made for different collectors that are designed to provide collector ΔT's that range from 5^{o} to 15 ^{o}C above a desired high side output temperature at the end of the feeder line. The optimum collector ΔT can be obtained from a set of these runs. Since the minimum costs for high pressure water systems were obviously going to be significantly higher than steam systems, the analysis of hot water systems did not proceed much beyond these computer runs. However, these computer runs do constitute a representative optimization analysis of pressurized water feeder lines.

The headings on these runs are also for the purpose of having a unique disk file identifier. All of the information in the header lines is contained in the query-response lines. The first query response line is:

KMX - The number of points in the high temperature grid

KMXL - The number of points in the low temperature grid

NMX - The maximum number of subsystems in a feeder line

FTYPE - 1 series piping arrangement, 2 single parallel piping arrangement, 3 double parallel piping arrangement and so forth.

SM - The collector mass flow rate, $\dot{m}$ (kg/sec.)

TO - The feeder line output design temperature (^{o}C)

TRISE - The collector ΔT (^{o}C)

TII - The high temperature side grid increment (^{o}C)

TIIL - The low temperature side grid increment (^{o}C)

The second query response line is:

YD - The collector length. The response 1 is used for point focus Collectors (m)

XD - The collector aperture (m^2 or m^2/m)

FNS - The North to South fill factor

FEW - The East to West fill factor

CC - The collector cost ($)

```
FILE NAME
? [illegible]                    TWO3IDI NEW
NEW [illegible]-ENT
 ? 1
ICON,KKYL,DIM,STYPE,CN,TT,TOISE,TII,TIIL
 ? 11,91,30,2,.1,.012,37,1,.25
YD,XD,FNS,FEN,CC
 ? 1,20.6,.5,.5,1154
QUE,S
JOB IN EXECUTION.
ACCUM. CPU SECONDS =  1025.525
TIME LIMIT CPU SECS=  1200.419
?
T=1000


QUE,S
JOB IN EXECUTION.
ACCUM. CPU SECONDS =  2057.510
TIME LIMIT CPU SECS=  2200.794
?
T=30--1000


TRACE BACK STAGE AND DESIGN T AND TL
 ? 20,200,175

TRACE BACK FROM STAGE  20  COST      27327  DESIGN T AND TL 200.00 175.

STAGE---HIGH SIDE DT, D, TI---LOW SIDE DT, D, TI
 20  0.    .0377  .0104   .25 .0353  .0263
 19  0.    .0367  .0104   .25 .0342  .0275
 18  0.    .0358  .0104   .25 .0330  .0286
 17  0.    .0348  .0104   .25 .0318  .0298
 16  0.    .0338  .0104   .25 .0305  .0311
 15  0.    .0327  .0104   .25 .0291  .0341
 14  0.    .0316  .0104   .25 .0277  .0365
 13  0.    .0305  .0106   .50 .0299  .0150
 12  0.    .0293  .0109   .50 .0286  .0160
 11  0.    .0280  .0113   .50 .0272  .0172
 10  0.    .0267  .0116   .50 .0258  .0186
  9  0.    .0253  .0120   .50 .0242  .0205
  8  0.    .0238  .0124   .50 .0224  .0220
  7  0.    .0223  .0128   .50 .0205  .0261
  6  0.    .0206  .0133   .50 .0182  .0307
  5  0.    .0187  .0136   .50 .0157  .0377
  4  0.    .0165  .0150   .75 .0161  .0254
  3  1.00  .0109  .0078   .75 .0120  .0359
  2  1.00  .0107  .0032  1.25 .0105  .0245
  1 -3.00  .0090  .0178  2.00 .0080  .0303

TRACE BACK STAGE AND DESIGN T AND TL
 ? 2*15,200,175

TRACE BACK FROM STAGE  15  COST      20308  DESIGN T AND TL 200.00 175...

STAGE---HIGH SIDE DT, D, TI---LOW SIDE DT, D, TI
 15  0.    .0225  .0093   .50 .0203  .0135
 14  0.    .0217  .0095   .50 .0211  .0142
 13  0.    .0206  .0097   .50 .0199  .0151
 12  0.    .0194  .0099   .50 .0186  .0161
 11  0.    .0181  .0101   .50 .0172  .0173
 10  0.    .0167  .0104   .50 .0158  .0187
  9  0.    .0154  .0106   .50 .0145  .0200
  8  0.    .0140  .0109   .50 .0124  .0220
  7  0.    .0124  .0111   .50 .0105  .0263
  6  0.    .0108  .0113   .50 .0190  .0300
  5  0.    .0129  .0121   .75 .0179  .0202
  4  1.00  .0131  .0452   .75 .0153  .0255
  3  1.00  .0125  .0225  1.00 .0135  .0220
  2  1.00  .0115  .0166  1.75 .0117  .0154
  1 -3.00  .0090  .0178  2.75 .0091  .0152

TRACE BACK STAGE AND DESIGN T AND TL
 ? 15,205,175

TRACE BACK FROM STAGE  15  COST      22604  DESIGN T AND TL 205.00 175.00

STAGE---HIGH SIDE DT, D, TI---LOW SIDE DT, D, TI
 15  0.    .0317  .0103   .25 .0291  .0345
 14  0.    .0306  .0102   .25 .0276  .0362
 13  0.    .0294  .0105   .25 .0261  .0397
 12  0.    .0282  .0109   .25 .0244  .0422
 11  0.    .0269  .0002   .25 .0225  .0479
 10  0.    .0256  .0006   .25 .0207  .0539
  9  0.    .0242  .0110   .25 .0187  .0604
  8  0.    .0227  .0113   .25 .0166  .0710
  7  0.    .0212  .0116   .25 .0140  .0765
  6  0.    .0195  .0120   .75 .0111  .1176
  5  0.    .0177  .0119   .25 .0090  .1417
  4  0.    .0133  .0129   .50 .0120  .0555
  3  0.    .0130  .0065   .50 .0099  .0831
  2  1.00  .0010  .1306   .75 .0010  .0739
  1 -2.00  .0080  .0501  1.00 .0080  .0724

TRACE BACK STAGE AND DESIGN T AND TL
 ? 10,200,175

TRACE BACK FROM STAGE  10  COST      13429  DESIGN T AND TL 200.00 175.00

STAGE---HIGH SIDE DT, D, TI---LOW SIDE DT, D, TI
 10  0.    .0270  .0079   .75 .0257  .0111
  9  0.    .0256  .0081   .75 .0252  .0121
  8  0.    .0242  .0084   .75 .0237  .0133
  7  0.    .0226  .0087   .75 .0220  .0149
  6  0.    .0210  .0091   .75 .0201  .0171
  5  0.    .0191  .0094   .75 .0179  .0204
  4  1.00  .0153  .0257  1.00 .0164  .0166
  3  1.00  .0142  .0166  1.25 .0142  .0159
  2  1.00  .0118  .0130  2.00 .0119  .0113
  1 -3.00  .0060  .0176  3.25 .0084  .0115

TRACE BACK STAGE AND DESIGN T AND TL
 ? 10,205,175

TRACE BACK FROM STAGE  10  COST      14218  DESIGN T AND TL 205.00 175.00

STAGE---HIGH SIDE DT, D, TI---LOW SIDE DT, D, TI
 10  0.    .0283  .0155   .25 .0307  .0538
  9  0.    .0269  .0155   .25 .0287  .0613
  8  0.    .0255  .0156   .25 .0265  .0715
  7  0.    .0219  .0164   .50 .0203  .0270
  6  0.    .0201  .0174   .50 .0181  .0318
  5  0.    .0182  .0185   .50 .0155  .0390
  4  0.    .0161  .0197   .50 .0125  .0527
  3  0.    .0134  .0235   .75 .0113  .0375
  2  1.00  .0002  .0778   .75 .0030  .0743
  1 -2.00  .0070  .0501  1.75 .0070  .0748

TRACE BACK STAGE AND DESIGN T AND TL
 ? 5,200,175

TRACE BACK FROM STAGE   5  COST       6562  DESIGN T AND TL 200.00 175.00

STAGE---HIGH SIDE DT, D, TI---LOW SIDE DT, D, TI
  5  1.00  .0190  .0109  1.25 .0190  .0102
  4  1.00  .0172  .0088  1.50 .0171  .0096
  3  1.00  .0150  .0076  2.00 .0149  .0092
  2  0.    .0124  .0057  2.50 .0122  .0036
  1 -4.00  .0095  .0107  3.75 .0096  .0093
```

```
 FILE NAME
  ?,T2,CIOS        TWOSIDI NEW
 NEW EXPERIMENT
  ? 1
 XMD,XMML,XMM,FTYPE,SM,T3,TPISE,TIL,TIIL
  ? 11,61,70,3,.1,215,65,1,.25
 YU,XD,FNS,FEN,CC
  ? 1,35.3,.5,.5,1747
 QUE,0
 JOB IN EXECUTION.
 ACCUM. CPU SECONDS =   802.039

TRACE BACK STAGE AND DESIGN T AND TL
 ? 20,200,150

TRACE BACK FROM STAGE  20  COST     40442  DESIGN T AND TL 200.00 150.00

STAGE---HIGH SIDE DT, D, TI---LOW SIDE DT, D, TI
 20  0.   .0371  .0152   .25 .0320  .0449
 19  0.   .0362  .0152   .25 .0307  .0472
 18  0.   .0352  .0151   .25 .0294  .0498
 17  0.   .0343  .0151   .25 .0280  .0529
 16  0.   .0332  .0150   .25 .0266  .0564
 15  0.   .0322  .0153   .50 .0312  .0221
 14  0.   .0310  .0155   .50 .0299  .0234
 13  0.   .0299  .0158   .50 .0285  .0249
 12  0.   .0287  .0161   .50 .0271  .0265
 11  0.   .0274  .0164   .50 .0255  .0290
 10  0.   .0261  .0166   .50 .0238  .0318
  9  0.   .0247  .0169   .50 .0220  .0354
  8  0.   .0232  .0171   .50 .0200  .0401
  7  0.   .0217  .0173   .50 .0178  .0468
  6  0.   .0201  .0175   .50 .0153  .0570
  5  0.   .0182  .0183   .75 .0160  .0357
  4  0.   .0161  .0191   .75 .0130  .0471
  3  0.   .0135  .0211  1.00 .0115  .0418
  2  0.   .0105  .0254  1.25 .0097  .0494
  1 -3.00 .0030  .0709  2.00 .0030  .0831

TRACE BACK STAGE AND DESIGN T AND TL
 ? 10,200,150

TRACE BACK FROM STAGE  10  COST     21003  DESIGN T AND TL 200.00 150.00

STAGE---HIGH SIDE DT, D, TI---LOW SIDE DT, D, TI
 10  0.   .0257  .0115   .75 .0259  .0135
  9  0.   .0253  .0117   .75 .0243  .0203
  8  0.   .0239  .0119   .75 .0225  .0225
  7  0.   .0223  .0121   .75 .0206  .0256
  6  0.   .0207  .0123   .75 .0184  .0300
  5  0.   .0188  .0128  1.00 .0175  .0233
  4  0.   .0168  .0133  1.00 .0148  .0296
  3  0.   .0144  .0144  1.25 .0128  .0287
  2  0.   .0115  .0165  1.50 .0097  .0349
  1 -4.00 .0080  .0318  2.50 .0080  .0442

TRACE BACK STAGE AND DESIGN T AND TL
 ? 10,205,150

TRACE BACK FROM STAGE  10  COST     22040  DESIGN T AND TL 205.00 150.00

STAGE---HIGH SIDE DT, D, TI---LOW SIDE DT, D, TI
 10  0.   .0256  .0203   .50 .0226  .0331
  9  0.   .0242  .0209   .50 .0218  .0365
  8  0.   .0227  .0215   .50 .0198  .0419
  7  0.   .0211  .0221   .50 .0175  .0490
  6  0.   .0194  .0226   .50 .0150  .0598
  5  0.   .0174  .0244   .75 .0158  .0373
  4  1.00 .0100  .0260   .75 .0127  .0495
  3  1.00 .0111  .0268  1.00 .0113  .0434
  2  1.00 .0101  .0313  1.50 .0096  .0359
  1

TRACE BACK STAGE AND DESIGN T AND TL
 ? 15,200,150

TRACE BACK FROM STAGE  15  COST     31976  DESIGN T AND TL 200.00 150.00

STAGE---HIGH SIDE DT, D, TI---LOW SIDE DT, D, TI
 15  0.   .0324  .0136   .50 .0311  .0223
 14  0.   .0313  .0138   .50 .0298  .0237
 13  0.   .0301  .0139   .50 .0285  .0252
 12  0.   .0289  .0141   .50 .0270  .0271
 11  0.   .0277  .0142   .50 .0255  .0294
 10  0.   .0264  .0143   .50 .0239  .0322
  9  0.   .0250  .0145   .50 .0219  .0359
  8  0.   .0235  .0145   .50 .0199  .0407
  7  0.   .0220  .0150   .75 .0206  .0251
  6  0.   .0203  .0155   .75 .0185  .0294
  5  0.   .0185  .0161   .75 .0159  .0360
  4  0.   .0163  .0173  1.00 .0149  .0291
  3  0.   .0139  .0137  1.00 .0115  .0415
  2  0.   .0110  .0216  1.25 .0057  .0483
  1 -3.00 .0080  .0709  2.50 .0080  .0433

TRACE BACK STAGE AND DESIGN T AND TL
 ? 15,205,150

TRACE BACK FROM STAGE  15  COST     35206  DESIGN T AND TL 205.00 150.00

STAGE---HIGH SIDE DT, D, TI---LOW SIDE DT, D, TI
 15  0.   .0310  .0237   .25 .0249  .0616
 14  0.   .0299  .0237   .25 .0233  .0667
 13  0.   .0285  .0238   .25 .0217  .0731
 12  0.   .0276  .0239   .25 .0199  .0812
 11  0.   .0254  .0239   .25 .0181  .0919
 10  0.   .0251  .0238   .25 .0162  .1063
  9  0.   .0236  .0247   .50 .0218  .0385
  8  0.   .0221  .0258   .50 .0198  .0414
  7  0.   .0204  .0269   .50 .0176  .0494
  6  0.   .0187  .0281   .50 .0151  .0590
  5  0.   .0168  .0294   .50 .0123  .0771
  4  0.   .0146  .0330   .75 .0128  .0490
  3  1.00 .0080  .1445   .75 .0092  .0763
  2  1.00 .0080  .0597  1.25 .0095  .0509
  1 -3.00 .0070  .0738  2.25 .0070  .0621

TRACE BACK STAGE AND DESIGN T AND TL
 ? 5,200,150

TRACE BACK FROM STAGE   5  COST     10384  DESIGN T AND TL 200.00 150.00

STAGE---HIGH SIDE DT, D, TI---LOW SIDE DT, D, TI
  5  0.   .0192  .0056  1.25 .0183  .0174
  4  0.   .0172  .0090  1.50 .0164  .0164
  3  0.   .0148  .0097  1.75 .0141  .0172
  2  0.   .0120  .0113  2.25 .0113  .0179
  1 -5.00 .0080  .0190  3.25 .0080  .0237

TRACE BACK STAGE AND DESIGN T AND TL
 ? 5,205,150

TRACE BACK FROM STAGE   5  COST     10505  DESIGN T AND TL 205.00 150.00

STAGE---HIGH SIDE DT, D, TI---LOW SIDE DT, D, TI
  5  1.00 .0155  .0095  1.00 .0174  .0240
  4  1.00 .0150  .0293  1.25 .0155  .0217
  3  1.00 .0136  .0216  1.50 .0135  .0202
  2  2.00 .0105  .0258  2.25 .0113  .0161
  1 -5.00 .0080  .0190  4.00 .0081  .0155

TRACE BACK STAGE AND DESIGN T AND TL
 ? STOP

  1967.049 /  15703.664 /      10673
```

5.0 TURBINE GENERATOR-COOLING TOWER OPTIMIZATION RUNS

The computer outputs of this section are examples of distributed systems and tower-heliostat systems. The headings on the outputs are self-explanatory. The inputs to these runs came from selected computer outputs described in Sections 3.0 and 4.2. These input runs may be identified by the steam flow rate and inlet temperatures.

5.1 Distributed Systems

The inputs from the field optimization runs of Section 4.2 are not all minimum-cost system runs. This is because a turbine-generator-cooling tower optimization run was made immediately after a group of field optimization runs had been made. This was done since the mass flow out of different shaped fields varied somewhat even though the same power plant size was being designed. Thus, without the turbine optimization, it was difficult to distinguish which field had a lower cost of power. The mass flow rate variation was caused by sizing the fields in multiples of 4 feeder lines to achieve symmetry.

1	2 *	3 *	4	5 *	6	7	8	9	10	11	12	13
ELECT POWER MW-E	STEAM FLOW KG/SEC	INL TMP D-C	ENG EFF	FIELD COSTS $/KWE	TUR-GEN COSTS $/KWE	COOLNG COSTS $/KWE	ELECT COST $/KWH	CONDENSER TEMP DEGREES	INL	OUT	RNG CENTIGRADE	APPR TMP
31.5	43.4	250	.34	282.19	92.43	27.97	.024	40	28	38	10	3**
31.5	43.4	250	.34	282.19	92.46	27.97	.024	40	28	38	10	3
31.6	43.5	250	.34	281.72	92.44	27.97	.024	40	28	38	10	3
31.7	43.6	250	.34	281.71	92.40	27.96	.024	40	28	38	10	3
110.1	148.1	250	.36	297.00	83.31	24.15	.024	40	28	38	10	3
110.2	148.2	250	.36	296.76	83.30	24.15	.024	40	28	38	10	3
110.4	148.5	250	.36	296.16	83.27	24.14	.024	40	28	38	10	3
110.7	148.8	250	.36	296.39	83.23	24.14	.024	40	28	38	10	3
95.3	147.8	200	.36	313.61	90.12	29.46	.026	40	28	38	10	3
95.4	147.9	200	.36	313.38	90.11	29.46	.026	40	28	38	10	3
95.6	148.2	200	.36	312.81	90.03	29.46	.026	40	28	38	10	3
96.4	149.5	200	.36	310.11	89.94	29.45	.026	40	28	38	10	3
75.7	147.6	150	.36	356.59	104.45	40.01	.030	40	28	38	10	3
75.8	147.7	150	.36	356.35	104.44	40.01	.030	40	28	38	10	3
75.9	148.0	150	.36	355.75	104.41	40.01	.030	40	28	38	10	3
76.0	148.3	150	.36	355.08	104.38	40.01	.030	40	28	38	10	3
27.3	43.4	200	.34	294.84	93.95	33.95	.026	40	28	38	10	3
27.4	43.4	200	.34	294.57	93.93	33.95	.026	40	28	38	10	3
27.4	43.5	200	.34	294.10	93.90	33.94	.026	40	28	38	10	3
27.5	43.6	200	.34	294.08	93.86	33.93	.026	40	28	38	10	3
21.7	43.4	150	.34	345.96	112.37	45.80	.030	40	28	38	10	3
21.8	43.4	150	.34	346.10	112.35	45.79	.030	40	28	38	10	3
21.9	43.5	150	.34	345.55	112.32	45.79	.030	40	28	38	10	3
21.8	43.6	150	.34	345.21	112.28	45.77	.030	40	28	38	10	3

* Columes 2, 3, and 5 are input data from collector field optimization.

** The 3 ^{o}C is a smaller approach than normally encountered in practice. This has resulted in part from the coarse grid (10^{o}) for condenser temperature and 5^{o} grid for range used in the initial run of this program.

5.2 Tower-Heliostat Systems

The inputs from the concentrator optimization runs of Section 3.0 were used for the optimization runs of this section. Example outputs from the computer optimization are included.

09/27/74. 09.52.53. C9628
PROGRAM NUMI

ELECT POWER MW-E	STEAM FLOW KG/SEC	INL TMP D-C	ENG EFF	FIELD COSTS $/KWE	TUR-GEN COSTS $/KWE	COOLING COSTS $/KWE	ELECT COST $/KWH	CONDENSER TEMP DEGREES	INL	OUT	ENG CENTIGRADE	APPR TMP
.9	1.7	150	.86	740.91	220.80	176.06	.063	40	28	38	10	3
.9	1.7	150	.86	751.03	220.80	176.06	.063	40	28	38	10	3
.9	1.7	150	.86	760.41	220.80	176.06	.063	40	28	38	10	3
.9	1.8	150	.86	727.91	218.64	168.41	.057	40	28	38	10	3
.9	1.8	150	.86	734.41	218.64	168.41	.057	40	28	38	10	3
.9	1.8	150	.86	746.22	218.64	168.41	.059	40	28	38	10	3
1.0	1.9	150	.86	709.07	216.62	161.57	.065	40	28	38	10	3
1.0	1.9	150	.86	717.31	216.62	161.57	.065	40	28	38	10	3
1.	1.9	150	.86	726.54	216.62	161.57	.065	40	28	38	10	3
1.0	2.0	150	.86	709.71	214.70	155.41	.065	40	28	38	10	3
1.0	2.0	150	.86	709.71	214.72	155.41	.065	40	28	38	10	3
1.1	1.7	200	.86	616.49	201.78	137.64	.057	40	28	38	10	3
1.1	1.7	200	.86	620.14	201.78	137.64	.057	40	28	38	10	3
1.1	1.7	200	.86	630.17	201.78	137.64	.058	40	28	38	10	3
1.1	1.9	200	.84	610.91	175.74	135.38	.055	40	28	38	10	3
1.1	1.8	200	.86	606.08	175.74	135.38	.056	40	28	38	10	3
1.2	1.9	200	.86	612.38	199.71	131.56	.056	40	28	38	0	3
1.2	1.9	200	.8	672.32	174.03	129.81	.054	40	28	38	10	3
1.2	1.9	200	.84	610.67	174.03	129.81	.055	40	28	38	10	3
1.2	1.9	200	.84	619.03	174.03	129.81	.055	40	28	38	10	3
1.3	2.0	200	.84	589.66	172.43	124.80	.053	40	28	38	10	3
1.3	2.0	200	.84	597.60	172.43	124.80	.054	40	28	38	10	3
1.2	1.7	250	.84	558.99	169.11	121.36	.051	40	28	38	10	3
1.2	1.7	250	.84	565.36	169.11	121.36	.051	40	28	38	10	3
1.2	1.7	250	.84	572.65	169.11	121.36	.052	40	28	38	10	3
1.3	1.8	250	.84	543.49	167.33	115.97	.050	40	28	38	10	3
1.3	1.8	250	.84	556.90	167.33	115.97	.050	40	28	38	10	3
1.3	1.8	250	.84	563.02	167.33	115.97	.051	40	28	38	10	3
1.4	1.9	250	.84	540.64	165.67	111.13	.049	40	28	38	10	3
1.4	1.9	250	.84	547.89	165.67	111.13	.049	40	28	38	10	3
1.4	1.9	250	.84	555.13	165.67	111.13	.050	40	28	38	10	3
1.5	2.0	250	.84	534.95	164.10	106.79	.048	40	28	38	10	3
1.5	2.0	250	.84	543.90	164.10	106.79	.049	40	28	38	10	3

STOP.

09/27/74. 12.38.58. C9628
PROGRAM TH

ELECT POWER MW-E	STEAM FLOW KG/SEC	INL TMP D-C	ENG EFF	FIELD COSTS $/KWE	TUR-GEN COSTS $/KWE	COOLING COSTS $/KWE	ELECT COST $/KWH	CONDENSER TEMP DEGREES	INL	OUT	ENG CENTIGRADE	APPR TMP
2.5	5.0	150	.84	546.05	161.56	99.10	.049	40	28	38	10	3
2.6	5.1	150	.84	547.97	161.02	97.25	.049	40	28	38	10	3
2.6	5.2	150	.84	559.79	160.49	96.35	.049	40	28	38	10	3
2.7	5.3	150	.84	542.36	159.97	95.48	.047	40	28	38	10	3
2.7	5.4	150	.84	543.41	159.46	94.64	.047	40	28	38	10	3
2.8	5.5	150	.84	540.73	158.96	93.83	.047	40	28	38	10	3
2.8	5.6	150	.84	531.13	158.47	83.05	.046	40	28	38	10	3
2.9	5.7	150	.84	532.32	158.00	82.30	.046	40	28	38	10	3
2.9	5.8	150	.84	530.02	157.53	81.53	.046	40	28	38	10	3
3.0	5.9	150	.84	531.19	157.08	80.80	.046	40	28	38	10	3
3.0	6.0	150	.84	528.89	156.63	80.20	.046	40	28	38	10	3
3.2	5.0	200	.84	463.48	146.15	67.66	.041	40	28	38	10	3
3.2	5.1	200	.84	465.34	145.62	66.91	.041	40	28	38	10	3
3.3	5.2	200	.84	460.91	145.11	66.19	.040	40	28	38	10	3
3.3	5.3	200	.84	464.20	144.62	65.50	.040	40	28	38	10	3
3.4	5.4	200	.84	464.42	144.13	64.84	.040	40	28	38	10	3
3.5	5.5	200	.84	455.77	143.65	64.20	.040	40	28	38	10	3
3.5	5.6	200	.84	453.50	143.19	63.59	.040	40	28	38	10	3
3.6	5.7	200	.84	456.68	142.73	62.99	.040	40	28	38	10	3
3.7	5.8	200	.84	440.62	142.28	62.40	.039	40	28	38	10	3
3.7	5.9	200	.84	443.82	141.84	61.85	.039	40	28	38	10	3
3.8	6.0	200	.84	433.18	141.41	61.31	.039	40	28	38	10	3
3.6	5.0	250	.84	424.10	137.41	57.01	.037	40	28	38	10	3
3.7	5.1	250	.84	423.33	137.03	56.67	.037	40	28	38	10	3
3.7	5.2	250	.84	426.33	137.43	55.94	.037	40	28	38	10	3
3.8	5.3	250	.84	420.99	136.99	55.34	.037	40	28	38	10	3
3.9	5.4	250	.84	423.14	136.58	54.77	.037	40	28	38	10	3
4.0	5.5	250	.84	418.52	136.05	54.21	.036	40	28	38	10	3
4.1	5.6	250	.84	415.55	135.69	53.67	.036	40	28	38	10	3
4.1	5.7	250	.84	418.67	135.15	53.16	.036	40	28	38	10	3
4.2	5.8	250	.84	418.71	134.72	52.66	.036	40	28	38	10	3
4.3	5.9	250	.84	403.75	134.29	52.17	.035	40	28	38	10	3
4.4	6.0	250	.84	401.61	133.87	51.71	.035	40	28	38	10	3

STOP.

24.174 / 69.436 / 0

702B